A Mechanistic Analysis of Naphthenate and Carboxylate Soap-Forming Systems in Oilfield Exploration and Production

Andrew G. Shepherd

Submitted for the degree of Doctor of Philosophy

Heriot-Watt University

School of Engineering and Physical Sciences

December 2008

ABSTRACT

This project entailed mechanistic aspects of the formation of oilfield soaps. An integrated approach to the study of field deposits was developed leading to an optimised analytical protocol which is one of the major contributions of this thesis. The philosophy behind the choice of techniques was to integrate measurements suitable for bulk and surface properties. The selected and optimised techniques were electrospray mass spectrometry (ES), energy dispersive X-ray (EDAX) and solid state ^{13}C nuclear magnetic resonance (NMR) as well as thermal analysis (TGA/DSC) and interfacial tension (IFT). These allowed for the differentiation of the two end-member types of soaps, namely, calcium naphthenate soap scales and sodium carboxylate soap emulsions, as well as for the identification of chemically-treated deposits and asphaltenes. It was concluded that the analysis of naphthenic acids from field soap deposits in mass spectrometry was a function of: ionisation source, solvent and instrument settings (e.g. voltages). These parameters had a direct effect on the relative detection of particular naphthenic acid species such as the Arn. Though the electrospray (ES) source was observed to lead to a more realistic fingerprint for naphthenic acid extracts, it was also suggested that the atmospheric pressure chemical ionisation (APCI) source could be used in conditions where identification of Arn was the ultimate objective. A series of static bottle tests were devised to simulate the pH changes associated with the occurrence of deposits in the field. The procedures focused on a number of model naphthenic acid systems, as well as acids extracted from field deposits and soap-forming crude oils. Soap formation was found to be a function of the precise aqueous phase (e.g. cations and pH) in addition to the oil phase (e.g. acyclic *vs.* cyclic/aromatic naphthenic acid content). It was possible to form soap deposits in the laboratory from both indigenous acids, as well as crude oils. Detailed speciation of certain indigenous acids allowed for the identification of Arn and the special properties of this species namely: four carboxylic acid groups by tandem mass spectrometry (MS/MS) and surface properties given by interfacial tension (IFT). Previous literature claims stated that Arn acid presence were solely responsible for the precipitation of calcium naphthenate soap scales. The results in this thesis show that although Arn acids have predominant surface properties, they compete with lower molecular weight acids for aqueous phase cations at high pH values. This was observed in static bottle tests as well as results from field precipitation samples. Fourier-Transform infrared (FTIR) spectroscopy showed potential as a technique for the prediction of soap deposition onset in the laboratory. Supporting experiments were designed to validate a simple thermodynamic model to predict the phase

behaviour of oil-water-naphthenic acid systems. A sensitivity study showed that the dissociation constants (pK_a) of the naphthenic acids were the most important model parameters and could affect predicted output pH values. For indigenous naphthenic acids, alternative procedures for both dissociation constant and partition coefficient were introduced. A comprehensive suite of crude oil analysis and water properties were employed for correlating field soap-forming systems. It was possible to obtain some trends which relate geochemical parameters with bulk crude oil properties, as well as naphthenic acid speciation. Based on this information, a preliminary attempt to establish prediction guidelines for soaps, one of the major contributions in this thesis to the current knowledge of soap-forming systems, is presented.

DEDICATION

For my mother

ACKNOWLEDGEMENTS

I would like to thank Dr. Robin Westacott, Dr. Gillian Thomson and Professor Ken Sorbie for their guidance, patience, support and encouragement throughout this project.

Thanks to all the Flow Assurance and Scale Team (FAST) members who I have worked with. In particular Dr. Eric Mackay and Lorraine Boak for being there when I most needed them.

I gratefully acknowledge the EPRSC and Professor Anne Neville for the PhD scholarship for this project. The support of FAST sponsors for the provision of samples is also acknowledged. Special thanks goes to Conoco-Phillips, Total, Statoil, Baker Petrolite, REP, BG, BP, Kerr-Maguee and Talisman. Petrobras is thanked for the opportunity of allowing me to work in their labs during the early stages of this work.

I am indebted to Colin Smith and Mike Turner of Oilplus (now Maxoil Solutions and BP respectively) for valuable discussions on soaps and for providing me with the industrial perspective of the soap precipitation problem.

A special thanks goes to Terry Halley of MScan for many enjoyable hours of mass spectrometry interaction and ionisation.

Jim Buckman, Marian Millar, Allan Boyd, Thomas Buchan, Vincent Jambon and Arnaud Durel, are also kindly thanked for experimental assistance in various different techniques carried out in this thesis.

Vassiliki Karali is thanked for her friendship and making my time in Edinburgh more enjoyable.

My parents, brother and grandmothers, for always believing in me.

ACADEMIC REGISTRY
Research Thesis Submission

Name*:*			
School/PGI:			
Version: *(i.e. First, Resubmission, Final)*		Degree Sought (Award **and** Subject area)	

Declaration

In accordance with the appropriate regulations I hereby submit my thesis and I declare that:

1) the thesis embodies the results of my own work and has been composed by myself
2) where appropriate, I have made acknowledgement of the work of others and have made reference to work carried out in collaboration with other persons
3) the thesis is the correct version of the thesis for submission and is the same version as any electronic versions submitted*.
4) my thesis for the award referred to, deposited in the Heriot-Watt University Library, should be made available for loan or photocopying and be available via the Institutional Repository, subject to such conditions as the Librarian may require
5) I understand that as a student of the University I am required to abide by the Regulations of the University and to conform to its discipline.

* *Please note that it is the responsibility of the candidate to ensure that the correct version of the thesis is submitted.*

Signature of Candidate*:*		Date:	

Submission

Submitted By *(name in capitals):*	
Signature of Individual Submitting:	
Date Submitted:	

For Completion in Academic Registry

Received in the Academic Registry by *(name in capitals):*			
1.1 Method of Submission *(Handed in to Academic Registry; posted through internal/external mail):*			
1.2 E-thesis Submitted (**mandatory from November 2008)**			
Signature:		Date:	

TABLE OF CONTENTS

LIST OF PUBLICATIONS

Full papers

Andrew G. Shepherd, Ken Sorbie, Robin E. Westacott and Gillian B. Thomson, *A Sensitivity Study Of Naphthenic Acids From Flow Assurance Deposits Characterized By Low-Resolution Mass Spectrometry*, in publication.

Andrew G. Shepherd, Gillian B. Thomson, Robin E. Westacott and Ken Sorbie, *New Insights Into The Chemistry Of Soap Formation In Exploration And Production*, presented at Royal Society of Chemistry, Chemistry in the Oil Industry X, Manchester, UK, 5-7 November, 2007.

Andrew G. Shepherd, Gillian B. Thomson, Robin E. Westacott, Ken Sorbie, Mike Turner and Patrick Colin Smith, *Analysis Of Organic Field Deposits: New Types Of Calcium Naphthenate Scale Of The Effect of Chemical Treatment?,* SPE 100517, presented at the 8th International Oilfield Scale Symposium, Aberdeen, UK, 31 May-1 June, 2006.

Ken Sorbie, Andrew G. Shepherd, Patrick Colin Smith, Mike Turner and Robin E. Westacott, Naphthenate Formation in Oil Production: General Theories and Field Observations, presented at Royal Society of Chemistry, Chemistry in the Oil Industry IX, Manchester, UK, 31 October-2 November, 2005.

Andrew G. Shepherd, Gillian B. Thomson, Robin E. Westacott, Anne Neville and Ken Sorbie, *A Mechanistic Study Of Naphthenate Scale Formation*, SPE 93407, presented at the International Symposium on Oilfield Chemistry, The Woodlands, Texas, USA, 2-4 February, 2005.

Extended Abstracts and presentations

Andrew G. Shepherd, Robin E. Westacott, Gillian B. Thomson, Colin Smith, Mike Turner and Ken Sorbie, *Novel Insights Into The Characterization Of Naphthenic Acid Deposits*, presented at the 7th International Conference on Petroleum Phase Behaviour and Fouling, Asheville, North Carolina, USA, 25-29 June, 2006

Andrew G. Shepherd, Robin E. Westacott, Ken Sorbie, Mike Turner and Colin Smith, *Naphthenate Soap Formation Analysis Under Laboratory Conditions*, presented at the 6th International Conference on Petroleum Phase Behaviour and Fouling, Amsterdam, The Netherlands, 19-23 June, 2005.

CHAPTER 1 – INTRODUCTION.

Abstract

In this chapter the soap precipitation problem is presented within the context of flow assurance operations. An introduction to naphthenic acids, focusing on geochemistry, engineering and process implications is also developed. The main thesis objectives are outlined and a brief summary of remaining chapters is also included.

1. 1. Soaps: the industrial perspective.

Flow assurance is the area within exploration and production concerned with the identification, prevention and mitigation of any event that might hinder the normal production of hydrocarbons (McMullen, 2006). Resistance to the flow of hydrocarbons can usually be induced by hydraulic and/or thermodynamic events such as slugging or emulsion formation. It can also manifest as solid deposits in reservoirs, pipelines or surface equipment. Within this last class, a large number of both inorganic and organic deposits occur. Deposits form due to specific production chemistry (e.g. oil and produced water content), as well as process or environmental variations (e.g. change in temperature or pressure). Inorganic deposits are commonly known as scale and the two most representative types are calcium carbonate and barium sulphate. The basic precipitation mechanism for conventional scales is well-established (Mackay and Sorbie, 2000). Organic deposits comprise a variety of compounds that includes asphaltenes and waxes. The understanding of precipitation mechanisms for these flow assurance problems has developed considerably over the last 20 years. This has been due to advances in deposit characterisation (Rodgers *et al.,* 2006), a better understanding of the effect of operational variables (Turner and Smith, 2005) and the use of novel technology such as molecular modelling (Jiang *et al.,* 2007) and quartz crystal microbalances (Chan *et al.,* 2004).

Soaps are a relatively new phenomenon in flow assurance. These are believed to form by the reaction between metal cations and particular crude oil components. Their precipitation and deposition in the field may represent a severe drawback for operations because:

- blockage of process equipment often requires shutdowns for remediation procedures,
- costs must be incurred by the operator due the use of chemical products (inhibitors and/or dissolvers) and
- loss of revenue as a consequence of interrupted oil production, or due to the recovery of crude oil below normal specification.

The understanding of the soap problem is of great practical significance given that many new exploration prospects are increasingly being developed in offshore deepwater operations, where unexpected mitigation costs could even jeopardise the future existence of the asset itself. In order to study the formation of soaps, a better understanding of naphthenic acids is also required. The next paragraphs will present a brief overview of these ubiquitous crude oil components.

1.2. Naphthenic acids: introduction.

It has been recognised for over a century that acids are present in a variety of diverse hydrocarbon sources such as crude oils and tar sands. A significant amount of work has been performed on these substances since Hell and Medinger first published their pioneering work in 1874 (Hell and Medinger, 1874). In 1883 Markownikoff recognised that acids present in crude oils from Azerbaijan contained the carboxyl group associated with carboxylic acids (*opere citato* in Kazanis, 1971). Since then, the term naphthenic acids has been used to account for all the acid species containing the carboxylic group in crude oils. Currently, the American Petroleum Institute definition of naphthenic acids includes structures with single and/or multiple fused cyclopentane and cyclohexane rings with a carboxylic group attached either to an aliphatic side chain or to a cycloaliphatic ring (American Petroleum Institute, 2003). Examples of these structures are illustrated in Figure 1.1.

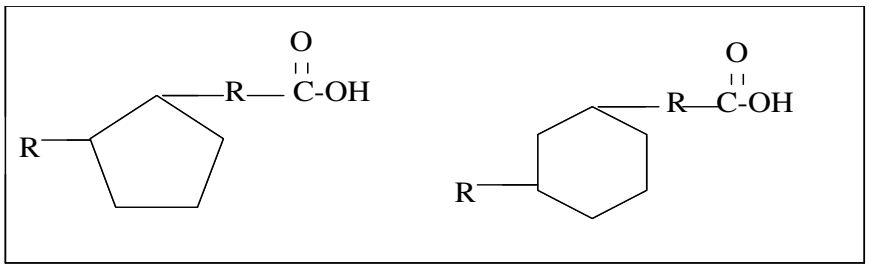

Figure 1.1. Illustration of common naphthenic acid structures present in crude oils (Robbins, 1998).

It has become common practice to represent naphthenic acids in crude oil by the following general formula:

$$C_nH_{2n+Z}O_2$$

Equation 1.1.

where, n is the carbon number and Z is the hydrogen deficiency. Z values can be 0 or a negative even integer. The value of Z reflects the loss of a hydrogen atom that occurs when

a cycloaliphatic ring is present in the acid structure. Thus, Z = -2 is equivalent to an acid with one ring (mono-cyclic), Z = -4 is equivalent to an acid with two rings (bi-cyclic), etc. More than one isomer will typically exist for a given Z value and this makes the correct identification of naphthenic acid species very challenging. However, it is generally accepted that crude oil naphthenic acids on average have molecular weights between 200 and 700 Daltons.

There are other acidic components present in crude oil that do not contain the types of naphthenic acid structures shown in Figure 1.1. These include components with phenol, amide, and sulphur derivatives to name only a few (Meredith *et al.,* 2000; Barth *et al.,* 2004). Acidic compounds in crude oil can also include more complex structures with up to 13 rings, two, three and even four carboxylic acid groups (Tomczyk *et al.,* 2001; Baugh *et al.,* 2004) as well as acidic structures with many heteroatoms (i.e. S, SO, SO_2, SO_3, N, NO, NO_2, N_2O) (Robbins, 1998; Tomczyk *et al.,* 1998 and 2001; Qian *et al.,* 2001; Rudzinski *et al.,* 2002). It is not known if these heteroatom species are a result of oxidation, thermal or biodegradation effects. Thus, the use of the terminology naphthenic acid comprises a wide variety of organic structures with unique chemical properties. In this thesis, the term naphthenic acid will be used to describe all organic acids containing the carboxylic group.

The measurement of a crude oil's acidic tendency is routinely carried out using total acid number assays (TAN). High TAN crude oils have been reported from many distinct geographical regions ranging from California, Mexico, Venezuela, the North Sea, West Africa and even the Far East and Russia (Robbins, 1998; Skippins *et al.,* 2000; Sartori *et al.,* 2001; Laredo *et al.,* 2004). Common TAN values for crude oils fall between 0.1 and 10 (Derungs, 1956; Sartori *et al.,* 2001). However, crude oils with TAN greater than 0.5 are considered high enough to have process implications (Robbins, 1998).

The exact origin of naphthenic acids and their implications in geochemistry have been the subject of much positive debate. Naphthenic acids are quite ubiquitous and can be found both in surface samples such as humic soil layers (Leenheer and Rostad, 2004) as well as in subsurface samples (Robbins, 1998). Figure 1.2 presents some examples of naphthenic acid structures identified in crude oils.

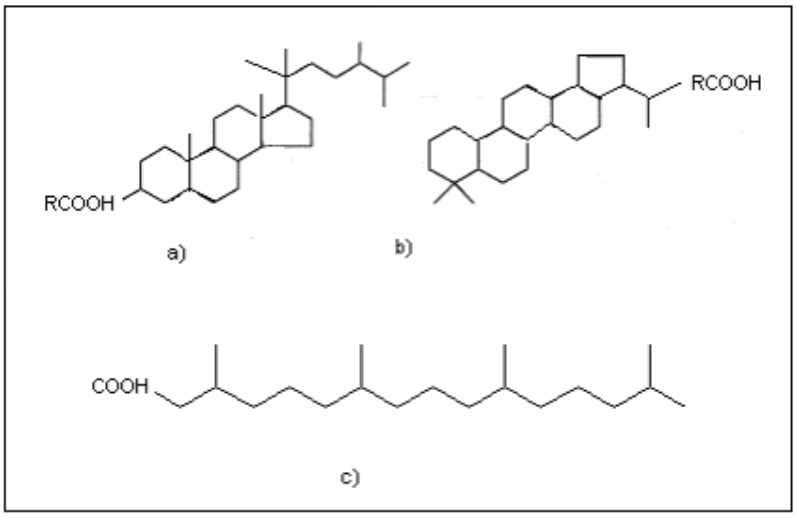

Figure 1.2. Naphthenic acid structures identified in crude oils. a) steroid-like acid, b) hopanoic acid, c) isoprenoid acid.

There have been few attempts to correlate naphthenic acids present in crude oils with other geochemical information or even bulk crude oil properties. Cooper and Bray (1963) suggested that acyclic acids could be precursors of n-paraffins in crude oils, and the conversion could occur via loss of CO_2. However, it was not until the work of Seifert *et al.* (1972) that the first carboxylic acids in crude oil had their structures confirmed and a clear link between steroid carboxylic acids and crude oil geochemistry was presented. Schmitter *et al.* (1978) were amongst the first to identify the relevance of hopanes-derived acids for petroleum geochemistry in particular for maturity correlations. They argued that the normal fatty acid patterns identified by gas chromatography (GC) did not give meaningful correlation data (when compared to n-alkanes). Jaffe *et al.* (1988) suggested naphthenic acids to be a result of geo-chromatographic processes and solubilization or washing effects, through which immature organic matter becomes incorporated into the oil through migration. Koike *et al.* (1992) also showed that traditional geochemical parameters were observed to correlate well with a reduction in low molecular weight acids in crude oil samples. The authors stated that acids were more sensitive to biodegradation and/or migration changes than hydrocarbons, and this would make their use in geochemical studies more relevant. Recently, hopanoic acids (carbon atoms between 30 and 32) have been shown to be present in high concentrations in severely biodegraded oils by Meredith *et al.* (2000). These authors used GC and gas chromatography mass spectrometry (GCMS) to compare hydrocarbon fractions with naphthenic acid fractions separated from crude oils. The GC spectra for these two classes of compounds showed an excellent match. Meredith *et al.* (2000) suggested two possibilities for the occurrence of the hopanoic acids: they could be a preserved signal of biodegradation heterogeneity within the field (before a

second charge of oil) or that they were due to processes other than biodegradation. Surprisingly certain non-degraded oils in the above-mentioned work had high TAN values, which suggested that other factors (e.g. sulphur content) might contribute to TAN. Barth *et al.* (2004) showed that naphthenic acids with molecular weight in the 300 to 500 Dalton range were predominant in biodegraded samples. Fan (1991) postulated the distribution of naphthenic acids in a crude oil could also be linked to the maturity of the sample. The author was able to show that acyclic acids were predominant in immature samples, and were said to originate from living organisms in recent organic sediments. Jones *et al.* (2001) also suggested that the relative higher amount of naphthenic acids in the biodegraded crude oil sample arose from newly formed species during reservoir processes. Two sources for the naphthenic acids were suggested: the incomplete oxidation of hydrocarbons, or, the lipid biomass of the microorganisms responsible for biodegradation itself. Gallup *et al.* (2005) identified a predominance of mono-carboxylic acids with carbon numbers between 16 and 34 in a soap emulsion-forming crude oil. The authors suggested they were derived from leaves of plants which contributed to the source rock of the oil (coal-derived with high pristane/phytane ratios). This was further confirmed by Gallup *et al.* (2007), where the analysis of a series of soap emulsion-forming crude oil samples was presented. Schouten *et al.* (2003) showed some data on core samples and compared the acid fraction with membrane lipid fraction from archaeal origin. There was a high abundance of hopanoic acids with carbon numbers of 32 and 33, as well as acyclic and cyclic acids. They suggested that certain acids are derived from the same archae organisms. The authors also postulated that acids could be either directly synthesised or be the product of biodegradation of the membrane lipids. Kim *et al.* (2005) analysed six oil samples and showed that the molecular weight distribution of polar compounds was greatly influenced by the level of biodegradation. In particular, the concentration of O_2, SO and S_2O species, increased with increasing biodegradation levels. As analytical hardware and tools develop, the exact role of naphthenic acid species in geochemistry and their true origin will become known, and their use in reservoir studies and flow assurance services will become common practice.

The decrease in conventional crude oil supplies means that fields with increasingly high sulphur content, lower API gravity, high viscosity, high nitrogen content and higher naphthenic acid content are being developed. Acidic crude oil supplies will grow by almost two million barrels per day by the end of this decade (Williams, 2003). These stocks are often known as opportunity crude oils. However, there are many process implications that arise because of the presence of naphthenic acids. Downstream, these organic compounds

tend to concentrate during crude oil distillation and most commonly reach a maximum level in the heavy gas-oil fractions (Turnbull *et al.,* 1998). In refineries, their presence may lead to deactivation of catalytic beds, emulsions and corrosion (Cressman *et al.,* 1995; Skippins *et al.,* 2000). When alkalis are used for naphthenic acid treatment, organic acid salts or "soaps" are formed from the reaction of the metal cations and the naphthenate anions. These soaps remain mostly water-soluble and are treated in the stripper unit where the caustic stream is extracted with alcohol (to remove compounds which did not form soaps) and acidified (usually with sulphuric acid) to liberate the bound acids in the soap structures (Brient *et al.,* 1995). Over long operational campaigns, soaps combine with other foulants and build up in desalter units. These can only be removed using mechanical intervention. Only a small fraction of the naphthenic acids recovered in refineries can be commercially used. These, however, have widespread applications in a number of industries. Crude oils with high naphthenic acid content are usually associated with naphthenic acid corrosion. As stated by Derungs (1956) this is an old enemy of the petroleum industry, observed since the 1920's. It is believed that the most important variables that contribute towards this are: TAN, acid distribution, sulphur content, temperature, fluid rates, metallurgy, equipment design and crude oil blends (Babaian-Kibala, 1994; Johnson *et al.,* 2002). The use of a technology to remove naphthenic acids from crude oils would provide many benefits for the processing of the parent hydrocarbons. Published accounts of commercial implementation of the naphthenic acid removal technologies on larger scales have not been found in the open literature. Naphthenic acids have also been identified as the main source of toxicity in refinery effluents for fish (Wong *et al.,* 1996). More importantly, naphthenic acids are suspected to be endocrine disrupting agents (Headley *et al.,* 2002). As higher resolution techniques are developed for the study of naphthenic acids it is hoped that a better understanding of the processes and implications due to naphthenic acids in hydrocarbons will become available.

1.3. Concluding remarks and thesis outline.

A number of gaps currently exist in understanding naphthenic acids in the petroleum and processes industries and this in turn is observed in the current lack of detailed knowledge of soap precipitation processes in oilfield operations. Few attempts have been made to analyse soaps as well as their parent naphthenic acids, under controlled conditions in the laboratory. Undertaking such a study would greatly aid in the development of a unified soap precipitation/prediction model, at present not known to be available in the open literature. Formation of soaps under laboratory conditions has also been limited and not used to explain field precipitation cases. Thus, the underlying mechanisms of soap formation have not been studied in the controlled environment of the laboratory. The role of specific crude oil components (e.g. naphthenic acids) in soap formation is also still unclear. This thesis will attempt to address the following issues:

- analysis of field soaps and their parent naphthenic acids with a view of obtaining more information of chemical structures and physical chemistry,
- soap formation in the laboratory and effect of the precipitation mechanisms,
- the role of crude oil components and water chemistry.

To this end, the thesis is divided into 9 chapters, as follows: Chapter 2 presents the literature review on the occurrence of soaps in the field as well as naphthenic acid phase behaviour and characterisation. Chapter 3 outlines the experimental strategy and methodologies specifically designed for use in analysing field soap samples. Chapter 4 is concerned with the results of the analysis of field soaps, and this includes a field precipitation case. The work undertaken in Chapter 5 presents the analytical tests to study the formation of soaps in the laboratory using a range of feeds. In Chapter 6 experimental results from the formation of laboratory soaps are presented which include model naphthenic acid solutions, indigenous naphthenic acids, as well as soap-forming crude oil samples. Chapter 7 discusses attempts to predict the naphthenic acid behaviour in oil-water systems using experiments and modelling. In Chapter 8 results of measurements on soap-forming crude oils and attempts to establish soap prediction guidelines are explained. Chapter 9 presents the thesis conclusions and recommendations. Finally, the references used in the thesis are listed.

CHAPTER 2 – LITERATURE REVIEW.

Abstract

The formation of naphthenic acid soaps is covered in detail in this chapter by using both field precipitation cases as well as more fundamental mechanistic studies from the literature. Special emphasis is given to the characterisation of naphthenic acids. The main information obtained here was organised and used as input in planning the remaining thesis chapters.

2.1. Naphthenic acid soaps in crude oil production.

A less publicised effect of naphthenic acids is the formation of soaps during crude oil production, and this is the main topic of this thesis. Within the area of flow assurance, operational problems with naphthenic acid soaps were first reported in the open literature in the mid 1990's (Vindstad *et al.,* 2003). It is very possible however, that soaps were formed in the oilfield before this date but were classified as other flow assurance deposits (Smith and Turner, 2004). In contrast to the soluble soaps that form downstream in refineries, soaps that occur during crude oil production can form rock-hard solid deposits. As a consequence they can lead to fouling and plugging of equipment such as heat exchangers, desalters, separator internals, sand cleaning systems, hydrocyclones, valves and pumps, in both the oil and water legs (Vindstad *el al.,* 2003; Smith, 2004; Pearson, 2004; Turner and Smith, 2005; Ubbels and Turner, 2005). There have also been reports of soap deposition leading to loss of process control due to blockage of level transmitters, valves and low pressure knock-out drums, resulting in unplanned shutdowns (Vindstad *et al.,* 2003). Certain types of soaps are also known to enhance the stability of emulsions which results in reduced production rates due to increased fluid viscosity (Turner and Smith, 2005). Increased viscosity can lead to entrainment of oil, water and solids, and may result in the formation of sludges in storage tanks (Gallup *et al.,* 2002). In severe cases, up to 20 vol% of total produced fluids can be composed of sludges. Soaps also cause a deterioration of discharge water and export oil quality (Vindstad *et al.,* 2003). Entrained cations (e.g. calcium) in crude oils from soaps can also affect the final market price of hydrocarbons in the export line and in refineries (Turner and Smith, 2005).

In field conditions the amount of soaps formed may be typically small, e.g. 10 mg solid /l of crude oil (Smith and Turner, 2004). This quantity may appear insignificant, but the flow assurance problem must be viewed as a cumulative effect (Vindstad *et al.,* 2003; Pearson 2004). As more oilfield production with crude oils having higher naphthenic acid content shifts towards deepwater fields employing subsea equipment (e.g. separators), the occurrence of soaps will have an increasing impact, and their prediction will become of

prime importance. As a consequence, several research groups have focused their attention on the scientific fundamentals underlying the formation of these soaps (Rousseau *et al.,* 2001; Havre, 2002; Dyer *et al.,* 2003; Ese and Kilpatrick, 2004; Brandal *et al.,* 2004; Baugh *et al.,* 2004, 2005a and 2005b; Brocart *et al.,* 2005; Brandal, 2005; Turner and Smith, 2005; Lutnaes *et al.,* 2006; Dyer *et al.,* 2006, Smith *et al.,* 2007). Most of these references were published in parallel to the work in the present thesis and they are reviewed next.

2.1.1. Conventional mechanism for soap formation.

The main factors believed to play a role in soap formation can be divided into flow assurance/production chemistry issues (e.g. crude oil composition, produced water pH) and operational parameters (e.g. pressure, temperature, co-mingling of fluids, shear, water-cut and electrostatic fields, Turner and Smith, 2005). The most important drivers are reviewed and discussed in the following section. However, the conventional view of how soaps are thought to form will be examined first. The assumed mechanism of soap formation is thought to be dependent on pH variations that occur during the production of crude oil, for example, as described by Rousseau *et al.,* (2001). Carbon dioxide (CO_2) contained in formation fluids in the reservoir controls the system pH. The solubility of CO_2 in water decreases with decreasing pressure. Pressure drops are encountered during the flow from reservoir to surface conditions and are necessary to ensure separation of oil (or condensate), gas and water. As CO_2 is released from solution, the pH of the produced water increases. The naphthenic acids collect at the oil-water interface since the main part of the molecules is hydrophobic, while the carboxylic acid group is hydrophilic. As pH increases naphthenic acids become deprotonated at values above the dissociation constant (pK_a). The pK_a is the constant used to distinguish the pH at which 50 mol% of a specific naphthenic acid is dissociated. The ionised naphthenic acids may react with cations from the produced water (calcium Ca^{2+} and/or sodium Na^+) at the oil-water interface to form soaps. Equations 2.1, 2.2 and 2.3 summarise what is believed to be the basic mechanism.

$$\mathbf{CO_2 + H_2O = HCO_3^- + H^+} \qquad \textbf{Equation 2.1}$$

$$\mathbf{HA = H^+ + A^-} \qquad \textbf{Equation 2.2}$$

$$\mathbf{A^- + Ca^{2+} \text{ or } Na^- = CaA_2 \text{ or } NaA} \qquad \textbf{Equation 2.3}$$

where HCO_3^- represents the bicarbonate ions in the produced water, HA represents a general naphthenic acid molecule and A^- represents the dissociated naphthenate anion.

From the mechanism outlined above, it would appear that the formation of soaps in the field should be both pressure dependent (which would have a direct effect on pH) and composition dependent (e.g. the variety of naphthenic acids present in the crude oil). Pressure and composition dependency are common in other flow assurance phenomena: for example, calcium carbonate precipitation, which is mostly a water-based problem, and asphaltene precipitation, which is a hydrocarbon-based problem (Zhang *et al.,* 2001; Idem and Ibrahim, 2002).

Based on the simple mechanism presented in equations 2.1 to 2.3, attempts have been made to obtain soaps under laboratory conditions (Rousseau *et al.,* 2001; Havre, 2002; Dyer *et al.,* 2003; Mediaas *et al.,* 2005; Dyer *et al.,* 2006). Both static and dynamic tests have been performed in which the pH change trigger for soap formation has been obtained using either alkaline addition (Dyer *at al.,* 2003), saturated CO_2 solutions (Mediaas *et al.,* 2005), or through shear and flow over valves (Dyer *et al.,* 2006). Formation of soaps in the laboratory would be very useful to support prediction models for application in field systems. This goal may be very ambitious since many crude oils which contain naphthenic acids often have hundreds or even thousands of such components (Tomczyk *et al.,* 2001). It is thought that current commercial scale thermodynamic pressure-volume-temperature (PVT) models do not include the precipitation of naphthenic acid soaps in their thermodynamic libraries. Clearly including all crude oil naphthenic acid in a predictive model would be practically impossible since the relative molar concentrations and properties of most of these acids are rarely known and vary considerably from one crude oil sample to another. For a realistic model to be developed, the phase behaviour of naphthenic acids and soaps needs to be better understood. A pseudo-component approach has been used in an attempt to model this behaviour. The model was first conceived by Ken Sorbie (Sorbie *et al.,* 2004) and was validated and further developed by supporting experiments, which will be discussed in more detail in Chapter 7.

2.1.2. Detailed review of mechanisms of soap formation.

Crude oil composition.

The acidic tendencies for a crude oil have traditionally been evaluated using TAN measurements as mentioned in Chapter 1. Figure 2.1 shows TAN values from the literature (Meredith *et al.,* 2000) for a number of crude oils plotted against their naphthenic acid concentrations (obtained by various analytical techniques such as gas chromatography and gas chromatography mass spectrometry). The straight line on the graph represents a theoretical naphthenic acid concentration which would be equivalent to the TAN of the crude oils. It is observed that there is some correlation between TAN and naphthenic acid concentration for these fields. Despite this, the measured naphthenic acid concentrations are not close to the expected value, as illustrated by the straight line, particularly for TAN values above 1. This is because TAN is an average value arising from all the acidic components in the crude oil (e.g. CO_2, H_2S, phenols) not just naphthenic acids. No information can be obtained from the TAN method in regards to precise naphthenic acid species found in the crude oils (Qian *et al.,* 2001). This makes the speciation of acidic moieties very challenging.

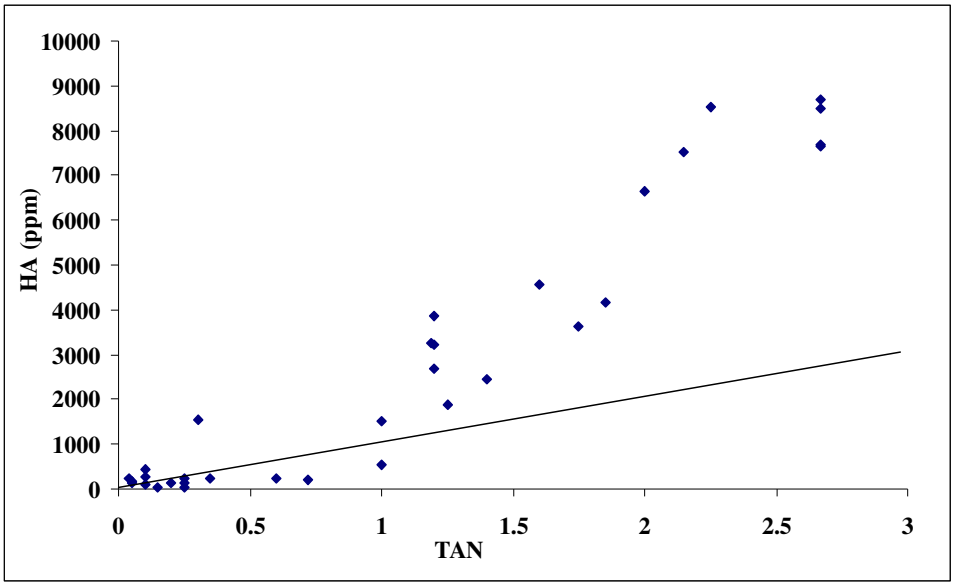

Figure 2.1. Naphthenic acid concentration in crude oils, HA (ppm), as a function of TAN from the same crude oils (Meredith *et al.,* 2000). Points represent samples from different geographical locations such as the North Sea and Mediterranean fields. The straight line is the theoretical predicted HA concentration, if TAN were a function of HA only.

Much of the initial work on soaps focused on the relationship between TAN and soap formation, where TAN was thought to be a predictor of soap formation. It was shown that for wells from the same soap-forming field, TAN was a function of both API gravity and

wax content of the parent crude oil (Rousseau *et al.,* 2001; Hurtevent, 2004). However, specific naphthenic acid content has been linked to source rock maturation and/or biodegradation which is not at present used for soap prediction purposes (Meredith *et al.,* 2000). Thus TAN would be of little use in fingerprinting soap-forming crude oils. Therefore, the study of more specific crude oil components has driven soap research in more recent work.

Specific naphthenic acid components in crude oils.

Until as recently as 1955 only two naphthenic acids with as many as ten carbon atoms had been identified from hydrocarbon sources (Brient *et al.,* 1995). The first naphthenic acids identified were acyclic species, including isoprenoid structures with between fourteen to twenty carbon atoms. This is most likely due to acid separation and identification hardware, which has vastly improved over the last fifty years (Cason and Graham, 1965). The separation of naphthenic acids from their bulk parent sources has been reported by Cason and Graham (1965), Seifert and Howels (1969) and Tomczyk *et al.,* (2001) using liquid and solid phase extractions. A number of authors have employed alkaline solutions for the extraction of naphthenic acids (Hoeiland *et al.,* 2001; Tomczyk *et al.,* 2001; Barth *et al.,* 2004), a disadvantage of which is the formation of emulsions. In addition, if naphthenic acids are complexed in crude oils, they may not be removed by contact with an alkaline system. Barth *et al.,* (2004) have reported low naphthenic acid recoveries (29 to 57 wt%) from crude oils using alkaline extraction methods. Long contact times might also be required for efficient acid extraction (Saab *et al.,* 2005). Solid extraction media have been tested using a wide range of materials including zeolites, clays, aluminosilicates, silica gel, granulated activated carbon, and ion exchange resins (Wong *et al.,* 1996; Gaikar and Maiti, 1996; Acevedo *et al.,* 1999; Mediaas *et al.,* 2003; Campos *et al.,* 2006). Resins may affect the identification of particular naphthenic acid structures because of their retention properties. In particular, acid-eluent-column interactions, the presence of functional groups in the matrix, electronic charges, eluent concentrations, ion exchange capacity and pH may affect the overall resin performance (Hajos and Nagy, 1998; Headley *et al.,* 2002). The adsorption of naphthenic acids appears to be strongly dependent on the polymeric backbone on the functional group and less on the ion exchange capacity of the resin (Gaikar and Maiti, 1996). Hajos and Nagy (1998) have shown a number of interesting effects of ion exchange chromatography and carboxylic acids: mono-carboxylic anions elute before bi-carboxylic anions. Increased solute charges lead to increased capacity charges and retention behaviour depends on the exact position of the carboxyl group.

Most of the characterisation of naphthenic acids from multicomponent sources has been carried out using mass spectrometry (MS). One of the major challenges when using MS is sample fragmentation, which is an unwanted by-product of ionisation. If the sample containing the naphthenic acids has low volatility, as is the case of crude oils, it may be possible to prepare a suitable naphthenic acid derivative to aid in molecular ion determination. Derivatization may be carried out using a number of chemicals (Cason and Graham, 1965; St John *et al.,* 1998; Jones *et al.,* 2001). A constant feature of certain derivatization procedures is the poor recovery of the high molecular weight naphthenic acid components (Meredith *et al*., 2000). There are at present a very limited number of studies looking at comparative derivatization effects for naphthenic acids (Jones *et al.,* 2001). In addition, most of the MS sources used for the analysis of naphthenic acids have been soft ionisation varieties. These include fast ion bombardment (FAB), electrospray (ES) and atmospheric pressure chemical ionisation (APCI). These have been used due to their tendency for low fragmentation (Fan 1991; Hsu *et al.,* 1998; Rogers *et al.,* 2002; Headley *et al.,* 2002). Direct comparisons of the effects of different ionisation sources on naphthenic acid studies are still required since they may affect fingerprinting of feeds.

The first reported work on the analysis of soap-forming crude oils in the oil industry dates from 2001 (Rousseau *et al.,* 2001). However, it was not until two years later that specific naphthenic acid components in both soap-forming crude oils and soaps were first identified in detail. Barrow, 2003 (*opere citato* in Hurtevent, 2004) used Fourier-Transform ion cyclotron resonance mass spectrometry (FTICRMS) to quantify the distribution of naphthenic acids in a range of soap-forming crude oils. His results showed that these crude oils contained species with mass-to-charge (m/z) ratios between 300 and 700 and with a predominance of hydrogen deficiency (Z values) of -2, -4 and -6 (the equivalent of species with one, two and three rings respectively). However, naphthenic acids with Z values between 0 to -24, and number of carbon atoms ranging from eighteen to forth eight were also identified. An unusual group of acids was present at m/z 1240, at high intensities for one of the samples, but this was not commented on. No discussions were presented over the relative importance of naphthenic acid species in the crude oils for soap formation. The pioneering work of Baugh *et al.* (2004) continued to investigate specific acid species present in calcium soap deposits. These authors studied both a soap-forming crude oil and field soap deposit from a North Sea location using a variety of techniques. TAN analysis on both crude oil and the naphthenic acids extracted from the soap resulted in the determination of average molecular weight for naphthenic acids between 330 and 430 Daltons. This was consistent with the results of Vindstad *et al.,* (2003). Somewhat

surprising results were obtained however from the analysis of the soap sample using liquid chromatography mass spectrometry (LCMS) by Baugh *et al.* (2004), which indicated that the soaps were in fact composed of two different groups of naphthenic acids: a lower molecular weight group with maximum m/z values close to 325 as well as a higher molecular weight group with m/z values close to 1230. MS settings did not however allow for a direct comparison of intensities of the low and high molecular weight groups. It was claimed that structures with four carboxylic acids would be present, and this was justified by vapour pressure osmmometry (VPO) and MS results. Both of these techniques resulted in molecular weight values for the naphthenic acids in the deposits of 1230 Daltons, which were higher than the value given by TAN measurements (since the latter technique cannot distinguish different carboxylic groups in the same sample). Moreover, it was also claimed that the group of acids around with 1230 Daltons was the predominant naphthenic acid group in the soap, though clearly more experimental data was needed to support this. These conclusions were mostly based on the analytical sequence of techniques applied to the naphthenic acid in the soap deposits: acid extraction using ion exchange, followed by derivatization with BF_3/methanol, liquid chromatography and ionisation with an atmospheric pressure photo ionisation (APPI) source in MS. The significance of this sequence of techniques is important because some of these are known to have different yields as a function of naphthenic acid structure (Jones *et al.,* 2001). For instance, no comments were made in regards to favourable ionisation of particular acid species during the MS parts of the experiments. No sensitivity studies were provided on the effect of these different analytical steps. Some of these issues will be addressed in this thesis. Nevertheless, an empirical formula, based on the analytical results for the high molecular weight naphthenic acids at m/z 1230 was proposed by Baugh *et al.* (2004). This was $C_{80\text{-}81}H_{142\text{-}130}O_8$, and the naphthenic acid was given the name Arn (meaning Eagle in Norwegian). In further studies, Baugh *et al.* (2005a) analysed soaps using FTICRMS, 2D-nuclear magnetic resonance (NMR), titrations and pyrolysis mass spectrometry. The authors reported the precise molecular weight of the Arn species together with certain initial information on the possible molecular structures. Again this work was carried out on the derivatized naphthenic acids extracted from the deposit. The Arn were said to have a predominant molecular weight of 1230 Daltons, and composed mostly of cycloaliphatic species (no aromatic or alkene functions were suggested to be present). Work indicated that the basic Arn unit (see Figure 2.2) consisted of four or more methylene groups, and that the carboxylic function was in a side chain attached to a ring structure. The carboxyl species within the Arn structure were shown to be equivalent in acid strength using titration

experiments. An illustration of a possible Arn structure, based on the 2D NMR of the naphthenic acid derivatives obtained from a field soap from Baugh *et al.* (2005b) is shown in Figure 2.2. Lutnaes *et al.* (2006) carried out an extensive characterisation of the Arn acid present in a soap sample from a North Sea field. The authors were able to establish a more precise structure of the Arn species, and suggested the predominant component within the Arn family would be composed of six rings. They also speculated that the acid would be of biological archaeal origin and suggested a few kinetic routes for Arn formation. An illustration of the structures proposed by the previous authors is shown in Figure 2.3. All the analysis of the acids was carried out using the same extraction and derivatization procedures employed by Baugh *et al.* (2005a).

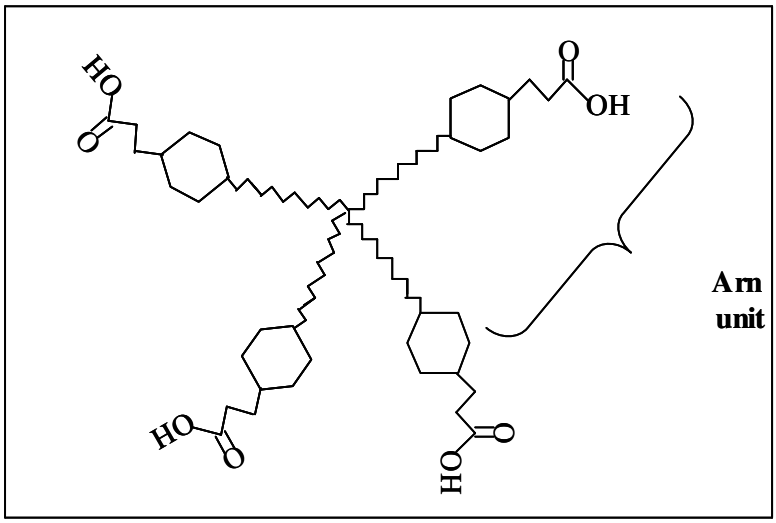

Figure 2.2. Proposed most likely structure of Arn acid based on results by Baugh *et al.,* 2005b. The Arn unit represents the hydrocarbon skeleton and the single carboxylic acid attached to a side chain, in turn attached to a cycloaliphatic ring.

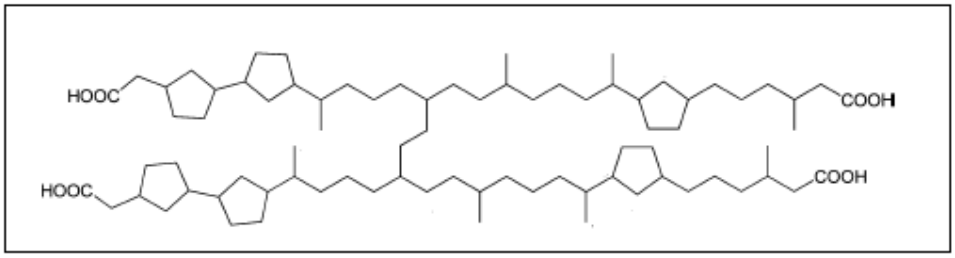

Figure 2.3. Proposed predominant structure of Arn acid (Lutnaes *et al.,* 2006).

Smith *et al.* (2007) have also identified additional Arn analogues with eighty one and eighty two carbon atoms, containing seven and eight rings during the analysis of two field soap deposits. The authors speculated that the relative distributions of the acids would be due to distinct reservoirs and growth temperature of the bacteria from which they originated. An example of one structure assigned by the previous authors appears in Figure 2.4.

The exact structures of Arn and their relative importance in the occurrence of soap deposits is subject to much debate. To the present date, no studies have been reported on the relationship between Arn and low molecular weight naphthenic acid species in the soap-forming crude oils or the impact of these on soap deposition.

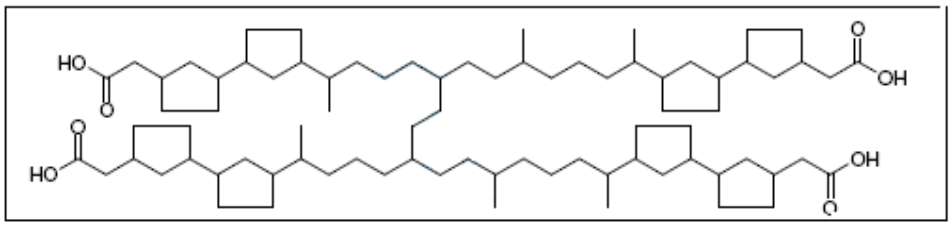

Figure 2.4. One of the Arn structures proposed by Smith *et al.* (2007).

In addition, Baugh *et al.* (2005a) stated that the Arn species needed to be present in the parent crude oil in order for soap to form, however the reasoning behind this was not explained. Brocart *et al.* (2005) performed an analysis of Arn acids extracted from various crude oils using a number of techniques including ion exchange and liquid extraction followed by LCMS. The authors claimed that Arn is present in soap-forming crude oils, typically in the ppm range, yet they did not comment on limit of detection. Mediaas *et al.* (2005) on the other hand suggested that Arn could be detected in crude oils using LCMS down to concentrations of 3 ppm. Brocart *et al.* (2005) noted that despite identifying Arn in a number of crude oils, not all of these were soap-forming under field conditions. In other words, the presence of Arn in crude oils would not be sufficient to lead to a soap deposition problem. Thus it was concluded that Arn in combination with operational variables were responsible for the formation of soaps in the field. This information will be revisited further in experimental results described in Chapters 6 and 8. Brandal, (2005) analysed soap deposits from a West African field using NMR, FTICRMS and Fourier-Transform infrared (FTIR). The NMR spectrum of the fraction isolated from the deposit showed a single peak in the carboxylic acid region, well-resolved peaks in the aliphatic region but no indication of aromatic carbons, which is consistent with the work of Baugh *et al.* (2005a). Brandal, (2005) also showed that Arn were the dominant species in the mass spectrum of the naphthenic acids from the soap deposit, although the spectrum for the lower molecular weight naphthenic acids was not shown for comparison. The author also suggested that Arn would have the potential to form polymer-like structures in with the presence of multivalent cations. This would be the direct result of the presence of the four carboxylic groups, which could then lead, in turn, to the formation of networks at the oil-water interface. Langmuir film measurements were presented by the same author which

might support this hypothesis. The occurrence of networks composed of Arn and cations was also supported by Brocart *et al.* (2005) by thermal analysis results.

Gallup *et al.* (2002, 2004 and 2005) analysed the composition of soaps, as well as soap-forming crude oils from Asian fields using techniques such as FTIR, NMR and gas chromatography mass spectroscopy (GCMS). It was surprising that they identified predominantly acyclic species in these field soaps. These consisted of mostly fatty acids containing between twenty eight and thirty carbon atoms, and molecular weights between 396 and 452 Daltons. They also analysed the soaps using ES and these measurements confirmed the previously reported predominance of acyclic species. The selectivity of these acyclic naphthenic acids towards soap formation has not been explained to date. Data from Gallup *et al.* (2005) also shows the wax content of the parent soap-forming crude oils to be above 5 wt%, and indicated that the deposits formed with a large quantity of entrained wax solids. It is not clear if the soaps behaved as binding agents for the wax and what the exact interaction between the two flow assurance issues might be.

The literature review presented in this chapter led to the development of a hypothesis to be explored in this thesis that one of the possible factors important in soap deposition could be the properties of Arn naphthenic acids in relation to non-Arn naphthenic acid species in a specific crude oil. Experiments were conducted in this thesis to evaluate this, the results of which are presented in Chapter 6.

Another specific observation in some soap-forming crude oils is the dramatic increase in cation content during production. The concentration of calcium ions in particular crude oils has been shown to reach very high levels of between 250 and 1000 ppm (Smith and Turner, 2004; Weers and Bieber, 2005). Ramstad, (2001) showed data from a North Sea crude oil where an increase in calcium content in the crude oil occurred with increase in water breakthrough. In this field, the naphthenic acid content of the crude oil remained constant while calcium content increased. This could also suggest that the naphthenic acids in the crude oil are becoming bound/complexed to calcium ions present in dispersed produced water which is entrained in the oil. It is understood that high calcium content in crude oils are a result of complexed oil-soluble soaps dissolved in the crude oil which result from bound naphthenic acids and calcium ions (which do not precipitate), as opposed to less oil-soluble soaps at the oil-water interface (which may have the potential to precipitate). This information implies that soaps may form from a range of naphthenic acid species: low molecular weight as well as high molecular weight. This hypothesis could also support the anecdotal evidence of formation of soaps downhole which do not precipitate as solids

(Smith and Turner, 2004). However, a definite scientific investigation of this (e.g. monitoring of calcium content in produced and virgin crude oils) is still to be presented.
There is therefore a clear need to distinguish the correct naphthenic acid species responsible for the different soap varieties: the Arn-containing soaps, the fatty acid soaps as well as the bound soaps in high calcium content crudes. This was one of the current gaps not available in the literature of soap-formation systems in exploration and production, during the course of this thesis.

Produced water chemistry – pH.

As described in the conventional mechanism for soap deposition (Section 2.1.1), pH plays a central role. This variable depends on pressure and the coupled carbonate/brine chemistry, i.e. CO_2/cations/HCO_3^- (Rousseau *et al.,* 2001). At higher downhole pressures where pH is often low, the majority of naphthenic acids are not ionised in the crude oil. However as the pH rises during production, naphthenic acid partitioning and dissociation is enhanced, and soap formation and deposition occurs. This has been reported at pH values above 6 for calcium-rich soaps (Rousseau *et al.,* 2001; Goldszal *et al.,* 2002; Turner and Smith, 2005). In contrast, sodium-rich soaps are suggested to occur at slightly higher pH, at or above 7 (Gallup *et al.,* 2005; Turner and Smith, 2005). The reasons for this discrepancy are probably a combination of issues such as the predominant naphthenic acid species and the relative solubility of soaps. These reflect either a majority of calcium or sodium cations combined with the presence of bicarbonate ions in the produced water. pH changes observed during soap formation may also be associated with the carbonate scale deposition mechanism. Rousseau *et al.* (2001) and Goldszal *et al.* (2002) have reported the possibility of mixed calcium carbonate and calcium soap deposits occurring in the field. This would imply competing kinetics between the bicarbonate and the naphthenate anions for the calcium ion. No compositional results of such mixed deposits have been reported in the literature. Rousseau *et al.* (2001) also suggested that the bicarbonate ion content is the critical kinetic variable responsible for the competition between carbonate or soap precipitation. It is widely known that bicarbonate ions can behave as pH buffers, and this could affect the balance of carbonate or soap species during production. The pH decrease observed after the precipitation of soaps from produced waters without bicarbonate ions, would prevent further soap formation due to diminished naphthenic acid partitioning. In the presence of bicarbonate ions, the formation of soap would be enhanced, due to pH being maintained at constant high values. The importance of bicarbonate ions in soap formation has been further demonstrated by Rousseau *et al.* (2001), who showed that these ions were

the limiting reagent in soap formation for a number of West African fields. The authors studied crudes and produced waters from soap-forming systems and correlated the amount of bicarbonate ions required to maintain critical pH values, based on the concentration of naphthenic acids in the parent crude oils. Surprisingly, the concentration of calcium ions in the produced water was shown not to be the limiting reagent, and thus claimed not to be affecting soap formation. Definite evidence of bicarbonate ion influence on soaps from other geographical locations is still to be presented.

Produced water chemistry – cation content.

As described above, most soap deposits in the field has been shown to contain predominantly divalent calcium ions. However, in certain cases, soap deposits contain mainly monovalent ions such as sodium or potassium (Gallup *et al.,* 2002; Turner and Smith, 2005). Turner and Smith (2005) have suggested that these comprise two defined varieties of soaps, or end-member cases, and have adopted the following definition: calcium-rich soaps are calcium naphthenate soap scales, and sodium-rich soaps are sodium carboxylate soap emulsions. This terminology is used hereafter in this thesis. These two varieties of soap have very different properties as will be described in the following paragraphs.

Calcium naphthenate soap scales have been shown to occur as separate phases at the oil-water interface (Vindstad *et al.,* 2003; Mediaas *et al.,* 2005). It has been suggested that these soaps contain a range of naphthenic acid species and possibly a predominant amount of Arn (Baugh *et al.,* 2004; Baugh *et al.,* 2005a and 2005b; Mediaas *et al.,* 2005). These soaps are observed as sticky soft pads at separator conditions, but solidify rapidly to rock-like hardness when exposed to ambient pressure and temperature (Pearson, 2004). This phenomenon is not fully understood, but is speculated be the product of oxidation (Smith and Turner, 2004). Vindstad *et al.,* (2003) used elemental analysis to study calcium naphthenate soap scales. It was found that the soap contained 2.6 wt% calcium with lower concentrations of barium, sodium, silica, and sulphur atoms. This type of soap has also been suggested to occur in conjunction with a number of other solids (i.e. sand, inorganic scale, waxes and asphaltenes) and also precipitate at the bottom of vessels (Vindstad *et al.,* 2003). It is useful to visualise naphthenates as binding agents for other solids, as well as solids in their own right (Turner and Smith, 2005). As stated before, it has been suggested that Arn are the predominant naphthenic acid species in these soaps. Because of the proposed four carboxyl groups in the Arn structure, and the fact that calcium is a divalent cation, the Arn species could be bound to one or even four different calcium ions forming a

sticky network. Thus an empirical formula for the calcium naphthenate soap scale may be difficult to determine with accuracy, despite the claims of Baugh *et al.* (2005a). The types of crudes where soap scales are usually observed comprise medium to high TAN oils, but there are exceptions, and crudes with TAN values of 0.5 have been shown to form calcium naphthenate soap scales.

Sodium carboxylate soap emulsions have been shown to consist of predominantly fatty acids (Gallup *et al.,* 2004; Turner and Smith, 2005). These are seen as ultra-stable viscous emulsions with incorporated materials such as paraffins, barite and clays (Gallup *et al.,* 2002). These soaps do not harden on exposure to air, but can consist of up to 10 vol% of the total fluid content (Turner and Smith, 2005). Gallup *et al.,* (2002) suggested 5 wt% of minerals in the production fluids would be sufficient to generate a viscous sludge from the soap emulsion. This suggests that the soap emulsion is also either stabilised by solid particles, or is itself a binding agent for other solid materials. Gallup *et al.,* (2005) analysed sludge resulting from a sodium carboxylate soap emulsion pad using a number of techniques. The authors suggested an empirical formula for the sodium soap, $C_{38}H_{78}O_4Na$, which would require the presence of a fatty acid containing thirty eight carbon atoms. These soaps have been linked to reduced production rates and may be deposited as sludges in storage tanks leading to less oil storage capacity. Soap sludges were analysed by X-ray diffraction (XRD) and energy dispersive X-ray (EDAX) by Gallup *et al.* (2002). The sludges were seen to be amorphous matrices composed of 50 wt% oil and 20 wt% sodium salts of linear fatty acids with between twenty eight and thirty carbon atoms. Crude oils normally associated with his type of soap have low TAN. In regards to fields which have high calcium content crude, no information is available in the literature detailing the precise associated water chemistry. In this thesis, the term bound soap scale will be used to describe this type of soap occurrence and further analysis of these systems will be presented in Chapter 8.

It can be concluded that the reported field soap varieties appear to be a function of both naphthenic acid types and formation water cations. A challenge for anyone attempting to predict soap problems from crude oil and cation data would be the possibility of a field initially having one soap problem (i.e. soap scale), but later in production life a different issue altogether (soap emulsion). In this case, the water composition as well as the naphthenic acid content of crude oils for the particular field would have to be surveyed over the entire life of the field for correct predictions. This information was used in this thesis to plan soap formation experiments in laboratory conditions (Chapter 5).

Produced water chemistry – bicarbonate content.

Gallup *et al.* (2002) have suggested that bicarbonate ions may be present in sodium carboxylate soap emulsions as complexes consisting of monovalent cations bound through hydrogen bonds of the carboxyl groups of fatty acids present in the crude oil. For soap emulsion-forming fields, Gallup *et al.* (2005) suggested that the high concentration of bicarbonate and CO_2 in the parent fluids would be a result of the de-carboxylation of the fatty acids present in the oil. If the complexation of the bicarbonate does occur then a possible structure for this molecular arrangement might be the proposed structure in Figure 2.5.

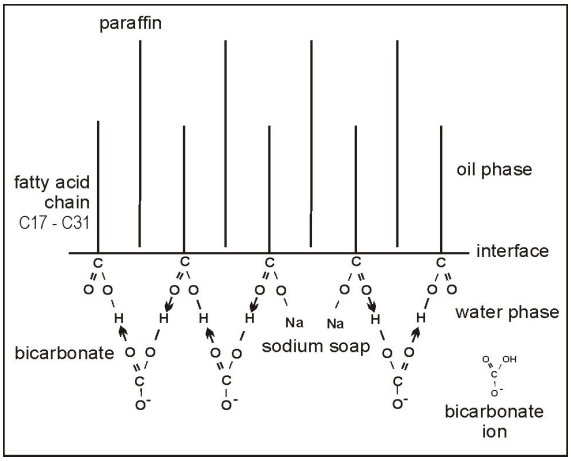

Figure 2.5. Sodium carboxylate soap emulsion structure proposed by Gallup *et al.,* 2004.

Clearly if the occurrence of the complex structure in Figure 2.5 can be proved, then the presence of bicarbonate ions would play a dual role in the mechanism for these soap emulsions: pH control as well as a complexing agent. Some of the experiments which have been designed in this thesis investigated the possible occurrence of the complex species suggested by Gallup *et al.* (2004). Figure 2.5 also shows that layers of paraffins are positioned adjacent to the fatty acid chain in the oil phase of the soap emulsion systems. The exact role of paraffins is however unclear but it is very possible they contribute towards emulsion stability, or changes in emulsion viscosity below the pour point of the crude oils.

Physical parameters – temperature, shear and electric fields.

The effects of various physical and operational parameters on soap formation, as well as possible mitigation options have been detailed by Turner and Smith, (2005). Temperature has been shown to be a key physical parameter in soap formation. Evidence of enhanced

soap generation at higher temperatures in heaters (50 to 80 ºC) has been observed for both soap scales and soap emulsions. Gallup *et al.* (2004) reported that temperature differences from offshore pipelines to land terminals (between 80 ºC to ambient) influenced the precipitation of the soap emulsion as sludge. The detailed mechanism of how temperature affects soap formation is not understood. Thus it is not known whether temperature affects the kinetics of soap formation and/or the thermodynamic behaviour of naphthenic acids or waxes in solution. Shear has a major impact on soap formation in the field (Turner and Smith, 2005), particularly for soap emulsions. This is especially true for fluids flowing across electric submersible pumps and through certain topside components. The effect of shear is to produce smaller water droplets that provide larger interfacial areas, which in turn, could lead to a more stable emulsion, and also encourage more soap formation. For a detailed review on the effects of shear on emulsion behaviour in the petroleum industry, the reader is referred to Petex (1990). Water cut has also been observed to influence the occurrence of soaps, although the precise mechanism for this is not known (Turner and Smith, 2005). During the course of this thesis, evidence has been obtained that supports the idea that this effect might be due to the balance of water-soluble/oil-soluble soaps, or a balance between the more water-soluble naphthenic acids and acids which are sparingly soluble in water. Soap emulsions have also been observed to agglomerate and deposit at faster rates under the influence of electric fields, as found in electrostatic coalescers (Turner and Smith, 2005). This could be an indication of the water-in-oil emulsion nature of these soap types, but no information was available to confirm this prior to the work in this thesis. The effect of shear was specifically taken into account when planning the best strategy for the analysis and formation of soaps in the laboratory. This is described in detail in Chapter 5.

2.2. Naphthenic acid chemistry, phase behaviour: possible factors in soap deposition?

It is widely accepted that naphthenic acid chemistry has not been the subject of extensive published research. Single commercial naphthenic acids and acid mixtures are either solids or liquids with molecular weights ranging from 100 to 400 Daltons (Brient *et al.,* 1995). As would be expected from their structure, naphthenic acids have polarity, and thus can form hydrogen bonds with each other. These strong hydrogen bonds result in a range of specific properties, including, for instance, high boiling points. Naphthenic acid behaviour in an oil-water system is governed by the oil-water partition coefficient (K_{ow}), given by Equation 2.4. and the dissociation constant (K_a) given by Equation 2.5,

$$K_{ow} = \frac{[HA]_o}{[HA]_w}$$

Equation 2.4.

$$K_a = \frac{[H^+][A^-]}{[HA]_w}$$

Equation 2.5.

where HA and A^- represent a generic undissociated naphthenic acid and the dissociated acid or naphthenate anion respectively, the subscripts w and o, the water and oil phases. The K_{ow} and the K_a for naphthenic acids are not widely available in the literature. A review of the publications shows there is no universal correlation between the type of naphthenic acid and its K_{ow}, although factors such as pH, temperature, cations present in the water, type of solvents used as the oil phase and the actual acid concentrations may be important. Many experimental techniques have been used in K_{ow} determination, including colourimetric titration and IR spectroscopy (Bitsh-Larsen *et al.,* 2004), as well as ultraviolet (UV) spectroscopy (Spildo and Hoiland, 1999). Volatile fatty acids (between two and four carbon atoms) have also been analysed with ion chromatography with reported values for K_{ow} between 1000 and 4.14 in oil-water systems (Reinsel *et al.,* 1994). Nevertheless, higher molecular weight acids and those with the structures shown in Figure 1.2 have been said to have much lower K_{ow} values in model oil-water systems, e.g. $5x10^{-5}$ (Bitsh-Larsen *et al.,* 2004). Reinsel *et al.* (1994) performed tests on low molecular weight acids and found a linear relationship between the logarithm of K_{ow} and the number of carbon atoms in the acid. pH was also seen to influence increases in K_{ow} and this was attributed to the formation of the naphthenate anion, which has a stronger affinity for water compared to the neutral acid molecule. Havre (2002), working with model naphthenic acids and acids extracted from crude oil, found K_{ow} values between 10^{-2} and 10^{-5}. The author observed that K_{ow} varied linearly with the number of methyl groups in the acid structure, however an effect caused by the number of cycloaliphatic rings was also suggested. In work with a model naphthenic acid in n-decane and water, Spildo and Hoiland (1999) showed a dependency of K_{ow} on the cation content of the aqueous phase. The presence of monovalent sodium ions did not affect K_{ow}, but divalent calcium ions were seen to have an influence when tested at the same pH. Standal *et al.* (1999) also confirmed this trend using a different acid compound and suggested the results were due to the salting-out effects (increased solubility of the acid in the water phase) in the presence of calcium ions. The various different behaviours of reported K_{ow} are thus probably a reflection of the variety of features in the different naphthenic acid structures such as number of carbon atoms, hydrogen deficiency as well as the number of unsaturations and carboxyl groups.

Naphthenic acid dissociation constants are more widely available in the literature. It is well known that for low molecular weight mono-carboxylic naphthenic acids, dissociation constants, K_a, usually have values between 10^{-5} and 10^{-6} (Brient, 1998). This means that these species are weakly acidic. The pK_a is usually calculated by titration of the naphthenic acids with a stronger acid or a strong base. It is determined as the pH of the solution at half neutralization volume. In other words, where 50 mol% of the hydrogen ions are removed from the carboxylic group by hydroxyl ions in solution (Kanicky and Shah, 2002). Any factor which stabilises the naphthenate anion by withdrawing electrons, increases the acidity as given by the pK_a. On the other hand any factor that makes the anion less stable is associated with electron release/sharing, and decreases acidity (Morrison and Boyd, 1979). Alternative methods for pK_a measurement have been tested. For instance, Sjoblom *et al.* (2003) reported pK_a values of naphthenic acids calculated with GC. pK_a values for naphthenic acids with ten to sixteen carbon atoms and one, two and three rings were determined to be 4.9 ± 0.1 at 25 °C.

It is not surprising that pK_a studies of fatty acids are more common in the literature than those of acids having the structures shown in Figure 1.2. Fatty acids are more water-soluble than species with cyclic rings. However, because electronic effects of the added carbon cannot be increased beyond three or four carbon atoms, the pK_a tends to become constant for acids with more than five carbon atoms and the same chemical backbone (Kanicky and Shah, 2003). Kanicky and Shah (2002) carried out a number of pK_a measurements for fatty acids with eighteen carbon atoms in model systems. They measured very high pK_a values, ranging from 8.28 (linolenic acid) to 10.15 (stearic acid). The lower values were found for acids with more unsaturations in their carbon chains. The authors suggested the results could be correlated to the packing of the acid at the interface. In crude oil mixtures, naphthenic acids will, however, dissociate over a range of pH values as reported by Rousseau *et al.,* (2001). This makes individual effects of acid groups more difficult to determine. Kanicky and Shah (2003) determined the pK_a for a number of mixed fatty acids in solution. Their results showed that if a fatty acid was added to a solution containing other acids of different carbon chain lengths, the final pK_a would be closer to that of the shortest chain. The authors argued that this would be because the unequal chain length would lead to disruption in molecular packing. Baugh *et al.* (2005b), have shown that the pK_a of the Arn naphthenic acids is of the same order of magnitude of that of a fatty acid with fourteen carbon atoms. They also showed that all four carboxyl groups in this naphthenic acid had equal strength. This is interesting because these results suggest that despite the high molecular weight (~1230 Daltons) and complex molecular structure of these species, their

positioning at the oil-water interface would not be affected by the different carboxylic acid groups. Nevertheless, in crude oils which may contain more than 3000 naphthenic acid components (Qian *et al.,* 2001; Kim *et al.,* 2005) it might be very difficult to ascertain with precision, the exact order in which each selected naphthenic acid partitions to the oil-water interface. It might also be possible that the dissociation of higher molecular weight naphthenic acids (i.e. Arn) is systematically affected by other lower molecular weight acids during this process. In Chapter 7 a more detailed analysis of the importance of K_{ow} and K_a on prediction of soap precipitation will be carried out, together with specially designed measurements.

Work on naphthenic acid chemistry has also used the solubility product (K_{sp}) of the soap as a tool for phase behaviour studies. This is shown in Equation 2.6.

$$\mathbf{K_{sp} = \frac{[MeA_x]}{[Me]^x.[A]^-}}$$

Equation 2.6.

where A^- is the naphthenate anion, Me represents the metal cation with charge x which forms the soap MeA_x. Beneventi *et al.* (2001) demonstrated that calcium soap solubility was a function of the presence of unsaturations on the hydrocarbon chain of the parent acid: the higher the number of unsaturations, the higher the solubility of the soap. Solubility at pH 9 and 67 °C for these soaps varied between $6x10^{-5}$ and $3x10^{-4}$ g/l obtained by surface tension measurements. Information on solubility products of oilfield soaps is less reported. Havre (2002) claimed it would be possible to study the formation of calcium soaps by induction time measurements. The pre-requisite to this was that the soaps formed through a crystallisation type mechanism. Thus near infrared spectroscopy (NIR) was used by Havre (2002) to gain information on the growth of calcium soaps and their solubility products in a bulk aqueous phase using dilute concentrations of acids in a single (water) phase. K_{sp} values were shown to vary between $6.4x10^{-13}$ and $2.8x10^{-8}$. However these results are qualitative since the formation of soaps occurs in a two-phase system in realistic conditions and may not even be governed by nucleation and crystal growth. The technique used by Havre (2002) was developed further to view the growth of soap particles (from model naphthenic acids) in oil-water interfaces created in laboratory conditions (Brandal, 2005). In Chapter 7 it will be shown that K_{sp} values are useful in modelling the formation of soaps in the laboratory.

An interesting aspect of naphthenic acid phase behaviour is their ability to self-organise through the formation of aggregates, such as micelles and dimers. An elegant review of the subject together with the first attempts to correlate these types of aggregates with soap deposition was carried out by Havre (2002) and extended by Brandal (2005). These aggregation properties result from the amphiphilic nature (presence of both hydrophobic and hydrophilic moieties (the organic chain or ring and the carboxyl group, respectively) of the naphthenic acid itself. One of the most interesting aggregation species are micelles, which are colloidal structures where the hydrophobic part of the molecule is directed towards the centre and the hydrophilic part directed towards the liquid phase. These aggregation structures can occur either in bulk organic or aqueous phases and result from hydrogen bonding and/or hydrophobic interaction of the hydrocarbon chains (a result of the balance of electrostatic and attractive van der Waals forces). Patist *et al.* (2001) presented an elegant review of the mechanism believed to be responsible for micelle formation. These and other aggregate varieties (e.g. reverse micelles) are believed to be restricted to a limited number of molecular species, and to be highly dependent on bulk phase pH, temperature, pressure and concentration. The critical micellar concentration (CMC) is the minimal concentration necessary for micellar formation (Kanicky *et al.,* 2001). This can be measured by a number of techniques such as surface tension, electrical conductivity, chemical means and even light interferometry (Nikolov and Wasan, 1989; Patist *et al.,* 2001). Micelles can be understood as aggregates with different shapes and diameters between 4 and 10 nm. They are said to be in equilibrium with single surfactant monomers in the bulk liquid. Ekwall (1969) showed that in a system consisting of water, caprylic acid and sodium caprylate, two clearly distinguishable regions could be observed: a L1 phase, where water was the solvent and micelles were observed, and a L2 phase, where the fatty acid was the solvent and reverse micelles were found with a water-core surrounded by amphiphile molecules with hydrophobic groups oriented toward the core. This phase behaviour is shown in Figure 2.6. In a series of papers, Stenius and Zilliacus (1971) and Stenius (1973a, 1973b, 1973c and 1978) studied the formation of micelles in fatty acid systems containing up to six carbon atoms. The basic experimental set-up was potentiometric and VPO evaluations of brine systems containing acids. Micellar stability was found to increase with chain length, although the smallest carboxylate molecule to form micelles was an acyclic acid with five carbon atoms. Association was seen to increase with temperature in the range 25 to 40 °C and decrease with increasing branching. Damas *et al*., (1999) studied the effect of changes of sodium carboxylate salts on their micellar properties. All unsaturated carboxylate salts formed aggregates in aqueous solutions at 0,

25 and 40 °C. Unsaturated salts had higher CMC values compared to saturated salts, and this was seen to increase with temperature and degree of unsaturation. This effect was attributed to increase in polarity and CMC values varied between $7.1x10^{-3}$ and $405x10^{-3}$ mol/kg. Havre (2002) obtained a number of CMC values for various single naphthenic acid solutions as well as commercial mixtures and these varied from $1.7x10^{-2}$ to $8x10^{-4}$ mol/l at pH 11 and 25 °C. Brandal (2005) reported CMC values for benzoic acid homologues between 0.83 and 0.01 mol/l. Certain correlations do exist to explain CMC values and the molecular weight of acids, related in turn to the hydrophobic part in the acid structure (Havre 2002). Beneventi *et al.* (2003) also argued that the presence of sodium oleate soap micelles in aqueous systems would play an important role in the foam stability mechanism. There is, however, a general lack of publications dealing with the micellization behaviour of naphthenic acid species and their soaps. Horvath-Szabo *et al.* (2001a) demonstrated that no CMC occurred for sodium naphthenates from commercial samples in the range from 0 to 0.3 mol/kg toluene. This was attributed to hydrotropic behaviour of soaps (the ability to increase the solubility of one solvent in another). The occurrence of micelles has the potential to affect the prediction and modelling of naphthenic acid oil-water phase behaviour as shown by Havre (2002). Kanicky and Shah (2003) argued that at concentrations below the CMC, pre-micellar aggregates reflect the molecular cooperation in the ionisation behaviour of the carboxyl groups. This was supported by larger than expected measured pK_a values for acid solutions which were below the CMC. CMC and surface activity are closely linked. In a surfactant system the CMC may be related to the stabilisation of the surface tension. The main problem is that if the solubility limit of the surfactant is below the CMC (i.e. at low temperatures, below the Kraft point), micelles cannot be formed and the surface tension trend is only due to lack of solubility, not micellization. The phase behaviour is also made more complex by the formation of multimeric species, such as dimers (Murkerjee, 1965).

Naphthenic acids are also closely associated with emulsions. An emulsion (macroemulsion) can be defined as a thermodynamically unstable mixture of two immiscible liquids (Iupac, 1997). Under the appropriate conditions of agitation, one of the liquids becomes dispersed in the other in the form of droplets. The most common type of emulsions found in crude oil production are water-in-oil emulsions (W/O), in which the crude oil is the continuous phase and water is the dispersed phase. Reversed emulsions, or oil-in-water emulsions (O/W), are those in which oil is the dispersed phase. Certain naphthenic acid species can be classed as surfactants. Surfactants within the petroleum industry are a class of compounds which accumulate at the oil-water interface and form an adsorbed film which may lower the

interfacial tension (IFT) of a crude oil-water system to very low values (Kanicky *et al.,* 2001). Their phase behaviour can be very complex, as illustrated by Kanicky *et al.* (2001). The actual phase behaviour of naphthenic acids in solution has been observed to be equally as complex. Horvath-Szabo *et al.* (2001b) examined commercial sodium naphthenate in toluene-water systems and found five overlapping phases in equilibrium as shown in Figure 2.6. This is also presented with the phase behaviour of a single naphthenic acid, its salt and water (solvent) as studied by Ekwall (1969). The presence of an additional solvent (toluene) leads to a more complex phase behaviour as illustrated in Figure 2.6. L1 represents the micellar region and L2 represents the reverse micellar region. It is interesting to note that the gel phase found in the presence of an oil phase only (toluene) is a birefringent structure containing liquid crystals. The overall phase behaviour would also necessarily be expected to be a function of the oil-water partition coefficient, degree of surface activity and molecular structure of the naphthenic acids.

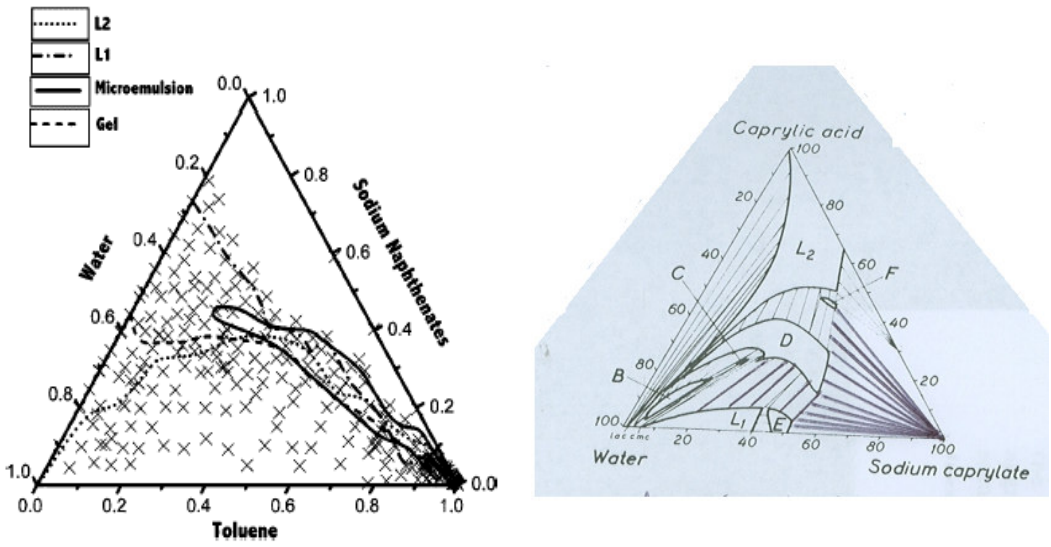

Figure 2.6. Left: phase diagram of toluene, water and commercial sodium naphthenate from Horvath-Szabo *et al.* (2001b). Right: phase diagram of caprylic acid, sodium caprylate and water from Ekwall (1969).

Further evidence of naphthenic acid surfactant behaviour has been presented by Mendez *et al.,* (1997). These authors reported Winsor transitions for a solution of fatty acids in toluene. Winsor systems I, II and III were also observed by Horvath-Szabo *et al.,* (2001b). Similar emulsion transitions were observed by Pickett and Ellway (1976) for soaps formed from oleic acid and magnesium ions, and this was shown to be a function of the concentration of salt in the system. Winsor systems represent either O/W, W/O or multiple emulsion transitions.

Naphthenic acids structures have also been described as forming liquid crystals. These are also additional surfactant association structures discovered by Reinitzer in 1888 (*opere citato* in Friberg *et al.,* 1974) which have been studied extensively since the 1960's mostly in attempts to explain the structure of biological membranes (Friberg *et al.,* 1974). They can be understood as systems exhibiting anisotropic properties associated with solid crystals as well as flow properties found in ordinary liquids, but usually with high viscosity values. Examples of compounds which behave in this fashion are cholesteryl esters, n-alkoxyazobenzenes and anisaldazine (Pope and Judd, 1980). Liquid crystals have been reported in a range of systems containing naphthenic acids, namely: water-commercial sodium naphthenates (41.8 to 74.5 wt%) (Horvath-Szabo *et al.,* 2001a), water-toluene-commercial sodium naphthenates (Horvath-Szabo *et al.,* 2001b), naphthenic acid in 1M NaOH solution, naphthenic acid in toluene or heptane with 0.5 to 1 M NaOH and bitumen in toluene or heptane with 0.1 to 1M NaOH (Horvath-Szabo *et al.,* 2002 and 2003).

It is still not certain whether the acid species responsible for soap formation also form dimers, micelles or behave as liquid crystals and if this has any significance in soap deposition under field conditions. However, as described above, crude oil contains a vast number of naphthenic acids. Therefore it is possible that even micelles from non-soap-forming naphthenic acids may also have an important role in soap deposition. No reports of liquid crystal structures for soap-forming systems could be found up to the work carried out in this thesis. The influence of these structures on the formation of soaps or on the stability of the emulsions formed from soaps remains unknown. More recently, specific acid structures have been suggested responsible for the occurrence of liquid crystal structures (Ese and Kilpatrick, 2004). Experimental evidence demonstrating the influence of liquid crystals on the stability of emulsions containing naphthenates has been presented by Horvath-Szabo *et al.* (2001b).

The surface properties of fatty acids in aqueous systems has been studied by a number of authors for more than 60 years. It is known that these molecules have an overall preference for interfaces. Langmuir and Schaefer (1937) studied the behaviour of stearic acid monolayers in water in the presence of calcium ions and at specific pH. The authors used specially designed troughs to study surface pressure. Calcium ions were seen to lead to a significant decrease of the monolayer area (the interface area where the acids are positioned) and to make the cation-acid film more rigid at pH values of 7. In the presence of sodium ions, more calcium ions needed to be added to make the film rigid again. Wolstenholme and Schulman (1950 and 1951) carried out some complimentary experiments using a similar set-up and studied the effect on the monolayer in air-water

systems. Myristic acid and a larger number of cations were evaluated as a function of pH. Iron, aluminium, copper, manganese, calcium, cobalt and magnesium were used. In these experiments pH was observed to have an important role in the behaviour of the monolayer under equal ionic strength conditions. Calcium and magnesium had more significant effects at pH values greater than 6, while iron and aluminium had greater effect at pH values less than 4. Enever and Pilper (1967a) studied the kinetics between stearic acid and calcium ions at the air-water interface. Their results pointed to a direct dependency on pH, the concentration of the calcium substrate, the area per molecule of the stearic acid, and temperature of the overall reaction. Moreover they stated that the overall process could be understood by four basic steps:

- diffusion of the metal (calcium) ions to the oil-water interface,
- reaction at the interface between the ionised carboxyl groups and the metal ions,
- structural reorientation in the mixed calcium naphthenate (stearate) and fatty acid film, and
- further reactions between calcium and carboxyl groups due to removal of steric hindrance.

Enever and Pilper (1967a) also claimed that the first two steps would occur within a few tenths of a second to two minutes, the last two steps would be dominant in the kinetics of the reaction. Moreover, they claimed this could be measured by surface viscosity measurements, which would be proportional to the amount of soap formed. Furthermore the same conclusions also held in a mixed system consisting of stearic acid, octanol and an aqueous phase with calcium ions (Enever and Pilper, 1967b). This data was also reinforced by surface potential measurements which proved to be a good indication of the ionisation of the stearic acid during the experiments. It is currently agreed that the presence of a net charge on a surfactant polar group affects its adsorption onto the monolayer. In the case of fatty acids, if all molecules become ionised, repulsion of molecules with similar charge may result in expansion of the monolayer leading to a weak/unstable film (Kanicky and Shah, 2002). Berg and Claesson (1989) conducted further studies on the forces within monolayers of acids in the presence of divalent cations using Langmuir-Blodgett films. Surface pressure-isotherms, contact angles and force versus distance curves were obtained for monolayers consisting of docosanedioic acid and eicosylamine in aqueous solutions. The effect of cadmium and calcium ions (concentrations from 10^{-5} to 10^{-3} M) was studied. It was observed that increasing the pH from 2.8 to 6 led to a change in the charge on the

mixed monolayer surface. In other work, Yazdanian *et al.* (1990) studied the effect of a wider range of cations at low ionic strength (~ 0.01 M) on stearic acid and arachidic acid monolayers. Surface pressure and surface potential measurements were obtained. It was seen that increase in the positive charge of the monolayer was induced by the presence of specific cations, based on the following order: magnesium < calcium < barium. Negative charges were however also observed to follow a specified order: cobalt < cadmium < lead. The cation order was shown to follow the expected degree of hydration of the atom (a function of ionic size). Ederth and Claesson (2000) carried out elegant work on the formation of soaps in the laboratory using thiohexadecanoic acid in hexadecane and water. The authors performed the measurement of the surface forces at a specially prepared carboxyl acid (charged) surface in the presence of calcium, magnesium and sodium ions. At very low ionic concentrations (~ 1 mM), DVLO (Derjaguin, Verway, Landau and Overbeek) theory was used to explain the effect of adsorped cations. This theory advocates the existence of an electric double layer for colloids in aqueous solutions (Adamson and Gast, 1997). Thus divalent cations were argued to be more efficient in reducing the surface charge than the monovalent sodium ions. At higher ionic concentrations it was shown that the DVLO theory was not adequate to predict the measured forces. In other words, the stability of the systems could not be determined by the sum of the electrical double layer forces and the repulsive van der Waals forces. Differences in adsorption for the divalent ions were rationalized in terms of hydration of the cation atom: magnesium is smaller than calcium, thus more strongly hydrated which in turn provides an energy barrier against adsorption. Havre (2002) also studied the influence of different cation species on the film formation of naphthenic acid solutions using the Langmuir technique at the air-water interface. His results showed that film formation from oil-water systems (containing naphthenic acids) was pH dependent with the more stabilising effect resulting from the presence of calcium ions at high pH. However, these experiments were based on the particular type of naphthenic acids forming a film, and this was structure dependent. The formation of the acid-cation monovalent complex was used by Brandal (2005) to explain the occurrence of oilfield soaps. A two-step mechanism was suggested to be occurring, in which the formation of the complex was the first as illustrated in Equation 2.7.

$$M^{2+} + 2 - RCOO^{-} \xrightarrow{k1} [RCOO - M]^{+} + RCOO^{-} \xrightarrow{k2} (RCOO)_2 - M$$

Equation 2.7. Two-step mechanism for soap formation proposed by Brandal *et al.,* (2004) and Brandal (2005). k_1 and k_2 represent the rate constants.

Moreover, the same author advocated that the rate of soap formation would depend on the stability of the monovalent complex $[RCOO\text{-}M]^+$ as a consequence of steric hindrance of acid monomers at the interface, as well as interfacial affinity of the cations towards the acids. The formation of such complexes was modelled in Langmuir systems by Bloch and Yun (1990) and Kovalchuck *et al.* (2001). The conclusions reached by Brandal (2005) resulted from a series of experiments using the Langmuir technique to investigate a larger variety of sensitivities such as pH and naphthenic acid type, as well as divalent cation type on soap-forming systems (Brandal *et al.,* 2004, Brandal 2005). These results showed the compression isotherms were a direct result of pH and of the type of acid used (model naphthenic acid or species extracted from field soaps). The authors tested a number of divalent cation sensitivities. The species with smallest ionic radius (magnesium), was shown to have the least stable film. This could be related to the larger hydration effects supporting preliminary conclusions on similar systems by Yazdanian *et al*. (1990). However, the same experiments did not show a clear effect for other larger atoms (e.g. there were no clear trends for barium and calcium ions). Further Langmuir film measurements for naphthenic acids isolated from soaps carried out by Brandal (2005) showed a dependency on pH, high stability in the presence of calcium ions compared to the model naphthenic acid solutions and uneven trends. The author related this to the suggested polymeric network behaviour of Arn.

Surface properties of model oil-water systems have been shown to be associated with the presence of naphthenic acids. The lowering of interfacial tension (IFT) in more complex two-phase (crude oil-water systems or model acid-water systems) occurs as a result of the particular type of naphthenic acid (Hoeiland *et al.,* 2001; Havre, 2002). Fatty acids have been shown to present typical surfactant behaviour (decrease of IFT with high pH). Much less has been reported in the literature on the surface activity for more complex acid structures from crude oils. Naphthenic acid fractions isolated from crude oils have shown interfacial tensions of less than 0.003 mN/m, even at concentrations as low as 0.14 wt% (Seifert and Howells, 1969). Direct dependence of interfacial activity on acid content of a crude oil was first established by Seifert (1969). No correlations exist at present which indicate the overall effect of naphthenic acid structures in crude oil on IFT. However certain conclusions may be reached by analysing specifically the length of aliphatic chains (which would allow the polar groups to be packed closer together), and the absence of bulky aromatic or cycloaliphatic structures. Hoeiland *et al.,* (2001) presented IFT trends as a function of pH for naphthenic acids extracted from crude oils. Measurements were carried out in the presence of NaCl using the drop-weight method. A gradual decrease in IFT as a

function of pH was observed, despite different acid types present in the extracts. Havre (2002) showed preliminary IFT data for a series of model naphthenic acid solutions and acids extracted from crude oil. The author's results showed that commercial naphthenic acids behaved similarly to those species extracted from crude oil. IFT trends were seen to decrease with increase in pH, and this was attributed to acid structure. This methodology was developed further by Brandal (2005) in experiments with naphthenic acids extracted from soap deposits. The author reported IFT for systems containing Arn acids as low as 12 mN/m and claimed that this would be one of the reasons behind the selectivity of this species towards soap formation. Yet, it is debatable if this reduction in IFT is significant, particularly when the IFT values for these Arn systems are three orders of magnitude higher than the results of Seifert and Howels (1969), who used different naphthenic acids.

There have been a number of attempts to model the changes in oil-water IFT due to the presence of naphthenic acid systems. Primarily, the lowering of IFT with pH is a result of the extent of naphthenic acid ionisation, and the accumulation of these ions at the oil-water interface. This can be represented in its simplest form by the Gibbs Equation:

$$\Gamma_{HA} = -\frac{1}{RT}\left(\frac{\partial\gamma}{\partial \ln C_{HA}}\right)$$

Equation 2.8.

where Γ_{HA} is the surface excess of the naphthenic acid, γ is the interfacial tension, C_{HA} is the concentration of the naphthenic acid in the bulk phase, R is the universal gas constant and T is temperature (Adamson and Gast, 1997). This simple equation has been used successfully to model the phase behaviour of naphthenic acids in oil-water systems. Through mathematical manipulation of the Gibbs equation, a relationship between interface behaviour and IFT can be established: tighter molecular packing in the adsorbed film decreases the IFT. More recent models attempt to correlate subtle surface property changes with bulk property variations as a result of naphthenic acid presence. The premise for these models is the occurrence of an ionised monolayer, formed at the oil-water interface in which both kinetic and electrostatic contributions are present. The general agreement is that IFT will be reduced in systems consisting of an organic solvent with a naphthenic acid which has been placed in contact with alkaline brine. IFT is then related to surface pressure (π), which can be due to two contributions as shown in Equation 2.9.

$$\pi = \pi_k + \pi_E$$

Equation 2.9.

The electrostatic contributions (π_E) result from the charging of the interfacial double layer, and the kinetic contributions (π_k) are due to the motion of molecules at the interface. Healey and White (1978) developed a mathematical model which employed no more than electrostatic effects. This model was used successfully by Spildo and Hoiland (1999) to explain experimental IFT trends in model naphthenic acid systems. In their assumptions, the authors considered electrostatic contributions to IFT could be modelled only with salt concentrations below 0.1 M (DVLO theory does not hold at high salinities). In a series of elegant experiments, Brandal (2005) showed dynamic IFT changes for a model naphthenic acid (in toluene/hexadecane mixtures) and acids extracted from soaps could be related to the size of the divalent ions present in the aqueous phase. Results were highly dependent on the structures of naphthenic acids used. The initial dynamic IFT decrease was attributed to the electrostatic forces exerted by the ionised acids on the unionised acids. They would react together to form less surface-active complexes, which could justify dynamic IFT increase. Trends were related to the results of Ederth and Claesson (2000) the degree of hydration in the aqueous phase, which followed the decrease in ionic size: barium > strontium > calcium > magnesium. Thus barium (larger ionic radius), being less hydrated would absorb faster at the interface leading to enhanced formation of the complexes. IFT data for the naphthenic acids isolated from a soap sample by Brandal (2005) show a clear dependence on pH and acid concentration. A value of 12 mN/m was found at equilibrium for these tests, but the influence of other cations (e.g. monovalent *vs.* divalent) was not reported. The lowering of the IFT data in these last tests was claimed to be a result of the presence of the Arn acids.

There is no information in the literature correlating the actual IFT trends for naphthenic acid from soap-forming crude oils with the actual measurements for the crude oils themselves. The correlation of model IFT trends (or indeed for any other surface-derived property) with more complex systems cannot be carried out without difficulties. This is because of the net effect on surface properties of other crude oil components such as phenols, indolic acids and bases such as pyridine (Standal *et al.,* 1999). Seifert (1969) has shown that phenolic hydroxyl groups have a diminishing effect on the surface properties of naphthenic acids. Acevedo *et al.* (1992) demonstrated that the IFT properties of selected crude oils matched more closely those of extracted asphaltene fractions, and less those of the carboxylic acid fraction. Therefore it could be possible that the most surface-active components of particular crude oil are not naphthenic acids, but asphaltenes. This presents an additional difficulty since asphaltenes are a solubility class (though certain sources

defined them also being colloids more akin to naphthenic acids), as opposed to carboxylic acids which are a chemical family which may even be present in the asphaltene fraction itself. In further work, Acevedo *et al.* (1999) also showed that IFT data for asphaltene fractions as a function of concentration was at least 50 % less than those of the extracted crude oil acid compounds. Even for the acids isolated from soap samples it is expected that their concentration would be many times that found in a soap-forming crude oil and thus their net effects could be somewhat artificially enhanced, in particular, in the absence of other surface-active crude oil components.

From the previous discussion, it becomes evident that the exact extraction and characterisation of naphthenic acids from soap samples is an ongoing challenge. As far as integrating this information into a prediction tool for soaps, it is also necessary to obtain precise information on the molecular arrangement of both naphthenic acid and calcium prior to deposition, if at all possible. Current understanding is that the reaction between the produced water cations and the naphthenic acids may occur either at the oil-water interface or in the bulk of the aqueous phase. No attempts have been made however to study the changes in both crude oil and/or water properties before the formation of soaps actually takes place. For instance it is not know if the thermodynamic properties of the oil change before soap deposition (i.e. the solubility of certain naphthenic acid species in the crude oil).

It is also not known if cation-naphthenic acid complex or chelate formation takes place in the oil, and if this could be used for predicting the precipitation problem. Carboxylates are a very important class of ligands and can occur in a variety of bonding modes, and some of these can be distinguished using FTIR or NMR (Cotton and Wilkinson, 1988). Organic acid chelated transition metals are actually very common structures and are used as important trace mineral source for human and animal applications as well as in soil studies (Trusovs, 2003; Collins, 2004). It is not know if naphthenic acids themselves do form complexes with metals in crude oil systems, despite the fact that copper carboxylates can be found in tetrameric form. Cotton and Wilkinson (1988) suggested that these carboxylates might be polymeric in form. There are currently a number of possible analytical techniques for metal complex identification. A good review of the available techniques for metal-acid complex measurement can be found in the work of Collins (2004). Techniques reviewed by the author included reversed phased high performance LC, reversed phase ion pair chromatography, size exclusion chromatography and ion exchange chromatography in addition to a detailed discussion of metal-organic acid kinetics. Yepez (2005) studied the reaction between elemental iron and naphthenic acids in a crude oil sample in a special

reactor with temperatures up to 380 °C. The author used inductively coupled plasma to measure the amount of iron taken up in the crude oil complexes and to study the effects on naphthenic acid corrosion. Brandal (2005) presented a very interesting discussion that suggested that the reaction between calcium ions and naphthenic acid anions occurs through a two-step complexation mechanism, as shown in Equation 2.7. These conclusions were reached using IFT measurements on the extracted acids from soap samples. It is unlikely however that IFT would be used for soap prediction since this does not provide any information of the onset of soap occurrence. Thus, the need for a more fundamental understanding of prediction of soaps is a major gap existing in the open literature. A very promising technique which has not been reported in the literature for soap prediction is FTIR. More details of this study will be given in Chapters 3 and 5. Raman spectroscopy was also evaluated in this thesis but the results were not encouraging. In Chapter 6 the results of trial tests on model solutions will be presented using these technologies.

2.3. Concluding remarks.

In this chapter, an extensive literature review was presented which included the current understanding of the basic mechanism of soap formation together with a detailed analysis of the most important variables believed to be implicated in the field occurrence of these flow assurance issues. Soap formation is said to occur both in the bulk of the continuous phases as well as at the oil-water interface. Precipitation is a result of the reaction between crude oil naphthenic acids and produced water cations and occurs at high pH during loss of CO_2. Calcium naphthenate soap scales are said to be composed primarily of Arn naphthenic acids. Sodium carboxylate soap emulsions are said to be composed of fatty acids.

Finally, the review focused on naphthenic acid and soap properties, as well as particular techniques for naphthenic acid extraction and characterisation. Particular gaps were identified in the understanding of the formation of naphthenic acid soaps:

- the knowledge of physical chemistry and basic phase behaviour or naphthenic acids, particularly Arn and non-Arn systems, which could impact on the precipitation mechanism.
- the correct identification of soaps and characterisation of naphthenic acid fractions in field samples,
- the modelling of soap deposition in realistic conditions and prediction tools.

This information presented in this chapter is seen as a platform for the discussion of the methodologies used in this thesis.

`

CHAPTER 3 – CHARACTERISATION OF FIELD DEPOSIT SAMPLES: MATERIALS AND METHODS.

Abstract

In this chapter tests to develop the protocol for the analysis of field soap samples in this thesis are described. The philosophy behind the choice of techniques was to integrate measurements suitable for bulk and surface properties. A number of techniques were compared for investigation of both the inorganic and the organic constituents of soaps. The optimised protocol and the results helped gain an understanding of mechanistic drivers for soap formation, as well as to devise suitable experimental matrices for the study of the formation of soaps in the laboratory using various different feeds.

3.1. Introduction.

3.1.1. The characterisation of soap samples.

One of the fundamental objectives of this thesis, as outlined in Chapter 1, is to understand the formation mechanisms for soap deposits. Chapter 2 presented an overview of the techniques reported in the literature that are used to characterise a variety of field soaps. However, major gaps in this area exist. With this in mind, it was decided to establish a protocol for the analysis of field soap samples under the same set of conditions. It was also hoped that the analysis would provide inputs into the experimental design for the formation of laboratory soaps from single model naphthenic acid solutions and aid in the interpretation of tests using the extracted naphthenic acids from field deposits, as well as their parent soap-forming crude oils (Chapter 6).

A number of field deposits were used in this thesis. These were all assumed to be soap samples at the start of the experiments, as provided by the sample owners. The following deposit samples were used as received: Field X (North Sea), Field Y (West Africa), Field Z (North Sea), Field W (South East Asia), Field T (North Sea). These samples were obtained from offshore locations in which no chemical treatment/mitigation procedures took place prior to precipitation. In addition, samples were also analysed from Field U (North Sea) and Field Z (North Sea), which formed when chemical treatment/mitigation procedures were in place to stop precipitation. The significance of this on the interpretation of analytical results will be explained in Chapter 4.

The techniques tested to develop the analysis protocol were chosen to allow for the measurement of key variables believed to influence the formation of field soaps, as outlined in Chapter 2. The literature review highlighted that few attempts have been made to correlate bulk soap properties, specific chemical constituents as well as surface properties,

and integrate this information within a prediction strategy. In addition, traditional analysis of oilfield deposits has focused on characterisation of either inorganic (e.g. barium content of scale deposits) or organic (e.g. paraffin distribution in wax). Soaps are both the result of organic and inorganic chemistry (Chapter 2), so the techniques used in this thesis were selected to integrate both these aspects. The following properties were therefore chosen to be studied in the field soap samples:

- chemical composition,
- thermal behaviour,
- elemental composition,
- diffraction behaviour and
- surface properties of soap components.

The techniques tested and employed in the protocol were designed to treat the soaps as presented to avoid deliberately concentrating any soap constituent and therefore potentially overestimating its importance in the mechanism of precipitation. Detailed separation of particular field soap components was however carried out for more specific analysis and this is described in Chapter 5. However, for the application of certain techniques, the soaps were converted back to their original parent naphthenic acids, prior to analysis.

3.1.2. Naphthenic acid extraction procedure.

Two different procedures were used to convert the soap deposits back to their original parent naphthenic acids from field samples. In the first method (Procedure A), 25 g of the field deposit sample was washed with toluene (100 ml), followed by treatment with 3 molar (M) hydrochloric acid/glacial acetic acid 50/50 vol/vol mixture (100 ml) under agitation for one hour. The mixture was placed in contact with toluene (250 ml) until full dissolution of the organic phase (usually no longer than eight hours), after which the toluene phase was separated from the aqueous acidic phase and the inorganics (sludge). A second and third batch of fresh toluene was added to the leftover sludge. The process was followed by direct electrospray mass spectrometry (ES) in the negative mode on the toluene fractions used in the extractions, until no detected naphthenic acids were observed in the spectra. This was to maximise the recovery of the acids from the deposits. The toluene phases containing the naphthenic acid solutions prepared as described here will be hereafter referred to as naphthenic acid extracts.

To focus on the identification of key naphthenic acid components a second procedure was developed. In this (Procedure B), 300 g of the field soap sample was ground using a mortar

and pestle, and stirred with acetone (500 ml) for one hour. The sample was filtered, reground and treated with a fresh volume of acetone. The process was repeated using different solvents such as methylene chloride, toluene and isooctane. At the end of the solvent wash treatment, the methylene chloride was removed in vacuum giving cleaned material (approximately 200 g). It was hoped that this would be the calcium naphthenate in its purest form. This material is hereafter referred to as clean calcium soap scale. The clean calcium soap scale (100 g) was added to 3M hydrochloric acid (400 ml) and toluene (300 ml). This mixture was stirred and heated under reflux (two hours), after which the deposit had (for the most part) become a fluid organic phase. Filtering gave a residue of approximately 7 g, including sand and other insoluble materials. This deposit was filtered and rinsed with water to wash out most of the hydrochloric acid and placed in a solvent extraction unit (rotary evaporator) for toluene removal. This phase will be hereafter termed indigenous acids. Procedure B therefore contains the most concentrated fraction of naphthenic acids since most of the crude oil contaminants are removed during the extraction. Further results of this procedure are presented in Chapter 6.

3.2. Chemical composition of soaps.

One of the key variables believed to be important for field soap formation is the precise chemical constituents of the parent crude oil, which are concentrated in the soap, as discussed in Chapter 2. Many techniques were reviewed with the purpose of obtaining information on the chemical composition of both soaps and their parent crude oils. No single modern analytical technique allows determination of the precise chemical composition of crude oils or their deposits. It was for this reason that more than one analytical technique was chosen in this thesis. The molecular weight of specific soap components was investigated with mass spectrometry (MS). The review of the literature did not present any comparative results of different MS ionisation sources as well as detectors or analysers for soap samples. Therefore, a sensitivity study was carried out using different ionisation sources. The choice of these sources was based on the following criteria:

- a soft ionisation with low sample fragmentation, and
- clear distinction of low and high molecular weight naphthenic acids.

A second sensitivity study was conducted using different mass analysers. The objective was to investigate the effect of using higher resolution equipment on the detection of specific soap naphthenic acids species. The presence of particular chemical groups was also

investigated using Fourier-Transform infrared (FTIR) and nuclear magnetic resonance (NMR).

3.2.1. Mass spectrometry.

Mass spectrometry (MS) is the technique in which samples are analysed as ions according to their mass-to-charge ratios (m/z). The resolution of a mass spectrometer is defined by the ratio of ion mass to the difference in mass between two resolvable peaks in a spectrum. Resolution can also be measured by considering two adjacent peaks of approximately equal intensity. These peaks should be chosen so that the height of the valley between the peaks is less than 10 % of the intensity of the peaks (Silverstein *et al.,* 1991). Low-resolution techniques usually allow for the differentiation of unit masses up to 2000 Daltons. Standard low-resolution instruments have resolution between 10^2 up to 10^5. High-resolution instruments can have resolution of above 10^6. As mentioned in Chapter 2, derivatization of the analyte of interest may be carried out to aid detection response, although this may also make the analyte more surface-active and lead to preferential ionisation. Typically, the MS hardware set-up consists of a variety of ionisation sources, detectors and mass analysers. For this thesis, a sensitivity study was carried using a series of ionisation sources and mass analysers/detectors to determine the best set-up for detailed analysis of soap-forming systems.

3.2.1.1. The ionisation source and analyser selection.

In this thesis, a number of ionisation sources were selected for the study of naphthenic acid detection in the field soap samples. The simplest source used was an electron impact (EI) in a pyrolysis gas chromatography mass spectrometry (GCMS) set-up. Chemical ionisation (CI) was also used, despite the relatively high fragmentation reported with this source with naphthenic acids (Dzidic *et al.,* 1988; Roussis and Lawlor, 2002). Most of the analytical sensitivity studies with MS were carried out using soft ionisation sources to avoid unwanted sample fragmentation. These sources were atmospheric pressure chemical ionisation (APCI), electrospray (ES), fast ion bombardment (FAB), and matrix-assisted laser desorption ionisation (MALDI). For detailed information on the operation of these sources, the reader is referred to the specialised equipment manufacturer literature (Waters, 2005; Massspec, 2005; New Objective, 2005). Naphthenic acid extracts from a soap deposit from Field Y acquired using Procedure A (Section 3.1.2) were used in these experiments. The choice of field deposit was based on sample availability.

The selection of mass analysers used was based on the different resolution of the instruments. The focus was also on the detection of the range of components in the naphthenic acid extracts obtained using Procedure A (Section 3.1.2). In this thesis, a sensitivity study was carried out using three analysers: a single quadrupole, a time-of-flight (TOF) and a Fourier-Transform ion cyclotron resonance (FTICR). The analysers were coupled to either electrospray or nanospray sources. The negative mode of operation was used with all analysers to enable the detection of acidic species. Detailed operation of the FTICR is beyond the scope of this thesis; however more information is available in Marshall *et al.* (1998). All mass spectra obtained during this sensitivity study were recorded up to m/z values of 1500. For the ionisation source study it was decided not to employ derivatization of the naphthenic acid components with the exception of selected tests conducted with the EI source where a silyl agent was used. The reason for this decision is that derivatization of naphthenic acids is highly sensitive to structure, and therefore it was opted not to include an additional experimental variable which could affect the final spectra. The EI source also has the potential to benefit more from a derivatization procedure on the naphthenic acids than other sources. This is because of the unwanted fragmentation effects reported with this source and non-derivatized naphthenic acid species

For the FAB experiments, a VGZABSE instrument with caesium iodide source having a resolution of 1200 was used. The voltage of the atom gun operation was 30 keV, the discharge approximately 3 mA, the orientation of the ion beam gun was close to 110 °. The pressure in the source housing was between 5.5 and 10 mbar. The first matrix used was nitrobenzylalcohol (m-NBA). However, due to poor sensitivity for Arn detection, a 50/50 vol/vol mixture of m-NBA and triethanolamine (TEA) was also tested. Standard commercial naphthenic acid mixtures were also used for instrument verification.

The APCI tests were carried out using a PE Sciex 150EX mass spectrometer with a heated nebulizer source. Tuning and calibration of the equipment was achieved using polypropylene glycols and verification with commercially available naphthenic acid mixtures. Nitrogen was used as both nebulizer and curtain gas, at gas pressures of 10 and 12 psi, respectively. The nebulizer current voltage and temperature were -6 kV and 400 °C, respectively. The focussing and extraction potentials used were -50 and -5 V. The analysis parameters were: 1.0 V ion energy, deflector voltage 300 V and electron multiplier 2 kV.

The CI experiments were carried out on a semicircular VG70SE spectrometer. About 10 ml of sample was placed into a quartz capillary tube which was then inserted into the probe cavity. The probe was inserted into the sources with pressures of 10^{-7} mbar. The source was heated to 160 °C and used at -8 kV. The carrier gases used were ammonia and isobutane.

Isobutane generates tert-butyl ions when ionised in the presence of naphthenic acids, which add 57 Daltons to the ionised naphthenic acid molecular structure, whilst ammonia generates ions with 1 Dalton less than the original molecular weight (Hsu *et al.,* 2000). Between each run the source is heated to 400 °C to remove any residue. The equipment was tested with calibration standard heptacosafluoro-tributylamine.

The MALDI experiments were run with an MX Micromass time-of-flight (TOF) instrument. Flight tube voltages were 5.2 to 12 kV and a Reflectron optics path length of 2.3 m. The matrix used was alpha-cyano-4-hydroxy-cinnamic acid. A nitrogen UV laser energy source with a 337 nm wavelength was used. The pulse energy used was 1950 μJ and the analyser pressure was 10^{-7} mbar. Samples were run at a rate of 10 pmol/ml. High molecular weight standards were used for the calibration of the MALDI equipment.

The EI source was a CDSAS2500 Pyroprobe coupled to a Hewlett Packard 6890 gas chromatograph. A Hewlett Packard 5973 mass selective detector was used. For these tests the deposits were used *in natura* (i.e. without conversion back to the original parent naphthenic acids). Pyrolysis was first conducted at 650 °C and then at 800 °C (since most field deposits remained stable at lower temperatures, as given by thermal analysis tests). The analytical column was DBFFAP with 30 m length, 0.32 mm i.d. and 0.25 μm film thickness. Temperature programming was set to 40 °C (for 5 minutes) then increased to 250 °C at 8 °C/min, and finally held for 5 minutes. A commercial naphthenic acid mixture was used to test the experimental set-up.

The ES instrument used was a PE Sciex 150EX single quadrupole mass spectrometer. Samples were infused using a Harvard Syringe pump with flow rates between 1 and 10 μl/min. The source temperature was 350 °C and the needle voltage for ionspray -4.5 kV. Nitrogen was used as both nebulizer gas and curtain gas at pressures of 6 psi and 60 psi, respectively.

For the analyser sensitivity study, a single quadrupole analyser was used with the ES settings mentioned above. The TOF analysis was carried out using a Waters LCT Premier. The ionisation source was a nanospray model from Sciex. Nitrogen was also used and the pressure was tuned to around $2x10^{-3}$ Torr. The following settings were used: capillary voltage 2.8 kV, sample cone voltage 60 V, desolvation temperature 300 °C, source temperature 100 °C, cone gas flow 50 l/hr and desolvation gas flow 200 l/hr. The cycle time used was 2.1 seconds, with a scan duration of 2 seconds (delay of 0.1 seconds). Calibration and tuning was achieved using sodium formate. This solution was prepared by dissolving formic acid (1 ml) in water (9 ml) to which 10 wt% sodium hydroxide (0.5 ml) was added

to aid ionisation. To this solution a mixture of 2-propanol and water (9/1 vol/vol, 9 ml) was added. The FTICR instrument used was a Bruker BioApexII with a 4.7 Tesla magnet containing an electrospray source (Analytica). Naphthenic acid extracts (20 µl) from Field Y soap were used and these were prepared according to Procedure A (Section 3.1.2). The naphthenic acid extracts were diluted into a methanol/acetonitrile mixture (50/50 vol/vol, 1 ml). Aqueous ammonia solution (10 µl, 35 vol%) was added to the sample to aid deprotonation. The conditions used were: trapping potentials PV1 and PV2 both -1.12 V and detection and excitation mass ranges between 86 to 5000 Daltons. Ions were retained in the hexapole ion trap of the source for 0.6 seconds (D1) prior to excitation, and an extraction pulse length P2 of 4000 µs was used. The sidekick mechanism was employed to detect ions that were off axis as they entered the cell, thus preventing them being redirected out of the path. The values used for EV1, EV2 and DEV2 were 7.94 V, 0.72 V and -1.12 V, respectively, where EV corresponds to the ICR cell extraction plates and DEV2 to the ICR cell delta extraction plate 2. Dipolar excitation was used to excite the ions to a detectable cyclotron orbit prior to detection. The duration of the excitation pulse length (P3) was 12 µs, and RF attenuation for excitation (PL3) was 4.62. The FTICR was calibrated with a solution of sodium iodide (2 µg/µl) in a 2-propanol/water 50/50 vol/vol mixture.

The electrospray source (ES), together with the single quadrupole analyser, was used in more detailed sensitivity studies where the effect of solvents and instrument parameters were investigated on the detection of the naphthenic acid extracts. Solvent sensitivity was examined by using three combinations: toluene, toluene-methanol and toluene-methanol-acetonitrile mixtures (note in all three cases 0.1 wt% aqueous ammonia solution was also added to aid ionisation). The rational behind this was to check for different solvent polarity and viscosity influences on the different naphthenic acid structures. The following operational variables were also examined using toluene only as a solvent: ion spray voltage, nebulizer and curtain gas flow rates.

From the sensitivity studies with the ES and the single quadrupole mass analyser, an optimum set of conditions were selected for the remaining analysis of the field soap samples. A representative aliquot of each sample (0.1 g) was taken and dissolved in a glacial acetic acid/toluene mixture (50/50 vol/vol, 5 ml). The resulting solutions were washed with ultra high quality water (1 ml, HPLC grade). This procedure was necessary to reduce acidity since this affects the ionisation procedure in ES because negative mode operates better in neutral or basic pH. However this procedure also removes some of the more water-soluble components, and therefore the washing procedure constitutes a trade-off. 0.1 wt% ammonia solution was also added to the organic phases prior to injection to

aid ionisation. The internal standard used initially for recovery calculations was benzoic acid (0.08 g/l). To improve sensitivity of particular soap scales, samples were further diluted where appropriate with toluene/2-propanol (50/50 vol/vol). This was important for naphthenic acids present in lower concentrations such as those from Field W. All apparatus were cleaned with toluene/2-propanol 50/50 vol/vol between sampling, until no trace of soap elements was observed in the MS spectra.

3.2.1.2. Statistical treatment of MS data – mapping the naphthenic acid distributions.

The molecular weights of the soap constituents can be obtained from the m/z ratios of the protonated or deprotonated ions generated from either negative or positive modes in MS. In this thesis, the data from the negative mode ES was used to obtain assignments of naphthenic acid constituents in the soap samples. The objective was to match the naphthenic acid species according to the number of carbons atoms and hydrogen deficiency groups. To this end, it was necessary to assume that each m/z value represented a naphthenic acid species which had become deprotonated. Thus the real naphthenic acid molecular weight (corrected m/z) is obtained by adding 1 Dalton to the spectrum data. This procedure does however consider equal ionisation sensitivity for all naphthenic acids in the ES process. Thus the assignments are not quantitative. In certain cases mis-assignment of acids due to fragmentation may occur (Clemente and Fedorak, 2004). In order to tentatively assign the m/z data to true naphthenic acid structures certain criteria has to be met. In this thesis, the standard naphthenic acid formula, $C_nH_{2n+Z}O_2$ (Equation 1.1.), was used to assign m/z values to all mono-carboxylic species below 1220 (i.e. all non-Arn species). This procedure was previously described by Holowenko *et al.* (2002) and Clemente *et al.* (2003). A few hypotheses are considered for this approach as put forward by Clemente and Fedorak (2004), namely:

- if the hydrogen deficiency (Z) is -2, one ring of at least five carbon atoms must be present,
- there must be at least one carbon atom available for a carboxyl group,
- there must be at least one carbon atom available for an alkyl group, and
- structures with more than 3 rings ($Z < -6$) may be fused on more than two sides.

A major limitation of this approach, however, is that it considers all naphthenic acids to be mono-carboxylic species. Baugh *et al.* (2005a) suggested that molecules in the Arn naphthenic acid family contain four carboxylic acid groups and have molecular weights in the region of 1230 Daltons. Thus in this thesis, m/z data between 1220 and 1250 were used

to assign Arn naphthenic acids species, and the empirical formula proposed by Baugh *et al.* (2005b) was used ($C_nH_{2n+Z}O_8$, with n set to 80). In addition, m/z data in the range of 615 to 627 were removed from the statistical calculations as these represent second ionisation species of the Arn acids (Brocart *et al.* 2005). Tables 3.1 and 3.2 present examples of m/z assignments to naphthenic acids using these procedures. Table 3.1 presents information from Clemente and Fedorak (2004). According to this data each calculated naphthenic acid molecular weight would differ by 14 mass units for every carbon number (n, CH_2) and 2 mass units for every hydrogen deficiency value (Z, H_2). According to the proposed formula of Baugh *et al.* (2005a), for a fixed number of carbon atoms (n set to 80) the Arn species would differ only by 2 mass units for every ring (Z) as shown in Table 3.2. However other papers have suggested Arn acids with carbon numbers of up to 82 may occur (Smith *et al.,* 2007). Nevertheless, all Arn species would be included in the m/z range specified earlier, regardless of the number of carbon atoms (i.e. m/z from 1220 to 1250). To simplify the statistical speciation of soap sample species, a carbon number of 80 and a hydrogen deficiency value of -10 were used to represent all Arn naphthenic acids.

				Z			
n	**0**	**-2**	**-4**	**-6**	**-8**	**-10**	**-12**
5	102	x	x	x	x	x	x
6	116	x	x	x	x	x	x
7	130	128	x	x	x	x	x
8	144	142	x	x	x	x	x
9	158	156	x	x	x	x	x
10	172	170	168	x	x	x	x
11	186	184	182	x	x	x	x
12	200	198	196	194	x	x	x
13	214	212	210	208	x	x	x
14	228	226	224	222	220	x	x
15	242	240	238	236	234	x	x

Table 3.1. Mono-carboxylic naphthenic acid molecular weights as a function of n and Z values. Formula used $C_nH_{2n+Z}O_2$. Molecular weights which do not represent naphthenic acids as per the hypothesis of Clemente and Fedorak (2004) are represented by x.

Arn (MW)	**Z**
1230	-18
1232	-16
1234	-14
1236	-12
1238	-10

Table 3.2. Arn naphthenic acid molecular weights (MW) as a function of Z values. Carbon number (n) set to 80. Formula used: $C_nH_{2n+Z}O_8$. (Baugh *et al.,* 2005a)

After naphthenic acid species have been assigned, qualitative statistical information for the soap samples is displayed in 3 dimensional graphs, which allows for good visualisation of the variation of naphthenic acid content (Clemente and Fedorak, 2004). The graphs are constructed by taking the raw mass spectra data, correcting for the loss of 1 Dalton, and matching this molecular weight with that of known mono-carboxylic acids (Table 3.1) or Arn species (Table 3.2). Carbon number and hydrogen deficiencies are then plotted as a function of the normalised percentages for each naphthenic acid species assigned. It was hoped that this qualitative procedure would allow for the fingerprinting of the naphthenic acid content of soaps.

3.2.2. Fourier-Transform infrared spectroscopy.

The spectroscopic analysis of naphthenic acids using IR is a well-documented procedure (Silverstein *et al.,* 2005). Naphthenic acid dimers display a very broad intense hydroxyl (O-H) stretching absorption in the region of 2500 to 3300 cm^{-1}. This is a result of the exceptional strength of the hydrogen bond present. Naphthenic acids also exhibit stretching vibrations due to the carbonyl group (C=O), for which the monomers of naphthenic acids absorb near 1760 cm^{-1}. The C=O group from dimerized acids absorbs in the 1720 to 1760 cm^{-1} region. The bands for C-O stretching and O-H bending appear in the spectra near 1210 to 1320 cm^{-1} and 1395 to 1440 cm^{-1}, respectively. The more intense band near 1280 to 1315 cm^{-1} for dimers appears as a doublet in the spectra of long chain fatty acids. Another feature of dimeric naphthenic acid solutions is the bending of the hydroxyl group at 920 cm^{-1} (Morrison and Boyd, 1979; Silverstein *et al.,* 1991). The application of FTIR to crude oils or emulsions for naphthenic acid identification is problematic due to the large number of interferences and contaminants: water, for instance, can be distinguished through the appearance of particular broad bands near 3450 cm^{-1}. From a practical perspective, if crude oil products have been in contact with plastics, phthalic acids may interfere (Yen *et al.,* 2004). FTIR can be used, under certain circumstances, for the analysis of acids in aqueous solutions (Yen *et al.,* 2004) and sometimes even directly on crude oils (Gorbaty *et al.,* 2000). The main disadvantage of FTIR for the analysis of naphthenic acids is that it cannot distinguish more than one carboxylic acid group per acid molecule. The technique cannot therefore, be used to distinguish mono-carboxylic from bi-carboxylic or other naphthenic acid species.

FTIR spectra were obtained in this thesis using a Perkin Elmer PERX instrument on the naphthenic acid extracts from the field soap samples obtained as per Procedure A (Section 3.1.2). The naphthenic acid extracts were evaporated with nitrogen and placed on a 0.015

mm sodium chloride cell to remove solvents used in preparation (i.e. toluene). Spectra were obtained in the absorbance mode between 500 and 4000 cm^{-1}. The background absorption was subtracted prior to each sample measurement.

3.2.3. Solution nuclear magnetic resonance.

Solution nuclear magnetic resonance (NMR) was chosen to be tested in the protocol developed in this thesis to provide insights into the main chemical groups present in the field soap samples. It was hoped that the technique would aid in the identification of the naphthenic acid groups present. NMR usage in flow assurance studies has been widely reported. The analysis of separated asphaltenes from crude oils for instance has been shown by Dehkissia *et al.,* 2004. Self-diffusion measurements by NMR have also been used to measure asphaltene aggregation and the interactions with naphthenic acids. This technique is known as pulse field gradient NMR (Sjoblom *et al.,* 2003). There are a few studies of NMR applications for the analysis of naphthenic acids from crude oils for example, Tomczyk *et al.,* 2001. For soap analysis, both ^{1}H and ^{13}C NMR have been reported (Brandal, 2005; Lutnaes *et al.,* 2006) for the identification of indigenous components at the same time the work in this thesis was being carried out. Carboxylic acid protons are easily identified with ^{1}H NMR by a narrow range of chemical shifts between 10 and 13.2 ppm. The C=O groups of carboxylic acids and derivatives can be seen with ^{13}C NMR in the range between 150 and 180 ppm. Two dimensional (2D) NMR was reported for the first time by Baugh *et al.* (2005a and 2005b), and this gave insights into the structure of the Arn naphthenic acid family. The main conclusions reached from this work were: no aromatic or alkene functions present in the Arn acids, the carboxylic acid function is primary, no presence of tetra-substituted carbons with the exception of the carbonyl, the carboxylic acid function are carried on a side chain attached to a ring. The basic NMR set-up is illustrated in Figure 3.1. For a detailed description of the technique the reader is referred to Silverstein *et al.* (1991) or Saunders and Hunter (1993). Typically, samples are placed in tubes located inside a powerful magnet that generates a static magnetic field. The nuclei contained in the sample have spins and associated magnetic moments (a reflection of their individual charges). The effect of different hardware changes on sample spins is the major output variable in NMR experiments. In this thesis samples were analysed using ^{1}H and ^{13}C NMR including Distortionless Enhancement by Polarisation Transfer (DEPT).

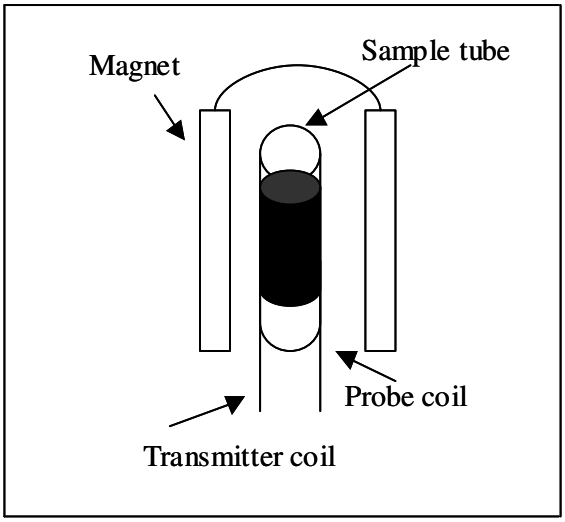

Figure 3.1. Simplified NMR lay-out (Silverstein *et al.,* 1991).

The solution NMR experiments were carried out on a Bruker DPX4000 instrument, and ^{1}H and ^{13}C nuclei were examined. The observing frequencies were 400 and 100 MHz respectively. The magnetic field strength was 9.4 Tesla. DEPT spectra were also acquired for ^{13}C NMR to obtain additional information on the carbon atoms in the naphthenic acids from the soap samples. All spectra were acquired using deuterated chloroform as a solvent and using the relative solvent shifts as reference. Preparation of the naphthenic acid extracts for solution NMR followed Procedure A (Section 3.1.2). In addition, removal of trace water was necessary. This was carried out by placing the naphthenic acid extracts in contact with chloroform (500 ml) and heating in a water bath at 50 °C for 30 minutes. Anhydrous magnesium sulphate (drying agent) was added to make a layer about 1 cm thick across the bottom of the conical flask. The suspension was stirred so that the magnesium sulphate reached the whole solution. Additional magnesium sulphate was added until the solution became clear. The liquid was filtered using a large Buchner funnel and the magnesium sulphate residue on the filter paper was also washed with fresh chloroform. The filtered liquid was then transferred to a flask and taken to evaporation using a rotary evaporator. A minimum amount of chloroform was used to dissolve the sample prior to NMR analysis. Since only qualitative spectra were obtained, no relaxation agent or pulse delays were used in the acquisition. To aid in interpretation, a literature survey of chemical shift information of naphthenic acids was carried out and is included in Chapter 5 for ease of comparison of the results.

3.2.4. Solid state nuclear magnetic resonance.

Solid state NMR is widely applicable to samples with solubility that is too low to be used in solution NMR. In general, the hardware used for solution NMR can be adapted for solid

state studies. The magnetic fields (usually much larger), the applied pulses (usually narrower) are inherent operational parameters required to generate good signal-to-noise ratios in solid state NMR. In the solid state, the chemical shifts can also be used to aid in structure determination, but this must be performed with reservations, since the values depend on both the magnitude and the angle of the applied magnetic field. This is in direct response to the orientation of the solid particles in the magnetic field. This effect is termed chemical shift anisotropy (CSA) and is much larger in solid state than in solution NMR. In addition, in solid samples, the effects of nuclei interactions play a significant role in data acquisition. More abundant ^{1}H nuclei with strong dipole-dipole interactions will dilute the effect of the less abundant ^{13}C nuclei. Static local fields can also be created in each nucleus as a result. The two effects described above can lead to detrimental line broadening effects and poor resolution. The methods used to reduce these effects are magic angle spinning (MAS), cross polarisation (CP) and dipolar decoupling (DD). MAS averages dipolar effects and reduces CSA to zero by setting the spinning of the atoms at a pre-selected angle which is tuned using a calibration standard, and the rotation must be at least the order of the CSA linewidth (~3 kHz). DD is a sequence of phase modulations in which nuclear spin coupling information is removed to increase spectral resolution. However, because of the level of interaction (tens of kHz for a solid state sample compared to 100 to 200 Hz for the same sample in solution), the decoupler power must be set to high levels, and these can be enough to induce residual broadening as a function of CSA only. CP is used to enhance the intensity of NMR signals from higher to lower magnetogyric nuclei. Essentially, the technique uses dipolar coupling (as opposed to spin-spin coupling in solution NMR experiments or direct polarisation DP). The combination of these techniques, or CPMAS, is particularly useful for identifying crystalline materials and zeolites, and to obtain mobility and conformational effects in polymers. Although solid state NMR has been used to identify humic naphthenic acids (Leenheer and Rostad, 2004), no mention of application of this technology to flow assurance studies could be found in the literature. Thus it is performed for the first time on soap deposits in this thesis.

Solid state ^{13}C NMR was performed on the field soap samples *in natura* as a complementary technique to solution NMR since it was not possible to distinguish the carboxylic carbons with the latter technique. The analysis was carried out using a Varian Unity Inova spectrometer and a 5 mm rotor i.d. MAS probe. CPMAS experiments were performed in addition to direct polarisation (DP). The objective was that the CP experiment would preferentially detect the least mobile components, and the DP experiment would detect preferentially the most mobile component. All spectral referencing are in respect to

tetramethylsilane. Additional dipolar decoupling (DD) experiments were also conducted to check for quaternary carbons. Because of the large amount of water present in sample from Field W the best spectrum for this deposit was obtained using slow-spinning direct polarisation (DP).

3.3. Thermal behaviour of soaps.

Thermal analysis comprises a range of techniques which are used to analyse enthalpies for changes in physical state (e.g. melting), transitions between crystalline forms (e.g. liquid crystals) or to accompany chemical reactions induced by temperature variations. This is achieved by heating both the sample and an inert reference material under controlled conditions. Thermal analysis has not been widely used for analysis of flow assurance deposits, but there are reports of the study of wax and hydrates deposition using these techniques (Pope and Judd, 1980). Thermal analysis is also used for the determination of wax appearance temperatures in distillate fuels as in the IP389 method (Riazi, 2005). Gallup *et al.* (2005) used differential scanning calorimetry (DSC) to study mixed wax and soap deposits. They found it possible to identify the occurrence of microcrystalline paraffin structures within these mixed deposits and treat the wax deposition problem accordingly. Huang (2006) used thermal analysis of asphaltene fractions deposited from a crude oil and was able to correlate asphaltene decomposition with boiling point cuts. The key advantage in applying thermal analysis to the study of soaps is to aid in the correlation of important bulk properties with specific soap components. Until this thesis, this information was not available in the open literature. Ushikusa (1990) used thermal gravimetric analysis (TGA) to study the behaviour of metal salts of fatty acids. Calcium, copper, cadmium and barium soaps of acids having carbon numbers between sixteen and eighteen were used. From initiation to 25 wt% loss, changes were shown to be the result of the degradation of the carboxylic group, either through the formation of CO_2 or ketones. At higher temperatures the authors suggested that polymerisation of the naphthenic acids was taking place. Two of the techniques which have widespread applications in thermal analysis are differential thermal analysis (DTA) and DSC. The main difference between these methods is that in DSC both sample and reference have individual heaters, and in DTA a single heater is shared. Figure 3.2 presents a typical simplified DSC layout. R_O represents the thermal resistance between pan and holder and R_S represents the thermal resistance between sample and pan. These must be minimised through design and are such that they are unaffected by changes in the sample. For more information the reader is referred to the work of McNaughton and Mortimer (1975).

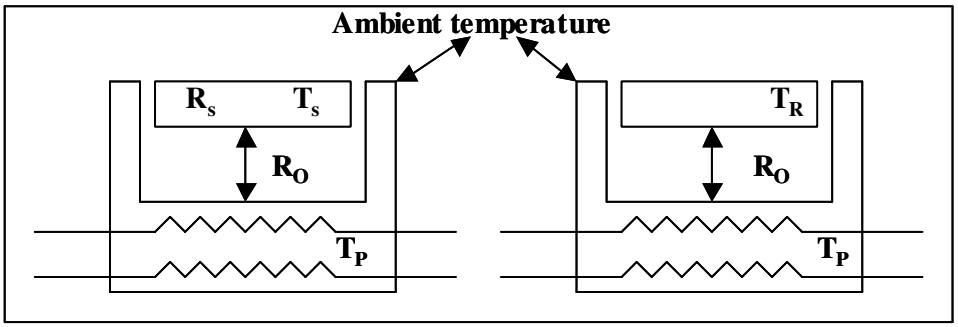

Figure 3.2. Typical DSC layout (McNaughton and Mortimer, 1975). T_s and T_R represent the sample and reference material temperatures, T_P the temperature of the pan. R_O represents the thermal resistance between pan and holder and R_S represents the thermal resistance between sample and pan.

The holder material, geometry, flushing gas as well as the contact surface between the holder and sample packing affect DSC operation (McNaughton and Mortimer, 1975). Thus holders with thin disks or films are preferred. The holder pans can be used with or without sealing. Sealing is necessary if specific heat capacities are to be calculated. Sample weights should be chosen so that they each absorb the same amount of heat on fusion. For DSC generally the smaller the sample size the better, provided the bottom of the pan is fully covered (to prevent loss of material since it is very common to use samples in the mg weight range). Careful attention should also be paid towards choosing an appropriate scanning heating rate. This is a function of the equipment available, but is usually a compromise between resolution and the time taken to acquire data. It can however affect the diffusion of volatile products to the surface of the sample being analysed. Calibration is usually performed using high purity metals (99.5 wt%) as standards with known enthalpies of fusion. Two common examples are indium and platinum (melting points 156.6 °C/1768.3 °C and enthalpy of fusion 28.5 Jg^{-1}/256.4 Jg^{-1}) (Pope and Jude, 1980; Cotton and Wilkinson, 1988). A calibration constant is obtained by heating a pre-weighed sample of the standard, measuring the area given by the thermogram and dividing this by the known enthalpy change. The sample atmosphere (type of gas and the use of static or dynamic measurements) is also a very important parameter in DSC analysis. The use of either nitrogen or oxygen gas leads to differences in acquired thermogram of up to 35 % (Pope and Jude, 1980). An atmosphere of flowing inert gases is preferred, since these remove decomposition products which could otherwise retard reactions in the samples. Current hardware design for DSC apparatus ensures that the temperatures applied to the sample and to the reference are maintained equal. Thus the heat input to the sample and reference with time (dH/dt) can be acquired accurately. Modern DSC instruments provide good

calorimetric response over temperatures up to 600 °C with accuracies within 0.2 °C. Temperature corrections arise if the calorimeter has been calibrated with a certain standard and the samples melt at significantly different values. Other sources of error lie in the temperature lag between the sample pan and the holder. The interpretation of DSC thermograms is made even more complex by the presence of multicomponent samples. DSC and TGA have been used in this thesis to obtain information on soap sample thermal stability, initially with a soap deposit sample from Field Y. Data is qualitative only since the relative influence of particular soap components is not known. This was in part minimised by using DSC/TGA of a clean calcium soap, as well as the separated indigenous acids from this sample as templates (obtained as per Procedure B Section 3.2.1). Because of sample heterogeneity, special attention was paid to the presence of impurities such as crude oil and water on the thermogram to avoid false interpretations. Thus, the DSC thermograms of the parent soap-forming crude oil from Field Y were also analysed. A DSC2920 (TA Instruments Ltd) was used to measure the calorimetric characteristics of the sample as a function of increasing temperature. A heating rate of 10 °C min^{-1} was used and a nitrogen-purged atmosphere was applied, over the temperature range from ambient to 300 °C. Samples were placed in open aluminium pans of 6.0 mm diameter, with side walls 1 mm in height. Samples were placed as close to the surface of the pan as possible and then tapped gently. For the TGA analysis, the TGA2950 (TA Instruments Ltd) was used to measure the weight loss of the sample as a function of increasing temperature. A heating rate of 10 °C min^{-1} under a nitrogen-purged atmosphere was applied, over the temperature range from ambient to 1000 °C. This higher temperature was chosen due to the inherent stability of many of the soap samples observed during preliminary TGA tests carried out up to 400 °C. Samples were placed in open platinum pans of 9.5 mm diameter, with side walls 1 mm in height. For both DSC and TGA, temperature corrections were carried out using indium standards (which are software implemented). Mass calibration for the TGA was carried out using Mettler and Toledo standards.

3.4. Elemental composition.

The objective of using elemental composition techniques was to gain information about the distribution of the soap sample components from an atomic perspective. There are a number of techniques which can be used for this purpose. Certain techniques probe the inner electronic structure of atoms, for example X-ray fluorescence (XRF), energy dispersive X-ray (EDAX), X-ray photoelectron spectroscopy and Auger electron

spectroscopy. Other techniques probe the mass of atoms generated during measurements, such as inductively coupled plasma mass spectrometry. Moreover, the outer electronic structure of atoms can also be investigated using flame atomic absorption, inductively coupled plasma atomic emission spectroscopy. An excellent review of most of these techniques is presented by Adamson and Gast (1997). The elemental composition study of inorganic scale deposits has traditionally relied on EDAX and XRF. Organic deposit analysis (i.e. asphaltenes) has relied on combustion type bulk elemental analysis for a qualitative indication of aromatic/aliphatic ratios in each sample. In this thesis, a sensitivity study was carried out using two soap samples from Fields Y and W, and three techniques for a qualitative elemental composition: XRF, EDAX (with environmental scanning electronic microscopy, ESEM) and elemental analysis.

3.4.1. Elemental analysis.

Elemental analysis is an important measurement in oilfield chemistry used to indicate the overall character of crude oil and petroleum stocks and to predict the hydrogen requirement to convert heteroatoms to their hydrogen analogues (Dehkissia *et al.,* 2004). There are many variants of this analysis, but they usually comprise the burning of the sample in a controlled environment and the analysis of the produced gas. The sample is typically wrapped in a tin capsule and inserted into a furnace where a steady stream of an unreactive gas (e.g. helium) is passed through. Oxygen gas is added as the sample capsule is inserted into the oven. The furnace may contain a catalyst that facilitates combustion. Copper turnings may also be added to ensure that any nitrogenous components in the sample are reduced to nitrogen gas. The technique is highly dependent on the weight of the sample used. Any elements which are not carbon, hydrogen, nitrogen or oxygen will not be identified using the technique. This method is applied in the correlation of asphaltene fractions and their parent crude oils done through comparison of atomic ratios such as hydrogen/carbon, nitrogen/carbon for instance (Acevedo *et al.,* 1992; Anchyeta *et al.,* 2002). It is common to use elemental analysis information to obtain the double bond equivalent (DBE) using Equation 3.1.

$$\mathbf{DBE} = (1 - \frac{\mathbf{H/C}}{\mathbf{2}})\mathbf{100} - \mathbf{1}$$

Equation 3.1.

where H/C is the hydrogen/carbon atomic ratio. Elemental analysis has been used by a number of authors to study naphthenic acids Average percentage values for carbon, hydrogen and nitrogen compositions for naphthenic acids separated from crude oils are: 80 %, 12 % and 0.3 %, with hydrogen/carbon (H/C) ratios of 1.7 (Acevedo *et al.,* 1992; Saab *et al.,* 2005). DBE for acids have also been reported between 8 and 13 (Tomczyk *et al.,* 2001; Saab *et al.,* 2005). Asphaltenes on the other hand, have been credited with much lower H/C ratios, such as 0.5 (due to their higher aromaticity) and oxygen levels from 0.3 to 10.3 %, sulphur from 0.3 to 4.9 % and nitrogen from 0.6 to 3.3 % (Speight, 2004).

Determination of carbon, hydrogen and nitrogen in this thesis was carried out using a Leco CHN932 analyser. The method used was a modified version of the ASTM D5291 (Riazi, 2005). The sample was burned at a temperature of 1000 ^{o}C in flowing oxygen. The carbon dioxide, water and nitrogenous oxide combustion gases (NO_x) are passed through a reduction tube with helium as the carrier gas. This converts the NO_x into nitrogen. The carbon dioxide and water are measured by selective IR detectors. After the absorption of these gases, the content of the remaining nitrogen is determined by thermal conductivity detection. For oxygen, a separate sample is decomposed in a pyrolysis furnace at 1300 ^{o}C because it is the combustion gas used in the technique itself. Oxygen was not therefore measured in this technique. Calibration of the instrument was made using high purity acetanilide standards of known compositions.

3.4.2. X-ray fluorescence.

X-rays are electromagnetic radiation with a wavelength of 0.003 to 3 nm with energy between 0.5 and 500 keV. The photoelectric effect is the name given to the absorption of a primary X-ray by an atom. During this process, inner-shell electrons are ejected which results in the atom becoming unstable. To return to a stable condition, there is a transfer of electrons between the atom's outer and inner shells. This process gives off a characteristic secondary (fluorescent) X-ray which is proportional to the difference between the two binding energies of the corresponding shells. Energy levels are an exact function of each element. Sometimes, as the atom returns to its stable condition, instead of emitting a characteristic X-ray, it transfers the excitation energy directly to one of the outer electrons, causing it to be ejected from the atom. The ejected electron is called an Auger electron. This process competes with X-ray emission. Auger electrons are more likely to occur in elements with atomic numbers larger than 10. Detection limits are a function of the element to be analysed and can be as low as 0.1 ppm (Fitton, 2000). The use of these phenomena to help identify unknown materials is called X-ray fluorescence spectroscopy (XRF). The

technique is widely applied for the characterisation of both solids and liquids. Some of the inherent advantages of this technique are that it is reasonably fast and in most cases, non-destructive. The XRF hardware set-up usually consists of a source (radioactive or X-ray tube) and a detector. Because X-rays are absorbed by air, it is usual for the XRF spectrometer chamber to be evacuated using a rotary pump. Two approaches can be used for calibration using either empirical or fundamental parameters. The empirical approach is based on standards with known elemental compositions. Yet the standards must be representative of the matrix, as well as the elemental concentration ranges of the sample. In the fundamental parameters approach, mathematical algorithms that describe the physics of the detector response to pure elements are used for sample identification. Thus, the typical concentration of the sample must be known and a single standard used to optimise the in-built model (Lachance and Claisse, 1995). Sample preparation for XRF analysis varies considerably, but is mostly a function of the type of instrument used and the method of analysis (intrusive, *in situ*, etc). It is common for solid samples to be polished, in order for surface homogeneity to be achieved. Powders are normally pressed into pellets in the laboratory using transparent supporting materials such as polyethylene, for instance.

In this thesis, the sample preparation techniques for XRF were similar to those described by Fitton *et al.* (1998), with modifications noted by Fitton and Godard (2004). Major element concentrations were measured on fused glass discs prepared by a method similar to that of Norrish and Hutton (1969). Element data is therefore presented on an organic-free basis and is corrected to the total sample basis using the mass loss on ignition (LOI). The soap samples were dried at 110 °C for at least two hours after which 1 g was ignited at 400 °C to determine LOI. The residue was then mixed with a lithium borate flux containing La_2O_3 as a heavy absorber, by a method similar to that developed by Norrish and Hutton (1969). The borate flux consisted of a commercial Johnson Matthey Spectroflux 105 mixture. This was added using a sample/flux ratio of 1/5 based on the LOI. The mixture was fused in a muffle furnace for twenty minutes at 1100 °C in a special crucible. After the initial fusion, the crucible was reweighed and any weight loss was made up with extra flux. Mass loss in fusion can be ascribed to volatiles such as water and carbon dioxide. A second sample fusion was then carried out over a Meker burner. During these procedures the molten mixture was swirled several times to ensure homogeneity, cast onto a graphite mold, and flattened with an aluminium plunger into a thin disk. The mould and plunger were maintained at a temperature of 220 °C on a hotplate. Trace element concentrations were determined on pressed-powder samples. Samples were made by compressing the fused samples to make a 40 mm diameter sample pellet. The binding agent consisting of a 2 wt%

aqueous solution of polyvinyl alcohol. The fused and pressed samples were analysed using a Philips PW 2404 automatic X-ray fluorescence spectrometer with a rhodium anode X-ray tube. The spectrometer was calibrated with reference standards, using the values given by Jochum *et al.* (1990) and Govindaraju (1994).

3.4.3. Energy dispersive X-ray and environmental scanning electron microscopy.

Scanning electron microscopy (SEM) has long played a central role in structural characterisation for flow assurance samples. When a sample is examined with an electron beam, three signal types can be created: secondary electrons, backscattered electrons and X-rays. Secondary electrons are sample electrons ejected after interaction with the primary electrons of the beam. These have low energy (less than 50 eV), and thus escape from shallow areas within the sample, resulting in the best imaging resolution. Back-scattered electrons (BSE) are primary beam electrons which have left the sample due to static collisions. They have energies from 50 eV up to the accelerating voltage of the beam. Because of their higher energy, they have higher specific volumes of interaction, thus lower resolution. SEM works by bombarding the surface of a material with a beam of electrons and detecting both secondary electrons or BSE's since X-rays provide poor spatial resolution compared to these types. A virtual image is constructed from the signals emitted by the sample and the resolution of SEM instruments is the measure of the smallest feature observable by the apparatus specified by Å or nm ranges. This is typically set by the size of the spot formed by the beam on the sample surface. In SEM, magnifications are decoupled from depth of field and are determined by the size of the beam scan. This is the main advantage over conventional transmission light microscopy.

Because of the need for high vacuum and extensive sample preparation with SEM, the environmental scanning electron microscopy (ESEM) mode of operation is often preferred in solid characterisation studies. High vacuums are a requirement for correct beam focusing to avoid the effects of ignitable gases due to the high voltages employed. Thus, only samples that are vacuum tolerant and conductive may be used in SEM. In ESEM no prior specimen preparation is required and even wet samples can be analysed. Multiple pressure limiting apparatus separate the sample chamber from the beam column. The column remains at high pressure, while the chamber sustains pressures of at least 4.6 Torr (Philips, 1996). Gas flow controls the pressure in the chamber and this is usually comprised of an inert species. Gas ionisation in the sample chamber eliminates the charging effects typically seen with non-conductive samples and this is used to amplify the secondary electron signal which is measured in the ESEM detector (Philips, 1996). Sample coating is often required

in ESEM to aid in conductivity/contrast and to avoid destabilising sensitive samples. However, one disadvantage of a coating, whilst enhancing the surface detail of the sample is the masking of internal structures (Philips, 1996). Most ESEM apparatus have in-built EDAX capabilities to make use of the energy produced as a result of the incidence of the primary electron beam. The EDAX detectors measure the quantity of emitted X-rays as a function of energy, which is characteristic of the element from which it is emitted. But EDAX provides only an elemental composition of the exact surface spot of the sample being analysed. Thus it becomes important to perform a surface scan of the sample under scrutiny. However, one of the advantages over XRF or elemental analysis is that EDAX can focus on different sample areas and help identify multiple contaminants. One of the most undesired effects during an EDAX analysis is the interference of skirt X-rays. These are produced from electrons scattered by gas molecules. The effect can be minimised by correct adjustments of the distance and angle between the X-ray detector and the sample. Elements with atomic numbers from that of beryllium to uranium can be detected due to low X-ray intensity. The minimum detection limits vary from about 0.1 wt% to a few percent depending on the element and matrix.

ESEM/EDAX was performed using an XLM Philips model in this thesis, operated with nitrogen. The objective was to obtain both soap morphology and elemental composition information. Copper and aluminium standards were used to verify the correct EDAX instrument operations. Gold coating was used initially, but discontinued owing to reasonable sample stability under vacuum and to avoid any interference from the potential absorption of gold. The beam energy was 20 keV. Three different measurements were carried out on each sample, thus atomic and weight percentages represent the average of these values. An EDAX spectrum of the stub holder used to place the samples in the gas chamber was also acquired to determine background interference.

3.5. Diffraction behaviour of soaps.

In X-ray tubes radiation is produced when a focused electron beam is directed at a stationary solid target within a high voltage field. This collision results in the ejection of inner shell electrons from the atom of the solid target. In the event of a free electron fitting the inner shell an X-ray of energy characteristic of the solid material is emitted and is measured by XRF (Section 3.4.2). Some photons from the incident beam are deflected after the collision with the electrons. The type of collision where no energy loss occurs is known as Thomson Scattering and the reflected X-rays can interfere constructively to produce a diffraction beam. Because the wavelength of the reflected radiation is of the same

magnitude of the size of atoms (in the Angstroms range), standard X-ray diffraction (XRD) can then be used to study atoms that are arranged in lattice planes. Crystalline material, in particular, will show as sharp peaks. Thus XRD is very suitable for fingerprinting unknown solid samples with crystalline content. The condition for a diffraction peak to occur is described by Bragg´s law:

$$2.d\sin\theta = n\lambda$$

Equation 3.2.

where d is the interplanar distance (also known as d-spacing), θ is the scattering angle and n is the integer representing the order of the diffraction peak. This equation is the basis for all diffraction pattern interpretation (Warren, 1969).

Powder X-ray diffraction in the reflection mode was applied to the study of field soaps in this thesis. Data was acquired using a type F Siemens diffractometer (NaI scintillation counter). The X-ray source was copper K_α and it was run at 40 keV and 30 mA power. Samples were packed in special glass capillary tubes 0.7 mm i.d. and 80 mm length supplied by Capillary Tube Supplies Ltd. Steps were in increments of 0.005 ° and counts were collected at 0.25 seconds for each step. Viscous soap samples which could not be packed were rolled onto the capillary tube. The software used to convert the frequency of the acquired spectra into the time domain was Siemens Diffrac AT.

3.6. Surface properties of soap components.

As shown in Chapter 2, surface properties of naphthenic acids can be measured using a variety of methods including interfacial tension measurements, force area curves with Langmuir films, interfacial viscosity and electrical measurements, to name a few (Langmuir and Schaefer, 1937). Measurement of surface properties in soap-forming systems is justified since it is agreed that deposition of certain soap types occurs primarily at the oil-water interface. At the start of this thesis, there had been no previous attempts to measure the surface properties of the acids found in soap deposits. However, some interesting work has been performed on model naphthenic acid solutions and acids extracted from crude oil systems (Havre, 2002; Brandal *et al.,* 2004). Langmuir films offer many opportunities for the study of the interactions at the oil-water interface. In this thesis a simpler technique for interfacial tension measurements was selected for studying naphthenic acid extracts with selected brine systems. Interfacial tension (IFT) can be understood as the physical quantity associated with the deformation of fluid interfaces. The adsorption of the surface-active species (i.e. naphthenic acids) at the oil-water interface can be described by the Gibbs

equation (Equation 2.8). Because the Gibbs equation is formulated on a thermodynamic basis, it does not take into account the time required for the molecules to diffuse and adsorb at the interface (Kanicky *et al.,* 2001). Thus static and dynamic values might be different if the time required to attain equilibrium between the two phases being measured is not taken into account. Equilibration time can vary from a few minutes to up to an hour or more. It is agreed that higher molecular weight naphthenic acids will have slower kinetics. However equilibration times will be shorter at higher pH values (Spildo and Hoiland, 1999), and thus this needs to be taken into consideration prior to planning experiments. An important insight from the work of Brandal *et al.* (2004) was that after an elapsed time of ten minutes, dynamic surface tension experiments for model naphthenic acid systems had reached equilibrium. If more than one surface-active component is present the variation in surface tension as represented by the Gibbs equation becomes complicated because the correct amounts of surfactants preferentially adsorbed cannot be determined (Langmuir and Schaefer, 1937). The Gibbs equation in this case needs to be formulated using chemical potentials and the modelling required to describe the system can become very complex (Somasundaran *et al.,* 1984).

There are many techniques for the measurement of IFT. Under certain circumstances these have been shown to give different results. Beneventi *et al.* (2001b) used an image analysis tensiometer and a Du Nouy ring for static and dynamic ST measurements in foams containing fatty acid soaps. Their results show that the longer the hydrophobic chain of the soap, the larger the differences between the results for these two ST techniques. This was attributed to different absorption kinetics. Standal *et al.* (1999) used the Du Nouy ring and the Wilhelmy plate to investigate the partition coefficient of selected polar components. They found that the exact cation types and concentrations had a direct effect on the polar component bulk and surface properties. The authors suggested that the stable IFT curve for the naphthenic acid could be due to the complexation between calcium cations and acid anions resulting in a monovalent complex in the alkaline range which would concentrate in the bulk phase rather than at the interface.

In this thesis, IFT experiments were carried out to investigate the effect of pH and salinity on the surface properties of naphthenic acid extracts from soaps dissolved in toluene, obtained according to Procedure A (Section 3.1.2). The Du Nouy ring with a platinum ring of the KSV Sigma 70 tensiometer was used. The water phases comprised pH adjusted brines and the contact times used were twelve minutes. All brines were prepared with deionised water, which was further purified with a Millipore Milli-Q plus 185 system. Preliminary tests were used to show that after this time interval the system was close to

equilibrium. The Du Nouy ring was cleaned with detergent and water, followed by treatment with a flame from a Bunsen burner between each measurement. Repeated water-air ST measurements were carried out with the cleaned ring until a value of 72.8 mN/m at 20 °C was recorded. The resolution for the IFT measurements can be considered to be 0.1 μN/m, as indicated by the equipment manufacturer (KSV, 2004). Brine temperatures and densities were measured at the start of the experiments. Variations in temperature were corrected using software implemented algorithms for density variation. All brine temperatures were measured with mercury thermometers prior to phase equilibration. Brine densities were measured using an Anton Paar DMA 4500 apparatus.

3.7. Special analysis of Field U and Field T deposits.

It was also necessary to carry out special analysis on selected field deposits from Field U and Field T. These deposits were not soaps but consisted of asphaltenes (Field T) and chemically treated resin-type deposits (Field U). The samples were studied using a SARA type separation procedure (Aske *et al.,* 2001; Speight, 2004). The objective was to obtain the relative distributions of saturates, aromatics, resins and asphaltenes. SARA separations are usually applied to crude oil samples not deposits. However, the use of the SARA separation in this thesis was aimed at fingerprinting differences between soaps and asphaltene samples. The SARA method used was the technique developed by the Norwegian Petroleum Directorate and published by Weiss *et al.* (2000). Additional whole oil gas chromatography (GC) was carried out on the maltene (saturate, aromatic and resin fractions) for each deposit to check for biodegradation fingerprints. GC is a well-established technique in geochemistry for the study hydrocarbon fractions (Peters and Moldowan, 1993). GC uses a stationary phase consisting of a column and a mobile phase (an inert gas) which are used in combination for compound separation. On injection, samples are vaporised into the carrier gas. Large molecules are retained at the head of the GC column in a process known as cold trapping. As the temperature of the column is raised, molecules are released and begin to elute as a direct function of their volatility. The GC column is usually coated with a non-volatile liquid and the release of compounds from the column is related to the interactions between the analytes and the stationary phase (including the coating) and the mobile phase. In this thesis GC was carried out on the n-pentane soluble fraction of the deposits from Field U and Field T. The equipment used consisted of a HP5890 with a FID detector. The column used was a DB1 phase 0.25 μm film 30 m by 0.25 mm, with helium as the carrier gas at a constant pressure of 15 psi and flow rate of 1.5 ml/min. Split Injection was used with 0.2 μl, 1/100 split. Injector and

detector temperatures were 320 and 350 °C respectively. The temperature programming range 50 to 320 °C at 10 °C/min was used with a final hold of 20 minutes. TOF-MS analysis was also conducted on both the maltene and the asphaltene fractions separated for each deposit above to verify the presence of naphthenic acid species and to establish favoured detection of these species in one of the solubility fractions. The conditions for TOF-MS analysis follow those described in Section 3.2.1.1. To help identify the asphaltene deposition tendencies for Field U, the parent crude oil from this field was also analysed using the basic methodology described in ASTM D3279 (Riazi, 2005), where the mass percentage of asphaltenes in a crude oil sample is defined as the total insoluble fraction in n-heptane solvent. The results of the ASTM D3279 method are not fully accurate indications of the asphaltene precipitation tendencies of a crude oil sample. This is because only a small fraction of the asphaltenes in a crude oil is responsible for flow assurance precipitation problems (Mullins *et al.,* 2007). Nevertheless, the method provides a preliminary assessment of asphaltene precipitation tendencies for hydrocarbons. The use of the techniques described above was very important in studying those samples identified not to fall in the soap category (i.e. soap scale or soap emulsion). The results also provided information to interpret the soap precipitation mechanism and this will be further discussed in Chapter 4.

CHAPTER 4 – CHARACTERISATION OF FIELD DEPOSIT SAMPLES: RESULTS.

Abstract

In this chapter the main results from the study and analysis of field deposit samples are presented. The techniques have been described in Chapter 3. The main contribution of this chapter to the overall thesis is an optimised analytical protocol for the study of soap samples under the same set of conditions. This is summarized at the end of the chapter and is termed Full Analysis of Soap Types (FAST). The data refers to deposits from Field X (North Sea), Field Y (West Africa), Field Z (North Sea), Field W (South East Asia), Field T (North Sea) and Field U (North Sea). The use of the protocol enabled the fingerprinting of the two end-member soap types: calcium naphthenate soap scales and sodium carboxylate soap emulsions. Moreover, chemically treated soaps and asphaltenes were also clearly identified by additional techniques selected.

4.1. Chemical composition.

The different techniques evaluated to gain insights into the chemical compositions of the field deposit samples are now discussed. For this purpose, the naphthenic acid extracts from each deposit were separated, according to Procedures A reported in Section 3.1.2, unless stated otherwise. Mass spectrometry, Fourier-Transform infrared spectroscopy and solid state nuclear magnetic resonance were used.

4.1.1. Mass spectrometry.

4.1.1.1. Ionisation source and analyser sensitivity study.

The EI mass spectrometry ionisation source was used in combination with pyrolysis and high-resolution gas chromatography (GC). The sample from Field Y was used *in natura.* To aid interpretation, a commercial Acros naphthenic acid mixture was also analysed. Further information on the composition and properties of this sample may be obtained from Hao *et al.* (2005) and Acros (2006). Figure 4.1 presents the chromatogram for this sample. It can be observed that the commercial naphthenic acid mixture resulted in a complex pyrogram, possibly due to the large number of components, eluting mostly between 11 and 30 minutes.

Pyrolysis for the field deposit was conducted at 850 °C, in response to thermal analysis studies. This high temperature programming significantly improved the detection of GC peaks in the field soap sample pyrograms. Figure 4.2 presents an example of the pyrolysis results for the field deposit.

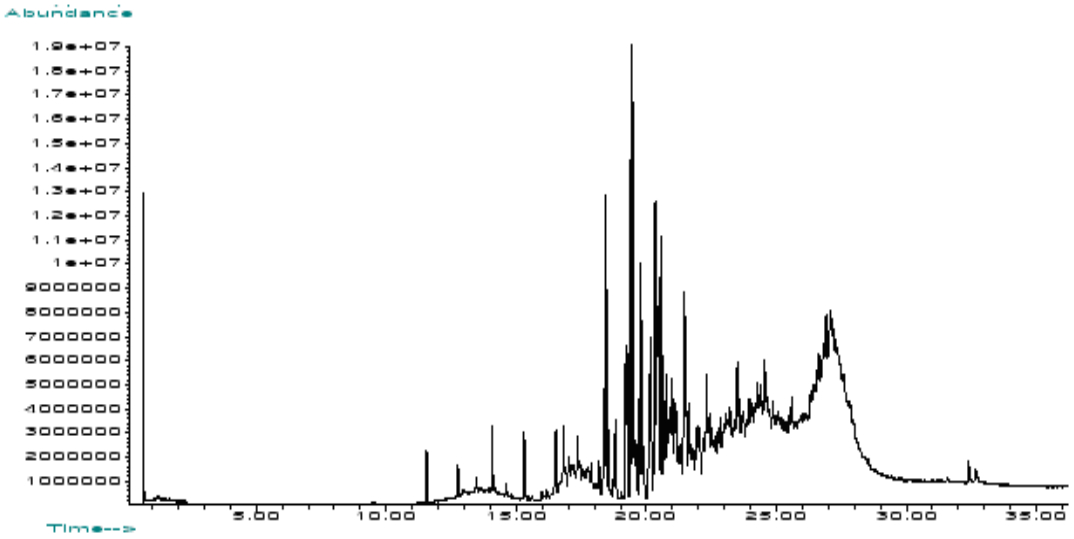

Figure 4.1. Pyrogram GC of commercial Acros naphthenic acid mixture at 650 °C.

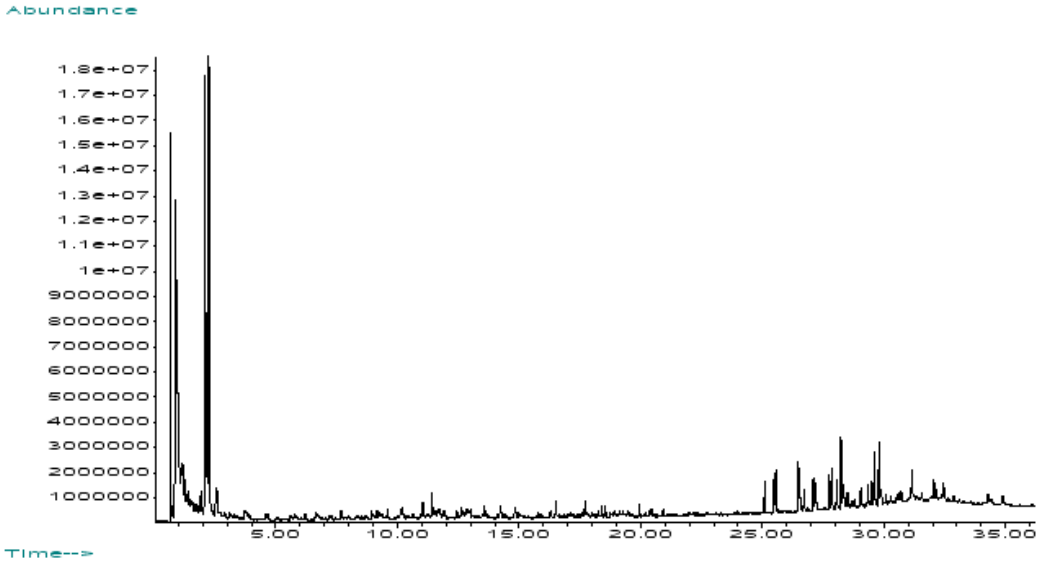

Figure 4.2. Pyrogram GC of deposit sample from Field Y at 850 °C.

A number of ions were extracted using MS equipment for interpretation of the Field Y soap deposit data. The following ions were used: 74, 88 and 101 Daltons. These ions were some of the most common components detected in the commercial Acros naphthenic acid mixture. These ions were also used in the work of Baugh *et al.* (2005a). The authors reported that fragments at 74 and 101 Daltons and lack of fragments at 88 Daltons would indicate the presence of derivatized Arn in a naphthenic acid extract from a field soap.

Very poor signals were obtained in the MS results in this thesis, particularly for the 88 and 101 Dalton ion overlays when compared to the commercial naphthenic acid. However, some peak matches were obtained for the 74 Dalton overlay. These results are presented in Figure 4.3.

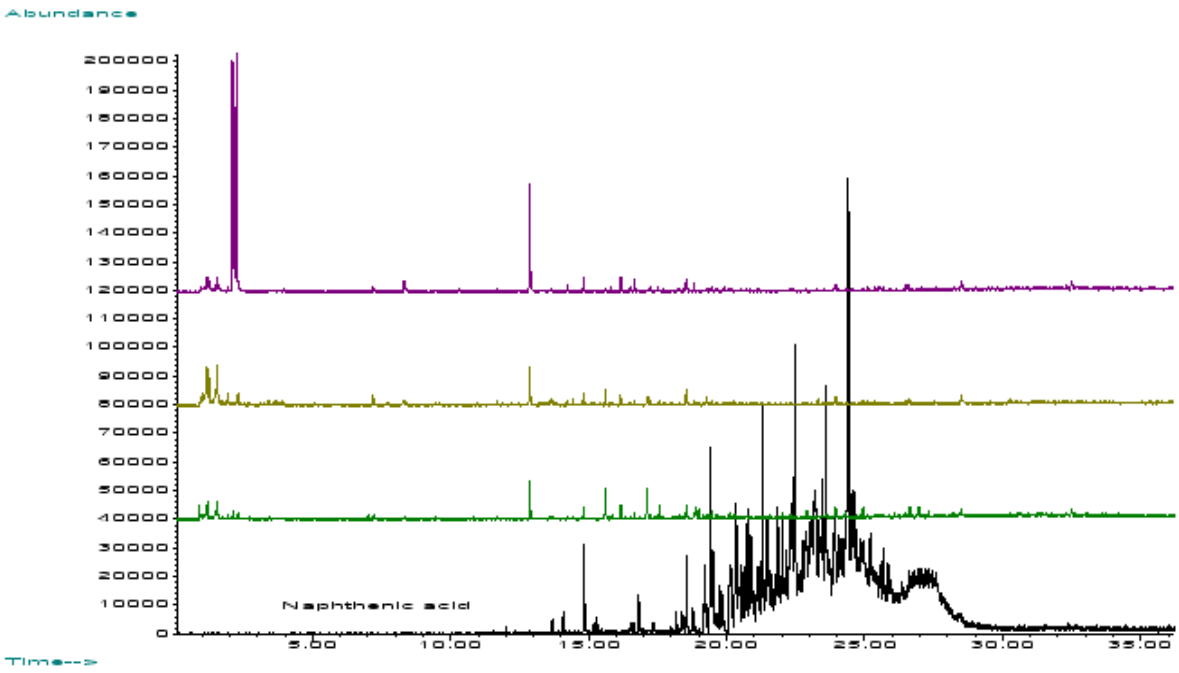

Figure 4.3. Pyrolysis GCMS at 850 °C of samples from Field Y (note each coloured chromatogram represents a sub-sample from the Field Y soap deposit) and commercial naphthenic acid standard (black chromatogram). Overlay of ion 74 Daltons.

The use of a commercial Acros naphthenic acid for fingerprinting did not allow any detailed conclusions to be made in regards the particular acid structures present in the field sample. This is probably due to the different naphthenic acid species present in the commercial mixture as well as the soap deposit. Because of the poor sensitivity of the above procedure, it was decided to carry out a test on the naphthenic acid extract from Field Y soap sample diluted in a mixture of toluene and n-o-bis-tri-methylsilyl acetamide. This derivatization agent was chosen to allow for better observation of silyl esters, which are preferably ionised, as opposed to the non-derivatized naphthenic acids structures. No pyrolysis was used for this experiment. The EI source was used with the same GCMS set-up as described in Section 3.2.1.1. The ion having 74 Daltons was extracted since it was common to all components detected in the derivatized commercial naphthenic acid mixture. An overlay of this data is presented in Figure 4.4. The peaks at retention times 7.9, 8.37, 8,5 and 11 minutes are observed in all tests with the naphthenic acid extracts from Field Y. These coincide with some peaks in the commercial naphthenic acid. Yet, many other peaks present in the commercial naphthenic acid are not observed in the field sample. Thus, despite better sensitivity obtained by the use of the silyl derivatization agent, it would appear that the field soap sample contains different groups of acid families compared to the

commercial naphthenic acid. Since the precise derivatization yield for each acid species is not known, it is very difficult to ascertain the predominant parent acid structures in the field soap deposit sample after derivatization. This is because derivatization is also a function of molecular structure. Although the composition of the commercial naphthenic acid is known (it was analysed with electrospray mass spectrometry, results presented later), the overall yields for derivatization are not. This makes a true comparison with the field soap sample difficult. Moreover, it is likely that the low energy of the EI source is unable to ionise high molecular weight acids efficiently. Given the poor resolution of the GCMS system, the decision was taken to focus on more selective ionisation sources for the analysis of the naphthenic acids in the field deposit.

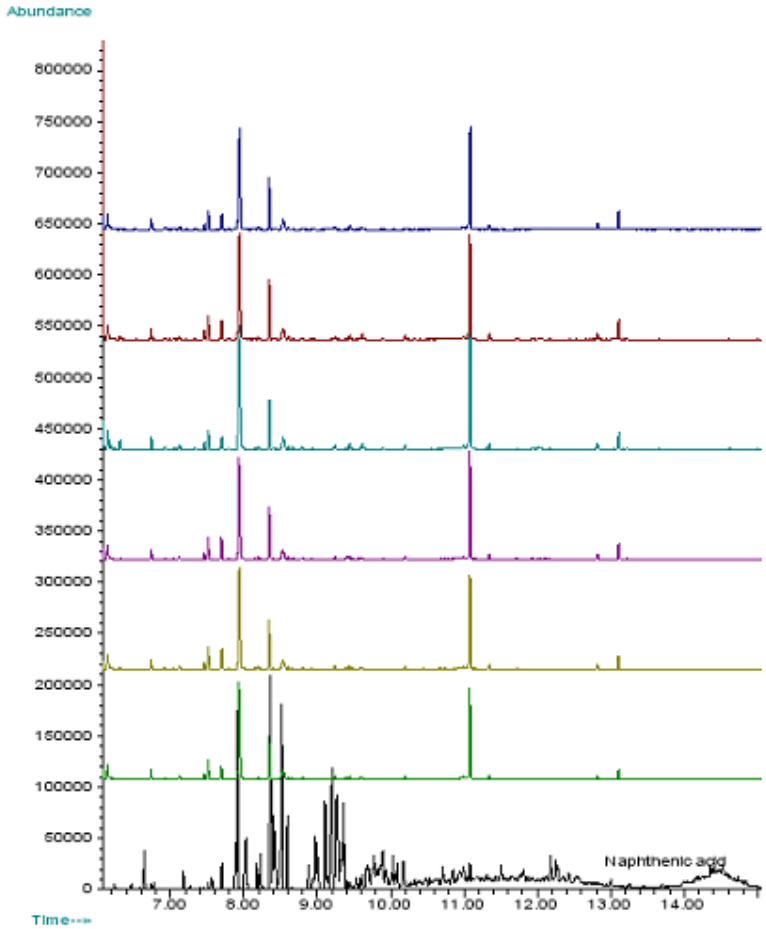

Figure 4.4. GCMS of silyl derivatized naphthenic acids from Field Y (note each coloured chromatogram represents a sub-sample from Field Y soap deposit) and derivatized commercial naphthenic acid standard (black chromatogram). Overlay of ion 74 Daltons.

The CI source was tested with the naphthenic acid extract from Field Y using isobutane and ammonia as the carrier gases. When isobutane was used, the spectrum showed very poor signal-to-noise ratio, probably due to fragmentation caused by the carrier gas. An attempt was made to correct this with little success. When ammonia was used there was less

fragmentation, and there appeared to be a broad Gaussian distribution of acids, including higher molecular weight species, but no Arn (m/z ~1230) naphthenic acids were detected. It has been reported that CI sources have poor ionisation yields for higher molecular weight naphthenic acids (Dzidic *et al.,* 1988). The results in this thesis confirm this observation and also show that the source does not favour the detection of Arn acids from soap samples. Thus the use of the CI source was discontinued in this thesis.

When the MALDI source was used, despite the low sample flow rates, the spectrum showed preferential ionisation of particular m/z species. There were repeating bundles of peaks starting at m/z 800 and going up to 1700. The presence of higher molecular weight species in this sample is most likely a consequence of multimerization of the naphthenic acids which combine after ionisation. These effects could result from the poor selectivity of the matrix material towards the components in the naphthenic acid extracts. Attempts were made to improve the spectra by using less matrix material. This was not successful due to poor signal-to-noise ratio. Thus the use of the MALDI source was discontinued in this thesis.

The next paragraphs discuss the FAB results on the analysis of the naphthenic acid extracts from Field Y. Two matrix materials were used in a sensitivity study for this source: nitro-benzylalcohol (m-NBA) and a 50/50 vol/vol mixture of m-NBA and triethanolamine (TEA). Figure 4.5 presents the spectrum of the Field Y sample analysed with the m-NBA/TEA matrix. The main matrix peaks can be identified at m/z 153 and 305. Figure 4.5 also shows two major clusters of ions around m/z 1226 to 1238 and m/z 1239 to 1248, which may be associated with the presence of Arn (Baugh *et al.,* 2004). When the 50/50 vol/vol m-NBA/TEA matrix mixture was used, the sensitivity of Arn detection was increased by around 30 % compared to the use of m-NBA alone (data not shown). This result is probably due to better charge transfer between the TEA matrix material (which contains three hydroxyl alcohols as opposed to one in the m-NBA) and the Arn. Given these results it would appear the FAB ionisation source would be suitable for the characterisation of naphthenic acids present in soap deposits, since no observable fragmentation or multimerization patterns are present.

Figure 4.6 presents the results of the APCI source used with the same naphthenic acid extract from Field Y. The spectrum is dominated by two clusters of ions around m/z 1230 to 1236 and from m/z 1240 to 1250, which may be attributed to Arn (Baugh *et al.,* 2004). Two other clusters were observed with m/z from 1325 to 1332 and from 1342 to 1346, however these cannot be ascribed to naphthenic acid species, according to Equation 1.1. It is likely these are multimer species artificially generated during the ionisation process. Thus

it would also appear that the APCI ionisation source would be suitable for the identification of high molecular weight acids, but would not be suitable for general identification of the naphthenic acid extracts because of this bias.

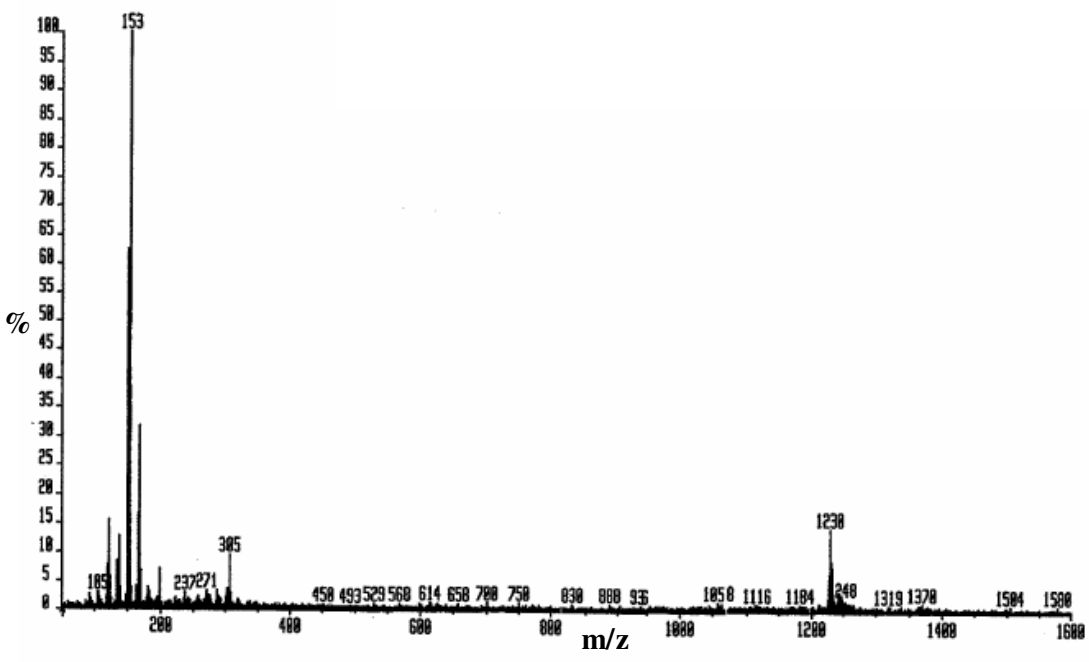

Figure 4.5. FAB spectrum for the naphthenic acid extract from Field Y soap sample. m-NBA/TEA matrix.

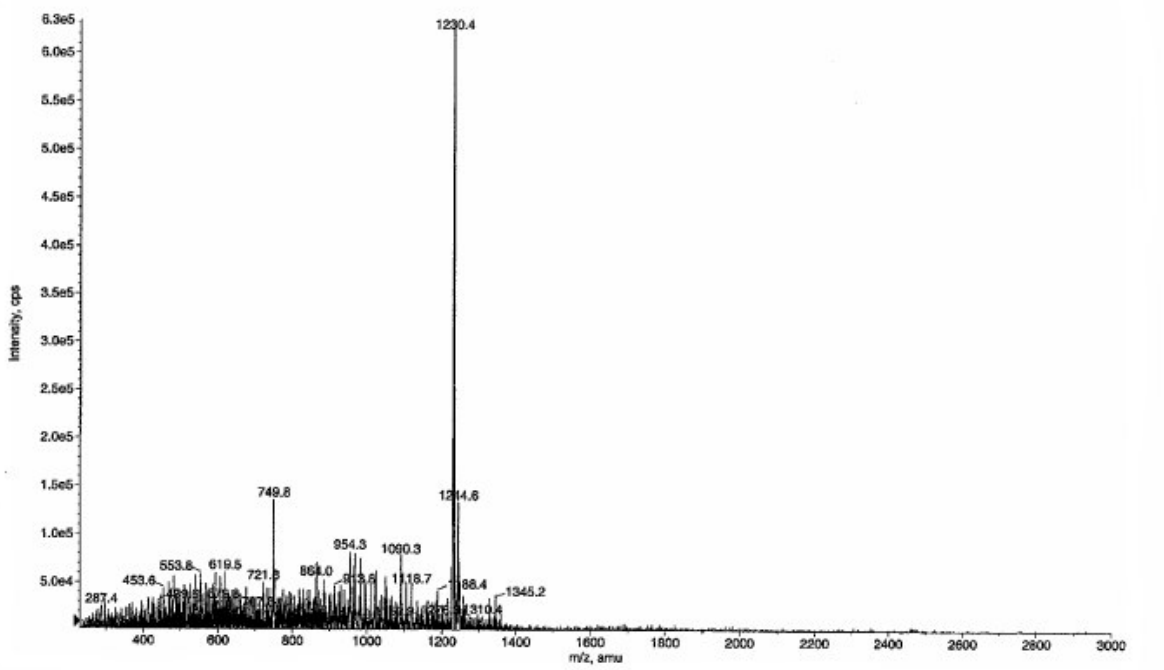

Figure 4.6. APCI spectrum for the naphthenic acid extract from Field Y soap sample.

Figure 4.7 presents the spectrum for the same naphthenic acid extract from Field Y using ES. In this spectrum, ions were detected which indicated the presence of acyclics (fatty acids) with 7 to 32 carbon atoms, mono-cyclics with 7 to 34 carbon atoms and bi-cyclics with 10 to 35 carbon atoms. This interpretation is based on the corrected m/z signals from the spectrum as well as the guidelines from Clemente and Fedorak (2004). The ion at m/z 126 is due to the presence of an internal standard. An additional cluster of ions between m/z 1228 to 1236 is also detected and this corresponds to Arn naphthenic acids (Baugh *et al.,* 2004). Note that the second ionisation species from Arn (between m/z 614 and 618) were also detected, but with weaker signals (not clearly observed in Figure 4.7). Thus, the ES technique can be used for the analysis of naphthenic acids from other similar field deposit samples.

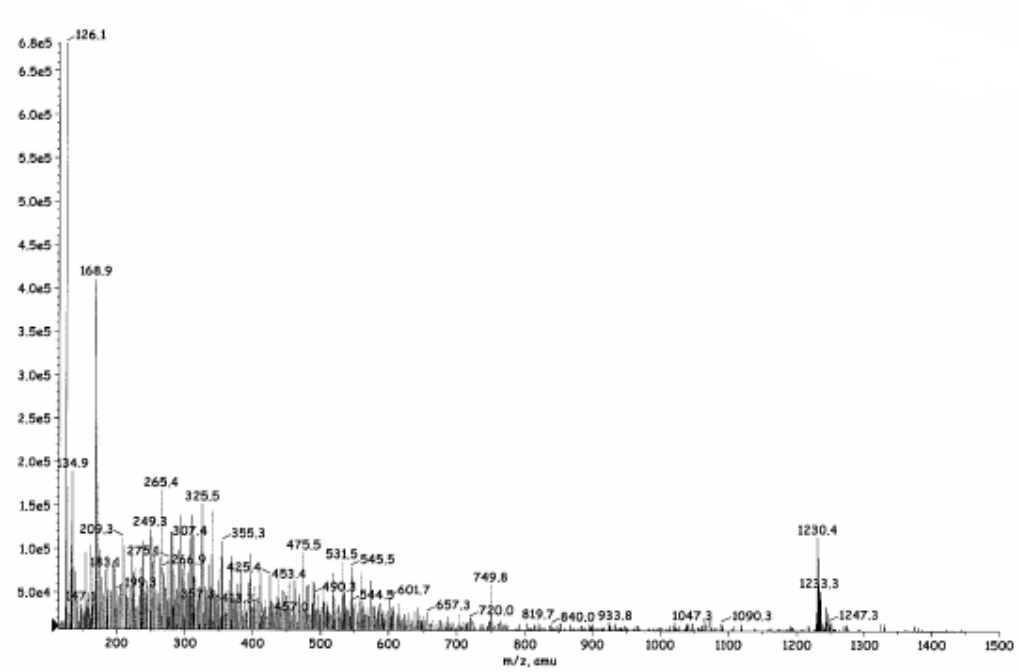

Figure 4.7. ES spectrum of naphthenic acid extract from Field Y soap sample.

Given that three soft ionisation sources, FAB, APCI and ES showed good potential for the analysis of naphthenic acids from field deposits (yet yielded different results particularly for Arn species and lower molecular weight naphthenic acids), the spectra for these three sources were compared. This was done using relative intensity percentages of each single spectrum as opposed to the absolute intensity values. Note, matrix and internal standard peaks were removed from these calculations. Although individual ionisation efficiencies for each naphthenic acid species are not known, conclusions can be obtained by looking at the relative proportions of detected MS species, both high and low molecular weights as relative percentages. To aid in the interpretations, a standard commercial Acros naphthenic acid mixture was also analysed with the same ionisation sources. Results are presented in Figures 4.8 and 4.9.

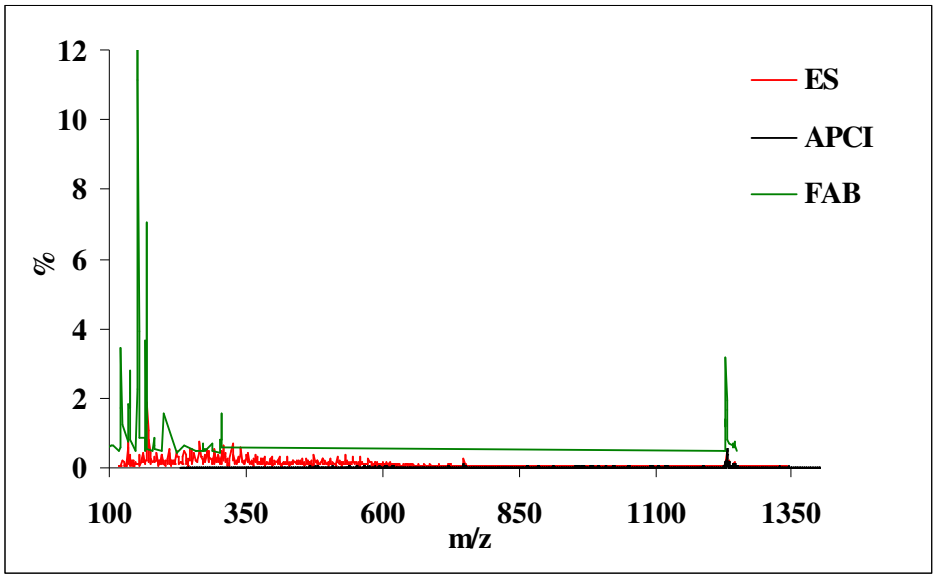

Figure 4.8. Comparison of ES, APCI and FAB spectra for naphthenic acid extract from Field Y soap sample.

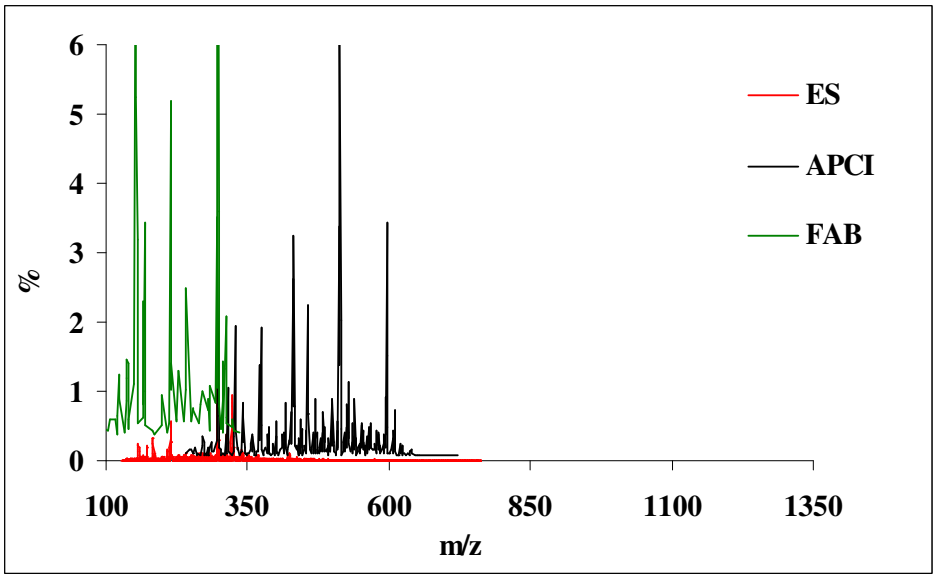

Figure 4.9. Comparison of ES, APCI and FAB spectra for the commercial Acros naphthenic acid mixture.

The overall detection of the naphthenic acids by MS is a function of the energy delivered by the ionisation sources. In this sensitivity study it was not possible to operate the sources using similar energy ranges due to hardware limitations. Nevertheless this was reconciled for comparison. The atom gun of the FAB source was operated at 30 keV. However the nebulizer current voltage for the APCI was -6 kV which was close to the ionspray voltage for the ES which was -4.5 kV. In Figure 4.8 it can be observed that the FAB spectrum shows a high percentage of Arn acids. In FAB, molecular ions are produced by deprotonation of naphthenic acids due to charge transfer with the matrix. For homogenous

ionisation, the matrix and the solute need to be well-mixed. The molecular weight of the matrix used in these experiments was 153 Daltons, thus it would be natural to assume a good affinity towards naphthenic acids with similar molecular weight. This can be observed both in the field deposit sample, as well in the commercial acid mixture. Figure 4.9 shows good recovery yields for the low molecular weight naphthenic acids in the commercial mixture when using the FAB source. Nevertheless charge transfer would also be facilitated with the Arn species, because of their high polarity if these species were to contain four carboxylic acid groups as suggested by Baugh *et al.* (2005a). Yet, as a result of this preferential ionisation, the naphthenic acid species with intermediate molecular weight would be less ionised and therefore not detected. For the APCI and ES sources, the percentages of Arn were comparable, but only the ES spectrum showed m/z groups between 100 and 500. In APCI, ionisation is a function of charge transfer between the solvent molecules and the sample molecules generated in a plasma by partial discharge around a conductor at a high potential. Samples are not injected in ionised form. Ionisation due to charge transfer is facilitated with polar molecules during the corona discharge. It can be expected that charge transfer will be favoured by the presence of Arn. This may explain the absence of low molecular weight species in the APCI spectrum compared to the FAB or the ES. No dielectric constant measurements were carried out on the Arn acids. Yet it can be suggested that this acid is more polar than the other naphthenic acid species in the soap sample, due to the presence of four carboxylic groups.

Particular solvents and solvent-solute interactions also play a role in naphthenic acid detection by MS. Hsu *et al.* (1998) compared FAB (using a TEA matrix) and APCI for commercial naphthenic acids with different solvents. It was found that the spectra were similar, but the APCI results were not as selective towards the lower molecular weight naphthenic acids found in the mixture. In further studies, Hsu *et al.* (2000) demonstrated that the ES signal was an order of magnitude lower than APCI, but only for solvents with low polarity. This might be attributed to enhanced charge transfer in the APCI source with more polar solvents. In ES samples are injected in ionized form by addition of an alkali, for instance. Rudzinski *et al.* (2002) compared both APCI and ES sources with standard acid mixtures as well as individual naphthenic acid solutions. In their experiments ES in the negative mode was shown to lead to ion generation with no fragmentation. Their results also showed that ES had higher sensitivity (three orders of magnitude) than APCI, but this was attributed to the addition of ammonia in the sample. The APCI was also observed to lead to the formation of dimers.

The average molecular weights for commercial naphthenic acid mixtures have a certain degree of statistical variation. Nevertheless, reported values in the literature have been between 220 and 239 Daltons, with bi-modal type distributions, as a result of a predominance of single charged ions (Hsu *et al.,* 1998; Roussis and Lawlor, 2002; Rudzinski *et al.,* 2002). This suggests that these commercial mixtures contain a very small amount of species above m/z of 400. Rudzinski *et al.* (2002) showed that higher m/z envelopes for the commercial naphthenic acid mixtures were due to dimer formation. In Figure 4.9 the spectra of a commercial naphthenic acid analysed with the same FAB, APCI and ES sources are presented. The FAB source again shows a high selectivity for low molecular weight acids. The ES shows low signal intensity, however the spectrum is consistent with the trends reported in the literature (Hsu *et al.,* 1998; Roussis and Lawlor, 2002; Rudzinski *et al.,* 2002). The APCI spectrum does not present many m/z species below 250, which is rather surprising since the average molecular weight for this sample is 230. In addition, the spectrum for this source shows m/z species above 400. These species are most likely multimers generated during the ionisation process. They do not represent true naphthenic acid species in the commercial mixture, since they do not have the proposed structure in Equation 1.1.

The optimum ionisation source for soap and crude oil analysis would ideally need to be used for a wide range of naphthenic acid molecular weights as well as feeds (i.e. crude oils and their soaps) for fingerprinting purposes. Given the effects discussed with reference to Figures 4.8 and 4.9, FAB and ES could potentially be used for this purpose. Despite this, the FAB source may present poor sensitivity for naphthenic acid detection with crude oil samples. FAB experiments conducted with soap-forming crude oils showed the only identifiable peaks were those due to the FAB matrices (data not shown). Thus, the charge transfer between the crude oil naphthenic acids (including Arn species) and the matrix did not allow for the detection of other naphthenic acids in the soap-forming crude oil sample. This could be caused by a combination of viscosity and/or concentration effects. Thus the FAB source would be discouraged for naphthenic acid analysis in crude oils given the current equipment and experimental conditions detailed in Chapter 3.

It is also suggested that the APCI source could be used with samples where the concentration of Arn acids was low. This is because of the enhanced ionisation effects observed for this species with APCI.

The previously discussed ionisation sources employed very similar low-resolution mass analysers. Use of higher resolution analysers with electrospray/nanospray sources is now discussed. The electrospray source (ES) was considered the optimum source for naphthenic

acid analysis, as a result of the non-biased performances towards the various different acid species.

Figure 4.10 and 4.11 show the spectra for the time-of-flight (TOF-MS) and the Fourier-Transform Ion cyclotron resonance (FTICRMS) analysers for the naphthenic acid extracts from Field Y soap sample, both operated in the negative mode. The resolution of these instruments was approximately 7.5 and 1000 times that of the single quadrupole analyser used in the acquisition of the spectrum shown in Figure 4.7.

In Figure 4.10 the TOF-MS spectrum is presented with intensity values on the same scale as that of the single quadrupole spectrum in Figure 4.7. It was possible to extend the current mass range to include ions up to m/z 3000 with this instrument. The spectrum shows the presence of acyclic acids, mono-cyclics and bi-cyclics based on the visible peaks on the spectrum as well as the guidelines of Clemente and Fedorak (2004). This is carried out using the assignment of the corrected m/z data from the spectra to naphthenic acid species. There is also some evidence of the presence of Arn species in the sample at m/z 1232. Nevertheless, the overall signals for these species are weaker than that for the single quadrupole analyser. The TOF-MS did however increase the sensitivity for the detection of lower molecular weight naphthenic acids.

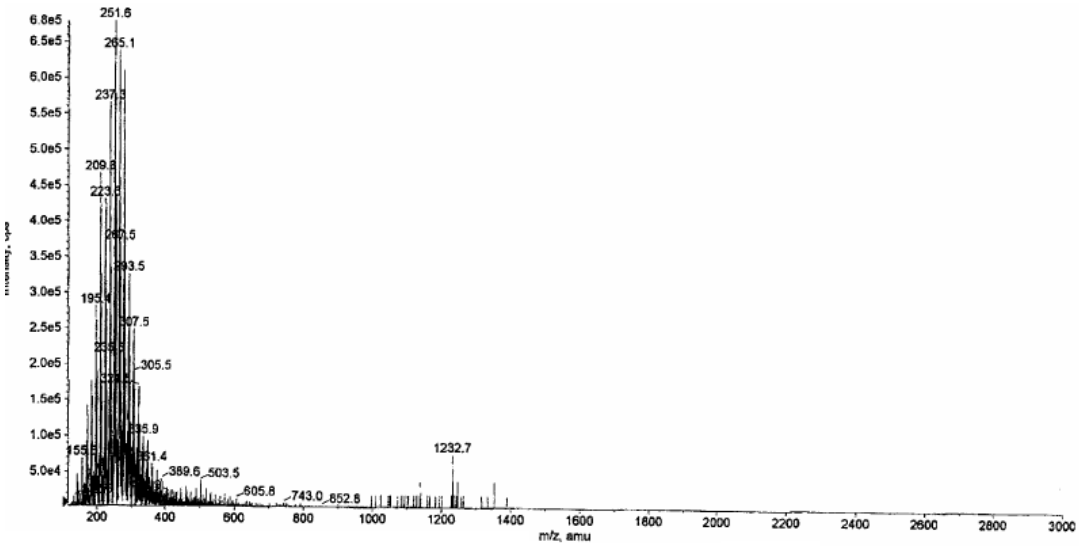

Figure 4.10. TOF-MS spectrum of naphthenic acid extract from Field Y soap sample.

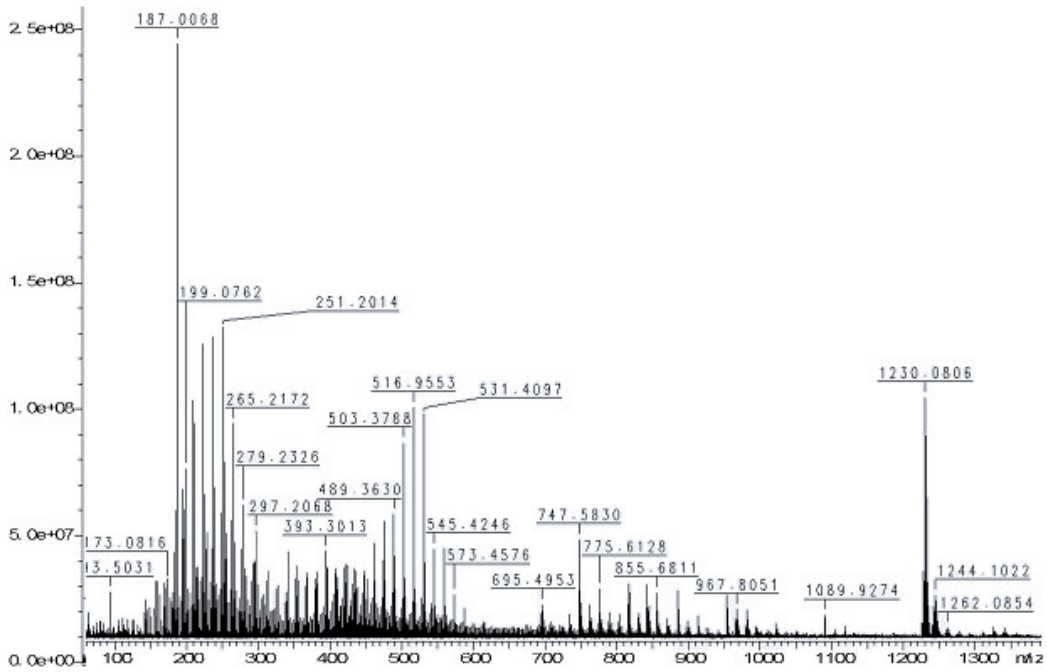

Figure 4.11. FTICRMS spectrum of naphthenic acid extract from Field Y soap sample.

Figure 4.11 presents the spectrum for the same sample as given by FTICRMS. The spectrum showed the highest sensitivity towards the Arn acid species, when compared to Figures 4.7 and 4.10. Despite this, it can be observed that there is a large amount of multimer formation, particularly between m/z 400 and 1000. Multimer formation in FTICR studies with naphthenic acids from crude oils has been reported in the literature (Rodgers *et al.,* 2006). They can be identified by the unusual bi-modal distributions in Figure 4.11, not observed in Figures 4.10 (TOF-MS) or 4.7 (single quadrupole). Many of the ions identified in this spectra do not correspond to naphthenic acid species according to the guidelines discussed in Chapter 3. It is possible that particular equipment fine-tuning could lead to an improved FTICRMS spectrum. However, given that the simple single quadrupole instrument produced spectra without multimer formation and with no bias towards any particular naphthenic acid species (Figure 4.7), it was chosen as the default instrument to analyse the remaining samples in this thesis.

4.1.1.2. ES sensitivity study.

Optimisation of the ES single quadrupole operation applied to the study of naphthenic acids was performed. The following variables were examined: ion spray voltage (ISV), nebulizer gas (NEB) and curtain gas flow rates (CUR). Table 4.1 presents the experimental matrix used in this optimisation.

Experiment	1	2	3	4	5
Ion spray voltage (ISV) kV	-4.50	-3.75	-3.00	-4.50	-4.50
Nebulizer gas setting (NEB)	10	10	10	10	5
Curtain gas setting (CUR)	12	12	12	6	12

Table 4.1. ES single quadrupole equipment setting sensitivity tests.

Data was acquired over the range m/z 115 to 3000 for each set of instrument parameters. The gas flow parameters (NEB and CUR) are digitally set and work off an array of internal valves. Exact flow rates can be calculated, but the digital values are most commonly used for comparative purposes. The gas pressure supplied to the instrument was 60 psi. The minimum value for CUR was 6, since a lower setting would result in collapse of the vacuum needed to operate the system. Other settings were kept constant as described in Section 3.2.1.1.

Figures 4.12, 4.13 and 4.14 present the results of the sensitivity study as a function of ISV. Spectra for experiments 4 and 5 (variation of NEB and CUR) are not displayed since these did not lead to any significant variations compared to that of experiment 1 (Table 4.1). The spectra in Figures 4.12, 4.13 and 4.14 show peaks at around m/z 1230 which can be attributed to the Arn. Nevertheless to understand the effect of ISV on the spectrum, maximum signal intensity as well as Arn signal intensity in the spectrum needs to be discussed. The Arn signal intensity is reduced from 7000 to 270 as the ISV is reduced from -4.5 kV to -3.0 kV, while the effect on the non-Arn species is different. In this case the signal is reduced from 16000 to 900. This signal deterioration is a direct result of incomplete ionisation of the non-Arn species. This can be explained if one considers preferential ionisation of the Arn acid due to the presence of four carboxylic acid groups compared to the other naphthenic acid structures. This would explain the lower variation in the Arn signal with ISV. The spectrum looks remarkably similar to the APCI spectrum presented in Figure 4.6 in regards to fragment distribution.

The results from this section would support the conclusion of preferential ionisation of the Arn acid by APCI and may also explain the large percentage of Arn detected in the work of Baugh *et al.* (2004). To support these conclusions a sensitivity test was also performed using three solvents: toluene, toluene and methanol (50/50 vol/vol) and toluene, methanol and acetonitrile (25/25/50 vol/vol/vol). Table 4.2 presents properties of these solvents to help in the interpretation of the results. The equipment used was the ES with the optimum

single quadrupole settings, with the exception of the ISV. Although the optimum setting for this variable was -4.5 kV, it was decided that the experiments would be conducted using a voltage of -3.75 kV, in order to force the preferential ionisation of the Arn (as per the results in Figure 4.13). The results for these tests are presented in Figures 4.15 and 4.16.

Solvent	Molar mass (g/mol)	Viscosity (cP at 20 °C)	Dipole Moment (D)
Toluene	92.14	0.59	0.36
Methanol	32.04	0.59	1.69
Acetonitrile	41.05	0.35	3.90

Table 4.2. ES solvent properties for sensitivity tests.

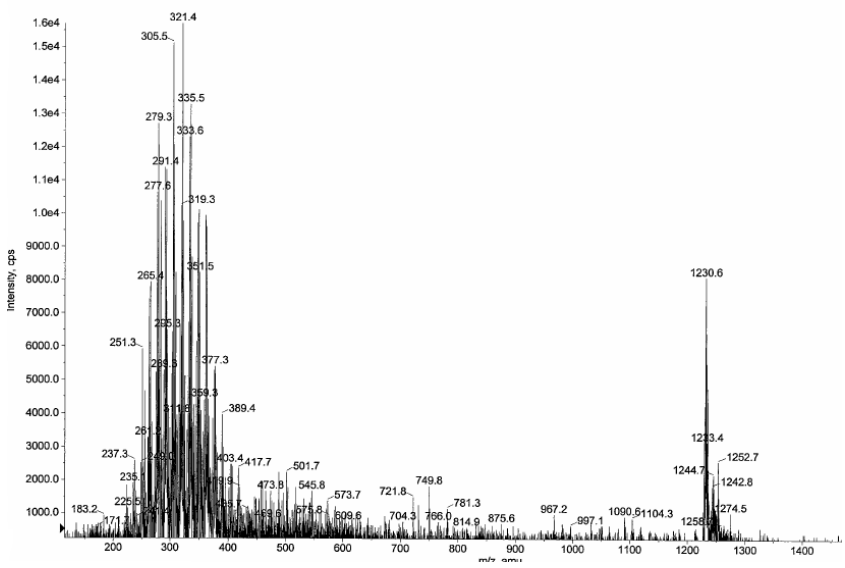

Figure 4.12. ES spectrum of naphthenic acid extract from Field Y soap sample for experiment 1. See Table 4.1.

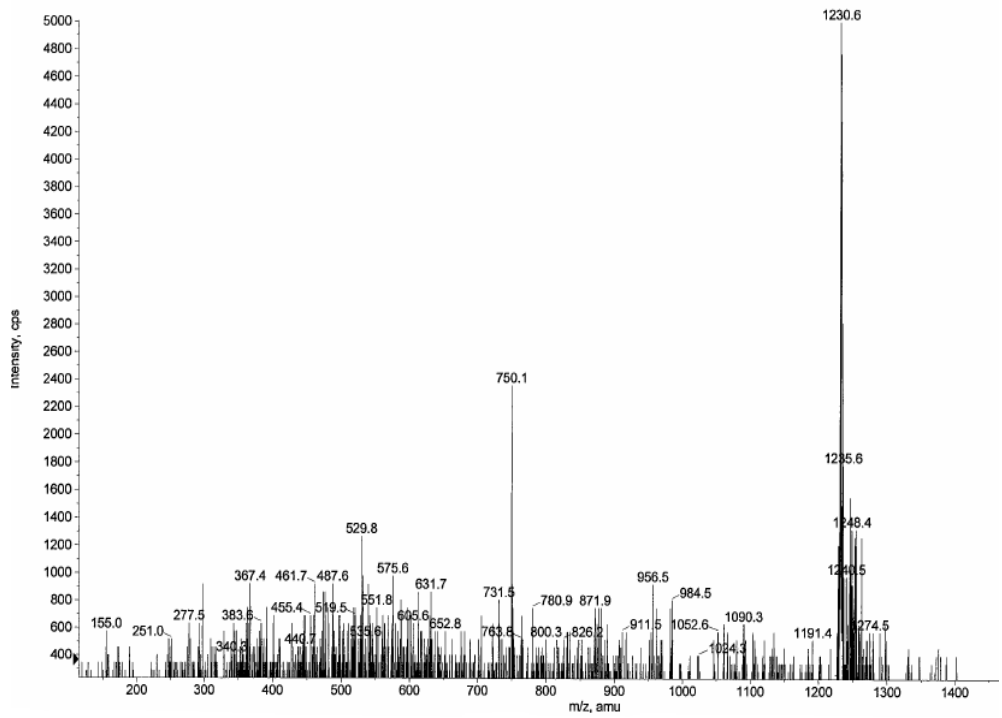

Figure 4.13. ES spectrum of naphthenic acid extract from Field Y soap sample for experiment 2. See Table 4.1.

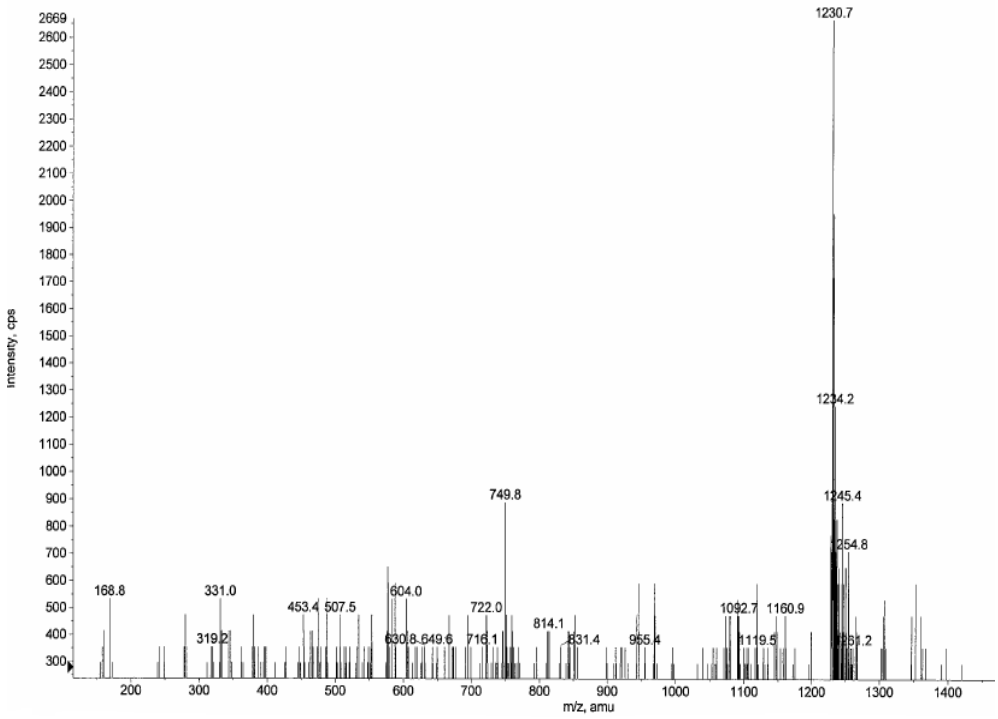

Figure 4.14. ES spectrum of naphthenic acid extract from Field Y soap sample for experiment 3. See Table 4.1.

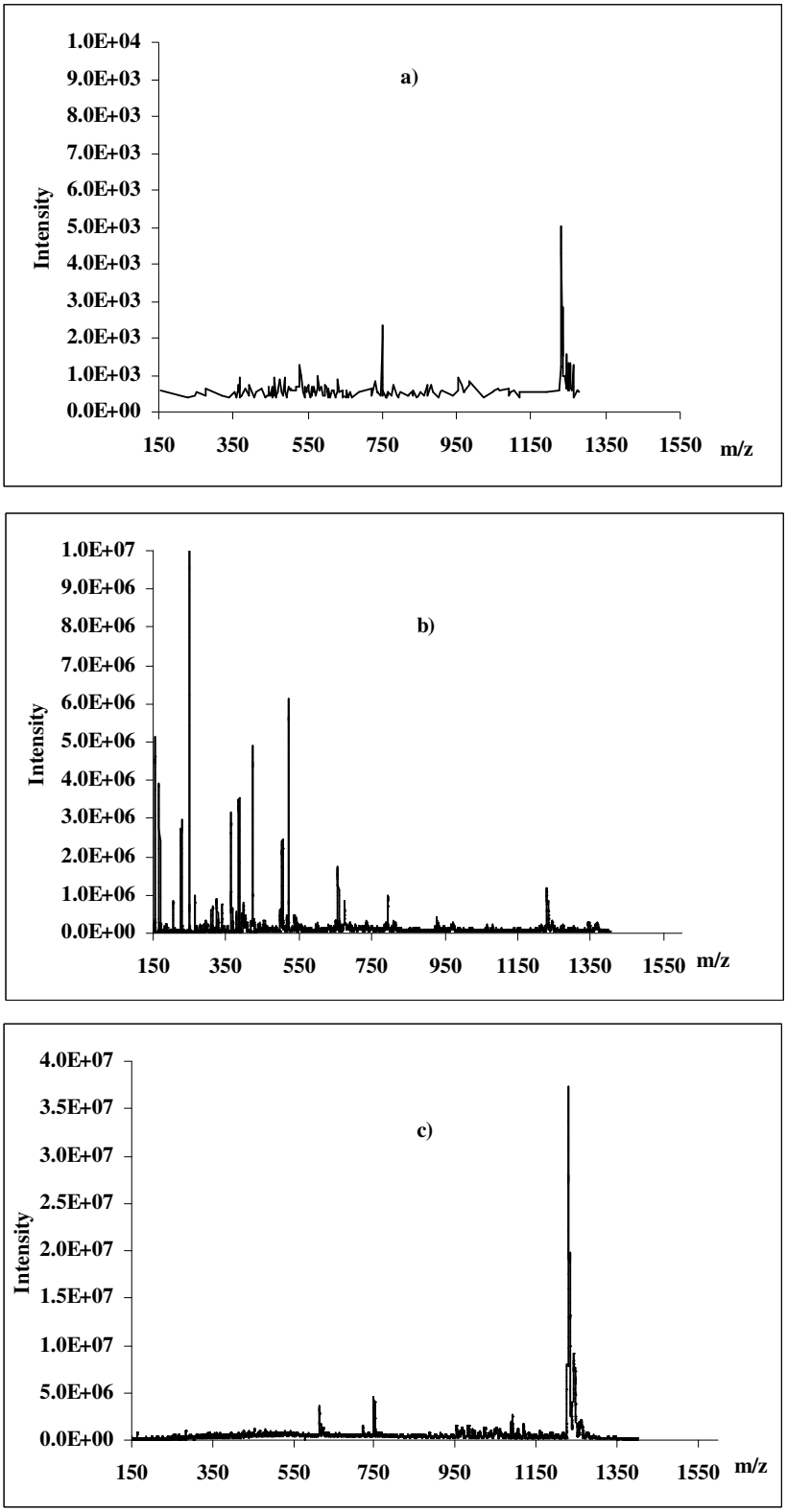

Figure 4.15. ES spectrum of naphthenic acid extract from Field Y soap sample in three solvents: a) toluene, b) toluene and methanol and c) toluene, methanol and acetonitrile.

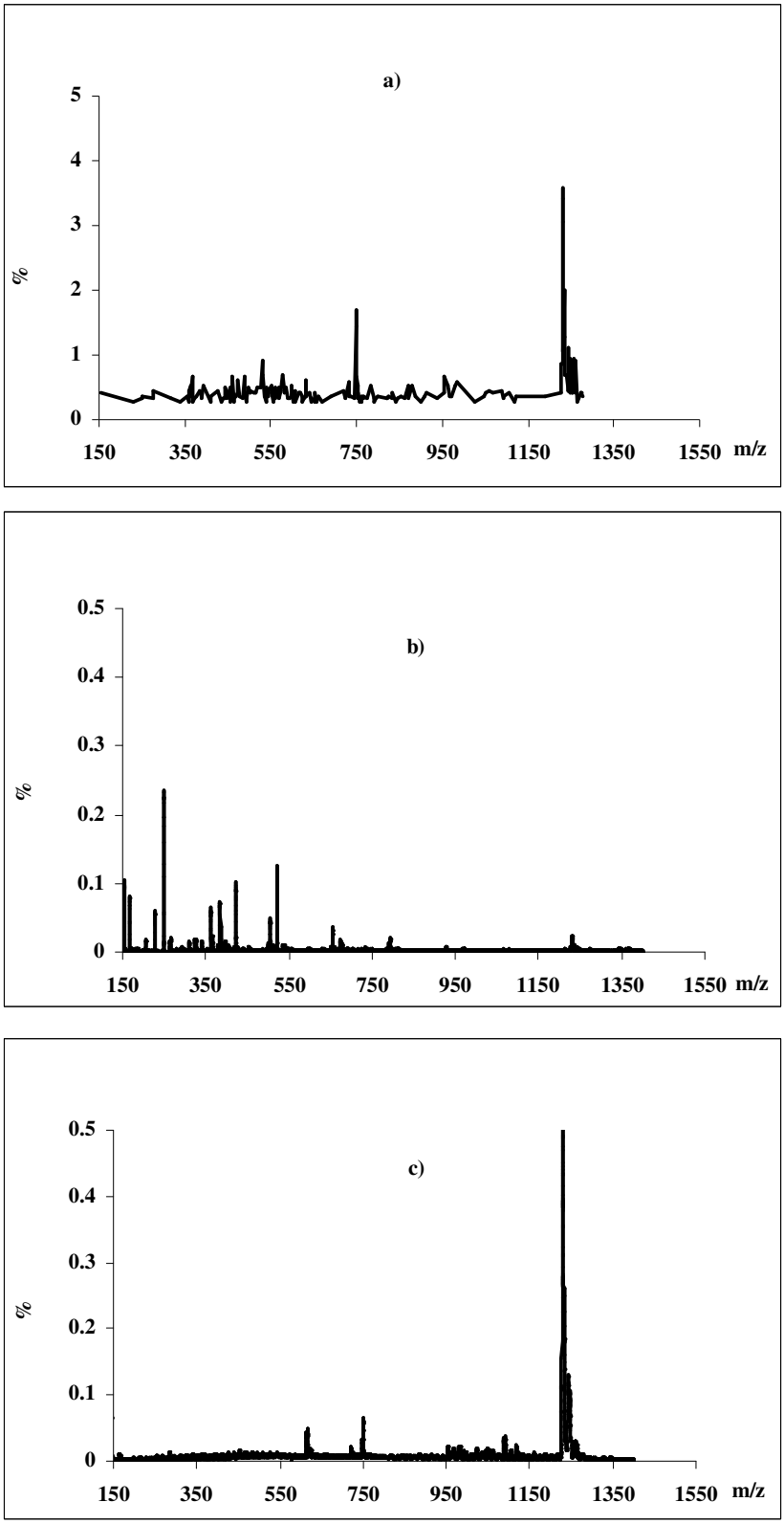

Figure 4.16. ES spectrum of naphthenic acid extract from Field Y soap sample in three solvents: a) toluene, b) toluene and methanol and c) toluene, methanol and acetonitrile.

Figure 4.15 shows the spectra for the three different solvent combinations plotted as a function of absolute intensity values. The overall signal intensity increases with the addition of methanol or a methanol/acetonitrile mixture (up to three orders of magnitude) compared

to when toluene alone is used. The intensity of peaks associated with the Arn naphthenic acid increases only when acetonitrile is present. Methanol and acetonitrile have higher dipole moments which aid charge transfer. Molecules of these solvents have lower molar mass compared to toluene. This would aid the formation of the aerosol spray used by the ES source (although this effect is less pronounced with methanol since its viscosity is very close to that of toluene). Nevertheless, with methanol, a higher percent of lower molecular weight naphthenic acids are ionised. When acetonitrile is added, it appears the high dipole moment of the solvent (3.9 D) is leading to preferential ionisation of the Arn acids. This has a direct effect on the detection of the remaining lower molecular weight naphthenic acids. Arn species may be considered more polar due to the suggested presence of four carboxylic acid groups as reported by Baugh *et al.* (2005a). The preferential detection of Arn can be observed in Figure 4.16. The Arn acids are predominant in the spectrum, yet their relative percentage is only 0.5 %, based on MS signal response. Toluene on the other hand produced the highest percentage of Arn acids (4 %) in addition to a range of other naphthenic acids at lower molecular weights. Arn is not the predominant species in this spectrum. The results thus point to favoured ionisation of the Arn species when high polarity solvents are used with ES.

An overall fingerprint of the naphthenic acid species would be required for a mechanistic study of soap deposition, as opposed to favoured detection of Arn acids. Thus, this information was used to select toluene as the main solvent for the remaining ES analysis in this thesis. Note however that acetonitrile was used in experiments to study the Arn acid in more detail and these are discussed in Chapter 6.

4.1.1.3. Naphthenic acid speciation of field soap samples.

Figures 4.17 to 4.21 present the ES spectra of the various field deposits studied in this thesis, using the optimum equipment and solvent settings detailed in Table 4.3. Interpretation was carried out by inspection of the m/z values using the guidelines of Clemente and Fedorak (2004).

ES	PESciex 150EX
Analyser	single quadrupole
Ionspray voltage (ISV) kV	-4.5
Nebulizer and curtain gas	nitrogen
Nebulizer gas (psi)	>10
Curtain gas (psi)	> 12
Pump flow rate (µl/min)	10
Source temperature (^{o}C)	350
Internal standard (g/l)	benzoic acid 0.08 g/l
Solvent	toluene & 0.1 wt% aq. ammonia *

Table 4.3. ES single quadrupole optimum settings.

Note* = a further dilution was carried out with 2-propanol to aid ionisation and increase sensitivity, but only for Field W samples, as described in section 3.2.1.1.

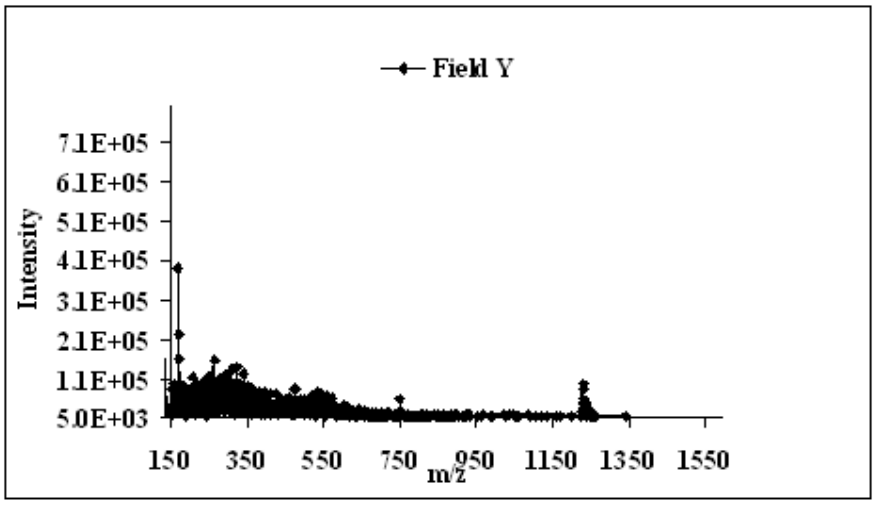

Figure 4.17. ES spectrum of naphthenic acid extract from Field Y soap sample.

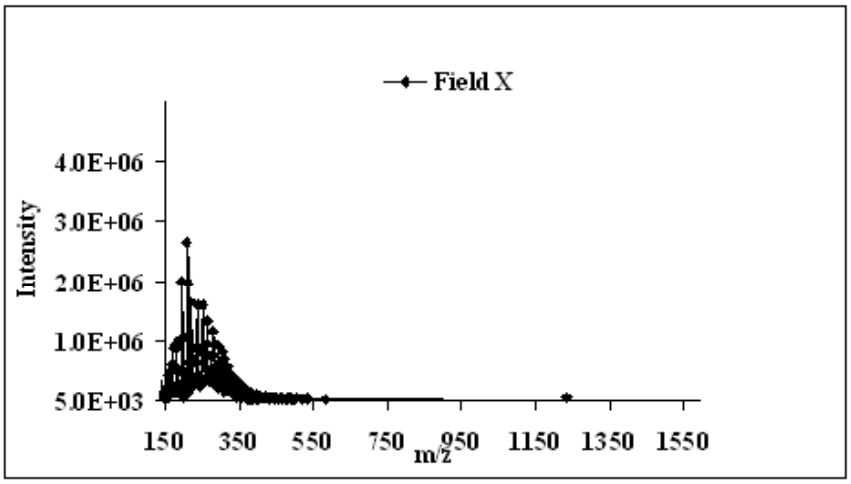

Figure 4.18. ES spectrum of naphthenic acid extract from Field X soap sample.

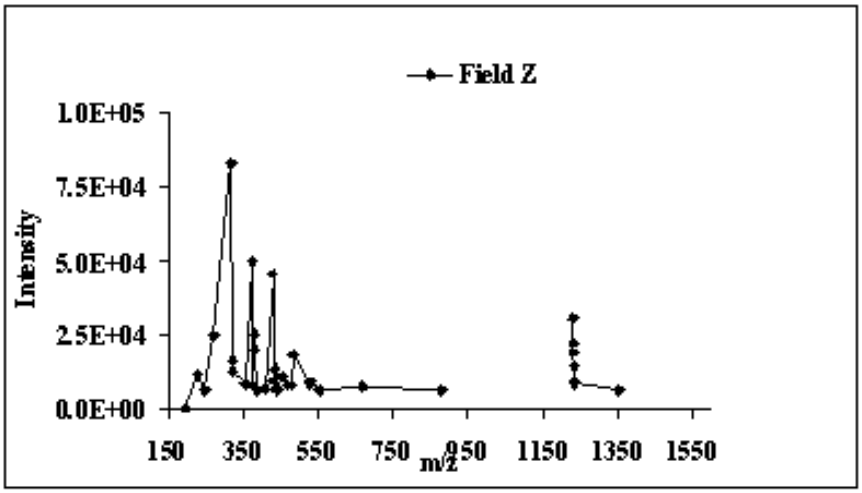

Figure 4.19. ES spectrum of naphthenic acid extract from Field Z soap sample.

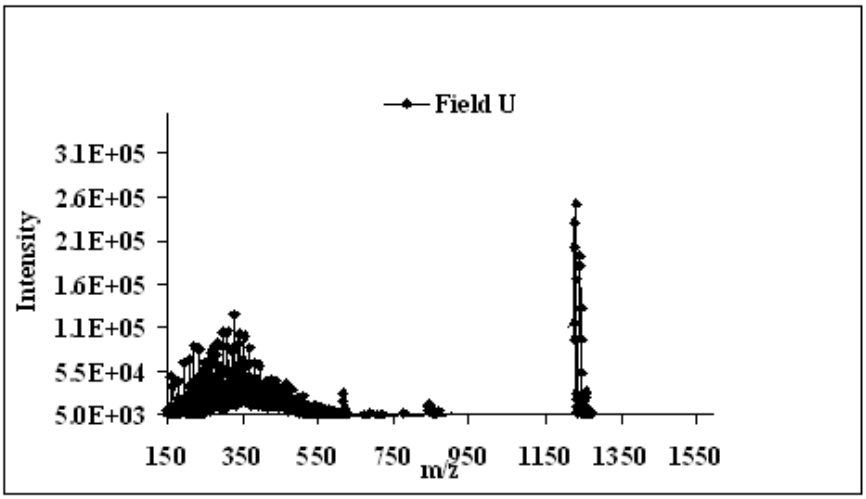

Figure 4.20. ES spectra of naphthenic acid extract from Field U soap sample.

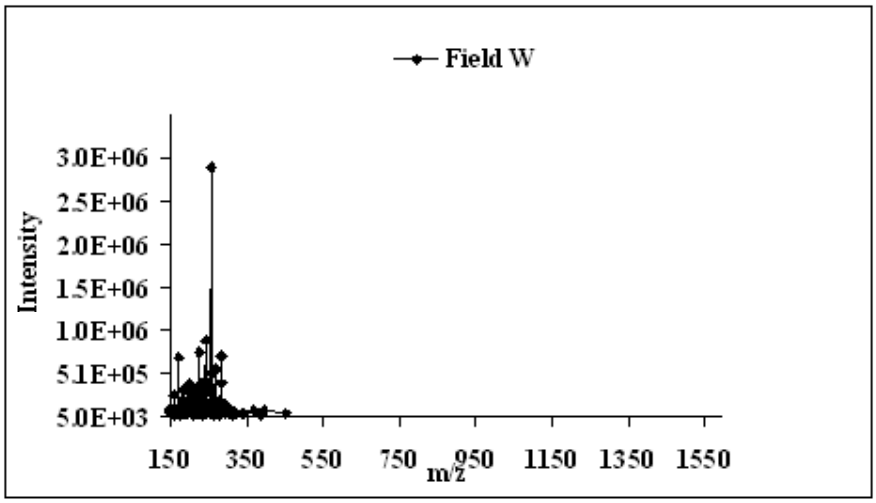

Figure 4.21. ES spectra of naphthenic acid extract from Field W soap sample.

The spectrum for Field Y sample in Figure 4.17 contains a cluster of ions at m/z 1230 associated with Arn, and a range of other low molecular weight naphthenic acid species. The spectrum for Field X sample (Figure 4.18) has m/z ions indicating the presence of acyclics, mono-cyclics and bi-cyclics, as suggested by the guidelines of Clemente and Fedorak (2004). Similar to the sample from Field Y, Field X sample also contains ions attributed to Arn species at m/z 1228 and 1236, but with lower intensity. Figure 4.19 shows the spectrum for the sample from Field Z, in which a range of acyclic and mono-cyclic species are predominant (Clemente and Fedorak, 2004). The ion clusters at m/z 1230 representing Arn are also observed. Figure 4.20 contains the spectrum for the Field U sample. The peaks associated with Arn acids between m/z 1226 and 1238 are observed and have high intensity, in addition to species between m/z 1268 and 1272. In Figure 4.21 the spectrum of Field W sample is presented, which shows a strong presence of acyclic acids with species between 7 and 33 carbon atoms. There was no evidence of higher molecular weight naphthenic acids or Arn, even after dilution, for this particular sample.

An MS spectrum for the deposit sample from Field T was acquired up to higher m/z values using different equipment. The set-up used for this purpose was a TOF-MS instrument and further equipment details have been included in Section 3.2.1.1. The justification for the use of this equipment was that Field T sample constituted an asphaltene deposit, and therefore could contain species outside of the m/z 1500 envelope given by the ES single quadrupole approach. Figure 4.22 presents the spectrum obtained for the sample from Field T. This sample shows one major ion at m/z 208 which can be attributed to a bi-cyclic naphthenic acid species (Clemente and Fedorak, 2004). There are other low intensity signals which may be assigned to naphthenic acid structures with more than one ring. Other m/z species could not be matched to naphthenic acid species using Equation 1.1, and thus probably represent other types of chemical families with even heteroatom structures.

Figure 4.22. TOF-MS spectrum of deposit sample from Field T.

Figures 4.23 to 4.27 present the statistical speciation of the naphthenic acids in the naphthenic acid extracts from Figures 4.17 to 4.21, according to carbon number and hydrogen deficiency (Z), following the procedures described in Section 3.2.1.1. It is assumed that all non-Arn naphthenic acid components (i.e. m/z values below 1220) can be assigned according to Equation 1.1. Isomers, however, cannot be distinguished using the low-resolution techniques employed for the soap sample analysis. Moreover, naphthenic acids are assumed to be the only acidic groups given by the low-resolution MS instruments used in this work. Validation of this needs to be carried out using other techniques such as MS/MS. Note that the results are qualitative, since the exact ionisation efficiencies of each individual naphthenic acid family are not known. In the statistical analysis, internal standards were removed from the calculations. The Arn species were assigned to molecular weights at or above m/z 1220 and below m/z 1250. The empirical formula proposed for the Arn naphthenic acids by Baugh *et al.* (2005b) was used: $C_nH_{2n+Z}O_8$, and the carbon number and hydrogen deficiency for this species was set to 80 and –10 respectively. Note that the Field T sample was not included in this speciation since many of the m/z species given in Figure 4.22 probably do not represent naphthenic acids.

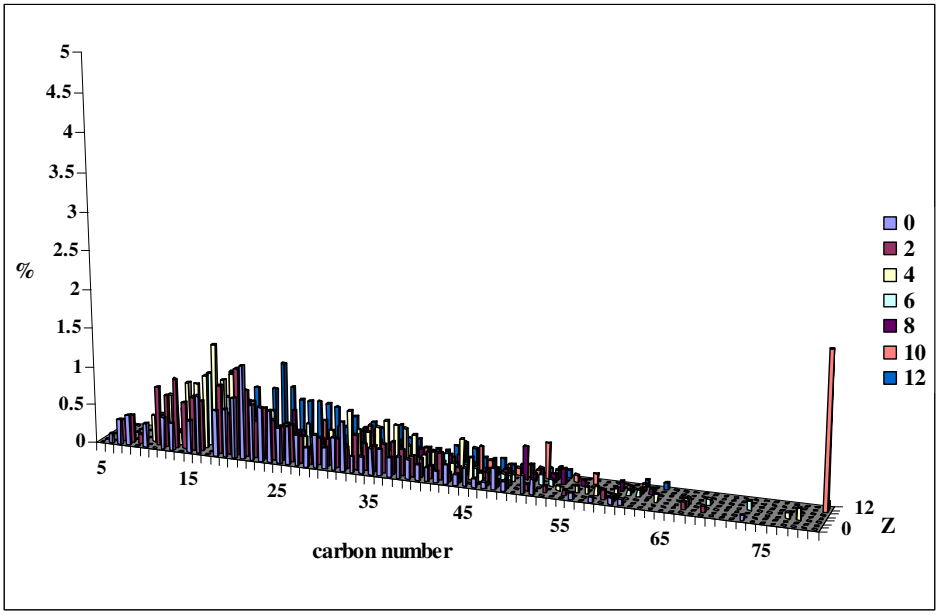

Figure 4.23. Speciation of naphthenic acid extract from Field Y sample in terms of carbon number and hydrogen deficiency (Z). Legend represents Z values.

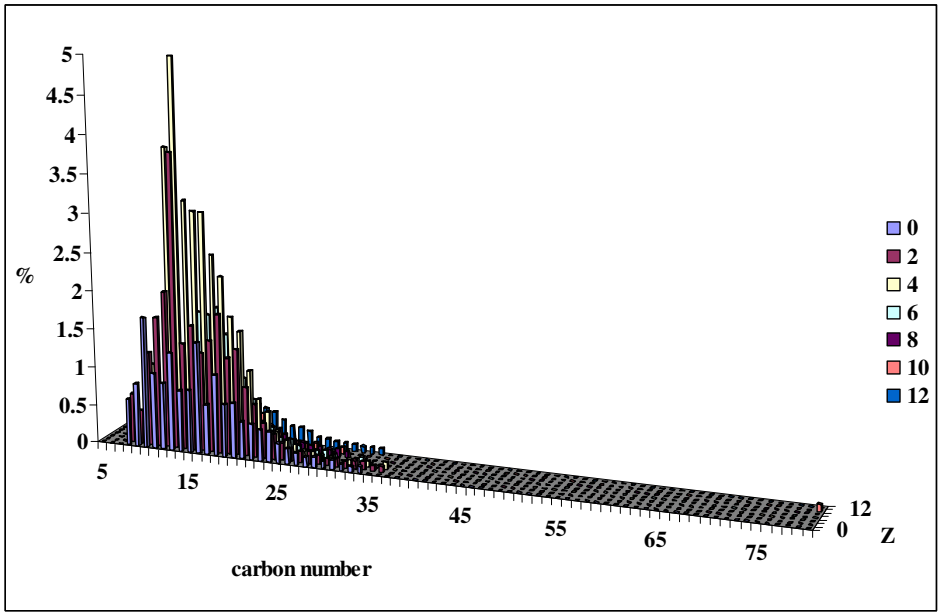

Figure 4.24. Speciation of naphthenic acid extract from Field X sample in terms of carbon number and hydrogen deficiency (Z). Legend represents Z values.

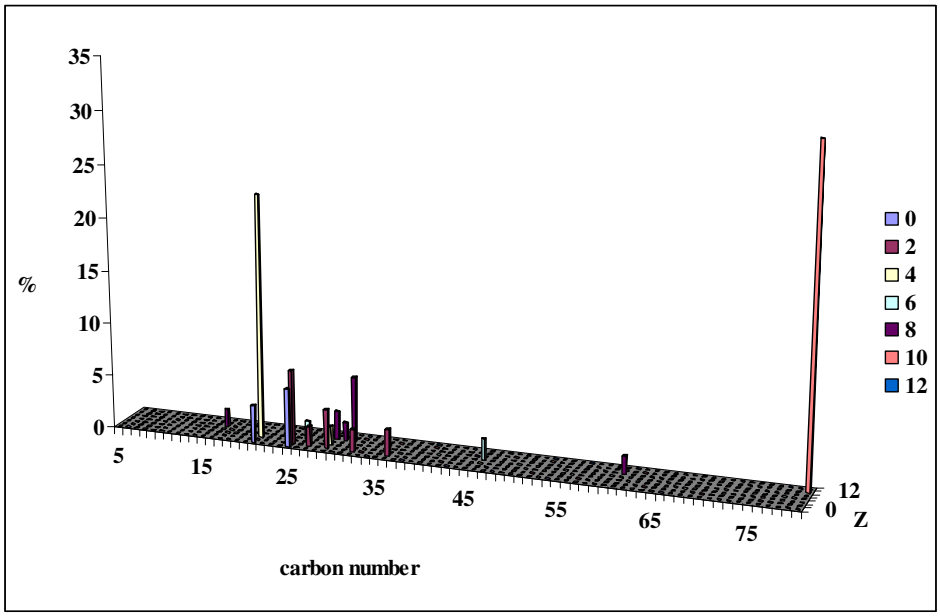

Figure 4.25. Speciation of naphthenic acid extract from Field Z sample in terms of carbon number and hydrogen deficiency (Z). Legend represents Z values.

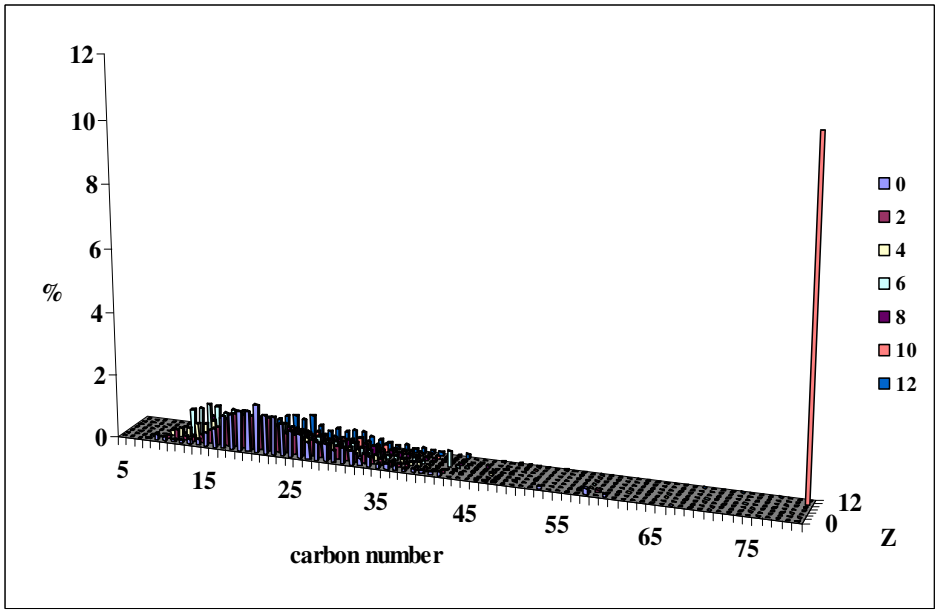

Figure 4.26. Speciation of naphthenic acid extract from Field U sample in terms of carbon number and hydrogen deficiency (Z). Legend represents Z values.

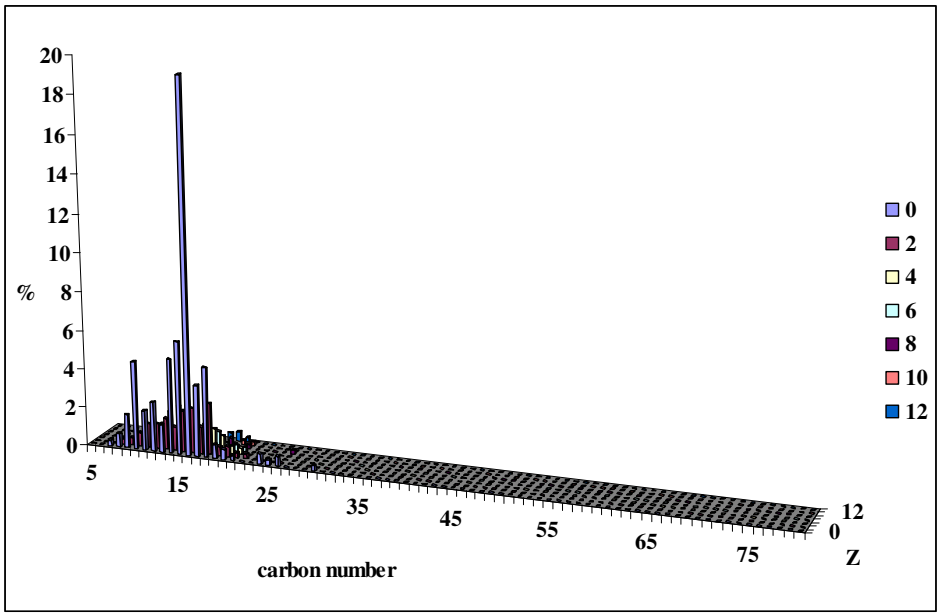

Figure 4.27. Speciation of naphthenic acid extract from Field W sample in terms of carbon number and hydrogen deficiency (Z). Legend represents Z values.

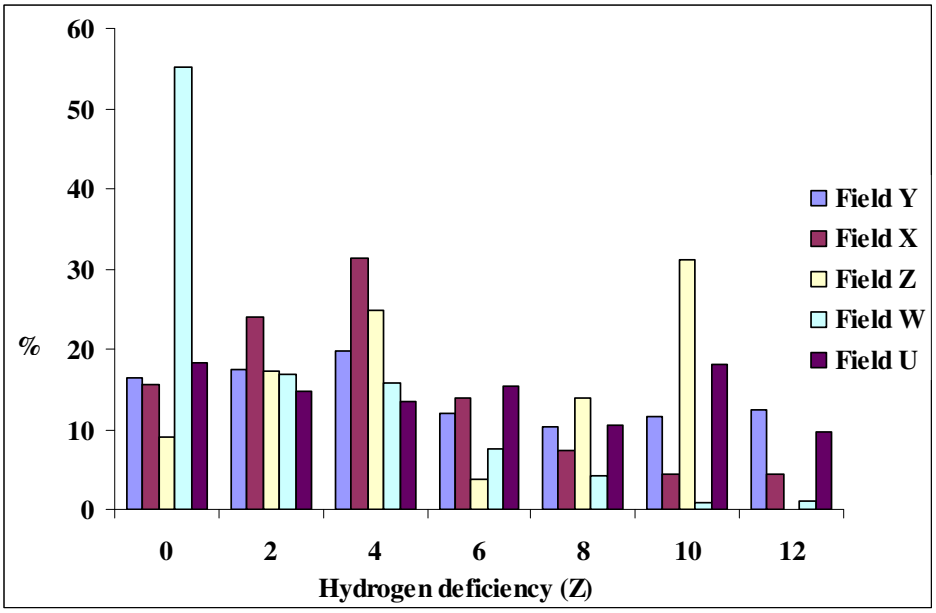

Figure 4.28. Naphthenic acid families in naphthenic acid extracts from field deposit samples as given by hydrogen deficiency (Z). Note, 0 = acyclics, 2 = mono-cyclics, 4 = bi-cyclics, 6 = tri-cyclics, 8 = tetra-cyclics, 10 = penta-cyclics and 12 = hexa-cyclics

Field	Arn %
Z	31.1
U	10.9
Y	2.0
X	0.1
W	0

Table 4.4. Arn percentage for different soap samples as a function of the ES signal intensity.

The speciation of soap samples from Fields Y, X, Z and U are presented in Figures 4.23 to 4.26. These samples showed a range of naphthenic acid components, mostly with 15 and 40 carbon atoms. According to the overall speciation in Figure 4.28, acyclics, mono-cyclics, bi-cyclics and penta-cyclics are predominant. This means that all major naphthenic acid groups (acyclic, one ring, two rings, etc) have similar concentrations in the samples. Arn naphthenic acids were observed for these samples, although high concentrations of these species were only found for samples from Fields U and Z as illustrated in Table 4.4. The percentage of Arn were calculated based on the normalised MS signals.

Field W sample however presents a different naphthenic acid distribution as given by Figure 4.27. Acyclic acids were observed to be the predominant in this sample (55 %) with the majority of species having between 9 and 19 carbon atoms. Field W sample is a sodium carboxylate soap emulsion sample from the Far East. Gallup *et al.* (2004) also reported analysis for a soap emulsion consisting of fatty acids and suggested they are responsible for stabilising emulsions. Data presented in Chapter 6 will support the effect of these naphthenic acid species on the formation of different types of soaps in the laboratory.

Mediaas *et al.* (2005) claimed the Arn acids were the main species which constituted the calcium naphthenate soap scale deposits based on the analysis carried out on derivatized acids from one field sample. The results in this thesis for calcium naphthenate soap scale samples (Fields X, Y, Z) clearly indicate that the Arn acid is not the predominant naphthenic acid in these samples. The differences in Arn detection in this thesis in comparison to other work are most probably due to the exact soap sample treatment and equipment settings. More specifically, Baugh *et al.* (2005a) and Mediaas *et al.* (2005) used a combination of polar solvents (i.e. acetonitrile) and sources which favour Arn ionisation (i.e. APPI). The results in this thesis show that Arn can be unequivocally identified using mass spectrometry. However, different source solvent combinations would be used for either a general crude oil fingerprinting as opposed to Arn focus and detection.

4.1.2. Fourier-Transform infrared spectroscopy of naphthenic acid extracts.

In Figures 4.29 to 4.32 the band intensities for different naphthenic acid extracts are presented expressed as transmittance [T]. The annotated bands are assigned in Table 4.5 and interpretation was carried out according to the guidelines of Silverstein *et al.* (1991). Note that Field U and Field T deposit samples were not tested using this technique since these are not soap deposits. Water was used to prepare the acetic acid solutions for the dissolution of the soap samples prior to analysis as per the procedures in Section 3.2.2. However, the vibration band of water at 3450 cm^{-1} is not observed in any of the samples analysed in this thesis. Thus, samples can be said to be reasonably free of water contamination.

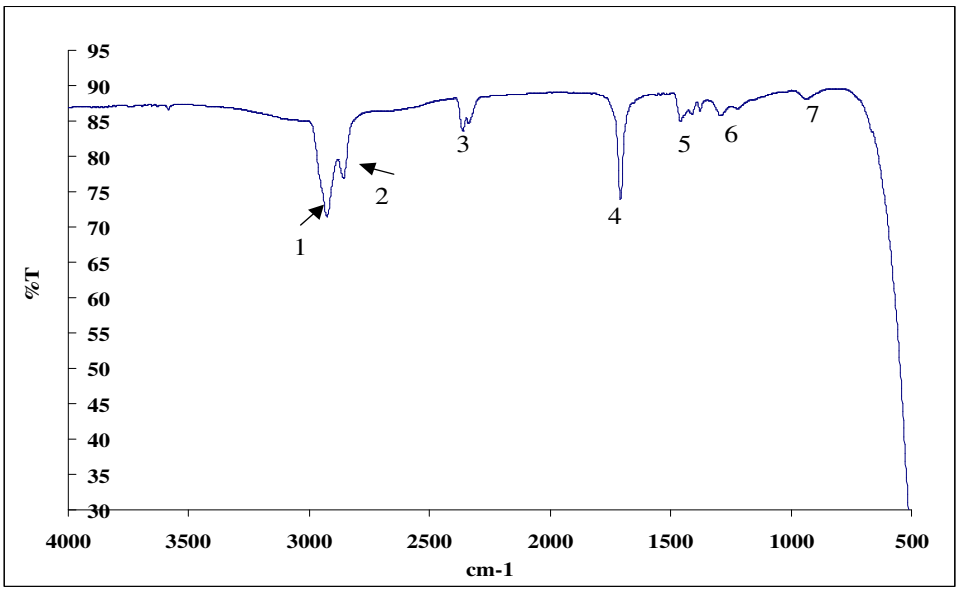

Figure 4.29. FTIR for naphthenic acid extract from Field X sample.

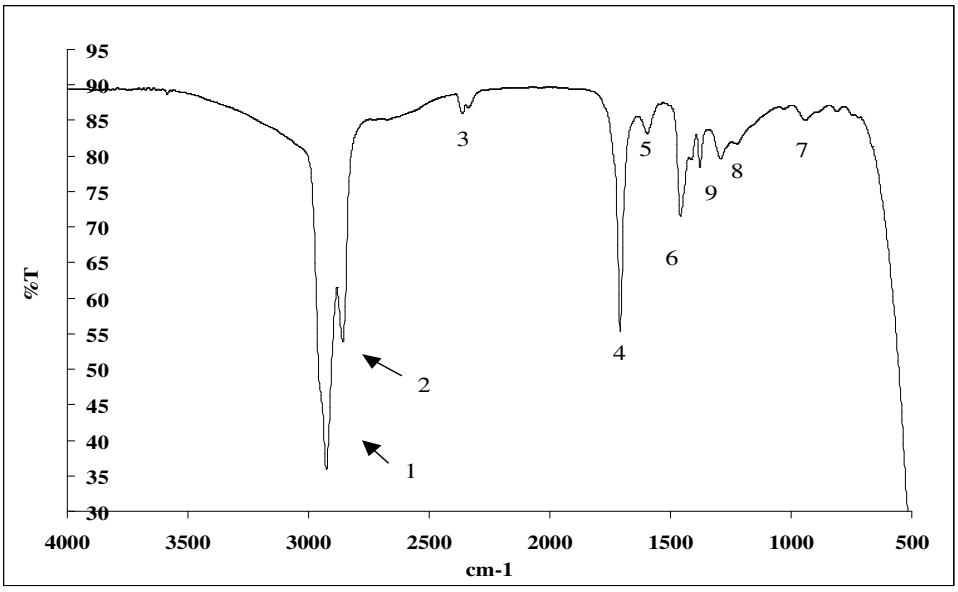

Figure 4.30. FTIR for naphthenic acid extract from Field Y sample.

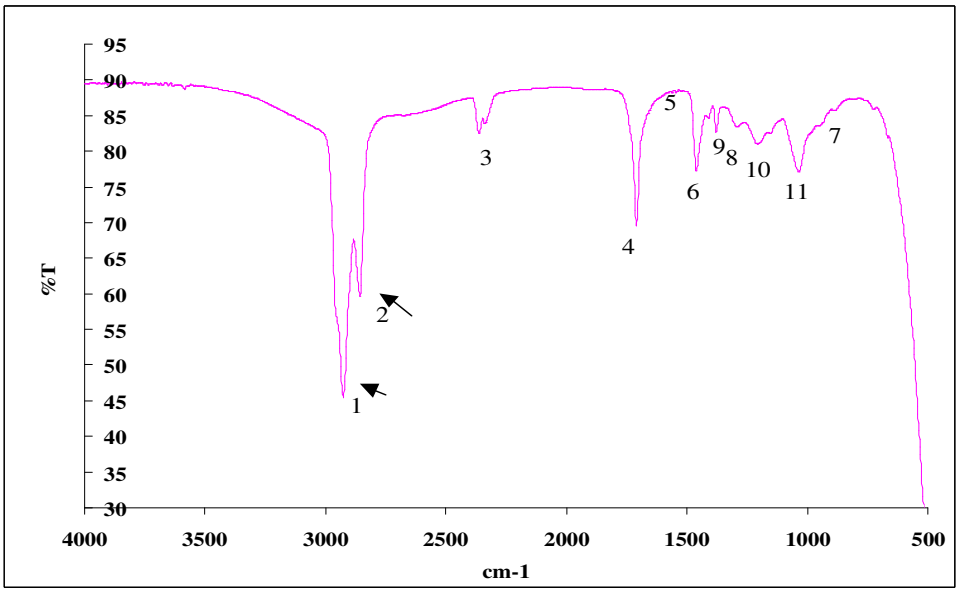

Figure 4.31. FTIR for naphthenic acid extract from Field Z sample.

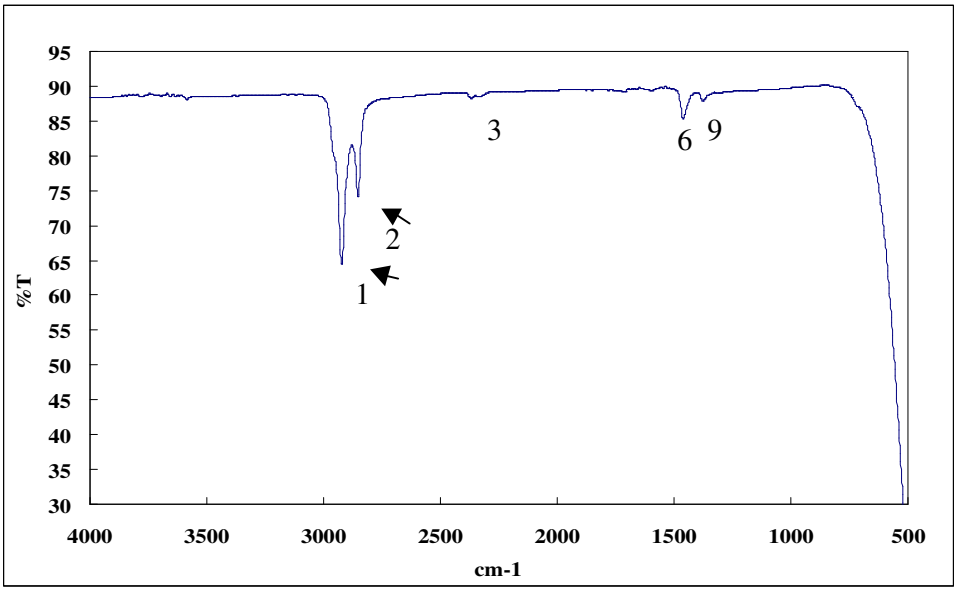

Figure 4.32. FTIR for naphthenic acid extract from Field W sample.

The spectra in Figures 4.29 to 4.31 show a number of common features. Peaks 1, 2 and 5 can be attributed to absorbance bands characteristic of CH, CH_2 or CH_3. CH and CH_2 stretches are usually observed in the 2926 to 2890 cm^{-1} range, as opposed to the CH_3 band which is usually observed in the 2962 to 2872 cm^{-1} range. However the current spectra do not allow these to be distinguished clearly. The exact differentiation of CH, CH_2 and CH_3 was however possible using NMR and this is shown in Section 4.1.3. In the spectra in Figures 4.29 and 4.31 there is also evidence of hydrocarbon in-plane bending or rocking given by peak 7. There is weak evidence of mononuclear aromatic hydrocarbons in the low frequency range. These are very weak signals (peak 6) for out-of-plane bending of the C-H aromatic bonds. There is also evidence of a weak band for C-C aromatic stretching (peak 3). It is likely these hydrocarbon peaks are a result of crude oil residue, which was originally embedded in the field deposits and was retained during the naphthenic acid extraction procedure.

Band	Wavelength (cm^{-1})	Assignment
1	~2900 to 2700	Symmetrical stretching CH, CH_2 or CH_3
2	~2900 to 2700	Symmetrical stretching CH, CH_2 or CH_3
3	~1600	C-H stretching (aromatics)
4	~1700	Dimer C=O stretch (carbonyl)
5	~1450	Scissoring vibration CH_2
6	~900 to 600	C-C stretching (aromatics)
7	~720	In plain rocking CH_2
8	~1200 to 1000	C-O stretch (carbonyl)
9	~1400 to 1350	Scissoring vibration CH_2 with some O-H bending (carboxyl)
10	~900	Bonded O-H groups (carboxyl)
11	~1000	Out-of-plane C-H bendings (aromatics)

Table 4.5. Assignment of FTIR bands in the naphthenic acid extracts.

Hydrogen bonding may occur in naphthenic acid solutions, particularly when dimers are formed. These may have a direct effect on the force of the carboxylic acid groups. In addition, concentration effects may affect both stretching and bending vibrations of naphthenic acids. Stretching C=O vibrations are usually reduced to a lesser extent than the stretching of the proton donor OH groups. For the naphthenic acid extracts in Figures 4.29 to 4.31, there are bands which may be attributed to C=O stretches (peak 4). Furthermore, an O-H stretch may also be attributed to carboxyl groups, usually at wavenumbers greater than 3200 cm^{-1}. There is evidence that this signal might be overlapping with the strong symmetrical C-H stretching bands. Thus, the O-H stretch could not be observed directly in any of the FTIR spectra for the naphthenic acids from the field soap samples. However, weak additional evidence of carboxylic acid functionalities can be observed in the C-O stretches in peak 8 (though only in Figure 4.30). In addition, O-H bending vibrations (between 1440 to 1395 cm^{-1}) occur as a moderate intensity band, but this is also superimposed with the scissoring vibration of the C-H groups (peaks 1 and 2). There is also evidence in some of the spectra of weak out-of-plane bends for bonded O-H groups, as can be observed in peak 10. This is typical fingerprinting for dimeric carboxylic groups, identifiable with a characteristic signal around 920 cm^{-1} (Silverstein *et al.,* 2005).

In Figure 4.32, the results for the naphthenic acids from Field W sample are presented. There are only hydrocarbon bands in this spectrum. The absence of the C=O carboxylic stretching bands at 1740 to 1750 cm^{-1} for monomers and from 1700 to 1735 cm^{-1} for dimers is probably an indication of low acid content in the naphthenic acid extract for this sample.

4.1.3. Solution nuclear magnetic resonance of naphthenic acid extracts.

Solution NMR results for the naphthenic acid extracts of the field deposits are now discussed. Samples from Field U and Field T were not evaluated since these did not represent soaps. Chemical shift assignments were carried out according to the published guidelines of Silverstein *et al.* (1991). Figure 4.33 presents the ^{1}H NMR spectra for all naphthenic acid extracts. Two well-resolved peaks between 1.5 and 0.8 ppm are observed which can be assigned to aliphatic alicyclic species. Some evidence of bi-substituted aliphatic species is also observed around 3.5 ppm. Very weak peaks which account for chemical shifts of trace impurities may be observed at around 1.5 ppm (water), 2.1 (acetic acid) and 2.3 (toluene). ^{1}H NMR is more sensitive than FTIR, and hence the reason that these contaminants were not observed in FTIR. A large peak at about 7.2 ppm was observed in all samples and can be ascribed to the deuterated chloroform used for preparation. Carboxylic protons are usually observed in ^{1}H NMR spectra between 13.2 and 10 ppm, as a result of stable hydrogen-bonded dimers formed from the OH groups. These peaks were not observed in any of the spectra. This result does not match the trends reported by Baugh *et al.* (2005a). It is likely this is due to concentration effects, which also resulted in poor FTIR spectra as discussed in Section 4.1.2. However, the presence of aliphatic alicyclic species given by the ^{1}H NMR results are in agreement with those reported by Baugh *et al.* (2004) and Brandal (2005) who analysed other soap samples.

Figure 4.34 presents ^{13}C NMR solution spectra for the same samples as those presented in Figure 4.33. The ^{13}C NMR traces consist of peaks between 40 and 10 ppm, centred around 30 ppm. These may be ascribed to acyclic hydrocarbons. The sharp peaks at 77 ppm may be assigned to the CH carbon from the deuterated chloroform used for sample preparation. The weak hump between 130 and 125 ppm is due to trace amounts of toluene, which was also used for sample preparation. Carboxylic carbons are usually found in the 185 to 150 ppm range; yet in the samples analysed in this thesis carboxyl groups were not identified. These results are in sharp contrast to the data of Baugh *et al.* (2004) who were able to show carboxylic carbons for derivatized naphthenic acids from soap samples. The derivatization procedure employed by these authors was aimed at producing methyl esters with lower boiling points compared to the original naphthenic acids. This was tailored to aid identification by MS, but also might have had an impact on detection of the carbonyl signal in NMR.

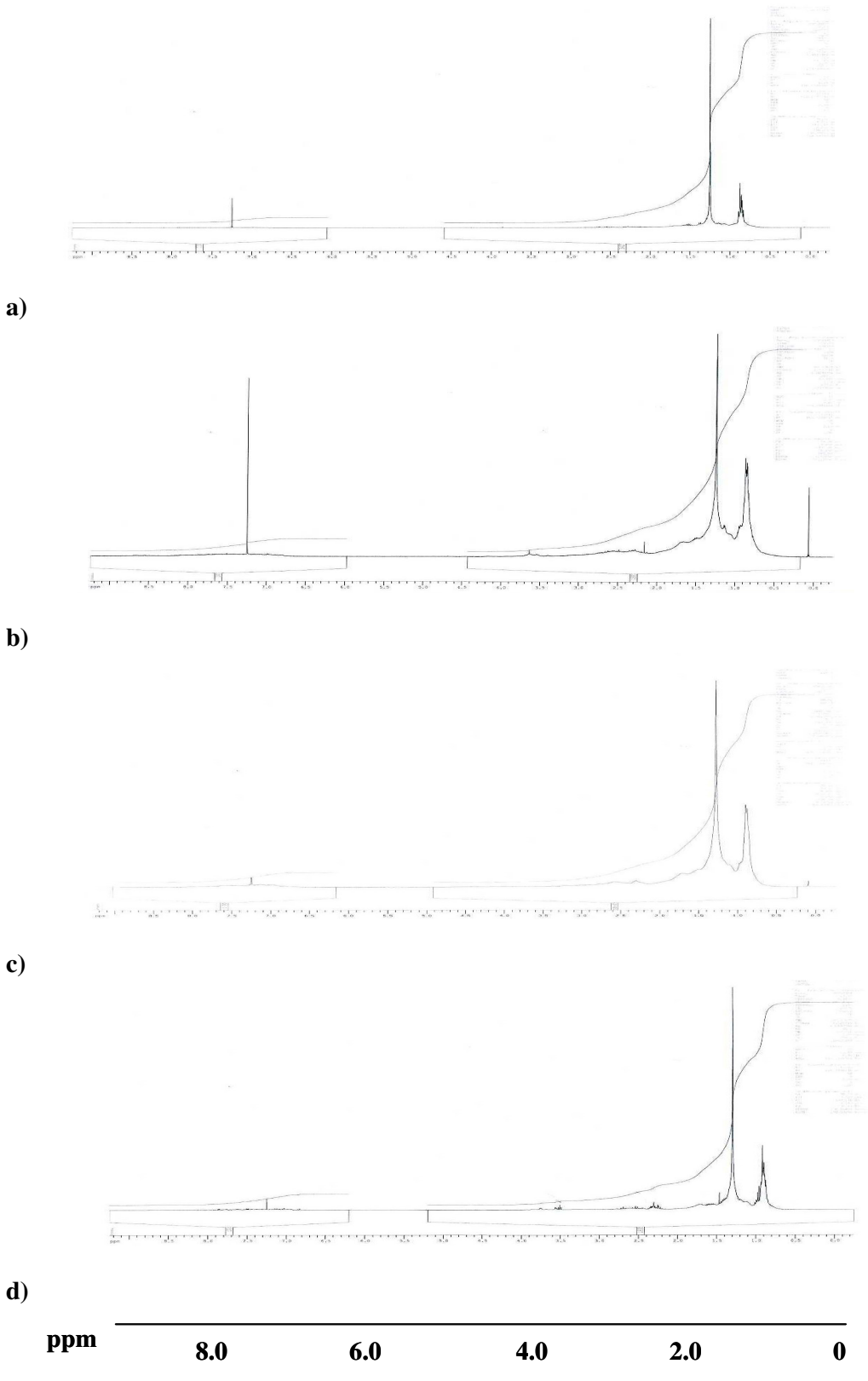

Figure 4.33. ^{1}H NMR spectra for naphthenic acid extracts from field deposit samples. a) Field Y, b) Field X, c) Field Z, d) Field W.

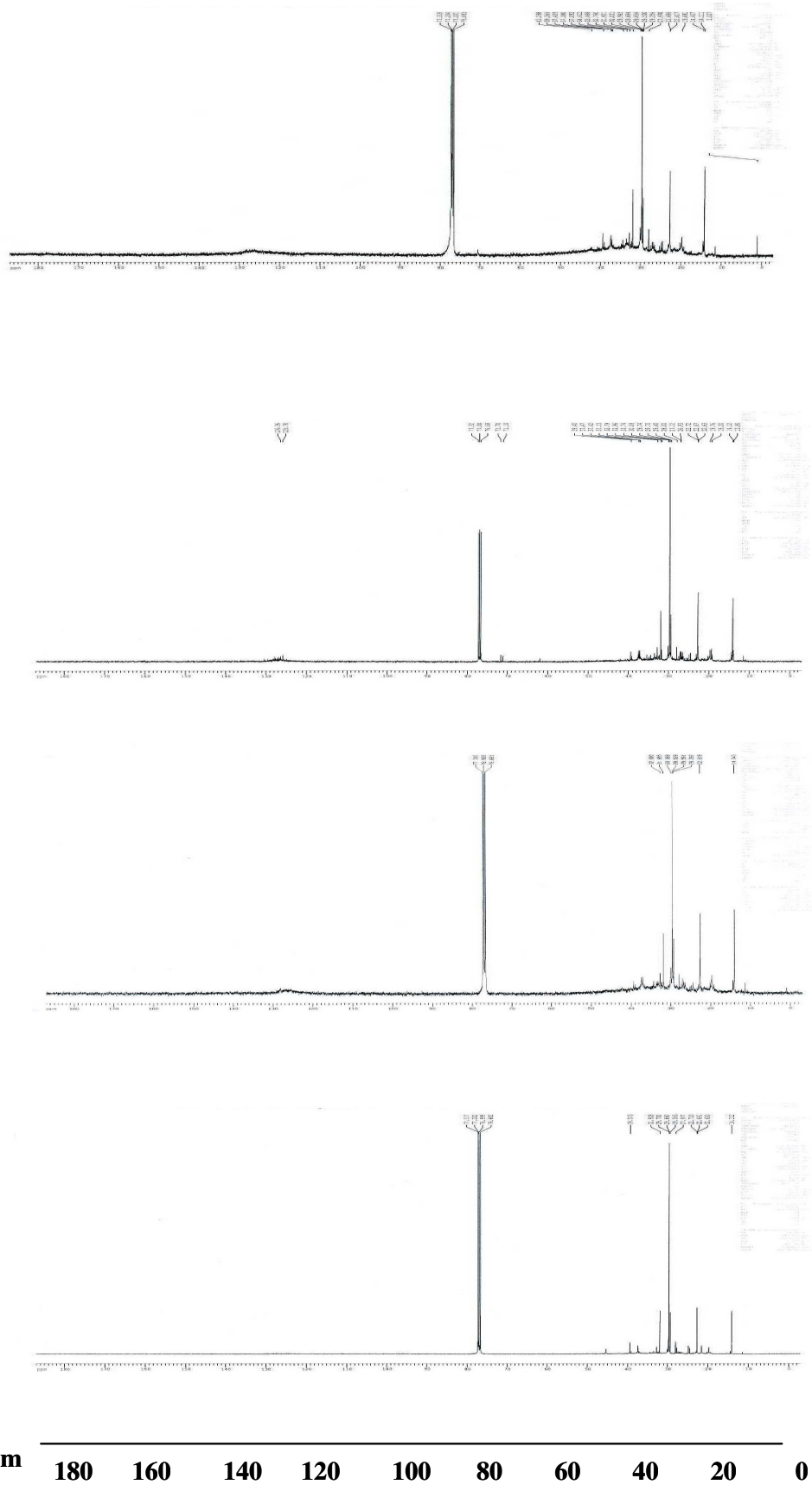

Figure 4.34. ^{13}C NMR spectra for naphthenic acid extracts from field deposit samples. a) Field Y, b) Field X, c) Field Z, d) Field W.

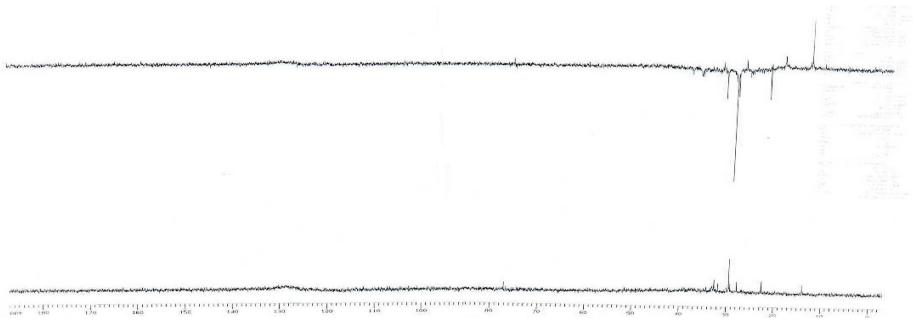

a)

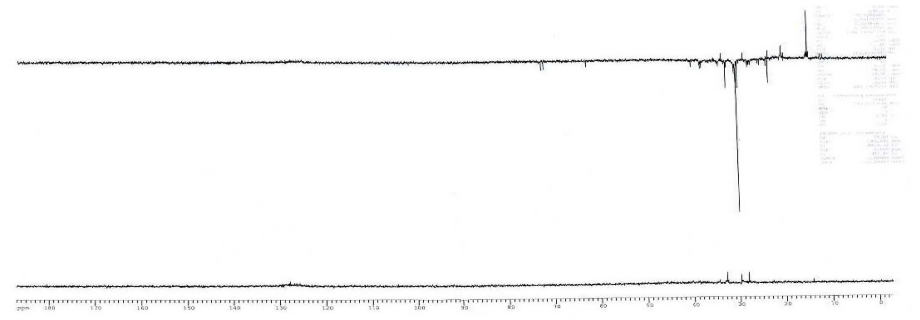

b)

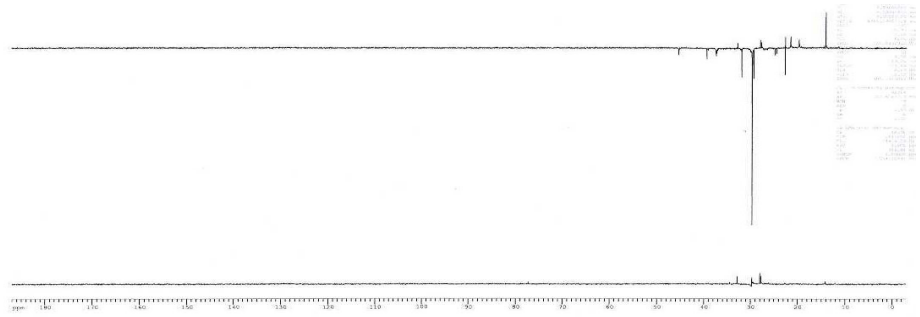

c)

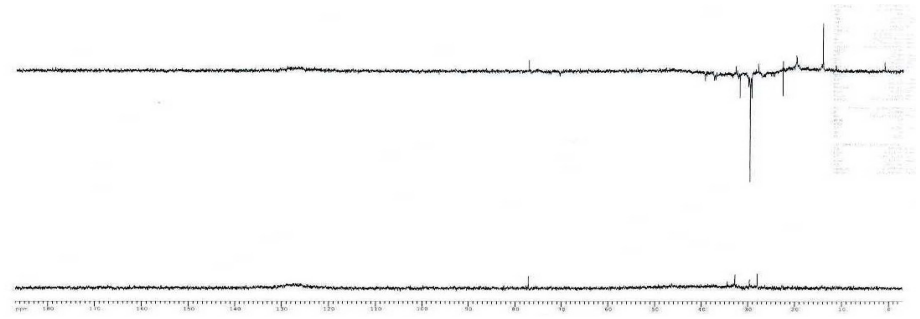

d)

ppm 180 160 140 120 100 80 60 40 20 0

Figure 4.35. DEPT ^{13}C NMR spectra for naphthenic acid extracts from field deposit samples. a) Field Y, b) Field X, c) Field Z, d) Field W.

The DEPT ^{13}C NMR spectra (Figure 4.35) allows the number of protons directly attached or coupled to an individual ^{13}C nucleus to be assigned. The spectra must be compared to the previous spectra in Figure 4.34 which presents the proton decoupled carbon information. In DEPT spectra, CH_3 and CH are phased up, whereas CH_2 are phase down. In Figure 4.35, it can be observed that the overwhelming majority of coupled peaks are resulting from CH_2 groups. There are also indications of CH and CH_3 groups, but the signals are less intense. No quaternary carbons were detected for the soap samples.

In conclusion, hydrocarbon resonances were observed to be predominant in the ^{13}C NMR solution spectra of the naphthenic acid extracts. This could not support the evidence of carboxylic groups in the acid extracts, as suggested by some of the FTIR results. In addition, no further conclusions could be reached in regards to possible structures in the naphthenic acid extracts in these samples. To eliminate the possible influence of concentration effects, solid-state ^{13}C NMR was employed with the field deposit samples *in natura*, and these results are discussed next. This also enabled the characterisation of the deposits sampled from Fields U and T which were not soap deposits *per se*.

4.1.4. Solid State nuclear magnetic resonance of field deposits.

Solid state ^{13}C NMR spectra were obtained for all field deposit samples. Figure 4.36 presents some of the results using the cross polarisation (CPMAS) method for the deposit sample from Field Y. Spectrum referencing was carried out relative to a tetramethylsilane reference. Peaks can be observed in two main ranges of the spectrum: 46 to 19 ppm and 185 to 178 ppm. Table 4.6 presents a compilation of chemical shifts taken from the literature for species containing carboxylic groups as well as some reference hydrocarbons (Silverstein *et al.,* 2005). It should be noted that the chemical shifts are for solution NMR. However this data should be close to solid state values, but not necessarily identical. This data may be used in the interpretation of the results for the deposit sample from Field Y, as well as the signals from the DEPT spectra in Figure 4.35. Table 4.6 shows that methyl-terminated linear chains (CH_3) result in a low-frequency signal between 14 and 9 ppm. There are no signals in this range for the deposit from Field Y in Figure 4.36. In addition, methyl-terminated linear chains do not give signals above approximately 36 ppm. There is a significant amount of these signals in Figure 4.36. The cycloaliphatic compounds detailed in Table 4.6 have signals in the range of those shown for the deposit sample from Field Y. This is true for species where the carboxyl group is a substitute of the ring (C acid) and when there is an aliphatic chain separating the ring and the carboxylic group (Ring CH). In addition, Figure 4.36 shows a signal at 19 ppm. A methyl group directly attached to a ring

could account for this, but a methyl in any other position would occur at significantly lower frequencies. The highest frequency signal from the carbon bonded to the acid occurs for secondary acids according to Table 4.6. Additional dipolar dephasing (DD) experiments confirmed the peak at 19 ppm could be the result of a methyl carbon (results not shown). The peak around 180 ppm is consistent with carboxylic acid carbons. Despite the lower sensitivity of solid state ^{13}C NMR, the results are comparable to those presented by Baugh *et al.* (2005a) using solution ^{13}C NMR. Thus the most likely structures present in the deposit sample from Field Y would be cyclic structures with aliphatic chains separating the ring from the carboxyl group, preferentially.

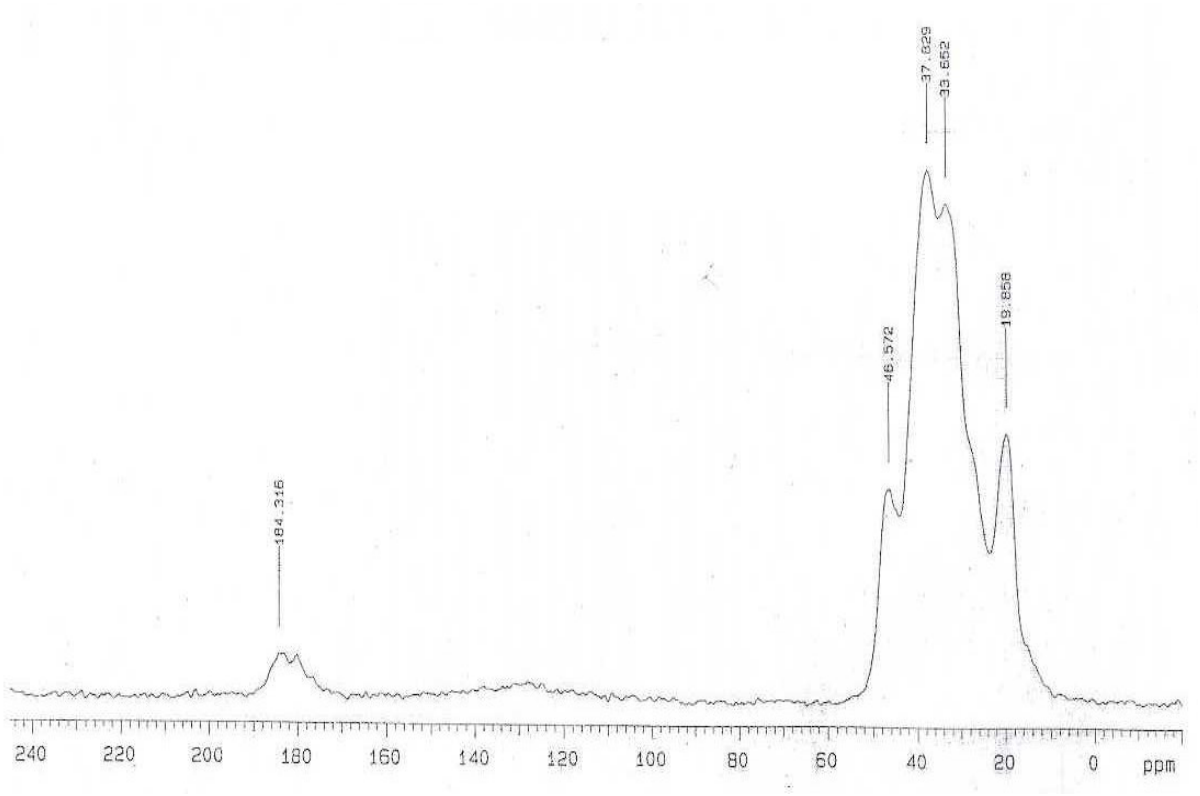

Figure 4.36. ^{13}C NMR CPMAS spectrum for deposit sample from Field Y.

Figure 4.37 presents the ^{13}C NMR spectra for two additional field deposit soap samples. The results support the previous conclusions in regards to the fingerprinting for the deposit sample from Field Y, e.g. the presence of a carboxylic acid carbon, and the presence of both cyclic and straight chain carbon backbones. The spectrum for the deposit sample from Field W is presented in Figure 4.38. Owing to sample viscosity, a normal spinning CPMAS experiment did not result in good spectrum. The only observable signal is consistent with CH_2 from a linear hydrocarbon chain. As a compromise, a slow-spinning direct polarisation (DP) experiment was carried out. This is very similar to a solution NMR

experiment but without cross polarisation. The spectrum is presented in Figure 4.39. The DP experiments produced a spectrum showing a range of aliphatic signals. In addition, the broad line at 110 ppm is a background signal from the material in the rotor (teflon). No carboxylic acid carbon signal was observed for this sample. This is also probably due to concentration effects, e.g. low carboxylic acid amounts in the sample.

Species	**CH_3**									**C Next to CH_3**	**Ring CH**	**C acid**	**COOH**
Dodecanoic	14.1	22.8	24.8	29.2	29.3	29.4	29.5	29.7		32.0		34.2	180.7
Octanoic	14.1	22.7	24.8	29.0	29.2					31.8		34.3	180.8
Hexanoic	13.9	22.4	24.5							31.4		34.2	180.8
Pentanoic	13.7	22.3								26.9		34.0	180.9
Butanoic	13.7									18.4		36.2	180.7
Propionic	8.9											27.6	181.5
Cyclohexane carboxylic		25.5	25.8	28.9								43.1	183.0
Cycloheptane carboxylic			26.3	28.4						30.7		44.9	183.9
Cyclohexyl ethanoic			26.1	26.2						33.1	42.1	34.7	180.0
Cyclohexyl butanoic		22.1	26.4	26.7						33.3	37.4	34.4	180.5
Methyl cyclohexane	23.0	26.5	26.6							35.6	32.9		
Ethyl cyclohexane	11.4	26.6	26.9						30.2[b]	33.2	39.7		
Butyl cyclohexane	14.2	26.6	26.9		29.3[b]	23.1[b]			37.4[b]	33.6	37.8		
2-ethylbutyric acid	11.8		24.9									48.9	183.3
2-ehtylhexanoic acid	11.8[b]	14.0	22.8	25.3	30.0				25.3[b]	31.6		47.3	183.3

Note: Blank cells = signal absent, b = branched, C acid = carboxyl group is a substitute to the ring, Ring CH = there is a chain separating the carboxyl group from the ring.

Table 4.6. Chemical shift template list for selected naphthenic acids and hydrocarbons (Silverstein *et al.,* 2005).

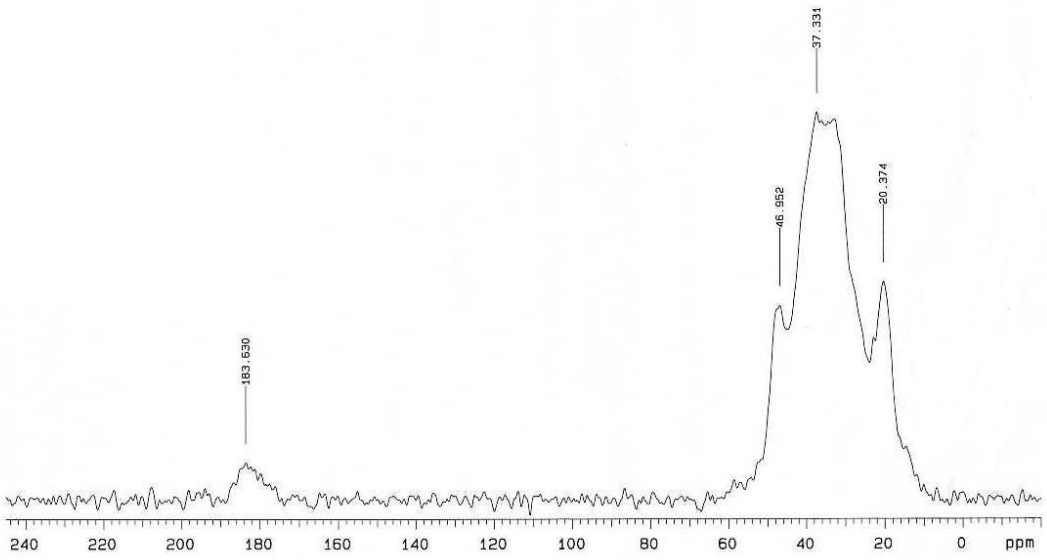

a)

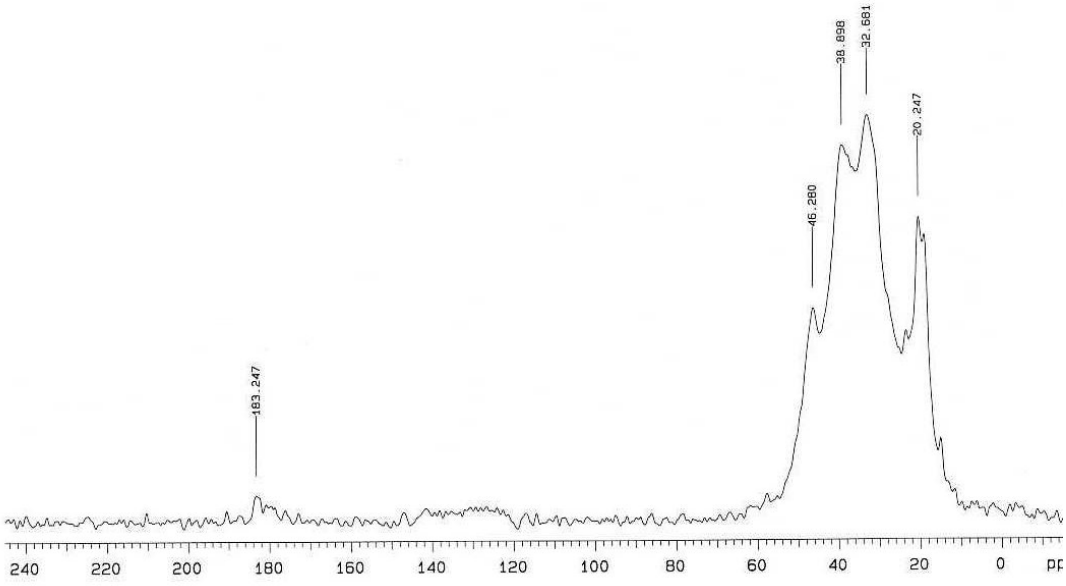

b)

Figure 4.37. ^{13}C NMR CPMAS spectra for deposit sample from Field Z (a) and Field X (b).

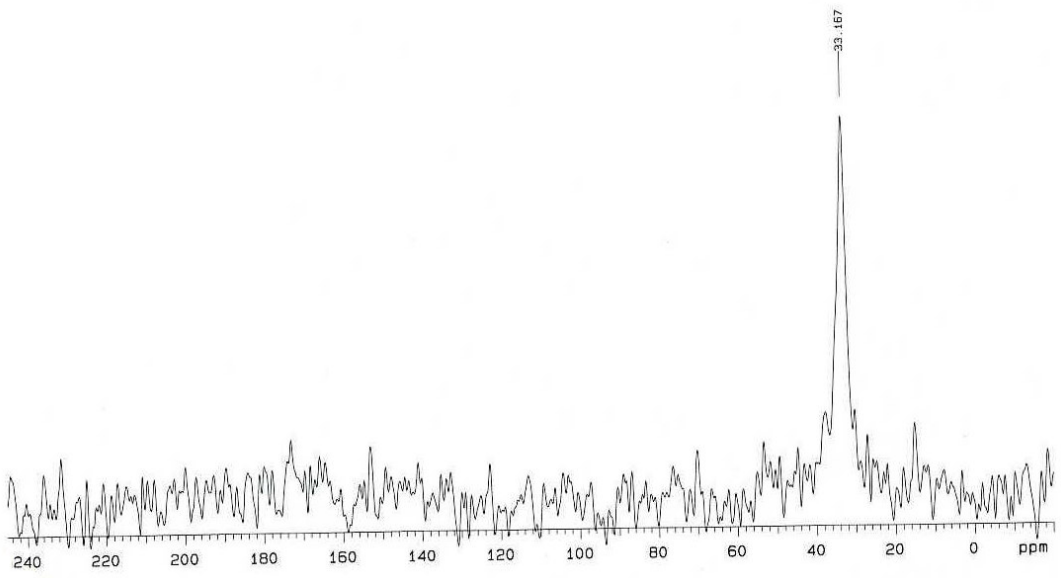

Figure 4.38. ^{13}C NMR CPMAS spectrum for deposit sample from Field W.

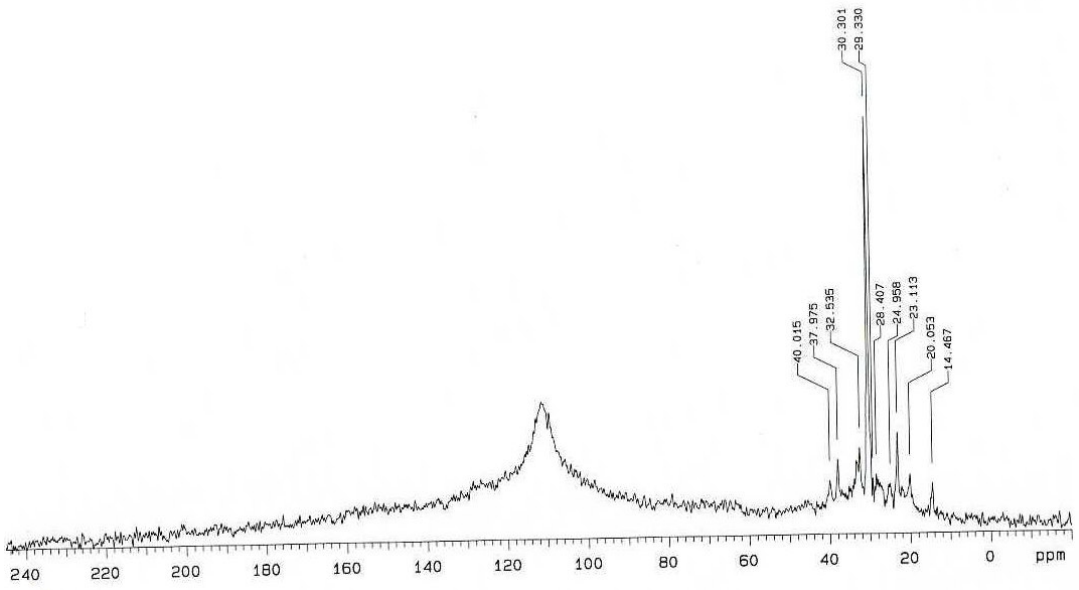

Figure 4.39. ^{13}C NMR DP spectrum for deposit sample from Field W.

Both CPMAS and DP experiments were also carried out for the deposit sample from Field U. The CPMAS spectrum produced very low signal-to-noise ratio and is shown in Figure 4.40. It can be observed that overall fingerprinting for this sample is very different to those of the soap samples shown in Figures 4.36 and 4.37. This sample is more gel-like and the

trace in Figure 4.40 suggests relatively mobile components, which is consistent with a large number of narrow lines in the DP spectrum shown in Figure 4.41. This sample also presents aliphatic signals between 40 and 18 ppm. Interestingly, a carboxylic acid carbon signal at 176 ppm can also be observed. This signal is somewhat sharper than those observed for the samples in Figures 4.36 and 4.37, which may suggest a smaller range of compounds is contributing to it. This sample also presents aromatic signals at 120 ppm and a signal at 110 ppm, the latter being due to background teflon material in the rotor. However, the biggest differences observed in this sample compared to those in Figures 4.36 and 4.37 are the presence of signals between 80 and 60 ppm. These may be attributed to alcohol or ether species. It is likely that the alcohol and ether peaks are due to the chemical inhibitor used to mitigate this soap in field conditions. Figures 4.42 and 4.43 show ^{13}C NMR spectra for the deposit sample from Field T. This deposit consisted of an asphaltene sample. Two sub-samples of this deposit were analysed by ^{13}C NMR: the first *in natura* (Figure 4.42), and the second which was treated with 100 ml of a toluene wash (Figure 4.43). The spectra in Figures 4.42 and 4.43 appear similar to the solution ^{13}C NMR of asphaltene fractions separated from crude oils in laboratory conditions (Anchyeta *et al.,* 2002). Two clear regions of aromatic carbons (between 135 to 115 ppm and from 200 to 95 ppm) and a region of aliphatic carbons (40 to 0 ppm) can be observed. The aliphatic signals are located in the same range as in the soap spectrum of Figure 4.36. The signals between 200 and 195 ppm correspond to spinning sidebands. The spectrum of the sample subjected to the toluene wash (Figure 4.43) contains weaker aromatic signals (which could indicate removal of many aromatic asphaltene components). Despite the toluene wash, no evidence of any signal due to naphthenic acids was observed in the asphaltene deposit (e.g. carboxylic acid carbon at 180 ppm).

In summary, the solid-state ^{13}C NMR spectra allowed for a better chemical differentiation of the parent naphthenic acids in the field soap deposit samples (Field X, Y, Z). In addition, ^{13}C NMR allowed for the observation of possible chemical inhibitor families used to mitigate field soap samples (Field U). An asphaltene deposit was also analysed for the presence of naphthenic acids (Field T). No evidence of naphthenic acids was observed from these tests in the asphaltene samples.

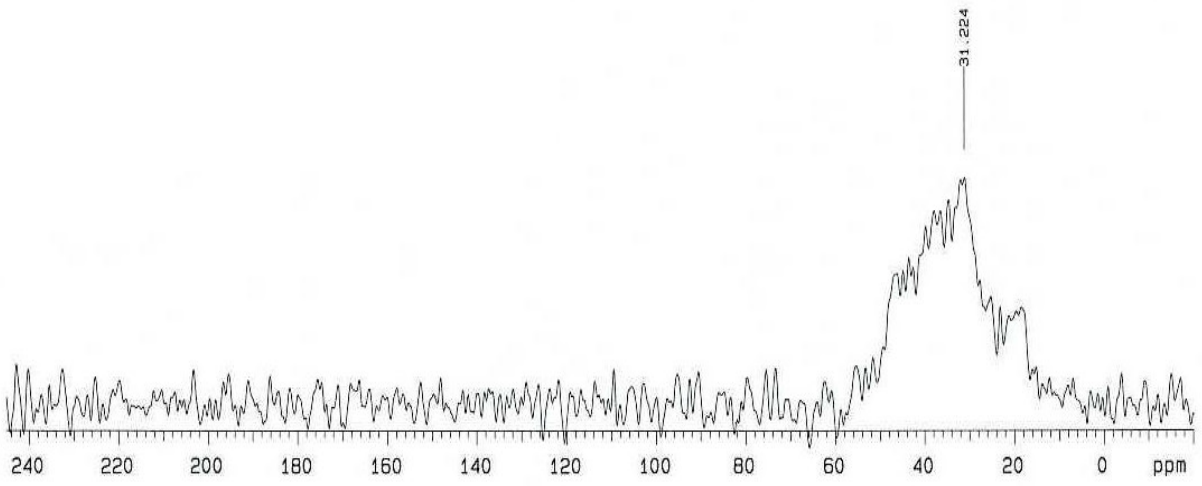

Figure 4.40. ^{13}C NMR CPMAS spectrum for deposit sample from Field U.

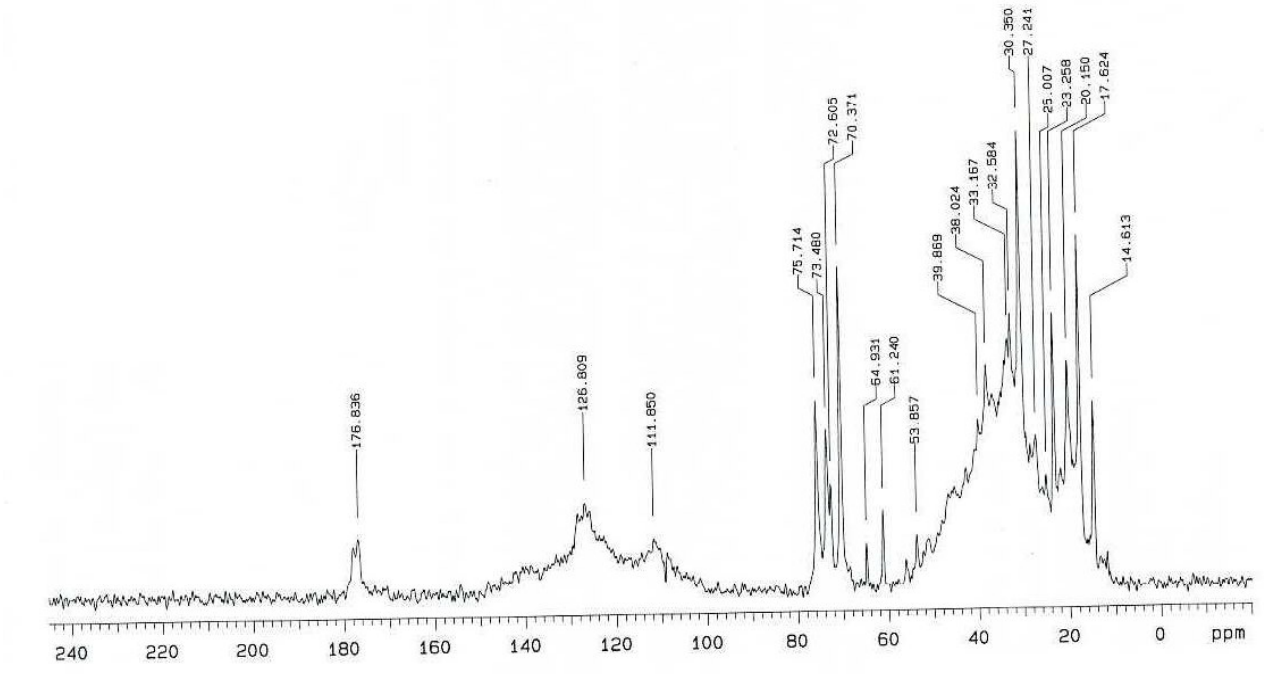

Figure 4.41. ^{13}C NMR DP spectrum for deposit sample from Field U.

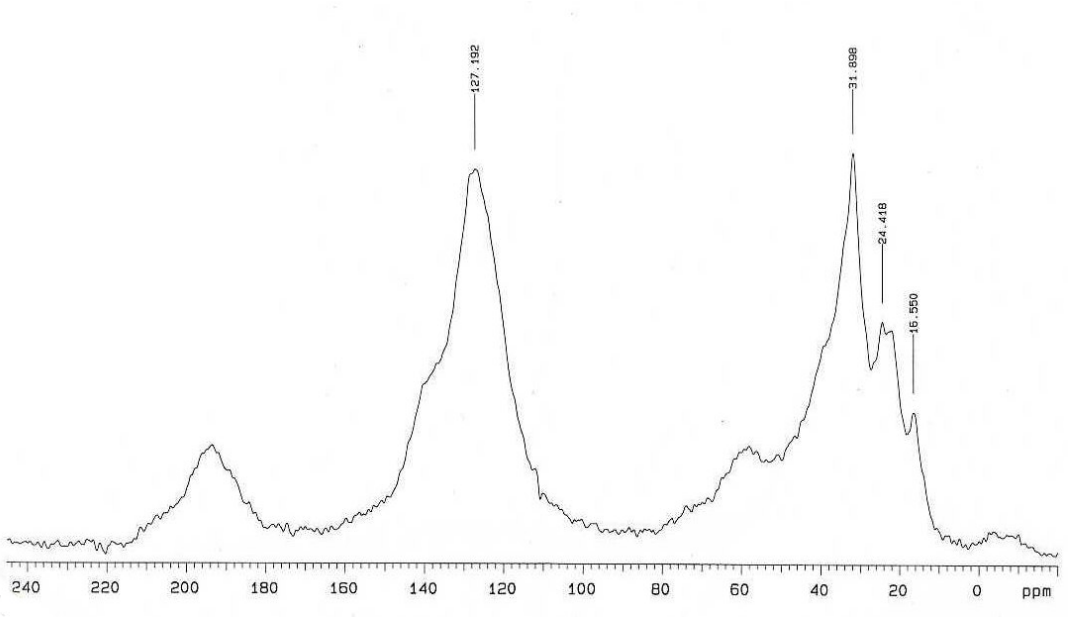

Figure 4.42. ^{13}C NMR CPMAS spectrum for deposit sample from Field T *in natura.*

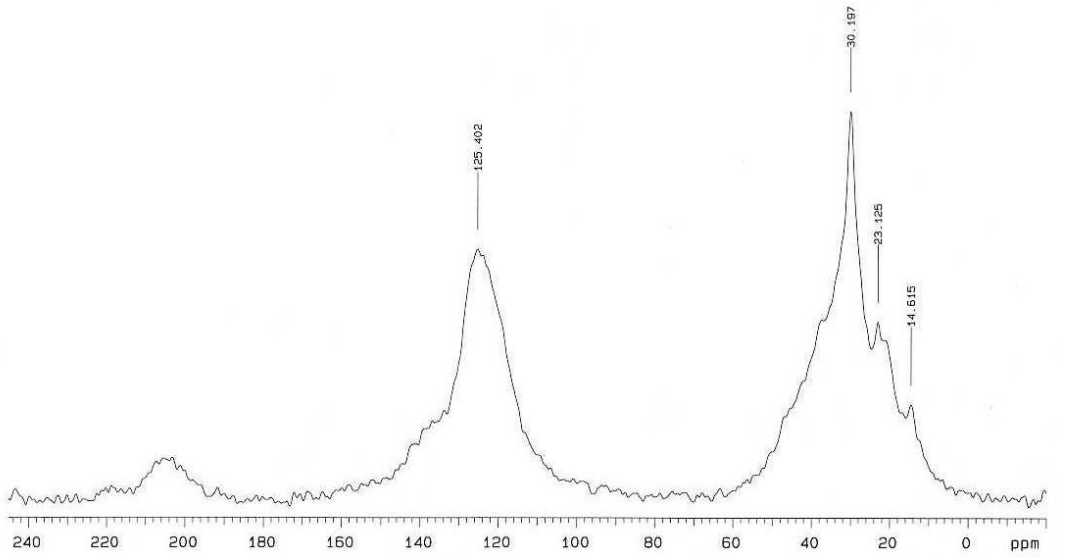

Figure 4.43. ^{13}C NMR CPMAS spectrum for deposit sample from Field T (after toluene wash).

4.2. Thermal behaviour of field samples.

The thermal analysis of the field samples are discussed next using results from both TGA and DSC. Figure 4.44 shows the TGA profile for a series of samples from Field Y namely: a separator crude oil, the corresponding field soap deposit, the clean calcium soap scale as well as the indigenous naphthenic acids from this deposit.

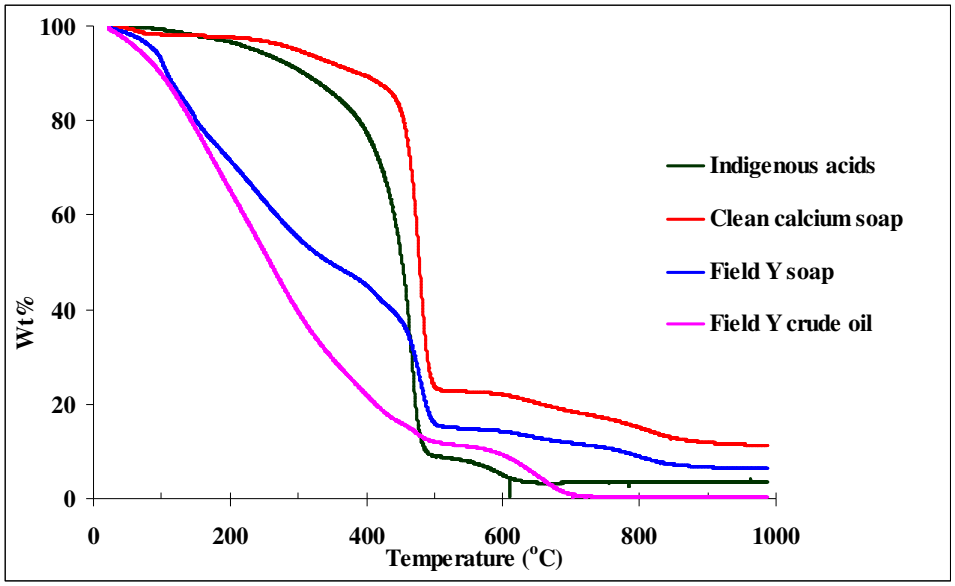

Figure 4.44. TGA of samples from Field Y. Indigenous acids refer to the acids extracted from the clean calcium soap. Clean calcium soap refers to the field soap sample after crude oil removal.

The trend of the indigenous naphthenic acids was used as a template for interpretation. It was expected that their properties would determine the overall thermal characteristics of Field Y samples. It can be seen in Figure 4.44 that the indigenous acids show gradual weight loss from ambient to around temperatures of 400 °C, whereupon more significant weight loss occurs. Further weight loss is observed between 500 and 600 °C. The TGA profile for the clean calcium soap is remarkably similar to that of the indigenous naphthenic acids. A major weight loss transition is observed at 470 °C, with a small weight loss prior to this at 50 °C. Two further weight losses are seen at 600 and 700 °C. Compared to the TGA of the indigenous naphthenic acids, it can be seen that the clean calcium soap is more thermally stable at 500 °C: 20 wt% of the original sample weight is present at this temperature, as compared to less than 10 wt% for the indigenous naphthenic acids. The high melting point of the indigenous naphthenic acids used in this thesis may be explained by the presence of carboxyl groups, which may be involved in strong hydrogen bonding (Morrison and Boyd, 1979). In salts of carboxylic acids, the strong electrostatic forces

holding the ions in the lattice can only be overcome by high temperatures. The temperature required for melting these salts is so high that carbon-carbon bonds may break, leading to the decomposition of the molecule around 300 to 400 °C (Morrison and Boyd, 1979). However, as can be observed in Figure 4.44, the clean calcium soap is stable at temperatures well above this. The DSC data for the same samples from Field Y are presented in Figure 4.45. The DSC results for the indigenous naphthenic acids are characterised by 4 or 5 endothermic transitions across the entire temperature range tested. The most significant is at 450 °C, but there are others at 91, 205 and 365 °C. There is good agreement with the TGA data from Figure 4.44, where a major weight loss transition was observed at 470 °C. It is very likely that the endothermic features observed above 400 °C represent phase transition from solid to vapour, where the soap structure begins to break. For the clean calcium soap, these endotherms are also observed, but two other features are also present: an endotherm transition at 71 °C and an exotherm at 196 °C. The transition at 71 °C represents a weight loss of 1.85 % which could be solvent evaporation. Since no weight loss occurred at 196 °C (as shown by TGA in Figure 4.44), it is likely that this exotherm represents crystallisation or a solid-solid phase transition associated with solvent removal. Weight losses above 600 °C could not be analysed due to DSC hardware limits.

The main thermal analysis feature of the clean calcium soap from Field Y, the endotherm at 470 °C, is also observed in the deposit sample from Field Y as shown in Figure 4.44. However it could not be identified in the parent crude oil. This may be attributed to components which are in higher concentrations in the soaps than in crude oils, such as naphthenic acids or their salts, which have been removed from the parent crude oil due to precipitation. Both TGA and DSC trends for the indigenous naphthenic acids (which are salt-free) are also observed in the clean calcium soap. It is likely that the thermal trends are therefore a result of the main structures present in the indigenous naphthenic acids.

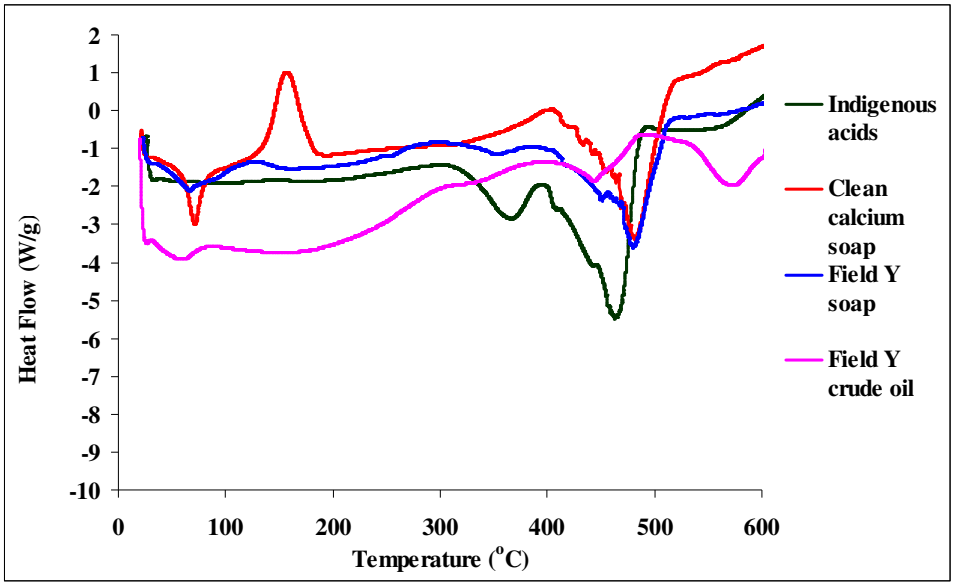

Figure 4.45. DSC of samples from Field Y. Indigenous acids refer to the acids extracted from the field soap. Clean calcium soap refers to the field soap sample after crude oil removal.

Figure 4.46 presents the TGA profiles for the field deposit samples from other geographical regions. The sample from Field T shows a very different trend from the other deposits. It can be observed that it is thermally stable even at 1000 ºC, where 40 wt% of the original sample remains. Work by Ali and Alqan (2000) has shown that asphaltene solids taken from field samples are stable up to 800 °C (45 wt% of the original sample remaining at this temperature). The authors attributed the stability above 650 °C to inorganic species entrained in the asphaltenes, although precise quantification and identification was not presented.

The deposit sample from Field W showed evidence of trends commonly associated with glass transitions around 36 and 56 °C in the DSC profile. This information is shown in Figure 4.47. The deposit sample from Field W also shows large endotherms between 100 and 150 °C which agree with the TGA profile, probably due to loss of water and solvent entrained in the deposit. The deposit samples from the remaining fields show a more gradual weight loss over the temperature range studied with noticeable changes occurring before 500 ºC. Samples from Fields X, Z and U, on the other hand, are characterised by one major weight loss transition at 470 °C (Figure 4.46). This is consistent with the pattern observed in Figure 4.44 for the sample from Field Y.

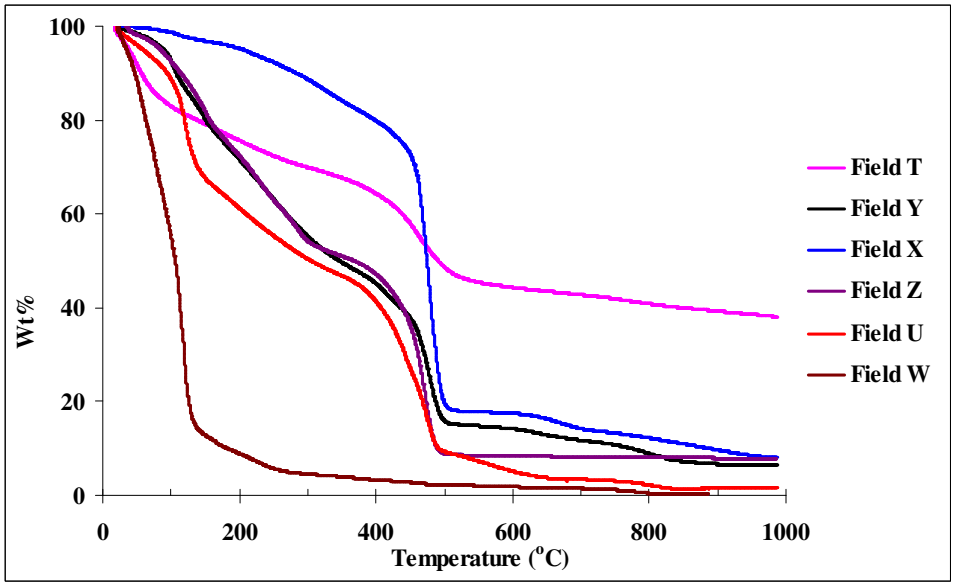

Figure 4.46. TGA of selected field deposits. Samples represent soaps from the different fields analysed in this thesis (note Field T is an asphaltene deposit).

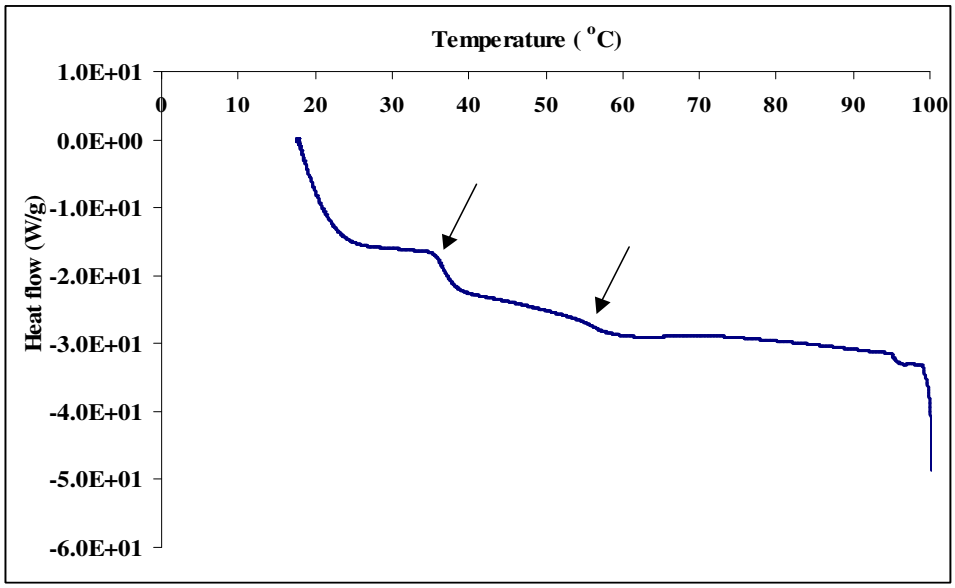

Figure 4.47. DSC soap sample from Field W. Arrows represent possible glass transition temperatures.

Figure 4.48 presents the DSC of the remaining field deposits analysed in this thesis. There is good qualitative agreement of the samples from Fields X, Z and U with that of Field Y shown in Figure 4.44, particularly above 150 °C, after water and other solvents have been removed. These deposits also show a major endotherm at around 470 °C, while the samples from Field T and Field W do not. The deposit sample from Field U also showed high thermal stability, even though this sample was not a calcium naphthenate soap scale deposit

per se (further EDAX results in this chapter will support this). Because this sample is not a soap, it can be suggested that its inherent thermal stability may be due to the indigenous naphthenic acids it contains. The deposit from Field U presented the highest concentration of Arn in the indigenous acids found in this thesis (see Table 4.4). Thus, results in this section suggest that thermal stability may be a result of the Arn present in these samples. However further tests would need to be carried out to support this claim, such as, thermal analysis directly on the separated Arn species from the indigenous acids.

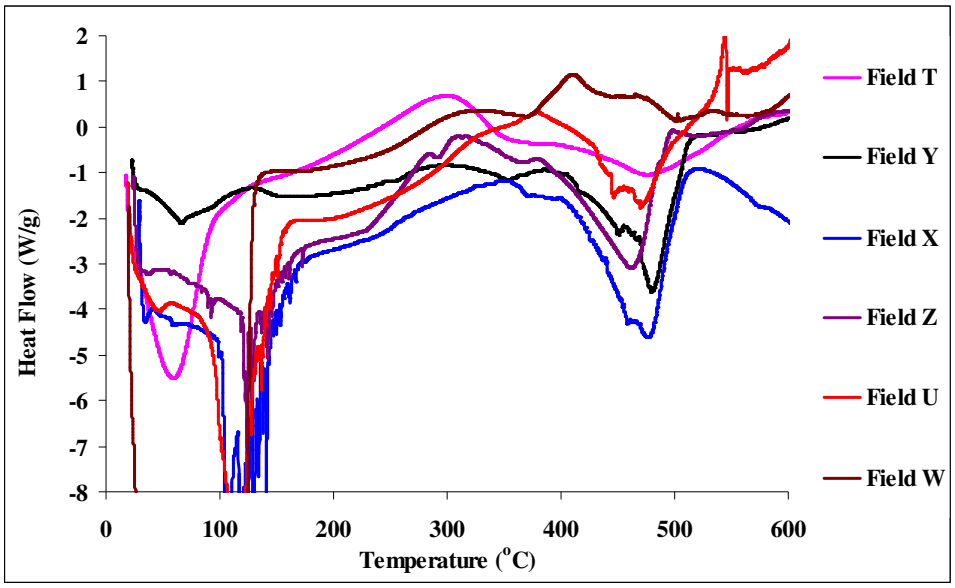

Figure 4.48. DSC of selected field deposits. Samples represent soaps from the different fields analysed in this thesis (note Field T is an asphaltene deposit).

4.3. Elemental composition.

Figure 4.49 contains digital images of the field deposits analysed in this thesis. The deposits showed two end-member types of textures: rock-hard consistency (Fields X, Y, Z and T) and soft sludge type (Fields U and W). Most deposits had a dark, black-brown colouring, with the exception of Field W which was a much lighter brown, similar in shade to a "café-latte". Field T also exhibited some differences in respect to the other samples since it was very shiny, flaky and brittle. A sensitivity study was conducted with samples from Field Y, Field W and Field T to gain information on the inorganic constituents present. Techniques used were elemental analysis, energy dispersive X-ray (EDAX) and X-ray fluorescence (XRF).

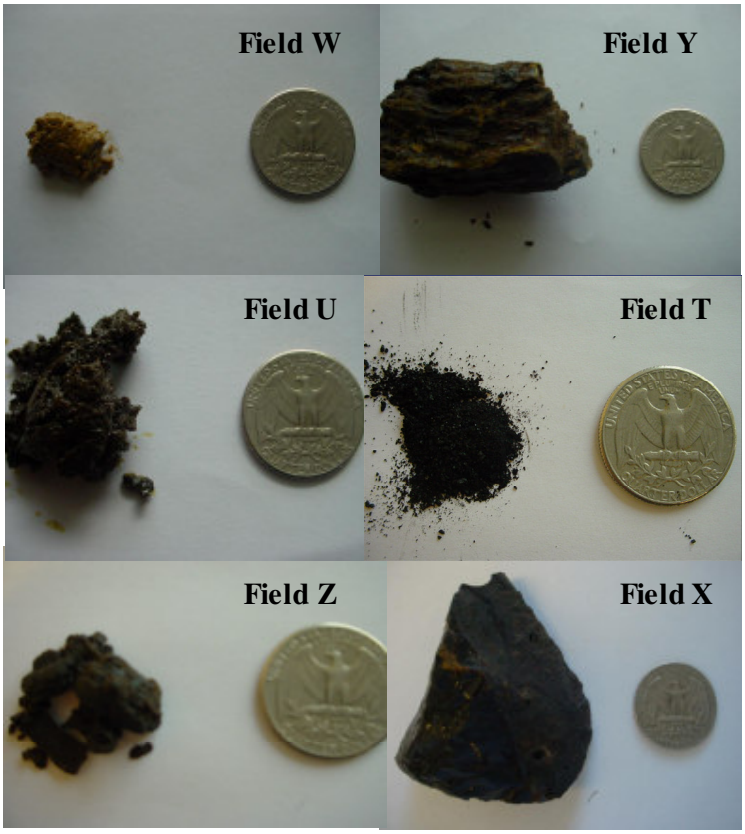

Figure 4.49. Morphological analysis of field deposits.

4.3.1. Elemental analysis.

Table 4.7 presents the elemental analysis of selected field deposits as given by the Leco instrument and procedure details in Section 3.4.1. Note oxygen was not measured in this test. Thus, empirical formulae for the deposit naphthenic acids will not be proposed.

Sample	C	H	N	C/H	DBE
Field W	52.9	10.7	0.4	4.9	88.9
Field Y	71.6	10.3	0.2	6.9	91.8
Field T	82.5	7.9	0.7	10.4	94.2

Note: C= carbon, H = hydrogen, N = nitrogen, DBE = double bond equivalent.

Table 4.7. Elemental analysis of selected field samples.

Saab *et al.* (2005) showed that naphthenic acids extracted from crude oils had C/H atomic ratios around 7.1. The three field deposits analysed here showed different elemental compositions as given in Table 4.7. Common crude oil solubility fractions (which contain naphthenic acids) may have low C/H values, as in resins (e.g. lower than 9), or high C/H

values, as in asphaltenes (e.g. higher than 10) (Acevedo *et al.,* 1985). The C/H data as well as the DBE values in Table 4.7 suggest increasing aromaticity in the order Field T followed by Field Y and Field W. This could be related to the precise type of naphthenic acids in the deposits. The sample from Field Y was shown to contain Arn acids as well as a high percentage of high molecular weight naphthenic acid species compared to the Field W sample which contained a predominance of acyclic acids (Table 4.4). In addition, the ^{13}C NMR analysis for the Field T sample showed a high content of aromatic material, which was not observed in either the Field Y or Field W samples. The C/H and N data for the Field T sample is consistent with the data for asphaltene deposits as reported by a number of authors (Escobedo and Mansoori, 1992; Sato *et al.,* 2005). These results confirm that Field T sample is an asphaltene deposit, as suggested by both the sample providers and the results of ^{13}C NMR, TGA/DSC and MS measurements shown in this chapter.

The C/H value for the Field Y sample (6.9) is in line with the reported value (6.8) for another calcium naphthenate soap scale as given by Baugh *et al.* (2005). C/H values for the Field W (4.9) are slightly lower than those reported by Gallup *et al.* (2004) for a sodium carboxylate soap emulsion (5.7). Of course the samples in this thesis cannot be precisely ascribed to calcium or sodium-containing soaps, given elemental analysis results only. Therefore it would be unlikely that this elemental analysis technique could be used as a fingerprint for soap deposits.

4.3.2. X-ray fluorescence.

Table 4.8 presents the XRF analysis of selected field deposits. The objective of using XRF for soap analysis was to examine the predominant cations. Prior to analysis, as described in Section 3.4.2, samples were fired at 400 ^{o}C overnight to remove hydrocarbons, then ignited at 1100 ^{o}C to obtain a loss on ignition (LOI) index. Silicon dioxide (SiO_2) was added if the LOI was very high. The Field T sample gave so little residual material after firing off the organics (less than 10 mg) that the XRF numbers are meaningless and thus are not presented. For this reason, the samples from Field X were included as a replacement in the XRF analysis.

Field	% SiO_2 added	SiO_2	Al_2O_3	Fe_2O_3	MgO	CaO	Na_2O	K_2O	TiO_2	MnO	P_2O_5	Totals %
W	0.50	2.75	1.62	2.08	2.91	5.03	36.25	0.81	0.10	0.01	0.15	51.71
Y	0.17	3.13	1.22	1.71	2.20	34.36	3.42	0.18	0.05	0.42	4.23	50.93
X	0.15	1.51	0.93	4.87	1.74	38.64	1.97	0.12	0.13	0.23	1.87	52.01

Note: % SiO_2 added denotes the amount on a weight basis used for topping.

Table 4.8. XRF results for field deposits samples.

In Table 4.8 samples are speciated as oxides following the ignition procedures described in Section 3.4.2. Field samples Y and X show low totals (about 51 %) with appreciable amounts of calcium, iron and magnesium oxides. This can be attributed to loss of carbon dioxide and may be interpreted as the decomposition of the naphthenic acids originally present. If all the calcium in these samples can be assigned to calcium naphthenate soap scales, then the amount of naphthenate scale in the soap deposits would be 34 and 38 wt% of the total values in Table 4.8, i.e. 74 and 67 wt% respectively. The Field W sample also shows the same order of magnitude of sample loss, yet the predominant oxide is sodium, with small amounts calcium oxides. The Field W sample could therefore be identified as a sodium carboxylate soap emulsion. One of the disadvantages of the XRF technique is that the organic portion of the soap sample is lost during analysis. Thus it becomes difficult to match the inorganic (cations) with the organic (naphthenic acids) components of the soaps. For this reason, it was decided to examine the remaining soap samples with a non-destructive technique such as EDAX/ESEM.

4.3.3. Energy dispersive X-ray and environmental scanning electronic microscopy.

Figure 4.50 presents the ESEM images acquired for the field deposit samples shown in Figure 4.49. Note the scale of the images which is 50 μm across. All field deposits produced similar ESEM images showing flaky rugged heterogeneous surfaces. These represent non-crystalline hydrocarbon matrices with a range of trace compounds.

Table 4.9 represents the mass and atomic percentages for the samples shown in Figure 4.50 as given by EDAX, where the results are the average values of three measurements. It is observed that most of the field deposits are composed of carbon and oxygen. The predominant cation species for samples from Fields X, Y and Z is calcium (average value of 2.83 wt%), while Field W sample contains a predominance of sodium cations. As shown in the ESEM images in Figure 4.50, some of the field deposits also contain entrained inorganic scales (i.e. barite), clays and sand.

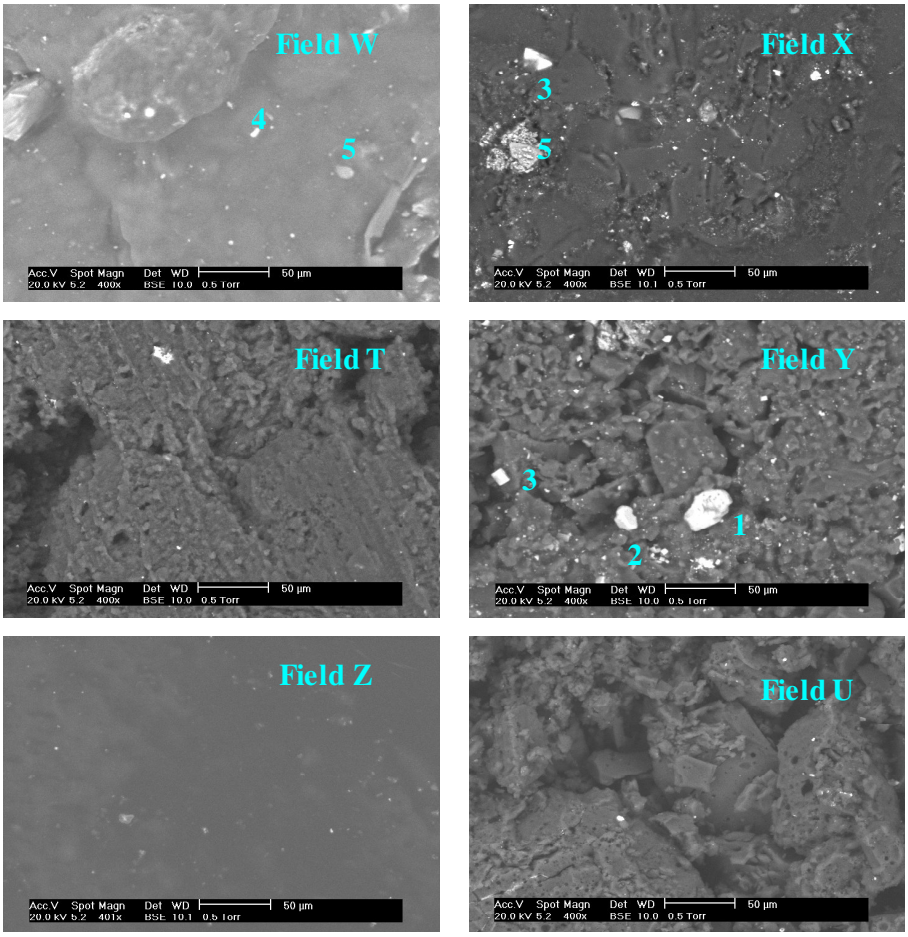

Figure 4.50. ESEM images of field deposit samples. Highlighted particles were assigned using EDAX as 1 = barite, 2 = iron carbonate, 3 = sodium chloride, 4 = alumina and 5 = silica.

Field	X	X	Y	Y	Z	Z	W	W	U	U	T	T
Element	Wt %	At %	Wt %	At %	Wt %	At %	Wt %	At %	Wt %	At %	Wt %	At %
C	85.77	92.72	85.86	91.84	91.41	94.70	85.02	91.86	99.08	99.67	93.3	96.27
O	5.54	4.50	6.71	5.39	5.39	4.19	3.85	3.13	x	x	2.79	2.16
Na	0.71	0.40	1.28	0.72	0.45	0.24	3.65	2.06	x	x	0.75	0.4
Al	0.25	0.12	0.21	x	x	x	0.49	0.23	x	x	x	x
Si	0.30	0.14	0.17	0.08	x	x	2.41	1.11	x	x	x	x
S	0.55	0.22	0.55	0.22	x	x	0.28	0.11	0.50	0.19	1.93	0.74
Cl	1.06	0.39	1.70	0.61	0.38	0.13	3.50	1.28	0.43	0.15	1.22	0.42
Ca	3.72	1.20	2.42	0.77	2.37	0.74	0.23	0.08	x	x	x	x
Fe	0.76	0.18	1.10	0.25	x	x	0.58	0.13	x	x	x	x
Mg	x	x	0.21	0.11	x	x	x	x	x	x	x	x
Ba	1.34	0.13	x	x	x	x	x	x	x	x	x	x
C/Ca		77.27		119.27		127.97		148.25		x	x	n.a.
C/Na		231.80		127.56		394.58		44.59		x	x	240.68

Note. x = not observed, blank cells indicate ratios not calculated, n.a. = not applicable.

Table 4.9. EDAX data for field deposits.

Figure 4.51 contains a comparison of some of the cations measured by EDAX and XRF for samples from Fields X, Y and W. EDAX measurements are specific to a few microns deep in the sample surface relative to an area covered by the electron beam, while XRF measurements are from the bulk of the soap sample used in a combustion cell. Despite the different measurement techniques, Figure 4.51 shows there is excellent correlation for the main cations present the field samples, i.e. sodium and calcium. It is assumed that calcium and sodium ions in these samples may be present as either calcium or sodium naphthenate molecules. If this is the case, the atomic carbon/calcium (C/Ca) or carbon/sodium (C/Na) ratios are likely to provide information on the precise naphthenic acid structures present in the naphthenate soaps. Table 4.9 shows that the carbon/calcium (C/Ca) ratios for samples from Fields X, Y and Z vary between 77.27 and 127.97. Calcium naphthenate molecules with mono-carboxylic acids have two naphthenate anions for every calcium cation. Thus if all calcium in the deposits are due to calcium naphthenates with mono-carboxylic species, these could have naphthenic acid structures with average number of carbon atoms between 38 and 64 (these are the C/Ca ratios divided by two). Thus the naphthenic acids in the field deposits would have molecular weights between 552 and 564 Daltons, and between 916 and 928 Daltons, respectively (the differences in molecular weight is due to the different Z values for each number of carbon atoms). The samples would therefore have a range of naphthenic acids. The carbon/sodium (C/Na) ratio for Field W is 44.59. Sodium naphthenate molecules for mono-carboxylic acids have one naphthenate anion for every sodium ion. Thus the field deposit could have an average number of carbon atoms of 44. The MS analysis for this sample did not suggest any naphthenic acids present in this sample with carbon numbers higher than 29 (Figure 4.27). Thus it is possible that the EDAX cation data do not represent naphthenate molecules, e.g. not all sodium in the sample is sodium naphthenate.

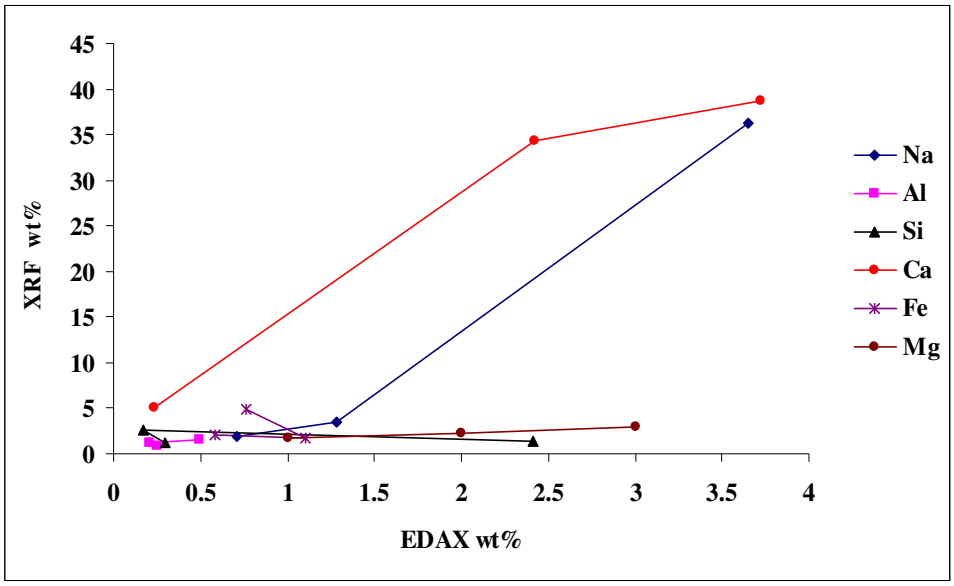

Figure 4.51. Cation EDAX wt% as a function of XRF wt%. Legend indicates different species identified using the two analytical techniques.

The EDAX data in Table 4.9 also shows the atomic and weight percentages for Field U and Field T field deposits. The Field U sample was not seen to contain any cations. The only elements present in this sample were carbon, sulphur and chlorine. This is rather remarkable since this field sample presented the highest concentrations of Arn naphthenic acids as given by Table 4.4. The significance of these results is due to the fact that Arn acids have not been reported in the open literature in non-calcium naphthenate deposits. Naphthenic acids cannot exist in ionised form as solids so it can be concluded the Arn present in the sample from Field U are in un-ionised form. It could be argued Arn might have precipitated in conjunction with other naphthenic acids and or waxes. However, the presence of wax compounds in this sample could also be ruled out due to the high temperatures required for sample melting as shown in the thermal analysis experiments (Figure 4.44). In conclusion, it is likely that the sample from Field U represents a resinous type deposit. The Field T sample contained some small amounts of oxygen and sodium. However, the remarkable feature of this sample is the large concentration of sulphur embedded in the hydrocarbon matrix. Given the DSC/TGA and ^{13}C NMR results shown in Figures 4.44, 4.45 and 4.42, it was thought that Field T sample could be an asphaltene deposit. This information was confirmed after discussions with the sample providers. A series of tests were carried out on the Field T and Field U deposits, in addition to the parent crude oil from Field U to further categorise these deposits (Section 4.6).

4.4. Diffraction behaviour of the field deposits.

Owing to high viscosity, the Field W sample could not be packed correctly in the XRD capillary following normal procedures. An attempt was made to centrifuge this sample prior to XRD analysis to aid in sample placement but this was not successful. Since no flat plate was available for the analysis of the Field W deposit, the sample had to be studied by rolling onto a glass capillary. Figure 4.52 presents and example of XRD pattern for a calcium-rich deposit identified in Table 4.9, namely, Field X. Lines 1 to 7 were common to all the calcium-rich deposits and have been highlighted on the diffraction pattern. Line 3 is a background reading and is a result of the silica capillary used for analysis. Line 7 was also found in the deposit from Field U but nevertheless, it is probably too broad to be considered a strong line from an ordered species. The pattern from Field W did not show identifiable strong lines other than those due to the silica glass capillary used in these experiments. Given the poor response for the field samples using XRD, it was concluded that the naphthenates present in the soaps are probably not crystalline and thus the XRD was discontinued as a means of fingerprinting deposits.

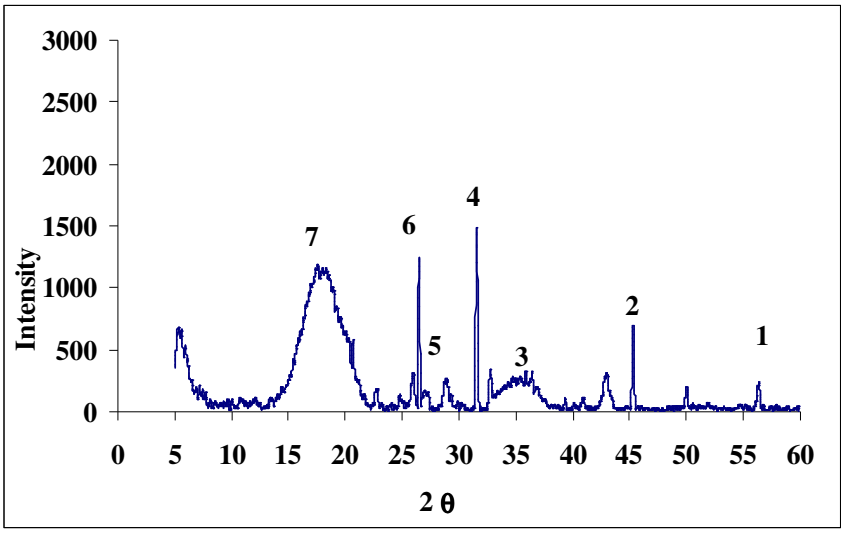

Figure 4.52. Powder XRD diffraction pattern for Field X sample (calcium-rich deposit).

In summary EDAX and XRF was more suited than XRD for the study of the inorganic portion of the field soap samples. The field soap deposits studied in this thesis could be separated into calcium-rich and sodium-rich samples. There was evidence of trace amounts of entrained sand, sodium chloride and other scales embedded on the soap samples. Two samples, Field U and Field T, did not show any predominant cation species and thus represent deposits which are not part of the end-member soap varieties.

4.5. Surface properties of soap components.

Figure 4.53 presents the surface properties of the deposit samples from Fields X, Y, Z, W and U as given by interfacial tension (IFT) measurements. Data was acquired using naphthenic acid extracts from each field as the oil phase. The aqueous phases used in the experiments comprised the brines containing 25000 ppm sodium ions, 20000 ppm calcium ions and 300 ppm bicarbonate ions. IFT measurements were carried out using these phases as a function of pH. Because of the high concentration of salts in the brine systems the IFT trends can be understood as resulting primarily in kinetic effects over electrostatic effects (Equation 2.9). Thus the changes in IFT as a function of pH are the result of the hydration of dominant cations in the aqueous phase, the positioning of the acid at the oil-water interface and steric hindrance of particular acid structures. Note the maximum pH values used in the tests were between 5 and 6. The reason for this was that solids were formed from the solutions tested at higher pH values.

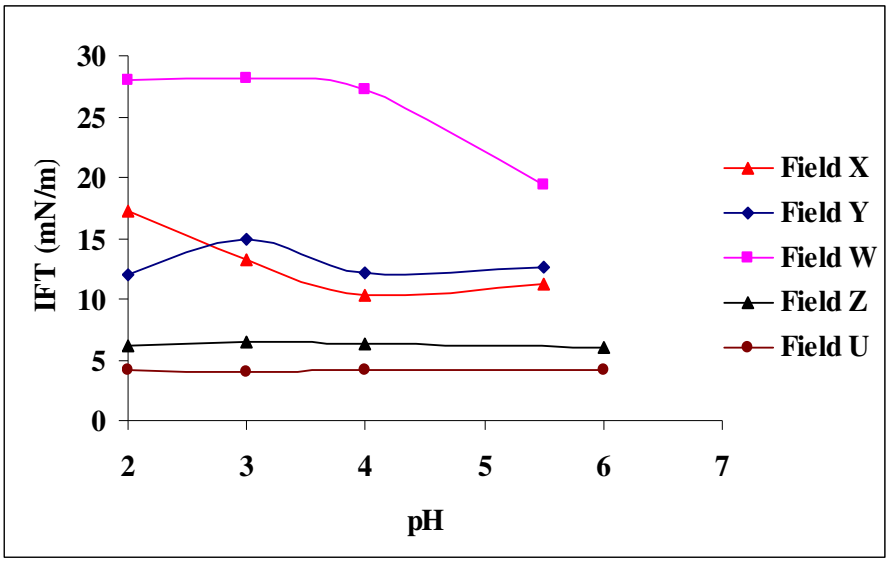

Figure 4.53. IFT of naphthenic acid extracts and pH adjusted aqueous phases as a function of pH.

Figure 4.53 shows some very distinctive IFT trends. Field W extracts have very high IFT values at higher pH compared to the other samples. As pH values were increased the IFT for this sample was seen to progressively decrease. This trend is very particular to fatty acids as shown by Cratin (1994). This supports the mass spectrometry analysis for Field W which showed the predominant species to be acyclic (Figure 4.27). Field Y and Field X measurements showed lower IFT trends as a function of pH. Mass spectrometry analysis in this thesis confirmed that these samples had a range of naphthenic acids. It is likely the IFT trends reflect the combined effect of the different naphthenic acids species present in these

samples. Field Z and Field U show the lowest IFT trends. Co-incidentally these samples had the highest concentrations of Arn acids, as shown in Table 4.4. Brandal (2005) suggested that Arn acids lowered IFT under laboratory conditions. Despite these results, the IFT values cannot be considered to be low or to mimic surfactant behaviour. Crude oil-water IFT values as low as 10^{-4} mN/m can be achieved with specific surfactant systems (Kanicky *et al.,* 2001) and certain model naphthenic acids (Rudin and Wasan, 1992). Based on this information alone, it is difficult to gain insights into the role of Arn acids in soap deposition. In addition, IFT trends are known to be a function of cation types and concentrations (Acevedo *et al.,* 2001). Chapter 6 will elaborate more on the precise effects of acid mixtures and cation influences on IFT.

4.6. Special analysis of Field U and Field T deposits.

A special range of analysis was conducted on deposits from Fields U and T. One of the objectives was to clearly fingerprint Field U deposit as either a soap or asphaltene sample. Previous results in Table 4.4 showed this sample contained a high concentration of Arn naphthenic acids, which would be more consistent with a soap scale. Yet EDAX data showed the same sample did not contain measurable quantities of calcium cations, but appreciable amounts of sulphur. Thus it would be more consistent with an asphaltene deposit, such as Field T.

The parent crude oil for Field U deposit was analysed for possible asphaltene precipitation tendencies. The first analysis was the quantification of n-heptane-insoluble asphaltene crude oil components by the ASTM D3279 method. Results showed that Field U crude oil had less than 0.2 wt% insolubles, which translated into a very low concentration of asphaltenes. The total acid number for this crude oil was measured at 2.5 mg KOH/g and its API gravity measured at 21.5. Usually crude oils with high naphthenic acid content are biodegraded, though more detailed analysis (e.g. GCMS) would need to be carried out to verify this. Risks for asphaltene precipitation for crude oils usually decreases with biodegradation. This information can only be supported with live fluid tests which could not be made available during the course of this thesis. Nevertheless, discussions with the sample providers concluded this particular crude oil had no asphaltene precipitation history under field conditions.

It was decided to carry out a SARA analysis on the both Field U and Field T deposits for an additional comparison. Table 4.10 presents the SARA results for both the samples tested according to the procedures of Weiss *et al.* (2000).

Sample	S	A*	R	A
Field U	19.35	34.12	4.92	41.61
Field T	10.75	11.52	2.29	75.45

Note: S = saturate, A* = aromatic, R = resins and A = asphaltenes.

Table 4.10. SARA data for Field U and Field T deposits. Solubility fractions in wt%.

The results indicate that the Field T deposit contains a majority of asphaltene fractions (about 75 wt%). Note these are considered to be all components which are insoluble in n-pentane, according to the method used. Thus it is likely these could include certain naphthenic acid components such as Arn species. Field U on the other hand, contained a lower amount of n-pentane insoluble compounds, as well as higher proportions of all other solubility groups. There are clear differences between these samples. This information would suggest that the Field U deposit sample is not likely to be an asphaltene deposit. Yet the ES data for this sample showed that there was a predominance of Arn species within the naphthenic acid components (Figure 4.26). Nevertheless, mass spectrometry in the negative mode would only provide an indication of the ionisable acidic polar molecules in the sample. Thus GC chromatograms were acquired for the n-pentane soluble fraction for both Fields U and T to aid in further identification of the deposits.

In the chromatograms for Field T and Field U samples in Figures 4.54 and 4.55, the peak at 6 minutes indicates carbon disulphide which was added to the sample to improve GC mobility. The peak at 10 minutes is the n-pentane solvent. Field U is the more biodegraded sample and the components observed on top of the GC hump are most likely branched, based on information available in the literature (i.e. isoprenoid alkanes, 2 and 3-methyl alkanes and cycloalkanes). This is typical of a biodegraded parent crude oil where n-alkanes are the first to be lost (Peters and Moldowan, 1993). Field T results indicate a less biodegraded sample, since some normal alkanes can still be observed in the system, and these are usually the first hydrocarbons to be affected by biodegradation. These trends support the conclusion that the Field U sample is not an asphaltene deposit.

What is most striking about the deposit from Field U are the large concentrations of Arn acid found (Table 4.4). The produced water analysis for this field indicates that conditions were favourable for calcium naphthenate soap deposition when the deposit was formed and collected. The surface pH was 6.3 and the calcium ion concentration in the produced water was 3000 ppm. Discussions with the field operator revealed that a soap inhibitor was used in this field to prevent calcium naphthenate soap scale formation. Thus the deposit analysed in this thesis was formed even during these inhibitor trials. Clearly the inhibitor was not successful, since despite inhibiting calcium naphthenate soap scale formation, it could not prevent a different type of flow assurance deposit being formed (a resinous type solid with large quantities of Arn). The generic inhibitor type used was a water-soluble calcium complexant. At high pH, naphthenic acids become dissociated and are positioned either at

the oil-water interface, or partitioned between the two phases. This would depend on a number of factors such as the solubility of the naphthenic acid species in both phases. Because the calcium ions would be complexed with the chemical inhibitor, naphthenic acids would not be able to precipitate as calcium soaps. Nevertheless, at low pressures, it is likely that the solubility of the acids and other resins in the crude oil is reduced. These compounds may co-precipitate and hence this would explain the high concentrations of naphthenic acids in the deposit from Field U including Arn. Thus the mechanism would have similarities to asphaltene precipitation.

The SARA results presented in Table 4.10 for Field U and Field T deposits are based on solubility groups. The correlation between solubility groups and specific chemical families (i.e. naphthenic acids) was attempted in this thesis by examining the differences between the time-of-flight mass spectrometry data (TOF-MS) for each sample *in natura* (using the procedures described in Section 3.2.1.1) and the n-pentane insoluble asphaltene fraction. This fraction was prepared by washing sub-samples with 100 ml of n-pentane. TOF-MS was chosen to allow for an analysis of a higher molecular weight range, both for the deposit *in natura* as well as the sub-sample insoluble in n-pentane.

Figures 4.56 and 4.57 present the analysis of the Field U samples as given by TOF-MS. It can be seen that there is very little difference between Field U sample *in natura* and the n-pentane insoluble fraction from the same sample. Moreover, both these sub-samples contain high percentages of Arn naphthenic acids. Given these results, it is likely Arn naphthenic acid species in this deposit are part of the asphaltene solubility fraction.

Figure 4.22 showed the analysis of the Field T deposit *in natura*. Figure 4.58 presents the n-pentane insoluble fraction (asphaltenes) of this sample. It can be observed that this sample contains certain amounts of species in the region of m/z 1220 to 1228 which may be assigned to Arn species. It would thus appear that the Arn species are entrained in the asphaltene matrix of this deposit. It is widely recognized that asphaltene samples do contain naphthenic acid functionalities (Mullins *et al*., 2007). However no Arn species have been identified in asphaltene deposits in the open literature prior to this thesis.

The presence of Arn species with asphaltenes is not entirely surprising from a chemistry point out view. Both asphaltenes and Arn contain polar/non-polar portions. Naphthenic acids have also been suggested to be linked to asphaltene stability (Havre, 2002). Nevertheless, soaps and asphaltenes have not been shown to be present in the same field samples. Yang and Czarnecki (2005) performed laboratory experiments on asphaltene samples separated from bitumens and commercial sodium soaps. It was found that sodium soaps were not present in re-precipitated asphaltenes under laboratory conditions. The

presence of naphthenic acids in the MS spectrum of Field T is however in clear opposition to the solid state ^{13}C NMR spectrum presented in Figures 4.42 and 4.43, which did not show measurable quantities of naphthenic acids in the asphaltene deposit. It can be concluded that the concentration of naphthenic acid in Field T is too low for detection by ^{13}C NMR. What is surprising is that the asphaltene deposits analysed in this thesis formed when the produced water pH was 6 and it contained 1000 ppm calcium ions, which are very suitable for calcium naphthenate soap scale formation. Yet the Arn naphthenic acids remained in the asphaltene matrix. These results suggest factors other than naphthenic acids may be responsible for soap deposition, as opposed to the concentration of Arn alone, as suggested by Mediaas *et al.* (2005). For instance, there may not be sufficient Arn in a particular crude oil to precipitate as soap, or the acid may not partition to the interface without help of other naphthenic acids or hydrocarbons. Chapter 8 will attempt to explore these issues further.

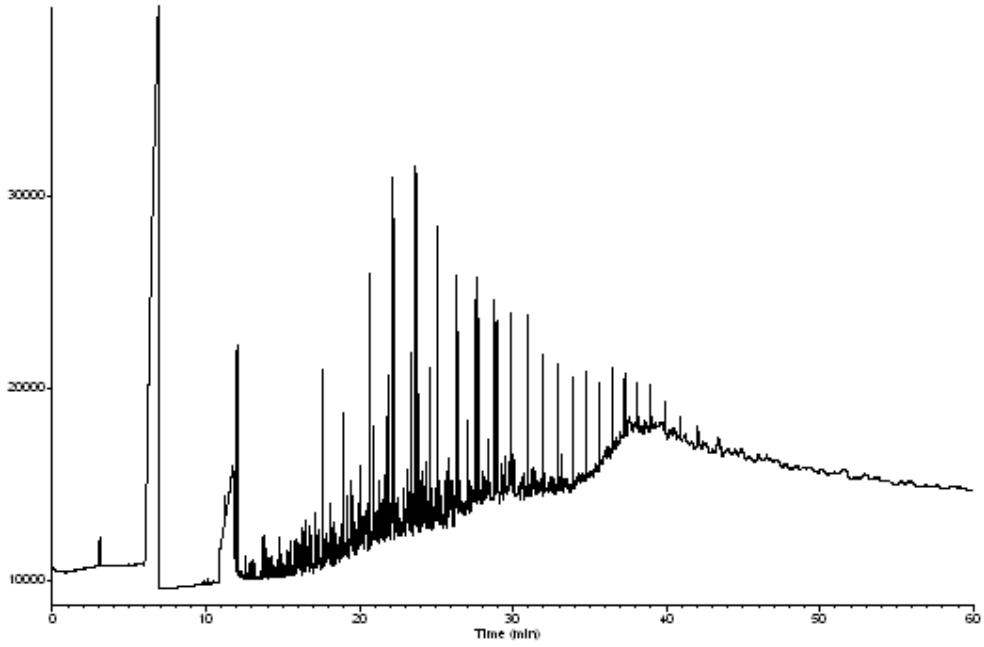

Figure 4.54. GC of n-pentane soluble fraction from Field T deposit.

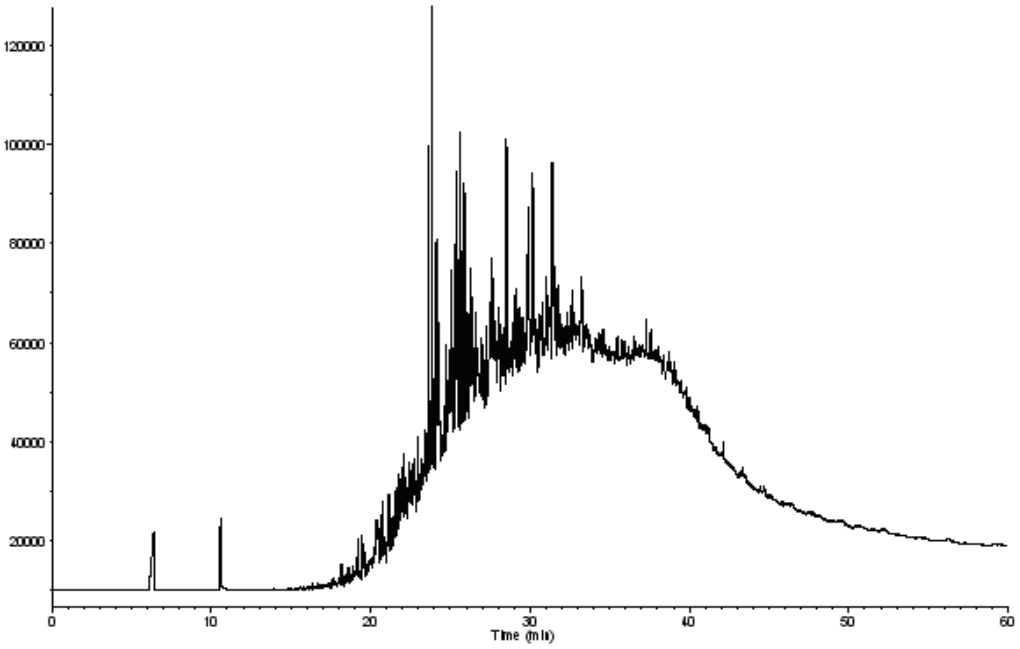

Figure 4.55. GC of n-pentane soluble fraction from Field U deposit.

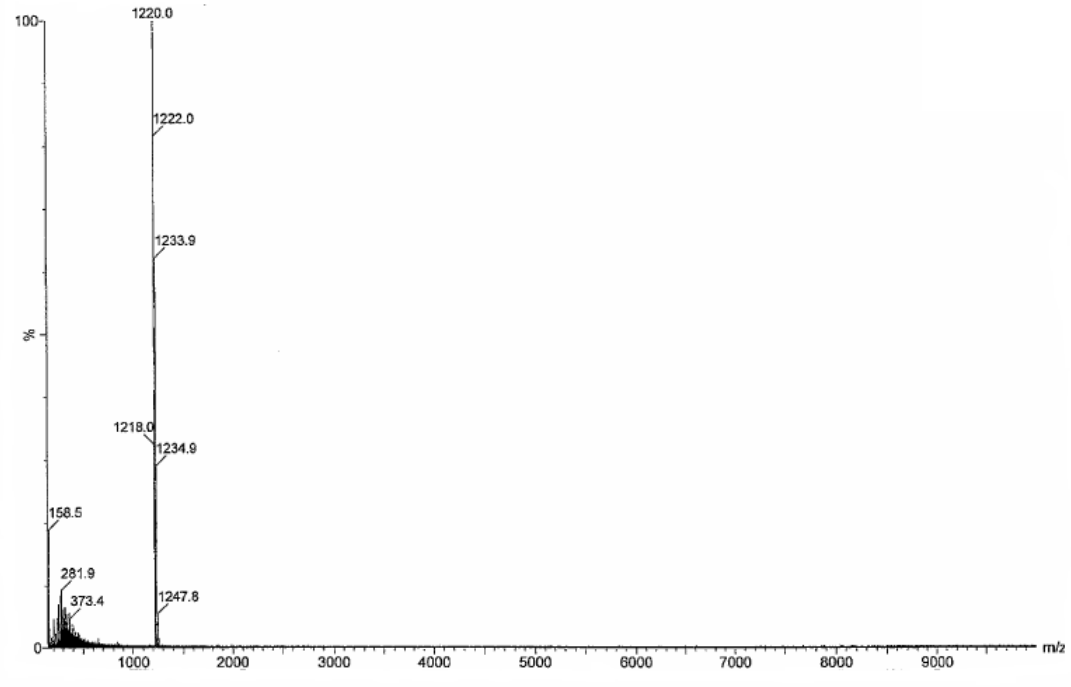

Figure 4.56. TOF-MS spectrum for deposit sample from Field U *in natura.*

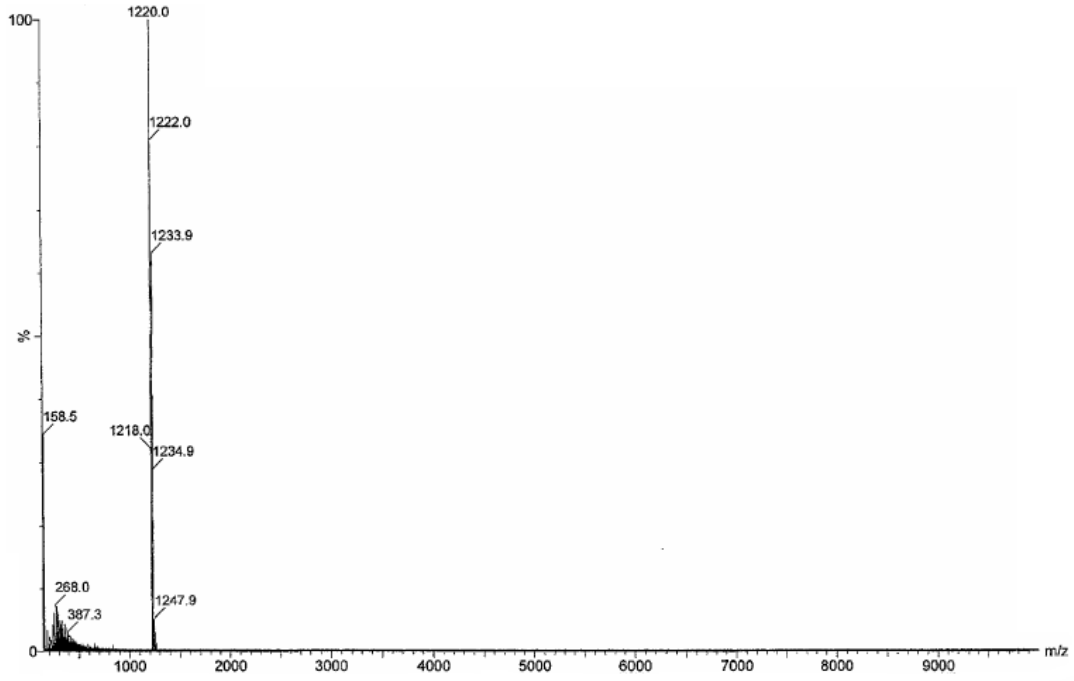

Figure 4.57. TOF-MS spectrum for deposit sample from Field U, n-pentane insoluble fraction.

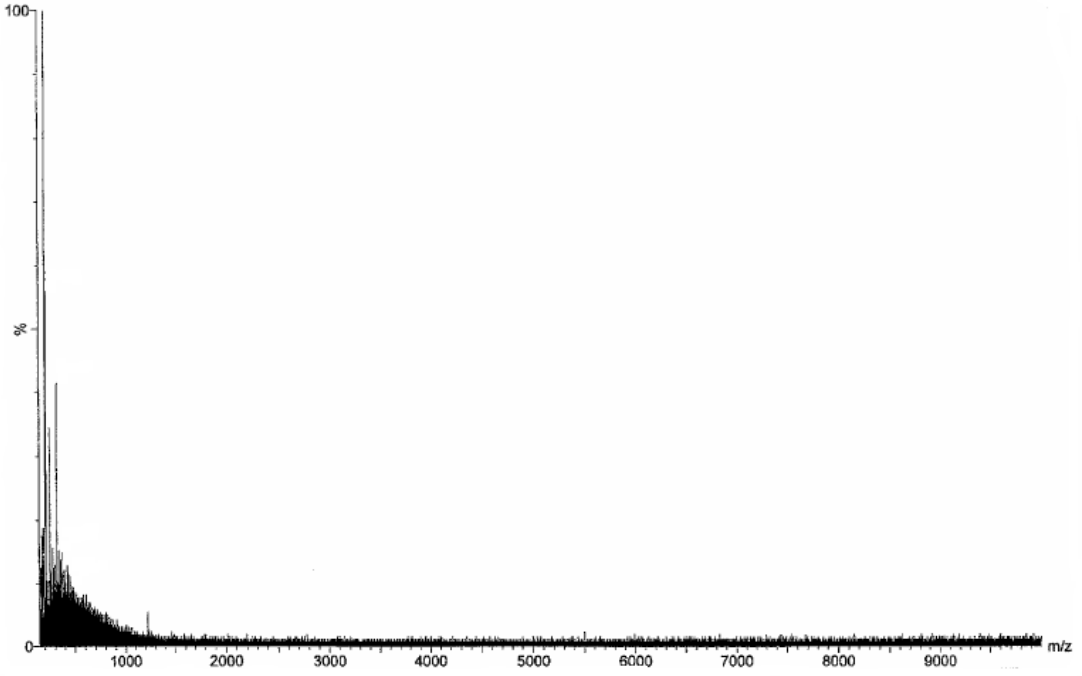

Figure 4.58. TOF-MS spectrum for deposit sample from Field T, n-pentane insoluble fraction.

4.7. Field Z deposition history.

Data and sample analysis from Field Z are now discussed. This was motivated by the analysis of various soap samples from this field, which showed different morphology over a period of time as in Figure 4.59.

Figure 4.59. Images of different soap deposits from Field Z. Morphologies Z1, Z2 and Z3 indicated in the images.

The soap morphologies were seen to vary between the rock-hard consistency (Z1), to softer sludge-like consistencies (Z2), and very viscous liquids (Z3). The techniques used to compare these deposits were ES, TOF-MS, EDAX, TGA/DSC and solid state ^{13}C NMR. Parent crude oils which were collected at the same time as the deposits were sampled under field conditions were also analysed using ES and EDAX.

Field Z is located in the North Sea. It produces crude oil with TAN values typically around 0.1 and produced water content containing on average 20000 ppm sodium ions, 1000 ppm calcium ions and 700 ppm bicarbonate ions (this information was obtained with the sample providers). The first soaps observed in this field in late 2003 were hard calcium naphthenate soap scales which deposited in the oil-leg of the topsides facilities. These deposits had the Z1 morphology shown in Figure 4.59. The mitigation treatment selected was acetic acid at various injection points. Until mid-2004, only acetic acid injection was used but this eventually led to a new problem with soap plugging, resulting in an unplanned shutdown. As a direct result, a chemical naphthenate inhibitor was injected at concentrations of 200 ppm together with acetic acid. This appeared to control the soap problem despite an increase in chemical expenditure. However, in early 2005 another unplanned shutdown occurred due to the deposition of soap. These deposits were now observed in the water-leg with the Z2 morphology. From February to April 2005, a number of injection strategies and treatment location ports were tested with varying degrees of success. In April 2005, another major shutdown occurred, previous to which the inhibitor had been injected into the main separator at concentrations between 500 to 600 ppm, together with acetic acid, which brought the brine pH to between 6.0 and 6.2. The soaps observed during this deposition campaign had the Z3 morphology. Since July 2005, the inhibitor has been applied at concentrations around 350 ppm with acetic acid to bring pH values to no higher than 6.0. This has not led to any unplanned shutdowns. However, water cut levels have increased slightly and soap material is still forming in the water-leg, although in manageable amounts.

Figure 4.60 presents the ES analysis of the water-leg deposits collected from Field Z in February 2005. The optimum ES settings described in Table 4.3 were used. The deposits were observed in various different topside locations and had the Z3 morphology shown in Figure 4.59. Most of these samples contained up to 20 wt% entrained crude oil as given by centrifugation experiments. It can be observed in Figure 4.60 that many of these soaps show a high percentage of the Arn (m/z ~1230). However these also showed a broad distribution of acids with lower molecular weight. Some samples also contained species with m/z values above 1400. These were not identified previously in any of the field soap samples analysed in this thesis as shown in Figures 4.23 to 4.27.

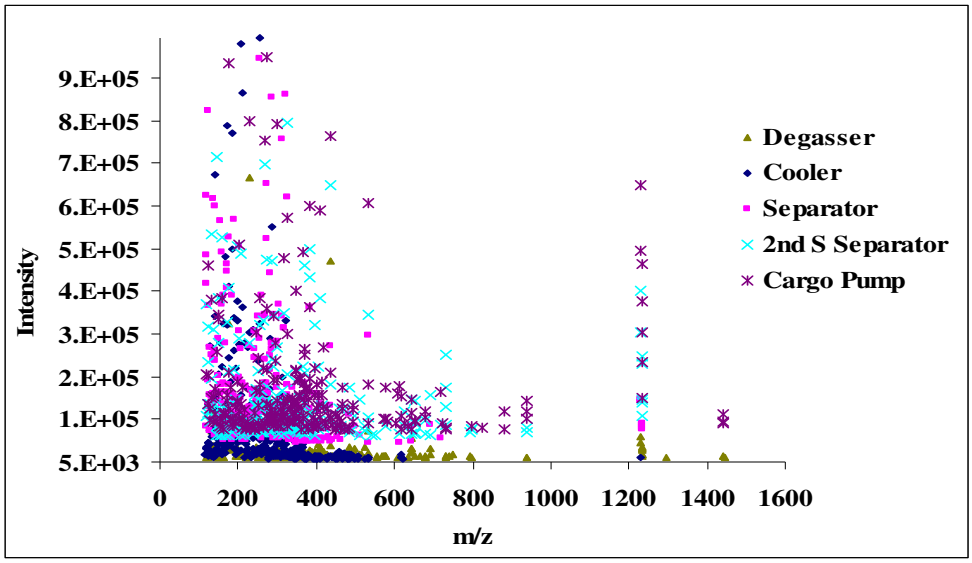

Figure 4.60. ES samples of Field Z water-leg deposits. February 2005. Legend indicates topsides location where the sample was collected.

It is interesting to note that the soaps analysed in Figure 4.60 had the Z3 morphology and were deposited after a period of six months during which time acetic acid and inhibitor were used to avoid deposition. The ES analysis of soaps deposited in the same topside unit (degaser) over a period of time are presented in Figure 4.61.

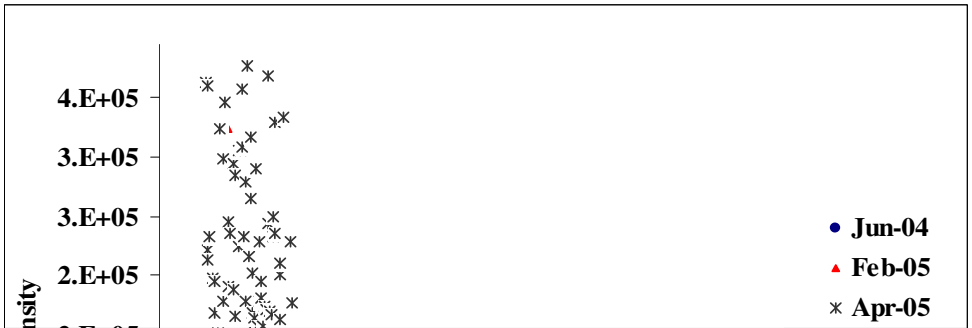

Figure 4.61. ES samples of Field Z degaser deposits. Note sample from Jun-04 corresponds to morphology Z1, sample from Feb-05 corresponds to Z2 morphology and sample from Apr-05 corresponds to Z3 morphology.

From Figure 4.61, it can be seen that there are changes in the naphthenic acid distribution of the deposits over time which also accompany the change in deposit morphology (Figure 4.59). The first deposits observed in Field Z (Jun-04) were hard calcium naphthenate soap scales (Z1 morphology) formed before chemical treatment begun. These show a large distribution of high molecular weight naphthenic acids including the Arn. There are clear shifts in the naphthenic acid species with soap morphologies Z2 (Feb-05) and Z3 (Apr-05). Note that these were formed during the inhibitor injection campaigns. Differences were observed in the ES spectrum of the crude oils sampled at the same time soap deposition for the samples shown in Figure 4.61 (data not shown). These may be due to statistical variations in the crude oils themselves. However the influence of chemical inhibitors is more likely to be affecting the naphthenic acid distribution which is concentrated in the soap, as shown in Figure 4.61.

The speciation of the Field Z soap samples is presented in Figures 4.62 to 4.64. In addition to high percentage of Arn, the sample with Z1 morphology presents other naphthenic acids species with carbon atoms between 15 and 35. Samples with Z2 morphology present a lower percentage of Arn, and there is a shift in the predominant lower molecular weight species to lower carbon numbers as compared to the sample with Z1 morphology. The sample with Z2 morphology also contained species in the spectrum identified with m/z values above 1400. These were not included in the speciation since they do not represent naphthenic acids with the formula given in Equation 1.1. The sample with Z3 morphology did not show any presence of Arn species. No naphthenic acids with more than 25 carbons were detected in this sample.

Figure 4.65 presents additional speciation for the three Field Z samples given by hydrogen deficiency (Z). In this analysis, it is assumed all species identifiable in the negative mode ES represent naphthenic acids. The sample with Z1 morphology presented lower percentage of species with hydrogen deficiency values of 0 (acyclics). The sample with Z2 morphology showed very high percentage of species with hydrogen deficiency values of -2 (mono-cyclics). The sample with Z3 morphology showed the highest percentages of species with hydrogen deficiency values of 0 (acyclics), in addition to very high percentages of species with hydrogen deficiency values of -4 (bi-cyclics). The higher concentration of these species could be responsible for the change in deposit morphology, and moreover, the deposit location (oil-leg to water-leg). Acyclics are the most water-soluble of the naphthenic acids found in crude oil. These are also present in the softer water-leg deposits

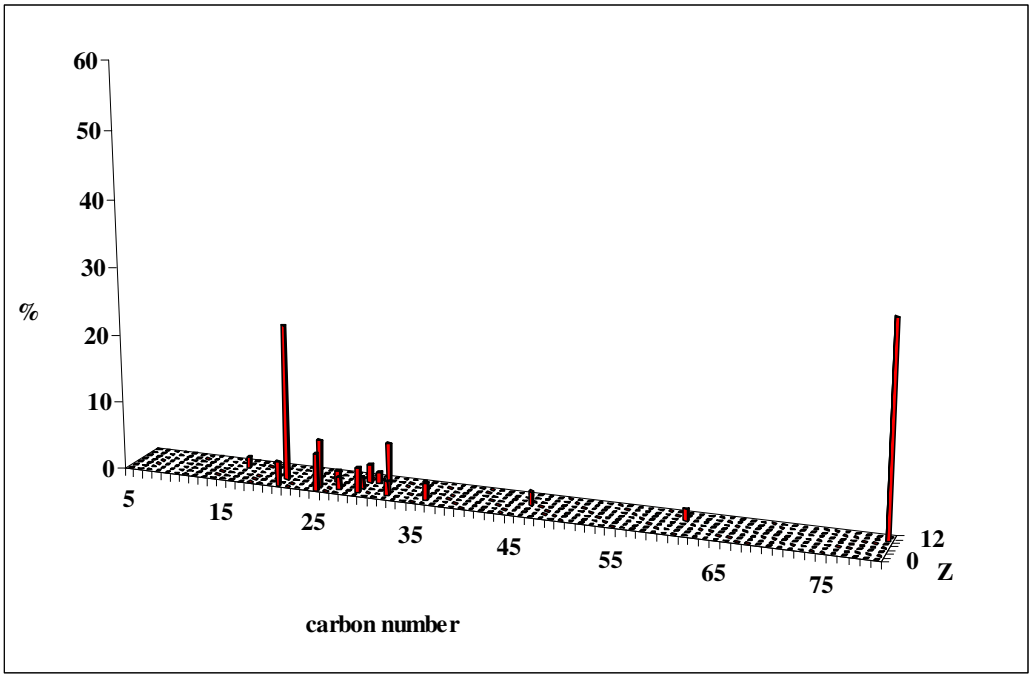

with morphologies Z2 and Z3.

Figure 4.62. Naphthenic acid speciation for Field Z sample, Z1 morphology.

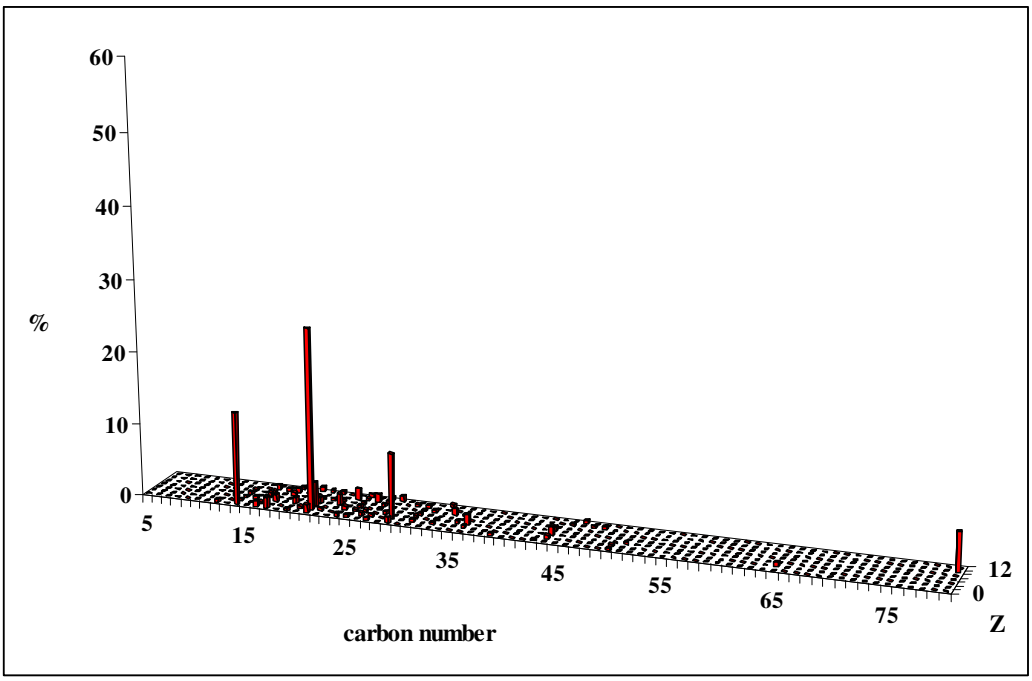

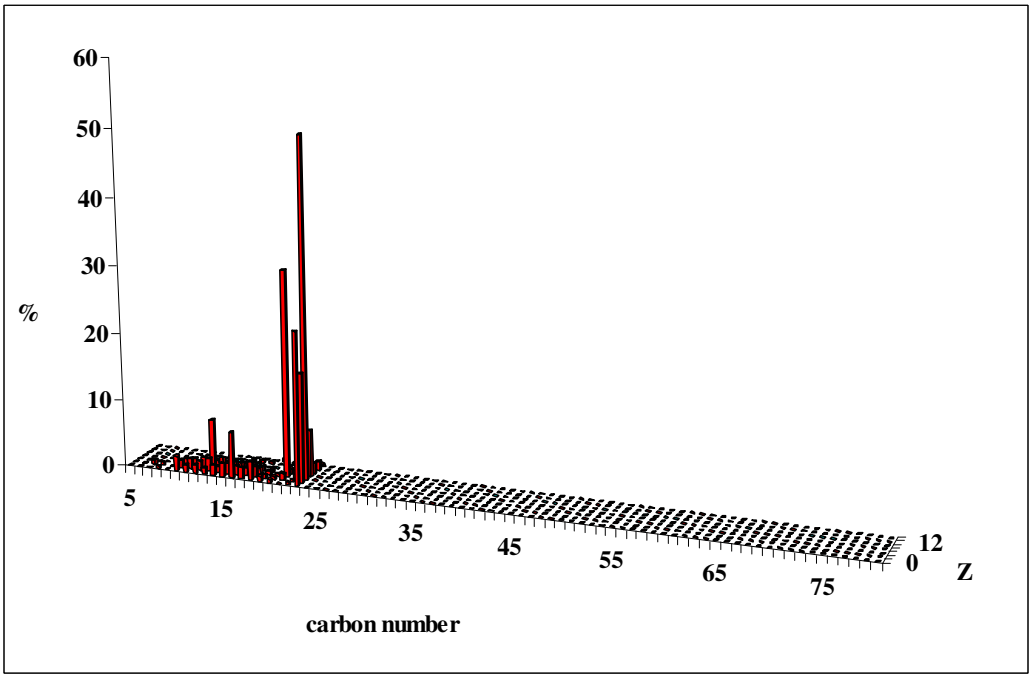

Figure 4.63. Naphthenic acid speciation for Field Z sample, Z2 morphology.

Figure 4.64. Naphthenic acid speciation for Field Z sample, Z3 morphology.

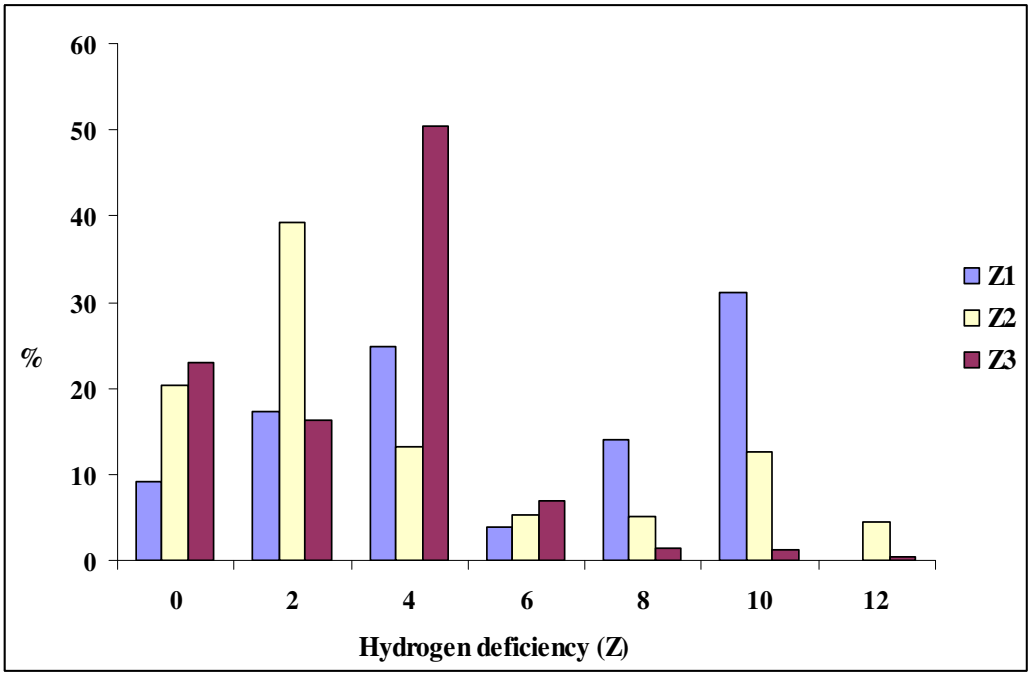

Figure 4.65. Naphthenic acid speciation for Field Z soap samples as given by hydrogen deficiency (Z).

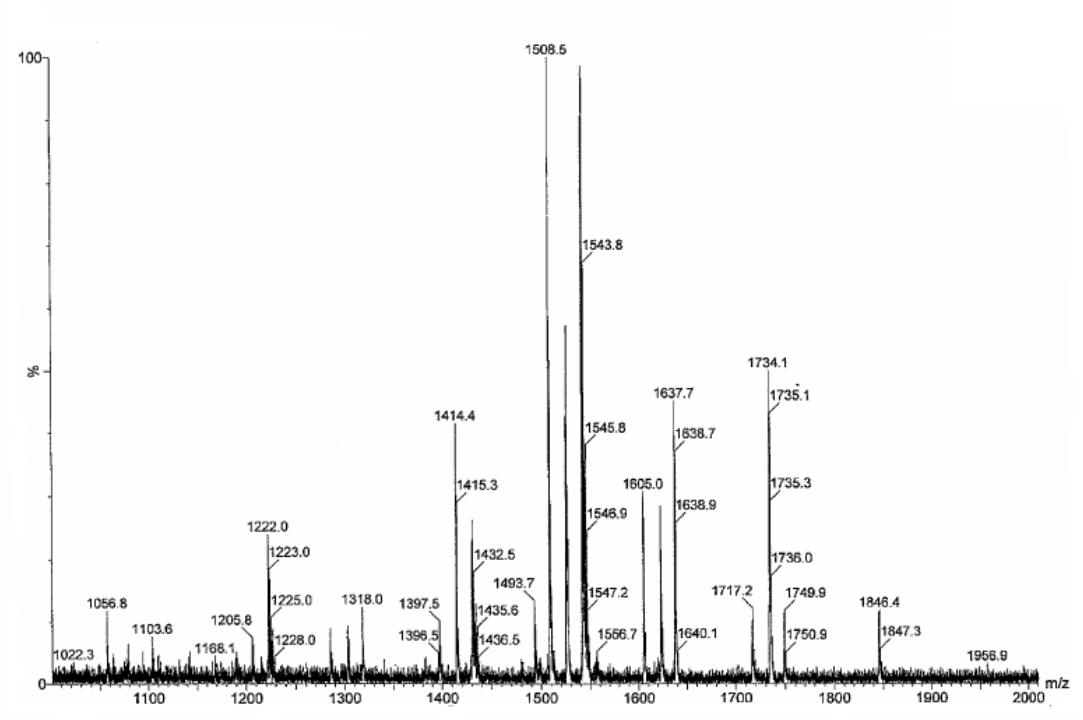

Figure 4.66. Expanded TOF-MS for Field Z sample, Z2 morphology.

The sample with Z2 morphology also presented ions above 1400 m/z as given by TOF-MS and this is shown in detail in Figure 4.66. It is very likely that these species are not true naphthenic acid species originally present in the parent soap-forming crude oil. The ions possibly represent the inhibitor chemicals used for soap mitigation, or even species resulting from complexed naphthenic acids with the inhibitor chemicals themselves. Note also the spectrum in Figures 4.23 to 4.27 in which no m/z species were identified above 1250 (non-chemically treated samples). It was not possible to gain access to the generic inhibitor chemistry used for soap mitigation in Field Z, so further work would be necessary to support the earlier conclusion.

The sample with morphology Z3 was also analysed by solid state ^{13}C NMR. Owing to the very high viscous nature of this sample only a DP experiment was carried out. This spectrum is shown in Figures 4.67. There is a range of lines in the aliphatic region which are in-line with those presented for the sample with morphology Z1 shown in Figure 4.37 (a). Based on the information in Table 4.6, shifts from linear components are dominant, but there is also some degree of contribution from branched species. The carboxylic acid signal is much less intense compared to the samples in Figure 4.37. A recycle delay change (from 0.5 to 10 seconds) was carried out but this did not increase the carboxylic acid signal. Since this is a sample that has been chemically treated, it can be suggested that the aromatic signals may account for traces of the chemical inhibitor used in the field.

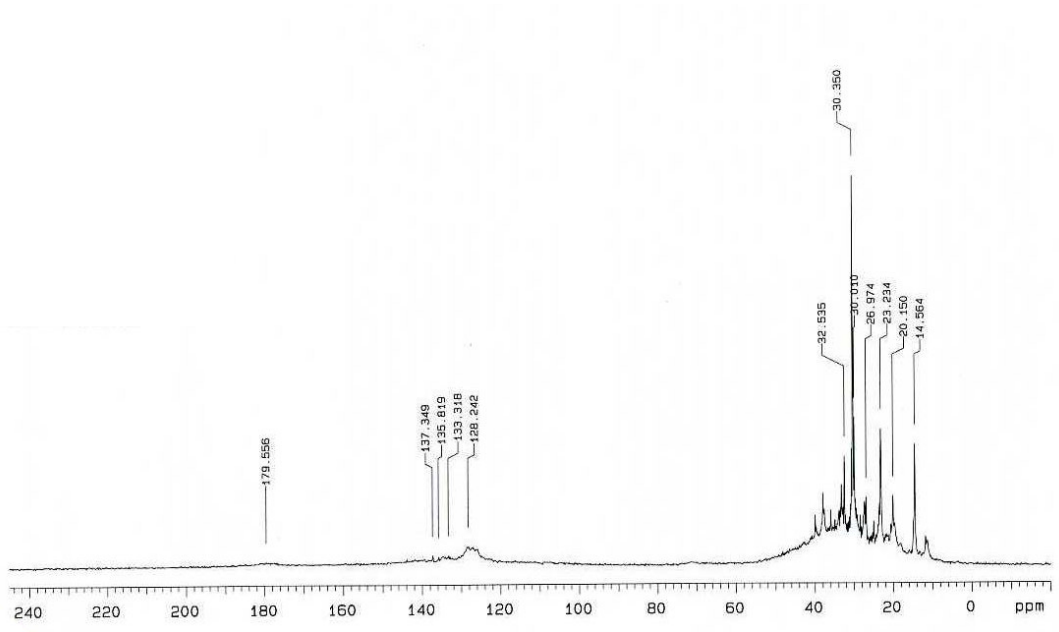

Figure 4.67. ^{13}C NMR DP spectrum for Z3 deposit sample.

Figures 4.68 and 4.69 present a comparison of the TGA and DSC analysis for the sample with Z1 morphology and that with Z3 morphology. The sample with Z3 morphology showed a faster weight loss until 470 °C, after which both samples degraded at a similar rate. The DSC peaks are all endothermic and correspond to evaporation of volatile materials which are confirmed by the TGA profile up to 200 °C. Four main endothermic peaks in the DSC profile are observed below 150 °C. These are consistent with the TGA data and correspond to a weight loss of 23.68 %. Two broad peaks are observed at 230 and 280 °C, which correspond to TGA weight losses of 13.56 % and 9.65 % respectively. The endotherm at 470 °C is not as pronounced in the sample with Z3 morphology. Based on the discussion presented in Section 4.2, this is may be a result of lower concentration of Arn found in the chemically treated sample (Z3 morphology). However, it is clear that the use of chemical mitigation has affected the thermal stability of the soap deposits.

A comparison of the atomic and weight percentages for the three Field Z soap samples given by EDAX is presented in Table 4.11. The sample with Z1 morphology contained the highest percentage of calcium ions (2.37 wt %). The deposits which were collected on the same equipment (but at the water-leg, Z2 and Z3 morphologies) showed different results. Both these chemically treated deposits showed a decrease in calcium content to values of 1.03 and 0.88 wt%, namely. Experiments were carried out where samples of the deposit with Z2 morphology were washed with toluene to check if the low percentages of calcium could be a result of entrained water or crude oil. Results are presented in Table 4.12. The sample with Z1 morphology and a sample from Field X were used as references. It can be observed that the relative percentage of calcium in sample with Z2 morphology remained low, even after washing with toluene. This means the lower percentages of calcium in the sample with Z2 morphology compared to the sample with Z1 morphology are not due to entrained solvent contaminants.

Phosphorus ions are also observed in the samples with morphologies Z2 and Z3 as shown in Table 4.11. These ions were not observed in sample with morphology Z1. The presence of phosphorus is believed to be evidence of chemical or corrosion inhibitors in the soap sample. Phosphate ester inhibitors are common active ingredients of corrosion inhibitors (Babaian-Kibala, 1994). Crude oil collected at the same time as the samples with Z2 morphology formed, was also analysed by EDAX and these results are presented in Table 4.13. No phosphorus ions could be observed in this sample, which suggests the phosphorus elements detected in the soap samples are not indigenous to the parent soap-forming crude oil.

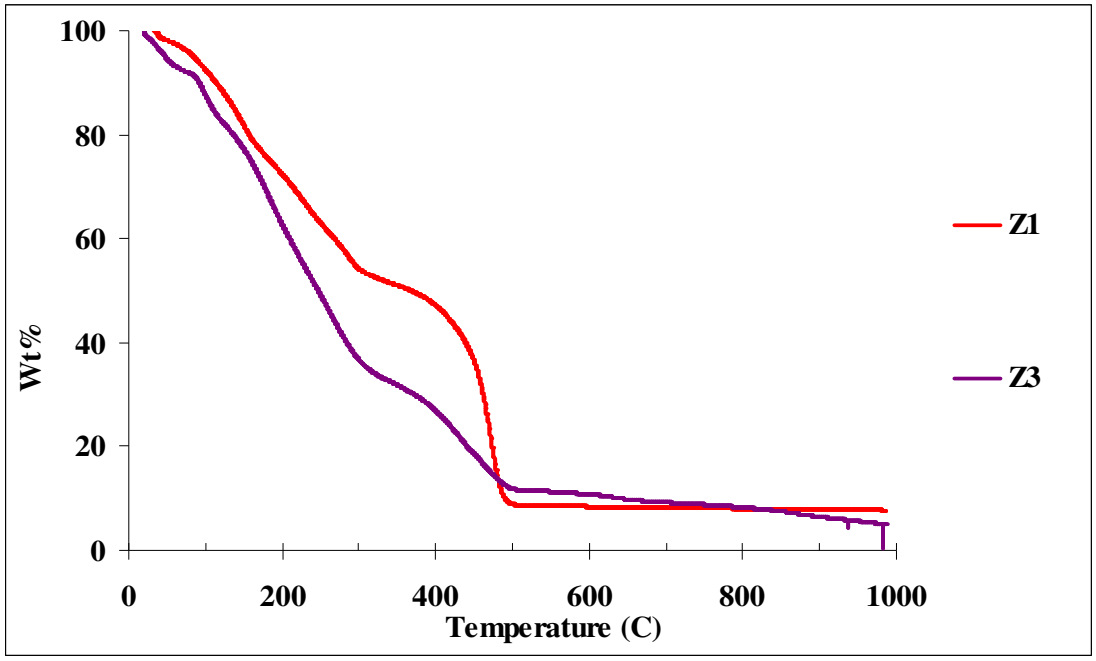

Figure 4.68. TGA of Field Z deposits. Z1 and Z3 refer to the samples with morphologies shown in Figure 4.59.

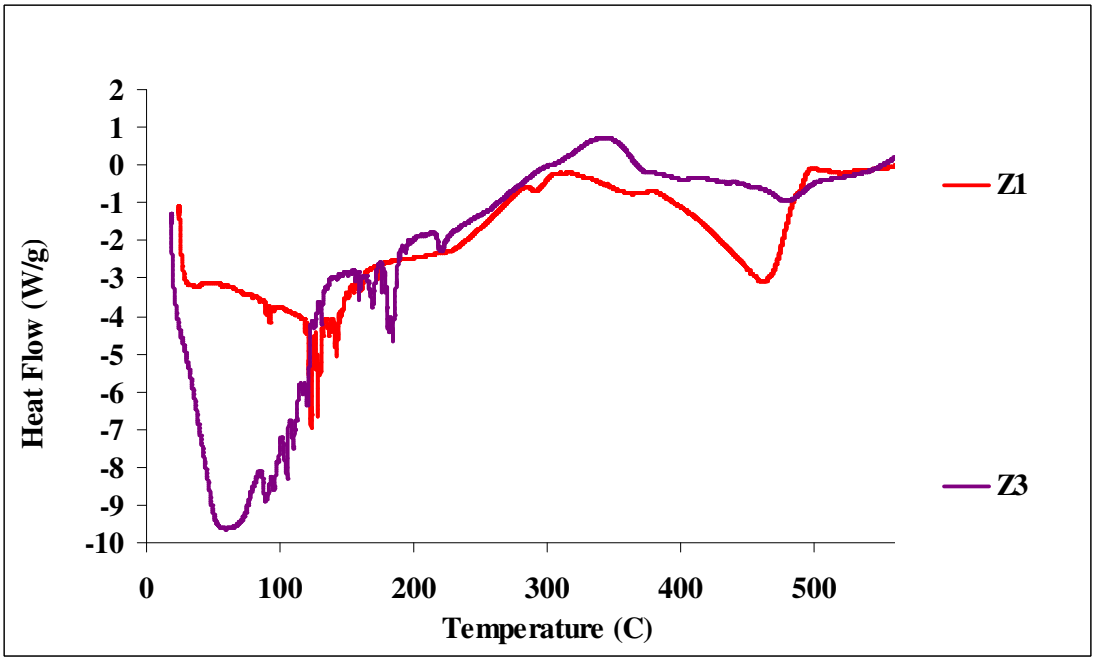

Figure 4.69. DSC of Field Z deposits. Z1 and Z3 refer to the samples with morphologies shown in Figure 4.59.

Field	Z1		Z2		Z3	
Element	Wt %	At %	Wt %	At %	Wt %	At %
C	91.41	94.70	93.15	95.72	93.01	94.99
O	5.39	4.19	4.44	3.43	4.76	4.01
Na	0.45	0.24	x	x	0.01	0.23
Al	x	x	x	x	x	x
Si	x	x	x	x	x	x
S	x	x	0.27	0.10	0.22	0.08
Cl	0.38	0.13	0.18	0.06	0.10	0.08
Ca	2.37	0.74	1.03	0.32	0.88	0.18
Fe	x	x	x	x	x	x
Mg	x	x	x	x	x	x
P	x	x	0.93	0.37	1.02	0.43

Note: x = not detected.

Table 4.11. EDAX analysis of Field Z deposits with different morphologies.

Soap	Calcium Before (wt%)	Calcium After (wt%)	Phosphorus Before (wt%)	Phosphorus After (wt%)	Weight loss (wt%)
Field X	3.72	3.92	x	x	5.3
Field Z (Z1 morphology)	2.37	2.65	x	x	7.2
Field Z (Z3 morphology)	1.03	1.37	0.93	1.05	19

Note: x = not detected. Before denotes the sub-sample prior to toluene washing. After denotes the sub-sample after toluene washing. Weight loss is that experienced during toluene washing.

Table 4.12. Calcium wt % and phosphorus wt% as given by EDAX of toluene washed soap samples with weight loss values.

Element	Wt %	At %
C	99.59	99.84
S	0.41	0.16

Table 4.13. EDAX analysis of Field Z crude oil sampled at the same time of the sample with Z2 morphology.

The reduced amount of calcium ions in the chemically treated soaps (morphologies Z2 and Z3) may reflect the precise naphthenic acid structures shown in each individual sample (Figures 4.62, 4.63 and 4.64). Arn acids have a special affinity towards calcium. Moreover, acyclic acids similar to those observed in samples with morphologies Z2 and Z3 have less affinity for calcium. It is likely that the inhibitor species used for soap mitigation in Field Z had a direct effect on the availability of Arn for soap formation. As a consequence, changes in soap morphology and composition occurred. Hurtevent and Ubbels (2006) commented on the mechanisms of soap inhibition under field conditions. According to these authors, the dedicated inhibitor chemicals act by stopping the reaction of calcium with naphthenic acids at the oil-water interface. This would further prevent the sticky network which forms (and then hardens) due to the presence of Arn. Presence of soaps with soft morphologies (Z2 and Z3) supports these claims.

4.8. Conclusions.

The analysis of field deposits in this chapter has lead to a development of a series of techniques resulting in a protocol for the correct analysis of field soap deposits (both organic *vs.* inorganic and bulk *vs.* surface properties). The current state-of-the-art for soap deposit analysis prior to this thesis had relied heavily on a limited number of measurements and procedures. Moreover the specialised literature had lacked detailed description of the exact sensitivity of these techniques on the identification of specific naphthenic acids (e.g. Arn and fatty acids). Thus in this chapter a range of ionisation sources, mass analysers and solvents were examined for the best optimum method for naphthenic acid identification by mass spectrometry using naphthenic acid extracts. The soft ionisation sources, FAB, APCI and ES showed good potential for use. Soap emulsion samples containing fatty acids were not affected by the use of the different sources. Yet the analysis of samples containing the Arn acid showed clear differences with the three ionisation sources. The ES was the optimum source leading to a spectrum which was not the result of preferential ionisation of

Arn or lower molecular weight naphthenic acids. Solvent effects, particularly on the detection of Arn, were seen to be a consequence of polarity and molecular weight. Nevertheless the APCI source would also be applicable for samples containing trace concentrations of Arn acid, due to the favoured ionisation effects. The statistical analysis of the mass-to-charge data for each deposit allowed for the identification of two clear end-member fingerprints as given by hydrogen deficiency and carbon numbers. Sodium carboxylate soap emulsions contained a strong presence of acyclic acids with carbon numbers between 7 and 33. Calcium naphthenate soap scales showed a range of species including mono-cyclics, bi-cyclics and varying percentages of Arn. These results are important since they point to possibly different interactions of the Arn and non-Arn naphthenic acid in the precipitation mechanism. The chemical characterisation of the naphthenic acids extracts by FTIR and solution NMR showed spectra of mostly hydrocarbons with minor naphthenic acid elements. This might be due to low naphthenic acid concentrations. Solid state ^{13}C NMR (applied for the first time in this thesis for the analysis of field deposits) allowed for a better fingerprinting of the field deposits and carboxylic carbon signals were observed for most samples (which supported the mass spectrometry results). Clear differences for the spectra from the end-member soap types as well as the asphaltene and chemically treated deposit were obtained. Though results are less sensitive when compared to the solution ^{13}C NMR data, the advantage of the solid state technique is that it can be applied on samples *in natura*. The TGA/DSC results (applied for the first time in this thesis for the analysis of field deposits) showed it was possible to trace thermal stability of field deposits to the indigenous acids present in these samples. Nevertheless it was not possible to ascribe this behaviour to Arn acids. The end-member soap types and the asphaltene deposit showed very distinct thermal behaviour. The elemental analysis and evaluation of the inorganic portion of the field deposits concluded the fatty acid soaps were sodium-rich *vs.* the predominantly cyclic naphthenic acid deposits which were calcium-rich, as shown by XRF and EDAX. Samples were identified which did not contain cations. These were chemically treated soap samples in addition to asphaltene deposits. This information is particularly important for the correct modelling of the interaction of the produced water cation species and naphthenic acids from the associated crude oil. The large concentrations of Arn in the Field U deposit suggest the soap deposition mechanism might also involve solubility group effects, of the type resin *vs.* asphaltene. Note no cation species were observed in the deposit even though production conditions in this field would lead to the precipitation of a soap. In this thesis it was shown that Arn acids would fall within the asphaltene solubility group from a deposit. Moreover

this was also supported in this thesis by the identification of Arn in an asphaltene deposit. The significance of this information lies in the potential for soap modelling via equation-of-state (EOS). The measurements of surface properties of naphthenic acid extracts from field samples using IFT, suggested the possibility of distinguishing the two end-member soap types as a function of pH. Samples containing Arn resulted in lowest IFT values, but these were not surfactant-like, since the lowest measured value was 5mN/m. Thus the results point to differentiated surface properties of the Arn which may contribute in the overall phase behaviour of the soap deposit (e.g. sticky nature). Analysis of deposits from Field Z (known calcium naphthenate soap scale-former) presented data which shows the clear influence of naphthenic acid compositions on the variation of soap properties as given by EDAX, ES, TGA/DSC and solid state ^{13}C NMR as well as the soap morphology. This is additional information pointing at the interactions between different naphthenic acid species during the precipitation mechanism. Previous published information has claimed Arn acids to be the sole species responsible for calcium naphthenate soap scale formation. The results in this thesis suggest this hypothesis need to be expanded by studying the effect of other naphthenic acids found in deposits during precipitation campaigns. Results suggest chemical inhibitors used in the field may complex with the Arn and prevent these species from forming a rock-hard deposit by the reaction with calcium. In contrast chemically treated samples tend to have a higher concentration of fatty acids as well as less calcium. The significance of these results is that the selected experimental techniques presented in this thesis would also have the potential to be used to follow inhibition trials. In this chapter, a range of experimental techniques was applied to the study of field deposits. The optimum method is presented next and is termed full analysis of soap types, FAST. The use of this protocol enabled the differentiation of the two end-member soaps: calcium naphthenate soap scales and sodium carboxylate soap emulsions. In addition, this protocol was used to distinguish chemically treated samples as well as asphaltenes. The results of this protocol represent the major contribution of this chapter to the knowledge of soap-forming systems. The conclusions from the current chapter served as guidelines and

interpretation for the results from Chapter 6 where the precipitation of soaps in the laboratory from various feeds was attempted. The most important analytical methods developed in this chapter for the FAST protocol, their sensitivities, applications and major contributions are included in Table 4.14.

Procedure	Technique	Preferred sample requirements	Errors/repeatability	Major thesis contribution
Naphthenic acid extraction	liquid-liquid extraction with HCl/glacial acetic acid and solvents (Section 3.1.2)	25 g of soap deposit (output is naphthenic acid extract)	Sensitive to solvent amounts. Inorganics must be removed via titration. Problems with deposits with low naphthenic acid concentrations	A quick and optimized method for naphthenic acid separation including chemically treated samples
Chemical identification by mass spectrometry	ES (Table 4.3 for optimum settings)	< 1ml naphthenic acid extract	Used with the single quadrupole, ES offers enough resolution for correct fingerprinting of naphthenic acids in deposits from m/z data. Non quantitative, but should be able to differentiate m/z values at least to 3 decimal places. Corrections need to be applied in mass assignment (addition of 1 Dalton). In the low-resolution tests employed in this thesis all m/z ratios were assigned to naphthenic acid species with either one or four carboxylic acids	Effects of settings and solvents on Arn detection
	APCI (Section 3.2.1.1)	< 1ml naphthenic acid extract	Preferential ionisation of Arn acids with polar solvents. Would be suitable for Arn identification in low concentration, not fingerprinting	Preferential ionisation effects particularly with acetonitrile.
	FAB (Section 3.2.1.1)	< 1ml naphthenic acid extract	Used with the single quadrupole offers enough resolution for correct fingerprinting of naphthenic acids in deposits, at least 3 decimal places. Not suitable for direct application on parent crude oils (mixing effects)	Matrix effects (NBA/TEA)
Chemical identification by nuclear magnetic resonance	solid state ^{13}C NMR (Section 3.2.4)	1 g of soap deposit	Non-destructive. Good repeatability providing major contaminants (e.g. water and solvents) removed. Lower sensitivity than solution NMR (but able to identify even low concentration of naphthenic acids)	Aliphatic *vs.* aromatic and carboxylic acid fingerprinting. Identification of samples with production chemicals. Identification of asphaltene *vs.* soap deposits
Inorganic analysis of deposit	EDAX (Section 3.4.3)	100 mg of soap deposit	Non-destructive spot test analysis and very repeatable. Detection limits down to a few ppm. No coating required. Gives surface compositional information and may miss bulk features of the sample. X-ray detector adjustment critical to avoid back scatter interference	Identification of calcium *vs.* sodium-rich samples. Fingerprinting non-standard deposits (e.g. Field U)
Surface properties	IFT (Section 3.6)	50 ml of naphthenic acid extract placed in contact with 50 ml pH adjusted brine	± 0.1 mN/m experimental error. Very sensitive to contaminants. Little application to crude oil naphthenic acid soap samples but potential for use in inhibitor evaluation. Time-consuming method with equilibration time of at least 12 minutes required. Du Nouy ring does not have sensitivity for low IFT. Fluid densities must be accounted for as well as temperature effects	Identification of surface properties of Arn-containing samples under different conditions. Fatty acid fingerprint clearly observed. Investigation of predominant Arn effects
Thermal properties	TGA/DSC (Section 3.3)	50 mg of soap deposit	Errors of ± 0.2 wt% (TGA) and ± 0.5 W/g (DSC). Accuracy of 0.2 °C Destructive techniques sensitive to contaminants such as water. Has the potential to be used in inhibitor evaluation	Observation of enhanced thermal properties of indigenous acids. Identification of samples with production chemicals. Identification of asphaltene *vs.* soap deposits

Table 4.14. Full analysis of soap types protocol (FAST).

CHAPTER 5 – FORMATION AND EVALUATION OF SOAPS UNDER LABORATORY CONDITIONS: MATERIALS AND METHODS.

Abstract

In this chapter, experiments to form soap deposits under laboratory conditions are described with the objective of understanding the fundamentals of this flow assurance occurrence. The procedures focused on a number of model naphthenic acid systems, as well as acids extracted from field deposits and soap-forming crude oils. Sensitivities which are covered in these tests include: the type and concentration of naphthenic acids used, cation and anion varieties in synthetic brines, as well as different modes of pH change mechanism (static bottle testing, dynamic tube blocking and a carbon dioxide injection rig). A number of particular tests were performed which provided insights into the phase behaviour of indigenous acids as well as Arn species. In addition, attempts to predict the onset of soap formation in model laboratory systems, with a range of techniques such as Fourier-Transform infrared are discussed.

5.1. Introduction.

In Chapter 2 the basic mechanism for soap precipitation under field conditions was presented. It was postulated that during the production of reservoir fluids, carbon dioxide (CO_2) evolution results in pH increase of the produced water. The crude oil naphthenic acids may then partition and dissociate across the oil-water interface. Naphthenic acids in turn may react with the cations in the produced water and lead to the formation of soaps. Thus pH variations play a key role in the initiation of the precipitation mechanism for soaps. A series of simulations of these pH changes using data from a soap-forming field were carried out using Multiscale thermodynamic software. These simulations were conducted to gain an understanding of the impact of fluid properties (hydrocarbon and produced water) on final pH. In Figure 5.1 the effect of CO_2 content in the hydrocarbon phase on final pH is presented. Small variations in CO_2 content (2.5 to 5 mol%) can lead to significant pressure decreases from subsurface to surface conditions. This in turn may result in pH changes, particularly for pressures below 50 bar, which are more often seen in topsides equipment. Note that the pH increase below 50 bar is due to gas separation. The final topsides pH values in the simulations shown in Figure 5.1 varied between 6.2 and 9. The actual measured onsite pH from the field is 6.4, and this is in agreement with 6.6 which is the value predicted in the simulations for the actual hydrocarbon CO_2 content.

Thus, if formation of soaps in the laboratory was to be attempted, similar pH variations would need to be targeted. However, there are limited references of formation of soaps in the laboratory using this methodology. Trusovs (2003) used the reaction between an

organic acid ligand with a metal selected from a group of oxides and hydroxides. In these tests, suspensions were formed which when filtered allowed for the separation of solid soaps. These reactions however occurred in a model oil phase only and are thus not consistent with the basic soap formation mechanism from the field examples described in Chapter 2, which occur at the oil-water interface. Attempts to form soaps from model oil and water mixtures were made by Dyer *et al.* (2003) using static bottle tests with adjusted pH brines at room temperature and pressure. More realistic conditions were employed by Rousseau *et al.* (2001) who showed it was possible to obtain deposits from crude oils and synthetic brines using specially adapted dehydration equipment operated at 60 °C. Mediaas *et al.* (2005) also formed soaps in the laboratory from crude oil and brine systems using a dedicated depressurisation rig which allowed for the use of CO_2, as well as realistic shear rates. Dyer *et al.* (2006) showed the possibilities of using a rig with shear conditions, thus establishing better control over the system pH. For the study of soap formation, it is debatable whether the use of field samples alone (crude oil and produced water) would aid in the understanding of deposition mechanisms. As reviewed in Chapter 2, crude oil systems contain a variety of naphthenic acid species. Produced water has equally many different ionic components. The use of model systems containing selected individual naphthenic acid species, as well synthetic brines, aims to limit the number of possible variables, and to allow for a more mechanistic approach to soap formation studies. Nevertheless there is a risk that model systems may not represent the totality of components present in crude oil. Moreover, unless high pressure, high temperature and multiphase conditions are used, results may not be truly representative of field conditions.

In this thesis, various sensitivity studies were conducted that had the objective of better replicating field deposition conditions, with increasing degrees of sophistication. Three techniques were chosen: static bottle tests, dynamic tube blocking and a static CO_2 rig. The basic principle and operation of these techniques is described briefly in the next paragraphs.

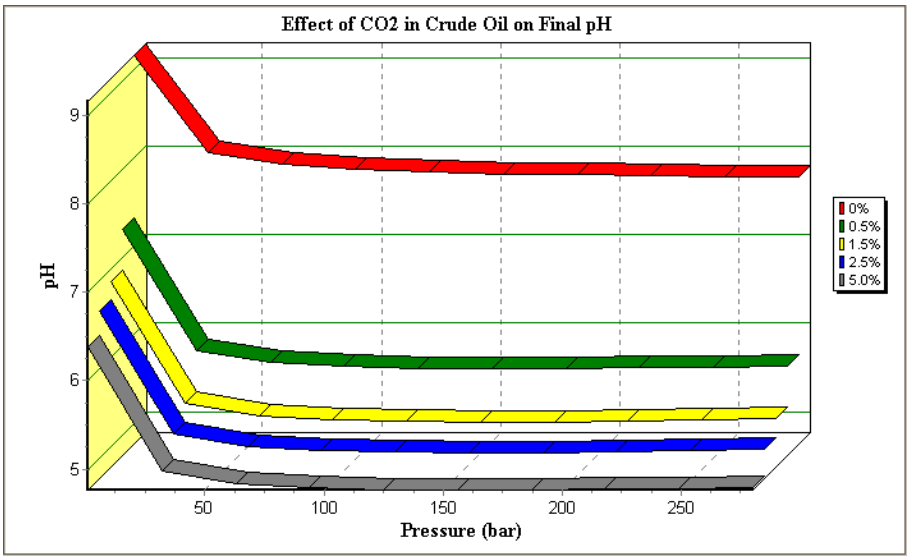

Figure 5.1. Multiscale simulation of pH as a function of pressure and CO_2 mol% in reservoir fluids. Hydrocarbon and water properties used from PVT report from Field X (North Sea).

5.2. Techniques for soap formation in the laboratory.

5.2.1. Static bottle tests.

Dyer *et al.* (2003) presented a series of fundamental static bottle tests on model naphthenic acid systems. In their experiments, acids were dissolved in toluene used as the oil phase, and mixtures of calcium and sodium ions in water (but not individual cation species) were used as the aqueous phases. Only two very high pH values were examined: 10 and 11.5. These were adjusted with alkaline agents. In this thesis it was decided to carry out more detailed analysis with the static bottle tests in order to obtain an optimum and reproducible set of conditions for overall testing. The preliminary variables chosen included: brine pH adjustment (alkalinity), the effect of agitation, time dependency (contact time between the oil and aqueous phases), the effect of acid concentration in the oil phase and the effect of cation concentration in the aqueous phase.

5.2.1.1. The effect of alkalinity.

It is known from the literature that alkaline agents in the presence of naphthenic acids affect the stability of any oil-in-water (O/W) emulsion formed, as a result of electrostatic effects. Verzaro *et al.* (2002) showed that the stability of emulsions containing naphthenic acids could be studied in terms of droplet size and viscosity due to variations in alkaline concentration and type (sodium or ammonium hydroxides). Li *et al.* (2004) showed that the use of sodium hydroxide (0.6 wt%) with particular crude oil samples could lead to the formation of not only O/W but also W/O emulsions. The authors also showed that the inversion point, and changes to interfacial tension and viscosity were mostly time

dependent. For these reasons, the effect of alkalinity was selected to be studied in this thesis. pH adjustment media and concentration were evaluated on the formation of soaps in the laboratory. An oil phase consisting of 1 wt% of stearic or myristic acid in toluene (analytical grade, VWR) was prepared. 50 ml of this was placed in contact with 50 ml of Milli-Q water (conductivity less than 18 mΩcm, equivalent to a three-times distilled water). The aqueous phase was adjusted to pH 12 using three different media: aqueous sodium hydroxide (NaOH) and potassium hydroxide (KOH) solutions of concentrations ranging from 0.1 to 10 wt% were used. A commercial pH 12 buffer solution, Normadose (VWR) was also used. Both oil and pH adjusted aqueous phases were shaken manually and vigorously for one minute and left in contact for 24 hours. Soap samples which formed were separated by filtration using a glass microfibre paper 1.2 μm retention diameter grade 1 qualitative (Whatman) and a BOC (Edwards) vacuum pump. The separated soaps were left for 24 hours to dry in a fume cupboard. To avoid the loss of any water-soluble material it was decided not to use a deionised water wash, which was the method carried out by Dyer *et al.* (2003). The output variables measured in these experiments were: the mass of soap formed, as well as the overall variations in pH.

5.2.1.2. The effect of agitation.

It was shown in Chapter 2 that the formation of soaps in the field is highly affected by shear and agitation. These are a result of both the evolution of gas from the produced fluids and the flow through restrictions such as valves, fittings and sharp bends (Petex, 1990). These effects are more noticeable in the formation of sodium carboxylate soap emulsions (Turner and Smith, 2005). The mechanism responsible for the increased stability to shear is the formation of droplets with smaller surface areas, which are less affected by coalescence. It was decided that the effect of agitation on soap formation would be investigated in this thesis. For this purpose, a 1 wt% stearic or myristic acid solution in toluene was used as the oil phase. The aqueous phase was a pH 12 adjusted solution with 10 wt% NaOH. Shear was induced by three methods: manually shaking the bottle samples vigorously for one minute, using an Ultra-Turrax mixer with two different rates, and a case consisting of leaving oil and aqueous phases in contact without shaking as a reference. For the evaluation of the effect of agitation, the mass of soap formed and pH changes were noted.

5.2.1.3. Time dependency.

Li *et al.* (2004) showed that changes at the oil-water interface for naphthenic acids and aqueous solutions containing NaOH were time dependent. This was reflected in variations in interfacial tension and viscosity which were explained by the delayed kinetics of soap formation. Equilibration times of above 10 minutes are required for surface properties to remain constant for such systems (Brandal, 2005). Dyer *et al.* (2003) carried out filtration experiments on soaps formed after a contact time of 5 minutes. Yet, this time interval was most likely below the necessary equilibration time for soap formation to occur in its entirety in the model systems. For the investigation of time dependency on soap formation, aqueous phases with pH values from 2 to 10 adjusted with 10 wt% NaOH and 10 wt% HCl were used. The oil phases consisted of either 1 wt% myristic or stearic acid in toluene. 50 ml of oil and water phases were placed together and manually shaken vigorously for one minute. A reference solution of toluene containing no naphthenic acid was used and also placed in contact with different water phases. pH values and the mass of soaps formed were taken at time intervals between 12 minutes and 24 hours of phase contact.

5.2.1.4. Acid and cation concentration.

Additional sensitivities examined for the static bottle tests consisted of the effects of naphthenic acid and cation concentration. In Chapter 2 it was discussed that some naphthenic acid structures can form micelles in solution. The formation of micelles would prevent the reaction of an acid monomer with a cation in detriment of soap occurrence. For the acid concentration tests, stearic acid concentrations ranging from 0.001 to 0.1 wt% were used. These concentrations are representative of crude oil naphthenic acid components found in crude oils and soap samples. The objective was to examine the influence of possible micelle formation on the precipitation of laboratory soaps. Aqueous phases used were adjusted to pH 12 with 10 wt% NaOH. Shear was induced by manually shaking both phases for one minute. Cations present in the water phase have a clear effect on the partition and dissociation of naphthenic acids. This effect is more noticeable for divalent cation species (Acevedo *et al.,* 2001). The effects of cation concentration on the phase behaviour of naphthenic acids in the static bottle tests was examined by using a 1 wt% stearic acid solution and aqueous phases adjusted to pH 12. The aqueous phases contained calcium ions with concentrations ranging from 10 to 2000 ppm. All pH measurements in the tests in this section were carried out using an Orion bench top pH/ISE meter model 920A, with a temperature compensated probe. The correct

temperature is obtained from a hand-held thermometer. The associated error for this temperature measurement was ± 1 °C according to the equipment manufacturers. The meter/electrode system was calibrated with standard buffers with set pH values of 4, 7 and 10 during every set of measurements. The probe was cleaned with deionised water between measurements. All pH measurements have an associated error of ± 0.1, according to equipment manufacturers.

5.2.2. Dynamic tube blocking tests.

One of the biggest disadvantages of the static bottle test procedures described in Section 5.2.1 is the lack of good pH control. For this reason it was decided to use a dynamic tube blocking rig. Tube blocking is a well-established technique for determining scale formation in laboratory systems. It has mostly been used for inorganic scaling tests, such as the formation of calcium carbonate (Zhang *et al.,* 2001). Dyer *et al.* (2003) presented some results on systems with stearic acid in tube blocking tests where two pH values (8.5 and 11.4) were evaluated using a brine consisting of 10000 ppm calcium ions with 25000 ppm sodium ions. The authors claimed it was possible to observe the formation of soaps using pressure readings across the mixing coil of their rig. Although pressure variations indicated possible formation of soaps during these tests, results were inconclusive since no actual analysis of precipitated solids was presented. The rig used in the present study was similar to the one described by Dyer *et al.* (2003). It consisted of a mixing vessel with a magnetic stirring bar. Owing to material limitations, tests could not be conducted at more than 200 psi. The apparatus is illustrated in Figure 5.2. Both oil and aqueous phases were mixed and passed into a micro-bore coil and an in-line filter. Two pumps were used, one for each phase. Differential pressure transducers were used to indicate the pressure fluctuations. Equilibration of the phases is done in small steps, where individual cation solutions at low pH are first injected into the rig, followed by the oil phase and higher pH aqueous phases. A 1 wt% myristic acid solution in toluene was used as the oil phase. For the aqueous phase, a brine consisting of 10000 ppm calcium ions and 25000 ppm sodium ions adjusted to pH 12 was used. Pressure in the rig was kept at 100 psi and temperature at 20 °C with flow rates at 10 ml/minute.

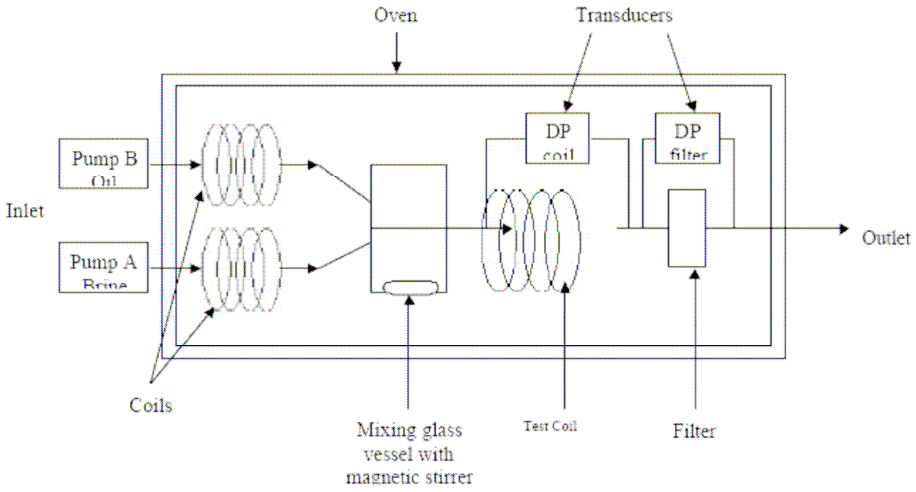

Figure 5.2. Tube blocking rig used for soap formation in the laboratory.

Dynamic tube blocking tests showed that pressure variations indicated possible formation of soaps, particularly in the rig coils, but also to some extent in the filters. Despite this, these tests did not lead to a blockage since no soaps could be detected from the analysis of the rig filters. Therefore the observed pressure fluctuations (which suggested soap precipitation), might have been caused by the changing of solutions in the rig. In additional experiments, the rig was left running over a period of over 24 hours, which would be sufficient for equilibrium to be achieved. Although pH control was more efficient in these experiments than bottle tests (owing to the slow equilibration of fluids), these did not, however, lead to the formation of soaps. It is likely that the tube blocking rig could not produce enough shear to lead to precipitation of solids, even when the aqueous phases were adjusted to high pH. Results are thus inconclusive and are in agreement with data from Dyer *et al.* (2003). Therefore the use of the dynamic tube blocking rig was discontinued for the remaining experiments in this thesis. During tube-blocking experiments, shear and turbulent conditions are dictated by the dimensions of the tubing, roughness of the tubing material as well as pump rates. Therefore additional equipment selection could attempt to encourage soap formation through better shear conditions.

5.2.3. Static CO_2 rig.

In the techniques described previously, pH control was attained by direct adjustment of the aqueous phase, with and without the presence of a buffer. In field conditions, pH is mostly a function of dissolved CO_2 and alkalinity, and variations occur as pressure varies during fluid production. According to Barth and Bjorlikke (1993), CO_2 in crude oils may be the

product of thermal degradation of kerogen. It is continuously generated through the maturity of source rocks.

Two types of tests with pressure equipment for soap formation were described by Dyer *et al.* (2006) which aimed at replicating the effects of CO_2 in the field. The first was an autoclave for pressure tests up to 100 bar where rapid depressurisation could be achieved. The disadvantages of this set-up were described as the large sample volumes required in addition to the time for experiment completion. The second was a flow-through cell, which had the advantage of being able to employ lower sample volumes, but at lower pressures (between 5 and 10 bar). Mediaas *et al.* (2005) also presented results from a dedicated rig for forming naphthenates. The equipment can operate at 200 ^{o}C and 275 bar. In this thesis, a static CO_2 rig was used and this is illustrated in Figure 5.3. It was composed of the following parts: reaction vessel, thermocouple, pressure gauge, pressure relief valve, needle valve, expansion chamber, hand pump and water bath. The experimental procedure consisted of adjusting the pressure in the vessel initially to 60 bar (limited through pump capability). The system is then left for a set duration of time after which pressure is released. Tests were carried out for the system being under pressure for 1 hour, 8 hours and 24 hours. Two different procedures of pressure release mechanism were investigated: releasing the pressure in one step after a fixed phase contact time had elapsed, or three pressure release steps evenly distributed throughout the duration of the experiment. Oil phases used with this equipment consisted of 1 wt% of either stearic and myristic acid solutions in toluene. Aqueous phases consisted of 20000 ppm calcium ions, 25000 ppm sodium ions with or without 70 ppm bicarbonate ions. Initial pH values for these were close to 6.5. Temperature was also investigated using systems at 20 and 70 °C. Maximum volumes used in these tests were 50 ml.

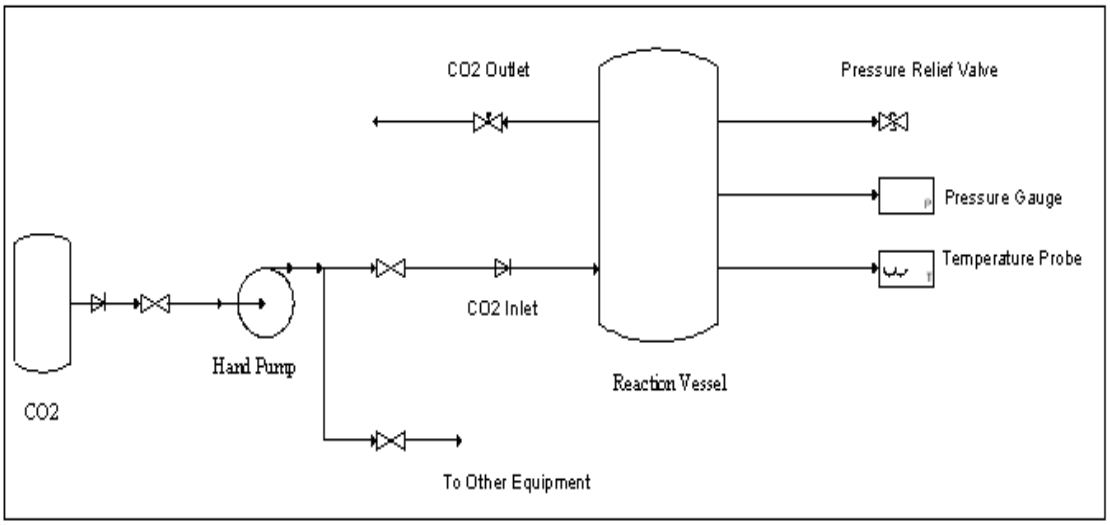

Figure 5.3. Static CO_2 rig used for soap formation in the laboratory.

The second pressure release mechanism did not lead to any significant changes on the experimental performance. This was probably due to the short equilibration times for dissolved carbon dioxide (CO_2) gas in aqueous systems. Thus, this pressure release mechanism was not used further. Tests were also initially devised to be carried out at two temperatures, 20 and 70 °C. Solubility of CO_2 is inversely proportional to temperature (Carroll *et al.,* 1991). Thus the use of higher temperatures did no lead to better experimental performance and thus only the temperature of 20 °C was used further. Table 5.1 presents the results of the static CO_2 rig experiments for tests where a single pressure release was carried out after the appropriate equilibration time had elapsed. The increase in equilibration time (e.g. from 1 to 8 hours) for the CO_2 rig experiments resulted in higher final pH values (pH_f), thus indicating better rig performance due to loss of CO_2. Nevertheless the overall pH difference was not sufficient to lead to the formation of any soap deposit.

Aqueous phase	Equilibration time (hrs)	pH_f
Deionised H_2O	1	5.45
25000 ppm sodium ions	1	4.48
25000 ppm sodium ions	8	4.78
20000 ppm calcium ions	1	4.25
20000 ppm calcium ions	8	4.48
20000 ppm calcium ions	24	4.49

Table 5.1. pH_f values for static CO_2 rig. All tests were conducted at 20 °C and maximum pressure of 60 bar.

Table 5.1 shows that there is a clear effect of cation presence on the solubility of CO_2, and higher pH values were obtained in the absence of cations. It is a well-known fact that the solubility of CO_2 is reduced in brines when compared to fresh waters (Crawford *et al.,* 1963). This could explain the pH values observed for brines in Table 5.1. However, there are no clear trends for the divalent and monovalent cations used in the tests in this thesis. An attempt was made to increase the final pH in the experiments by the addition of bicarbonate ions in the initial aqueous phase. This however did not lead to significantly different pH changes or the deposition of soaps. Thus the change in pressure could not lead to differential solubility of the CO_2 in solution. The average partitioning of CO2 from the gas phase to the aqueous phase is 0.8. Nevertheless, it is known that the kinetics of carbonic acid formation from CO_2 in the aqueous phases is slow. Hence the experiments with longer contact times in this thesis. Despite these modifications, no significant pH changes were observed during depressurization. The reason for this may also be the poor mixing of the CO_2 with the aqueous phase used in the experiments. It is likely that pressure effects on pH would only be observed in live fluids, where CO_2 his equilibrated across both hydrocarbon and produced water phases. Nevertheless, during the course of this thesis, live fluids were not available for testing. For this reason, the use of the static CO_2 rig was discontinued.

In conclusion, the results for tests employing the three experimental set-ups suggested that the simple static bottles would be sufficient for the formation of soaps in the laboratory and for mechanistic studies.

5.3. Optimisation and fine-tuning of static bottle tests.

5.3.1. Optimisation.

Static bottle tests were selected as the optimum method of choice for the study of the formation of soaps in the laboratory due to the fact this was the only method which resulted in sufficient pH changes. The optimum conditions for alkalinity, agitation, time dependency, acid and cation concentration were used in further sensitivity tests with model naphthenic acids, as well as more detailed aqueous phase conditions. Preliminary selection of naphthenic acids for the formation of soaps in the laboratory was based on the literature survey presented in Chapter 2. A series of candidate acid structures were chosen to account for the following variables: aliphatic *vs.* aromatic species, degree of unsaturation, number of carbon atoms as well as number of carboxylic groups. It was decided however, to focus on commercially available naphthenic acids and the selection of structures for the optimised bottle tests took into consideration a preliminary scan carried out by Dyer *et al.* (2003). The authors targeted primarily straight chain acids, and structures with 11 carbon atoms. Based on the literature review, it was decided to include a selection of the species tested by these authors, as well as others more representative of naphthenic acids found in crude oils. The concentration of the acids used in the tests was 0.01 wt% in toluene, which was chosen because it was similar to the total acid concentration found in a number of crude oils in the literature. In addition, this concentration would necessarily be below the critical micellar concentration (CMC) of most acids. This is important to force the formation of soap at the oil-water interface and not of micelle aggregates. Acyclic acids were also prepared in concentrations of 0.001, 0.1 and 1 wt%. In all tests, toluene was chosen as the solvent since it is both immiscible with the aqueous phase and has good solvency power towards most of the naphthenic acids. Figure 5.4 shows the acid structures used. All acids were purchased from Sigma Aldrich with the exception of numbers 9, 10, 19 and 20 which were purchased from Chiron. The acid purity may be considered to be higher than 98 wt% for all samples.

From the list of naphthenic acids tested, the following were selected for further optimisation experiments for the static bottle tests: stearic acid (SA), myristic acid (MA), cyclohexane pentanoic acid (CHP), 4-tert butylcyclohexane carboxylic acid (TBC), 4-tert-butylbenzoic acid (TBA) and 5-phenyl valeric acid (PVA). These were chosen because of the clearly observable formation of soaps at the oil-water interface in the preliminary tests and significant pH variations. The aqueous phases used in the additional tests contained 25000 ppm sodium ions added as NaCl (Merck) or 25000 ppm calcium ions added as $CaCl_26.H_2O$ (Merck). All aqueous phases were adjusted to pH 12 with 1 wt% NaOH,

aqueous solution. The objective of using these cations was to investigate the tendency of different acids to form either sodium or calcium soaps as indicated in the literature review in Chapter 2. These brines were prepared following the dissolution of the respective salts in Milli-Q water. After 24 hours the brines were filtered under vacuum using a cellulose acetate membrane with 0.45 μm retention diameter (Whatman). Measurements taken during these bottle tests were final pH and the observation of any soap deposits. It has been reported that temperature has an effect on the formation of soaps under field conditions (Turner and Smith, 2005). Nevertheless, it was decided that the effect of temperature in the bottle tests would not be investigated to avoid the inclusion of another variable. Thus all experiments were carried out at 25 °C. This decision was also based on health and safety implications of using highly flammable fluids as the oil phase (toluene).

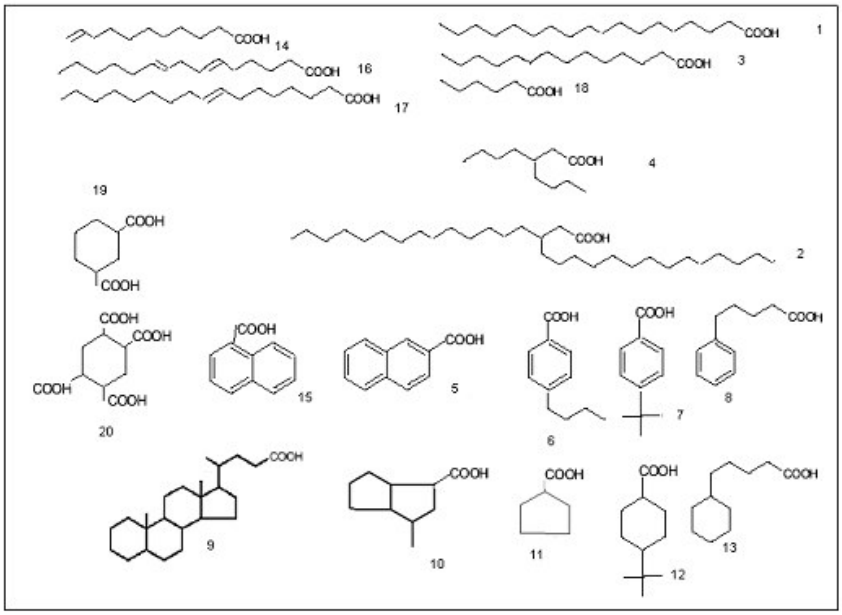

Figure 5.4. Naphthenic acid structures selected for screening. 1 = stearic acid, 2 = triacontanoic (melissic) acid, 3 = myristic acid, 4 = undecanoic acid, 5 = 2-naphthoic acid, 6 = 4-butylbenzoic acid, 7 = 4-tert-butylbenzoic acid, 8 = 5-phenyl valeric acid, 9 = β-cholanoic acid, 10 = 3-methyl octahydro pentalene carboxylic acid, 11 = methyl pentanoic acid, 12 = 4-tert-butylcyclohexane carboxylic acid, 13 = cyclohexane pentanoic acid, 14 = undecylenic acid, 15 = 1 naphthoic acid, 16 = oleic acid, 17 = linoleic acid, 18 = hexanoic acid, 19 = cyclohexane dicarboxylic acid, 20 = cyclohexane tetracarboxylic acid.

5.3.2. Fine-tuning.

Fine-tuning experiments were conducted on the effect of pH on the phase behaviour of calcium and sodium ion-rich systems in static bottle tests. This was carried out using systems with pH adjusted to values from 2 to 12, and with fixed naphthenic acid concentrations of 1 wt%. The next paragraphs will briefly discuss common measurements for the analysis of oilfield waters to support the techniques used in this section.

Basic produced water analysis comprises the following: specific gravity, resistivity, pH, total dissolved solids (TDS), total alkalinity, cations and anions, volatile fatty acids and oil content. The alkalinity of water samples is due to the carbonate, bicarbonate and hydroxide ions amongst others, and can be defined as buffering capacity. The most common technique for analysis of carbonate and bicarbonate ions employs a potentiometric titration which leads to a titration curve from measurements of pH versus volume of strong acid titrant (e.g. sulphuric acid). The reader is referred to the work of Barnes (1964) for details of the calculation of bicarbonate, carbonate and alkalinity concentrations. Inductively conductive plasma atomic emission spectroscopy (ICP AES) is the most common technique for the analysis cations and anions in oilfield waters. The choice of cations and anions selected for use in the fine-tuning of static bottle test procedures was based on typical compositions of produced waters found in soap-forming fields. An example is shown in Table 5.2. Bicarbonate ions (HCO_3^-) were selected to be added to aqueous phases for fine tuning testing. These are an integral part of the overall pH control. The inclusion of bicarbonates ions in aqueous phases would also help study the hypothesis of Gallup *et al.* (2005), namely that they would be part of the complex soap structure. The concentrations of bicarbonate ions and cations used in the different experimental cases in this thesis are included in Table 5.3. Note it was not possible to fully exclude sodium ions from certain tests, given that bicarbonate ions were added as excess $NaHCO_3$. Concentrations of additional sodium ions were topped up using NaCl. Any excess calcium carbonate solute was removed by filtration from the brine prior to the tests. Thus, the concentrations of bicarbonate in Table 5.3 are calculated values with Multiscale thermodynamic software, after removal of excess calcium carbonate solute. The final effect on calcium ion concentration was observed to be minimum.

pH	7.88
Ion	**ppm**
Sodium	19400
Potassium	1180
Lithium	4.7
Calcium	940
Magnesium	310
Iron (II)	0.05
Strontium	290
Barium	115
Sulphate	7.7
Chloride	33570
Bicarbonate	1140

Table 5.2. Produced water analysis of soap-forming field (Field Z).

Case	Ion concentrations (ppm)		
	Ca^{2+}	Na^{+}	HCO_3^-
1	2000	25000	11
2	2000	25000	72
3	20000	25000	200
4	x	25000	11
5	x	25000	72
6	x	25000	200

Note x = not tested.

Table 5.3. Experimental cases with aqueous phase concentrations used in bicarbonate tests.

Both divalent-rich and monovalent-rich aqueous phases were considered for the purpose of soap formation in the laboratory. Calcium and sodium ions were chosen since these were shown in Chapter 4 to be the predominant species present in field soap samples. Barium was also selected to provide an additional divalent ion for comparison with the calcium results. Barium has a larger ionic radius than calcium which affects the hydration of the cation and the availability for reaction at the oil-water interface as discussed in Chapter 2. Effects of other divalent ions such as magnesium were not investigated. Magnesium has a small ionic radius compared to calcium. Previous literature results have indicated the predominance of calcium effects in oil-water systems compared to magnesium (Brandal, 2005).

Mixed aqueous phases with monovalent and divalent ions were used to investigate particular competition of cationic species. The effect of cation concentrations was also investigated. Calcium and sodium ions were added as the chloride salts mentioned

previously. Barium ions were added as $BaCl_2$ (Merck). Table 5.4 presents the different aqueous phase compositions used. These were placed in contact with the naphthenic acids selected from Figure 5.4. In addition, two cases were used as references: a naphthenic acid solution mixed with an aqueous phase with no cations, and a pure toluene solution (with no naphthenic acids) mixed with an aqueous phase with no cations. Variation in divalent cation concentrations in the aqueous phases was investigated using ICP AES.

Case	Cation Concentration (ppm)		
	Ca^{2+}	Na^{+}	Ba^{2+}
1	1000	x	x
2	10000	x	x
3	20000	x	x
4	x	1000	x
5	x	10000	x
6	x	25000	x
7	x	x	1000
8	x	x	10000
9	x	x	20000
10	1000	25000	x
11	10000	25000	x
12	20000	25000	x
13	1000	x	20000
14	10000	x	20000
15	20000	x	20000
16	x	25000	1000
17	x	25000	10000
18	x	25000	20000
19	20000	x	1000
20	20000	x	10000

Note x = not tested.

Table 5.4. Experimental cases with aqueous phase concentrations used in cation tests.

The effect of aqueous phase pH was also examined in detail. It was decided to use values which would span the whole possible range of oilfield water values, in addition to those which would encourage the partitioning of the naphthenic acids across the oil-water interface (values above the pK_a, i.e. 5). Thus aqueous phases having pH values of 2, 4, 6, 8, 10 and 12 were used. All pH adjustments were carried out using either 10 wt% NaOH and 10 wt% HCl in aqueous solution. If during a test a particular phase behaviour such as the formation of a second phase (e.g. solid or emulsion) was observed, these were also analysed *in situ*.

5.4. Treatment of soaps formed in the laboratory.

5.4.1. Basic morphological analysis.

During the static bottle tests a number of soap-forming systems were observed over the phase contact period of 24 hours. These were examined first *in situ* using transmission microscopy and environmental scanning electron microscopy (ESEM with freeze fracturing). The theory of ESEM operation has already been described in Section 3.4.3. Transmission microscopy on the other hand is perhaps one of the oldest techniques for the study of particle morphology. It uses optics, through a combination of light and lenses for sample examination. In the study of emulsions, the technique relies on the sample being relatively transparent and the continuous phases having different refractive index. The resolution of transmission microscopy is a function of the wavelength of the illumination. In this technique, the divergence angle of the cone of light by the objective lens from each point in the sample determines the depth of field (loss of resolution with distance above or below the plain of best focus). Thus, there is a trade-off between magnification and depth of field. One of the most important sampling issues when studying liquids and emulsions is the loss of sample through evaporation. Thus, if temperature control is not available, examination must be carried out as soon as possible in order to avoid excessive sample loss.

Soaps obtained in the laboratory were examined with transmission microscopy. Sample optical properties (birefringency) were tested using cross polarisation filters in a procedure similar to that described by Horvath-Szabo *et al.* (2001a). A secondary objective was to check for the presence of liquid crystals, which are known to be associated with certain soaps and naphthenic acids (Ese and Kilpatrick, 2004). The microscope used to view and record the samples was an Olympus BH2 UMA model with polarisation filter lenses (A type). Objectives and lenses used were 0.9-0.25 and MSPLAN 10IC10 (0.3 μm) and MSPLAN 20IC20 (0.4 μm), respectively. Samples were transferred onto slides and observed at room temperature. Slides were rotated to avoid false interpretation of emulsion clusters in respect to the polarised light (Horvath-Szabo *et al.,* 2002). Photographs were taken by coupling an Olympus Camera C5060 Camedia to the microscope.

The environmental scanning electron microscopy (ESEM) was also used as a means of analysing the morphology of soaps formed *in situ*. The equipment details were presented in Section 3.4.3. For the examination of liquid samples, the freeze-fracturing of the soaps generated in the laboratory was carried out with liquid nitrogen. Sample freezing in this case was necessary because of the need to work at lower vapour pressures (to avoid

vaporisation) and to aid the flow of electrons in the instrument chamber. A potential drawback of this technique is the risk of induced structural changes in the sample under observation.

5.4.2. Particle size analysis.

Further tests on selected soap systems were conducted with the objective of correlating certain emulsion properties related to stability, to specific bulk aqueous phase and oil phase properties (e.g. cation content and naphthenic acid concentration). There are currently a variety of techniques available for emulsion droplet size analysis on which Sjoblom *et al.* (2003) have published a good review. The techniques include light scattering, nuclear magnetic resonance and acoustics. Droplet size measurements and distribution can be used as indicators of emulsion stability. This is in part due to the net effect of forces acting on the droplets, such as gravity induced sedimentation and diffusion. It is agreed that the mean droplet size of a kinetically stabilised emulsion system is linked to the emulsion viscosity. Droplet sizes are also a function of the surfactant concentration in the emulsion (below the CMC), the surfactant head group, and presence of cations in the aqueous phase. Measurement techniques which may be used include the Coulter principle, laser diffraction and photon correlation spectrometry (Malvern, 2005). In the Coulter principle, particles are made to flow through a small orifice and displace a volume of electrolyte solution. Electrical pulses which are generated are proportional to the volume of the particles. Particle size distributions as a function of frequency are reported. Volume or mass against distribution can also be reported if all particles have uniform density distribution across their size range. Particles in the size range 0.4 to 1200 μm can be measured and the exact range is a function of the aperture used in the equipment. One of the major disadvantages of using Coulter instruments is the compatibility of the material under analysis and also the flow effects (high viscosity solutions). In addition, if solid matter is present, this can lead to error and therefore a technique such as pulse field gradient NMR is preferred. For Coulter measurements, the sample needs to be diluted either in water or in the electrolyte used in the instrument. An additional technique of measuring droplet sizes is light scattering. In this method a laser beam is focused on the dispersed samples to be analysed. Light scattered by the particles is directed onto an optical detector. Detector arrays carry out the summation of scattered light distributions as a function of scattering angle, and this is treated mathematically to obtain particle size distribution using a theoretical model for the scattering process. One of the most widely used models uses Mie theory which solves Maxwell's equation for the

boundary conditions of a spherical particle. Light scattering techniques may be used for particles size ranges from 0.02 to above 3000 μm (Trainer, 2001).

Particle size analysis measurements for selected laboratory soaps formed from model naphthenic acid systems, were carried out using a Coulter Mastersizer MX3 apparatus. Laboratory soaps formed from Field W crude oil were also examined using light scattering with a Malvern Mastersizer 2000 in conjunction with a Hydro S dispersion unit. In this instrument diffraction patterns are converted to particle size distributions using Mie theory. The following parameters were used: particle reflective index of 1.3300 (an estimation for the soap sample tested), absorption of 1.000 and dispersant (continuous phase) reflective index of 1.465.

5.4.3. Elemental composition.

The characterisation of deposits formed in the laboratory was carried out by conducting filtrations of the whole system, thus separating them from the bulk aqueous and oil phases. The rationale behind the use of filtration was to enable the destabilisation of any emulsions formed. The set-up for the ESEM/EDAX and XRD used for the analysis of laboratory soaps was identical to that used for the field soaps described in Sections 3.43 and 3.5. To aid in the interpretation of the XRD results, a series of commercial naphthenic acid soaps, calcium stearate and sodium stearate (Crestchem) and barium stearate (SPCIE), were used. All soaps used were 95 wt% purity. No soaps of the aromatic and cycloaliphatic acids used in the experiments were found to be commercially available. It was hoped that by comparing the powder XRD patterns of these samples, the identification of soaps formed in the laboratory (particularly with mixed commercial naphthenic acid systems) would be made easier.

5.4.4. Surface properties of naphthenic acids in soap-forming systems.

In Chapter 3 experiments were described with the objective of gaining an understanding of the naphthenic acids in soap sample deposits and their surface properties. To be able to compare this behaviour with known systems, parallel tests were also conducted on selected model naphthenic acid systems and pH adjusted brines. Interfacial tension measurements using the Du Nouy ring were used following the set-up described in Section 3.6. The following experimental variables were analysed: concentration and type of naphthenic acids, concentration and types of cations and pH. The experimental matrix for these tests therefore followed that presented earlier for static bottle tests in Tables 5.3 and 5.4.

5.5. Formation of soaps using indigenous acids and crude oil systems.

5.5.1. Tests on indigenous acids.

Section 3.2.1 presented the two extraction procedures applied to the field soap deposits used in this thesis. A number of materials were obtained by applying these procedures to the deposits: the clean calcium soap, the indigenous naphthenic acids and the naphthenic acid extracts. Chapter 4 presented the results of the analysis of the naphthenic acid extracts from the field soap sample as analysed by mass spectrometry. In these, peaks at m/z 1230 were identified and these were assigned to Arn naphthenic acid species. It is also of interest to better understand the detection of the indigenous acids, particularly for the purpose of conducting mechanistic tests where both soap scales and soap emulsions are re-precipitated under laboratory conditions. Thus, the maximum solubility of the indigenous acids in toluene was determined. This was carried out using indigenous acids obtained as per Procedure B in Section 3.2.1. Subsequent dilutions with fresh toluene were used and samples analysed by electrospray mass spectrometry (ES) in the negative mode. The indigenous acids were analysed using the optimum settings included in Table 4.3, in addition to solid state and solution NMR. A number of additional tests were performed specifically on the indigenous acids: tandem mass spectrometry (MS/MS), two dimensional nuclear magnetic resonance (2D NMR) and liquid chromatography mass spectrometry (LCMS). These additional techniques are discussed briefly in the next paragraph. All tests were conducted on the indigenous acids from Field Y soap sample.

5.5.1.1. Tandem mass spectrometry.

This is a fast analytical method primarily used to obtain structural information (Castiglioni *et al.,* 2005). The basis of the technique is to induce fragmentation on a particular species and this can be achieved by ion/molecule collisions. Usually the mass analysers in tandem spectrometers are separated by a collision cell into which an inert gas (e.g. argon, xenon) is admitted to provide fragmentation. With sources using collision-induced dissociation (CID), this is accomplished by selecting an ion of interest with a mass analyser and introducing that ion into a collision cell which is used to link mass spectrometers in series. This is known as ion trap. A selected m/z (parent ion) from the first MS collides with a gas (e.g. argon or helium) resulting in fragmentation which can be carried out in different modes. The fragments are then fed to the second MS and analysed to obtain a fragment spectrum (daughter ion). The procedure is abbreviated to MS/MS or MS^n where n refers to the number of generations of fragment ions being analysed. There are limited references of MS/MS in the literature for characterisation of naphthenic acids (Rudzinski *et al.,* 2002;

Ohlenbusch *et al.,* 2002). The instrument used in this thesis was a hybrid quadrupole-time of flight (Q-TOF) in which ions are selected using a quadrupole analyser and fragmented in a quadrupole collision cell. Detection and separation of the ions is carried out in the TOF sector. The resolution of this instrument is routinely between 5000 and 8500. The full equipment settings are presented in the Table 5.5.

Mode	CID
Collision gas	argon
Energy	50-60 V
Collision gas thickness (molecules/ml)	$2.19x10^{12}$
Ionisation source	electrospray
Scan time (ms)	500
Ionisation gas	nitrogen
Declustering potential (V)	-30
Focus potential (V)	-130
Entrance potential (V)	8
Collision energy TOF (eV)	-19
Air pressure in cell (torr)	$2x10^{-3}$
Exit potential (V)	4

Table 5.5. MS/MS settings.

5.5.1.2. Two-dimensional nuclear magnetic resonance.

Very elegant two-dimensional nuclear magnetic resonance (2D NMR) procedures were used to gain insights into the structures of Arn by Lutnaes *et al.* (2006). The acids used were extracted from a field soap sample using the QAE Sephadex ion exchange resin. These acids were further analysed with and without derivatization using $BF_{3/}$methanol. Molecular modelling and ES were also used in establishing the best possible structures. In this thesis, NMR studies were carried out on the indigenous acids from Field Y sample. The hardware and settings for this was the same as the solution NMR presented in Section 3.2.3. In addition to the one dimensional experiments described in Chapter 3, the following 2D sequences were carried out on the indigenous acids separated from Field Y soap: graded heteronuclear multiple bond correlation (gHMBC) which looks at long range carbon and proton correlations by shifting polarisation through carbon atoms, thus identifying proton nuclei with carbon nuclei that are separated by more than one bond; graded heteronuclear molecular quantum coherence (gHMQC), in which proton magnetisation is transferred to the directly-bonded ^{13}C atoms; and graded heteronuclear molecular quantum coherence total correlated spectroscopy (gHMQC-TOCSY) which looks at bond correlations via spin-spin coupling. In the experiments one drop of

dimethylsulphoxide was added to the acid solution for homogenisation. No additional 2D NMR sequences were attempted (e.g. ADEQUATE) because most of the spectra acquired with the techniques described previously resulted very complex signals.

5.5.1.3. Liquid chromatography mass spectrometry.

The combination of liquid chromatography (LC) and mass spectrometry (MS) offers one of the most powerful analytical techniques for the characterisation of organic compounds (Covey *et al.,* 1986). In LC, the solvent (which most often also doubles as the mobile phase) is used to dissolve the components of the sample to be analysed. It is essential that the solvent used is pure and filtered prior to analysis, but in addition, it is also preferred to have low viscosity and chemical inertness. The choice of solvent is also a function of the LC mode: non-polar solvents are used for normal phase operation as opposed to polar solvents for reversed-phase operation. The solvent and dissolved samples are forced to flow through a stationary phase (chromatographic column) under high pressure, if applicable. In the column, the mixture is resolved into its components and this is dependent upon the extent of interaction between the sample and the column packing material. These interactions can be manipulated through choice of material and mobile phase. This is because of the competition of sample components for adsorption in the column surface due to hydrophobic as well as dipole-dipole interactions which leads to retention of particular species. The most commonly used detector in LC is the ultraviolet (UV) absorption detector. Liquid chromatography mass spectrometry (LCMS) has been used for the separation and identification of naphthenic acids by Ohlenbusch *et al.* (2002) and Yen *et al.* (2004). The particular identification of soap naphthenic acid components using LCMS was reported by Mediaas *et al.* (2005) and Baugh *et al.* (2004).

In the present work, an Agilent 1100 LCMS ion trap SL model equipment with an APPI interface was used. HPLC mode was used with a small with Zorbax 300 SB-C3 (20 by 40 mm) column. This was followed by flow into a Purospher RP 18 column (250 by 4 mm) with a 5 μm coating. The column oven temperature was 35 °C. The eluents (mobile phases) used were acetone, acetonitrile and combinations. Acetonitrile/acetone volume ratios were varied from 100/0 to a 20/80 over 35 minutes and the flow rates of 0.5 ml/min. Note that the use of polar solvents where shown to lead to enhanced ionisation of Arn in mass spectrometry, as described in Chapter 4. These conditions are however necessary to ensure correct structural characterisation of the species which is the focus of the experiments in this section. The source temperature used was 300 °C and the needle voltage for ionspray was -5.5 kV. Nitrogen was used as both nebulizer gas and curtain gas

with flowrate 10 l/min and pressure 40 psi. Indigenous acids from Field Y sample were tested using this procedure with the objective of gaining a better understanding in the detection of Arn naphthenic acids. A separated fraction from the LCMS procedure was collected and analysed using a NMR Bruker Avance 400. ^{1}H NMR, ^{13}C NMR with DEPT experiments were carried out. MS/MS analysis as per the strategy described Section 5.5.1.2 was also carried out on this fraction.

5.5.2. Mechanistic studies and the role of Arn in soap formation.

The naphthenic acid extracts from the Field Y deposit prepared according to the Procedure A in Section 3.2.1 were used in sensitivity mechanistic tests. The objective was the study of different experimental variables on the formation of laboratory soap deposits. The experimental cases studied were detailed in Tables 5.2 and 5.3. Tests were also carried out with a range of soap-forming crude oils. Soaps formed in the laboratory, either from naphthenic acid extracts or crude oils, were examined using ES, transmission microscopy, particle size analysis and EDAX/ESEM.

The surface properties of the naphthenic acid extracts and indigenous acids were evaluated using IFT measurements as described in Section 3.6. Lutnaes *et al.* (2006) suggested that Arn acids were more prone to reaction with inorganic cations across the oil-water interface than mono-carboxylic acids. According to Mediaas *et al.* (2005), 93 to 96 % of Arn acid present in a crude oil could be precipitated as calcium naphthenate deposits in deposition trials. Tests were also carried out in this thesis to investigate the relationship between Arn acids in conjunction with mono-carboxylic model naphthenic acids, both from a surface property perspective as well as on the formation of soaps in the laboratory. The following oil phases were used for this purpose:

- naphthenic acid extracts from Field Y deposit sample (refer to Figure 4.22 for composition) in combination with those from Field W (refer to Figure 4.26 for composition),
- naphthenic acid extracts from Field Y deposit sample in combination with 1 wt% stearic acid (SA) and
- naphthenic acid extracts from Field Y deposit sample in combination with 1 wt% 4-tert-butylbenzoic acid (TBA).

5.6. On establishing a protocol for soap formation under laboratory conditions.

The experiments described in Sections 5.2, 5.3 and 5.5 were designed to investigate the formation of soaps under laboratory conditions. Crude oils contain other surface-active molecules such as phenols and amides which may affect the oil-water-naphthenic acid equilibria under conditions of soap deposition. Thus, the use of surface properties of crude oils for the prediction of soap precipitation would have to be regarded with reservations. The preferred technique for the prediction of soaps would need to indicate the transitions which occur prior to precipitation: from free acids (at low pH values) to bound acids or soaps (at high pH values). A similar strategy was proposed by Zyskowski and Kamdem (1999) for the study of wood copper naphthenates with UV and FTIR spectroscopy. In this thesis, two spectroscopy methods were evaluated for the prediction of soap formation from laboratory systems: Fourier-Transform infrared (FTIR) and Raman. The application of FTIR to the analysis of naphthenic acids extracted from field samples was described in Section 3.2.2. The naphthenate anion (cation bound acid) has IR features which make it distinct from those due to naphthenic acids. The naphthenate ion has two coupled carbonyl bonds (C=O), with strengths intermediate to those between a single C=O and a C-O bond. Thus a strong asymmetric stretching band near 1650-1550 cm^{-1} arises. A weaker signal is also seen due to a symmetrical stretching band near 1400 cm^{-1} (Silverstein *et al.,* 2005).

Two oil phases were used in the FTIR and Raman spectroscopy experiments. The first was a 1 wt% stearic acid solution and the second comprised naphthenic acid extracts from Field Y deposit. These were placed in contact with aqueous phases containing 25000 ppm sodium ions, 1000 ppm calcium ions and 72 ppm bicarbonate ions, with pH adjusted to 2, 6 or 10. By taking aliquots of the oil phases after 24 hours of phase contact with the aqueous phases, it was hoped that IR and Raman spectra could be used to examine the transition from naphthenic acid to naphthenates. In other words, the onset of soap formation under laboratory conditions.

For the work in this thesis, a Bomem MB-series FTIR instrument was used with a resolution of 4 cm^{-1}. The instrument used a DTGS detector and the solutions under study were placed in a KBr liquid cell with a 1 mm PTFE spacer. 50 scans were obtained for the background spectrum and for the individual solutions tested. Spectra of the solutions were converted directly to absorbance units after background measurements. Raman spectroscopy depends on bond polarisation (how tightly electrons are bound to the nuclei) rather than molecular dipole changes due to absorption which are observed in FTIR. In Raman measurements are made of wavelength and intensity of inelastic scattered light. Molecular vibrations provide energy which results in the scattered light with shifted

wavelengths compared to the incident light. Both rotational and vibrational spectroscopy are possible with Raman. The overall energy amounts will determine the exact type of transition. However, as a rule, rotational transitions are three orders of magnitude slower than vibrational transitions. Basic Raman hardware set-up comprises a source of monochromatic radiation (usually laser), sample holder and a detector. The reader is referred to the work of Smith and Dent (2005) for a more detailed description of the technique and instrumentation. Raman is useful for the analysis of samples without a permanent dipole moment (not observable in IR), particularly in solution since transitions are more characteristic than IR. For the work in this thesis the Raman instrument used was a Renishaw 1000 with 780 nm excitation and a 25 mW laser output. A 40 μm wide slit was used and the charge couple device binning box set to 20 pixels wide sensitivity.

CHAPTER 6 – FORMATION AND EVALUATION OF SOAPS UNDER LABORATORY CONDITIONS: RESULTS.

Abstract

This chapter describes the results of techniques developed to reproduce the formation of oilfield soaps in the controlled environment of the laboratory. Static bottle tests were chosen because they allow for a simple study of soap systems with reproducible effects such as final pH and soap mass. Soaps were obtained in the laboratory from model systems including single and mixed calcium, sodium and barium solutions, as well as bicarbonate-containing systems. Soap formation was found to be a function of the precise aqueous phase (e.g. cations and pH) in addition to acid content of the oil phase (e.g. acyclic *vs*. cyclic/aromatic naphthenic species). This information is of significant importance for future development of a precipitation model using realistic feeds. In addition, bottle testing also shows excellent potential as a suitable technique for the evaluation of inhibitor chemistries. It was possible to form soap deposits in the laboratory from both naphthenic acid extracts, as well as certain crude oil samples. Nevertheless, only soap emulsion formation was possible from soap-forming crude oils. From a molecular perspective, the analytical results of these laboratory soaps are in line with the field deposit data presented in Chapter 4. Detailed speciation of particular indigenous acids allowed for the identification of Arn and the special properties of this species. For instance, the four carboxylic groups of the Arn acids were clearly identified with MS/MS experiments, as well as surface properties identified by IFT. FTIR spectroscopy showed potential as a simple technique for the prediction of soap precipitation onset in the laboratory with possible applications to crude oil and produced water systems.

6.1. Techniques for soap formation in the laboratory.

Three techniques were short-listed as described in Chapter 5 for the evaluation of the formation of soaps in the laboratory, together with the sample preparation procedures: static bottle tests, dynamic tube blocking and a static carbon dioxide rig. The optimum set-up for static bottle tests was studied further using a range of conditions in optimisation experiments. Soaps that formed under laboratory conditions were analysed using procedures similar to those described in Chapter 3 for the study of field deposits. At least three repeats were conducted for each experiment.

6.1.1. Static bottle tests.

6.1.1.1. The effect of alkalinity.

Table 6.1 presents the results of the variation in soap mass as well as pH for different alkaline agents (NaOH and KOH) used for pH adjustment in the bottle tests. Note pH_i is the initial adjusted experimental value and pH_f is the final value measured after 24 hours of phase contact. Both alkaline solutions showed a decrease in pH_f with increase in alkali concentration of the aqueous phase. The NaOH solutions resulted in consistently lower pH_f

than the KOH solutions. Therefore the dissociation of the naphthenic acids used in the model systems was favoured by the presence of sodium ions. This can be explained by the larger ionic radius of potassium compared to sodium (227 pm as opposed to 186 pm). This results in less hydration effects which prevent the full dissociation of the naphthenic acid. The deposit masses formed from the different alkalis did not however show major variations. This is because soap formation is likely to be limited, in all but one case (e.g. 0.1 wt% alkali), by the naphthenic acids in the oil phase. These deposits were identified as naphthenate soaps with either sodium or potassium (EDAX and XRD data not shown). The Normadose solution exhibited a different effect. A large mass of deposit was formed with this pH adjusting medium; however the pH_f value was higher than the pH_i value. Naphthenate soaps are composed of naphthenic acids and either calcium or sodium cations as shown in Chapter 4. The Normadose buffer used in this case is of unknown composition (however the MSDS information indicates that it contains borates). Therefore if any deposits were to form with this buffer they would not be calcium or sodium naphthenates, but other salts. Use of EDAX and XRD on the samples formed from the Normadose buffer could not indicate the precise composition of these solids. Thus the NaOH solutions were chosen to be used in the remaining bottle tests due larger pH variations, and because of the formation of a deposit with composition more similar to those found in field conditions.

pH media	pH_i	pH_f	Deposit mass (g)
Normadose	11.87	12.00	1.02
0.1 wt% NaOH	12.00	11.34	0.12
1 wt% NaOH	12.00	11.04	0.14
5 wt% NaOH	12.00	10.86	0.12
10 wt% NaOH	12.00	10.64	0.16
0.1 wt% KOH	12.00	11.56	0.13
1 wt% KOH	12.00	11.43	0.12
5 wt% KOH	12.00	11.23	0.14
10 wt% KOH	12.00	10.89	0.15

Table 6.1. pH_f values and deposit masses for alkalinity sensitivity study.

6.1.1.2. The effect of agitation.

Three distinct agitation methods were used for the static bottle tests. Repeatability of final pH values and soap mass were ± 0.2 pH units and 1 wt% respectively in the experiments in this section. Bottles were manually shaken vigorously for one minute. This is represented by the "shake" notation in Table 6.2. Samples were also treated with an Ultra-Turrax mixer

with two different rates, namely 10000 and 25000 rpm. The reference test consisted of leaving both oil and aqueous phases in contact but without agitation.

Shear media	pH_i	pH_f	Deposit mass (g)
NaOH - reference	12.00	11.62	0.02
NaOH - shake	12.00	10.64	0.16
NaOH - 10000 rpm	12.00	10.75	0.17
NaOH - 25000 rpm	12.00	10.78	0.16

Table 6.2. Effect of agitation methods on soap formation tests. 10 wt% NaOH used for pH adjustment.

The data set for the reference test shows a pH_f value well above those obtained in the tests where shear was employed. Moreover, the mass of soap formed in this test was very low. The pH_f measurements for the Ultra-Turrax mixer tests are slightly higher than the value measured for the manually shaken test. Table 6.2 shows that the deposit masses were also very similar for the two agitation methods. Therefore, for the purpose of soap generation, it could be concluded that the total absolute shear for the Ultra-Turrax and manually shaken tests are probably the same. Soap formation is said to occur at the interface between oil and produced water (Vindstad *et al.,* 2003), and this is indeed what is observed with the soaps generated in the laboratory, as exemplified in Figure 6.1 which shows the reference test, as well as the manually shaken test, both after 24 hours of phase contact. Although both tests were adjusted to the same pH_i (12), the mixing energy transferred to the system to promote soap formation was not the same. This may be related to the enhancement of contact areas when the system is manually shaken (which results in greater soap mass) as a result of shear. The higher pH_f values for the reference test, (Table 6.2), indicate that not enough naphthenic acid was partitioned across the oil-water interface. Thus, by manually shaking both phases, sufficient mixing of the two liquids occurred to promote soap formation.

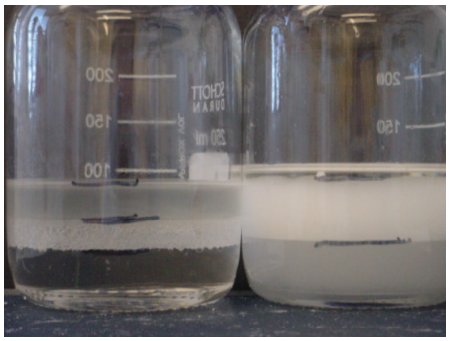

Figure 6.1. Effect of agitation on sensitivity tests. The sample on the left is the reference test (without shaking). The sample on the right is the manually shaken test. In both cases the oil phase was 1 wt% myristic acid in toluene. The aqueous phase was adjusted to pH 12 with 10 wt% NaOH.

6.1.1.3. Time dependency.

The time dependency of the results of the static bottle tests is presented in Figure 6.2. No differences in pH_f values were observed for tests with and without added naphthenic acids in the oil phase up to 12 minutes of phase contact. For contact times above 1 hour the presence of a naphthenic acid led to consistently lower pH_f, for the higher pH_i values. This effect is more noticeable for pH_i values of 6, which are close to the dissociation constant (pK_a) of the naphthenic acid used in the tests. Differences between the trends over time may be a result of diffusion effects (which are time-dependent) of the naphthenic acids to the oil-water interface, in-line with the results of Li *et al* (2004). No soaps were obtained by filtration from the pH 12 adjusted systems up to 12 minutes of phase contact. This is because the system is most likely not at equilibrium. This data is in sharp contrast with the trends presented by Dyer *et al* (2003). These authors used a phase contact times of 5 minutes for their tests. In this thesis, additional tests were conducted with contact times of 1 minute, 12 minutes, 1 hour, 6 hours and 24 hours. No major pH_f trend differences were observed for the contact times of 6 and 24 hours. Thus it is assumed the system has reached equilibrium at some point between these two time intervals.

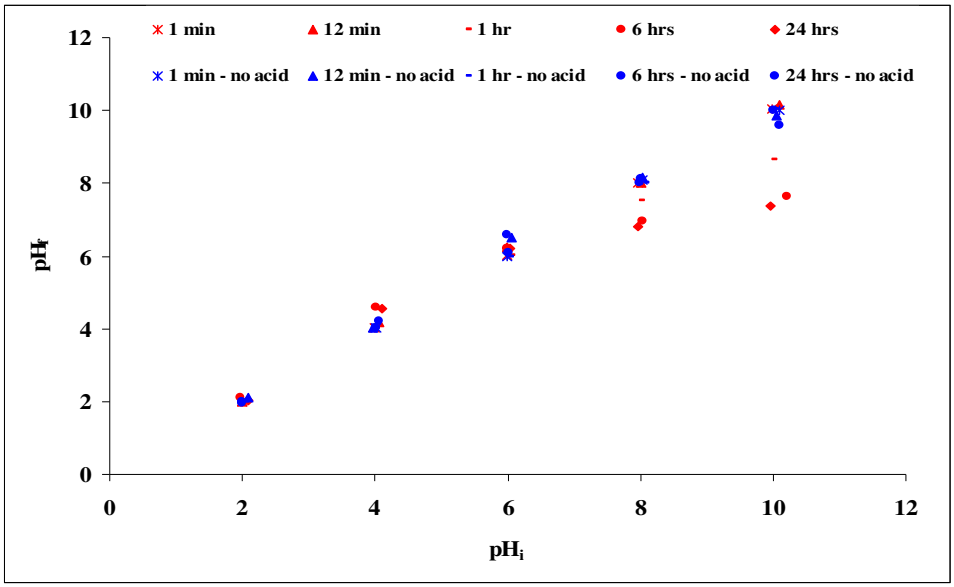

Figure 6.2. Time dependency on static bottle tests. pH_f as a function of pH_i, for contact times of 1 minute, 12 minutes, 1 hour, 6 hours and 24 hours, with and without the presence of naphthenic acids in the toluene (oil phase).

6.1.1.4. Acid and cation concentration.

The effect of acid concentration was tested using the shear and phase contact parameters described in the previous paragraphs (manual agitation and 24 hours of contact time). In

Figure 6.3 the mass of soap deposit formed in the laboratory is shown as a function of the available naphthenic acid in the oil phase. At acid concentrations below 0.05 wt%, the toluene oil phase became very turbid. The deposits formed under these conditions are particles with diameters of less than 45 μm, determined by transmission microscopy. The analysis of these deposits using EDAX and XRD showed that they were composed of solid naphthenic acid flakes. Thus, conditions exist for the formation of naphthenic acid micelles in solution as discussed in Chapter 2, and it is most likely these are being formed in detriment of naphthenate soap. Note the critical micellar concentration (CMC) for the acid used in the experiments is marked on Figure 6.3 and this value is 0.019 wt%. Thus it would be recommended to use naphthenic acid concentrations above this value in deposition tests, to enable maximum amounts of soap formation to occur, as opposed to micelles.

The effect of cation concentration was investigated using calcium ions and pH_i adjusted values of 12. As the concentration of calcium in the aqueous phase was reduced from 2000 to 10 ppm, a clear shift in the phase behaviour at the oil-water interface was observed. The interface which had appeared cloudy at first, changed to a thick gel-like layer at lower calcium concentrations. This was identified as a sodium naphthenate. This can be explained by the presence of NaOH used as the pH adjustment agent which leads to the addition of 200 ppm of sodium ions to the aqueous phase. These ions compete with the calcium ions for the naphthenic acids and soap formation. When the amounts of calcium ions are reduced in the aqueous phase, the dissociated acid will react with the sodium ions and deposit as a sodium soap. These tests demonstrated that calcium ion concentrations of at least 1000 ppm were necessary to ensure the reaction of the naphthenic acids with calcium ions in the static bottle tests.

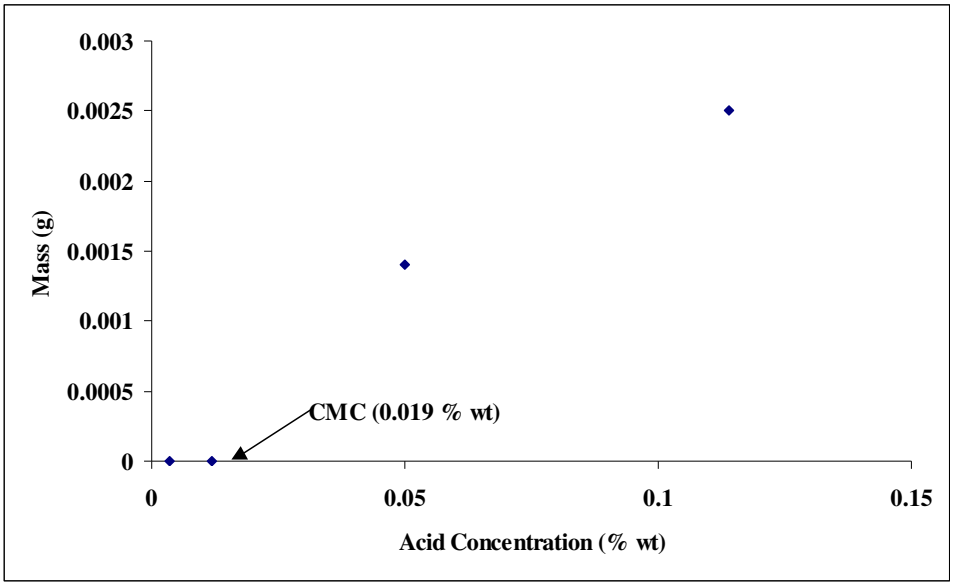

Figure 6.3. Mass of deposit as a function of naphthenic acid concentration. Deposit formed from aqueous phase pH 12 adjusted with 10 wt% NaOH, and oil phase consisting of various concentrations of stearic acid. CMC = critical micellar concentration.

6.2. Optimisation and fine-tuning of static bottle tests.

6.2.1. Optimisation.

The conditions for alkalinity, agitation and time dependency (10 wt% NaOH for pH adjustment, manual shaking and phase contact time of 24 hours) were used for the optimisation of oil phase compositions in the static bottle tests. A shortlist of different naphthenic acids was used to account for the majority of species in crude oil (Figure 5.4). No trends could be observed for particular acid species such as acyclics and mono-cyclics in terms of deposit mass and pH_f. Moreover, no conclusions could be reached in regards to the effect of molecular weight, number of carboxylic acid groups or polarity. Generally speaking, the calcium aqueous phases showed lower pH_f values compared to when sodium aqueous phases were used with the same oil phase. The only soaps observed to form during these experiments were for certain acyclic species such as oleic, myristic, linoleic, stearic, and melissic acids. Figure 6.4 presents an example of pH_f trends as a function of naphthenic acid concentration in the oil phase from the above-mentioned tests. All pH_i values were adjusted to 12. The acyclic species were chosen for this experiment since they were the only naphthenic acids that led to an observable soap deposit with low acid concentrations. It can be observed in Figure 6.4 that the increase in acid concentration in the oil phase, leads to a lowering of pH_f, which arises because of more partitioning and dissociation across the oil-water interface. Soaps were clearly visible in these tests. The trends in pH_f decrease followed a specific order according to the chemical nature of the naphthenic acid moiety. Acids with unsaturations, such as oleic and linoleic acid, led to smaller pH variations. This

is because the presence of the double bonds prevents extensive ionisation of the acids. Thus the pH variations were also a function of the number of unsaturations in the species. Acids with an acyclic structure led to lower pH values, and this trend was also a function of molecular weight (Figure 6.4). Note the differences between hexanoic acid (6 carbons) and myristic and stearic acids (14 and 18 carbons respectively). The pH_f was lower in the presence of calcium ions than sodium ions, despite the slightly higher ionic radius of calcium compared to sodium (197 pm as opposed to 186 pm). This is a reflection of the enhanced dissociation effects of divalent species on acids as discussed by Acevedo *et al.,* (2001). Thus the trends in the above-mentioned experiments are a reflection of the solubility and dissociation of the saturated naphthenic acid species at the oil-water interface.

Attempts were made to carry out similar experiments for other groups of naphthenic acids, such as those containing bi-cyclic structures and different number of carboxylic groups (see Figure 5.4). However, the difficulties encountered in these tests were in regards to the solubility of the acids in toluene. All acid species with more than one cyclic or aromatic ring, or more than one carboxylic group were sparingly soluble in toluene at or above concentrations of 0.01 wt%. Therefore, a trade-off between solubility and structure was necessary for the selection of acid species for the optimised procedures for the remaining experiments. Although unsaturated acyclics showed good potential for soap formation, these are not representative of major naphthenic acid species found in many crude oils. Saturated acyclics were selected because they were present in the field soap samples examined in (Figure 4.23). Mono-cyclic acids were also selected with two variants: a carboxylic group attached either directly to the ring or to an alkyl side chain. Acids with an aromatic ring with the same carboxylic group positioning were also chosen to allow for the study of differences in polarity and aromaticity. The selected species are illustrated in Figure 6.5.

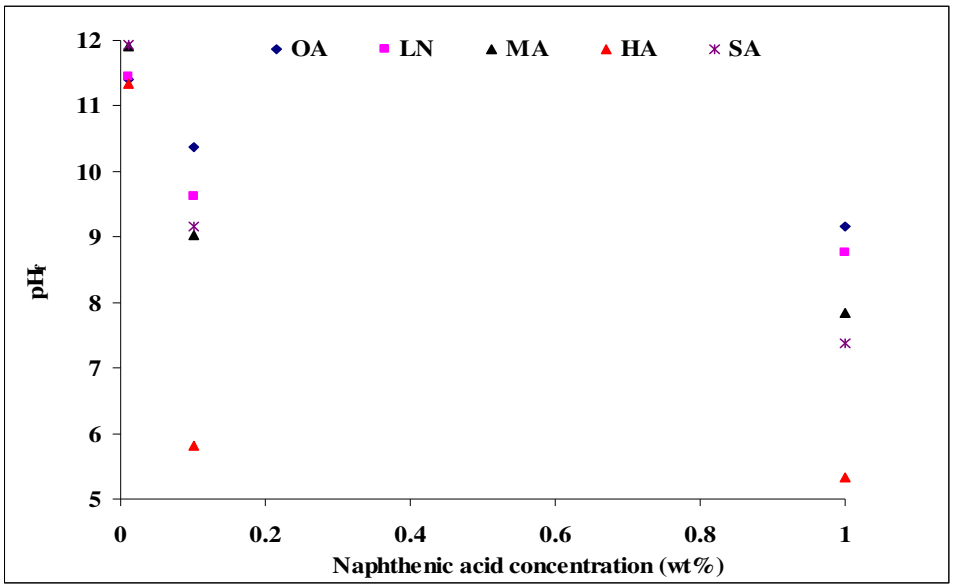

Figure 6.4. Final pH value as a function of naphthenic acid concentration for acyclic species. Oil phases: OA oleic acid, LN linoleic acid, MA myristic acid, HA hexanoic acid, SA stearic acid. Aqueous phase: 25000 ppm sodium ions pH 12 adjusted with 10 wt% NaOH.

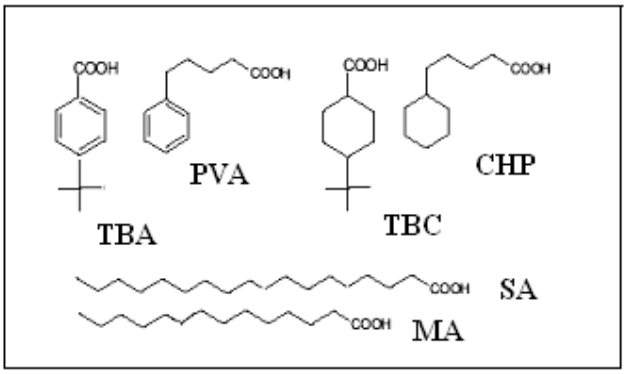

Figure 6.5. Naphthenic acid structures selected for fine-tuning static bottle tests. SA stearic acid, MA myristic acid, TBA 4-tert-butylbenzoic acid, PVA 5-phenyl valeric acid, TBC 4-tert-butylcyclohexane carboxylic acid, CHP cyclohexane pentanoic acid.

6.2.2. Fine-tuning.

During the fine-tuning experiments, the use of aqueous phases with pH_i values below 12 did not produce visible soap deposits in the static bottle tests. Both oil and aqueous phases remained clear and no deposit was recovered even after filtration of the system. There was however evidence that the naphthenic acids were partitioning and dissociating at pH values above the pK_a. Cratin (1993) showed that pH at the oil-water interface may be many units lower than the bulk pH. This is because ionisation of acids is at a maximum at the oil-water interface. This trend is observed in Figure 6.6 at pH_i values above 8. The acyclic species (MA and SA) show lower pH_f values in these experiments compared to the other

naphthenic acid structures, prior to the deposition of soaps (which occurs close to pH 12 in these experiments). These experimental observations suggest that the acyclic species are interacting preferably with cations at the oil-water interface.

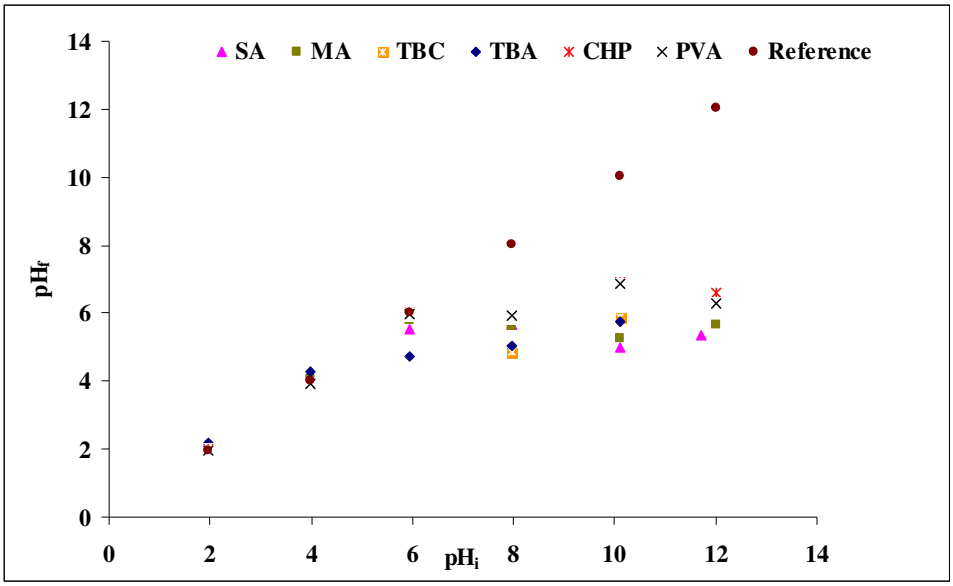

Figure 6.6. pH_f as a function of pH_i. Aqueous phases containing 20000 ppm calcium ions. Oil phases consisting of 1 wt% naphthenic acids. Key for the legend is in Figure 6.5. Note the reference case consists of toluene with no naphthenic acids placed in contact with the same aqueous phase.

Thus fine-tuning investigations were also carried out to study the effect of cation concentrations on pH_f and deposit mass, namely: calcium, sodium and barium ions (individually and in mixed cationic solutions as detailed in Table 5.4). It can be seen in Figure 6.7 that clear differences exist for the naphthenic acids in the presence of calcium ions obtained during the static bottle tests. The aqueous phases containing divalent ions (calcium and barium) showed largest pH_f variations, as a function of increasing cation concentration (compared to the monovalent sodium ions). This can be observed in Figures 6.7, 6.8 and 6.9. For the aqueous phases containing only sodium cations, there were less noticeable changes in pH_f. Only the acyclic species showed significant pH_f variation with increase in sodium concentration. Divalent cations lead to additional dissociation of naphthenic acids since one cation is bound to two naphthenate anions under the appropriate conditions. The acyclic species (MA, SA) showed the overall largest pH_f differences compared to the other naphthenic acid species used.

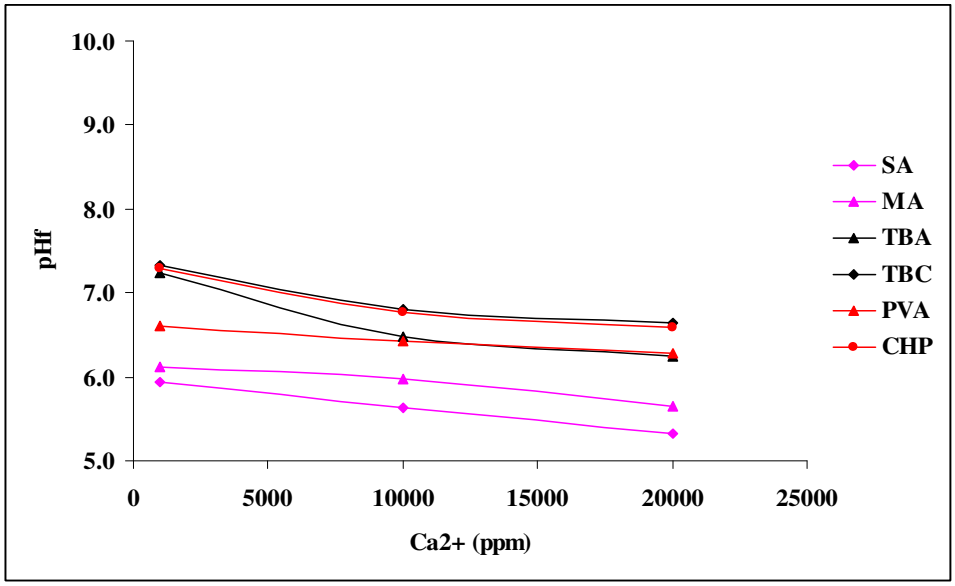

Figure 6.7. pH_f as a function of calcium ion concentration, Ca^{2+} (ppm) in the aqueous phase for a range of model naphthenic acids. The key to the legend can be found in Figure 6.5.

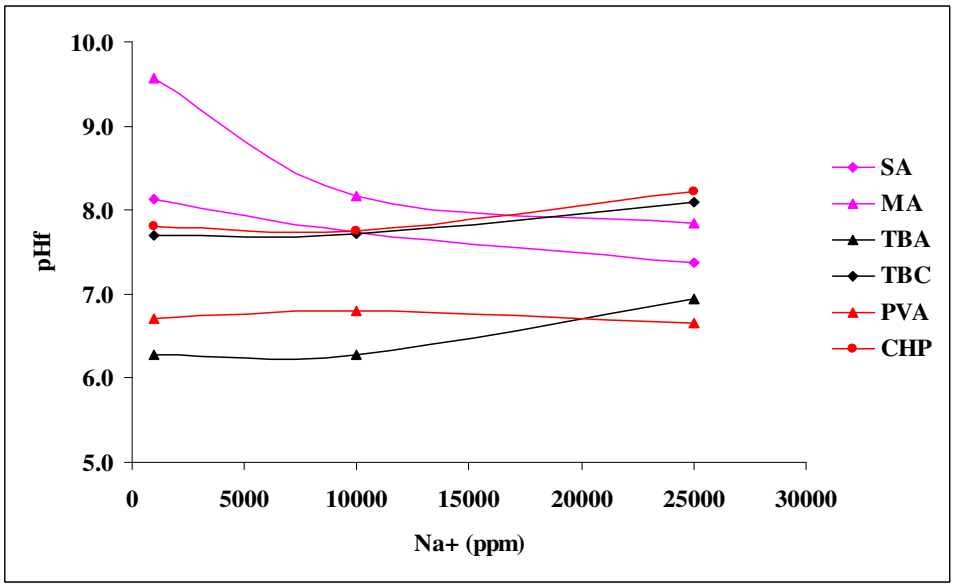

Figure 6.8. pH_f as a function of sodium ion concentration, Na^+ (ppm) in the aqueous phase for a range of model naphthenic acids. The key to the legend can be found in Figure 6.5.

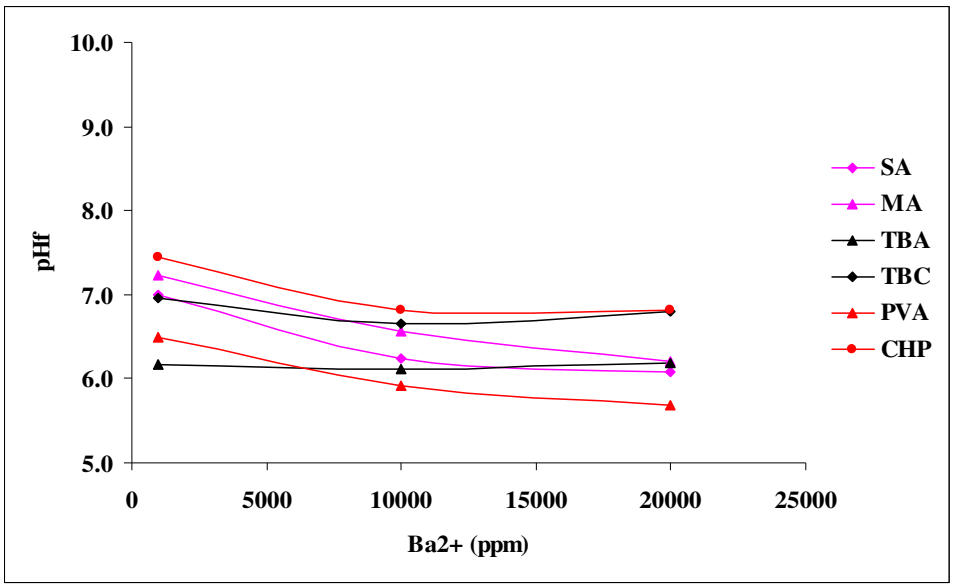

Figure 6.9. pH_f as a function of barium ion concentration, Ba^{2+} (ppm) in the aqueous phase for a range of model naphthenic acids. The key to the legend can be found in Figure 6.5.

Figure 6.10 presents an example of the soap deposit mass obtained from the same set of fine-tuning experiments conducted to obtain the pH trends presented in Figure 6.7. All but the acid species with the carboxylic acid attached to the alkyl side chain produced a deposit in the presence of calcium-rich aqueous phases. The possible explanation for this is steric hindrance caused by bulky naphthenic acid structures. The overall mass of deposit in these experiments remained practically constant as a function of calcium concentration. In the presence of sodium ions however, only the acyclic species produced a deposit which increased with the amount of sodium ions in the aqueous phase (results not shown). The amounts of deposit produced as a function of barium ion concentration were very low. Only acyclic species lead to deposits in the presence of barium ions (results not shown). These results represent combinatory effects of cation species and naphthenic acids.

Experiments conducted on mixed cation species resulted in equally interesting results. In all experiments, pH_f trends followed those of the individual divalent cation present. When two divalent species were present (i.e. calcium and barium), the trend followed that of calcium ions. Examples of these trends are shown in Figure 6.11 where pH_f values are presented for mixed calcium and sodium aqueous phases. It can be observed there is good qualitative agreement with the pH_f data shown in Figure 6.7. The deposit mass in the mixed cation experiments also followed particular trends; for example in Figure 6.12 it can be observed that the deposit mass trends are in qualitative agreement with those in Figure 6.10. Combinations of calcium and sodium ions lead to a range of deposits for all but the species with the carboxyl group attached to the alkyl side chain (possibly owing to reasons discussed earlier). Combination of barium and sodium ions only led to deposit formation

when acyclic acids were present in the oil phase. When combinations of calcium and barium ions were present, increases in deposit mass were only observed with the increase of calcium ions in the aqueous phase.

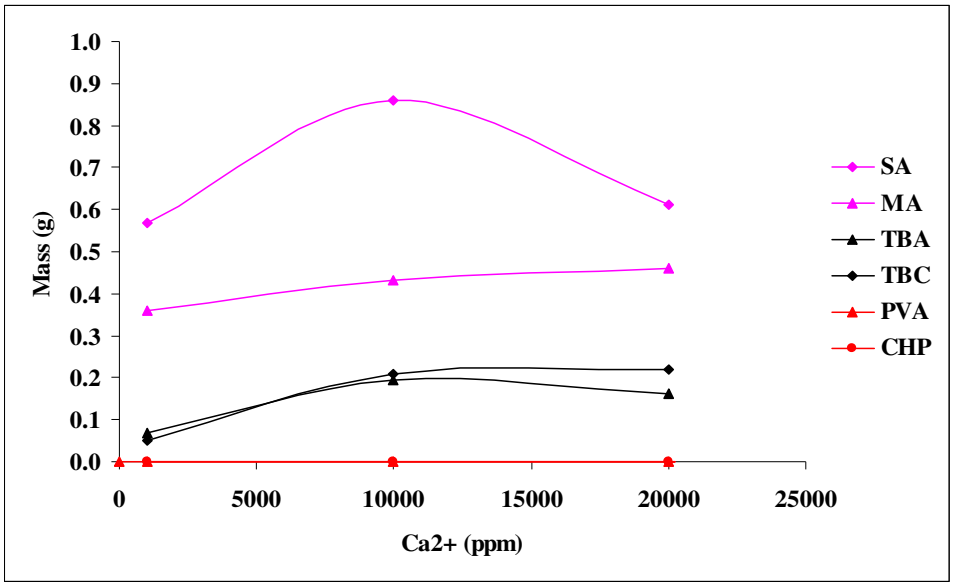

Figure 6.10. Mass of deposit (g) as a function of calcium ion concentration, Ca^{2+} (ppm). Deposits formed from calcium-rich aqueous phases pH 12 adjusted, and oil phases comprising 1 wt% naphthenic acids. The key to the legend can be found in Figure 6.5.

This data can be interpreted in light of the theory discussed in Chapter 2 in regards to the relationship between acids and cations at the oil-water interface and this is illustrated in Figure 6.13. The presence of divalent cations (e.g. calcium or barium) leads to a variation in pH_f with increasing or decreasing cation concentration in the static bottle tests. Because the ionic radius of the barium (222 pm) is larger than that of the calcium (197 pm), decreased hydration effects are present in the aqueous phase. Brandal (2005) suggested this would result in highly stable films at the interface. In tests conducted with barium aqueous phases in this thesis, a very small emulsion layer was seen to form at the oil-water interface. However this was unstable and broke after 12 minutes. Steric hindrance effects probably explain why only acyclic acids formed a deposit with barium ions and more bulkier naphthenic acid species did not. In other words, structures such as those with carboxylic groups attached to the alkyl side chain (e.g. PVA) would not pack favourably at the oil-water interface. In this case the hydration of the barium ions resulted in the presence of unstable soaps. This explains the larger deposit masses observed with calcium-rich aqueous phases, as opposed to barium-rich aqueous phases. When barium and calcium are present in mixed aqueous phases in static bottle tests, the calcium effect is predominant and thus higher deposit masses are observed with increasing calcium concentration (for a fixed

barium concentration). However this is only seen for the acyclic acids, owing to less steric hindrance compared to bulkier naphthenic acid species as per Figure 6.13.

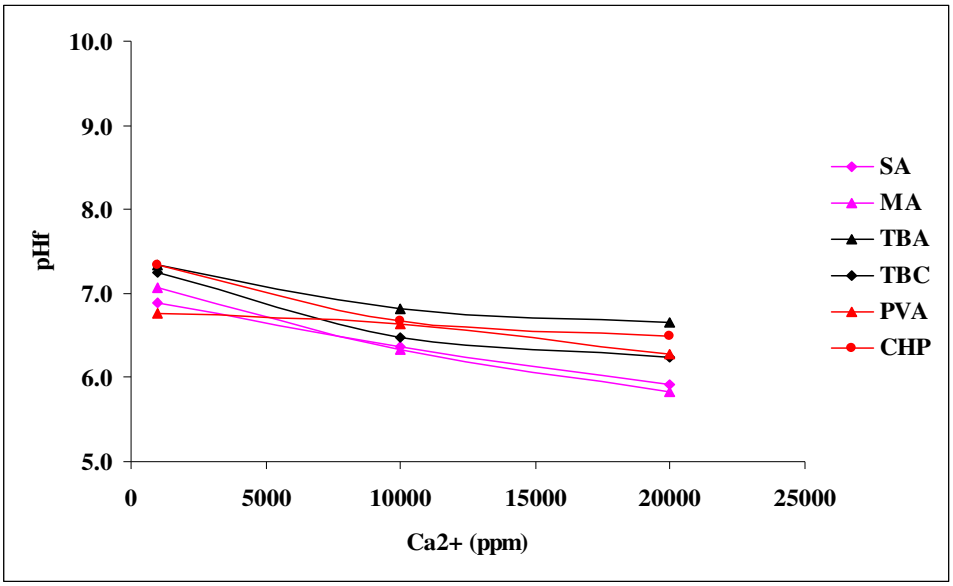

Figure 6.11. pH_f as a function of calcium ion concentration, Ca^{2+} (ppm). Aqueous phase containing 25000 ppm sodium ions and increasing concentrations of calcium ions. The key to the legend can be found in Figure 6.5.

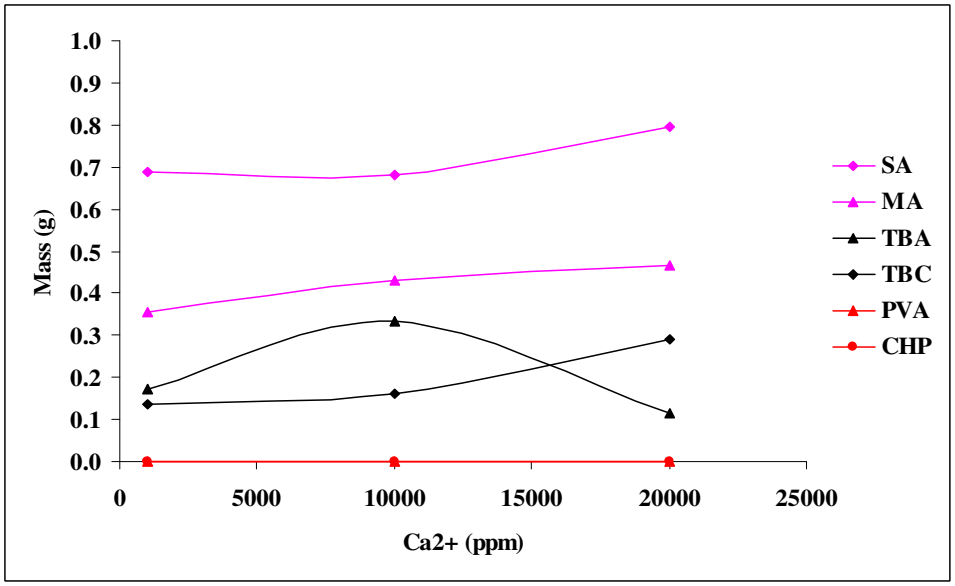

Figure 6.12. Mass of deposit (g) as a function of calcium ion concentration, Ca^{2+} (ppm). Deposits formed from aqueous phase containing 25000 ppm sodium ions and increasing concentrations of calcium ions, and oil phases comprising 1 wt% naphthenic acids. The key to the legend can be found in Figure 6.5.

Further evidence of the precise influence of naphthenic acid-cation interactions on the phase behaviour of the static bottle tests may be observed in Figure 6.14. The images show the different features when two acyclic acids, stearic acid (SA) and myristic acid (MA), where placed in contact with either a sodium-rich or a calcium-rich aqueous phase. A thick

turbid and viscous emulsion was formed when sodium ions and the acyclic acids were placed in contact. The oil-water interface in the presence of calcium ions was reduced to a thin flaky turbid layer. Lower pH values result from greater concentration of hydrogen ions. Thus the presence of divalent ions leads to increased ionisation of the naphthenic acids, compared to monovalent ions. An example of this ionisation effect can be seen in the pH trends in Figures 6.7 and 6.8. This would then destabilise the emulsion formed at the oil-water interface. Calcium has a slightly larger ionic radius compared to sodium ions (197 pm as opposed to 186 pm); yet two naphthenic acid ions are bound to one calcium ion, as opposed to one naphthenic acid ion bound to one sodium ion. Thus divalent ion presence would favour dissociation.

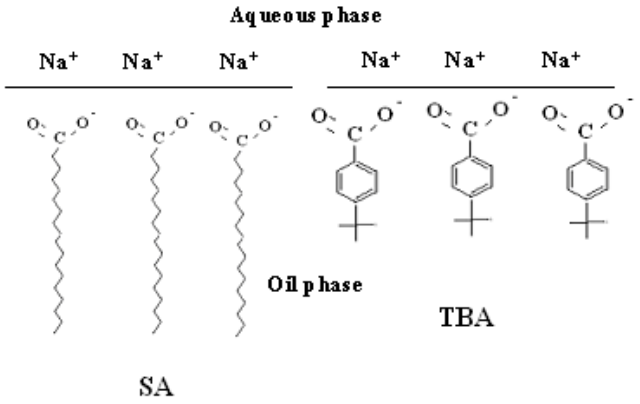

Figure 6.13. Illustration of the alignment of naphthenic acids and cations under high pH conditions at the oil-water interface. SA stearic acid, TBA 4-tert-butylbenzoic acid. Note the bulkier TBA acids would lead to steric hindrance at the interface.

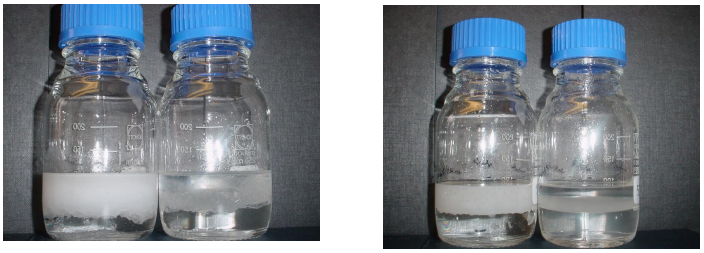

Figure 6.14. Phase behaviour of static bottle tests. Aqueous phase: pH 12 adjusted, left image bottle stearic acid (SA), right image myristic acid (MA). Comparison of the effect of different aqueous phases: 25000 ppm sodium ions (right bottle), 20000 ppm calcium ions and 25000 ppm sodium ions (left bottle).

In Chapter 4 it was shown that particular sodium-rich field deposit samples consisted predominantly of acyclic acids (Figure 4.27). Tests were devised to evaluate the selectivity of these particular acids towards sodium ions in mixed naphthenic acid solutions. In these tests all aqueous phases were adjusted to pH 12 to force the deposition of soaps. The total

concentration of individual acid species was 1 wt%. For comparison purposes, similar experiments where calcium was the main cation in the aqueous phase were also carried out. There were no major differences in pH_f values for the experiments in Figure 6.15 for each individual cation used, which would minimise structural type effects. This indicates no differential dissociation effects, probably owing to the high concentrations of naphthenic acids used. Stearic acid (SA) leads to the higher amounts of deposit mass, and there is little difference in deposit mass between the calcium and sodium cases for this species. The use of cyclic or aromatic acids (i.e. TBA or TBC) leads to reduced amounts of deposit mass for the calcium aqueous phases as observed in Figure 6.15. Yet the most striking effect was the absence of deposit masses for the case when sodium aqueous phases were placed in contact with cyclic and aromatic acid structures, in all but one case (SA/TBC mixture as shown in Figure 6.15).

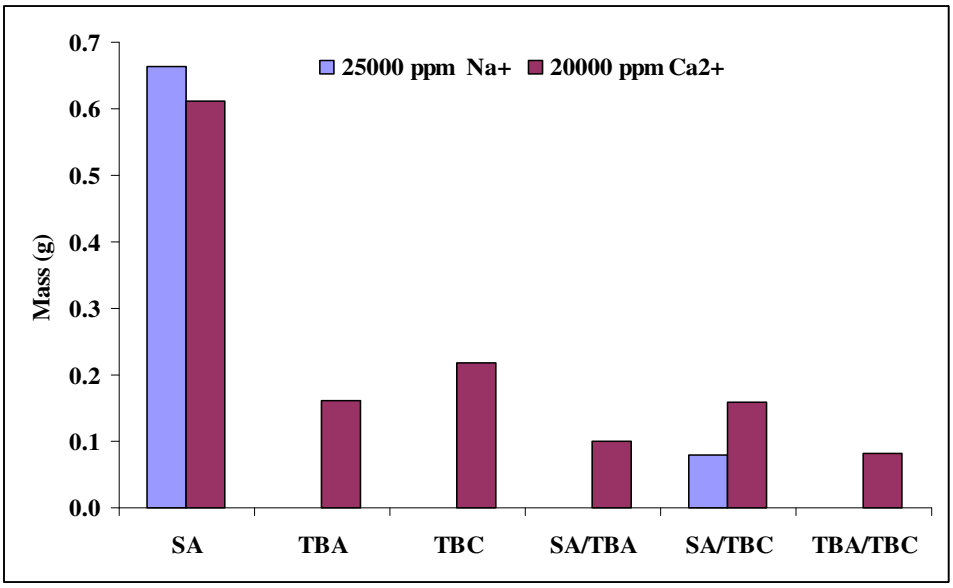

Figure 6.15. Mass of deposit (g) as a function of naphthenic acid and aqueous phase cation properties. Deposits formed from aqueous phases containing either 25000 ppm sodium ions or 20000 ppm calcium ions pH 12 adjusted. Oil phases containing 1 wt% naphthenic acids: SA stearic acid, TBA 4-tert-butylbenzoic acid, TBC 4-tert-butylcyclohexane carboxylic acid.

Experiments were also performed using model solutions where the ratio of acyclic/aromatic (SA/TBA) acid in the toluene oil phase was varied (i.e. SA and TBA acids were used in combination). The aqueous phase consisted of 25000 ppm sodium ions adjusted to pH 12 to force the formation of soaps. These results are presented in Figure 6.16. There were no major pH_f differences in the experiments as a function of naphthenic acid ratio. The presence of TBA acids in the oil phase leads to reduced deposit masses. This data is

additional evidence for the dissociation/steric hindrance effects discussed earlier and illustrated in Figure 6.13.

Based on the experimental results in this chapter, formation of deposits in the laboratory is a combination of acid dissociation effects (directly related to cation presence in the aqueous phase), cation hydration effects (related to the ionic size of the aqueous phase cation) and steric hindrance effects (resulting from the size and structure of the naphthenic acid). These effects are particularly noticeable with multi-component naphthenic acid and cation solutions. Under these conditions, an additional effect caused by the competition between acyclic *vs.* cyclic/aromatic structures for the formation of sodium or calcium soaps occurs.

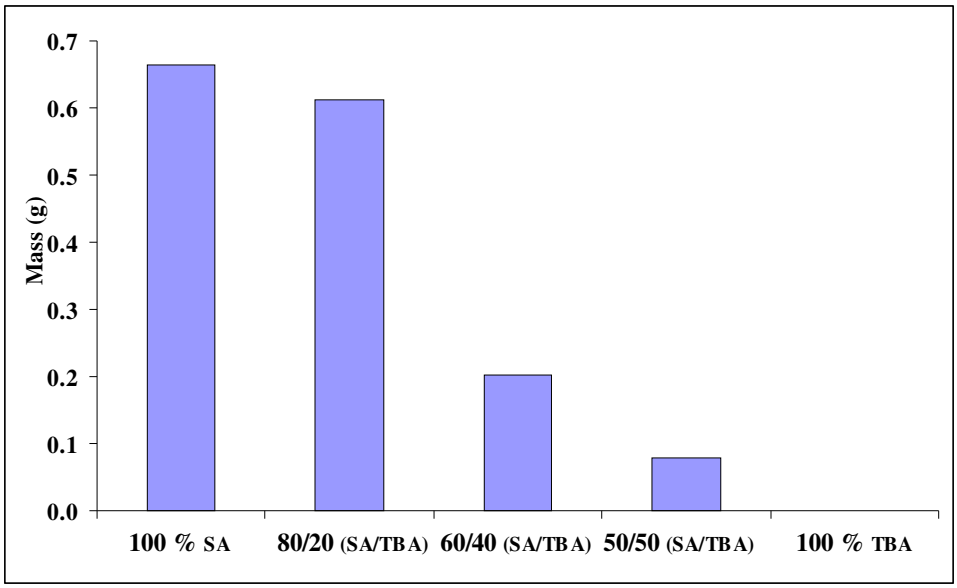

Figure 6.16. Mass of deposit (g) as a function of SA/TBA ratio in the oil phase. Total concentration of naphthenic acids kept constant in the oil phase at 1 wt%. Deposits formed from aqueous phases containing 25000 ppm sodium ions pH 12 adjusted.

Figure 6.17 presents the results of the experiments detailed in Table 5.3. For the experiments with both calcium and sodium ions, there is an increase in pH_f with increase in bicarbonate concentration. This is more evident for the oil phases consisting of TBA and SA/TBA naphthenic acids. Dissociation of the naphthenic acids is increased by the presence of a combination of calcium and sodium ions in the aqueous phase as shown in Figure 6.11, in the absence of a buffer. However, buffers should act to keep pH_f high. At higher bicarbonate concentrations, there are more buffer ions in the system to counter-balance the hydrogen ions resulting from the dissociation of the naphthenic acids. Thus pH_f increases with excess bicarbonate. Less TBA may dissociate compared to SA (due to steric hindrance, the TBA acid may not pack as well at the oil-water interface). This could explain

why less bicarbonate ions were required to keep pH_f values high. For the experiments with only sodium ions, pH remains reasonably constant with increasing bicarbonate concentration. Since there are only sodium ions are present in the aqueous phase, less naphthenic acids dissociate (see Figure 6.8). Thus, less buffer is required to maintain a high pH_f value. All deposit masses in the bicarbonate-containing experiments (Figure 6.18) were small compared to those without bicarbonate buffers (i.e. Figure 6.12). The only exception was when stearic acid (SA) was placed in contact with bicarbonate-containing sodium aqueous phases. Because of high precipitation yields, less naphthenic acid is available for dissociation, thus pH_f values for SA are higher than the other experiments owing to buffers, and this is also shown in Figure 6.17. Gallup *et al.* (2004) claimed sodium soaps would be formed by complex bicarbonate structures. The deposits obtained in the laboratory with bicarbonate buffers may represent realistic soap precipitates, since their deposition occurred with no prior pH adjustment. The morphological and compositional features of these deposits will be examined in the next section.

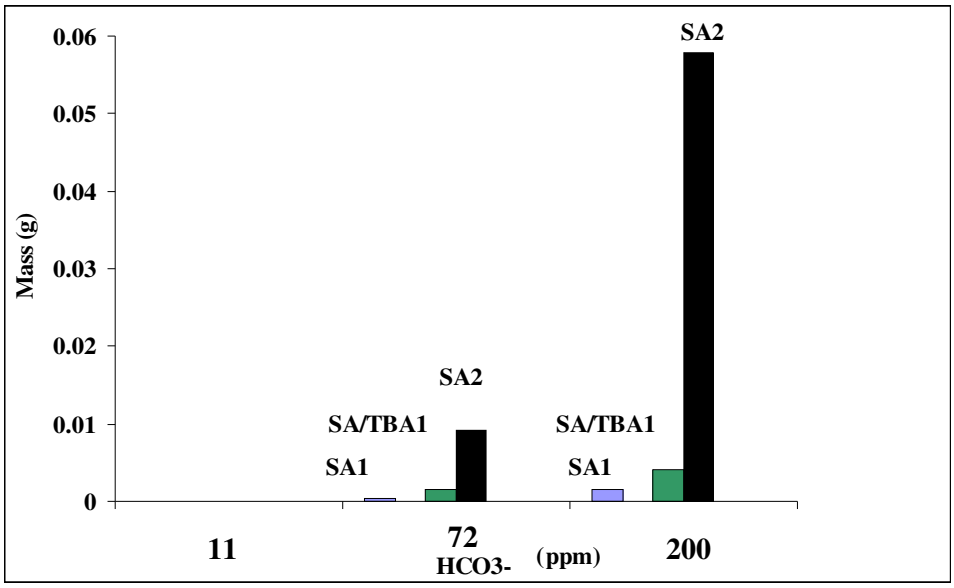

Figure 6.17. pH_f as a function of bicarbonate concentration (ppm). Aqueous phases containing 25000 ppm sodium ions and 20000 ppm calcium ions (legend " 1") or 25000 ppm sodium ions (legend "2"). All oil phases containing 1 wt% of naphthenic acids, SA stearic acid, TBA 4-tert-butylbenzoic acid.

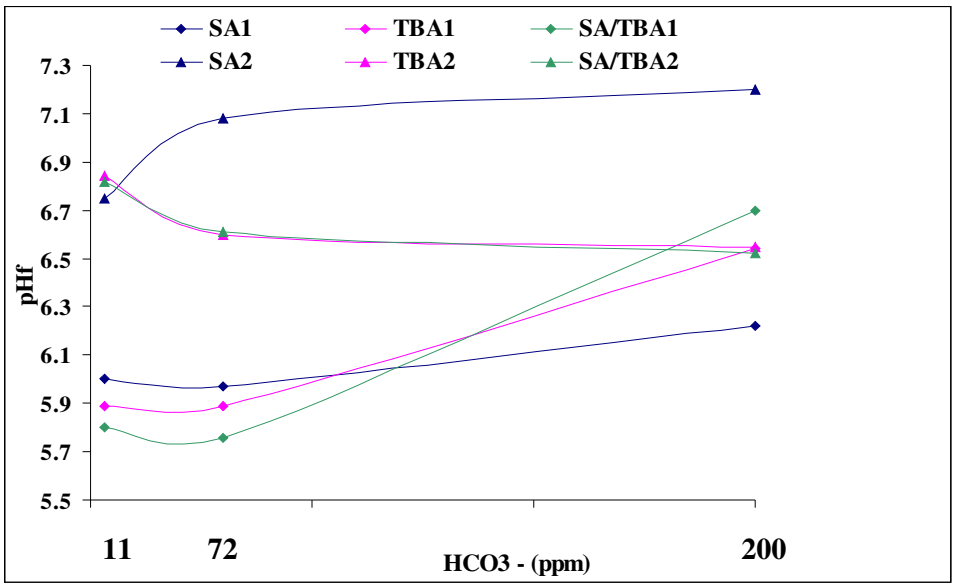

Figure 6.18. Mass of deposit (g) as a function of bicarbonate. Deposits formed from aqueous phases containing: 25000 ppm sodium ions and 20000 ppm calcium ions (legend "1") or 25000 ppm sodium ions (legend "2"). All oil phases containing 1 wt% of naphthenic acids, SA stearic acid, TBA 4-tert-butylbenzoic acid.

6.3. Treatment of soaps formed in the laboratory.

6.3.1. Basic morphological analysis.

Sub-samples of soaps formed *in situ* under laboratory conditions were separated for microscopic analysis. Figure 6.19 contains images that show the results for tests conducted with stearic acid (SA) in the toluene oil phase. Oil-in-water (O/W) emulsions were formed in these tests and the continuous phase was verified by the dissolution of an aliquot in an aqueous phase of the same composition used.

6.3.2. Particle size analysis.

As discussed in Chapter 2, O/W emulsions are stabilised by electrostatic interactions, governed by the type and concentration of ions in the bulk and oil-water interface. Presence of divalent ions (e.g. calcium) and sodium ions (Figure 6.19a) leads to a reduction in droplet size compared to the case where only sodium ions are present (Figure 6.19d). The addition of bicarbonate ions in the aqueous phase leads to further reduction in droplet sizes due to counter-ion effects (Figures 6.19b and 6.19e as compared to Figure 6.19a and 6.19d). Bicarbonate buffer ions balance the hydrogen ions which result from the dissociation of the naphthenic acids at high pH values. The precise effects of cations on droplet size distributions can be observed in more detail in Figure 6.20. The addition of calcium ions has an effect on the distribution and size of emulsion droplets. The cut-off value for emulsion diameter appears to be 100 μm since sodium and calcium based emulsions only have droplets above or below this value respectively. Additional morphological features of

the emulsion formed from sodium ions were acquired using freeze fracturing ESEM. Results suggested the emulsion droplets are surrounded by an amorphous layer, which was previously described as a thick turbid emulsion in Figure 6.14. The emulsion analysed collapsed under the ESEM high vacuum so no elemental analysis was conducted. It is possible that these structures may represent sub-micron soap particles which would not be detected by the particle size analysis equipment used to generate the data in Figure 6.20. The smallest particle sizes which can be detected using the current set up are in the order of 0.1 µm.

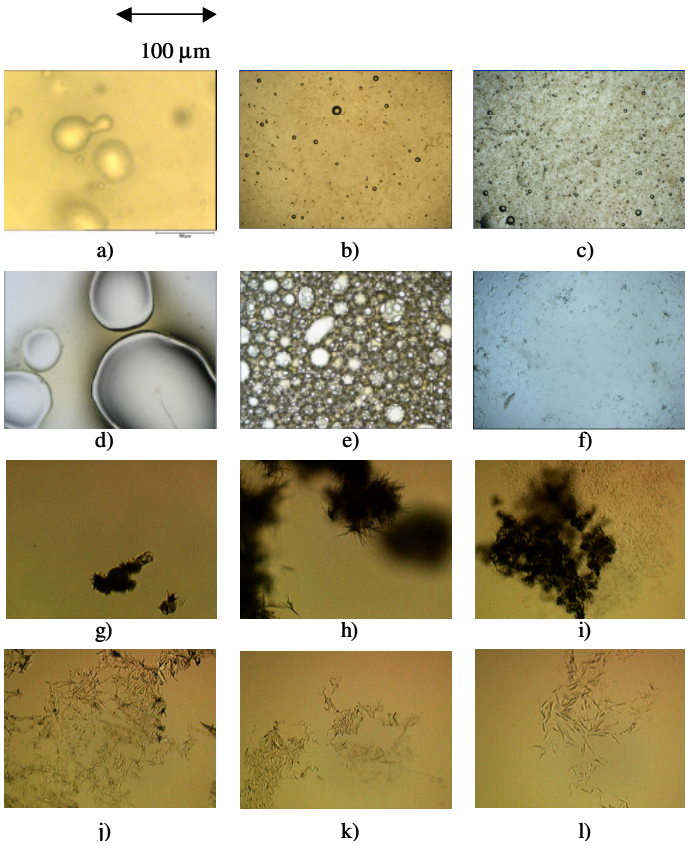

Figure 6.19. Transmission microscopy images of *in situ* deposits. a) Oil phase SA 1 wt% - aqueous phase 25000 ppm Na^+ and 20000 ppm Ca^{2+}, b) Oil phase SA 1 wt% - aqueous phase 25000 ppm Na^+, 20000 ppm Ca^{2+} and 72 ppm HCO_3^-, c) Oil phase SA and TBA 1 wt% - aqueous phase 25000 ppm Na^+, d) Oil phase SA 1 wt% - aqueous phase 25000 ppm Na^+, e) Oil phase SA 1 wt% - aqueous phase 25000 ppm Na^+ and 72 ppm HCO_3^-, f) Oil phase SA and TBA 1 wt% - aqueous phase 25000 ppm Na^+, 20000 ppm Ca^{2+} and 72 ppm HCO_3^-, g) Oil phase TBC 1 wt% - aqueous phase 1000 ppm Ca^{2+}, h) Oil phase TBC 1 wt% - aqueous phase 1000 ppm Ca^{2+} and 25000 ppm Na^+, i) Oil phase TBC 1 wt% - aqueous phase 1000 ppm Ba^{2+} and 20000 ppm Ca^{2+}, j) Oil phase TBA 1 wt% - aqueous phase 1000 ppm Ca^{2+}, k) Oil phase TBA 1 wt% - aqueous phase 1000 ppm Ca^{2+} and 25000 ppm Na^+, l) Oil phase TBA 1 wt% - aqueous phase 1000 ppm Ba^{2+} and 20000 ppm Ca^{2+}.

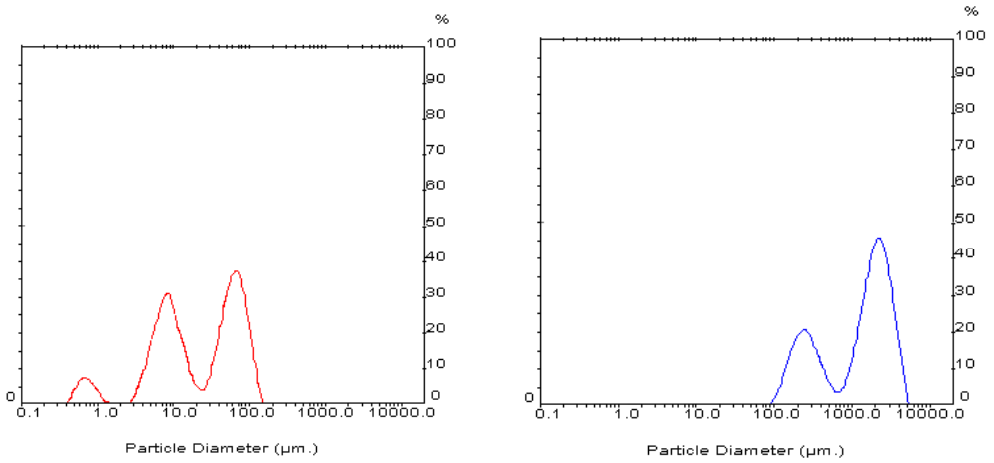

Figure 6.20. Particle size distribution of *in situ* deposits formed from oil phase SA 1 wt%. Aqueous phase: left 25000 ppm sodium ions and 20000 ppm calcium ions, right 25000 ppm sodium ions.

6.3.3. Elemental composition

The images in Figure 6.19 showed soaps formed with distinct morphology as a function of naphthenic acid and cation type and concentration. For the cyclic and aromatic structures (TBC, TBA), solid deposits were present in the oil phases. The solids formed from TBC acids are more compact and resemble clusters of needle-like crystals (Figures 6.19g, 6.19h and 6.19i). The solids formed from TBA acids are more dispersed and resemble long thin needles (Figures 6.19j, 6.19k and 6.19l). It was thought that these changes in morphology could be attributed to different amounts of calcium ions in the original aqueous phase used for soap formation. For this purpose, many attempts were made to analyse the cation composition of aqueous phases using ICP, to check for calcium depletion. The only observable changes in calcium concentration were those with low initial cation content in the aqueous phase (~ 100 ppm). The differences at higher calcium concentrations were within the experimental error of the ICP measurement. ESEM/EDAX as well as XRD measurements showed the deposits formed from TBA and TBC acids were all calcium naphthenates (data not shown). Therefore the analysis of the remaining deposits formed in the laboratory was carried out using both ESEM/EDAX as well as XRD.

When the soap systems (such as those in Figure 6.19a) were filtered, solid soap particles were formed. No clear morphological differences were observed with ESEM for these deposits in all tests. This was consistent with the field soap deposits presented in Figure 4.50. Therefore the use of ESEM was discontinued as a means of fingerprinting laboratory deposits. Commercial naphthenic acid soaps (stearates only) were used as templates for the interpretation of the XRD patterns. For the EDAX studies, the theoretical atomic carbon/cation (C/Ca or C/Na) ratios for naphthenate soaps were used. The ratios are shown in Table 6.4.

Naphthenic acid	C/Na	C/Ca or C/Ba
SA	18	36
TBC/TBA	14	28

Table 6.4. Theoretical carbon/monovalent cation (sodium) atomic ratio, C/Na. Theoretical carbon/divalent cation (calcium or barium) atomic ratio, C/Ca or C/Ba. SA stearic acid, TBA 4-tert-butylbenzoic acid, TBC 4-tert-butylcyclohexane carboxylic acid.

Calcium, sodium and mixed calcium-sodium aqueous phases.

An example of the use of the measured EDAX atomic ratios for the analysis of laboratory deposits is presented in Figure 6.21. In these experiments calcium-rich aqueous phases were used. The carbon/calcium (C/Ca) for the laboratory soaps formed were between 18 and 36 and are close to the theoretical ratios, 28 and 36 shown in Table 6.4. No other cations were found in the deposits. The cases where the carbon/calcium was lower than the theoretical ratio (i.e. TBC acid) indicate that there are more calcium ions in the sample than in pure calcium naphthenate soaps. In this case, the additional calcium ions are a result of the formation of calcium hydroxide formed due to the pH adjusting medium.

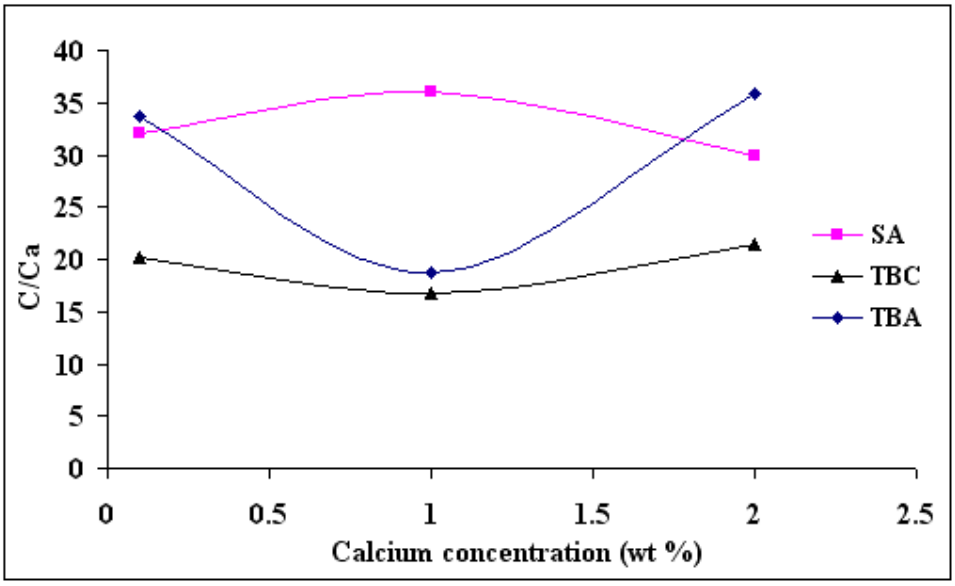

Figure 6.21. Carbon/calcium (C/Ca) atomic ratios. Deposits formed from aqueous phases containing calcium ions pH 12 adjusted. Oil phases containing 1wt% acid solutions. Legend in Table 6.4. Cation concentrations are plotted in wt% for ease of interpretation.

One of the XRD patterns for the deposits formed from calcium-rich aqueous phases in contact with an oil phase containing stearic acid is shown in Figure 6.22. It can be observed that the laboratory deposit pattern is very similar to the pattern of the commercial calcium stearate also plotted in the figure. This supports the conclusions reached from the analysis

of the EDAX data, that the deposits formed in the laboratory were mostly calcium naphthenate soaps.

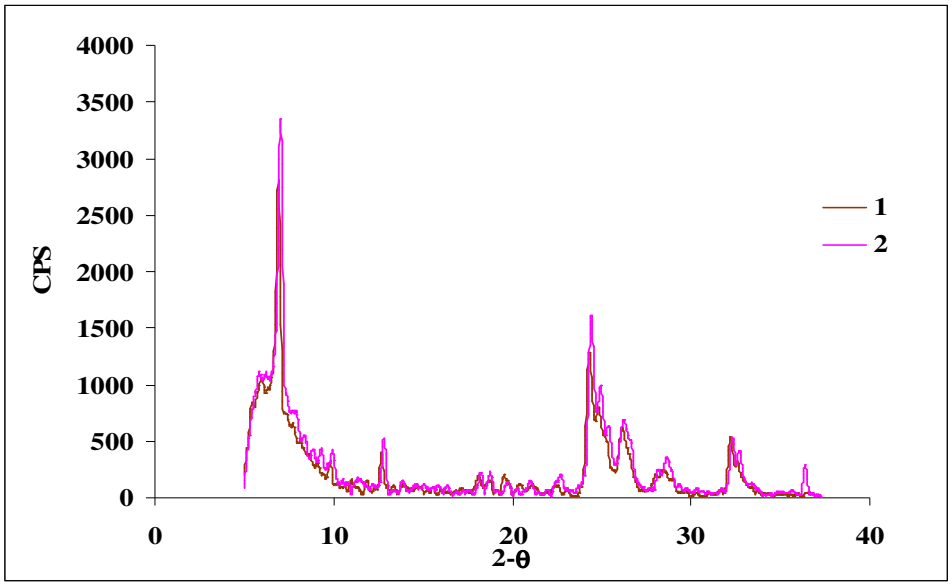

Figure 6.22. XRD patterns. 1 is the pattern from the deposit formed from aqueous phase containing 20000 ppm calcium ions pH 12 adjusted, oil phase 1 wt% SA, 2 is the pattern of a commercial calcium stearate.

Figure 6.23 presents the XRD pattern for the laboratory deposits obtained from an aqueous phase with sodium ions and an oil phase with stearic acid. The deposit pattern is very similar to that of the commercial sodium stearate also plotted in the figure. This indicates that sodium stearate was formed in this static bottle test, as a consequence of sodium-rich aqueous phases.

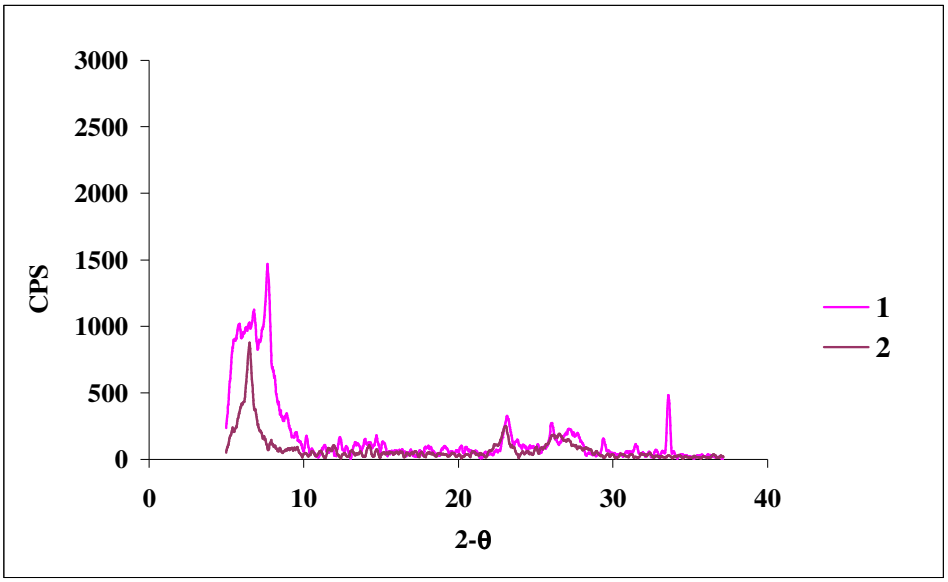

Figure 6.23. XRD patterns. 1 is the pattern from the deposit formed from aqueous phase containing 25000 ppm sodium ions pH 12 adjusted, oil phase 1 wt% SA, 2 is the pattern from a commercial sodium stearate.

The effect of using mixed calcium and sodium aqueous phases on the composition of the deposits formed in the laboratory is shown in Figure 6.24. The carbon/calcium (C/Ca) ratios are similar to the data presented in Figure 6.21. This means that the deposit contains predominantly calcium naphthenates. Figure 6.25 presents the carbon/sodium (C/Na) ratios for the same samples analysed in Figure 6.24. The carbon/sodium (C/Na) ratios for these samples were only close to the theoretical ratio shown in Table 6.4 for certain cases, when acyclic acids were used with aqueous phases with lower calcium concentrations (0.1 wt%). In other words, mixed calcium and sodium naphthenates may form under these experimental conditions, and this is a function of the availability of acid types and cations. At higher calcium concentrations the C/Na ratio increases due to the formation of calcium soaps (in which two naphthenate ions bind to one calcium ion). Figure 6.26 and 6.27 present examples of XRD patterns for these deposits which support the conclusion of mixed naphthenate formation. These results suggest that naphthenic acids may precipitate as sodium or calcium salts given the right combination of pH and cations in the aqueous phases. The use of non-acyclic acids structures did not lead to any deposit formation when placed in contact with sodium-rich aqueous phases. Under field conditions, soap emulsion samples are monovalent cation-rich, owing to the very large sodium concentration in the produced waters. The predominant naphthenic acids in these field deposits are acyclics (Figure 4.27). The results presented in this section point to the favoured reactions between acyclic acids and monovalent sodium ions.

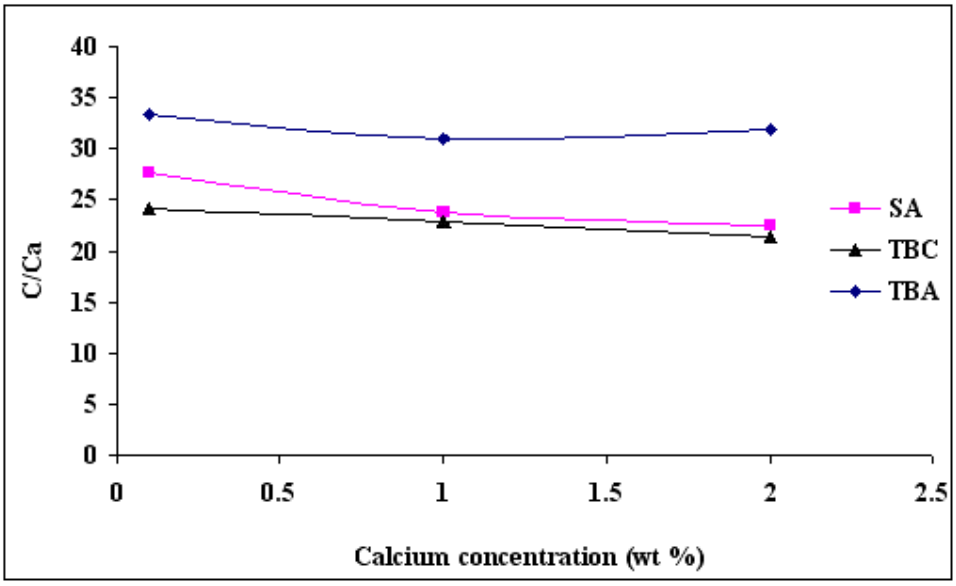

Figure 6.24. Carbon/calcium (C/Ca) atomic ratios. Deposits formed from aqueous phases containing 25000 ppm sodium ions and various concentrations of calcium ions pH 12 adjusted. Oil phases containing 1 wt% acid solutions. Legend in Table 6.4.

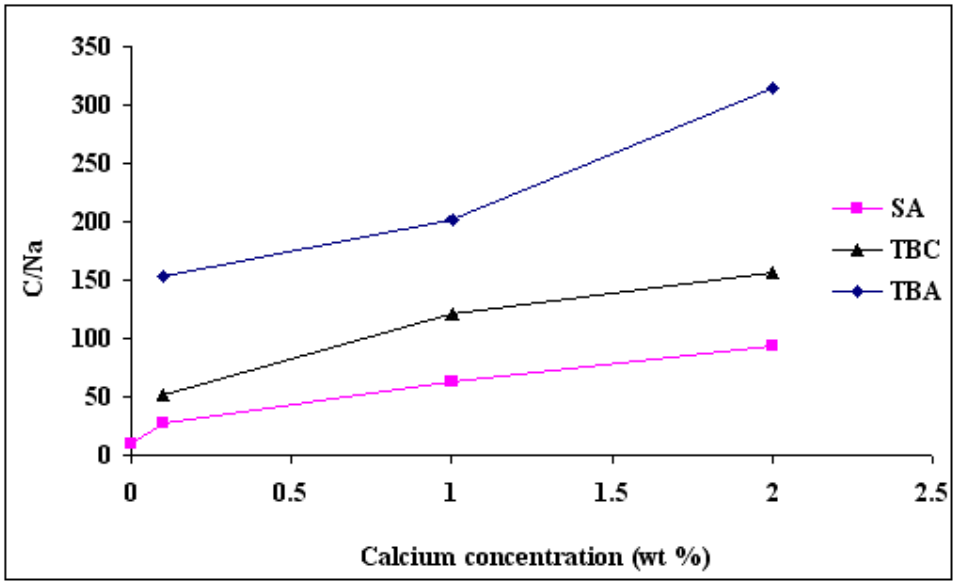

Figure 6.25. Carbon/sodium (C/Na) atomic ratios. Deposits formed from aqueous phases containing 25000 ppm sodium ions and various concentrations of calcium ions pH 12 adjusted. Oil phases containing 1 wt% acid solutions. Legend in Table 6.4.

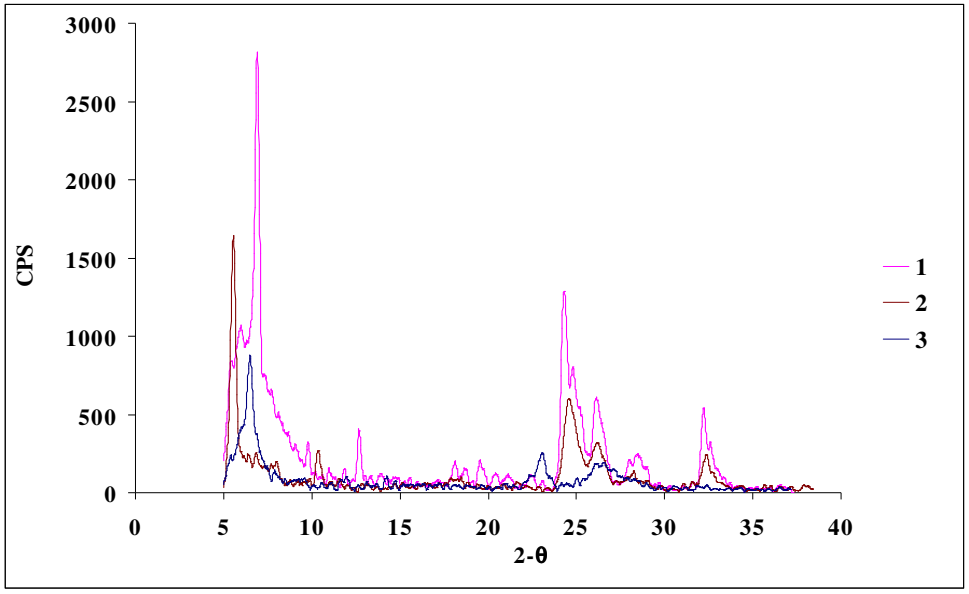

Figure 6.26. XRD patterns. 1 is the pattern from the deposit formed from aqueous phase containing 25000 ppm sodium ions and 20000 ppm calcium ions pH 12 adjusted, oil phase 1 wt% SA, 2 is the pattern from a commercial calcium stearate and 3 is the pattern from a commercial sodium stearate.

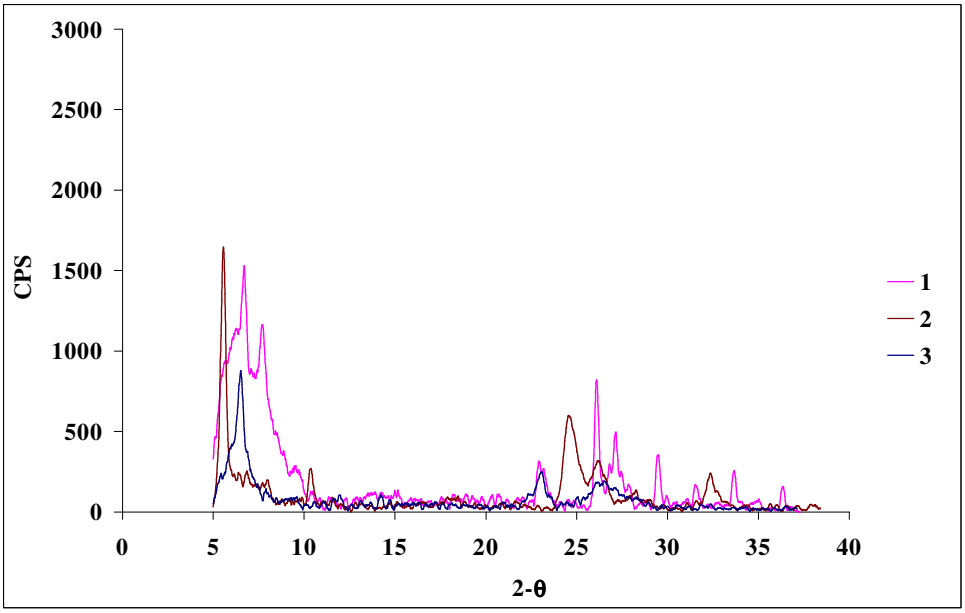

Figure 6.27. XRD patterns. 1 is the pattern from the deposit formed from aqueous phase containing 25000 ppm sodium ions and 1000 ppm calcium ions pH 12 adjusted, oil phase 1 wt% SA, 2 is the pattern from a commercial calcium stearate and 3 is the pattern from a commercial sodium stearate.

Mixed barium-sodium and calcium-barium aqueous phases.

Precipitates formed from mixed barium and sodium aqueous phases were only obtained when the acyclic naphthenic acid species were present in the oil phase. However, even for

these samples, the precipitate yields were small. The EDAX measurements suggest that the precipitates are composed of barium stearate when higher barium concentrations are in the aqueous phase. For lower barium concentrations in the presence of sodium, the deposits formed were sodium naphthenates. This was also supported by XRD patterns, and by the proposed stability of the divalent cation films reported by Brandal (2005). The steric hindrance caused by the fast absorption of acids at the oil-water interface with barium ions, would prevent the formation of large amounts of deposits (note since barium has the largest ionic radius, hydration effects are minimized, and absorption of acids maximized).

The deposits formed from aqueous phases with a mixture of calcium and barium ions are presented in Figure 6.28 and 6.29. The carbon/calcium (C/Ca) atomic ratios in Figure 6.28 obtained for the acyclic acid species (SA) were in the range of the theoretical values presented in Table 6.4. This suggests that in all cases calcium naphthenates were present in the deposit, even in the presence of barium ions in the original aqueous phase. At lower calcium concentrations however (0.1 wt%), barium naphthenate could also form and this is supported by data in Figure 6.29. This is mostly because the carbon/barium (C/Ba) ratio for the case of low calcium concentration is within the theoretical range shown in Table 6.4. For higher concentrations of calcium (i.e. 2.0 wt%), the barium in the deposits is owing to the formation of barium hydroxide. This was concluded by the analysis of EDAX/XRD (data not shown). The results are probably an indication of the different interactions occurring between the acid and the two divalent cations (barium and calcium) in solution. The presence of barium ions in the aqueous phases leads to decrease in precipitate amounts, in particular for the cyclic and aromatic acids. Thus, when mixed divalent ions are present, calcium ions are favoured in the formation of soaps, particularly with non-acyclic species. This is also observed from the analysis of the field deposit samples, which have a predominance of calcium ions (Table 4.9).

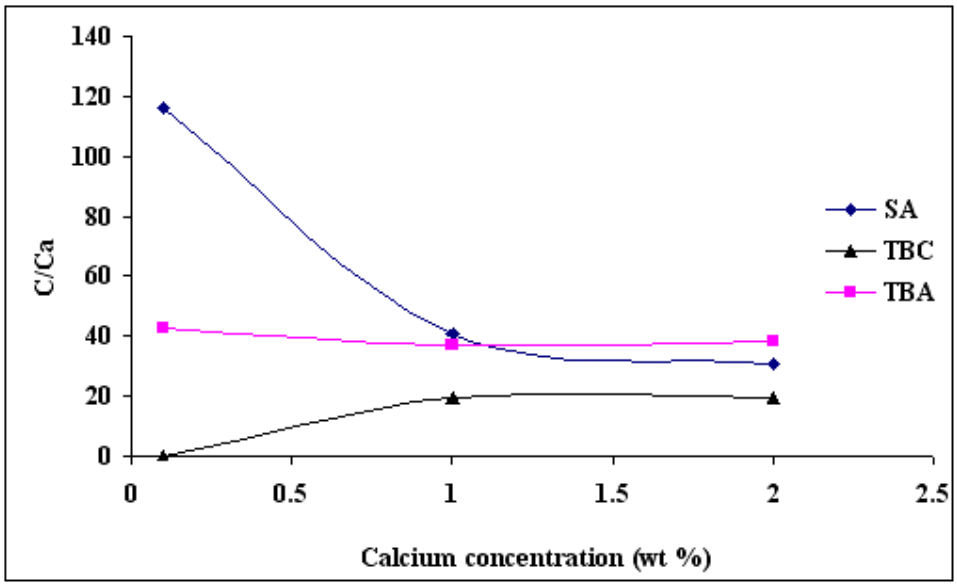

Figure 6.28. Carbon/calcium (C/Ca) atomic ratios. Deposits formed from aqueous phases containing 20000 ppm barium ions and various concentrations of calcium ions pH 12 adjusted. Oil phases containing 1 wt% acid solutions. Legend in Table 6.4.

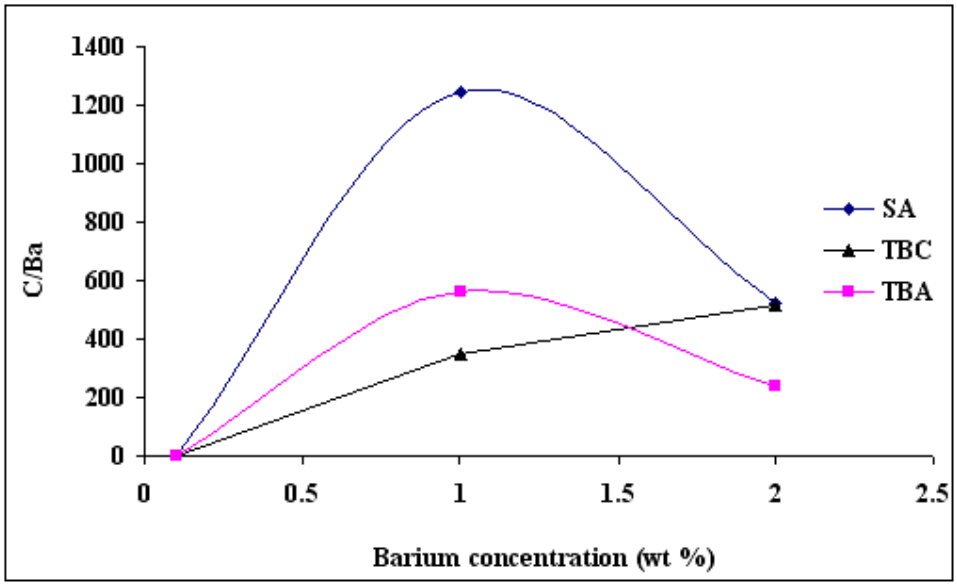

Figure 6.29. Carbon/barium (C/Ba) atomic ratios. Deposits formed from aqueous phases containing 20000 ppm calcium ions and various concentrations of barium ions pH 12 adjusted. Oil phases containing 1 wt% acid solutions. Legend in Table 6.4.

Bicarbonate-rich aqueous phases.

Table 6.5 presents the measured carbon/cation ratios for the deposits formed in the laboratory from aqueous phases containing bicarbonate ions, i.e. those which gave rise to Figures 6.17 and 6.18.

Oil Phase	Aqueous	Phase
	20000 ppm Ca^{2+}, 25000 ppm Na^{+} and 72 ppm HCO_3^-	25000 ppm Na^{+} and 72 ppm HCO_3^-
	C/Ca	C/Na
SA	43.1	39.8
SA/TBA	31.7	n.a.

Note. n.a. = not available due to absence of deposit formation.

Table 6.5. Carbon/calcium atomic ratio (C/Ca), carbon/sodium atomic ratio (C/Na) for laboratory deposits formed from bicarbonate-containing aqueous phases. Oil phases containing 1 wt% naphthenic acids (SA stearic acid, TBA 4- tert-butylbenzoic acid).

For the cases where only sodium ions are present in the aqueous phase in the presence of bicarbonate, the carbon/sodium ratio (C/Na) for the laboratory deposit is 39.8 which is above the theoretical ratio of 18 in Table 6.4. This suggests the deposit formed in the presence of sodium and bicarbonate does not contain the same atomic distributions as the sodium naphthenates formed from sodium-rich aqueous phases discussed earlier. Nevertheless, when calcium ions are present in the aqueous phase, the carbon/calcium ratios (C/Ca) are 43.1 and 31.7. These are close to those shown in Table 6.4 formed when no bicarbonate was present. This suggests the deposits formed in the presence of calcium and bicarbonate are most likely calcium naphthenates. Moreover, the presence of bicarbonate ions in the aqueous phase did not affect the atomic distribution in the deposit formed in the laboratory.

The work of Gallup *et al.* (2005) postulated that sodium carboxylate soap emulsions form owing to the complexation between the sodium ions, bicarbonate ions and acyclic acids. Bicarbonate ions are not implicated with the formation of calcium naphthenates under field conditions (Smith and Turner, 2004). The carbon/calcium ratios (C/Ca) in Table 6.5 appear to support this conclusion. Figure 6.30 presents a comparison of the diffraction patterns for a commercial sodium stearate, and that of a deposit formed from an aqueous phase consisting of 25000 ppm sodium ions and 72 ppm bicarbonate ions and oil phase of 1 wt% stearic acid. Note in Figure 6.30 that the XRD pattern is also different from the one shown in Figure 6.23 for the laboratory soap formed from an aqueous phase containing 25000 ppm sodium ions and oil phase with 1 wt% stearic acid. The XRD pattern in Figure 6.30 suggests the presence of bicarbonate ions led to the formation of a deposit which does not have the same crystalline arrangement as sodium stearate, which also supports the EDAX data in Table 6.5. These results were independent of the concentration of bicarbonate used in the experiments. The theoretical carbon/sodium ratio (C/Na) for the bicarbonate-

containing complex structure, from the work of Gallup *et al.,* (2005) is 39 (this was calculated using the average molecular weight of the predominant naphthenic acid in the soap emulsion sample reported by the authors). The measured ratio for the deposit precipitated in the laboratory in the presence of bicarbonate ions was 39.8 as presented in Table 6.5. The results in this section therefore suggest that the deposits formed in the laboratory in the presence of bicarbonate ions may lead to soaps containing naphthenic acid-sodium ion-bicarbonate ion complexes.

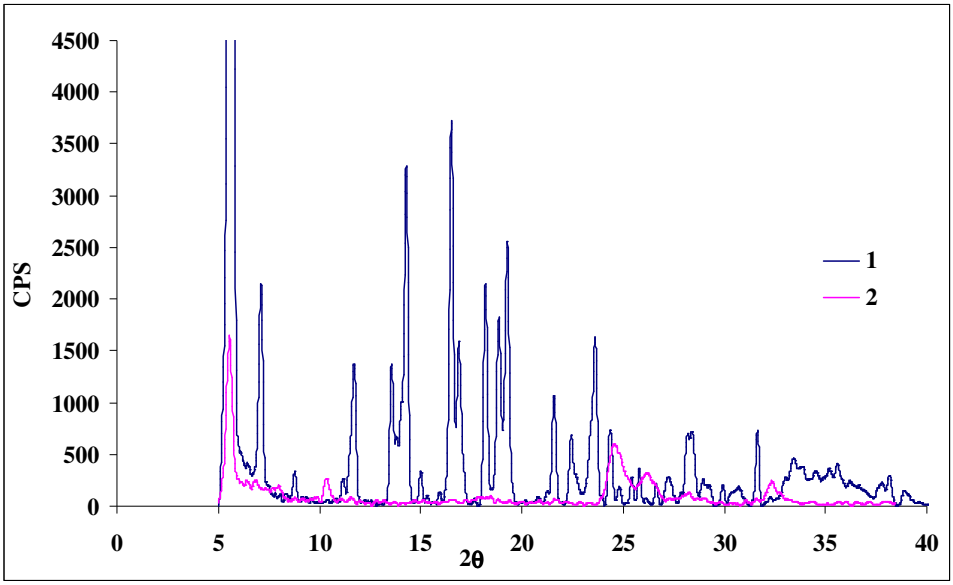

Figure 6.30. XRD patterns. 1 is the pattern of the deposit formed from: aqueous phase containing 25000 ppm sodium ions and 72 ppm bicarbonate ions, oil phase 1 wt% stearic acid (SA), 2 is the pattern of a commercial sodium stearate.

In conclusion, in this section a series bottle tests was optimised to investigate the formation of soaps under laboratory conditions. Phase behaviour and precipitation of deposits was shown to be a function of:

- cation species and their concentrations, particularly divalent/monovalent and bicarbonate in the aqueous phases,
- the pH adjustment media and the initial pH used and
- the type and concentration of naphthenic acids used in oil phases.

Both calcium naphthenate soap scales and sodium carboxylate soap emulsions were obtained in the laboratory and the specific phase relationships in this section generally support the data obtained for the field deposit sample analysis presented in Chapter 4.

6.3.4. Surface properties of naphthenic acids in soap-forming systems.

Interfacial tension (IFT) measurements between oil phases with naphthenic acids and aqueous phases containing pH adjusted brines were carried out. The experiments were conducted at pH values prior to the formation of deposits in solution. These values were pH 6.5 and 12 for the systems with and without bicarbonate ions respectively. Figure 6.31 presents the IFT data for sodium-rich aqueous phases. Clear differences are observed as a function of pH and precise naphthenic acids present. The acyclic SA acid showed a gradual decrease in IFT, more pronounced at pH values above 8. This is in-line with the results of Cratin (1994), who was able to explain the initial high constant IFT at low pH by the presence of unionised, non-surface active SA. Decreases in IFT were said to be owing to the formation of surface-active species or the ionised SA. In this thesis, acids having structures other than saturated acyclics, such as TBA, showed constant IFT values as a function of pH and this was in-line with the data of Gomari and Hamouda (2006). Because of constant IFT values it could be concluded that the change in pH does not lead to significant partitioning and dissociation of these acids species. The results in this section suggest the prevailing influence in the IFT trends is of steric hindrance. This may be a result of the packing of the particular naphthenic acid at the oil-water interface. Constant IFT values are also observed in mixed acid systems and this is also shown in Figure 6.31. In this case it can be observed that the predominant effect is that of the non-acyclic over the acyclic species.

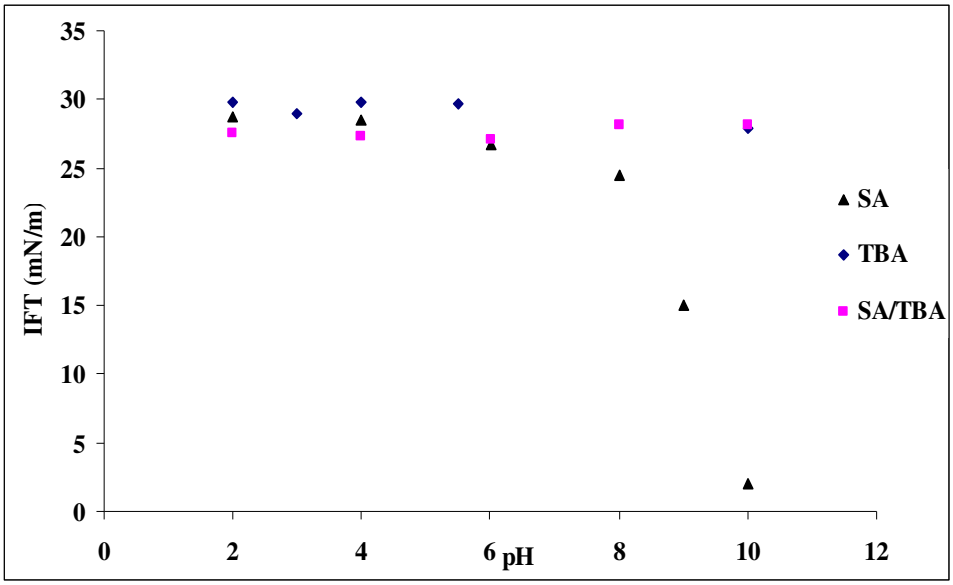

Figure 6.31. IFT measurements. Aqueous phases containing 25000 ppm sodium ions, oil phases 1 wt% naphthenic acid solutions in toluene. SA stearic acid, TBA 4-tert-butylbenzoic acid.

Figure 6.32 shows the IFT results for the calcium-rich aqueous phases. There is some scatter in the data, although it can be observed that there are no major variations in final IFT values as a function of pH. Values are between 24 to 32 mN/m. Because calcium ions are divalent, they are bound to two acid groups as opposed to just one for the sodium ions. As presented in Figures 6.7 and 6.8, this leads to an increase in dissociation of acids (as measured by lower pH_f values). Thus there would be less ionised naphthenic acids available for reduction of IFT. This would make the oil-water interface more rigid, hence higher IFT.

Figure 6.33 presents the IFT values for mixed calcium and sodium aqueous phases. Previous pH_f data as in Figure 6.11 has shown that the dissociation and partitioning of naphthenic acids is a direct function of the presence of the divalent species. The IFT data in Figure 6.33 is in qualitative agreement with that in Figure 6.32. The overall effect on IFT is therefore also a function of the presence of divalent species. However, the IFT for the SA acid decreases slightly with increase in pH_i followed by an increase at higher pH_i values. An explanation for this could be the competition of sodium and calcium ions for the stearate ions, as indicated in the previous section with the mixed naphthenate laboratory soaps. As pH increases, sodium acid pairs might be formed preferentially at first (monovalent cations require only one naphthenate anion). As the pH increases further, more acid becomes dissociated, and calcium acid pairs start to form preferably. This may lead to a more stable film at the interface, which helps revert the IFT back to high values.

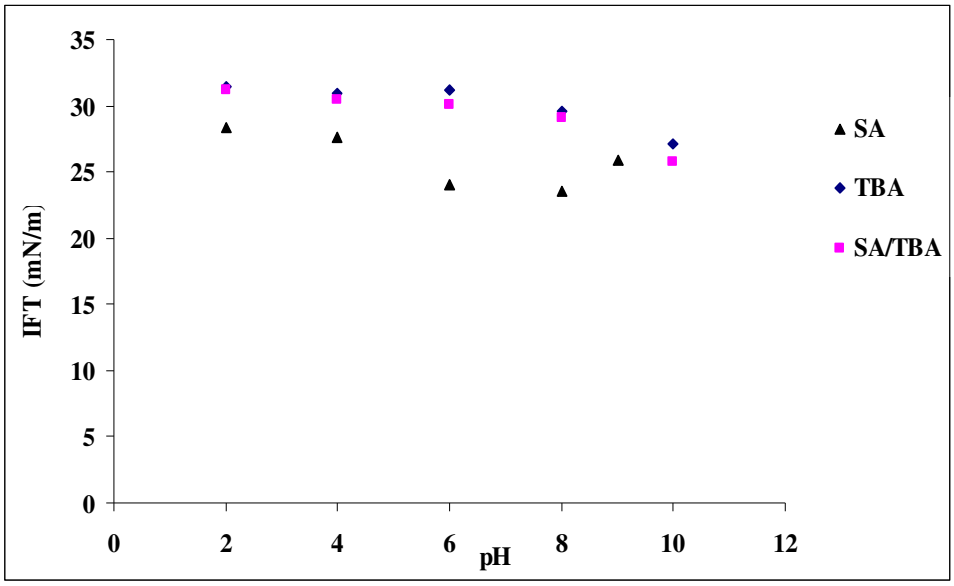

Figure 6.32. IFT measurements. Aqueous phases containing 20000 ppm calcium ions, oil phases 1 wt% naphthenic acid solutions in toluene. SA stearic acid, TBA 4-tert-butylbenzoic acid.

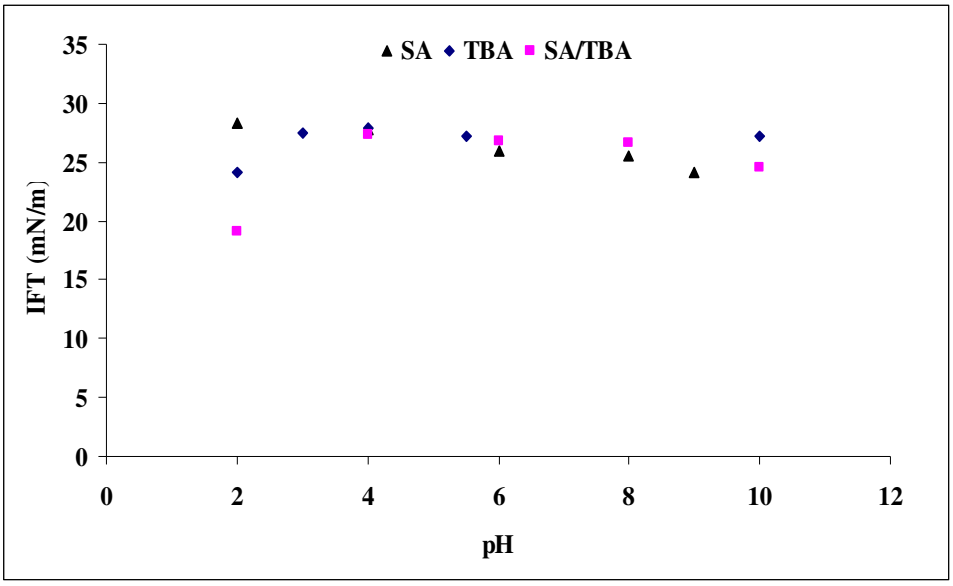

Figure 6.33. IFT measurements. Aqueous phases containing 20000 ppm calcium ions and 25000 ppm sodium ions, oil phases 1 wt% naphthenic acid solutions in toluene. SA stearic acid, TBA 4-tert-butylbenzoic acid.

The IFT values for barium-rich aqueous phases follow the trends for calcium solutions shown in Figure 6.33, despite the higher hydration radius for barium ions (data not shown). It is likely that this is caused by unstable films effects caused by rapid absorption at the oil-water interface with barium ions.

Figure 6.34 presents the IFT trends for selected bicarbonate-containing systems. When sodium is the only cation present with bicarbonate ions, the IFT remains high and constant as a function of pH. When calcium is added to the bicarbonate aqueous phase an interesting effect occurs. Calcium leads to an enhanced effect on naphthenic acid phase behaviour, yet buffer ions would act to keep pH at constant high values. The combined effect is significant naphthenic acid partitioning and dissociation. When acid-cation pairs are formed the IFT values remain high. As pH values are increased further, the excess dissociated acid then leads to the precipitation of the solid. The IFT trends in Figure 6.34 are consistently higher than those presented in Chapter 4 for naphthenic acid extracts separated from field soap deposit (Figure 4.53). The trends in Chapter 4 may be justified by the presence of more surface-active species, such as Arn in the naphthenic acid extracts. The results would thus also point to very specific naphthenic acid phase behaviour together with combinatory surface activity effects. Because IFT trends in the presence of bicarbonate did not show major variations (Figure 6.34) it is unlikely these surface properties could be used for the prediction of soap formation onset.

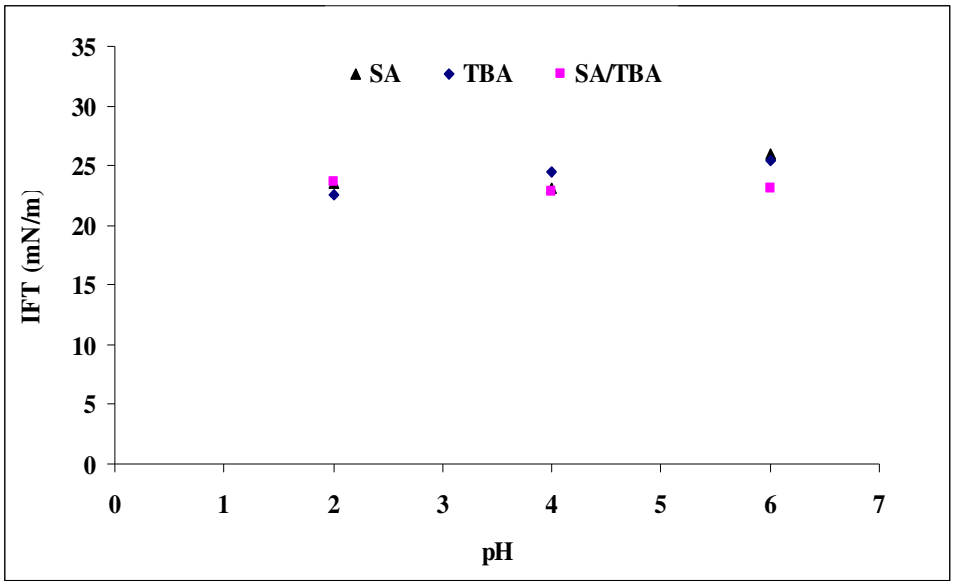

Figure 6.34. IFT measurements. Aqueous phases containing 25000 ppm sodium ions, 20000 ppm calcium ions and 72 ppm bicarbonate ions, oil phases 1 wt% naphthenic acid solutions in toluene. SA stearic acid, TBA 4-tert-butylbenzoic acid.

6.4. Formation of soaps using indigenous acids and crude oil systems.

6.4.1. Tests on indigenous acids.

6.4.1.1. ESEM/EDAX results.

The next paragraphs discuss the characterisation of indigenous acids separated from a soap deposit sample from Field Y prior to using this in static bottle tests. Procedure B (Section 3.1.2) described the preparation of this material. The preliminary step was to obtain a clean calcium soap scale which appears as a flaky light brown solid (Figure 6.35). The ESEM image shows a fairly homogeneous surface with embedded crystals of sodium chloride, sands and fines. The EDAX analysis of the clean calcium soap is presented in Table 6.6. The sample is composed of 8.5 wt% calcium which is much larger than the values reported for the field deposits in Table 4.9 (2-3 wt%). The reason for this is that the clean calcium soap is free from contaminants.

Baugh *et al.* (2004) suggested that there would be around 80 carbon atoms and four carboxylic acid groups in the Arn acid of a calcium naphthenate deposit. Thus Arn could be bound to different numbers of calcium ions. Some of the possible configurations are shown in Figure 6.36, where the Arn is schematically displayed bound to 4 or 2 calcium ions.

The carbon/calcium ratio (C/Ca) of 30 for the clean calcium soap (which is the most concentrated sample of calcium naphthenate obtained in this thesis) is shown in Table 6.6. This is also the average value of the carbon/calcium ratios (C/Ca) shown in Figure 6.36 (i.e. the average of 20 and 40). It has been suggested by Baugh *et al.* (2005a) that the Arn acid contains four carboxylic acid groups. If this is true, then the C/Ca ratio above suggests at least two or more calcium ions are involved in the Arn molecule (Figure 6.36). This could result in calcium-Arn networks growing in a polymer like fashion, and may explain the sticky network-like structure reported for field calcium naphthenate soap scale deposits (Vindstad *et al.,* 2003). On the other hand, if the clean calcium soap does not contain a high percentage of Arn species, then the carbon/calcium ratio (C/Ca) of 30 could be assigned to naphthenic acid species with an acyclic chain and fifteen carbon atoms (i.e. 30/2, 15, or the number of carbon atoms in naphthenate anion chain unit). The possible molecular weights for this naphthenic acid structure would be between 234 and 242 Daltons. Additional measurements in this chapter will provide more information on the correct distribution of Arn species in the indigenous acid samples.

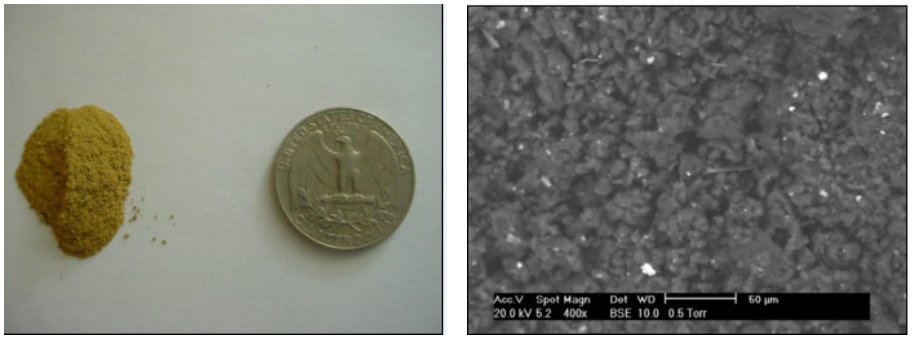

Figure 6.35. Left: Image of clean calcium soap from Field Y soap sample. Right: ESEM image of clean calcium soap from Field Y soap sample.

Element	Clean soap Wt %	Clean soap At %
C	78.57	88.39
O	7.48	6.32
Na	1.22	0.72
Al	0.22	0.11
Si	0.49	0.24
S	0.48	0.20
Cl	3.05	1.16
Ca	8.49	2.86
C/Ca		30.91
C/Na		122.76

Table 6.6. EDAX/ESEM analysis of clean calcium soap scale. From Field Y soap sample.

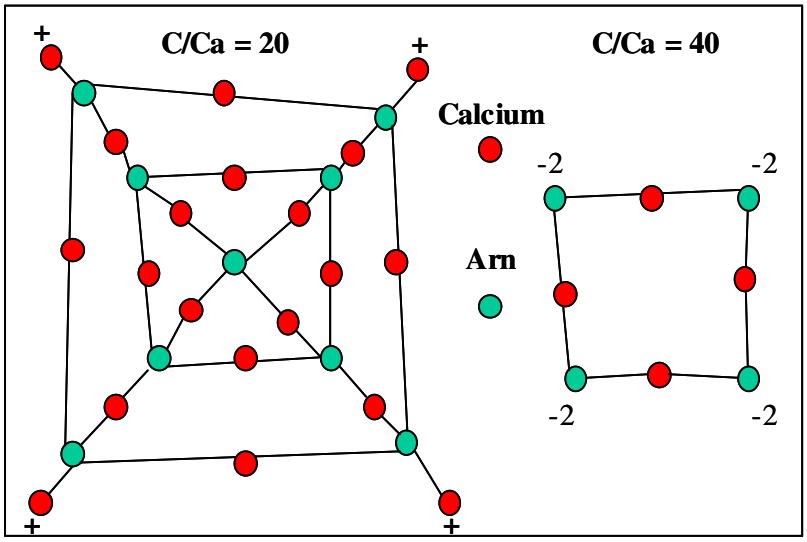

Figure 6.36. Illustration of possible carbon/calcium ratios (C/Ca) in a calcium naphthenate soap scale containing predominantly Arn naphthenic acid species.

6.4.1.2. ES results.

Figure 6.37 presents the ES of the indigenous acids obtained from the clean calcium soap described in the Section 6.4.1.1. The blue spectrum shows that the indigenous acids from the deposits are composed of a range of naphthenic species since the m/z ratios may be assigned to specific acid molecular weights. A cluster of ions around m/z 1230 is present and these represent Arn (Baugh *et al.,* 2004). Figure 6.37 also shows a spectrum where no Arn was detected (pink trace). Individual ionisation efficiencies for particular naphthenic acid species are not known and these effects on sample spectra have been discussed in Chapter 4. However, in the blue spectrum the concentration of Arn was estimated to be around 80 ppm. This was based on dissolution of indigenous acids in increasing volumes of toluene. The sample that gave rise to the blue spectrum was diluted 50 vol% to generate the pink spectrum. Thus it can be concluded that the maximum concentration of Arn identifiable with the ES set-up in this thesis was 80 ppm, without additional separation of the naphthenic acids (e.g. LCMS).

Figure 6.38 presents the speciation of the indigenous naphthenic acids, as given by hydrogen deficiency (Z) and carbon number, according to procedures discussed in Section 3.2.1.2. The amount of Arn in this sample is 4 wt% based on MS signals. This value is very close to the amount of found in the naphthenic acid extracts from Field Y deposit, which was 2 wt% (Table 4.4). The increase may be attributed to the removal of contaminants such as crude oils. It is clear that although the Arn acids have the highest percentage within the indigenous acids, there is no clear predominance of this species in the spectrum. Acyclic species account for almost a quarter of the total acids present, most of which have carbon numbers below 40. The presence of a wide distribution of naphthenic acid species may reflect the deposition mechanism itself, as was discussed in Section 4.7. Moreover this could be related to diffusion effects towards the oil-water interface (a function of naphthenic acid molecular weight and structure) and the relative affinity towards the calcium ions. Data in Figure 4.53 and Figure 6.34 showed that the IFT of naphthenic acid extracts from field deposits was significantly lower than those for model solutions.

It is likely that indigenous acids containing Arn would be favoured over other structures for the precipitation of a calcium salt due to: preferential surface properties, and the possibility of binding with up to four calcium ions due to the presence of the claimed four carboxylic acid groups. However, lower molecular weight acids would diffuse faster to the oil-water interface. Thus a competition could be established between the high and low molecular weight naphthenic acids for the formation of calcium naphthenate soap scale.

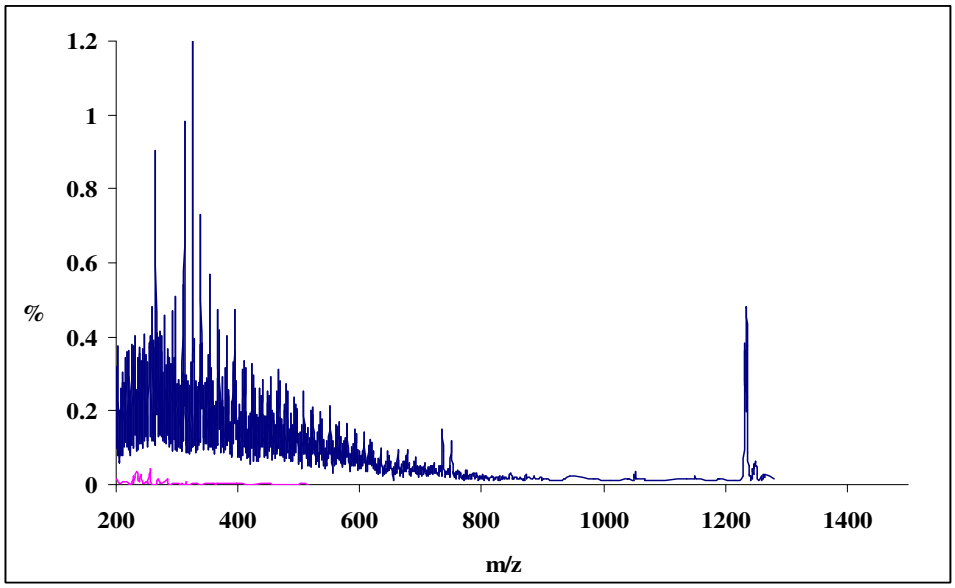

Figure 6.37. ES spectra of indigenous acids from Field Y soap sample. Blue spectrum is for a sample containing 80 ppm Arn. Pink spectrum represents a 50 wt% dilution of the 80 ppm sample.

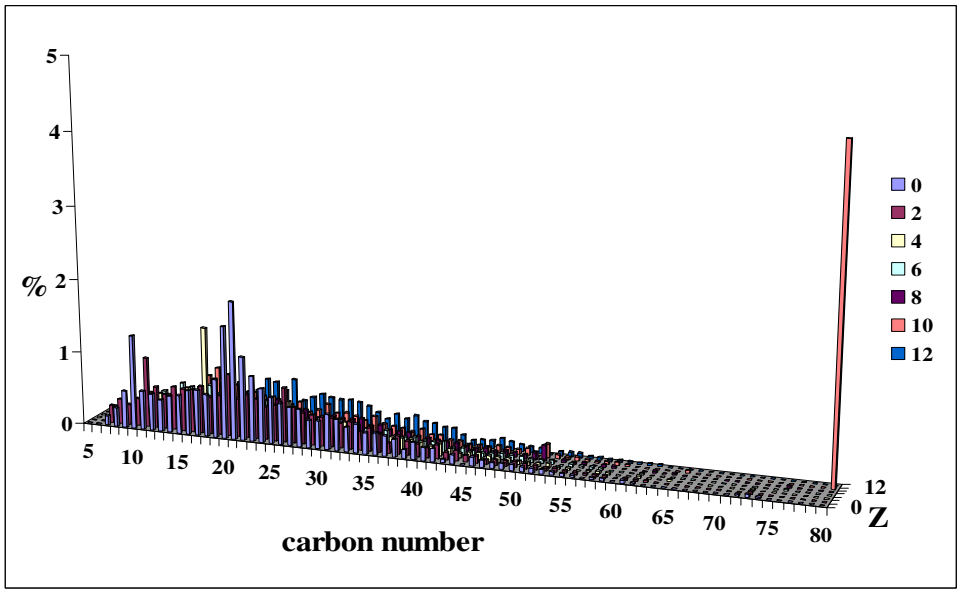

Figure 6.38. Speciation of indigenous acids from Field Y soap sample as given by hydrogen deficiency (Z) and carbon number. Legend represents Z values.

6.4.1.3. MS/MS results.

Initially it was intended to fragment the Arn precursor ion with m/z 1230 and 1234 since these were some of the most intense peaks present in the indigenous acid spectrum (Figure 6.37). However, all attempts to fragment the ions were unsuccessful, even with very high collision energies. As a compromise, it was decided to use the doubly charged ions with m/z 617 (these represent the second ionisation of the Arn which has m/z around 1234). The daughter ion spectrum, MS^2, from the precursor with m/z 617 is shown in Figure 6.39, and

expanded in Figure 6.40. The most intense daughter ions are those forming a cluster from m/z 563 to 617. The ion at m/z 617 may be ascribed to the ionisation of two carboxyl groups. This is evidence for the presence of two carboxyl groups in the Arn species, and confirms the suggestions of Brocart *et al.* (2005). Ions from one of the carboxyl groups in the Arn which were not ionised in the first MS experiment show doubly charged pairs 1 Dalton apart. Table 6.8 presents possible assignments for the mass losses from the major products observed. The doubly charged species would account for loss of carbon dioxide (CO_2), carbon monoxide (CO) and water (H_2O). For these experiments, it is likely that the highest intensity at m/z 585 represents the loss of both H_2O and CO_2. This is illustrated in Figure 6.41. Nevertheless these daughter ions do not provide additional information on the structure of the Arn itself. But it would appear that the fragmentation of the Arn acids is favoured at the carboxyl groups, which is probably a result of their high polarity as compared to the hydrocarbon backbone chains.

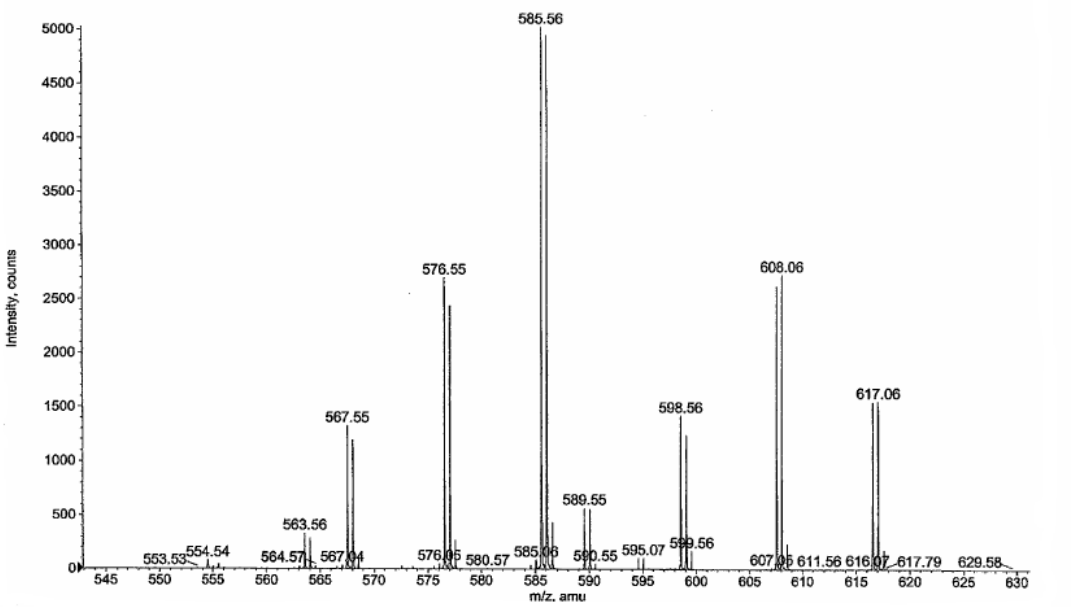

Figure 6.39. MS^2 from precursor ion m/z 617.

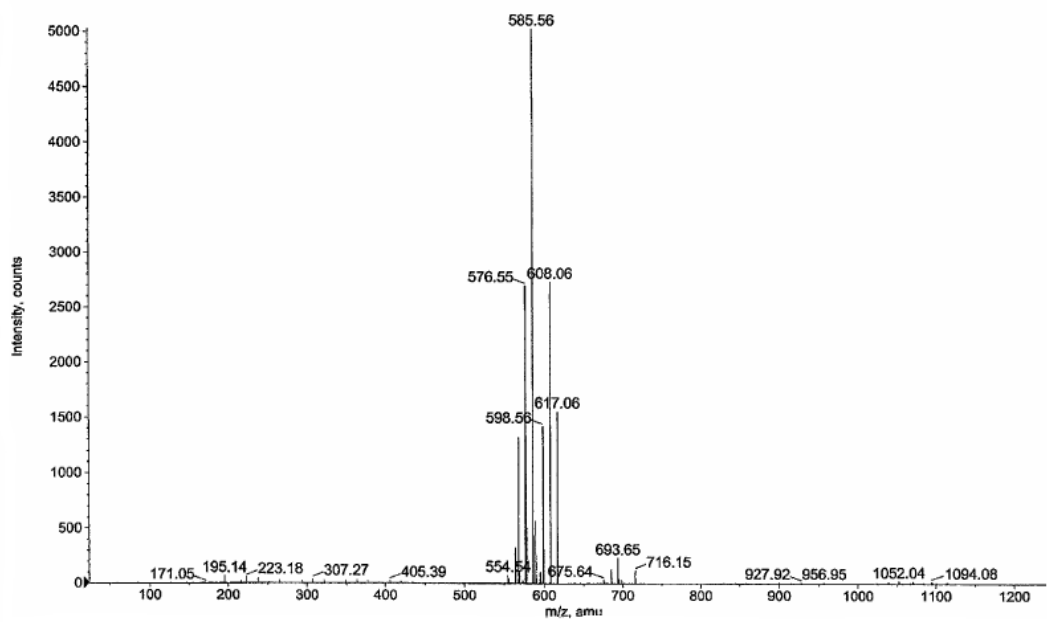

Figure 6.40. MS^2 from precursor ion m/z 617, expanded view.

m/z of product ion	Cumulative mass loss	Assignment
563	105	Loss of 2 CO_2 , H2O
567	96.9	Loss of 2 CO, CO_2
576	78.9	Loss of CO_2, CO
585	62.9	Loss of H_2O, CO_2
589	52.9	Loss of 2 CO
607	16.9	n.a.

Table 6.8. Assignment of m/z ions in MS^2 experiment.

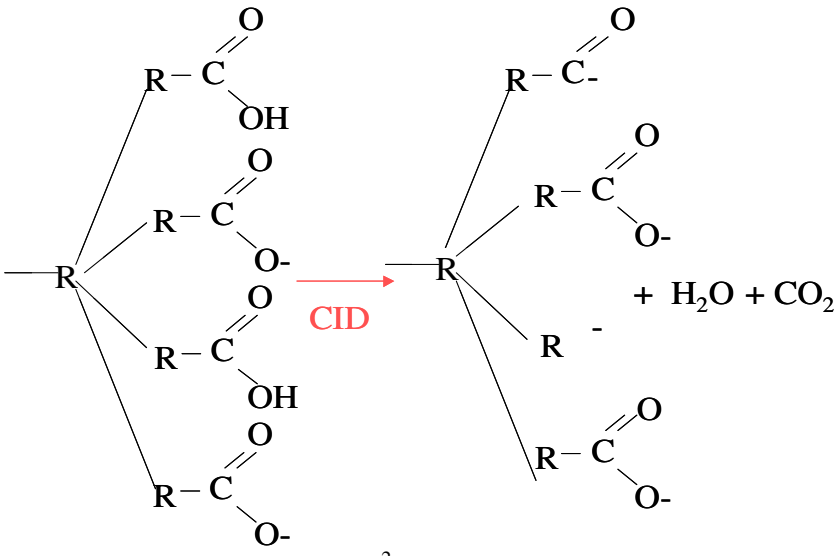

Figure 6.41. Possible assignment of MS^2 of precursor ion m/z 617. Note CID is collision-induced dissociation which generates the ion fragments. This figure shows a possible fragmentation path of the 4 carboxyl groups in the Arn which occurs with loss of water and carbon dioxide. Note R represents the groups which link the different carboxyl groups together in the Arn unit.

A series of low m/z product ions from Figure 6.39 which are singly charged, are shown in the expanded spectra of Figure 6.42. This series is dominated by ions with m/z from 195 to 433. The only mono-carboxylic acids identified in this cluster were at m/z 155 and 295, but the intensity for these species is very low. These can be assigned to bi-cyclic naphthenic acids with carbon numbers ranging from 12 to 29. Two possible structures for the predominant bi-cyclic naphthenic acid species identified are shown in Figure 6.43.

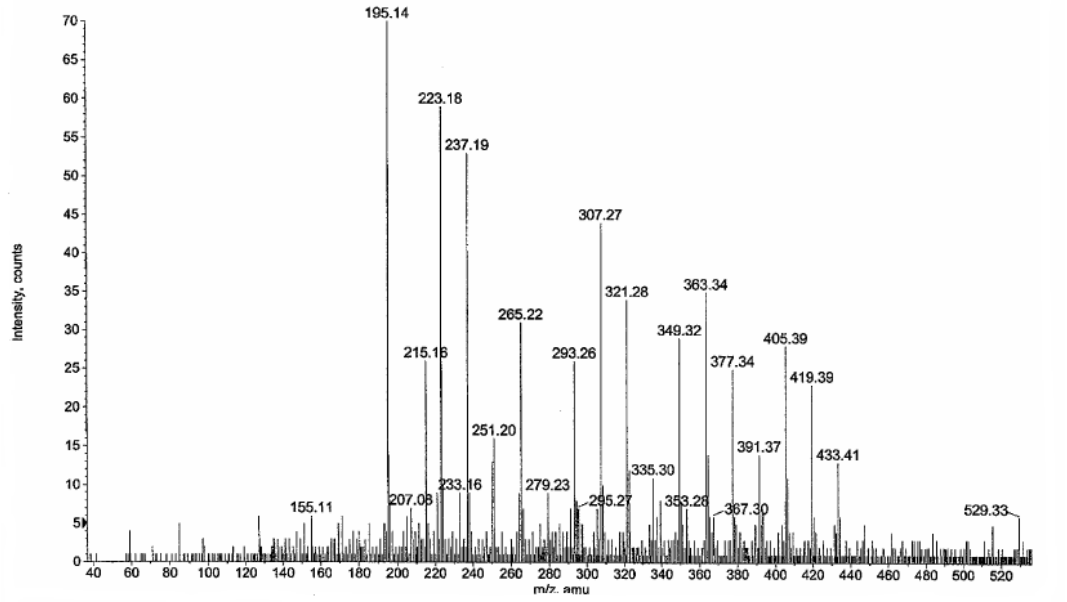

Figure 6.42. MS^2 from precursor ion m/z 617, expanded view.

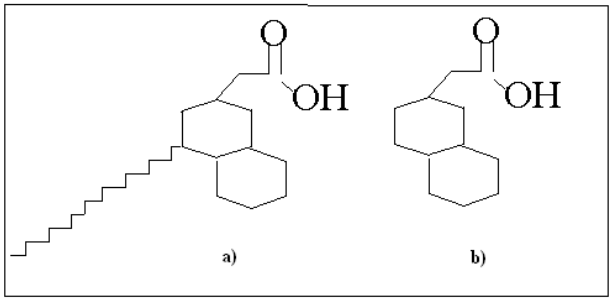

Figure 6.43. Possible structures present in the MS^2 of precursor ion m/z 617, assigned from Figure 6.42.

The structures in Figure 6.43 could represent the basic structures present in Arn (i.e. one of four groups containing one carboxylic acid). Structure a) in Figure 6.43 is a bi-cyclic naphthenic acid with 29 carbons. This is consistent with the structures suggested by Lutnaes *et al.* (2006) from 2D NMR experiments. Given the MS/MS results it can be concluded that the carboxyl groups in the Arn show preferential ionisation. The MS/MS results presented here indicate the presence of two carboxylic acid groups and suggest that the basic Arn unit (e.g. the single ionisable group at around m/z 1230) consists of a bi-cyclic naphthenic acid, with an alkyl side-chain with up to 29 carbon atoms. The precise determination of molecular structure for each daughter m/z species would assist in the correct assignment of the fragmentation patterns.

6.4.1.4. 1D and 2D NMR results.

Figure 6.44 presents the ^1H NMR solution spectrum of the indigenous acid sample from Field Y.

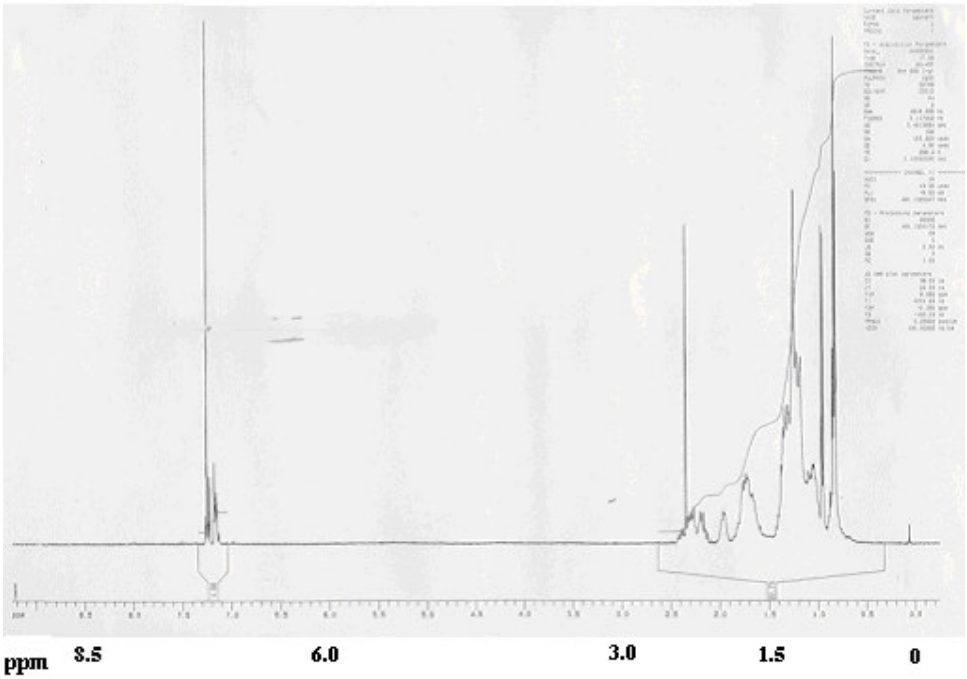

Figure 6.44. ^{1}H NMR solution spectrum for the indigenous acids from Field Y soap sample.

This spectrum shows similarities to those presented in Figure 4.33. At least 4 distinct peaks can be seen in the aliphatic region between 2.3 and 0.8 ppm. There are two peaks at 7.2 and 2.4 ppm which indicate the presence of aromatics. These peaks are from traces of the solvent (toluene) used to extract the acids from the sample as described in Chapter 3. Figure 6.45 presents the ^{13}C NMR solution spectra for the same sample, which indicates the presence of aliphatic carbons between 40 and 15 ppm, and is also similar to the spectrum shown in Figure 4.34. A peak was observed at 180 ppm, which is an indication of carboxylic acid groups, and is consistent with those reported by Baugh *et al.* (2005) and Brandal (2005a). This peak was not observed for the field soap sample reported in Figure 4.34. This is probably because of the reduced contamination in the indigenous acids after removal of crude oil. Figure 6.46 presents an enhanced image of the spectrum in Figure 6.45, showing the carboxylic acid carbon region, which shows at least four defined peaks and could be an indication of at least four distinct carboxylic acid groups in the indigenous acid sample. The indigenous acids consist of a range of structures, including Arn, although it is impossible to ascertain to which acid structures these carboxylic groups actually correspond to. DEPT spectrum for the indigenous acids was also acquired, and is shown in Figure 6.47. The data indicates that most of the species in the indigenous acids are composed of CH_2 and CH. The exact signature point to branched cyclic species, according to the guidelines of Silverstein *et al.,* 2005. This result is also consistent with the data presented in Chapter 4.

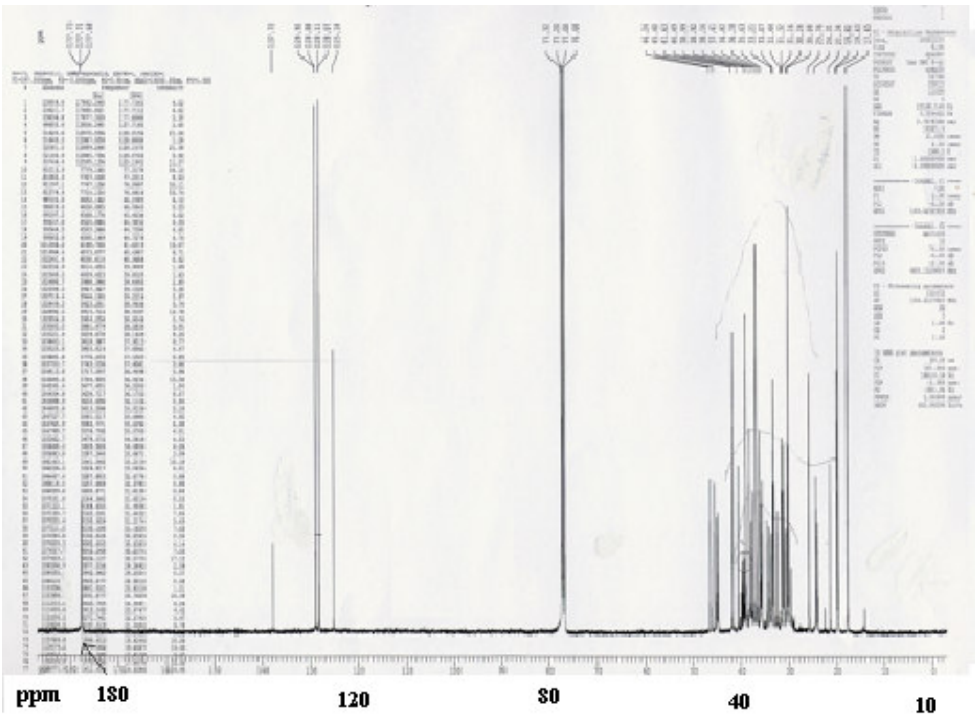

Figure 6.45. ^{13}C NMR solution spectrum for the indigenous acids from Field Y soap sample.

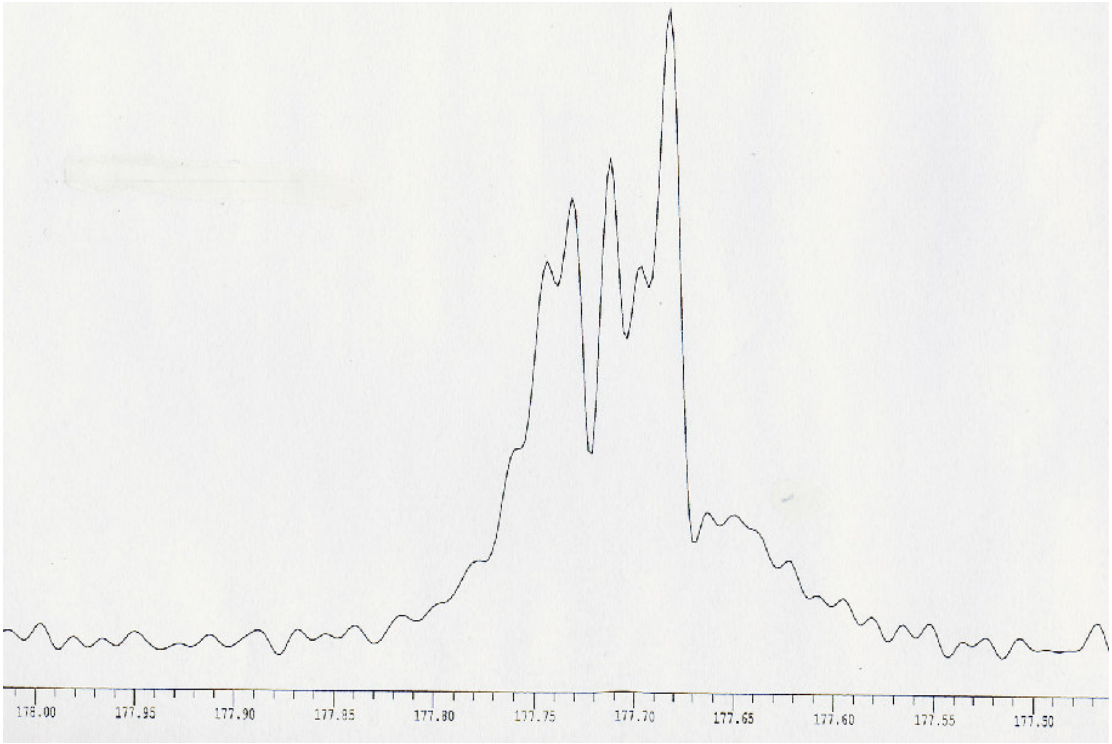

Figure 6.46. ^{13}C NMR solution spectrum for the indigenous acids in the carboxylic carbon range (expanded view) from 178 to 177.5 ppm.

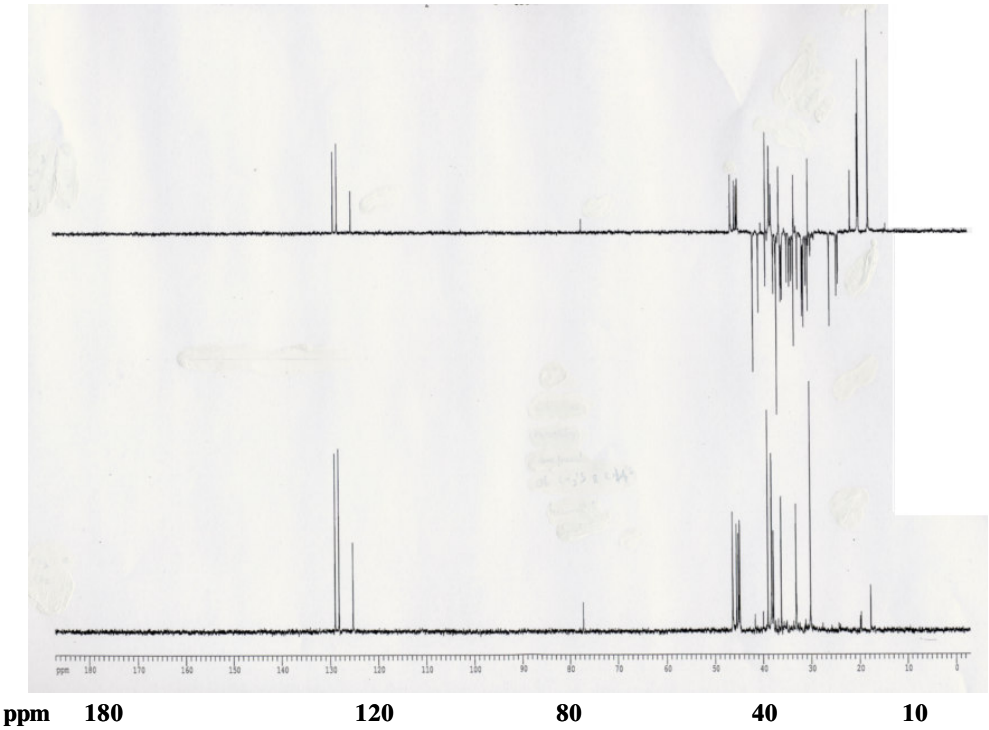

Figure 6.47. DEPT ^{13}C NMR solution spectrum for the indigenous acids from Field Y soap sample.

Figure 6.48 presents a cross polarisation (CP) solid state ^{13}C NMR spectrum acquired from the indigenous acid species. The result is consistent with the spectrum from the ^{13}C NMR solution spectrum in Figure 6.45. There is a group of signals at around 180 ppm from carboxylic acid carbons. In addition, there is a broad low intensity band from 150 to 120 ppm which is evidence of trace aromatics, possibly from the solvents used in sample preparation. There is also an intense band from 60 to 10 ppm from aliphatic carbons. Figure 6.49 presents the results of a dipolar dephasing experiment (DD). In principle this should give signals only from quaternary carbons. However, in practice any mobile species also tends to contribute to this spectrum, in particular, methyl carbon groups. The DD spectrum contains the signal from the carboxylic acids, a reasonable amount of the aromatic signal, methyl groups at 28 to 20 ppm and some signals between 50 to 30 ppm. The latter may originate from quaternary carbons, yet it is more likely to be unsuppressed C-H signals. It can be concluded that the indigenous acids consist mostly of cyclic aliphatic acids with the carboxylic acid. There is also suggestion of methyl groups attached to the cycloaliphatic rings as was concluded from the analysis of the field soap samples presented in Table 4.6.

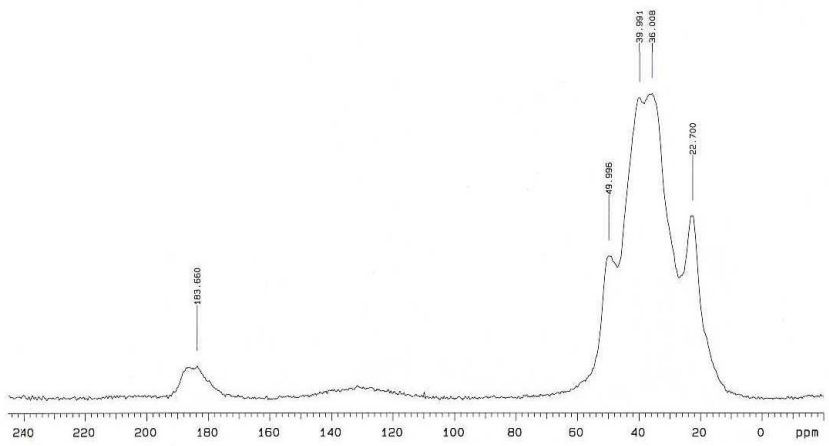

Figure 6.48. ^{13}C NMR CP spectra of indigenous acids from Field Y soap sample.

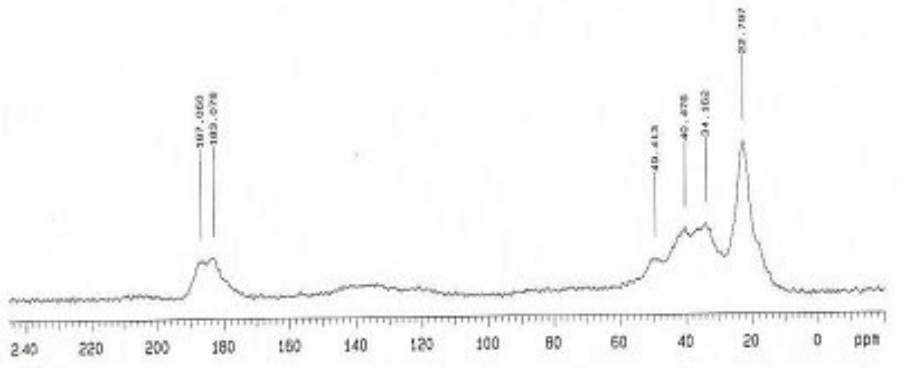

Figure 6.49. ^{13}C NMR DD spectra of indigenous acids from Field Y soap sample.

Figures 6.50 to 6.52 present the result of the 2D NMR experiments carried out on the indigenous acids. Three experiments were conducted: g-HMBC, which investigates long range correlations through polarisation transfer through the carbon atoms, g-HMQC which investigates single bond correlations and g-HMQC TOCSY which looks at spin-spin coupling correlations, where polarisation transfer is carried out through pairs of hydrogen atoms attached to carbons which are close together. The interpretation of the 2D NMR spectra was carried out according to the guidelines in Silverstein *et al.* (2005). Figure 6.50 presents the g-HMBC spectrum for the indigenous acids. The x-axis is the ^{1}H spectrum and the y-axis is the ^{13}C spectrum and two particular regions are annotated. Regions A are resonances due to the toluene solvent. Regions B show the correlations between the carboxylic acid carbon, the aliphatic carbons and the hydrogen atoms which are bonded to them. The results suggest that the carboxyl groups in the indigenous acids are bonded to a

CH_2 carbon. This is due to the location of the points close to the x-axis region associated with this structure. The results also suggest that the carbons in the acyclic region of the ^{13}C spectrum are also CH_2 species.

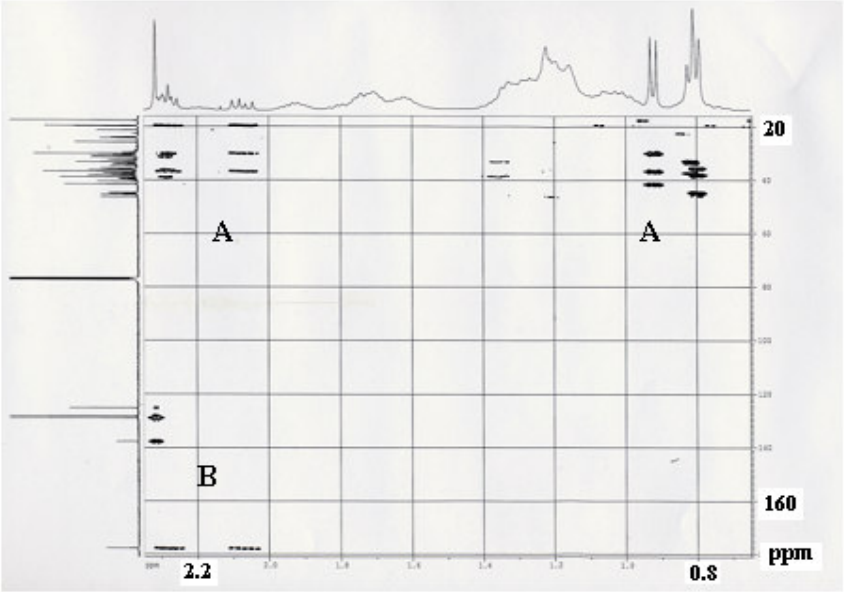

Figure 6.50. g-HMBC (long-range C-H correlation) for indigenous acids from Field Y soap sample.

Figure 6.51 presents the g-HMQC spectrum for the indigenous acids. There are many features in the spectrum which makes interpretation difficult. Two regions however can be clearly highlighted. Regions A are due to the presence of the toluene solvent. Regions B appear to be present for three separate groups of carbon atoms. They also suggest clusters of CH_2 carbons in cyclic structures and the absence of methyl terminated groups (Silverstein *et al.,* 2005).

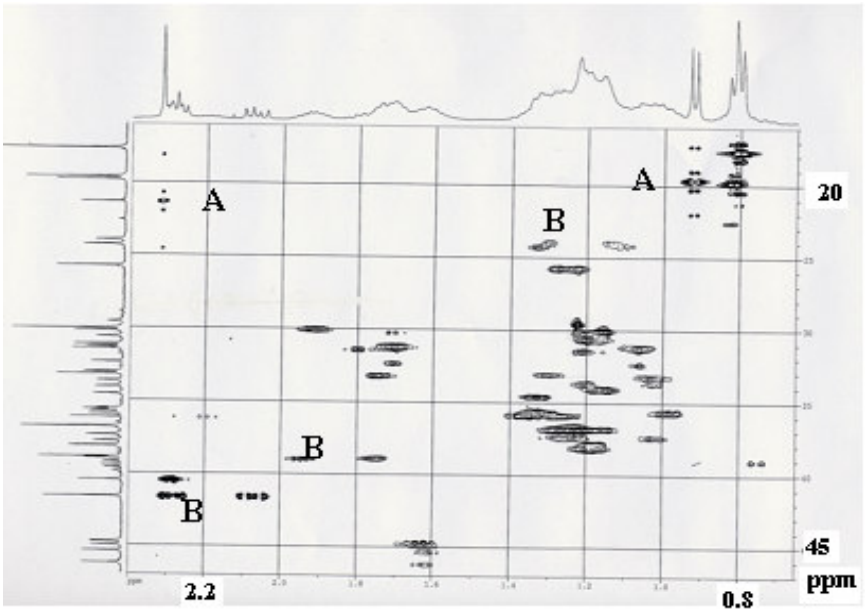

Figure 6.51. g-HMQC (C-H correlation) for indigenous acids from Field Y soap sample.

Figure 6.52 presents the g-HMQC TOCSY for the indigenous acids. There are also many features in the spectrum which are a result of the different naphthenic acid structures present in the indigenous acid samples. The interpretation of this spectrum is therefore focused on the 3 clusters identified by the letter B. These suggest the presence of hydrocarbon chains of at least four carbon atoms in the aliphatic region according to published guidelines (Silverstein *et al.,* 2005). The spin-spin correlations are an indication that cyclic hydrocarbon structures are present in the sample, with attached branched side-chains. Additional interpretation would only be possible with further separation of particular naphthenic acid species. For this reason, no experiments with the ADEQUATE technique were attempted.

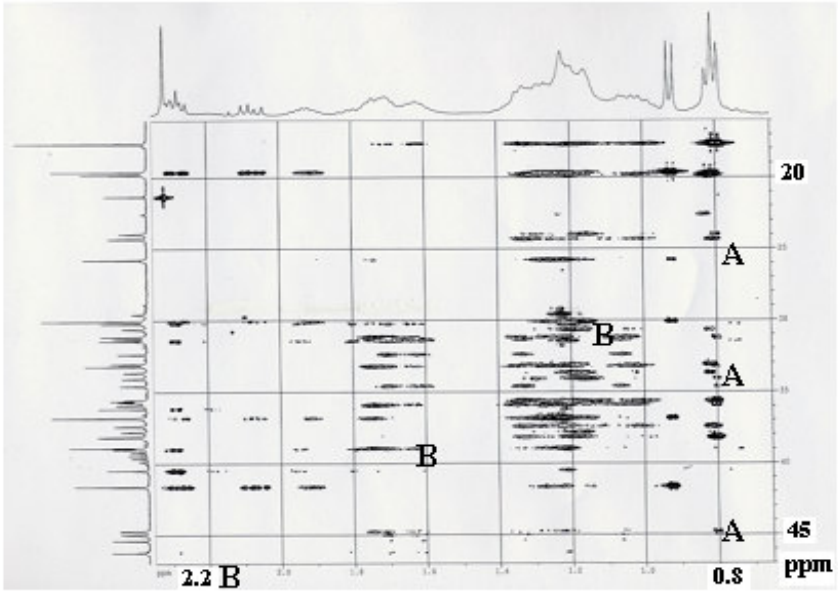

Figure 6.52. g-HMQC TOCSY (spin-spin correlation) for indigenous acids from Field Y soap sample.

The heavily populated spectra in Figures 6.51 and 6.52 are in sharp contrast with the data of Lutnaes *et al.* (2006), where these authors carried out experiments with acids separated from a field deposit using an ion exchange resin and derivatization with BF_3/methanol. They did not address the effect of acid separation and derivatization on the 2D NMR spectra they obtained. The main results in this thesis for the NMR evaluation of the indigenous acids showed the presence of at least four carboxylic carbons, and a predominance of aliphatic groups. The carboxyl groups were shown to be attached to CH_2 carbons. Hydrocarbon chains in the aliphatic range were identified to contain at least four carbon atoms. The results therefore suggest the main average structure in the indigenous acid is a cycloaliphatic structure, with alkyl side chains. An example is shown in Figure 6.53.

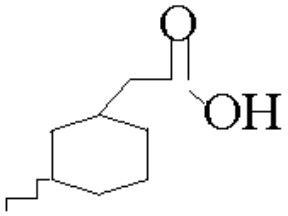

Figure 6.53. Illustration of average structure in indigenous acids given by the 2D NMR experiments.

6.4.1.5. LCMS results.

Mass spectrometry sensitivity results in Chapter 4 indicated that atmospheric pressure sources and polar solvents (such as acetonitrile) lead to preferential detection of Arn to the detriment of lower molecular weight naphthenic acid species in the soap sample. Thus it was opted to use this source-solvent combination to ensure high ionisation of Arn in the indigenous acids to allow for further characterisation by LCMS. Figure 6.54 presents the ion chromatogram obtained for the indigenous acids using acetone as the eluent. Acetone was included in the testing owing to HSE and cost reasons (dilution of the acetonitrile solvent) since it was also used to calibrate the LC column.

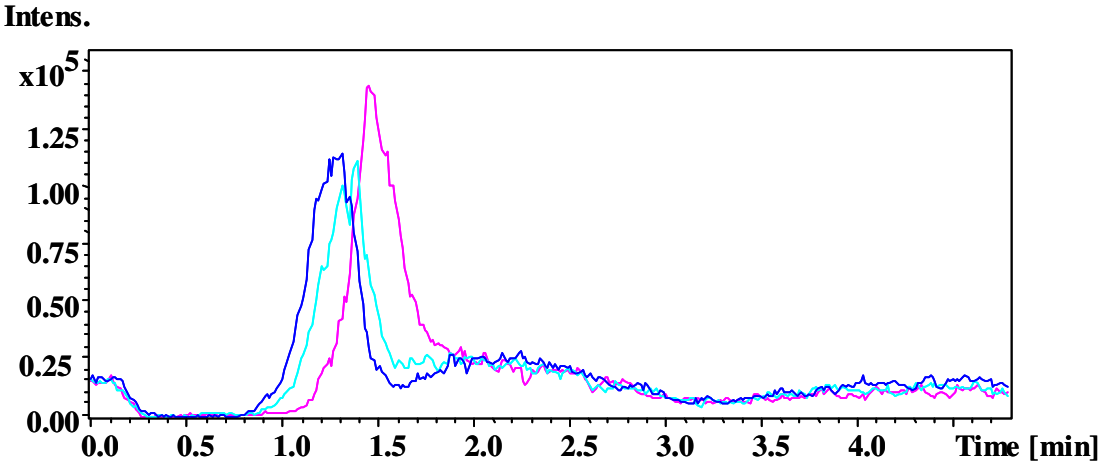

Figure 6.54. Ion chromatogram for indigenous acid samples with acetone as the eluent. Different colours represent distinct LC sample runs.

The chromatograms shows 3 major components in the indigenous acids with retention times of 1.2, 1.4 and 1.5 minutes. The mass spectrum for each of these components was also studied. The indigenous acid fractions show major concentration of species between m/z 1228 and 1248, an example of which is presented in Figure 6.55, for the component with retention time 1.2 minutes. The results in Figure 6.55 suggest different groups of Arn naphthenic acids present in the sample: from m/z 1230 to 1236, and from m/z 1240 to 1247. Nevertheless the use of acetone as an eluent did not allow for the concentration of samples for further analysis. Therefore the use of this solvent alone for LC was not pursued further.

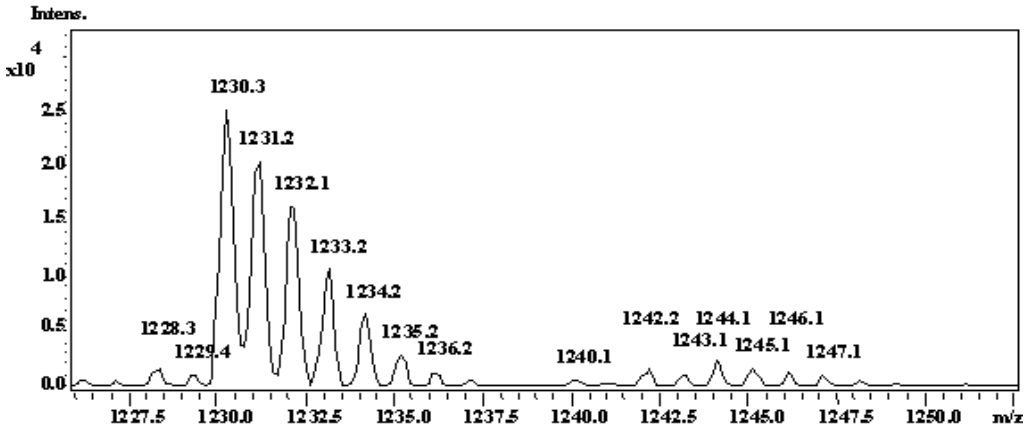

Figure 6.55. Mass spectra of sample from retention time 1.2 minutes from Figure 6.54.

Additional LCMS experiments were conducted using a more polar solvent combination (acetone/acetonitrile 1/4 vol/vol). Results in Chapter 4 pointed to the advantages of using acetonitrile for the identification of Arn acids. The ion chromatogram for one of these experiments is presented in Figure 6.56.

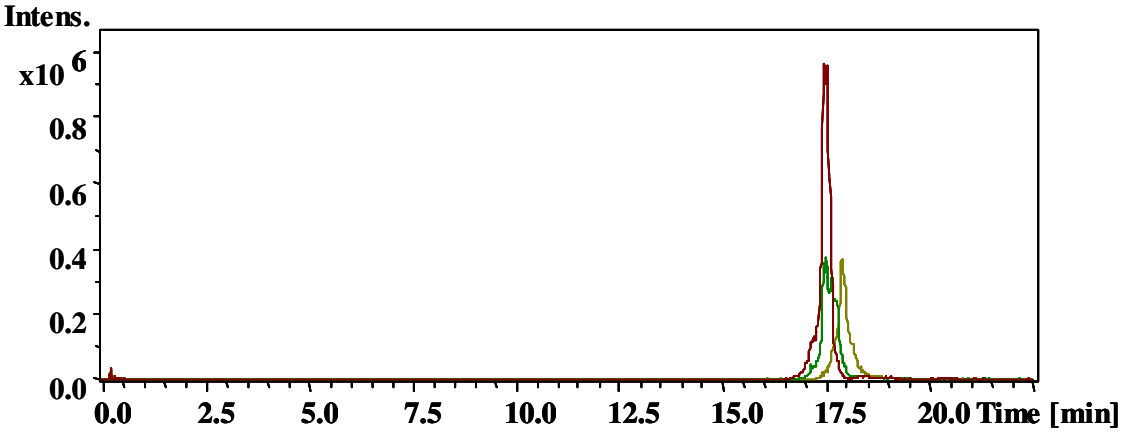

Figure 6.56. Ion chromatogram for indigenous acids with acetone/acetonitrile 1/4 vol/vol as eluents. Different colours represent distinct LC sample runs.

The results in Figure 6.56 show that the addition of a more polar solvent (acetonitrile) during the LC experiments results in different trends. Most of the indigenous acid species are observed with retention times around 17.5 minutes. The intensities of these peaks are an order of magnitude higher than those in Figure 6.54, since acetonitrile has a very good affinity towards Arn (Figures 4.15 and 4.16). It was possible to concentrate the sample eluting at 17.5 minutes using an automatic collector. This sample was analysed by NMR and MS/MS in order to gain a better understanding of the precise molecular structure of the Arn. ^{1}H NMR, ^{13}C NMR and DEPT were conducted on the LCMS fraction. However no additional information was obtained to that already discussed from Figures 6.44 and 6.45

(NMR experiments conducted on the indigenous acids without LC separation). Hence they are not discussed here.

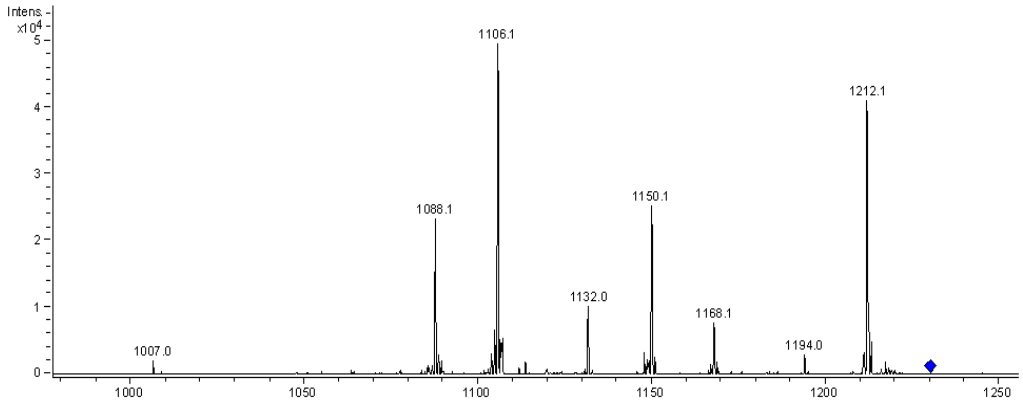

Figure 6.57. MS/MS spectra of m/z 1230 ion from the component with retention time 17.5 minutes from Figure 6.56 (blue diamond). Peaks represent daughter ions.

Figure 6.57 presents the fragmentation spectrum of the parent ion m/z 1230 from the component with retention time 17.5 minutes. At least 4 major daughter ions (m/z 1212, 1150, 1106 and 1088) were obtained from this fragmentation procedure, each of which was further fragmented, thus leading to a sequence of MS^4 experimental data. The assignment of these daughter ions is presented in Table 6.9.

Data suggests the loss of three carbon dioxide groups, two water groups, and one carbon monoxide group for the sequence of fragmentation experiments. These losses may be assigned to fragmentation of four carboxylic acid functionalities, and an example is illustrated in Figure 6.58. In summary, tandem MS data suggested the presence of four carboxylic acid groups in the indigenous acids at m/z 1230. Moreover the results suggest that the acid groups are affected differently by the collision dissociation energy. This could be a result of the different alkyl groups attached to each carboxylic group, as suggested in Figure 6.43.

m/z of product ion	m/z of daughter ion	Cumulative mass loss	Assignment
1230	1212	18	Loss of H_2O
	1168	44	Loss of CO_2
	1150	18	Loss of H_2O
	1132	26	Loss of CO
	1106	44	Loss of CO_2
	1088	44	Loss of CO_2
1212	1168	44	Loss of CO_2
	1150	18	Loss of H_2O
	1132	18	Loss of H_2O
	1106	26	Loss of CO
	1088	18	Loss of H_2O
1150	1132	18	Loss of H_2O
	1106	26	Loss of CO
	1088	18	Loss of H_2O
1106	1090	16	Loss of O
	1064	26	Loss of CO
1088	1072	16	Loss of O

Table 6.9. MS/MS parent and daughter ions and mass assignments.

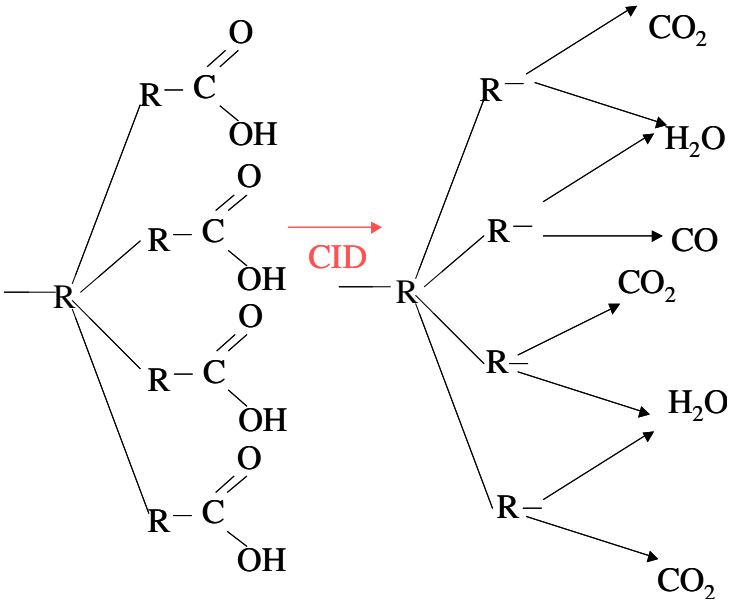

Figure 6.58. Possible assignment of precursor ion m/z 1230. Note CID is collision-induced dissociation which generates the ion fragments. Daughter ions represent m/z 1212, 1150, 1106 and 1088 from Table 6.9. Note the four carboxyl groups represent those in an Arn structure with alkyl side chains and rings given by R.

6.4.2. Mechanistic studies and the role of Arn in soap formation.

6.4.2.1. Mechanistic studies.

The next paragraphs discuss the tests conducted on naphthenic acid extracts obtained from the soap from Field Y sample. These were obtained using the Procedure A described in Section 3.1.2. A sensitivity analysis was conducted and the effect of solvent volumes used for the extraction of naphthenic acids was carried out. The base case was 100 ml of toluene added to the field soap for extraction. After separation of the toluene phase from the soap, fresh batches of solvent (100 ml each) were added, thus conducting additional extractions of naphthenic acids from the sample which were also separated and analysed. Figure 6.59 shows the ES spectra for each extraction for a fixed amount of field deposit (25 g).

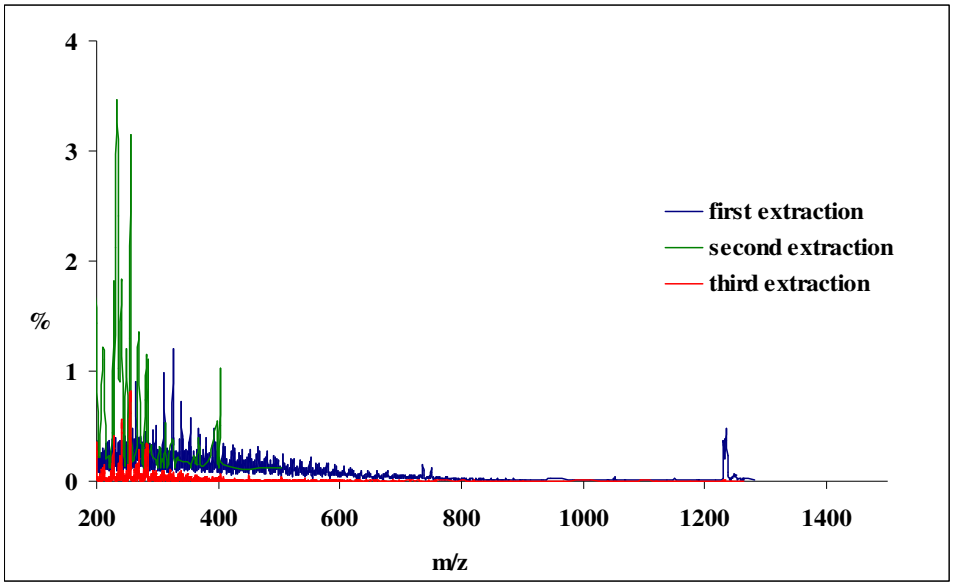

Figure 6.59. ES spectrum of naphthenic acid extract from Field Y soap sample washed obtained from three subsequent extractions using fresh toluene (100 ml each).

The spectra in Figure 6.59 show that the first extraction with toluene contains significant amounts of Arn, in addition to other naphthenic acid species. Only very small amounts of Arn were observed in the second toluene extraction. The third toluene extraction did not contain any Arn, but a range of lower molecular weight naphthenic acids. The results therefore suggest that two extractions of toluene (200 ml total volume) are sufficient for the recovery of most of the naphthenic acids contained in the field deposit samples. Therefore, the naphthenic acid extracts obtained from the first and second toluene extractions were combined and used with aqueous phases for mechanistic studies, following the static bottle procedures described in Section 6.2.2. The effects of pH, cation content and bicarbonate were investigated.

Figure 6.60 presents the final pH values (pH_f) for different aqueous phases used in the static bottle tests conducted with the naphthenic acid extracts from Field Y soap sample.

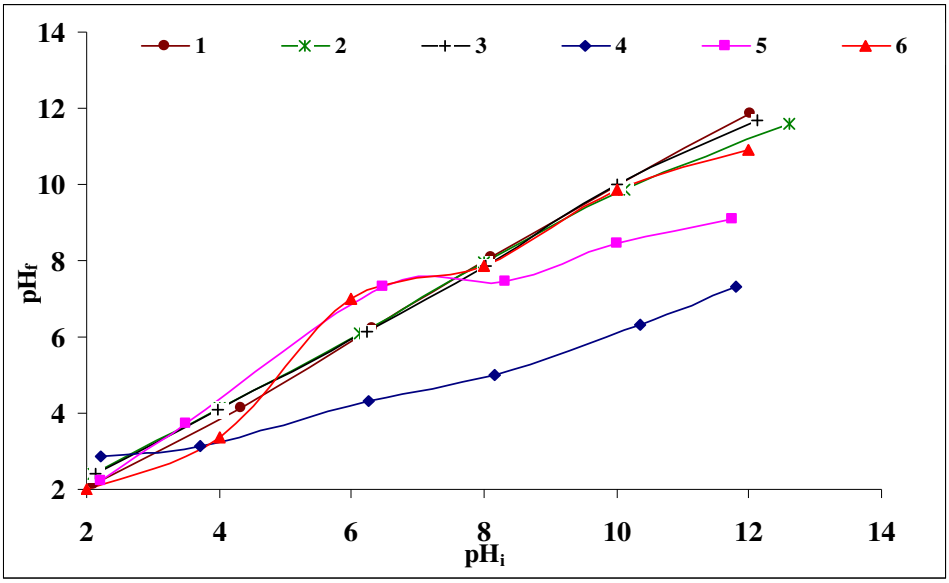

Figure 6.60. pH_f values as a function of pH_i values for naphthenic acid extracts from Field Y soap sample. All pH adjustments with 10 wt% NaOH and 10 wt% HCl. Aqueous phases consisting of, 1) reference deionised water, 2) 25000 ppm sodium ions, 3) 20000 ppm barium ions, 4) 20000 ppm calcium ions, 5) 25000 ppm sodium ions, 20000 ppm calcium ions and 72 ppm bicarbonate ions, 6) 25000 ppm sodium ions and 72 ppm bicarbonate ions.

There are clear observable effects of cation species on the pH_f values in the static bottle tests. The calcium-rich aqueous phase without bicarbonate (case 4) showed lower pH_f values. The sodium and barium aqueous phases do not show significant pH_f variations. Calcium ions have a direct influence on the partition and dissociation of naphthenic acids across the oil-water interface. The buffered systems (with bicarbonate) present different trends. For pH_i values around 6, these aqueous phases showed pH_f values higher than those found for the non-buffered systems. The bicarbonate ions help to maintain high pH_f values during acid partitioning and dissociation. This results in additional amounts of acid available for soap formation (since pH is maintained above the naphthenic acid pK_a). For very high pH_i, the presence of calcium ions in the systems results in additional dissociation, which cannot be balanced by the bicarbonate ions. Thus, the pH_f are lower for the aqueous phases containing calcium, sodium and bicarbonate ions (case 5), but higher when sodium and bicarbonate ions are in the aqueous phase (case 6). The effect of buffers on the overall amounts of deposit formed can be observed in Figure 6.61. The presence of bicarbonate ions in the aqueous phase leads to deposit formation at lower pH values (i.e. 6). This pH is consistent with those values found in cases where field deposits occur (Turner and Smith, 2005). The absence of bicarbonate ions only leads to deposit formation at higher pH (i.e.

12). Deposits are however formed from calcium, sodium and barium aqueous phases. It was observed that higher deposits masses were obtained with the following aqueous phase cation order: calcium > sodium > barium. This is in agreement with the results presented for the model naphthenic acid solutions discussed in Section 6.3. The results would therefore suggest that the naphthenic acid extracts are partitioning in the same fashion as the model naphthenic acids. When buffers are present, these are the limiting reagents for deposit formation. This can be further observed in Figure 6.62. Increasing amounts of calcium ions in the aqueous phase leads to increases in deposit mass, as well as decrease in pH_f in the absence of bicarbonate ions. Deposit mass and pH_f remain constant in the presence of bicarbonates. This observation agrees with data from Rousseau *et al.* (2001), who postulated that bicarbonate ions (not calcium ions) are the limiting reagents in soap forming systems in the field. This information will be used as part of a more detailed analysis of soap-forming systems, in Chapter 8.

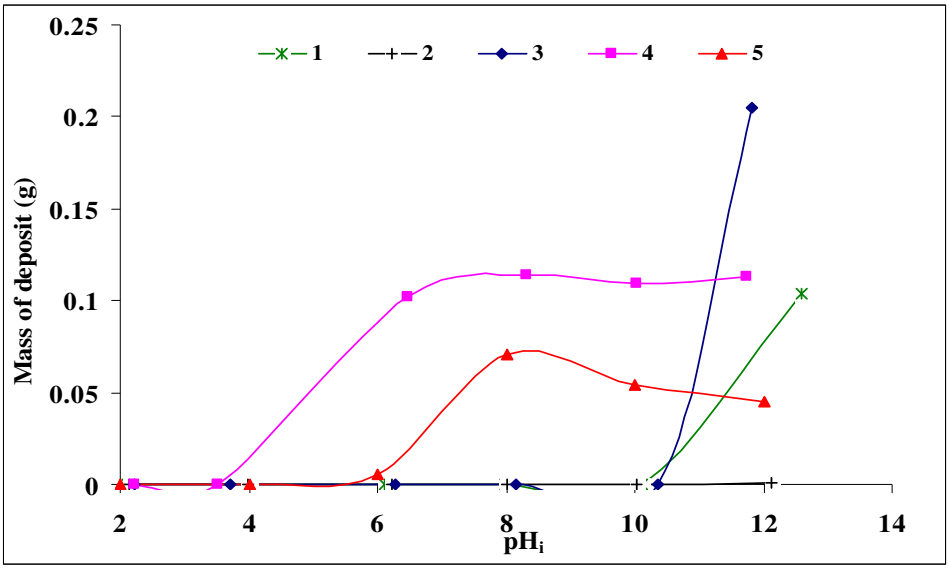

Figure 6.61. Mass of deposit (g) as a function of pH_i values for naphthenic acid extracts from Field Y soap sample. All pH adjustments with 10 wt% NaOH and 10 wt% HCl. Aqueous phases consisting of, 1) 25000 ppm sodium ions, 2) 20000 ppm barium ions, 3) 20000 ppm calcium ions, 4) 25000 ppm sodium ions, 20000 ppm calcium ions and 72 ppm bicarbonate ions, 5) 25000 ppm sodium ions and 72 ppm bicarbonate ions.

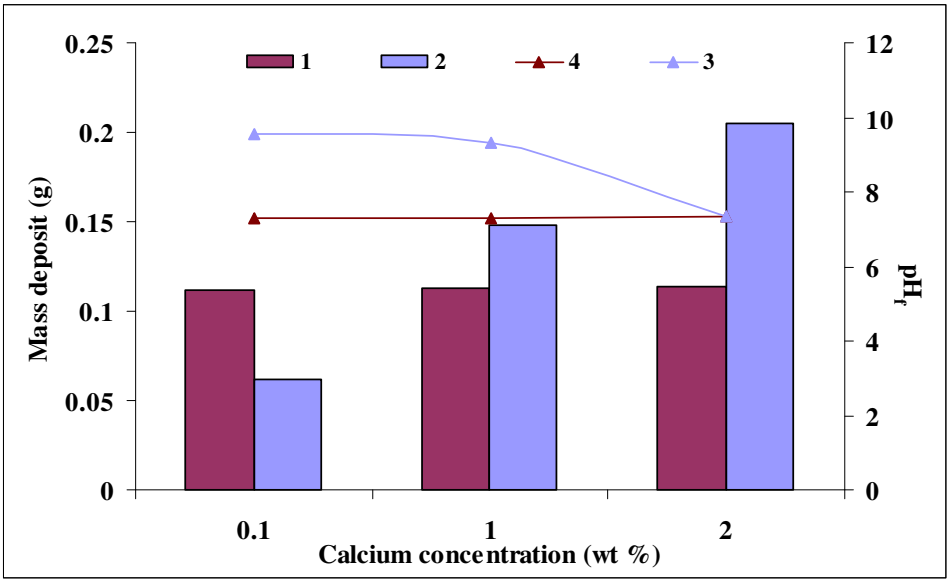

Figure 6.62. Mass of deposit (g) and pH_f as a function of calcium concentration in the aqueous phase. 1) mass of deposit formed from aqueous phase containing 20000 ppm calcium ions, 25000 ppm sodium ions and 72 ppm bicarbonate ions and 4) associated pH_f, 2) mass of deposit formed from aqueous phase containing 20000 ppm calcium ions only and 3) associated pH_f. Oil phases consisting of naphthenic acid extracts from Field Y soap sample.

Figure 6.63 presents an image of the deposit formed in the static bottle tests using an aqueous phase consisting 20000 ppm calcium ions, 25000 ppm sodium ions and 72 ppm bicarbonate ions. No pH adjustment was necessary for the formation of this deposit and it formed as a third phase at the oil-water interface at pH 6. Close examination revealed a sticky, rubbery cluster similar to that reported under field conditions for calcium naphthenate soap scale formation (Vindstad *et al.,* 2003).

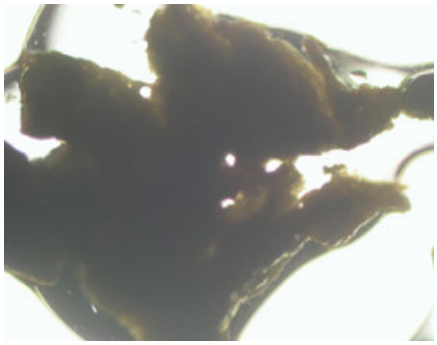

Figure 6.63. Microscopic image of laboratory deposit formed from: Oil phase consisting of naphthenic acid extract from Field Y soap sample. Aqueous phase consisting of 20000 ppm calcium ions, 25000 ppm sodium ions and 72 ppm bicarbonate ions.

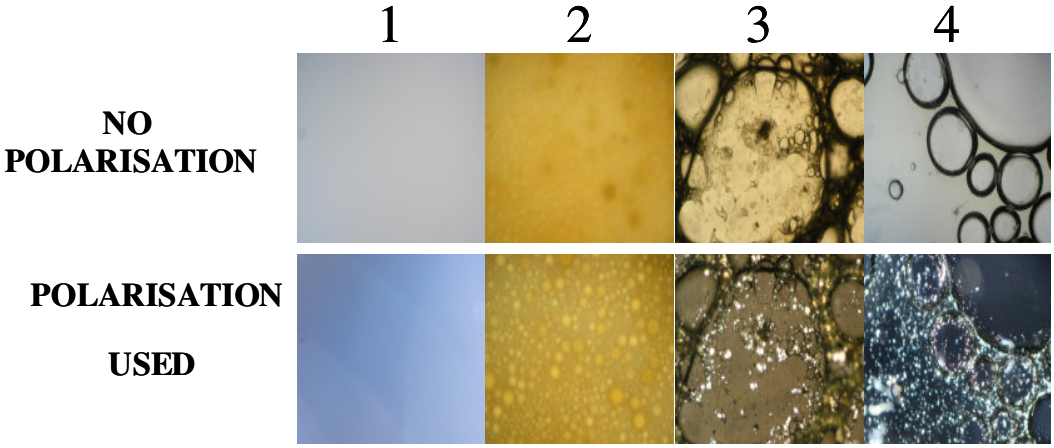

Figure 6.64. Cross-polarisation microscopic images. All oil phases consist of naphthenic acid extracts from Field Y soap sample. Aqueous phase cases: 1) blank cell, 2) deionised water, 3) 25000 ppm sodium ions and 20000 ppm calcium ions, 4) 25000 ppm sodium ions. All phases pH 10 adjusted with 10 wt% NaOH.

During the static bottle test experiments with the naphthenic acid extracts, a number of additional interesting features were observed. Figure 6.64 presents cross-polarisation microscopy images of selected non-buffered bottle tests with naphthenic acid extracts from Field Y soap sample. The use of an aqueous phase in cases 3 and 4 in Figure 6.64 resulted in the formation of liquid crystals at the oil-water interface. These structures were only observed at the onset of soap formation (e.g. at pH values close/prior to those where soap formation occurred, e.g. 10), and were also only observed for non-buffered systems. Liquid crystals seem to occur in the presence of particular naphthenic acid groups. For instance Ese and Kilpatrick (2004) reported β-cholanic acid was responsible for this type of phase behaviour. The presence of liquid crystals is most likely to due the combination of different species in the naphthenic acid extract. It is speculated that the liquid crystal structures have a transient stability behaviour and thus are not be observed when buffers are used in the aqueous phase because soap formation would occur very quickly at constant high pH. Table 6.10 presents the EDAX analysis of the laboratory deposits using the naphthenic acid extracts.

Sample	25000 ppm Sodium ions		20000 ppm Barium ions		20000 ppm Calcium ions		20000 ppm Calcium ions and 25000 ppm Sodium ions		20000 ppm Calcium ions and 25000 ppm Sodium ions and 72 ppm Bicarbonate ions		25000 ppm Sodium ions	72 ppm Bicarbonate ions
Element	**Wt%**	**At%**	**Wt%**	**At%**	**Wt%**	**At%**	**Wt%**	**At%**	**Wt%**	**At%**	**Wt%**	**At%**
C	83.16	88.77	85.7	93.33	41.07	59.22	77.28	87.74	49.23	64.65	82.77	89.45
O	9.27	7.43	7.21	5.89	23.37	25.3	6.59	5.61	24.51	24.16	7.25	5.88
Na	6.81	3.53	x	x	x	x	3.17	1.88	2.47	1.69	5.49	3.1
Cl	0.77	0.28	0.35	0.13	1.5	0.73	7.34	2.82	2.54	1.13	3.47	1.27
Ca	x	x	x	33.83	33.83	14.62	5.53	1.95	21.25	8.36	x	x
Ba	x	x	6.74	x	x	x	x	x	x	x	x	x

Note: x = not present.

Table 6.10. EDAX analysis of laboratory deposits formed from naphthenic acid extracts from Field Y soap scales and various aqueous phases listed in the table.

It can be observed in Table 6.10 that the major cations in the deposits correspond to the predominant cations present in the parent aqueous phase. Chloride ions are due to trace salts used for brine make-up. When calcium ions are used in the aqueous phase the relative percent of calcium present in the deposit is very large compared to the other cations. This supports the relative affinity of the naphthenic acid extracts towards this cationic species as suggested in Figures 6.60 and 6.61.

The presence and distribution of naphthenic acids in the deposits formed in the laboratory was examined by ES. The effect of aqueous phases containing single cationic species without buffers is presented in Figure 6.65, where clear differences can be observed in regards to the overall naphthenic acid distributions. When calcium-rich aqueous phases were used with the naphthenic acid extracts in the static bottle tests, the deposit formed contained Arn (m/z 1230) and a broad distribution of other species between m/z 300 and 600. The presence of a barium-rich aqueous phase leads a reduction in relative percentage of Arn species present in the deposit formed. When sodium ions are used no naphthenic acid species are observed in the laboratory deposits with m/z values above 300.

The effect of aqueous phases containing bicarbonate ions is shown in Figure 6.66, where it can be observed that the presence of calcium ions in the aqueous phases is necessary to obtain a deposit that contains Arn. When calcium ions are not present, but the aqueous phase contains bicarbonate ions, naphthenic acids with lower m/z values are found in the deposit. Thus the results point to the effects of naphthenic acids and aqueous phase composition in the final content of laboratory deposits.

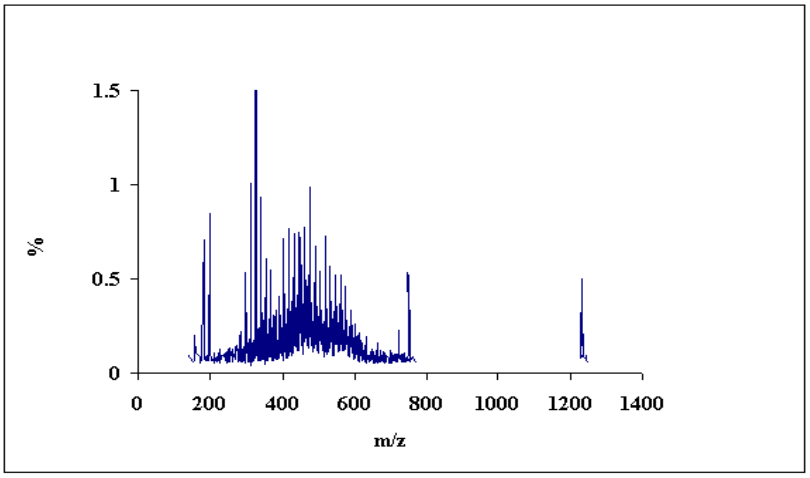

a) 20000 ppm calcium ions.

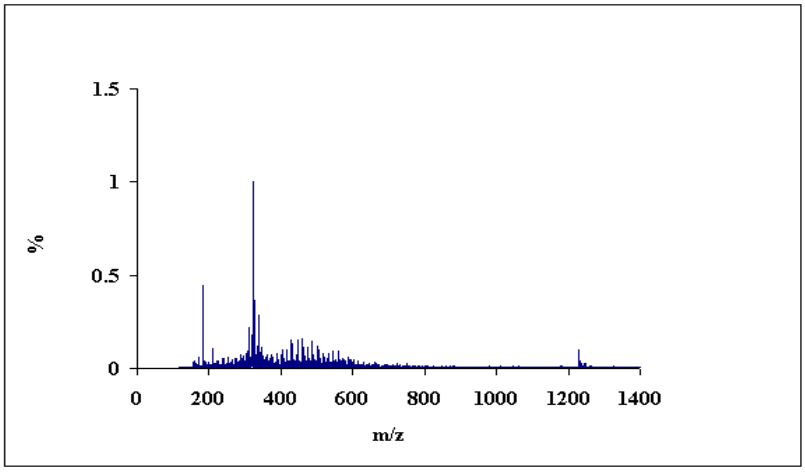

b) 20000 ppm barium ions.

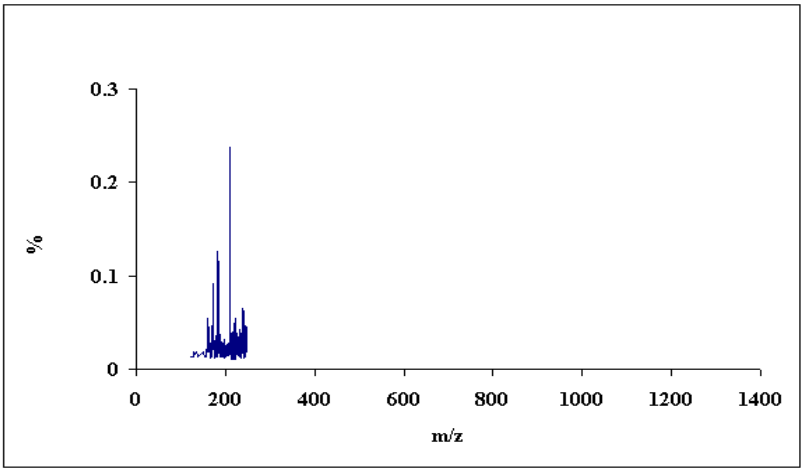

c) 25000 ppm sodium ions.

Figure 6.65. ES spectra of laboratory deposits formed from pH 12 adjusted aqueous phases placed in contact with naphthenic acid extracts from Field Y soap sample. Specific aqueous phase compositions are indicated.

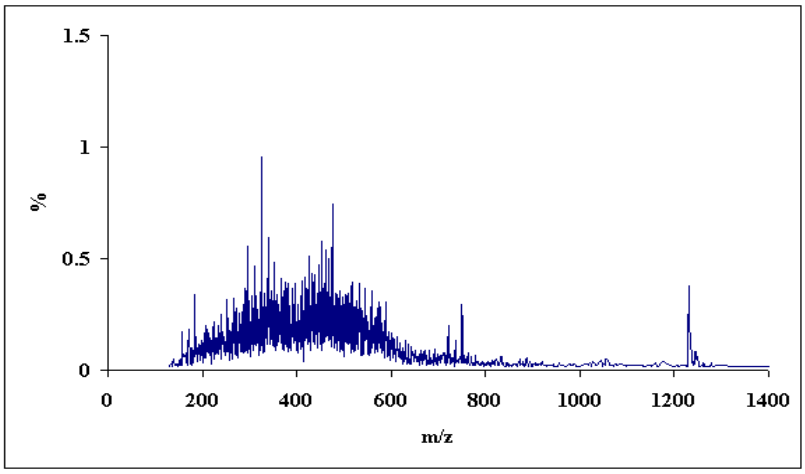

a) 20000 ppm calcium ions, 25000 ppm sodium ions and 72 ppm bicarbonate ions.

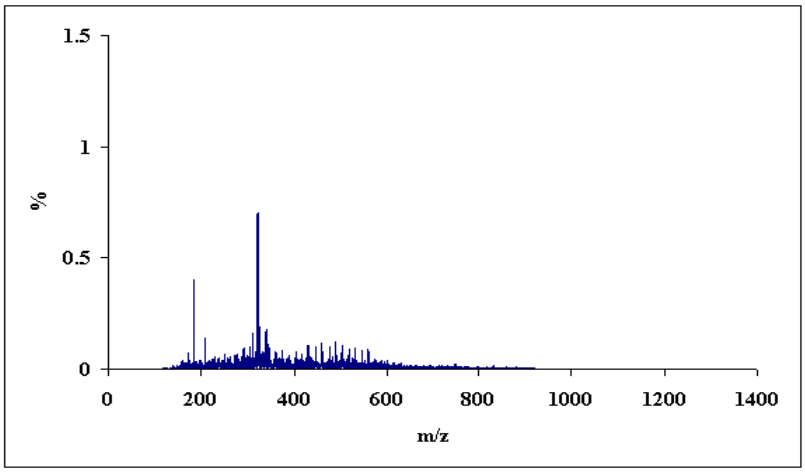

b) 25000 ppm sodium ions and 72 ppm bicarbonate ions.

Figure 6.66. ES spectra of laboratory deposits formed from bicarbonate containing aqueous phases with pH 6.5 placed in contact with naphthenic acid extracts from Field Y soap sample. Specific aqueous phase compositions are indicated.

Figure 6.67 presents examples of the results of the static bottle tests conducted on a number of soap-forming crude oils, in terms of pH_f data. With the exception of one crude oil sample (Field W), pH_f values did not show major variations during the experiments, which is different to that obtained for the naphthenic acid extracts presented in Figure 6.60. This probably reflects the lack of naphthenic acid partitioning and dissociation across the oil-water interface, under the conditions tested.

With the exception of samples from Field W, no other crude oils were shown to lead to the formation of deposits in the laboratory in the static bottle tests. This is despite the presence of Arn in at least one of the soap-forming crude oils (Field Z), as will be discussed in Chapter 8. The formation of deposits with Field W crude oil occurred for a range of aqueous phases and pH values, and an example is shown Figure 6.68.

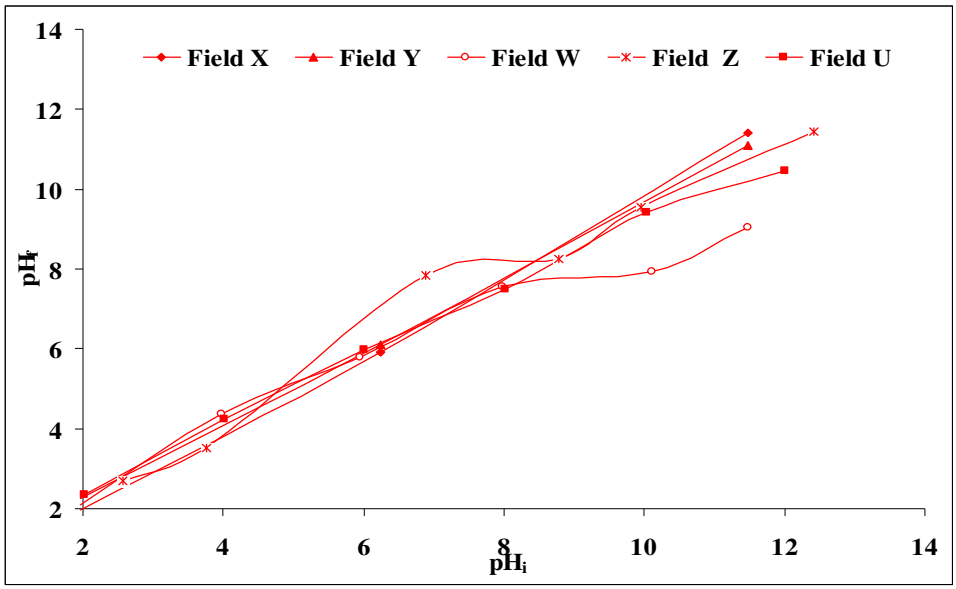

Figure 6.67. pH_f values as a function of pH_i static bottle tests with soap-forming crude oils and aqueous phase consisting of 25000 ppm sodium ions, 20000 ppm calcium ions and 72 ppm bicarbonate ions.

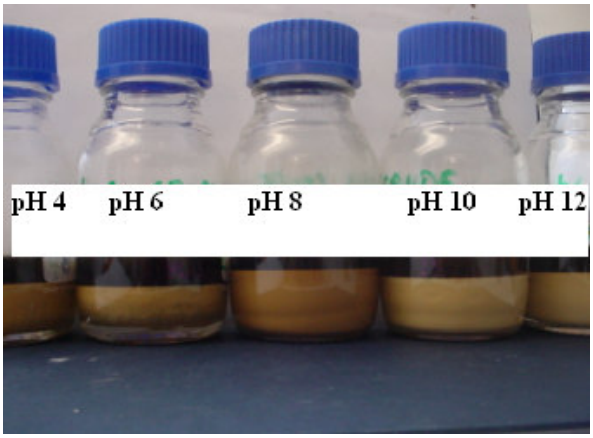

Figure 6.68. Static bottle tests with Field W crude oil sample. Aqueous phase consisting of 20000 ppm calcium ions, 25000 ppm sodium ions and 72 ppm bicarbonate ions.

Figure 6.68 shows that deposits are formed when aqueous phases are used with high and low pH values. Naphthenic acid crude oils are most surface-active at pH values above the pK_a (i.e. 5-6) since only the ionised form of the naphthenic acid has the ability to lower IFT values (Rudin and Wasan, 1992). Formation of deposit at pH values higher than 6 can be explained by the mechanisms discussed in Sections 6.2 and 6.3. The formation of deposits at pH values lower than 4 is difficult to explain without a full analysis of other chemical components in the crude oil itself. Straasner (1968) and Seifert (1969) have shown that basic crude oil species (nitrogen-containing) also have an effect on surface properties at lower pH values. It is likely that the formation of the deposits at low pH values in Figure

6.68 is not related to naphthenic acid groups. At low pH values, the naphthenic acids are not ionised and thus remain soluble at the oil-water interface where soap formation occurs (but in these conditions they have less of an effect on IFT as the ionised acids). The deposit from Figure 6.68 formed at pH 8 was analysed using laser diffraction particle size analysis. Figure 6.69 presents these results.

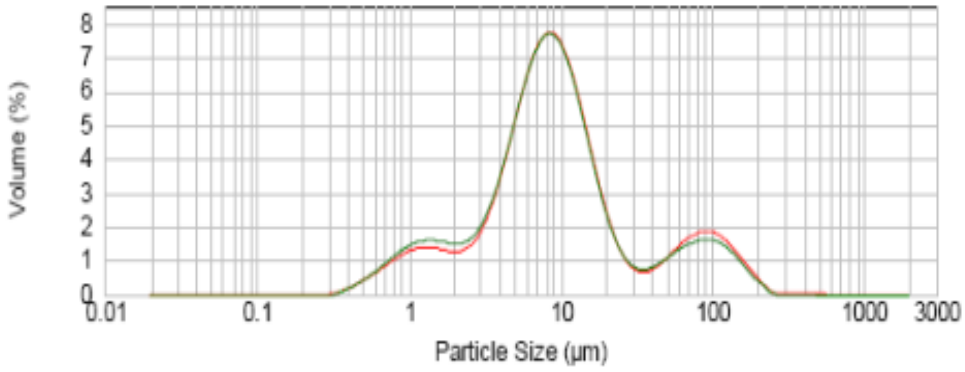

Figure 6.69. Particle size analysis of laboratory deposit formed from oil phase consisting of Field W crude oil and aqueous phases consisting of 20000 ppm calcium ions, 25000 ppm sodium ions and 72 ppm bicarbonate ions, pH 8.

Figure 6.69 shows a tri-modal particle size distribution and the majority of particles can be observed to be around 10 µm. A similar distribution was reported for laboratory soaps formed from model solutions (Figure 6.20). The difference is that the deposits analysed in Figure 6.69 are water-in-oil emulsions (W/O) as opposed to oil-in-water (O/W) emulsions which formed from the model systems. This conclusion was reached after the dissolution of the emulsion in a mineral oil. The W/O emulsions are shown in more detail in Figure 6.70.

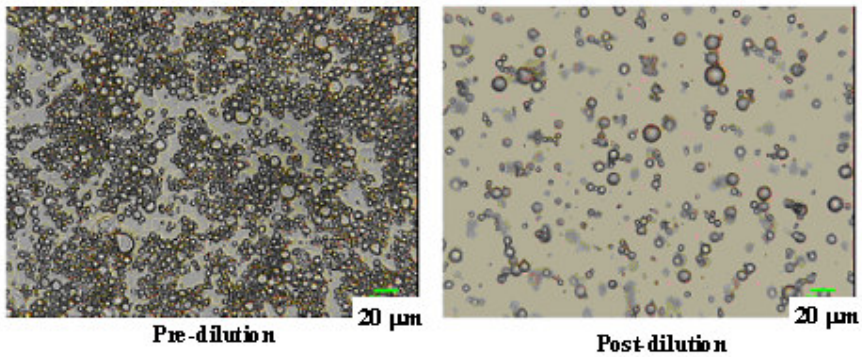

Figure 6.70. W/O emulsion images for laboratory deposit formed from oil phase consisting of Field W crude oil and aqueous phases consisting of 20000 ppm calcium ions, 25000 ppm sodium ions and 72 ppm bicarbonate ions, pH 8.

O/W emulsions are known to be stabilised by electrostatic effects which may be modelled by the double layer theory. W/O emulsions are known to be stabilised by non-polar and

aggregate interactions which have been known to include the formation of liquid crystals (Becker, 1997). Liquid crystals were not however identified in the W/O emulsions formed from Field W crude oil, yet these emulsions remained stable for many weeks. It is possible that the increased stability of these systems is a result of bicarbonate presence, as proposed by Gallup *et al.* (2004). Similar deposits were also formed for Field W crude oil samples in the absence of bicarbonate species. Van der Waals type forces between surface-active components are very likely to be responsible for the stability of the emulsions, however this would need to be confirmed by additional experiments such as atomic force microscopy or dielectric measurements. The W/O emulsions formed in the above experiments in this thesis were filtered and the residue analysed by EDAX. The atomic and weight percentages are presented in Table 6.11. The predominant cation species in the deposit is sodium. The data is in-line with the result of the field deposit sample shown in Table 4.9. Figures 6.71 and 6.72 present the naphthenic acid speciation of the deposit as given by ES.

Element	**Field W Wt%**	**At%**
C	91.55	92.87
O	3.55	3.33
Na	4.15	2.85
Cl	0.75	0.97

Table 6.11. EDAX analysis of laboratory deposit formed from oil phase consisting of Field W crude oil and aqueous phases consisting of 20000 ppm calcium ions, 25000 ppm sodium ions and 72 ppm bicarbonate ions, pH 8.

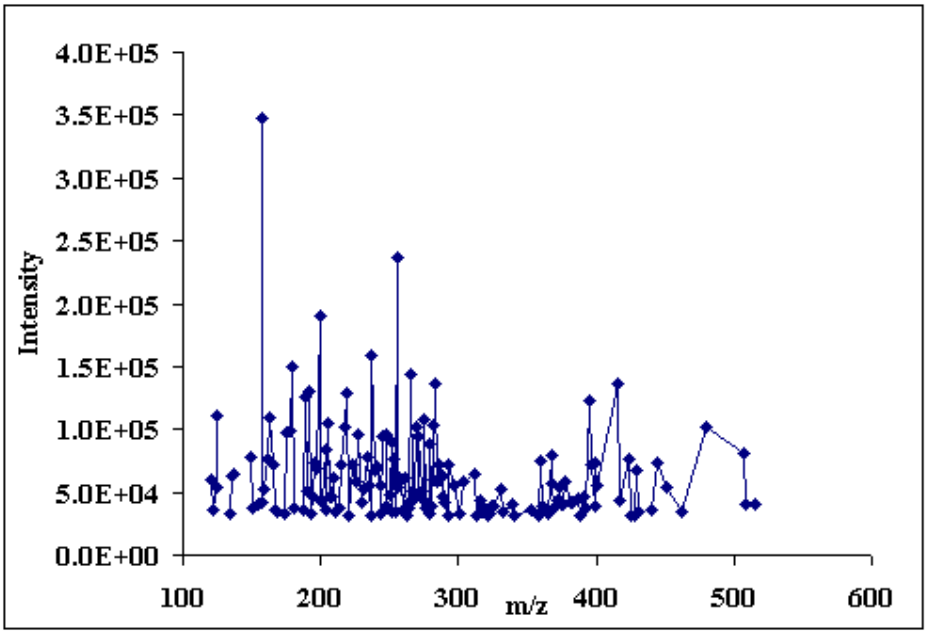

Figure 6.71. ES analysis of laboratory deposit formed from oil phase consisting of Field W crude oil and aqueous phases consisting of 20000 ppm calcium ions, 25000 ppm sodium ions and 72 ppm bicarbonate ions, pH 8.

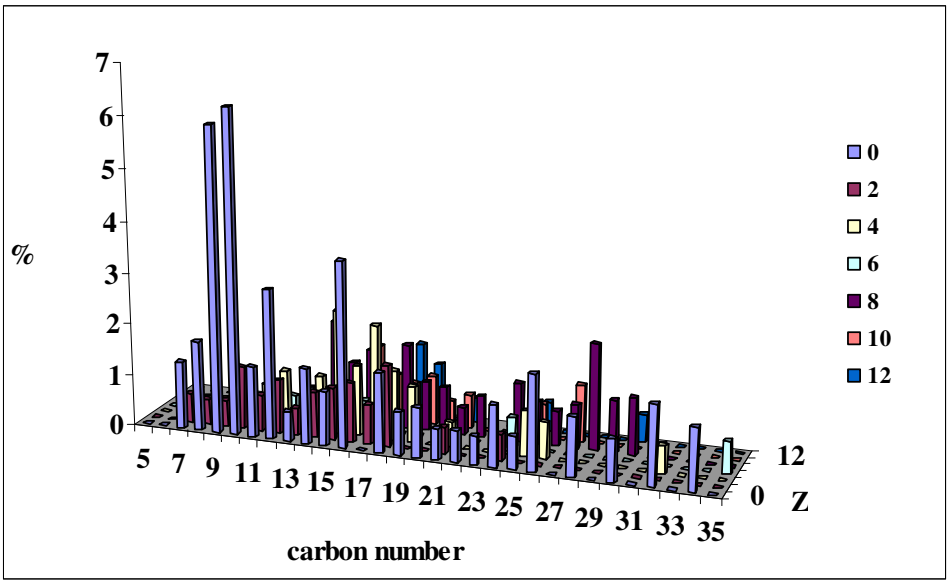

Figure 6.72. Naphthenic acid speciation given by hydrogen deficiency (Z) and carbon number of laboratory deposit formed oil phase consisting of Field W crude oil and aqueous phases consisting of 20000 ppm calcium ions, 25000 ppm sodium ions and 72 ppm bicarbonate ions, pH 8. Legend refers to Z values.

In Figure 6.71 it can be observed that there is a bi-modal distribution of naphthenic acids with two clear groups between m/z 150 to 300 and further to m/z 400 to 500. From the data in Figure 6.72, acyclic acids (Z = 0) represent 39 percent of the overall acid speciation, with

carbon numbers ranging from 7 to 33. These results are in qualitative agreement with the analysis presented for the deposit soap sample from Field W in Figures 4.21 and 4.27.

In conclusion, the soap formed in laboratory conditions from Field W was shown to be a sodium carboxylate soap emulsion, similar in composition to the sample obtained in the field.

6.4.2.2. The role of Arn in soap formation.

A number of experiments have been presented in this chapter showing the formation of laboratory soaps. The results in Figures 6.65 and 6.66 suggested that soap deposits containing Arn were only formed when divalent cation species were present in the aqueous phase. Additional experiments were carried out to examine in more detail the role of the Arn in soap formation. In the first set of experiments, the surface properties of naphthenic acid extracts were examined using interfacial tension measurements with the focus on different cation and bicarbonate effects. In the second set of experiments, naphthenic acid extracts from Field Y (containing Arn as shown in Figure 4.17), were mixed with naphthenic acid extracts from Field W (with no Arn as shown in Figure 4.21) in different ratios, and used in static bottle tests where pH_f, deposit mass and composition were studied. Figure 6.73 presents the IFT values for oil phases consisting of naphthenic acid extracts from Field Y and pH adjusted aqueous phases, with a variety of conditions.

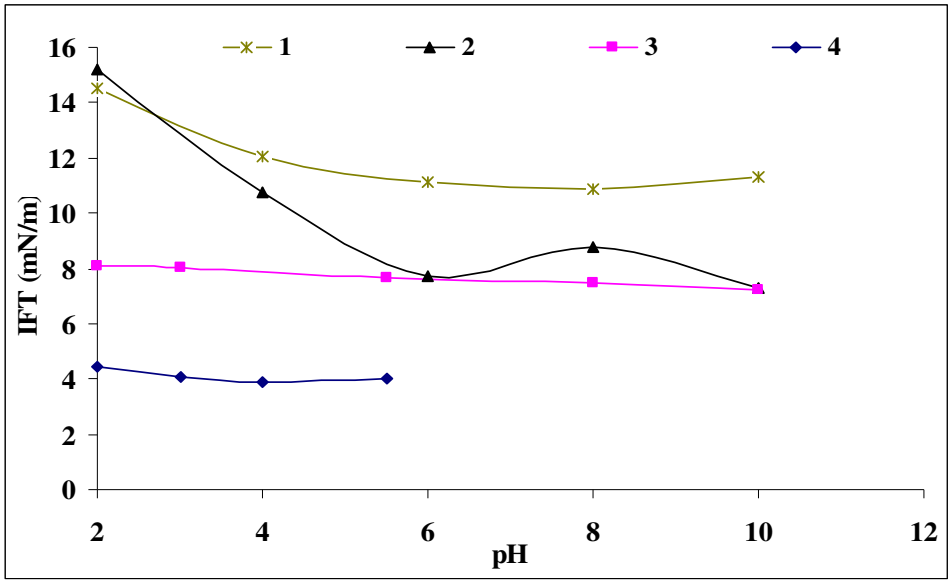

Figure 6.73. IFT as a function of pH. Oil phase consisting of naphthenic acid extracts from Field Y soap sample (containing Arn). Aqueous phases consisting of: 1) 20000 ppm barium ions, 2) 25000 ppm sodium ions, 3) 20000 ppm calcium ions and 4) 20000 ppm calcium ions, 25000 ppm sodium ions and 72 ppm bicarbonate ions.

The lowest IFT values were found for the aqueous phases with bicarbonate ions. These buffer ions result in pH_f values high enough to allow for additional naphthenic acid partitioning and dissociation. The IFT values in this case remain constant, around 5 mN/m. At pH values above 6, laboratory soaps form with this particular aqueous and oil phase combination. The second lowest IFT trend is for the calcium-rich aqueous phase (but without bicarbonate ions). The order of magnitude for these values is in agreement with that reported by Brandal (2005). It is interesting to note that barium ions led to higher IFT values. This is also a direct consequence of hydration effects on the cation itself at high pH. In the presence of bicarbonate ions, the naphthenic acids from the deposit from Field Y (containing Arn) behave like surfactants.

Figure 6.74 presents the IFT values for tests where the naphthenic acids extracts from Field Y soap sample were mixed with both stearic acid (SA) and 4-tert-butylbenzoic acids (TBA) both at 1 wt%. The results should be compared to those in Figure 6.34 where these model naphthenic acids were used. The IFT trends shown in Figure 6.74 suggest the addition of the model naphthenic acids does not lead to changes in the overall surface properties of the naphthenic acid extracts. This is despite the IFT values of the single model naphthenic solutions (under the same conditions) being five orders of magnitude higher. It would appear that the naphthenic acid extracts (containing Arn) have the predominant influence on the surface properties in mixed solutions.

Nevertheless, it is debatable if these effects could be observed with real crude oils samples under conditions of soap deposition in the field. Arn acids are found in very small concentrations in soap-forming crude oils, as opposed to the higher concentrations present in the naphthenic acid extracts used in this thesis. In Chapter 8 this hypothesis will be explored further to investigate the use of IFT properties for the prediction of soap formation in crude oils.

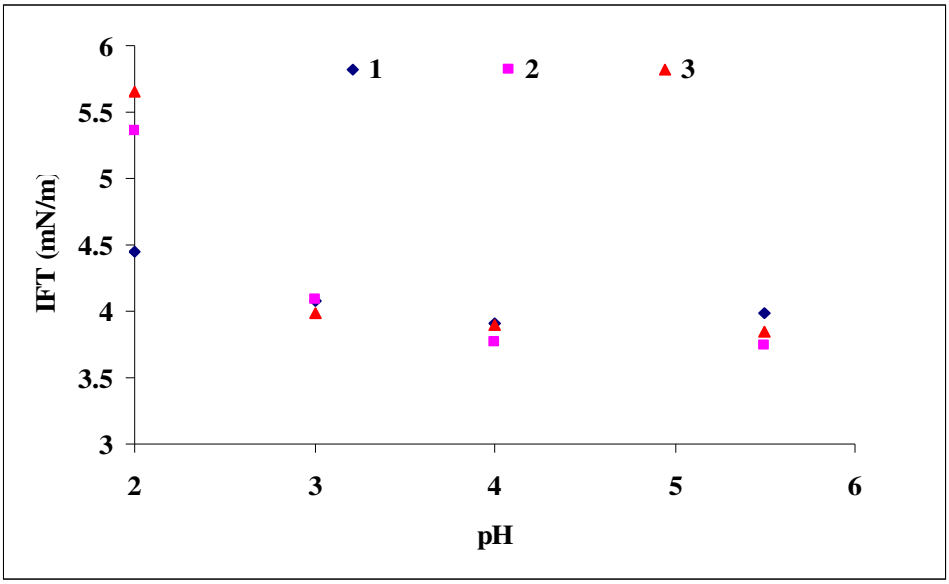

Figure 6.74. IFT as a function of pH. Aqueous phases consisting of 20000 ppm calcium ions, 25000 ppm sodium ions and 72 ppm bicarbonate ions. Oil phases consisting of: 1) naphthenic acid extracts from Field Y (~ 80 ppm), 2) naphthenic acid extracts from Field Y (~ 80 ppm) in combination with SA (1 wt%), 3) naphthenic acid extract acids from Field Y (~ 80 ppm) in combination with TBA (1 wt%).

Figure 6.75 and 6.76 present the results of static bottle tests in which naphthenic acid extracts from Field Y (containing Arn) and Field W (with no Arn) were used. The trends in Figure 6.75 show that as the percentage of naphthenic extracts from Field W is increased, there is a decrease in deposit mass. Moreover, the overall calcium percentage in the deposit is also reduced.

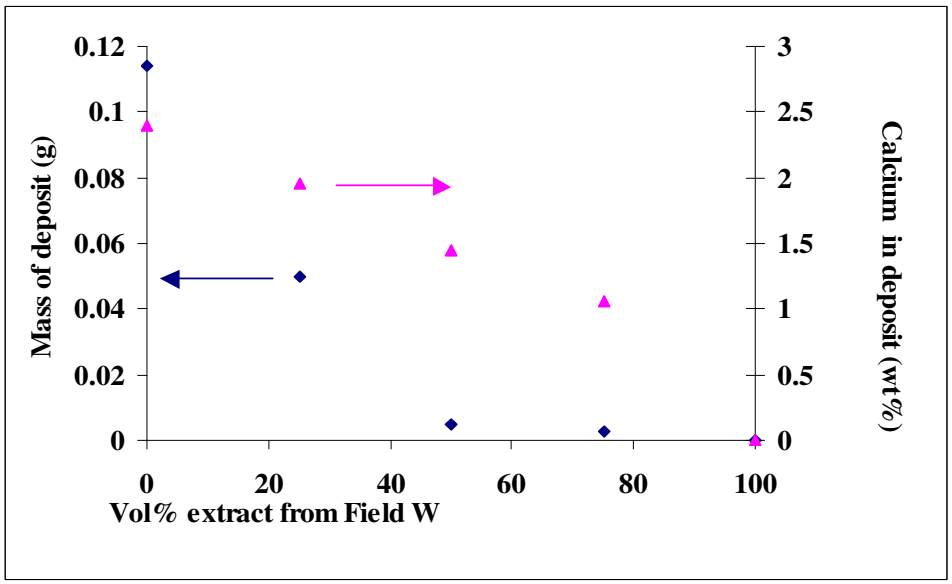

Figure 6.75. Mass and calcium wt% in deposit as a function of naphthenic acid extract from Field W soap sample mixed to the naphthenic acid extract from Field Y soap sample (vol%).

Figure 6.76 presents the speciation of naphthenic acid species of the ES spectra of the laboratory soap formed from Field Y extract and Field Y/Field W naphthenic acid extracts. The differences in Arn percent can be clearly observed. Note Arn is represented by species with 80 carbon atoms and 5 cyclic rings (hydrogen deficiency of -10).

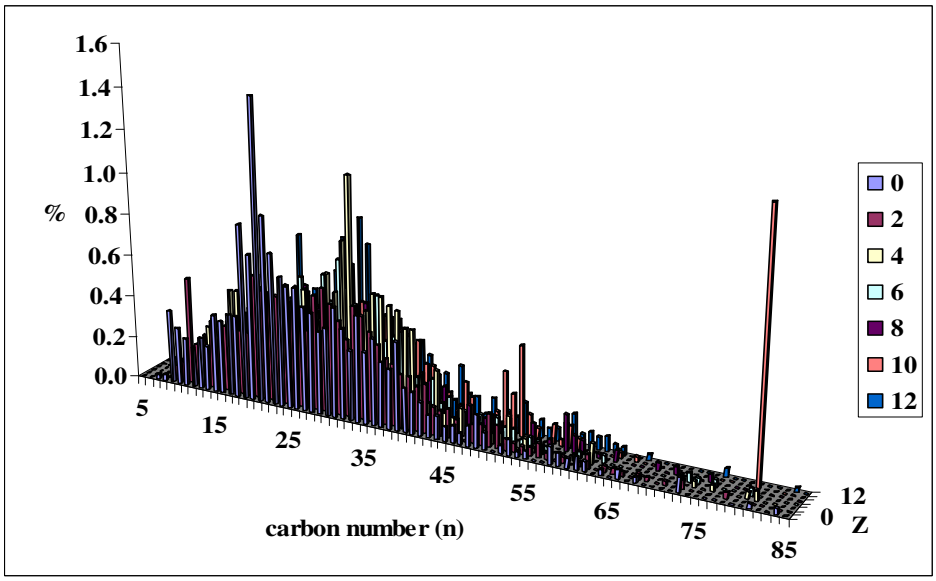

a)

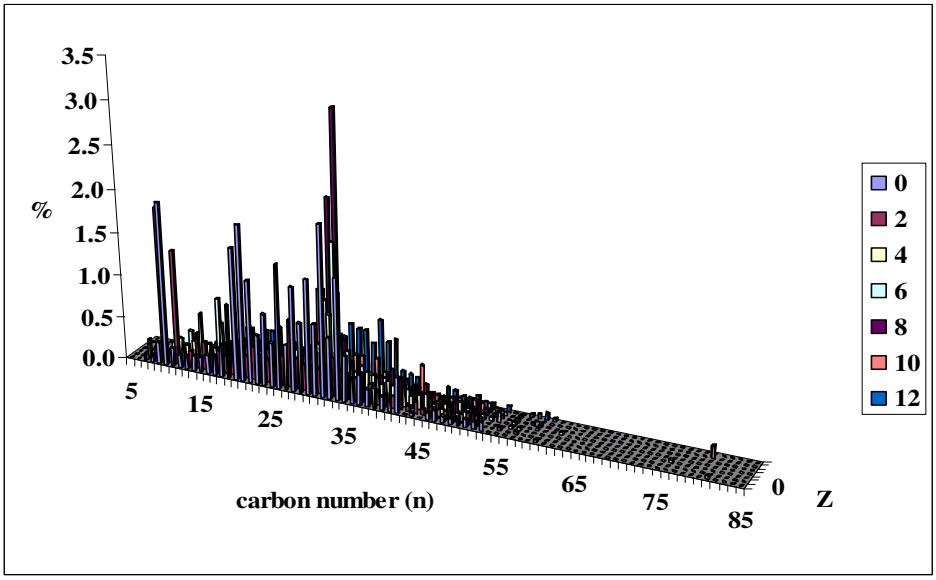

b)

Figure 6.76. Speciation of naphthenic acids from laboratory soap deposits formed from: a) Field Y naphthenic acid extract, b) Field Y and W naphthenic acid extracts. Speciation given by hydrogen deficiency (Z) and carbon number. Legend represents Z values.

Figure 6.77 presents a comparison of the different naphthenic acid species present in both the laboratory soaps formed from the naphthenic acid extracts from Field Y and FieldY/Field W in terms of hydrogen deficiency.

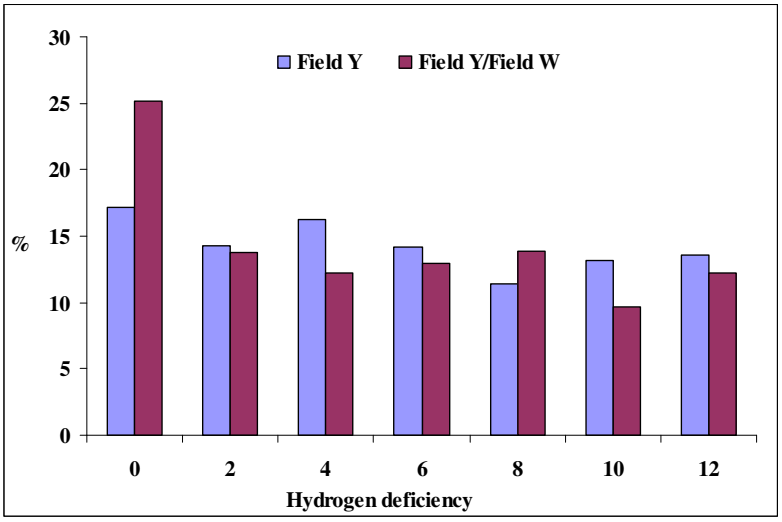

Figure 6.77. Speciation of naphthenic acids from laboratory soap deposits formed from Field Y naphthenic acid extract and Field Y/Field W naphthenic acid extracts. Speciation given by hydrogen deficiency (Z).

Based on the information in Figures 6.76 and 6.77, addition of extracts from Field W resulted in an increase in the percentage of acyclic acids in the deposits, and a decrease in the amounts of Arn in the laboratory soaps. Thus, the decrease in deposit mass and calcium content shown in Figure 6.75 may be interpreted as the effect of the presence of acyclic acids in the mixture, in detriment of the Arn species. As illustrated in Figure 6.36, Arn acids may bind with up to 4 calcium ions in a soap molecule. Thus the decrease in calcium content accounts for less overall Arn acids present. These effects were also observed in the analysis of Field Z deposits as discussed in Section 4.7.

Figure 6.78 shows the final pH values of a series of experiments where the naphthenic acid extracts from Field Y and Field W were mixed and diluted with toluene and used in static bottle tests. Two reference tests are also presented where the individual naphthenic acids extracts from each field are diluted with toluene (tests 1 and 2). There is a decrease in pH values for all data sets, but the extracts from Field W showed the lowest pH trends and Field Y extracts lead to the higher pH trends. These are a direct result of the partitioning

and dissociation of the naphthenic acid species present. Field W extracts contain mostly acyclic acids. Owing to well-documented stearic hindrance effects (Becker, 1997), acyclic species are more favourably positioned at the oil-water interface then cyclic structures. It is questionable if this advantage would also hold in the presence of Arn naphthenic acids. Arn acids in this thesis were shown on contain four carboxylic acid groups (Figure 6.57). However, diffusion to the oil-water interface may favour lower molecular weight

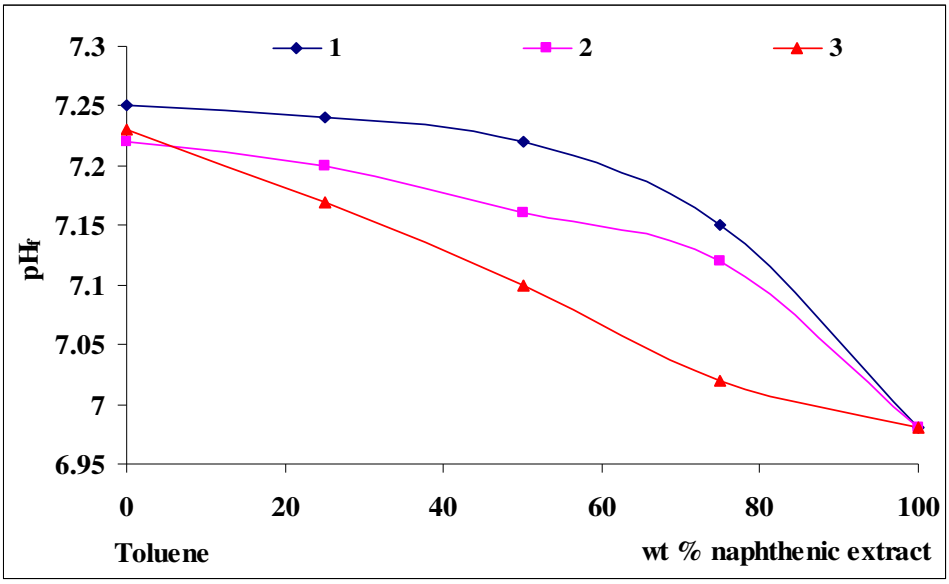

naphthenic acids. This discussion could support the results in Figure 6.75, and the formation of soaps in the experiments with increasing amounts of acyclic acids, Figure 6.77.

Figure 6.78. pH_f as a function of increasing naphthenic acid extract wt% in toluene. Aqueous phase consisting in 20000 ppm calcium ions, 25000 ppm sodium ions and 72 ppm bicarbonate ions. Oil phases consisting of: 1) naphthenic acid extracts from Field Y soap sample, 2) naphthenic acid extract from Field W soap sample, 3) combined naphthenic acid extracts from Field W and Field Y soap samples.

The data presented in Figures 6.73 to 6.78 provided insights into the role of Arn in soap formation. It is clear that the surface properties of Arn are enhanced by the presence of calcium and bicarbonate ions in aqueous phases. However, the surface properties of Arn are not affected by the addition of other naphthenic acids. This is despite the fact that acyclic species such as stearic acid (SA) would have less steric hindrance at the oil-water interface, than the bulky Arn acid. Acyclic acids such as SA are themselves surface-active under the conditions tested. However, they also have the potential to affect the phase behaviour of a soap-forming system, in detriment of the effect of the Arn naphthenic acids. They would compete with the Arn for calcium ions, and would be favourably partitioned and

dissociated. Thus, a deposit may be formed in the laboratory which contains increasing amounts of acyclics and decreasing that of Arn acids. Clearly particular naphthenic acid combinations, not just Arn, may be responsible for the formation of soaps in the laboratory but also in field deposits as was examined in Section 4.7. Chapter 8 will attempt to obtain information on specific naphthenic acid ratios and correlate this with the tendency for soap formation.

6.5. On establishing a protocol for soap formation under laboratory conditions.

It would be very useful to have a technique which could be used to predict the formation of soaps for a particular set of oil and aqueous phases. This technique would be used to detect the onset of soap precipitation. In the static bottle test experiments conducted in this thesis, it was shown that even in the cases where soaps were not formed reduction in pH was observed (e.g. Figure 6.6). A technique for soap prediction could be based on the pH transitions which occur, from unionised acids at low pH to ionised acids at higher pH. This could be carried out by observing the particular fingerprint for both free ionised acids as well as those acids which are bound as complexes with calcium ions, prior to the precipitation of a soap. Two spectroscopy methods were evaluated for this purpose: Fourier-Transform infrared (FTIR) and Raman. Various solutions were prepared containing indigenous acids with and without model naphthenic acids in toluene. These were then placed in contact with aqueous phases with increasing pH values between 2 and 10, and left for 24 hours. Toluene phase aliquots were then collected and examined for the presence of free or bound naphthenic acid fingerprints.

Figure 6.79 presents the FTIR calibration curve (red line) constructed using the percentage of monomer and dimer peak areas of the commercial naphthenic acid solutions in toluene used in this thesis prior to the examination of the test aliquots. The best correlation was found when both peaks were combined.

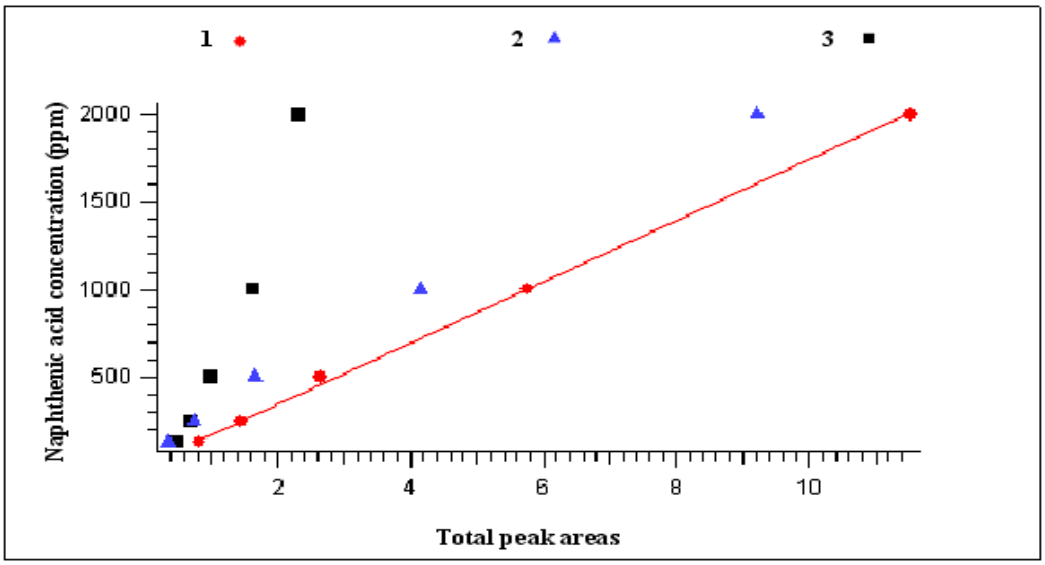

Figure 6.79. FITR naphthenic acid calibration curve. Peak areas versus naphthenic acid concentration (ppm). 1) combined dimer and monomer areas, 2) monomer areas, 3) dimer areas.

The construction of a calibration curve with Raman spectra for model naphthenic acids was not possible. The reason for this was the weak dimer peak response in addition to the lack of an identifiable monomer fingerprint. During the examination of the toluene test aliquots which had been in contact with the various different aqueous phases, it was not possible to observe bound acids peaks in the FTIR spectra. It was however possible to observe differences in the spectra within the region where peaks owing to free acids were expected. A possible explanation for this is that the toluene aliquots were taken from the bulk of the oil phase. Bound acids may be positioned closer to the oil-water interface. The FTIR intensities as a function of wavelength for these samples are shown in Figure 6.80. The measured carbonyl areas were used to calculate the naphthenic acid concentrations in the different oil phases. This assumes that the IR absorption coefficient for both carbonyls in the aliquots is identical to those of the naphthenic acid standard. The Raman instrumentation was more sensitive towards the different naphthenic acids and naphthenate ions compared to FTIR. However, there were no clear differences for the Raman spectra for the oil phases as a function of pH since a calibration curve was not obtained. Thus Raman was discontinued for the purpose of onset of soap precipitation. Figure 6.81 presents the acid concentrations in toluene as a function of aqueous phase pH calculated from the FTIR spectra. The results show that for both the indigenous acids, as well as the model naphthenic acids there are decreases in the amount of measured free acid present in the oil phases. This is an indirect effect of the formation of cation bound acid complexes at the oil-

water interface. There is a reduction in more than 50 % of the free naphthenic acid bands at the onset of precipitation, i.e. at a pH value just below the formation of a soap. This technique therefore would have the potential to be use for the prediction of soap formation in the laboratory.

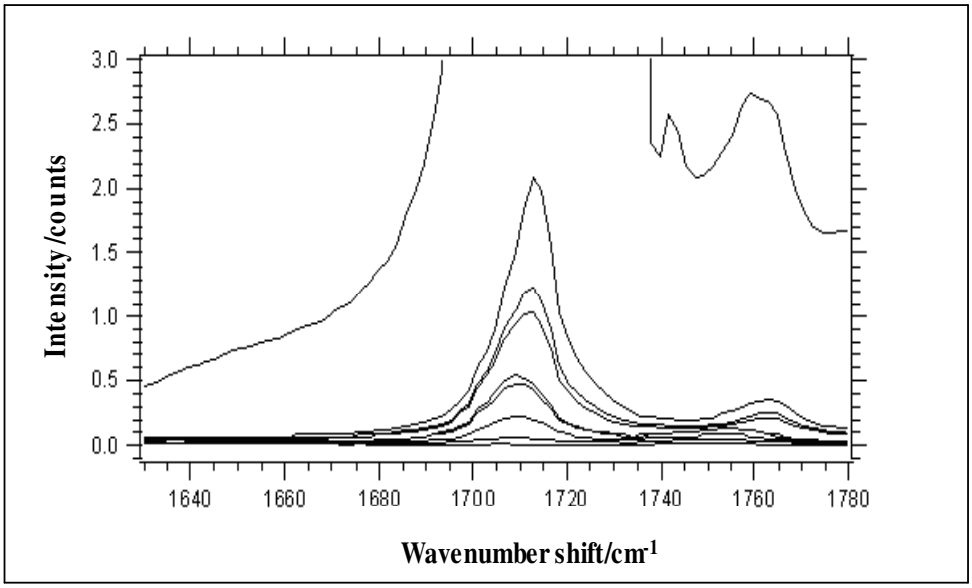

Figure 6.80. FTIR difference spectra of naphthenic acids from the aliquots used in the static bottle tests experiments.

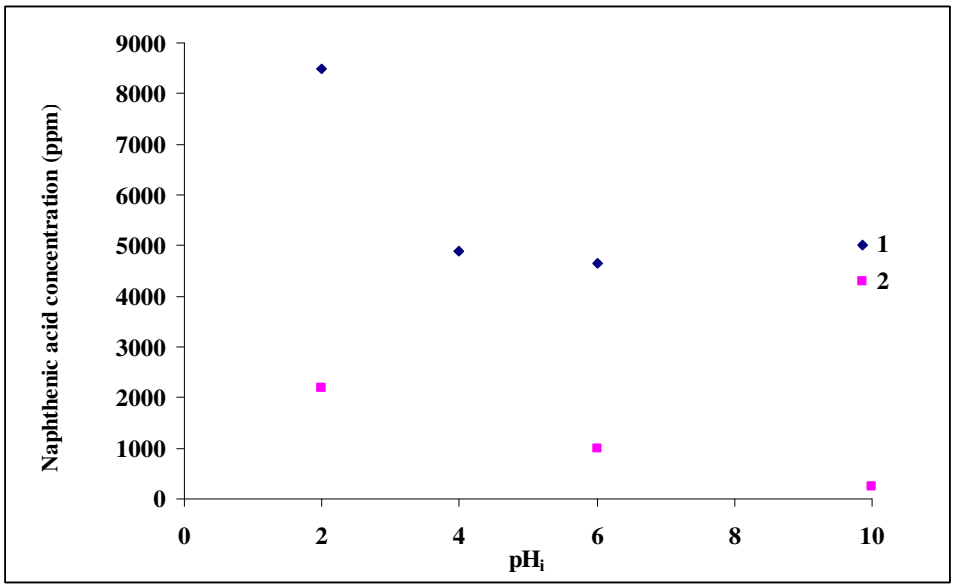

Figure 6.81. Naphthenic acid concentration in toluene phase as a function of pH_i for 1) naphthenic acid extracts from Field Y soap sample 2) stearic acid.

6.6. Conclusions.

Prior to the development of the tests detailed in this chapter, soap formation in the laboratory had been attempted by few researchers (e.g. Dyer *et al.,* 2003). Nevertheless, the results presented in this chapter, discuss many sensitivities and effects which had been overlooked in previous publications.

It was not possible to form soaps (even from model systems) using tube-blocking and the CO_2 static rig. Thus it was opted to employ bottle tests where the soap formation mechanism was simulated by a pH trigger resulting from an alkali agent. A main challenge during the optimisation of the bottle tests was to ensure that the addition of alkali agent was not affecting the final composition of soaps formed in the laboratory.

The optimised static bottle test procedure for soap formation in the laboratory consisted of adjusting pH with either 10 wt% NaOH or 10 wt% HCl, shaking both phases manually for one minute, and leaving oil and aqueous phases in contact for 24 hours prior to taking any measurements. It was shown that the mechanistic formation of soaps could be studied by pH changes even if no deposit was observed. Partitioning and dissociation of naphthenic acids was observed to be a function of divalent and monovalent cations. Nevertheless, one of the main challenges was to ensure that the laboratory soaps formed in these tests could represent the deposits which precipitate in the field, such as those analysed in Chapter 4.

Phase behaviour of naphthenic acid systems in static bottle tests indicated very distinct end-member type features: acyclic acids/sodium pairs as opposed to cyclic acids/calcium pairs. Sodium-rich deposits from model acids were observed to be O/W emulsions. Calcium-rich deposits from model acids were observed to be solids. This supported the results of the field deposits presented in Chapter 4.

Particle size and surface properties were shown to be a clear function of the cation type and concentration. EDAX allowed for the identification of the deposits as either calcium, sodium or mixed soaps. The presence of bicarbonate ions in the aqueous phases resulted in deposits which were most likely complexes but only in the presence of sodium. This information supports the hypothesis put forward by Gallup *et al.,* 2002 for field deposits. Thus it would appear that buffer ions enabled formation of soaps at low pH and participate in the soap formation mechanism (but only for fatty acid-containing systems).

In order to test competing effects of Arn *vs.* non-Arn acids, indigenous acids from a field deposit were also used in bottle tests. This also allowed additional contributions to the physical chemistry of Arn acids to be investigated. MS/MS attempts to fragment the Arn species were not successful. Yet results confirmed the degradation of the carboxylic acid group, as a result of favoured ionisation and polarity. 1D and 2D NMR enabled only basic

carboxylic and hydrocarbon skeletal structure for the indigenous acids to be identified, but LCMS allowed for the clear determination of the presence of 4 carboxyl groups, using sequential MS/MS. The MS/MS results represent an independent confirmation of the presence of the 4 carboxyl groups in this species.

It was observed that Arn naphthenic acids were approximately 4 percent of the indigenous species from Field Y soap sample and could be detected at concentrations down to 80 ppm in model systems. Acyclic acids (Z = 0) accounted for a quarter of the indigenous species. These results point to possible interactions between these species during the precipitation of calcium naphthenate soap scales. When this information was extended to bottle tests, it was observed that Arn acids were the predominant surface-active species present in indigenous acids from soap deposits. Nevertheless, there was a range of bulk phase behaviour observed. It was possible to form calcium naphthenate soap scale deposits in the laboratory from naphthenic acid extracts. The deposits contained Arn as well as other naphthenic acid species. The acid distribution was suggested to be a direct result of the competition of calcium and sodium ions in the water phase and the exposure to naphthenic acid types. The distribution of naphthenic acids (Arn and non-Arn) in the laboratory soaps was equivalent to the distribution of naphthenic acids found in field deposits. Moreover the results in this chapter are clearly in-line with the results from the Field Z deposition case discussed in Chapter 4. The results are important since the agreed mechanism of soap deposition has relied (prior to the thesis) on a qualitative description of the physical chemistry of Arn only. Nevertheless, formation of calcium naphthenate soap scales in the laboratory was not possible using soap-forming crude oils. Thus it is likely that factors such as total Arn concentration in the crude oils is affecting the performance of these tests. Field W crude oil did however lead to the formation of W/O emulsions in laboratory experiments. These matched the composition of sodium carboxylates soap emulsions from the field given in Chapter 4. Bottle tests in this case would also have the potential to be used in inhibitor studies.

Another major contribution of this chapter was the development of special test procedures used for the prediction of the onset of soap formation in the laboratory. FTIR was the technique which enabled the measurement of naphthenic acid depletion in the model oil phase and water phases containing naphthenic acids, as a function of pH. This was a direct result of the difference in FTIR signals between free naphthenic acids and cation-bound naphthenic acids. If tested on more realistic feeds (e.g. crude oils) the results would have potential impact on surveillance predictions, where the onset of soap precipitation would be accompanied through simple measurements.

CHAPTER 7 – PREDICTION OF NAPHTHENIC ACID BEHAVIOUR IN OIL-WATER SYSTEMS.

Abstract

In this chapter preliminary attempts to predict the behaviour of naphthenic acids in oil-water systems are presented. The equilibria model used was developed by Ken Sorbie and further details are available in Sorbie *et al.,* 2004. To support this initial modelling strategy, the formation of soaps in the laboratory using pH change experiments were studied using a range of sensitivities. Titration tests were used to simulate the phase behaviour of naphthenic acids across model oil-water interfacial systems. The results show that the equilibria model agree well with the experimental results. A sensitivity study showed that the dissociation constants (pK_a) of the naphthenic acids were the most important model variables and could affect predicted output final pH values. For indigenous naphthenic acids, which are mostly water-insoluble, alternative procedures for both pK_a and K_{ow} determination were also introduced which may help to explain the competing mechanisms of soap formation under field conditions.

7.1. Introduction.

The modelling of flow assurance deposits such as inorganic scales and asphaltenes allows reasonable predictions to be made in regards to possible operational problems which may be encountered during the life of a field. Modelling of asphaltene deposition is substantially advanced and can be carried out using predictions derived from polymer solution thermodynamics, colloidal stability and fractal aggregation theories (Mullins *et al.,* 2007). This information is used to predict the onset of asphaltene precipitation when a particular fluid approaches its bubble point (Idem and Ibrahim, 2002). Modelling of inorganic scales takes into consideration different mineral saturation ratios given particular water chemistry, hydrocarbon PVT information as well as reservoir details (Mackay, 2005).

Attempts to model the interactions of carboxylic acids and metal cations are not new. Langmuir and Schaefer (1937) presented a preliminary model to describe the adsorption of a stearic acid monolayer as a function of pH. Further modelling of fatty acids in aqueous brine systems was carried out by Stenius and Zilliacus (1971) to investigate soap aggregation. Somasundaran *et al.* (1984) modelled changes in interfacial tension to obtain a thermodynamic understanding of the formation of pre-micellar soap aggregates. Bloch and Yun (1990) modelled Langmuir monolayer structures to explain the forces between cations and carboxylic acids. Havre (2002) performed interesting modelling of naphthenic acids in solvent-brine systems. Basic thermodynamics could not explain differences in predicted and calculated values of bulk properties. The author explained that this was possibly due to micelle formation. Kuzmanovic *et al.* (2005) presented an interesting phase equilibria

model for the extraction of carboxylic acids from solvent systems using CO_2 which matched experimental data in pressure regimes as low as 5 bar. Nevertheless, models to predict the formation of soaps either in the laboratory or under field conditions are currently not available in the open literature. The objective of the work in the current chapter is to present the results of prediction experiments which were devised to study naphthenic acid phase behaviour, in laboratory conditions. It is hoped that as the information on the phase behaviour of naphthenic acids progresses, models may be developed which include pressure and temperature values closer to those found in oilfield operations, and possibly incorporated in PVT simulation suites.

7.2. Model description.

The modelling employed to describe the naphthenic acid phase behaviour across oil-water systems was based on an approach used by Havre (2002). The model was devised by Ken Sorbie and further details are available in Sorbie *et al.,* 2004. It attempts to describe the basic mechanism for soap formation presented in Chapter 2 (i.e. depressurisation and pH change) using simple thermodynamics.

When a naphthenic acid in an oil or organic phase is placed in contact with an aqueous phase, it may partition into the latter. This is a function of molecular weight of the acid, its chemical structure and also the associated water chemistry. The phenomena may be described by the partition coefficient, K_{ow}, which was presented in Equation 2.4.

It is difficult to be precise about the exact effects of a particular acid species on the overall K_{ow} in a multicomponent acid mixture. This is because of mutual solubility effects resulting from the different interactions between the acids themselves. Thus in the procedure used in this thesis, the concentrations of each single molecular species in both the aqueous phase and the oil phase at equilibrium were considered to have a constant ratio to each other. The implication of this assumption is that it entails no variation of the activity coefficient with temperature or pressure, i.e. ideal systems. Based on this assumption, aggregate forms of the naphthenic acid such as dimers or micelles are not considered. However, the presence of aggregation species can be minimised owing to the high acid concentrations used in the supporting experiments, which are above the critical micellar concentration (CMC), as reviewed in Section 6.1.1.4. Despite this, the total concentration of naphthenic acids in the oil phase (at both initial conditions and at equilibrium) should be understood as the sum of the concentrations all naphthenic acid species which also include the monomers, dimers and higher aggregate forms.

As shown in Chapter 2, when partitioned into a water phase (either in the bulk of this phase or at the oil-water interface), the naphthenic acids may dissociate and this may be described by the dissociation constant, K_a, presented in Equation 2.5.

Cratin (1994) pointed out the pitfalls in measuring the K_a value of naphthenic acid systems and this was also summarised in Chapter 2. Attempts to measure pK_a for model naphthenic acids and indigenous species will be presented further in this chapter.

It is reasonable to assume that the equation describing the ionic product of water (K_w) will also need to be included in any system where pH changes occur in naphthenic acid systems. This term is $1x10^{-14}$ at 25 °C.

Soaps may form at the interface between oil phases containing naphthenic acids and aqueous phases. These may be described by the solubility product, K_{SP} (Equation 2.6). For the examples used in this chapter, calcium soaps (formed from calcium ions, Ca^{2+}) will be used, however, the general approach may be equally applied to sodium soaps. It has been assumed that the naphthenic acid used in the experiments is mono-carboxylic; however the general methodology is also applicable for species with more than one carboxylic group.

The overall system for predicting naphthenic acid phase behaviour in oil-water systems, may be illustrated by Figure 7.1 which depicts an oil and a water phase placed in contact at an arbitrary initial condition (i) and at a final equilibrium state (f). It is assumed therefore that no phase dispersion occurs, i.e. both phases are well-separated and a clear interface exists. Other assumptions are that naphthenic acids are initially present only in the oil phase volume (V_o) and the cations in the water phase volume (V_w). Final conditions will include cations present in the water phase only and in any solid mass of soap formed (m_{sol}).

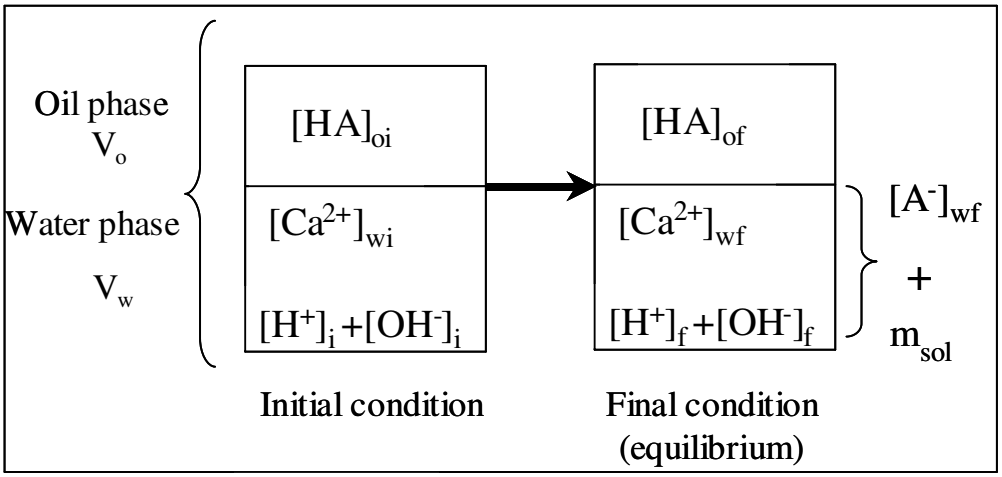

Figure 7.1. Illustration of oil-water-naphthenic acid system in two conditions: i) initial, f) final at equilibrium, with soap formation.

Conventional modelling says that in order for systems such as the one illustrated in Figure 7.1 to be mathematically solved, mass balances in addition to charge balances must be developed to account for the different species. For mass balances, naphthenic acids and calcium species (or the main cations present) must be considered.

The mass balances for the naphthenic acid species in initial conditions and final conditions are:

$$\mathbf{m_{Ai} = [HA]_{oi} M_{HA} V_o}$$

Equation 7.1.

$$\mathbf{m_{Af} = [HA]_{of} M_{HA} V_o + [HA]_{wf} M_{HA} V_w + [A^-]_f M_A V_m + m_{sol}\left(\frac{2M_A}{M_{CaA_2}}\right)}$$

Equation 7.2.

where m_{Ai} and m_{Af} are the masses of naphthenate ions in the initial and final conditions, M_{HA} is the molecular weight of the naphthenic acid, M_A is the molecular weight of the naphthenate anion, and M_{CaA2} is the molecular weight of the naphthenate soap. The law of conservation of mass dictates that m_{Ai} is equal to m_{Af}. Similar equations may be established for the calcium species, and, owing to conservation of mass, the initial and final masses of calcium ions must also be equal (m_{Cai} and m_{Caf}). Equations 7.3 and 7.4 show the mass conservation equations for the calcium species.

$$\mathbf{m_{Cai} = [Ca^{2+}]_{wi} M_{Ca} V_w}$$

Equation 7.3.

$$\mathbf{m_{Caf} = [Ca^{2+}]_{wf} M_{Ca} V_w + m_{sol}\left(\frac{M_{Ca}}{M_{CaA2}}\right)}$$

Equation 7.4.

For the charge balance of the species present in the system in Figure 7.1, equations are required to describe the aqueous phase considering the active ions, which are the cation species for calcium naphthenate, as well as the products of the ionisation of water and naphthenic acid dissociation; these are represented by Equation 7.5 and 7.6.

$$C_i = (2[Ca^{2+}]_{wi} + [H^+]_i - [OH^-]_i)V_w$$

Equation 7.5.

$$C_f = (2[Ca^{2+}]_{wf} + [H^+]_f - [OH^-]_f - [A^-]_f)V_m$$

Equation 7.6.

where C_i and C_f represent the total charge of the system at initial and final conditions. Because of charge conservation, C_i and C_f are also equal.

During the modelling of systems such as those shown in Figure 7.1 it can be expected that certain variables describing the initial conditions will be known, such as: the initial concentration of naphthenic acid in the oil phase $[HA]_{oi}$, the initial concentration of calcium in the aqueous phase $[Ca^{+2}]_{wi}$ and pH. In controlled laboratory systems the phase volumes (V_o, V_w) as well as the molecular weight of the naphthenic acid and that of the expected soap (M_{HA} and M_{CaA2}) would be expected to be known. Thus, in the model systems studied in this thesis, there would be 7 unknown terms:

- the final concentration of calcium ions $[Ca^{2+}]_{wf}$,
- the final pH or $[H^+]_f$,
- the final concentration of hydroxyl ions $[OH^-]_f$,
- the final concentrations of naphthenic acids in the oil and water phases, $[HA]_{of}$ and $[HA]_{wf,}$
- the concentration of naphthenate anions $[A^-]_f$, and
- the mass of soap formed m_{sol}.

Seven equations namely, 2.4, 2.5, 2.6, 7.1, 7.2, 7.5 and 7.6 may be used to describe the system.

To corroborate this modelling strategy, a number of supporting experiments were designed (Section 7.3). Examples of the application of the model and a comparison with experimental data are presented later (Section 7.4).

7.3. Supporting experiments.

It was decided that two titration-type methods would be tested with the objective of gaining information on the partitioning and dissociation of naphthenic acids across model oil-aqueous systems. The ASTM potentiometric D664 method (Riazi, 2005) was used together with an alternative method developed specifically during this thesis. For the ASTM D664, a Metrohm solvotrode combined LL pH glass electrode was used. The titrations were made with 0.1 M potassium hydroxide (KOH) in 2-propanol. This procedure was applied to a

range of naphthenic acid species in toluene solutions (refer to Figure 5.4 for specific acid structures). A toluene phase was also used as a reference during the titrations. During the titrations, the mass of potassium hydroxide used was measured (mg KOH/g oil phase sample). This was converted to moles equivalent of naphthenic acids, and then compared to the original naphthenic acid concentration used in the titrations. Figure 7.2 presents the original concentration of naphthenic acid in the toluene solutions plotted as a function of the acid concentration calculated using the ASTM D664 procedure. Data is the result of duplicate analyses. The concentrations of naphthenic acids measured in the titrations would be expected to be the same as the initial concentrations used in the oil phases. The straight line in Figure 7.2 indicates where the data points for acid concentrations would be expected to be located. The data points not only fall outside this expected trend, but there is also no correlation between the original acid concentration and the concentration of naphthenic acid given by the ASTM D664 titrations. It was thought at first that the different trends could be due to equipment malfunction (i.e. pH glass electrode), yet this was found not to be the case. The reason for the data scatter was that even for the lowest concentrations of naphthenic acid used in the procedures, the total concentration would be above the limit of the ASTM D664 method which is roughly 8 mg KOH/g crude oil. The conclusion is that the ASTM D664 method could not be used for study of laboratory systems. Thus, alternative techniques were required to aid in model development and the study of the oil-water interfaces containing naphthenic acids.

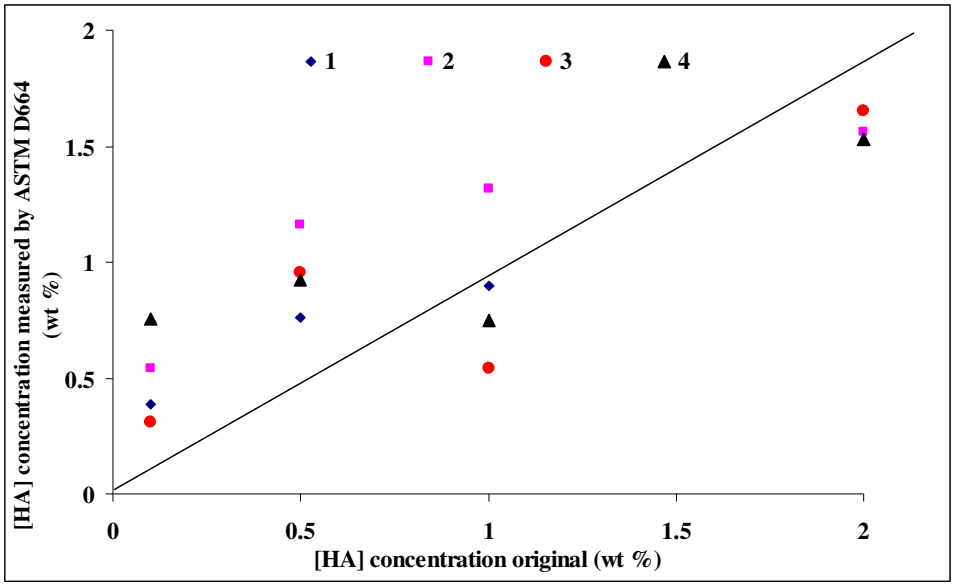

Figure 7.2. Concentration of naphthenic acid [HA] measured by ASTM D664 as a function of the original naphthenic acid [HA] concentration in toluene solution. Numbers refer to model naphthenic acids used: 1 stearic acid, 2 myristic acid, 3 4-tert-butylbenzoic acid, and 4 4-tert-butylcyclohexane carboxylic acid. Refer to Figure 5.4 for exact structures.

The ASTM procedure described above was therefore adapted to be used for higher acid concentrations. Titrations were thus carried out using KOH in a 1-propanol solution. Instead of titrating the naphthenic acid solutions in toluene directly, titrations were performed on water phases which were left in contact with toluene phases for a pre-determined equilibration period. One of the advantages of this procedure is that by titrating the water phase a distinction between dissociated and non-dissociated acid could be made. In order to gain insights into the sensitivities of this method described, the screening of a number of alkali concentrations from 0.1 to 0.0001 M was performed. The optimum concentration of 0.001 M was selected to enable a sufficient number of data points, and added in 0.5 ml volume aliquots.

The choice of aqueous phase used in the extraction of naphthenic acids from the toluene solutions was based on the pH observations described in Figures 6.7 to 6.9. Initially, distilled water was tested as the aqueous phase for naphthenic extraction, where low initial pH (between 5 and 6) was used to avoid soap formation. However, the results indicated that insufficient acid was being extracted. Results in Figure 6.7 to 6.9 also indicated that the presence of divalent cations in the aqueous phases results in more partitioning and dissociation of naphthenic acids across the oil-water interface. Thus an aqueous phase with dissolved cations was preferred over distilled water. This brine consisted of 25000 ppm sodium ions and 1000 ppm calcium ions, added as NaCl and $CaCl_2.6.H_2O$ respectively (Merck), leading to an original pH of around 6. Oil phases used in the titrations consisted of

solutions similar to those described in Section 5.3.1. Naphthenic acid concentrations ranging from 0.1 to 2 wt% in toluene were used. The oil phases (100 ml) were placed in contact with the aqueous brine phase (30 ml) with the aim to extract the largest amount of naphthenic acids. The initial pH was measured prior to addition of the toluene. After 24 hours the aqueous phase was separated into a clean beaker (by means of a separating funnel) and the pH was measured. This procedure was repeated by placing a fresh volume of the aqueous phase in contact with the original oil phase, depleted of naphthenic acids after each extraction. Both extracted aqueous phases (original and fresh volume) were then mixed. A titration using 0.001 M KOH in 1-propanol was carried out on the resulting aqueous phase until the original pH of the aqueous phase was reached (i.e. pH ~ 6), after which a further 3 volume additions (i.e. total of 1.5 ml) were added.

Sensitivity tests were also performed on the procedure described above. It was thought that a source of error could be the actual phase separation of the extracted aqueous phases after they had been in contact with the toluene. However, there were no significant differences between the measured volumes of the extracted aqueous phases during the different tests. The number of extractions for this procedure was optimised using the information presented in Figure 7.3, where it is observed that after the third extraction, the value of the final pH of the extracts is close to the original pH of the aqueous phase used.

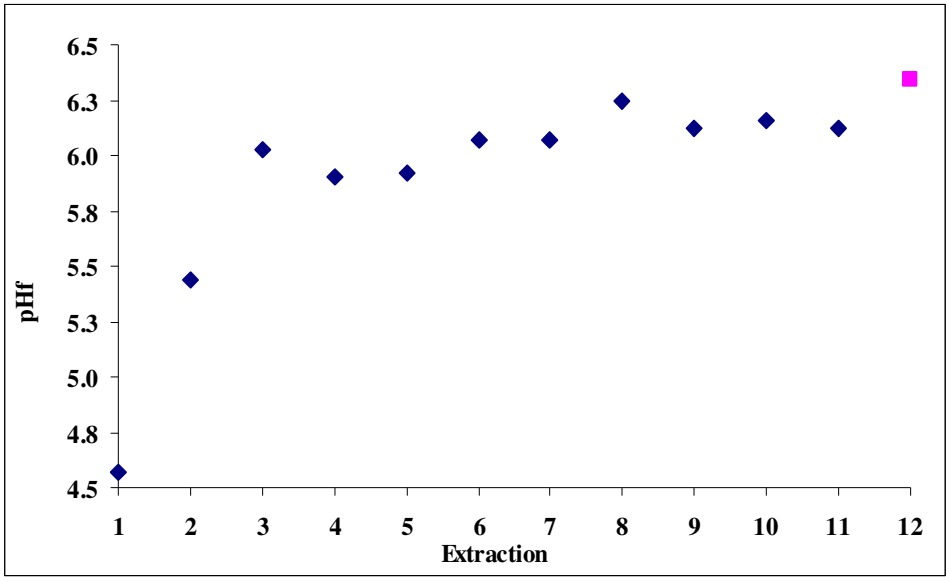

Figure 7.3. pH values for extracted brines used in titration procedures. Original aqueous phase pH prior to extraction indicated by the square (pH 6.3). Oil phase myristic acid 1 wt%, aqueous phase 25000 ppm sodium ions and 1000 ppm calcium ions.

A further sensitivity test was carried out to determine if there was a variation in the amount of naphthenic acid extracted from the oil phase into the aqueous phase as a function of time.

This was motivated by the results in Section 6.1.1.3, which showed longer phase contact times are needed to establish equilibrium. For this purpose, the pH of the extracted aqueous phases from individual titration tests were measured after phase contact times between 24 hours and up to 11 days. Figure 7.4 shows the results for an original aqueous phase pH of 6, prior to contact with the toluene phase with different acid concentrations. As expected, samples with lower naphthenic acid concentrations showed higher pH values over the same time interval. However, there is only a slight pH increase over time for each individual naphthenic acid concentration tested. These results indicate that a single pH measurement performed on a freshly extracted aqueous phase after 24 hours of phase contact was sufficient to validate titration data for these tests.

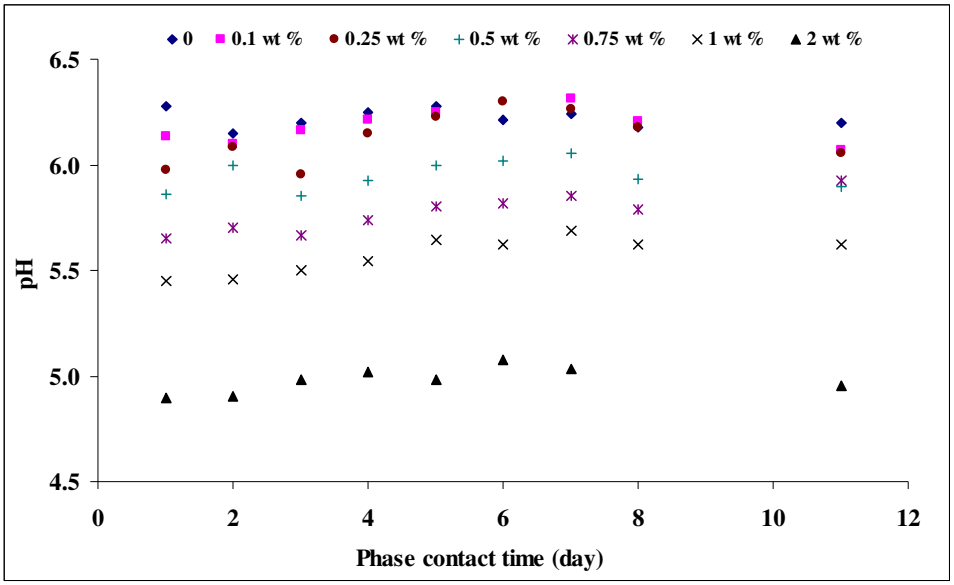

Figure 7.4. Measured pH values for different phase contact time (days) between oil and aqueous phases in extraction experiments. Oil phase myristic acid (concentrations from 0.1 to 2 wt%), aqueous phase 25000 ppm sodium ions and 1000 ppm calcium ions. Reference case (0) consisting of toluene with no added myristic acid.

The data obtained from the titration results, i.e. pH changes with known volume additions of KOH, was fitted with a third degree polynomial curve using Maple software (Heck, 2003). The point of inflection of this curve was used to calculate the mass of KOH consumed in the titration with the naphthenic acids. A minimum of three titrations was used for each test. Figure 7.5 shows an example of the measured pH used in the titrations of aqueous phases which were employed to extract acids from a 1 wt% myristic acid solution in toluene. Data for first and second extractions and the mixed aqueous phases (obtained by combining the two aqueous extracts) are used. The initial pH of the aqueous phase used was 6. It can be observed in Figure 7.5 that there is a decrease in pH with increase in acid

concentration. In addition, the first extraction pH values are the lowest in the experiments. Results from the reference test using a toluene sample with no acid, showed an increase in pH from 6 to 6.3, after the first extraction, and a decrease to 6.1 after the second extraction. The addition of the two extracts resulted in a final pH value of 6.3. This confirms the decrease in pH observed in the titration tests is the result of the presence of naphthenic acids partitioning from the oil phase into the brine and not due to the toluene solvent. The increase in pH with the presence of toluene might have occurred due to solvent contaminants.

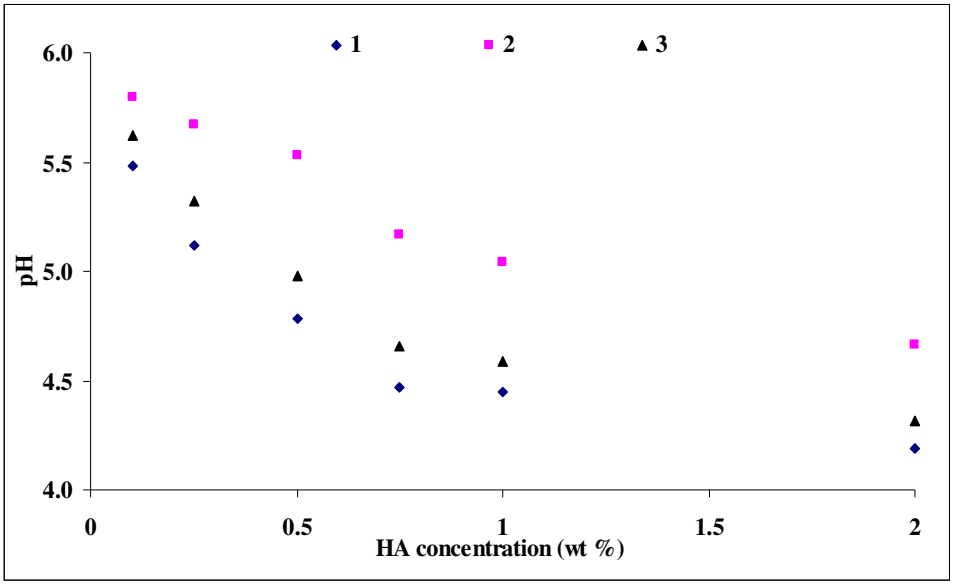

Figure 7.5. Final pH values measured for aqueous phase extracts as a function of naphthenic acid (HA) concentration used. Aqueous phase 25000 ppm sodium ions and 1000 ppm calcium ions. 1 refers to the first extract, 2 refers to the second extract and 3 refers to the mixed first and second extracts.

Figure 7.6 shows an example of naphthenic acid concentration determination (calibration curve) using the titration procedure described in this section. A linear correlation between the titration volumes and the predicted naphthenic acid concentration was observed. The modified titration example method described here was used in support of the analysis of the modelling strategy described in Sorbie *et al.,* 2004.

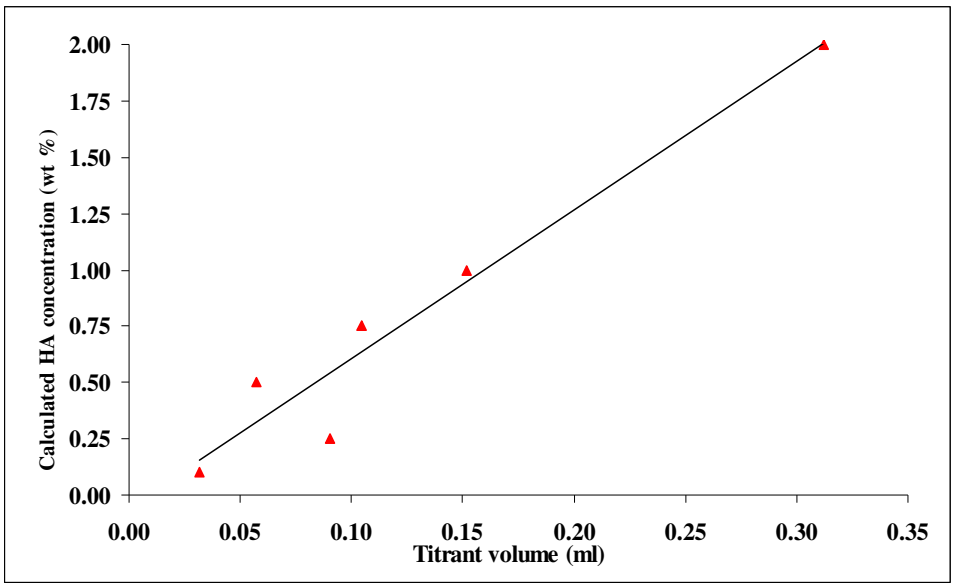

Figure 7.6. Example of calibration curve for naphthenic acid. Calculated HA concentrations based on titrant volumes of KOH in propanoic solution. Line represents bet fit for the experimental data points.

7.4. Preliminary model sensitivity analysis.

Because very little data can be found in the literature for naphthenic acids, it was of particular interest to examine whether any one physical term could affect the modelling of soap formation, based on the description in Section 7.2. In summary, the system comprises a simple oil phase consisting of toluene and acids, placed in contact with a pH adjusted aqueous phase. A sensitivity analysis was conducted on this basic model considering an oil phase with 1 wt% myristic acid and an aqueous phase consisting of 25000 ppm sodium ions and 1000 ppm calcium ions, initially adjusted to pH 6. The parameters investigated in this study were the partition coefficient of the naphthenic acid, K_{ow}, the dissociation constant, K_a, and the solubility parameter of the naphthenate soap K_{CaA2}. Figure 7.7 presents the selected results. Varying the values of the K_{ow} and K_{CaA2} parameters within the range 10^{-4} to 10^{-6} did not affect the predicted final concentration of naphthenic acid in either the oil phase, $[HA]_{of}$, or the water phase, $[HA]_{wf}$. However as Figure 7.7 also shows, increase in K_a for a given naphthenic acid, decreases the concentration of the acid in both the oil and water phases, $[HA]_{of}$ or $[HA]_{wf}$ respectively. More acid appears to be present in the oil phase than in the water phase as would be expected since most naphthenic acids are sparingly soluble in water.

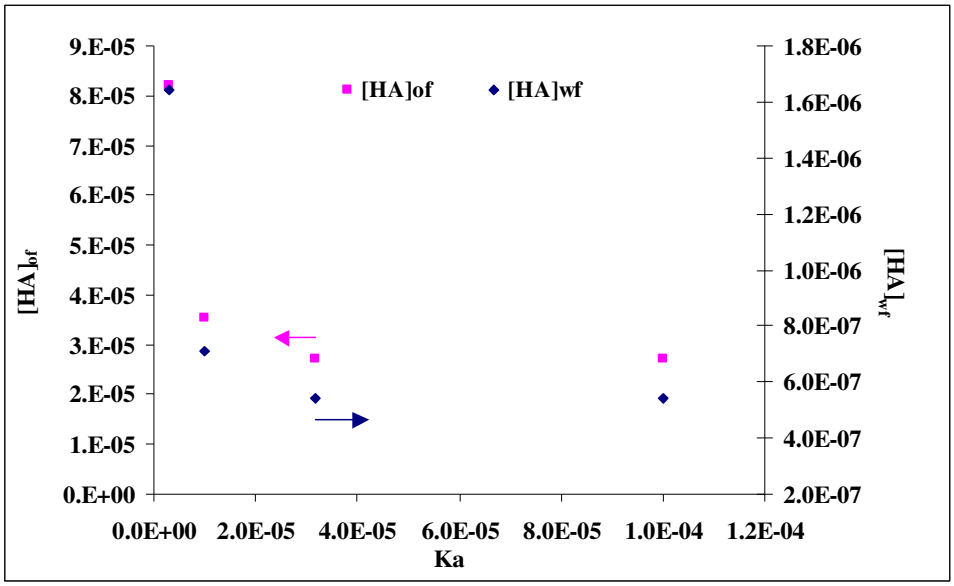

Figure 7.7. Effect of K_a on the concentration of the acid in the oil phase, $[HA]_{of}$, and the water phase, $[HA]_{wf}$.

By solving the seven equilibrium equations 2.4, 2.5, 2.6, 7.1, 7.2, 7.5 and 7.6 with values for parameters K_{ow}, K_a and K_{CaA2} (as in Table 7.1) the final pH (pH_f) and final hydrogen ion concentration, $[H^+]_f$, can be obtained. Results showed that variations in K_{ow} and K_{CaA2} did not affect the calculated pH_f and $[H^+]_f$ values. However, lowering K_a values resulted in a gradual decrease in $[H^+]_f$, which also resulted in pH values between 8 and 10 as displayed in Figure 7.8. The concentration of the dissociated acid species in the water phase, $[A^-]_f$, did not change when the three parameters K_{ow}, K_a and K_{CaA2} were varied. These results are summarized in Table 7.1. It appears that K_a is the only influential parameter for the prediction of soap precipitation and phase behaviour predictions using this model. This in turn stimulated further experimental tests to determine values for K_a for the different naphthenic acid species. These results are discussed in Section 7.5.

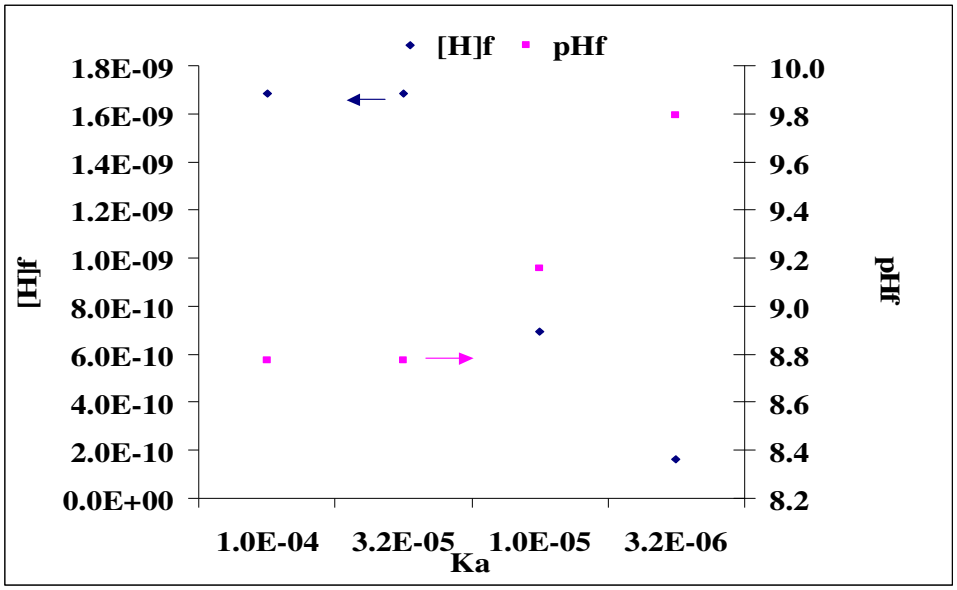

Figure 7.8. Effect of K_a on the pH_f, and $[H^+]_f$.

Variable Parameters	Calculated Parameters				
K_{ow}	$[HA]_{of}$	$[H^+]_f$	$[A^-]_f$	$[Ca^{2+}]_f$	m_{sol}
1.00E-04	2.71E-05	1.68E-09	3.22E-02	0.97	21.70
2.00E-04	2.71E-05	1.68E-09	3.22E-02	0.97	21.70
4.00E-04	2.71E-05	1.68E-09	3.22E-02	0.97	21.70
8.00E-04	2.71E-05	1.68E-09	3.22E-02	0.97	21.70
K_a					
1.00E-04	2.71E-05	1.68E-09	3.22E-02	0.97	21.70
3.16E-05	2.71E-05	1.68E-09	3.22E-02	0.97	21.70
1.00E-05	3.54E-05	6.95E-10	3.22E-02	0.97	21.69
3.16E-06	8.20E-05	1.61E-10	3.22E-02	0.97	21.68
K_{CaA2}					
3.16E-03	2.71E-05	1.68E-09	3.22E-02	0.97	21.70
3.16E-04	2.71E-05	1.68E-09	3.22E-02	0.97	21.70
1.00E-04	2.71E-05	1.68E-09	3.22E-02	0.97	21.70
1.00E-05	2.71E-05	1.68E-09	3.22E-02	0.97	21.70

Table 7.1. Results from sensitivity test using K_{ow}, K_a and K_{CaA2} at the specified values.

7.5. pK_a and K_{ow} determination.

In order to predict naphthenic acid oil-water equilibria, a number of variables are required as detailed in Section 7.3. The dissociation constant, pK_a, is amongst the most important terms which may influence the modelling of the systems as presented in Section 7.4. The pK_a for a particular naphthenic acid must be determined when the sample is dissolved in pure water, which is difficult because many naphthenic acids are only sparingly soluble in

water. Thus additional solvents must be used and their effects on the pK_a determination must be known.

There are a few methods for pK_a determination available in the open literature: the half-neutralisation method, the potentiometric method, Yesuda-Shedlovsky plots and the spectrometric-UV method, amongst others (Ege, 1994). The methods use distinct sample requirements and are applicable to various levels of naphthenic acid concentrations. In the half-neutralisation method, pH measurements are taken during the titration of an aqueous solution containing naphthenic acids. The pH at the midpoint of the titration (or the 0.5 wt% base equivalent) is equal to the pK_a. In other words, the pK_a corresponds to the pH at which the concentrations of ionised and unionised forms of naphthenic acids are equal. At a given temperature, the pK_a is therefore a thermodynamic ionisation constant (Earll, 2006). The half-neutralisation description is illustrated in Figure 7.9.

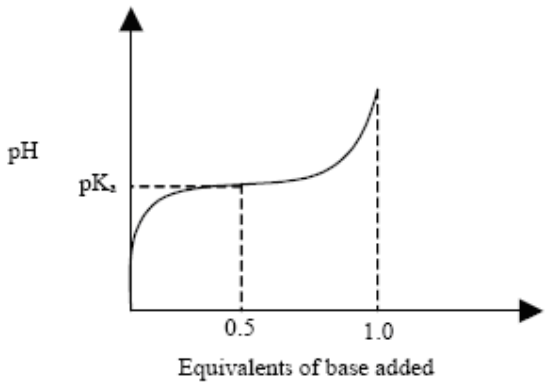

Figure 7.9. Half-neutralisation method of pK_a determination (Elvidge and Sammes, 1966).

The pK_a of water-insoluble compounds cannot be measured by the common half-neutralisation method. In addition, an inherent disadvantage of this technique is that low pK_a values (below 3), as well as overlapping pK_a cannot be determined. To improve this, proprietary pK_a methods use a back titration to determine the apparent pK_a in the presence of an alternative solvent (usually octanol). The technique can be performed on samples at concentrations of 0.0001 M or above (Sirius Analytical Instruments, 1993).

The pK_a of poorly water-soluble compounds may also be measured in mixed solvent solutions, such as water and methanol. Bjerrum difference plots are graphical methods originally used for the calculation of the stability constants of metal-ligand complexes (Sirius Analytical Instruments, 1993). The method consists of the plot of dissociable protons bound to the naphthenic acid versus pH. Equation 7.7 defines the Bjerrum plot, where n_H (number of dissociable protons) is a function of both pK_a and pH, independent of

any concentration other than protons. Equation 7.8 presents the Bjerrum plot expressed in experimental form.

$$\bar{n}_H = \frac{1}{1 + \frac{10^{-pK_a}}{10^{-pH}}} = \frac{1}{1 + 10^{pH - pK_a}}$$

Equation 7.7. Theoretical Bjerrum equation.

$$\bar{n}_H = 1 + \frac{A - C_b \upsilon - \left(10^{-pH} - 10^{-pK_w + pH}\right)\left(V_0 + \upsilon\right)}{L}$$

Equation 7.8. Experimental Bjerrum equation.

where A is the amount of excess of strong acid, C_b is the concentration of the base titrant, υ is the added base titrant volume, V_0 the initial volume and L is the concentration of the solute. The pK_a is determined by a comparison of the theoretical and experimental equations and n_H is obtained from the appropriate technique. In order to be able to use mixed solvents for pK_a determination, the Yasuda-Shedlovsky plots are employed, from which the apparent pK_as of naphthenic acids are calculated for various water/solvent mixtures. The pK_a is determined by extrapolating experimental values back to zero solvent volume. Thus the method consists of plots of apparent pK_a and log $[H_2O]$ against $100/\varepsilon$, where ε is the dielectric constant of the solution containing the compound of unknown pK_a. The method is valid for solutions with dielectric constants greater than 50 and can be performed on samples at concentrations of 0.0005 M or above.

The D-PAS probe (Sirius Analytical Instruments, 1994) enables spectrophotometric determinations of pK_a with lower sample concentrations, increased sensitivity and lower interference of electrodes when compared to other methods. The values obtained from this determination are measured ignoring activity effects and are therefore dependent on concentration. These are referred to as pK_{ac} (Earll, 2006). These terms may be related to the thermodynamic ionisation constants (pK_a) by:

$$K_a = K_{ac} \cdot \left(\frac{\lambda_A \lambda_H}{f_{HA}}\right)$$

Equation 7.9.

where f represent the fugacity and λ are activity coefficients.

Sorbie *et al.,* 2004, reported pK_a values for single model commercial naphthenic acids in water/methanol mixtures. The authors used Bjerrum and Yasuda-Shedlovsky plots. The pK_a values for these acids were found to be between 3.62 and 5.97. This is consistent with values reported in the literature (Morrison and Boyd, 1979). Nevertheless, the authors also reported that the selected method was not suitable for the determination of the pK_a of certain model naphthenic acids (e.g. oleic acid). Therefore, for the tests conducted in this thesis with indigenous naphthenic acids from field deposits, alternative procedures were devised. With this in mind, further tests were developed with the indigenous acid from Field Y soap scale sample, obtained as described in Procedure B (Section 3.1.2). Two techniques were tested to measure the pK_a of these indigenous acids: a pH-metric titration (potentiometric) and a UV method. For the potentiometric method a Sirius GlpKa titrator was used. It employs a proprietary Ag/AgCl double junction electrode for accurate pH measurement. For the UV method the same instrument was used with an added D-PAS probe. All reagents were flushed with argon gas prior to measurement and all titrations were performed at 25 °C with a 0.15 M KCl solution. The base titrant was 0.5 M KOH and the acid titrant was 0.5 M HCl.

A range of different titration-friendly co-solvents was used in attempts to dissolve the indigenous acid from the Field Y soap sample at sufficient concentrations (i.e. around 1 mM for the pH-metric assays and 50 μM for the D-PAS assays). The sample was initially titrated using the pH-metric technique with water in a triple titration, from high pH to low pH, over a range of pH 12.1 to 1.9 with a sample concentration of 1 mM. The acid was successfully dissolved at pH 12.1, but precipitation was observed in all assays at pH below 8. Confirmation of the indigenous acid insolubility in water was obtained by measuring the UV/Visible spectrum of the solution. An example of one of these titrations is shown in Figure 7.10, which is a 3D plot of pH *vs.* absorbance *vs.* wavelength. There is a general scattering of the absorbance over most of the pH range, and a sharp increase when the pH is below 8. The increase in absorbance at this value suggests that some precipitation is occurring. This is most likely owing to the formation of insoluble soaps.

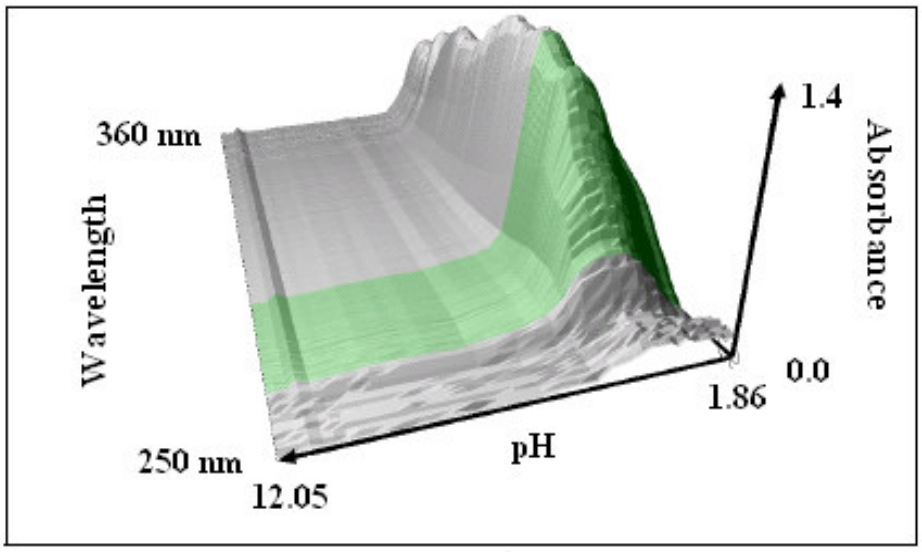

Figure 7.10. 3D plot of indigenous acid water titration procedure. Absorbance *vs.* wavelength *vs.* pH.

The precipitation and turbidity indicate certain components of the indigenous acid species are not fully soluble in the water. If this is ignored, two preliminary pK_a values (7.68 and 3.46) can be resolved from the data. The lower value is more in-line with naphthenic acid pK_a values reported in the literature (Morrison and Boyd, 1979). The titration plot is shown in Figure 7.11.

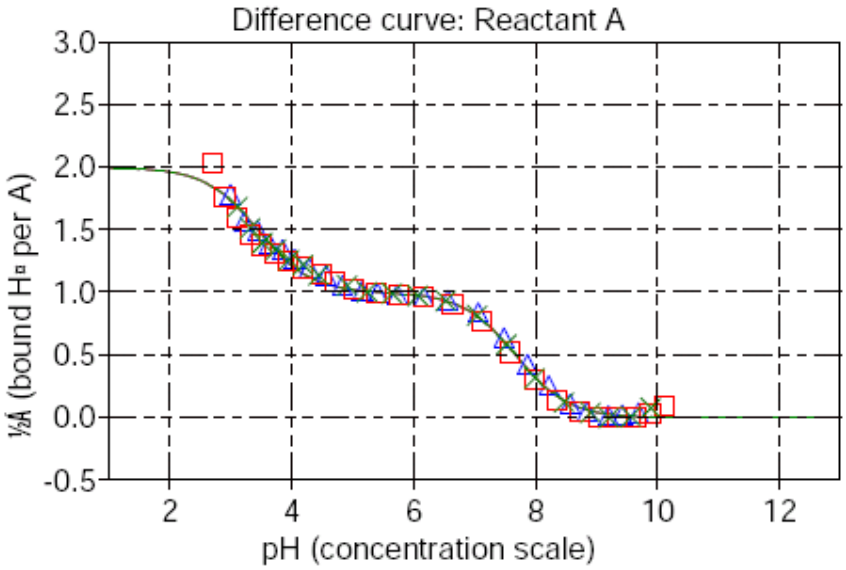

Figure 7.11. Titration plot for indigenous acids from Field Y soap scale in water (y-axis represents bound hydrogen atoms per naphthenic acid molecule). Points represent three separate titrations. Line represents fitted data.

In the second step of the titration procedures, the indigenous acids were titrated using a single solvent mixture until full dissolution (or no precipitation during titration) was obtained. This is a necessary step for accurate pKa determination. The indigenous acid

samples were titrated using the pH-metric technique in various methanol/water solutions (49.1 to 26.2 vol% methanol) in a triple titration, from pH 12.2 to pH 1.7, with sample concentrations in the range 1.0 to 0.7 mM. The indigenous acids were successfully dissolved at pH 12.2 in all cases, but precipitate was again observed at pH below 8 during the titrations. Thus, the indigenous acid samples were titrated again by the pH-metric technique in dimethylsulphoxide (DMSO)/water and dioxane/water mixtures but these were not successful either. Finally, the sample was titrated using the pH-metric technique in various tetrahydrofuran (THF)/water mixtures (56.3 to 32.3 vol% THF) in a triple titration, over the pH range 11 to 0.6 with sample concentrations between 0.60 and 0.42 mM. In the assays with lower THF concentrations, precipitation was observed below pH 8. In the assay with 56.3 vol% THF, no precipitation was observed, and two pK_as could be resolved at 7.84 and 4.42. Figure 7.12 presents the titration plots for the results for the 56.3 vol% THF experiment.

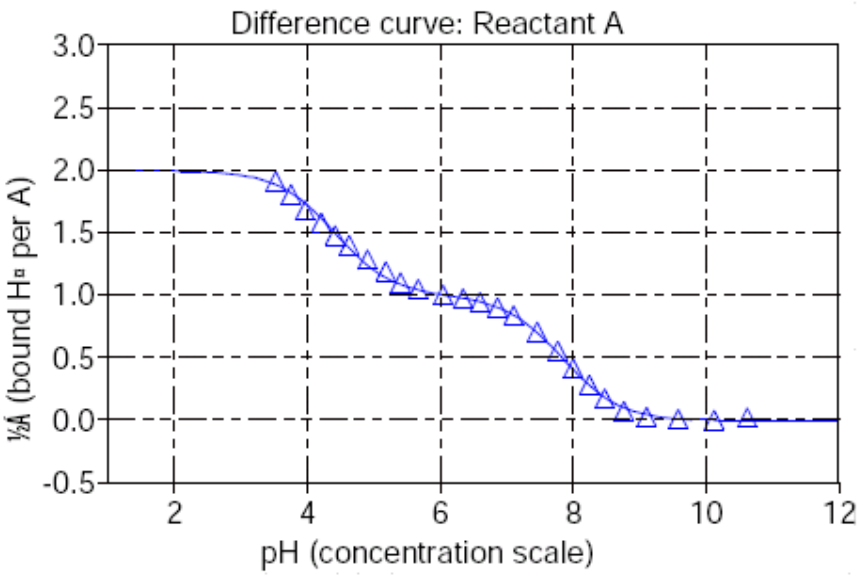

Figure 7.12. Titration plot for the indigenous naphthenic acids from Field Y soap sample in THF/water (56.3 vol% THF). The y-axis represents bound hydrogen atoms per naphthenic acid molecule. Line represents fitted data.

It is typical for acidic pK_a values to shift to higher pH values by 0.02 pH units for each percent of co-solvent added (Sirius Analytical Instruments, 1994). Applying this to the values obtained in the 56.3 vol% THF titration in Figure 7.12 would result in extrapolated aqueous pK_a values of 6.71 and 3.29 for the indigenous acids.

The indigenous acid samples were also titrated using the D-PAS spectroscopic technique under aqueous and co-solvent conditions in three triple titrations. Methanol (48.7 to 26.0 vol%) and THF (56.5 to 33.6 vol%) were used as co-solvents. A total pH range of 1.8 to

12.1 was investigated, with sample concentrations varying between 50.6 and 31.3 µM. Turbidity was observed in all assays at pH values less than 8, and no useful pK_a information could be resolved. Thus, only the pH-metric (potentiometric) method could be used to determine pK_a values for the indigenous acids tested in this procedure. Average values from the aqueous titration data and those extrapolated from the mixed aqueous/THF data indicate two pK_a values:

$$\mathbf{A^{2-} + H^{+} \Leftrightarrow HA^{-} = 7.20}$$
$$\mathbf{HA^{-} + H^{+} \Leftrightarrow H_2A = 3.37}$$

Equation 7.10. pK_a values for indigenous acids separated from Field Y soap sample.

It would appear that the indigenous acids from Field Y soap scale sample present two distinct pK_a values. This result is in sharp contrast to the work of Baugh *et al.* (2005a and 2005b), who carried out potentiometric titrations on Arn acid separated from a soap sample. The potentiometric curve for Arn was similar to a fatty acid with 14 carbon atoms and also showed that the acid strengths of the four carboxylic groups were similar. Thus one pK_a was found indicating an equivalence of the four carboxylic acid groups. The difference in pK_a values found in the present work can be explained in a number of ways. Firstly, it should be noted that this work used different indigenous acids to that of Baugh *et al.* (2005a and 2005b). The indigenous acids from Field Y used in this thesis were shown to contain 4 wt% Arn by mass spectrometry measurements (Table 4.4). In the work of the above-mentioned authors, Arn was the predominant species in the field soap deposit. Since Arn is thought to be a group of compounds it could be possible that the predominant species in the sample used in this thesis was not the same as that analysed by the previously mentioned authors. The LCMS results in Figure 6.55 appear to support this since it indicated more than one group of Arn acids present in the deposit used. In addition, if the carboxylic groups are quite close to each other in the Arn structure, it is possible that the ionisation of one would affect the other, causing the pK_a to shift to a different value. Lutnaes *et al.* (2006) suggested that carboxylic groups in an Arn species may be distant from each other, which would mean that pK_a values would be approximately the same. However these authors used derivatized acids species in their tests. It is more likely that the results presented in this thesis represent different species of Arn than those studied by the previous authors. In addition the indigenous acid species contain Arn and other mono-carboxylic naphthenic acids which might explain the presence of two pK_as.

The determination of K_{ow} was also carried out for the indigenous acids from Field Y. The techniques available for K_{ow} measurement include: potentiometric, ion pair LogP, filter

probe LogP (titrations) and HPLC LogP. Provided the LogP is high enough, it may be determined by titration by adding the sample to octanol followed by back partition into a prepared aqueous phase. If this fails then spectroscopic methods have to be employed since more dilute solutions have to be used. Note that these methods measure K_{ow} indirectly defined as:

$$\mathbf{LogP = Log10\ (K_{ow})}$$

Equation 7.11.

For the purpose of K_{ow} determination, the same GlpKa titrator and conditions mentioned earlier in this section were used. The best data obtained was that from the LogP titrations where the sample was titrated in the presence of octanol in a double titration. The apparent pK_a in octanol, poK_a is then measured. The logP is determined by quantifying the shift between the poK_a and the aqueous pK_a (in a procedure similar to a Bjerrum plot). The datasets were grouped together to calculate the logP for the neutral and ionic species using the average approximate pK_a values determined from the above procedure. The more lipophilic species lead to a bigger shift between the aqueous pK_a and the apparent pK_a in the presence of octanol. Figure 7.13 illustrates the Bjerrum plot for LogP determination

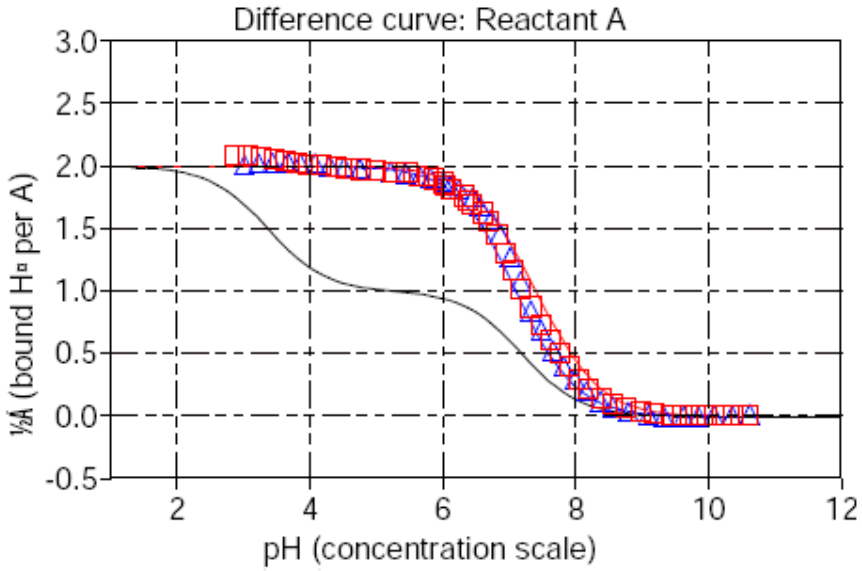

Figure 7.13. Bjerrum plot for indigenous naphthenic acids from Field Y soap scale sample. Data points represent aqueous octanol titration results. The y-axis represents bound hydrogen atoms per naphthenic acid molecule. The aqueous titrations data is represented by the solid black line.

In Figure 7.13, the ionisation of indigenous acids is illustrated. and the data points are from the aqueous octanol titration (0.25 ml of octanol in 10 ml of water). At low pH, the indigenous acids are neutral and the results suggest 2 bound hydrogens per acid molecule.

As the pH increases, the pK_a of the acid is reached and it becomes ionised, with one bound proton, and then with no bound protons after the higher pK_a has been reached. Thus, the data points range from 0 bound protons to 2 bound protons, confirming that the indigenous naphthenic acids do indeed have two pK_a values (refer to Equation 7.10). The pK_a of ionised naphthenic acid species with a -1 charge (HA^-) does not shift much in the presence of octanol (i.e. it does not shown enhanced partitioning), but the neutral H_2A shows a very large shift from the aqueous pK_a value, suggesting that it is highly lipophilic.

The logP result for the neutral species was calculated to be 5.28 mg/l (if pK_a values of 7.20 and 3.37 are used as the basis for the calculation from Equation 7.11). This seems a reasonable value, because the aqueous solubility of the acid is very low, but the solubility in octanol is better. The solubility of the ionic species (HA^-) is determined to be 1.48 mg/l. It should be noted that the logP values are dependent on the pK_a values used in the calculations, therefore any error in the pK_a values is carried directly through into the logP results. Thus, the following K_{ow} values are calculated from this procedure.

H_2A (neutral species) LogP = 5.28 $K_{ow} = 5.25 \times 10^{-6}$
HA^- (ionic species) LogP =1.48 $K_{ow} = 3.31 \times 10^{-2}$

Equation 7.12. K_{ow} values for indigenous acids separated from Field Y soap scale sample.

The significance of these results is twofold. Firstly, it suggests the indigenous acids in their dissociated (ionic) forms have a higher solubility in water than the undissociated acid. Thus the pK_a values for these acids would necessarily need to be reached before any partition into the water phase could occur. Secondly, the K_{ow} for the indigenous acids is quite close to that of acyclic acids such as myristic or stearic, which vary between 5.98 and 7.74, respectively (Morrison and Boyd, 1979). In Figure 6.38, it was shown that a quarter of the indigenous acid species were acyclic acids. This may explain the predominant K_{ow} values found in this section.

7.6. Model *vs.* supporting experiments development.

Sorbie *et al.,* 2004, contains further details of the application of the equilibria models to systems with and without soap precipitation under laboratory conditions. In summary, when no soap precipitation occurs, the five unknowns in this system are: $[H^+]_f$, $[OH^-]_f$, $[A^-]_{of}$, $[HA]_{of}$ and $[HA]_{wf}$ and these quantities must be calculated given the various input constants (K_{ow}, K_a and K_w) and known initial concentrations of the system ($[HA]_{oi}$, $[H^+]_i$

and $[OH^-]_i$). An example of pH trends generated with the equilibria model (when no precipitation of soaps occurred) is shown in Figure 7.14.

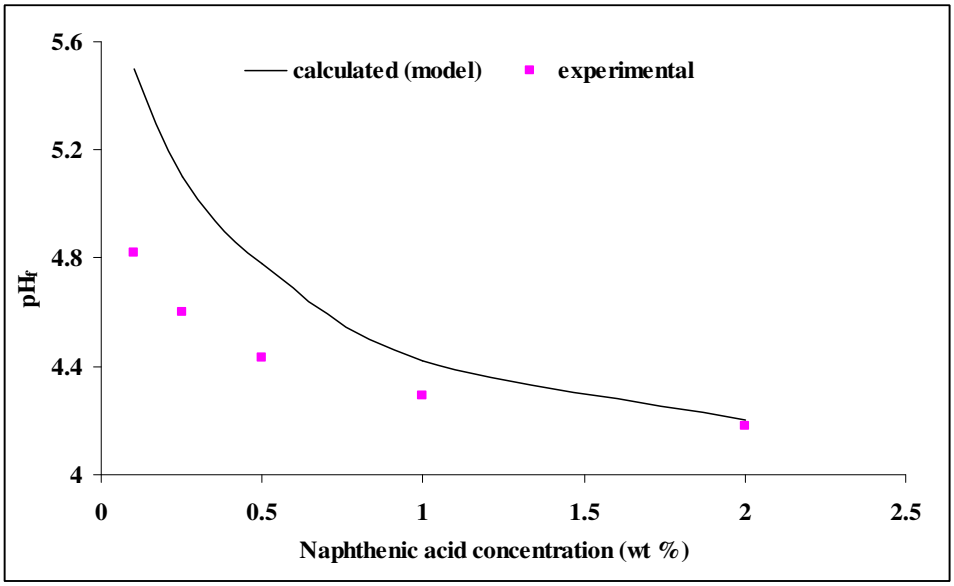

Figure 7.14. Final pH values [pH_f] plotted as a function of naphthenic acid concentration. Calculated (model) *vs*. experimental values.

From Figure 7.14 it can be observed there was a reasonable match of predicted and calculated pH_f, trends particularly at higher naphthenic acid concentrations. Yet at lower pH_f values, the model predicts values which are larger than the experimental error associated with pH measurements (± 0.1). The reader is referred to Sorbie *et al.,* 2004, for further details of model fine-tuning. For instance, an absorption isotherm was used to correct the pH_f trends shown in Figure 7.1.4. Nevertheless this approach needs to be extended to cases where soap formation occurs. In this thesis, the model described in Section 7.2 was also applied for cases where the formation of soaps did occur under laboratory conditions. A few adjustments were made to the basic experimental set-up described in Section 7.3 to support this modelling case. The results in Chapter 6 showed that higher adjusted pH values were necessary to induce soap formation with model solutions (Figure 6.6). Thus in the supporting extraction experiments for soap formation, pH_i was adjusted to 12. Any soap formed during the experiment was filtered prior to the separation of the aqueous and oil phases. These were weighed for comparison with calculated (model) results. A total of 20 bottle tests were carried out to account for the high volumes of oil phases, V_o (1 litre), used in the calculations. This was also necessary due to the low amounts of soap formed on a per bottle basis. The model equations for the case of soap precipitation are derived from the basic equations presented in Section 7.2. In this case

two equations may be obtained after algebraic manipulations, and these are the mass balance and charge balance equations:

$$\mathbf{m_A = \frac{1}{K_a}\left(\frac{M_{HA}V_O}{K_{OW}} + M_{HA}V_w\right)[H^+][A^-] + M_A V_w[A^-] + \frac{2M_A}{M_{Ca}}\left[m_{Ca\,A2} - \frac{K_{CaA2}M_{CaA2}V_w}{[A^-]^2}\right]}$$

Equation 7.13.

$$\mathbf{C_f = \frac{2K_{CaA2}}{[A^-]_f^{\,2}} + [H^+]_f - [A^-] - \frac{K_w}{[H^+]_f}}$$

Equation 7.14.

where M_{CaA2} is the molecular weight of the calcium soap. Note, only the final conditions in Equations 7.13 and 7.14 will be different to the case with no soap formation. For the purpose of illustration, the application of these equations will consider a laboratory calcium myristate soap with molecular weight of 496 Daltons. Though soap formation is both a surface and bulk phenomena, as discussed in Chapter 6, no absorption term is included in the model of soap precipitation. Absorption at the oil-water interface would only be owing to naphthenic acids in the un-ionised form which would assemble in a monolayer type arrangement (Brandal, 2005). The two variables used to predict soap formation in the laboratory are: $[H^+]_f$ and $[A^-]_i$. Similar to the case with no soap precipitation, the constants used were: K_{ow} (partition coefficient), K_w (ionic product of water), K_a (acid dissociation) and K_{CaA2} (solubility product of the calcium soap).

Figure 7.15 presents the results of a soap precipitation simulation and supporting experimental data. For this example the variation in calcium ions in the aqueous phase, $[Ca^{+2}]_i$, was studied and the final outputs analysed were pH_f and mass of calcium soap (m_{CaA2}). From Figure 7.15 it can be seen that the variation of calcium ions has a significant effect on the mass of soap produced, yet there is no variation in terms of pH_f. These trends may be explained by considering the relative proportions of acid and cations available for soap formation. Concentrations of calcium ions below 3 mol/l mean that these are the limiting reagents in the soap formation reaction; hence the gradual increase in mass values. Final pH, on the other hand, reflects the state of ionisation of naphthenic acids in the bulk aqueous phase and/or the oil-water interface. At very high initial pH (above the pK_a) all of the naphthenic acid would be ionised. Because of soap formation, the amount of free acid available would be restricted to amounts below the stochiometric naphthenic acid/cation ratios. The experimental pH is a very close match to the calculated data (model) shown in

Figure 7.15. Nevertheless, differences exist for the experimental and calculated (model) soap mass values. As discussed in Chapter 6, some soap particles are formed which have sizes below that of the filter paper used for soap separation, which could account for the mass differences. Note the varying soap mass trends are also different to what was presented in Table 7.1 and this is because of the larger value of K_{ow} used in the calculations.

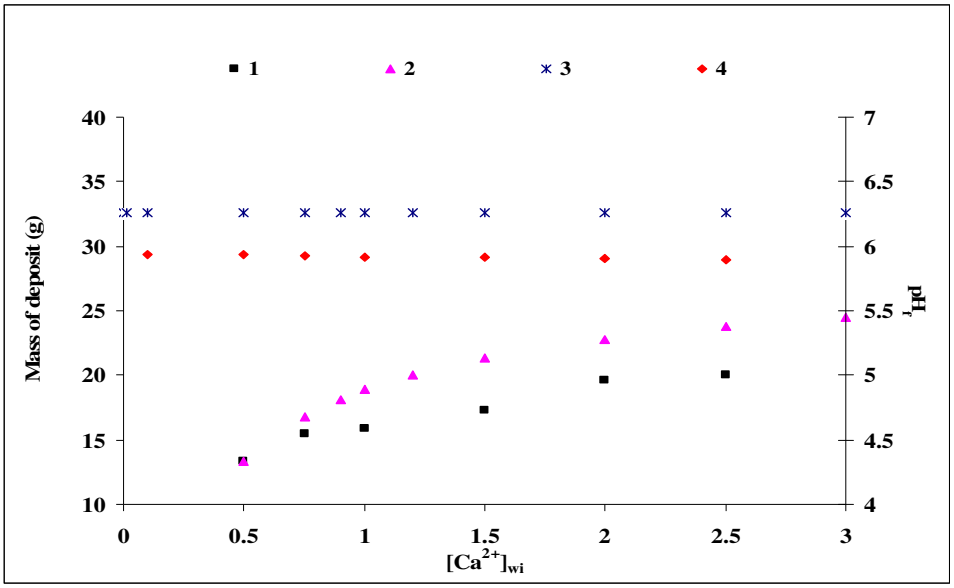

Figure 7.15. Effects of the variation of the initial concentration of calcium ions in the aqueous phase, $[Ca^{2+}]_{wi}$, on the final pH and on the mass of CaA_2 precipitate. 1 refers to experimental soap mass values, 2 refers to model soap mass values, 3 refers to experimental pH_f values, 4 refers to model pH_f values.

7.7. Conclusions.

In this chapter the combination of basic equilibrium thermodynamic modelling and supporting experiments has enabled a better understanding of oil-water interface systems in the presence of naphthenic acids. A preliminary model for the study of naphthenic acid behaviour was developed. The following terms were considered to be important for equilibria and balance equations: final pH, final concentrations of naphthenic acids in the oil and water phases, final concentration of cations, concentration of dissociated naphthenic acids and mass of soap formed.

A series of titrations were performed to enable the study of naphthenic acid equilibria. The main experimental strategy was the use of an equilibrated aqueous phase left in contact with an oil phase containing naphthenic acids. Titrations were carried out on these aqueous phases. This method allowed for analysis of systems where acid concentrations were above the limit of existing ASTM procedures.

The pK_a was shown to be the term with most impact on soap precipitation modelling. pK_a and K_{ow} determination for model naphthenic acids was shown to be possible using conventional techniques. Yet pK_a values for non-soluble species such as indigenous acids had to be determined by alternative methods. This is one of the major contributions of this chapter. Indigenous acids resulted in two distinct pK_a values which may suggest a combination of various different species present.

The supporting titration phase behaviour experiments in this chapter were shown to be a useful tool in matching modelling results for both non-precipitation as well as precipitation conditions. Results indicate that the formation of soaps occurs at constant pH and with increasing mass up to stochiometric ratios. In principle the model and supporting experiments could be used to test inhibitor performance, through the measurement of pH_f, and mass of soap formed. The application of the model to more realistic systems could be carried out using a naphthenic acid pseudo component (e.g. with defined molecular weight, pKa, etc) into a scale thermodynamic package (e.g. Multiscale). One of the main challenges would be the competing inorganic scale and naphthenate kinetics. Supporting experiments would therefore need to be conducted, preferably, with multiphase systems under the presence of CO_2. Such an approach would also allow for the testing of equation of state (EOS) modelling, given the existing information on naphthenic acid and solubility group discussed in Chapter 4.

CHAPTER 8 – ON THE ANALYSIS OF SOAP-FORMING SYSTEMS.

Abstract

In this chapter the results of data acquisition and analysis from a number of soap-forming fields are presented, in particular both crude oil and water properties. The main objective was to obtain correlations which would enable the prediction of both calcium naphthenates soap scales and sodium carboxylate soap emulsions based on only static measurements of parent fluids. A comprehensive suite of crude oil analysis, together with the understanding of mass spectrometric response to naphthenic acids (e.g. ionisation source effects, solvents and speciation) developed in previous chapters was employed. It was possible to observe some trends which relate geochemical parameters with bulk crude oil properties, as well as naphthenic acid speciation and water properties. Based on this information, an attempt to establish prediction guidelines for soaps is presented.

8.1. Introduction.

At the time of writing of this thesis, there were no commercially available tools for prediction of soap formation from fluid systems. Oilplus (Oilplus, 2006) advertised a method which is claimed to be applicable to the screening of crude oils only. Details of the method are not available in the open literature. Nevertheless, as discussed in Chapter 2, water properties are also strongly implicated in soap formation, since the precipitation mechanism is pH driven. One of the objectives of this thesis is to construct a simple prediction method which may be used as a guideline for soap formation from crude oil samples. Turner and Smith (2005) present preliminary assessments for specific field cases, but they do not support this with direct analysis of either crude oil or water samples to corroborate their conclusions. It was decided to proceed with an examination of crude oil as well as produced water properties with supporting field information. To obtain the most representative information, samples used in this work were from soap-forming fields in distinct geographical regions. These fluids were either obtained using drill stem tests (DST), or wellhead and topsides samples collected during the precipitation of soaps. Samples were used as received and thus no assessment could be made in regards to sampling conditions, which might have affected the overall fluid composition. In addition, no information was available with regard to reservoir parameters such as mineralogy, gas-to-oil ratios, compartmentalisation and stratigraphic levels. Thus, if the samples for analysis belonged to different reservoirs, the analysis in this thesis would not take this into consideration. No drilling mud samples were made available for analysis with the sample oils tested. Drilling mud components (in particular certain oil-based muds) may contain soaps and acyclic acids added as demulsifiers or defoamers which may interfere within crude oil characterisation techniques (Ogden, 1983). Nevertheless, it is estimated through direct communication with the sample providers, that drilling mud contamination in the

crude oil samples used in this thesis may be considered low. To aid in the interpretation of the results presented in this chapter, a crude oil and its associated water samples from a field in current production and known to be non-soap-forming (but from a geographical region known to be associated with soap formation) was also examined. This allowed for a verification of trends found for soap-forming samples.

8.2. Crude oil measurements.

The objectives of the analysis performed on the crude oil samples were twofold: to obtain basic crude oil properties and geochemical information, and to attempt to correlate this data with that of naphthenic acid speciation.

8.2.1. API gravity.

API gravity is related to relative density (specific gravity) at 60°F/15.56°C. This may be expressed as:

$$\mathbf{API}_{\mathbf{gravity}} = \frac{\mathbf{141.5}}{\mathbf{sp}_{\mathbf{gravity}} @ \mathbf{60}\boldsymbol{F}} - \mathbf{131.5}$$

Equation 8.1.

where $sp_{gravity}$ is the specific gravity measured at 60°F/15.56°C. API gravity has been shown to be correlated with the thermal maturity as well as biodegradation of crude oils (Jaffe and Gallardo, 1993). Barth *et al.* (2004) tested a few crude oil samples from similar sources and noted that certain biodegraded oils usually have high API gravity and higher viscosity when compared to non-biodegradable oils. This was suggested to be owing to the relative increase in heavy components as lighter components are removed (microbial activity), or owing to a production of heavier components by microbial biomass. API gravity data must be used with reservation since it is a function of many different parameters and processes (e.g. reservoir depth, sulphur content) and exceptions to these qualitative correlations occur (Peters and Moldowan, 1993).

API gravity can be measured using a variety of methods such as: ASTM D287, ASTM D1298, ASTM D5002, IP 160 and ISO 3675 (Riazi, 2005). Some of the most important parameters to influence the choice of technique are: sample volatility (determined by vapour pressures), temperature limitations and colour. If hydrometers are required for the measurement, meniscus corrections must be applied according to the density range expected (Lagendijk, 1998). In this thesis the ASTM D287 method, which uses a glass

hydrometer, was selected since it is one of the most accurate methods currently available for API gravity determination.

8.2.2. Total acid number and naphthenic acid concentration.

The total acid number (TAN) has been used for many years as an indication of acid properties of a crude oil. It is defined as the amount (in milligrams) of strong base (e.g. KOH) required to neutralise the acidity in one gram of hydrocarbon sample. The end point of this procedure is known as the total acid number (TAN) and is described mathematically as:

$$\mathbf{TAN} = \frac{\mathbf{base}_{\mathbf{volume}} * \mathbf{base}_{\mathbf{concentration}} * \mathbf{base}_{\mathbf{M.W}}}{\mathbf{crude\ oil\ sample\ weight}}$$

Equation 8.2.

where the $base_{concentration}$ is the molar concentration of the base and $base_{M.W}$ is the molecular weight of the base used. TAN measurements employ potentiometric or colourimetric procedures to indicate the endpoint of the titration. The two most commonly used ASTM procedures are D664 and D974, in addition to a micro-colourimetric method (IP 431). This last method is only used under special circumstances (e.g. small sample volumes). The ASTM methods are prone to experimental error, the most common of which is the incorrect identification of inflexion points, and often do not give the same results even with the same sample. Piehl (1988) showed that for samples of the same California crude oil, the potentiometric method gave acid numbers 30 to 80 % higher than the colourimetric method. This can be understood because the different TAN procedures are affected by the distinct acidic species in the oil, i.e. they are not selective to naphthenic acids alone. Dissolved hydrogen sulphide (H_2S), dissolved carbon dioxide (CO_2), hydrolysable salts (including calcium and magnesium chlorides), inorganic acids and many other contaminants, such as inhibitors or detergents, will affect the final measured TAN value (Meredith *et al.,* 2000). However, the precise effect of particular components on TAN is also most likely to be time and concentration dependent. For instance sulphur compounds like thiols rapidly oxidise in air and may lead to erroneous TAN results for crude oils (Barth *et al.,* 2004). If a particular crude oil has a predominance of naphthenic acid species, then TAN is a function of the number of carboxyl groups per naphthenic acid molecule, since it determines acid amount on a mole basis. Naphthenic acids obtained from crude oils in extractions (liquid-liquid, or solid phase as discussed in Chapter 2) are quantified on a weight basis and thus most

probably affected by the molecular weight of the acids present in the crude oil. Nevertheless, certain correlations between TAN and naphthenic acid concentration have been reported for selected crude oils (Figure 2.1). These correlations are better observed in high TAN crude oils. At low TAN the experimental error associated with the method (± 0.1) may be equal to or even larger than the TAN value itself (Meredith *et al.,* 2000). In this thesis, the total acid number (TAN) measurement was carried out on crude oil samples as a preliminary indication of degree of acidity. The ASTM D664 (potentiometric) technique was used, which is the most commonly used method for TAN determination, and 20 g of each crude oil sample was used for each analysis. For the titration procedures, a metrohm solvotrode combined LL pH glass electrode was used. The titrations were made with potassium hydroxide in 2-propanol with concentration 0.1 mol/litre.

A better quantification of naphthenic acids in crude oils can be carried out using more selective techniques, which target the carboxylic chemical family. These usually include a preliminary separation of naphthenic acids using either liquid-liquid or solid phase extraction techniques (detailed in Chapter 2), followed by Fourier-Transform infrared FTIR (detailed in Chapter 3) or gas chromatography (GC)/gas chromatography mass spectrometry (GCMS). In this thesis, naphthenic acid concentrations were measured using FTIR. Acid extraction from crude oils was carried out using liquid-liquid extractions as detailed in Brocart *et al.* (2005). Instrument details are similar to those described in Chapter 5.

8.2.3. Naphthenic acid speciation.

For the purpose of soap prediction, the identification of crude oil acidity has developed over the last couple of years from simple TAN measurements (Rousseau *et al.,* 2001), to acid speciation by mass spectrometry (Goldszal *et al.,* 2002) and to the identification of particular bad-actor species (Brocart *et al.,* 2005).

In this thesis, the analysis of the naphthenic acids in the soap-forming crude oils was carried out using a number of techniques. Firstly, electrospray mass spectrometry (ES) in the negative mode was used directly on the crude oils according to the settings obtained from the sensitivity study detailed in Table 4.3. A limited number of crude oils were also treated with QAE-Sephadex ion-exchange resin for the extraction of the naphthenic acids. It was hoped that this procedure would allow the identification of acids in low concentrations, in particular those implicated in soap deposition (i.e. Arn). The extraction was carried out as described by Mediaas *et al.* (2003). The basic principle of this technique is that the acids are selectively extracted onto the resin and recovered by back-extraction. Mediaas *et al.*

(2003) did not, however, present any data on the selectivity or yields of the resin in regards to the different naphthenic acids. The use of this method for very heavy, high TAN or very viscous oils, as well as very low TAN crude oils has also not been reported. Thus, the tests carried out in this thesis were also useful in gaining further information on the behaviour of the ion-exchange resin. The resin capacity used was 2.5 mmol acid equivalents per gram. The acid extracts obtained from this procedure were also analysed by ES, using the settings in Table 4.3.

The assignment of the mass-to-charge ratios (m/z) to naphthenic acid structures was carried out according to the procedures and equipment described in Section 3.2.1.2. All mass peaks in the negative mode were considered to arise due to naphthenic acids. In other words, the presence of other acidic species in the crude oil samples which are ionisable during mass spectrometry (e.g. phenols) was ignored. Arn acids were assigned the m/z range from 1220 to 1250 following the guidelines in Mediaas *et al.* (2005).

The third technique, which was applied to a limited number of soap-forming crude oil samples, was high-resolution Fourier-Transform ion cyclotron mass spectrometry (FTICRMS) in the negative mode. Sample preparation consisted of taking the crude oil (10 µl) and diluting into a methanol/water mixture (1 ml of a 50/50 vol/vol solution). The solution was shaken and allowed to stand prior to analysis. The methanol/water layer was used for analysis so any oil that separated out was not used. Aqueous ammonia solution (10 µl, 35 vol%) was added to the samples to aid deprotonation. The conditions for negative ion analysis were: cell trapping potentials PV1 -1.12 V and PV2 -1.12 V, detection and excitation mass range: 86 to 5000 Daltons, ions retained in hexapole ion trap of source for 0.6 seconds (D1), extraction pulse length (P2) 4000 µs. The sidekick mechanism was employed to detect ions off-axis as they enter the cell, thus preventing them "bouncing out again". The parameters for this were: EV1 7.94 V, EV2 0.72 V (where EV corresponds to the ICR cell delta extraction plates), DEV2 -1.12 V (ICR delta extraction plate 2). The duration of dipolar excitation pulse length (P3) 12 µs (this is a requirement to excite the ions to a detectable cyclotron orbit prior to detection), RF attenuation for excitation (PL3) 4.62. Note that no assignment of m/z data from the FTICRMS instrument was carried out, since the purpose of this analysis was to observe the presence of Arn species only.

Dyer *et al.* (2006) commented on the need for accurate crude oil sampling prior to the analysis of naphthenic acids for soap prediction. To avoid problems with non-representative aliquots, two sub-samples of each crude oil were analysed in this thesis in all mass spectrometry measurements.

8.2.4. Geochemical analysis.

Petroleum geochemistry can be defined as the study of naturally occurring hydrocarbons and the source rocks from which they are generated. These measurements entail identification of maturity, origin, thermal evolution and degree of biodegradation. Traditionally, geochemistry has involved the study of particular hydrocarbon fractions in crude oils, but not naphthenic acids. The correlation of naphthenic acids in crude oils with basic geochemistry parameters has been attempted by a few researchers (Fan, 1991; Nascimento *et al.,* 1999; Kim *et al.,* 2005), but only recently was this attempted for the purpose of soap prediction (Gallup *et al.,* 2007). Some of the most fundamental measurements for geochemical analysis include carbon isotopes and vitrinite reflectance (Peters and Moldowan, 1993). More advanced analysis includes biomarker identification.

The speciation of saturated and aromatic hydrocarbon, and other biomarkers in crude oil, is an important aspect of geochemical analysis. Many of these compounds can be analysed directly from whole crude oils. However, because of the trace concentrations of some species, separation of particular fractions prior to any analytical identification is sometimes necessary. De-asphaltation of the crude oil samples is also usually carried out, followed by thin layer or short column chromatography (Meredith *et al.,* 2000). Internal standards are then added if quantitative work is desired.

Gas chromatography (GC) and gas chromatography mass spectroscopy (GCMS) are well-established techniques in geochemistry for the study hydrocarbon fractions. GC finds wide applicability in geochemical analysis because it is sensitive to organic matter secondary processes such as biodegradation and thermal maturation (Peters and Moldowan, 1993).

The fundamentals of GC have been reviewed in Chapter 3, Section 3.7. Certain crude oil components may be resolved by GC alone, particularly for trace concentrations. In addition, n-paraffins and isoprenoids which may dominate the GC spectra are readily altered by secondary processes. In these cases, GCMS is preferred. In GCMS, the capillary column used for chromatographic separation is coupled to an ionisation source. Most GCMS instruments use electron impact ionisation sources. The limitations of this source for naphthenic acid identification have been presented in Chapter 4. Hence the source is better suited for the identification of hydrocarbons. A mass spectrum is obtained by holding a scan number (total number of number of scans per seconds) and by plotting mass-to-charge ratios (m/z) against detector response. The technique can be operated in different modes such as selected ion monitoring (SIM), full scan and parent mode. SIM is the most common method for biomarker analysis. Stearanes and terpanes can be easily monitored using their principal fragment ions at m/z values of 217 and 191, respectively. Some of the most

important parameters for GCMS operation include resolution, signal-to-noise ratio, ion sampling frequency, column bleed and overload. The identification of hydrocarbon compounds using GCMS uses the retention times in the GC column, the elution patterns, in addition to the mass spectrometry information.

Biomarkers may be described as molecular fossils and are useful for a number of reservoir studies, particularly if the source rock is not available. It is thought that organic compounds in a source rock can be transmitted to the oils. Despite their low abundance in crude oils when compared to other species, biomarkers are the most structurally defined compounds in petroleum (Peters and Moldowan, 1993). Typical applications in which biomarkers are used include: relative amount of oil-prone and gas-prone organic matter in the source kerogen, the age of the source rock, the environment of deposition (e.g. marine, lacustrine, fluvio-deltaic or hypersaline), lithology of the source rock (e.g. carbonate, shale) and thermal maturity of the source rock during generation (Peters and Moldowan, 1993). The basic structure of all biomarkers consists of the isoprene (methyl butadiene) skeleton. Compounds which contain the isoprene subunits include terpenoids and isoprenoids, for instance. Most biomarkers elute in the GC range between nC_{24} and nC_{36}, with the exception of pristane and phytane (acyclic isoprenoids), which elute earlier. For the purposes of correlating source rocks, depositional environments and crude oils, terpanes (e.g. C_{29} and C_{30}), hopanes and their ratios as well as the pristane/phytane ratio are used. An example of the identification of these compounds in a GC chromatogram of a whole crude oil is included in Figure 8.1.

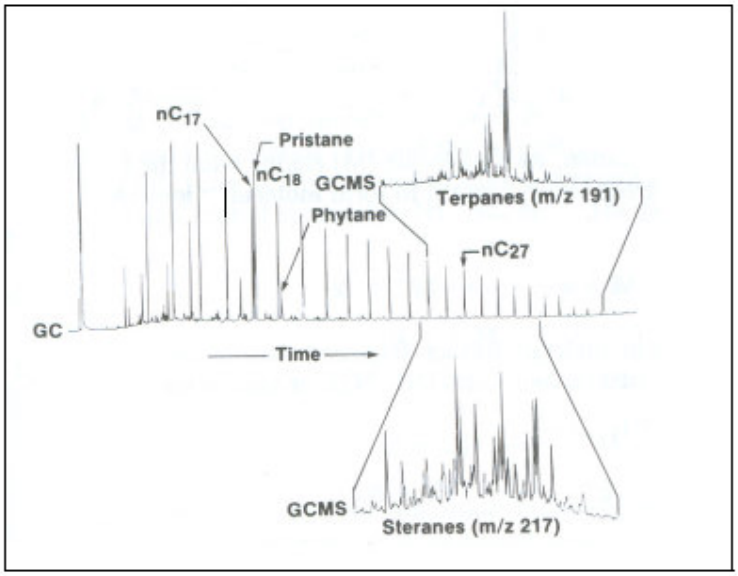

Figure 8.1. Identification of hydrocarbon biomarkers during GC analysis (Peters and Moldowan, 1993).

For the study of biodegradation there is an equally large range of biomarkers available. Meredith *et al.* (2000) used the pristane/nC_{17} ratio, but this is affected by other reservoir fractions, and it may be very difficult to measure in heavily degraded oils. Most of the oils tested by Meredith *et al.* (2000) were of marine origin. However the authors were able to show qualitative correlations between TAN, acid amounts and biodegradation. Biodegraded oils are associated with subsurface accumulations usually in shallow reservoirs at temperatures below 80 °C and low water salinity (Barnard and Bastow, 1991; Kim *et al.,* 2005). Nascimento *et al.* (1999) used the following ratios for accessing crude oil biodegradation: pristane/phytane, pristane/nC_{17} and phytane/nC_{18}. They were able to correlate these ratios with the presence of specific naphthenic acid families. Peters and Moldowan (1993) developed a scale for biodegradation in which level 1 represents undegraded oil (unaltered n-alkanes) and level 10 represents severely degraded oil. According to these authors the increase in resistance to biodegradation of biomarkers would be in the order: n-paraffins, isoprenoids, steranes, hopanes, diasteranes, aromatic steroids and porphyrins. Severely biodegraded petroleums cannot however be resolved by GC alone due to large amounts of unresolved organic matter, thus GCMS is also necessary.

In the elegant work by Kim *et al.* (2005) a series of crude oils were analysed with the purpose of establishing a correlation between biodegradation and naphthenic acid species identified by FTICRMS. The authors reported the use of a new biodegradation index, the acyclic/cyclic naphthenic acid ratio which was a reasonable match for the Peters and Moldowan (P&M) index. These trends were further supported by the work by Klein *et al.* (2006) who presented data on 16 crude oils which were suggested to have a low biodegradation index with high acyclic/cyclic ratios. Highly biodegraded crude oils on the other hand had low acyclic/cyclic ratios with an abundance of species with 2, 3 and 4 rings as well as double bonds.

Maturity of crude oils can be assessed with biomarker as well as non-biomarker parameters. Meredith *et al.* (2000), for instance, used C_{29} steroidal hydrocarbon information to study a range of acidic crude oils. The results of these authors showed that maturity did not vary with oils from the same region even with increasing TAN. One of the most common non-biomarker parameters used is n-paraffins. Less mature oils may show a bi-modal n-paraffin distribution (associated with higher plant waxes), as compared to more mature oils which may present uni-modal distributions (Peters and Moldowan, 1993).

GCMS was carried out in this thesis using a VG70VSE model with the electron impact source at an energy of 70 eV. The following settings were also used: trap current 200 μA, accelerating voltage 8 kV, source temperature 280 °C.

8.2.5. Solubility group analysis.

The classification of crude oils into solubility groups is a very well-established flow assurance procedure. Speciation of crude oil components into solubility fractions can be achieved using the Saturates, Aromatic, Resins and Asphaltenes (SARA) method (Riazi, 2005). The separation of these components from crude oil may be carried out using a variety of techniques such as liquid or thin plate chromatography. High performance liquid chromatography (HPLC) can also be used and has the advantages of being less time consuming, and less prone to sample losses (Sjoblom *et al.,* 2003; Hemmingsen *et al.,* 2005).

SARA methods are highly dependent on the exact nature of the solvent used and the time of contact with the crude oil sample, in particular, for asphaltene speciation. Other disadvantages include losses owing to evaporation during solvent removal, which are particularly noticeable in low density crude oils (Hemmingsen *et al.,* 2005). The classification of crude oils using SARA techniques has allowed for interesting correlations to be established; for instance, biodegradation usually increases the asphaltene content (relative to the saturated and aromatic hydrocarbon content). Miller *et al.* (1987) observed increases in asphaltene content from 2 to 21 wt% from a non-biodegraded to a heavily biodegraded tar sand. Many reports treat SARA data statistically for crude oil property prediction. Aske *et al.* (2001) have shown that the highest uncertainty of the results is in the saturate and aromatic fraction determination. Hurtevent (2004) attempted to use SARA information from soap-forming crude oils using multivariate analysis, but results did not indicate clear trends. Hemmingsen *et al.* (2005) used SARA information in order to study crude oil emulsion formation tendencies using multivariate analysis. It was decided in this thesis not to employ statistical methods for analysis given that insufficient data was available from soap-forming fields. It is estimated that the total number of soap-forming fields in the world is approximately 30 (Smith and Turner, 2004). Even if all the data from these fields were available in this thesis, the use of statistical tools (e.g. principle component analysis) would still be questionable because of over-parameterisation. Nevertheless, at the time of this work, there had been no reported publication on the correlation of SARA data with naphthenic acid information and other geochemical information.

In this thesis SARA was performed on the selected soap-forming crude oils. De-asphaltened samples were injected in isooctane for normal phase HPLC using an 8 μm silica column. Solvents used include isooctane, toluene and a dichloromethane/methanol mixture. Weight fractions were determined gravimetrically after the controlled evaporation

of solvent using nitrogen gas. GC settings for the saturate and aromatic fraction were similar to those described in Section 3.7 with the exception of the temperature programming, which was 70 °C for 3 minutes then to 320 °C at 5 °C/min, then a final hold for 20 minutes.

8.2.6. Wax content.

The separation of crude oil solubility classes using the SARA methods described earlier does not provide information on the wax content of crude oils. Waxes (paraffins) are crude oil components which are soluble at high temperatures, but which may crystallise when the oil is cooled during production. Wax crystals may result in non-Newtonian flow properties of the oil and represent one of the most important flow assurance issues, particularly for deep water prospects where gelling or restart after shut-in may be critical.

Crude oil waxes and naphthenic acids have been linked, in particular, during the formation of sodium carboxylate soap emulsions (Gallup *et al.,* 2004, reviewed in Chapter 2). Gallup *et al.* (2002) used GC to show that a dried sludge formed from soap emulsions contained a series of n-alkanes with predominant species having carbon numbers between 11 and 17. Gallup *et al.* (2005) presented studies on wax and soap deposits formed in a different field. This paper reported the wax deposition problem continued even after the soap emulsion problem had been resolved, which suggested that the primary flow assurance problem in this field was wax. This could mean that the soap emulsions formed in the process contribute to the emulsion stabilisation problem, but are not the main cause of the deposits. Li *et al.* (2004) suggested the possibility of soap occurrence as a justification for the formation of water-in-oil as well as oil-in-water emulsions during enhanced oil recovery. Interestingly, in their work the crude oil had very low TAN (0.18) and very high paraffin content (18.6 wt%). The authors also showed the presence of carboxylic acids and their salts in a separated aliphatic fraction of the crude oil. A definite correlation between wax content and naphthenic acids in soap formation is not at present available in the literature. Further attempts to correlate wax with API gravity and acidity were presented by Rousseau *et al.* (2001). The authors showed that for fields within the same geographical region, the wax content increased with the increasing API gravity and was inversely proportional to the TAN of the crude oil samples.

Wax content is an empirical value dependent upon the conditions under which it is separated. In addition, wax properties of oils are strongly dependent on the mechanical and thermal histories of the samples under study. Thus when preparing a sample for analysis, it is important that it is pre-heated to remove any solid wax already formed. The choice of

solvent is of critical importance in this procedure since non-removed asphaltenes may increase the amount of wax determined, for instance. In this thesis the UOP 46 method for wax determination was used. This is the most widely used method in the petroleum industry. In summary, the wax is determined in an asphalt-free crude oil in methylene chloride, during cooling.

8.2.7. Sulphur and metal content.

On a molecular basis, petroleum contains hydrocarbons, as well as organic compounds containing sulphur, nitrogen and oxygen. Metallic constituents may also be present, but only to a minor extent. Sulphur content is the primary heteroatom elemental measurement in crude oils. According to Speight (1991) sulphur levels in crude oils vary between 0.05 and 6 wt%. Most sulphur originates from early diagenetic reactions between deposited organic matter and aqueous sulphide species (Peters and Moldowan, 1993). The analysis of sulphur in crude oils can provide interesting information to oil producers, particularly in regards to corrosion tendencies. From a geochemical perspective, sulphur can also be used to classify crude oils in biodegradation studies. It has been suggested that sulphur is incorporated in crude oil during secondary processes (Meredith *et al.,* 2000). High sulphur content (higher than 1.3 wt%) is usually found in biodegraded crude oils. Sulphur may also be used as a secondary source indication. Marine and lacustrine environments usually have low or zero sulphur concentration (Hughey *et al.,* 2002).

Meredith *et al.* (2000) attempted to correlate sulphur content with other geochemical properties and acidity. A large range of sulphur content for crude oils was found, varying between 0.24 to 4.8 wt%. Meredith *et al.* (2000) could not find a clear relationship between sulphur levels and TAN, and suggested that sulphur could be related to particular source rock instead of acidity. Techniques employed to measure sulphur in crude oils include X-ray fluorescence (XRF), X-ray photoelectron microscopy (XPS) as well as inductively coupled plasma (ICP) (Laredo *et al.,* 2004; Yepez, 2005). Micro-colourometry may be used for concentrations between 1 and 100 ppm. The largest interferences in this method are from nitrogen and chlorine in concentrations above 1000 and 10000 ppm, respectively. Bromine and metal organic compounds may also interfere. XRF is the recommended method particularly if volatile sulphur is present in high concentrations. Wavelength dispersive XRF is used in the IP 407 method and is suitable for concentration ranges between 1000 and 20000 ppm. Energy dispersive XRF is used in the IP 336 method for concentrations varying between 100 and 50000 ppm, although samples containing heavy metal additives such as lead may interfere (Riazi, 2005). ICP may be the preferred method,

particularly if the analysis of the crude oil will also require components other than sulphur to be assessed. This may be carried out using the ASTM D4951 method. In the present thesis, it was decided that sulphur would be analysed in conjunction with other elements present in crude oil and therefore ICP was used.

Metal analysis, in particular iron, nickel and vanadium is quite a common practice in flow assurance studies, particularly to correlate asphaltene deposition (Idem and Ibrahim, 2002). Nickel and vanadium exist in crude oils largely owing to porphyrin complexes and they may be used to determine depositional environments as well as oil-rock interactions (Peters and Moldowan, 1993). Analysis of these elements is also required due to their tendency to poison downstream catalysts (Speight, 1991). Vanadium and nickel may be analysed with XRF using the IP 433 method for concentrations between 5 to 1000 ppm (vanadium) and 5 to 100 ppm (nickel). Barium at concentrations above 300 ppm may interfere with the analysis. For vanadium and nickel concentrations between 4000 and 40000 ppm, the IP 413 method is preferred. In this method the crude oil sample is ashed and the residue analysed with atomic absorption spectroscopy (AAS).

The direct comparison of metal content in crude oils must take into consideration the thermal maturity of the samples. This is because metal and sulphur content decrease with increasing maturity. There are numerous methods for analysis of metals in oilfield samples. Complexometric methods such as IP 339 may be used. However this has many disadvantages: alkali metals are not determined, in addition to poor reproducibility compared to other techniques. XRF methods include IP 407 (for the determination of lead in gasoline) and the IP 352 (for the determination of barium, calcium, phosphorus, sulphur and zinc). When analysing trace metals in hydrocarbons, one of the largest interferences occurs due to the presence of halogens. This is particularly observed in ICP with atomic absorption spectrometry (AAS) (Russel and James, 1997). Thus it is common practice to correct for halogens in these measurements. Chlorine in crude oil is measured using separate techniques which will be reviewed in Section 8.2.8. The use of crude oil metal content for the purpose of soap prediction has not been reported in the open literature. Determination of particular metal species (i.e. calcium) may be justified because it is believed that naphthenic acids may be complexed with metals in the crude oil prior to soap deposition. Results in Chapter 6, Section 6.5 suggested this is occurring both with commercial mode acids as well as indigenous naphthenic acids extracted from soap samples. It has also been reported that particular soap-forming crude oils contain very high concentrations of metals (Turner and Smith, 2005). These may represent an additional soap type (neither calcium naphthenate soap scale or sodium carboxylate soap emulsion) and are

hereafter referred to as bound soap scale. The operational problems associated with this type of soap behaviour include poor separation at topsides and off-spec samples. For the purpose of soap prediction, the analysis of divalent and monovalent metals in soap-forming crude oils might provide insight into the field deposition mechanism. In addition, nickel, vanadium and sulphur were also be analysed because of possible geochemical correlations. A full crude oil assay (21 elements) was carried out using ICP atomic emission spectroscopy (AES) using Perkin Elmer Optima 5X00DV in accordance to ASTM D4951 method. The test covers the determination of barium, boron, calcium, copper, magnesium, molybdenum, phosphorus and zinc. Sulphur can also be determined if the instrument operates with a wavelength of 180 nm.

8.2.8. Chlorine and water content.

In this thesis, it was thought that the water and chlorine content of crude oil would provide additional insights into the measurements of calcium and other metals presence in soap-forming samples. In other words, these analysis would enable the differentiation of, for instance, organic metal content as opposed to inorganic metal content. Different types of chlorides are found in crude oils and these are classified as inorganic, organic salts and chlorinated organic compounds. Inorganic chlorides are present mainly in the associated water and are usually removed with desalting. Organic chlorides are incorporated in crude oils as additives or production chemistry products. Chlorides are known to cause corrosion and catalyst poisoning in oilfield operations (Ye, 2000). The analytical measurements employed for chlorides in crude oils must take into consideration the exact species to be measured (e.g. inorganic *vs.* organic). Some of the methods that can be used to determine organic chlorides are reviewed in the next paragraph.

The ASTM D4929 method is used for concentrations above 1 ppm. This encompasses the distillation of a particular crude oil cut followed by the conversion of the organic chlorides to inorganic chlorides via chemical or combustion methods. The UOP 77992 method may be used for chloride concentrations from 1 to 1000 ppm. It entails sample combustion and automatic titration by colourimetry. The IP AK/81 method uses micro-colourimetric detection for organic chloride measurement. It works by converting organic chloride to hydrochloric acid. The total chloride content in petroleum may be analysed using XRF methods, such as ASTM D6443, using hardware described in Section 3.4.2. The use of XRF for liquids has the advantage that the technique requires little sample preparation. However one of the most important sources of error is the interference caused by matrix effects, which can lead to errors as high as 15 %, and can be minimised by the use of

alumina matrices (Russell and James, 1997). The analysis of liquids by XRF presents a number of additional challenges such as evaporation, stratification and precipitation effects. Samples should be mixed thoroughly and preferably allowed to stabilise for a few days prior to analysis. Potentially volatile samples such as oils should be analysed one at a time, and the transfer times must be kept to a maximum of a few seconds. An alternative adopted by many instrument manufacturers is to place a cover cap over the lid of the sample cup, yet this may cause poor reproducibility due to liquid film bulging. Other alternatives are baffled cups or pierced lids. There are a few alternative sample preparation methods which may be used when there is a risk of poor reproducibility as a result of sample volatility. Thin films are made by depositing the sample on a support, with or without drying. However, this procedure must be carried out with care, since light ends and other volatiles may be lost.

In this thesis XRF analysis of soap-forming crude oils was performed using the IP 503 method with bismuth as an internal standard. Matrix effects were corrected mathematically. The method is for the analysis of total chlorides (and bromides) in petroleum products with a guaranteed accuracy for concentrations between 5 to 1000 ppm. The largest contaminants for this method are lead ions. The equipment used for this procedure was a Philips PW2400 WDXRF instrument with a 3 kW rhodium source.

Crude oils usually contain water either in emulsified form or dispersed, and the knowledge of this is important in refining, purchase, sale and transportation of products. There are a number of methods which can be used for water determination in crude oils, including ASTM D4006 and ASTM D4377. The determination of water content using the distillation method is covered by ASTM D4006 (Riazi, 2005) for contents up to 1 vol%. The method uses a co-solvent to separate water from oil. An inherent disadvantage of the technique is the fact that large volumes of samples may be required. The Karl Fischer method for determining water content relies on the reaction of water with iodine (generated by colourimetry). This is carried out between two platinum electrodes using an iodide reagent in the presence of sulphur dioxide and a suitable base buffer. Water concentrations between 0.02 to 5 wt% can be measured with this approach. Sulphur interferences, particularly mercaptans and ionic sulphides, may cause incorrect measurement. The ASTM method D4928 uses a colourimetric technique for the Karl Fisher determination of water content, but may also be carried out using potentiometric titration (ASTM D4377). In this thesis the determination of water content in the selected crude oil samples was carried out using ASTM D4928, with a Metrohm 774 sample processor and 831 Karl Fischer coulorimeter. Only free and extractable water were determined. For samples with moisture content up to

1 wt%, the instrument repeatability (standard deviation) is ± 0.01 %. The choice of technique was based on the limited crude oil sample volumes available for analysis.

8.3. Water properties.

The importance of oilfield water analysis was discussed in detail in Chapter 5, as well as the implication of precise water constituents on soap formation in Chapter 2. For the purpose of soap screening, the following water parameters from a series of soap-forming fields were assessed: pH, cations (sodium, calcium) and anions (bicarbonate). Sodium and calcium concentrations were selected since they are the most important cations present in the field soap samples (Table 4.9). Also, sodium is usually the most predominant cation in oilfield water samples. The determination of bicarbonate ions was carried out for two reasons: these ions are part of the controlling elements in pH of the soap-forming system; and they are believed to play a role in soap emulsion structures (Gallup *et al.,* 2004). pH measurements are critical for the agreed basic mechanism of soap deposition (Rousseau *et al.,* 2001). It is also suggested that volatile fatty acids (VFA) may play an important part in predicting soap emulsion systems (Turner and Smith, 2005; Gallup *et al.,* 2007). However, this information was not available for the fields studied in this thesis and thus it was decided to exclude these variables from the analysis of water properties. Note that the water analysis used in this thesis comprised of cations (analysed using ICP AES), anions (bicarbonates analysed using titration techniques detailed in Chapter 5), and onsite pH measurements (mostly separator samples). It is expected that the largest source of error in these measurements will be the onsite pH measurements, since these values are highly dependent on the evolved CO_2 gas which may have been lost prior to the actual measurement itself (i.e. during sampling). Figure 5.1 showed the variation of pH at surface with CO_2 content and provided an assessment of this effect. In order to verify the accuracy of the pH values, it would be necessary to perform a re-equilibration of each water and hydrocarbon sample phase at reservoir conditions. This would be followed by a flash calculation to ambient or separator conditions. To carry out this calculation, access to PVT and reservoir data would be necessary, and this was not available.

8.4. IFT measurements.

It has been suggested in the literature (review in Chapter 2) and shown in tests with indigenous acids obtained from field deposits (Chapter 6), that particular naphthenic acids (e.g. Arn) present some degree of surface activity. These conclusions were obtained from a range of techniques, e.g. Langmuir troughs and interfacial measurements (Brandal, 2005) in

parallel to the results presented in Chapter 6. The application of interfacial tension (IFT) to crude oils provides useful information for oil recovery projects, demulsification studies and mixing of streams. Arla *et al.* (2007) presented work which aimed to correlate the different solubility classes of crude oil which the tendency for emulsion formation. TAN, API and SARA information of the crude oils was used. Emulsions maps showed a strong dominance of O/W systems at pH greater than 9, separated by regions where W/O systems were observed (at low pH) and a small area at pH values close to pH 14 (an inversion point caused by excess sodium ions). Naphthenic acids were suggested to be the main amphiphiles responsible for the formation of stable O/W emulsions at high pH. The resin and asphaltenes fractions were said to be the main components in the stability of W/O components at low pH.

IFT measurement of the selected soap-forming crude oils has been included in the proposed soap screening methodology. An additional objective of these measurements was to correlate the surface activity of the field deposits (presented in Figure 4.53) with that of the parent crude oils. Thus, the selected soap-forming crude oil samples were used in Du Nouy ring experiments, with synthetic brines containing the exact sodium and calcium concentrations from the actual water samples from these fields. Bicarbonate concentration was kept at 72 ppm. Brines were pH adjusted and measurements were carried out at 25 °C and in the pH range from 2 to 10. Details of the apparatus are identical to those presented in Section 3.6.

8.5. Results.

Basic crude oil properties: API, TAN, naphthenic acid content.

There is no clear trend correlating TAN and API for the series of soap-forming crude oils evaluated in this thesis (Figure 8.2). Soap scale-forming crude oils tend to have lower API than soap emulsion-forming crude oils. Figure 8.2 also shows an example of bound soap scale-forming crude oil, which occupies a separate region: high TAN and very low API. This would however need to be confirmed with similar crude oils from other fields. Figure 8.2 also includes the data for a non-soap-forming crude oil. This data point is located in the region of soap-scaling crude oils. This suggests that soap emulsion-forming crude oils can be identified because they have higher API than the three other types of crude oil samples used. Bound soaps tend to have very high TAN, but similar API to soap scale-forming crude oils. There is, however, an intermediate range of API where soap emulsion and soap scale-forming samples behave in a similar way, so only the extremes of API (i.e. greater than 30 or less than 25) can be used with any confidence.

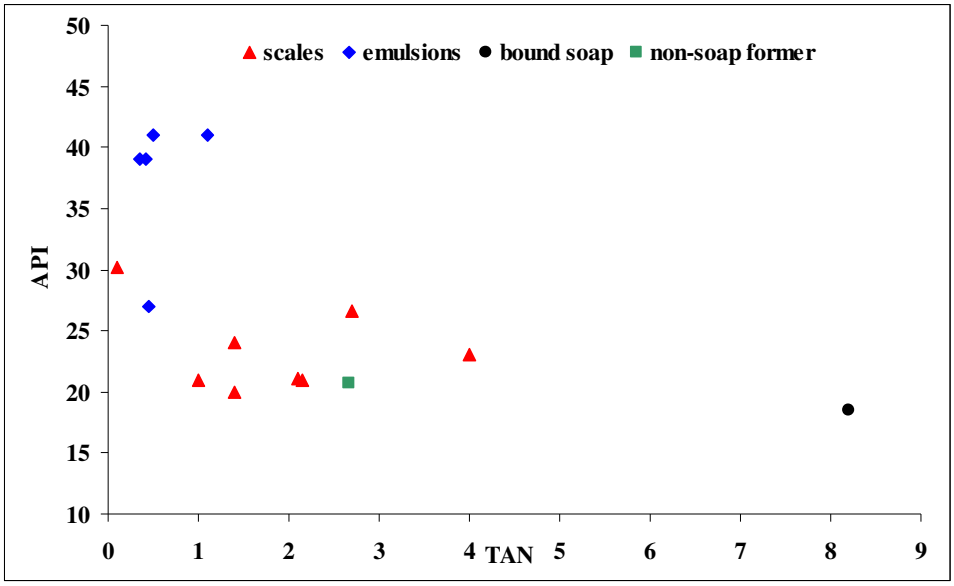

Figure 8.2. API as a function of TAN for selected crude oils. Scales refers to soap scale-forming crude oils, emulsions refers to soap emulsion-forming crude oils and bound soap refers to bound soap scale-forming crude oils.

Figure 8.3 presents the TAN values for the soap-forming crude oils plotted as a function of naphthenic acid concentration. No correlation can be observed between TAN and acid concentration in the soap-forming crude oils. This is probably a combination of the overall effect of bound acids in the crude oil, particularly in the high TAN samples. Yet in the low TAN crude oil samples this may also be a reflection of other acidic components which affect the TAN values (e.g. phenols). The naphthenic acids from the crude oils are measured as free ions, so there is a possibility that some might be combined with cations as salts, thus affecting the overall measurement. The bound soap scale-forming crude oil shows the largest concentration of naphthenic acid. This is probably due to large quantities of acid liberated from the cation-acid complexes during measurement.

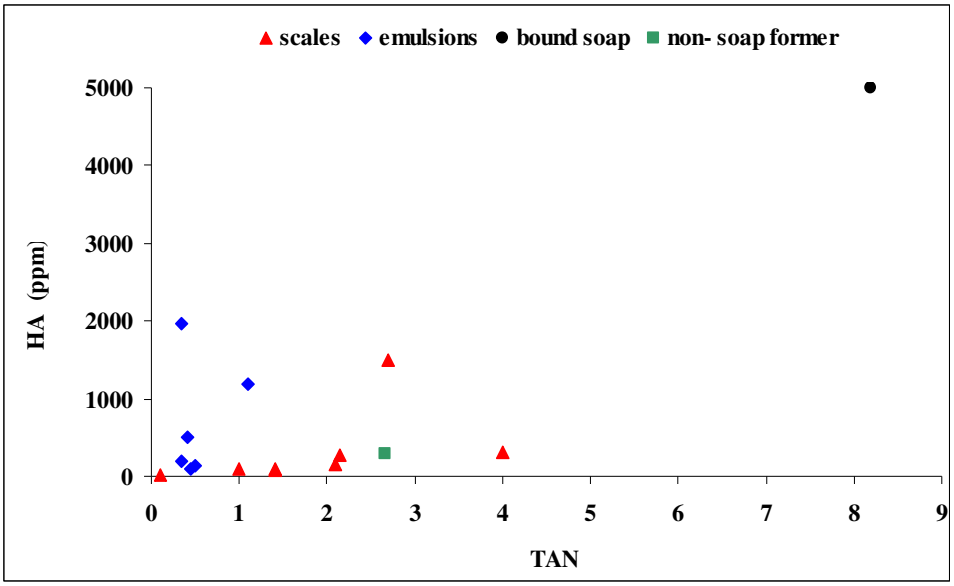

Figure 8.3. Naphthenic acid HA concentration (ppm) as a function of TAN for selected crude oils. Scales refers to soap scale-forming crude oils, emulsions refers to soap emulsion-forming crude oils and bound soap refers to bound soap scale-forming crude oils.

Naphthenic acid speciation.

Figures 8.4 to 8.7 present examples of the direct ES spectra (negative mode) on selected soap-forming crude oil samples. All spectra were recorded to m/z 1500. These samples were chosen because they represent examples from the major soap-forming crude oil types used in this thesis. All samples are soap-forming, yet their mass spectra show very clear distinct fingerprints. In mass spectrometry ionisation in the negative mode, not all m/z data can be assumed to be due to naphthenic acids. There are other acidic species in crude oils which do not contain the carboxylic acid functionality. Nevertheless, it has been assumed in this work that each peak in the spectra represents a naphthenic acid species. The overall ionisation of the sample is a function of the interaction between the solvent and the different naphthenic acids. Because the individual ionisation efficiencies of each naphthenic acid species are not known, mass spectrometry data should be regarded as qualitative only. Naphthenic acid species were assigned by using the m/z data with the guidelines of Clemente and Fedorak (2004), discussed in Section 3.2.1.2.

In Figure 8.4, which presents the results for crude oil from Field X, ions were detected which indicated the presence of the following species: acyclic acids, mono-cyclics and bi-cyclics. Naphthenic acid species are however detected in this sample up to 650 Daltons. The predominance of naphthenic acids with the formula described in Equation 1.1, would indicate an oil sample with certain degree of biodegradation (Kim *et al.,* 2005).

Figure 8.5 presents the results for crude oil from Field W, which has different trends to that of Field X. A larger distribution of acyclic species was detected compared to Field X. The proportion of mono-cyclics was also considerable with species ranging from C_8 to C_{32} and bi-cyclics from C_{10} to C_{34}. Based on the higher percentages of acyclics and the presence of higher carbon number species, this sample could represent a non-biodegraded oil. Other geochemical analysis would need to be carried out to support this conclusion.

In Figure 8.6, the results from crude oil from Field Z are presented. Very low levels of acyclic acids were evident and there was no major presence of mono-cyclic and bi-cyclics with carbon numbers below 50. In addition, species were detected in the range m/z 613 to 622 and from m/z 1230 to 1236 as well as m/z 1244. Observation of these ions is usually associated with the second and first ionisation of the Arn naphthenic acid species (Baugh *et al.,* 2004; Brocart *et al.,* 2005). This is highlighted in the expanded spectra in Figure 8.7. Based on the presence of substantial acyclic species in this sample, it is suggested that this represents a non-biodegraded crude oil sample.

The sample from Field Z was the only crude oil where the first ionisation of the Arn species at m/z 1230 was observed. Initially it was thought this could be owing to detection limits of the Arn species using conventional ES with a single quadrupole instrument. Results were shown in Section 6.4 which discussed tentative tests for the limit of detection of Arn acids with ES with a conventional low-resolution single quadrupole. It was determined that the Arn acid could be detected in samples using conventional ES at a concentration no lower than 80 ppm (Figure 6.37). From the results in Chapter 4 it was known that the detection of Arn species was also a function of the exact nature of the ionisation source and solvent used in MS (Figures 4.8 and 4.15). In order to optimise the usage of ES for the speciation of naphthenic acids from the soap-forming crude oils, the use of a selective ion-exchange resin (QAE-Sephadex) was justified. The primary objective was to verify if the lower concentrations of the Arn species could be observed after selective extraction. It was decided that the application of this resin to the crude oils could aid in the selective separation of the crude oil naphthenic acid content and help with the identification of the Arn species not seen using ES directly on the crude oils. In addition high-resolution FTICRMS was employed since it was claimed that the Arn family could be detected directly in crude oils using this technique in concentrations above 3 ppm, without prior separation (Mediaas *et al.,* 2005).

The results of the ES spectra of the naphthenic acids separated from crude oil from Field Y, with the ion-exchange resin are presented in Figure 8.8. To aid in the interpretation of the results, the spectra of the original parent crude oil is also presented. Two important

observations can be made in regards to the overall performance of the ion-exchange resin from Figure 8.8. From the results in this thesis it was observed that the resin extraction yields for naphthenic acid species is far from ideal. This is because many of the naphthenic acid species present in the parent crude oil were not observed in the naphthenic acid extract. This can possibly be attributed to irreversible losses of naphthenic acids during the extraction procedure. Borgund *et al.* (2007) have shown that the exact nature and distribution of acidic species separated from crude oils is a function of the extraction technique employed (liquid or solid phase). Secondly, it can be seen that no Arn naphthenic acid was recovered from the crude oil sample using the ion-exchange procedure. That many naphthenic acids have not been recovered is surprising and could be used to question the selectivity of the resin. This was the case for all the crude oils used in this thesis. The further absence of Arn acids in all of the QAE-Sephadex extracts as analysed by ES was also somewhat puzzling given many of the crude oils tested are known to be soap-forming. Mediaas *et al.,* (2005) have stated that presence of Arn in crude oil is a necessary requirement for calcium naphthenate soap scale formation. The results in Chapter 6 support this conclusion, given that a sticky polymer-like interfacial deposit was only observed when this acid was present in the oil phase during bottle tests. It would thus appear that the resin method is not be suitable for the accurate acid extraction of the soap-forming crude oils tested in this thesis, in particular those with higher TAN values. Nevertheless no optimisation of the ion-exchange method was carried out, such as an increase in resin capacity or contact time, since this falls outside of the original scope of the experimental work in this chapter.

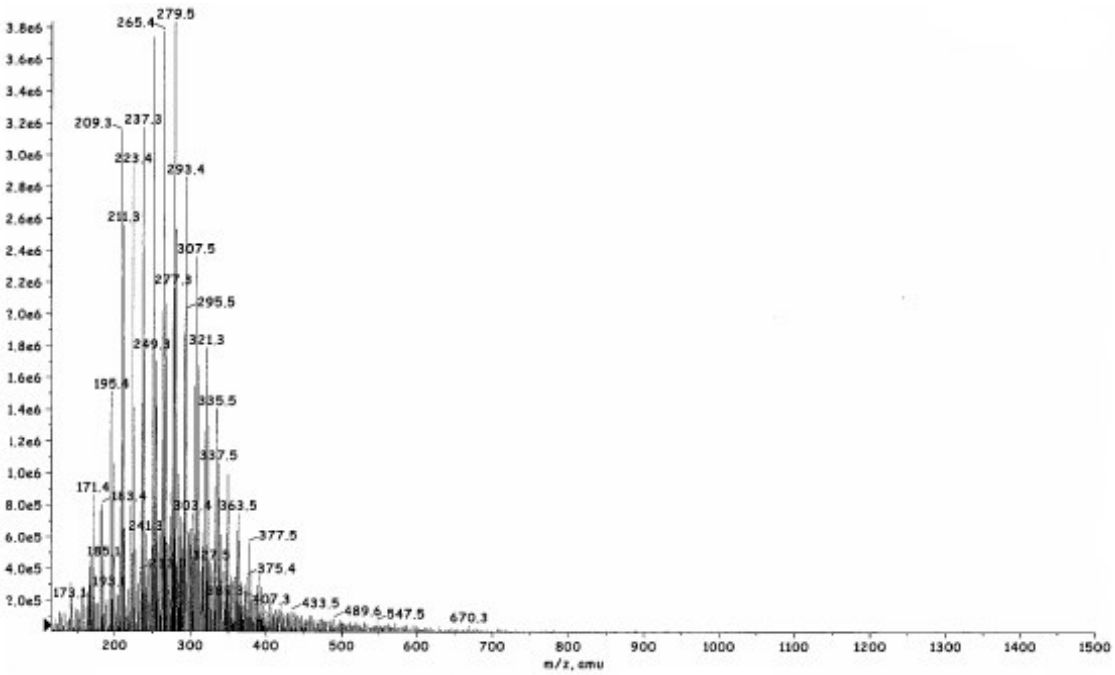

Figure 8.4. Direct negative mode ES of crude oil from Field X (soap scale-former).

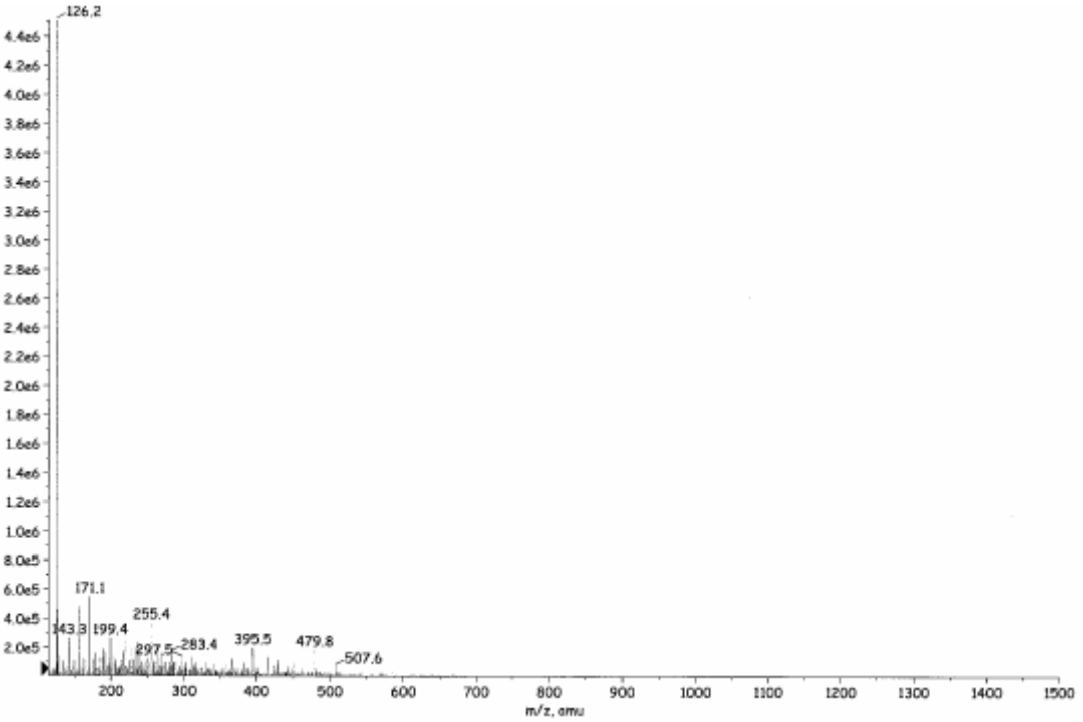

Figure 8.5. Direct negative mode ES of crude oil from Field W (soap emulsion-former).

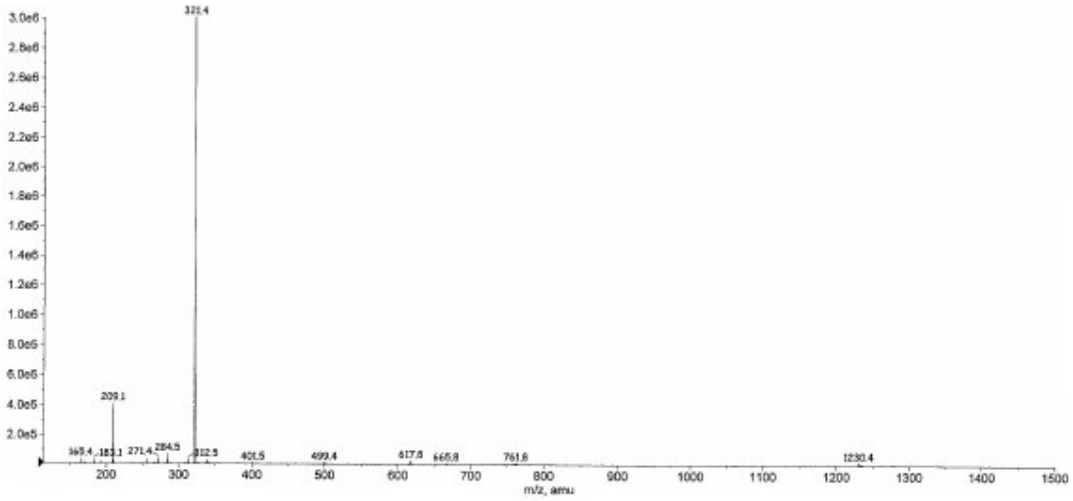

Figure 8.6. Direct negative mode ES of crude oil from Field Z (soap scale-former).

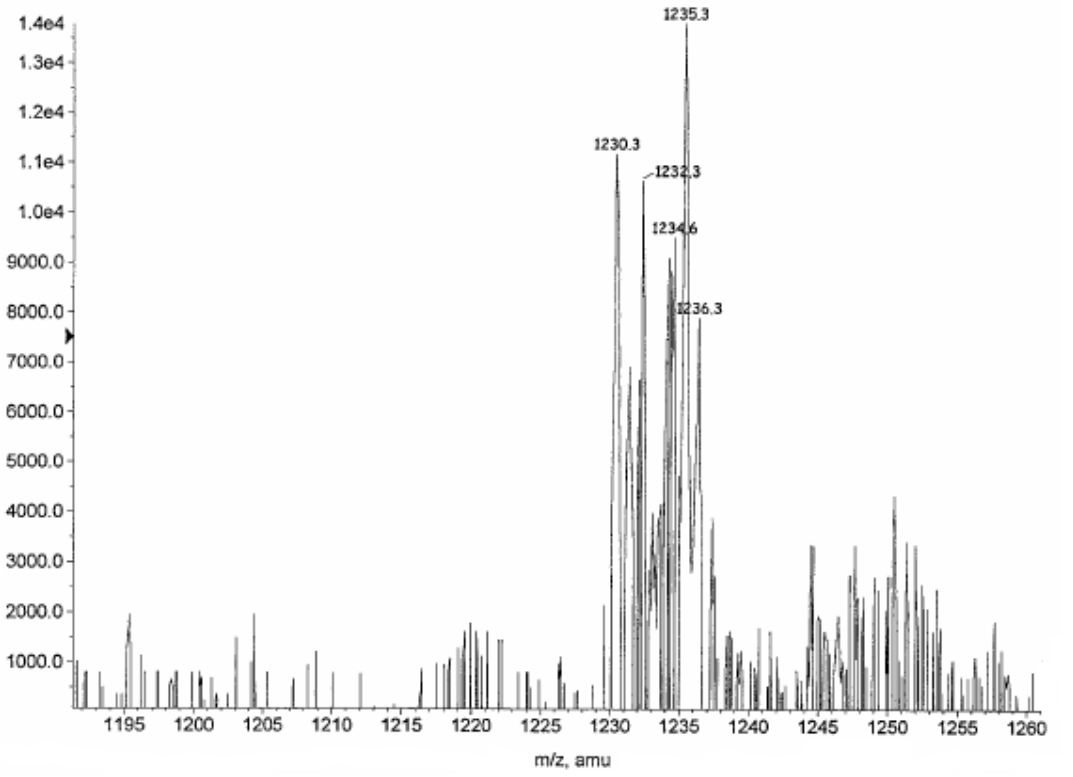

Figure 8.7. Expanded direct negative mode ES of crude oil from Field Z (soap scale-former).

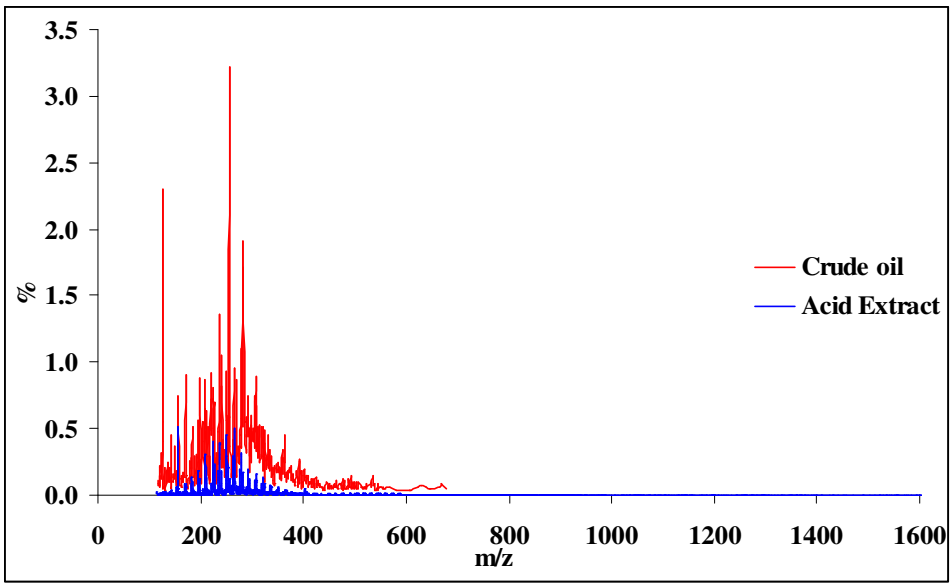

Figure 8.8. Negative mode ES spectra of naphthenic acids extracted from crude oil from Field Y using QAE-Sephadex. Comparison with direct negative mode ES of parent crude oil (soap scale-former).

No additional Arn species could be detected by ES in naphthenic acid extracts taken from the soap-forming crude oils. It was thought that the Arn acid could be in a concentration range below the limit of detection using single quadrupole ES for particular crude oils (detected to be around 80 ppm as per Section 6.4.1.2). Thus it was decided to use a high-resolution instrument (FTICRMS). Figure 8.9 shows a comparison of the high-resolution results with that obtained via conventional single quadrupole ES. The spectrum from the high-resolution is more intense than the low-resolution instrument, as expected, where at least two orders of magnitude higher are observed for the most intense naphthenic acid species. The spectra are however equivalent for m/z values of up to 550. For values above this, the FTICRMS shows a low distribution of species to about m/z 900. Rodgers *et al.* (2006) suggested this type of trend is a result of multimers which form due to lower molecular weight naphthenic acids in combination with ionisation effects. Yet, in the experiments conducted by the same authors, multimer formation could not be attributed to any particular naphthenic acid species. No Arn family was detected in the experiments in this thesis with the soap-forming crude oil even with the FTICRMS. This was also surprising, given that this technique is known have the highest resolution for the mass spectrometry of naphthenic acids.

In summary, the selective extraction of the naphthenic acids using QAE-Sephadex resin and the application of ES and high-resolution FTICRMS were unable to show evidence of Arn in all but two crude oil samples. This interesting result has suggested that these species in fact were no longer present in the crude oil samples. Because of the low concentration of

Arn acids in crude oil, it is very likely that during soap deposition in field conditions, these acids were selectively removed from the oil to during the formation of soap deposits. Figure 6.38 showed the indigenous acids from the same field as the crude oil analysed by the techniques in Figure 8.9 contained 4 wt% Arn. This would represent a very large depletion effect in the parent crude oil's Arn content.

For these reasons, it was decided not to include the Arn in the acid speciation for the purpose of soap prediction in this chapter. Brocart *et al.* (2005) have also shown data on crude oil samples where Arn was detected, but this did not result in a soap problem under field conditions. The authors did not mention possible mechanisms for this. Results presented in Chapter 4 and 6 support the idea of the competition of Arn and other acids for soap formation, in the field and laboratory condition. Yet when Arn was detected (Figure 8.6 and 8.7), the relative mass spectra signal of these acids was very low compared to the other naphthenic acid species.

Figure 8.10 presents an example of naphthenic acid speciation of a selected soap-forming crude oil used in this thesis. The acid species are presented according to the carbon numbers (n) and hydrogen deficiencies (Z), as per Equation 1.1. In Figure 8.10 it can be observed there is a range of naphthenic acid species in the crude oil, however with no predominance of Z groups or carbon numbers. The information in this graph was used to obtain a detailed speciation of naphthenic acid families for the soap-forming crude oils and this was used in additional screening.

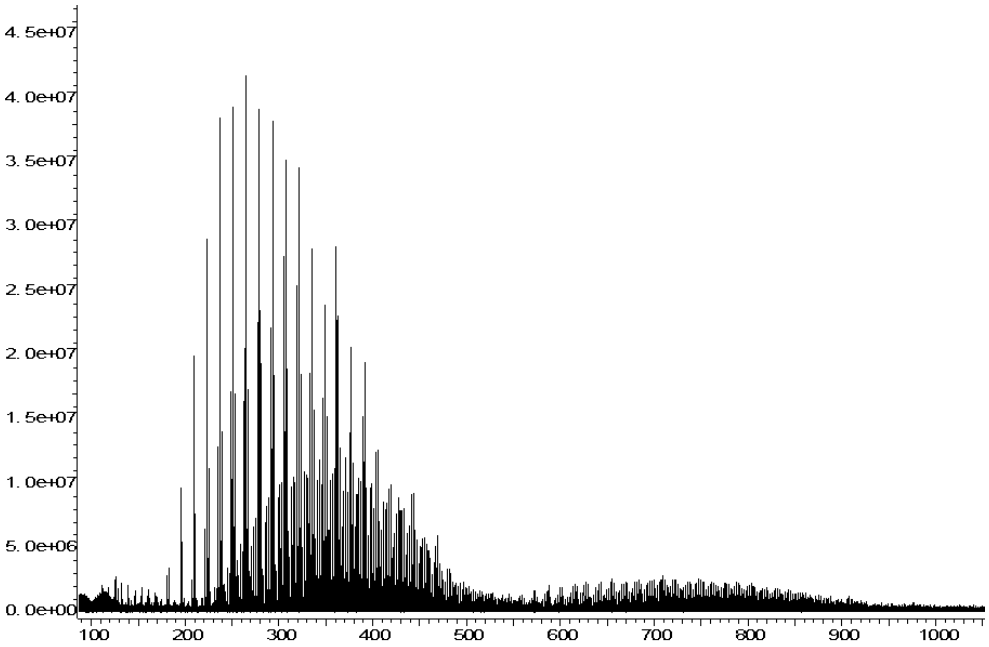

a)

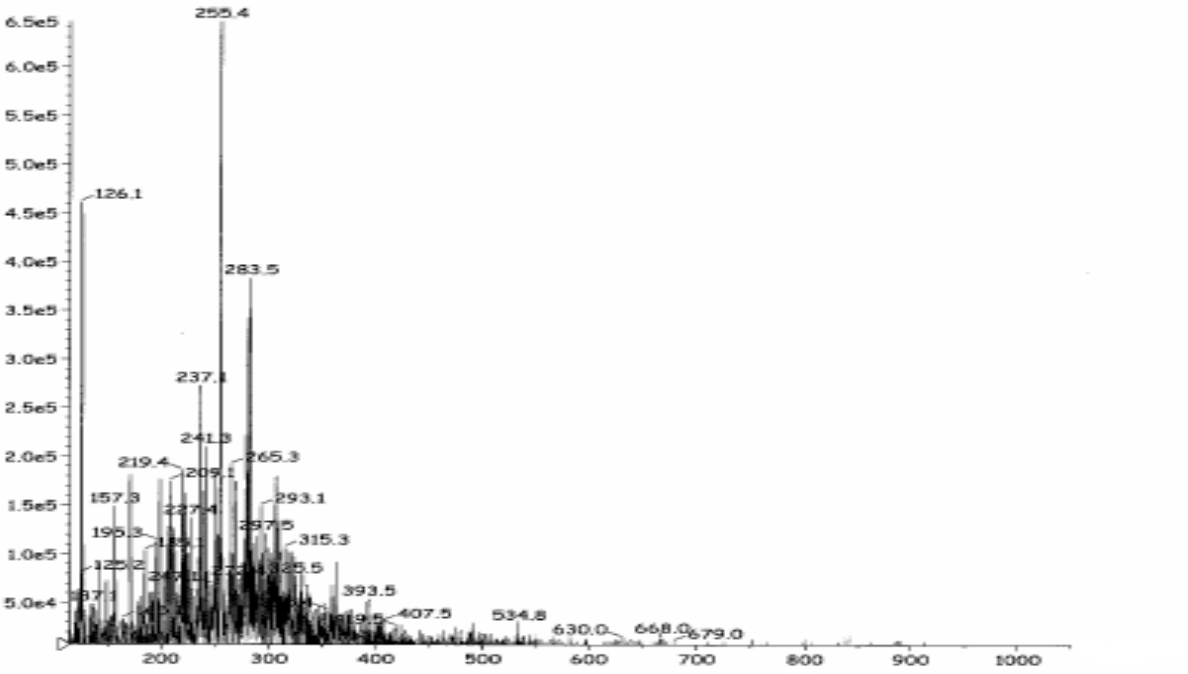

b)

Figure 8.9. Field Y crude oil spectra, a)FTICRMS and b)ES single quadrupole spectra (soap scale-former).

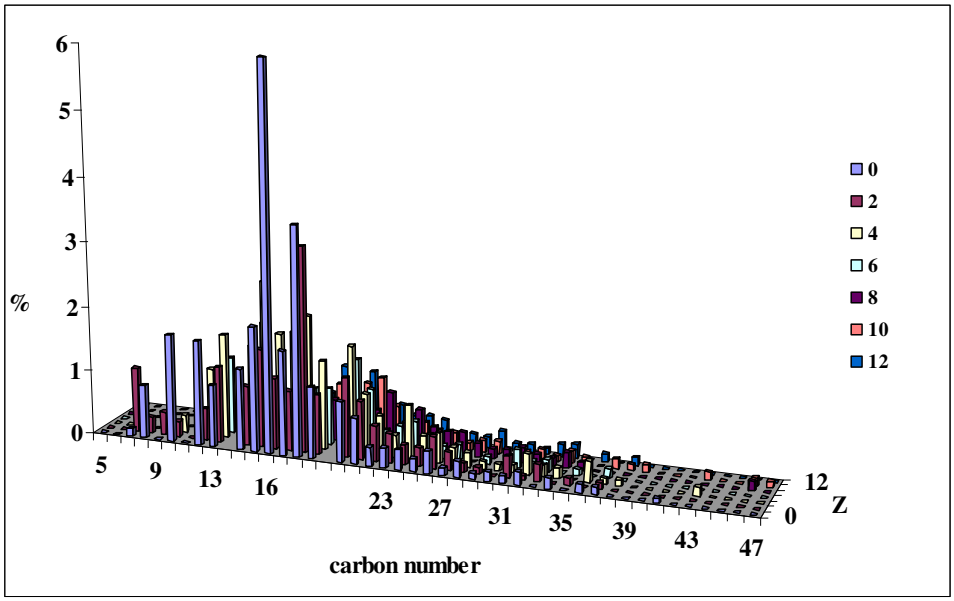

Figure 8.10. Speciation of naphthenic acids in crude oil from Field Y sample (soap scale-former) according to carbon numbers (n) and hydrogen deficiencies (Z). Legend represents Z groups.

Figure 8.11 presents the detailed speciation of naphthenic acids in the crude oil samples used in this thesis using the data illustrated in Figure 8.10. Fatty acids (acyclics) and mono-cyclics were used since they were amongst the most predominant species in soap emulsion field samples (Figure 4.27). The acyclic/cyclic ratio was first proposed by Kim *et al.* (2005) to be a reasonable biodegradation parameter based on six generically related crude oils. Figure 8.11 shows that by plotting the acyclic plus mono-cyclic acid content as a function of the acyclic/cyclic naphthenic acid ratio, it is possible to distinguish the two major soap-forming samples (scales and emulsions). Clearly, soap emulsion-forming crude oils contain higher concentrations of acyclics as well as higher acyclic and monocyclic acid concentrations compared to soap scale-forming crude oils. Cut-off values can be seen at an acyclic/cyclic ratio of 0.5 and acyclic plus mono-cyclic value of 50 %. Figure 8.11 also shows the data for a non-soap-forming crude oil and this falls within the area associated with soap scale-forming crude oils. More data on non-soap-forming systems would be required to evaluate this trend further. The implication of this is that Figure 8.11 may be used to predict soap emulsion-forming crude oils, but not soap scale-forming crude oils. It was not possible to examine the naphthenic acid speciation for bound soap scale-forming crude oils, due to volume limitations.

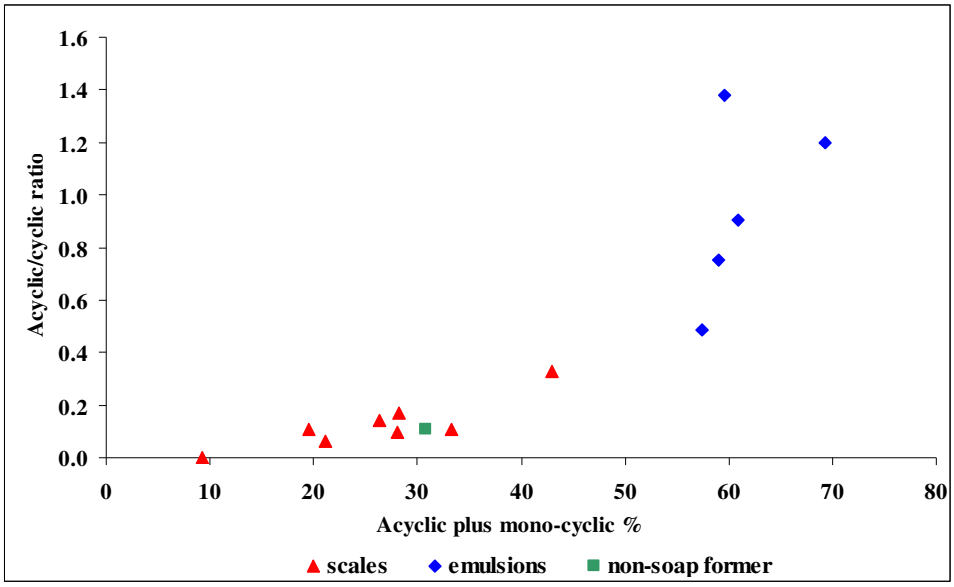

Figure 8.11. Naphthenic acid speciation of crude oils by MS. Acyclic/cyclic ratio as a function of acyclic and mono-cyclic acid percentage for selected crude oils. Scales refers to soap scale-forming crude oils, emulsions refers to soap emulsion-forming crude oils.

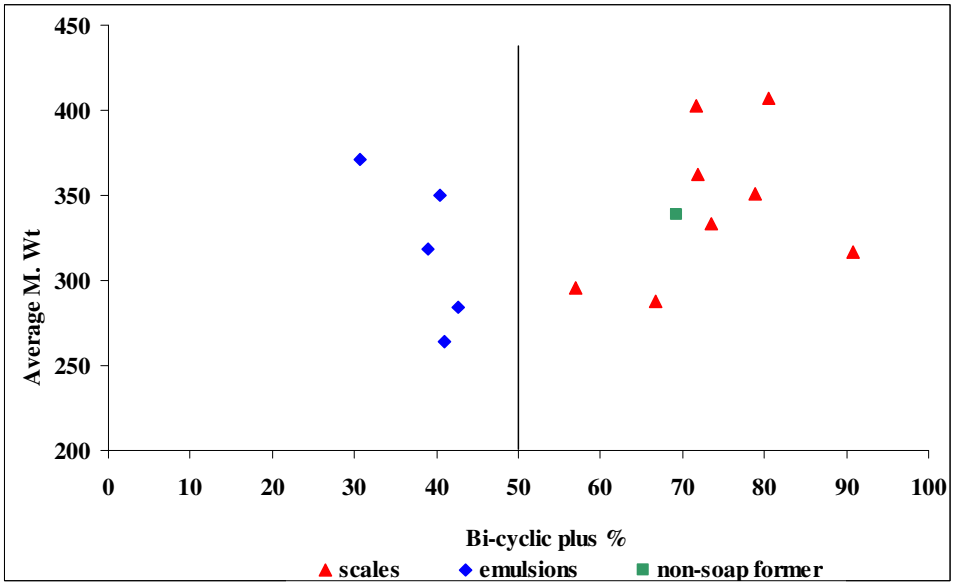

Figure 8.12. Number average molecular weight of naphthenic acids as a function of the bi-cyclic plus fraction for selected crude oils. Scales refers to soap scale-forming crude oils, emulsions refers to soap emulsion-forming crude oils.

Figure 8.12 shows a second approach to distinguishing soap emulsion-forming crude oils and soap scale-forming crude oils using another hydrogen deficiency parameter and the number average molecular weight of the naphthenic acids obtained from the m/z data from MS. In this case the naphthenic acids with hydrogen deficiency lower or equal to -4 (corresponding to species having 2 or more rings bi-cyclics) were used. There is a large

scatter in the data, but it can be observed that there is a clear separation between soap scale-forming and soap emulsion-forming crude oils. Based on the samples evaluated, a general cut off of 50 % bi-cyclic plus fraction can be used to distinguish between the two flow assurance cases. However, a non-soap-forming crude oil is also seen within the soap scale-forming region. Thus the graph could in principle be used to predict soap emulsion-forming crude oils, but not soap scale-forming crude oils and more data from non-soap-forming crude oils is required to investigate this further. Speciation attempts with carbon numbers were also carried out. However these did not result in clear trends that could be used to fingerprint the crude oil samples.

Geochemistry.

Whole oil GC as well aromatic and saturate GCMS were used to examine the degree of biodegradation and maturity for the samples according to the parameters of Peters and Moldowan (1993). Figure 8.13 presents whole oil GCs of soap-forming crude oils, which clearly show different fingerprints. Sample a) represents a typical soap emulsion-forming crude oil. This is a non-biodegraded oil which has characteristics of deltaic or lacustrine source rock with a significant input of land plant organic matter younger than Barremian. This conclusion is based on two major observations. Firstly, a high pristane/phytane ratio (5.6) is characteristic of a less anoxic depositional environment, where organic matter has had slightly greater oxygen exposure such as river systems into a delta. Secondly, the GCMS for this sample shows that steranes are predominant compounds with 29 carbon atoms, with the presence of oleanane, biomarkers characteristic of land plant derived sterols (Peters and Moldowan, 1993). These properties may be considered a very distinct guideline for the prediction of soap-emulsion crude oils. These results are consistent with the analysis of soap emulsion-forming crude oils presented by Gallup *et al.* (2007). The four remaining sample chromatograms in Figure 8.13 (b, c, d and e) represent soap scale-forming crude oils. Sample b) is non-biodegraded probably sourced by a siliciclastic source rock and formed from a normal marine source system. Presence of 28,30-bisnorhopane shown by GCMS is consistent with generation from Kimmeridge clay. This was the only non-biodegraded soap scale-forming crude oil sample analysed in this thesis. Sample c) is a slightly biodegraded oil sourced from a normal marine siliciclastic shale rock. This sample shows some indications of lower thermal maturity than the others given the particularly low sterane isomerization ratios. Sample d) is a biodegraded crude oil, generated again from a marine shale (pristane/phytane higher than 1, with high diasteranes). The predominance of diasteranes over regular steranes suggests a more thermally mature oil than sample b). The

presence of significant amounts of 25-norhopane suggests cycles of severe biodegradation and topping up with fresher oil to restore the n-alkanes. Sample e) is a heavily biodegraded oil. Remaining hopane and sterane distributions are typical of a crude oil sourced from marine shale generated from a siliciclastic depositional environment. This is shown by high amounts of diasteranes relative to regular steranes. The degree of sterane isomerization and conversion of mono to tri-aromatic steranes is consistent with a maturity of peak oil generation. Most of the soap scale-forming crude oils studied were shown to contain indicators of siliciclastic source rock in normal marine environment. However, deltaic or land plant dominated lacustrine facies source systems were also observed for the other samples examined.

The degree of biodegradation was further assessed using the pristane/nC_{17} ratio and on the scale proposed by Peters and Moldowan (1993). This type of approach was suggested by Meredith *et al* (2000). Level 1 in the Peters and Moldowan (P&M) scale represents an undegraded crude oil (unaltered n-alkanes), and level 10 severely degraded oils (hopanes and diasteranes absent, $C_{26\text{-}29}$ steroids attacked). Figure 8.14 presents the plot of the pristane/nC_{17} ratio as a function of the naphthenic acid concentration and Figure 8.15 presents the acyclic/cyclic ratio as a function of the P&M index. From Figures 8.14 and 8.15 it can be seen that there is no clear correlation between the acid concentrations, acid speciation and the biodegradation scales and biomarkers. Factors other than biodegradation must thus be affecting the overall naphthenic acid concentration and distribution in the crude oil samples studied in this thesis.

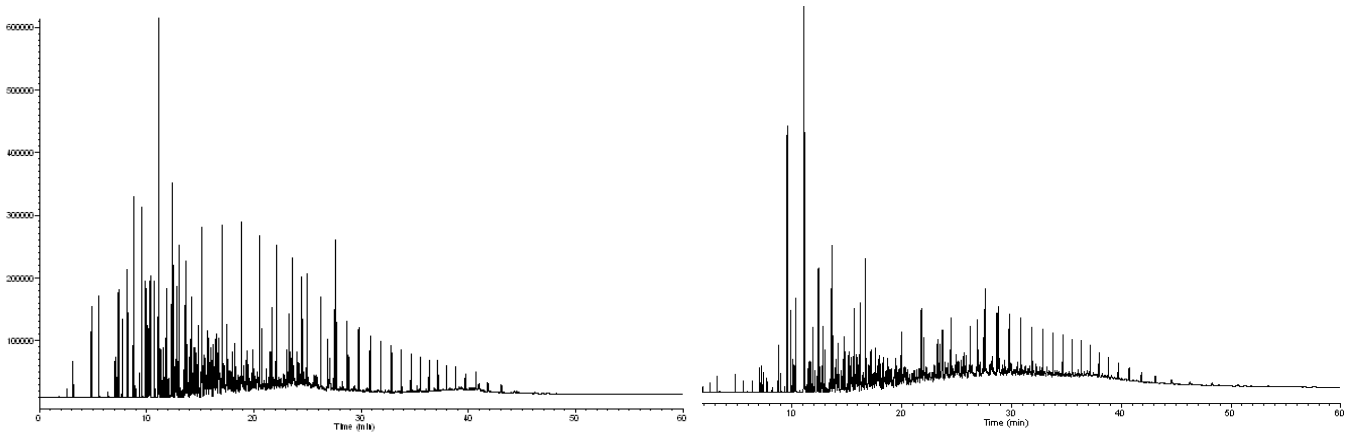

a) **b)**

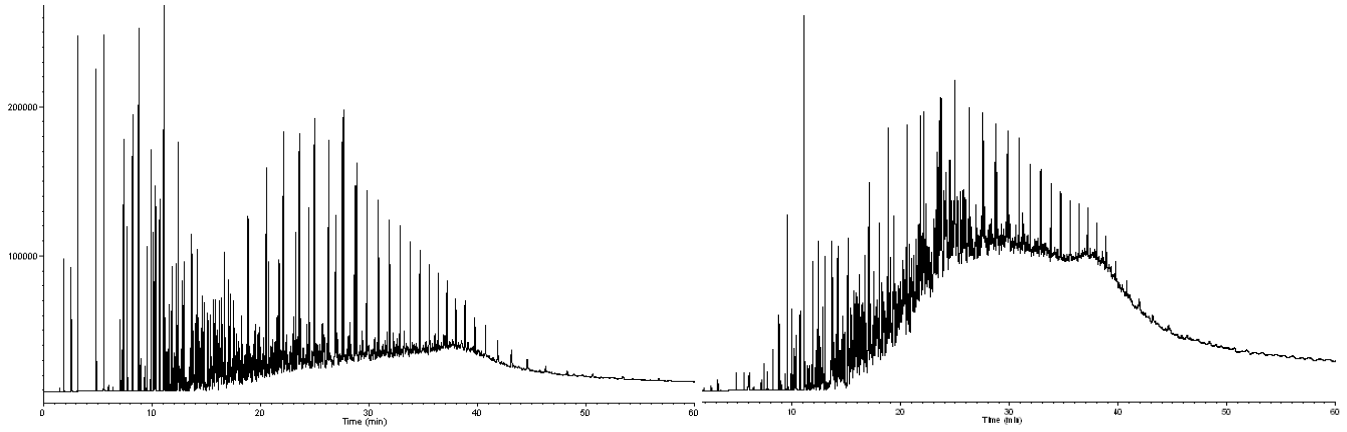

c) **d)**

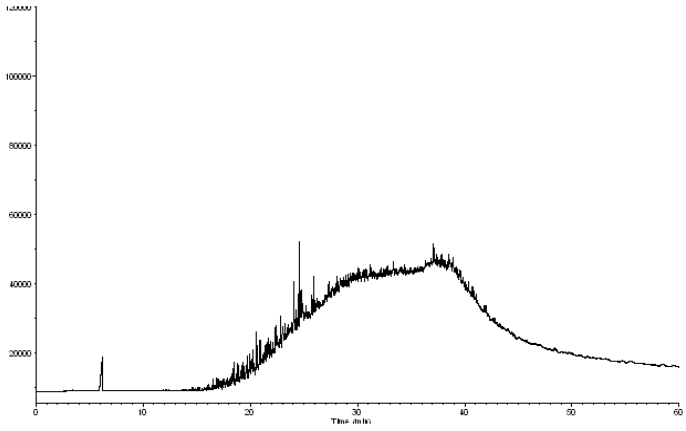

e)

Figure 8.13. Whole oil GC's of sample crude oils. a) soap emulsion-forming. b), c), d) and e) soap scale-forming.

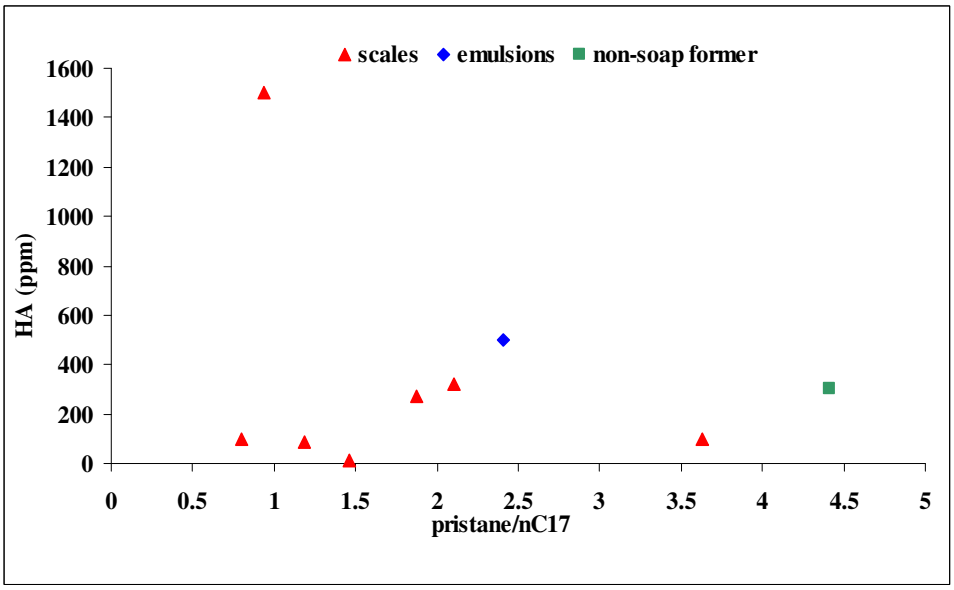

Figure 8.14. Naphthenic acid concentration HA (ppm) as a function of the pristine/nC17 ratio for selected crude oils. Scales refers to soap scale-forming crude oils, emulsions refers to soap emulsion-forming crude oils.

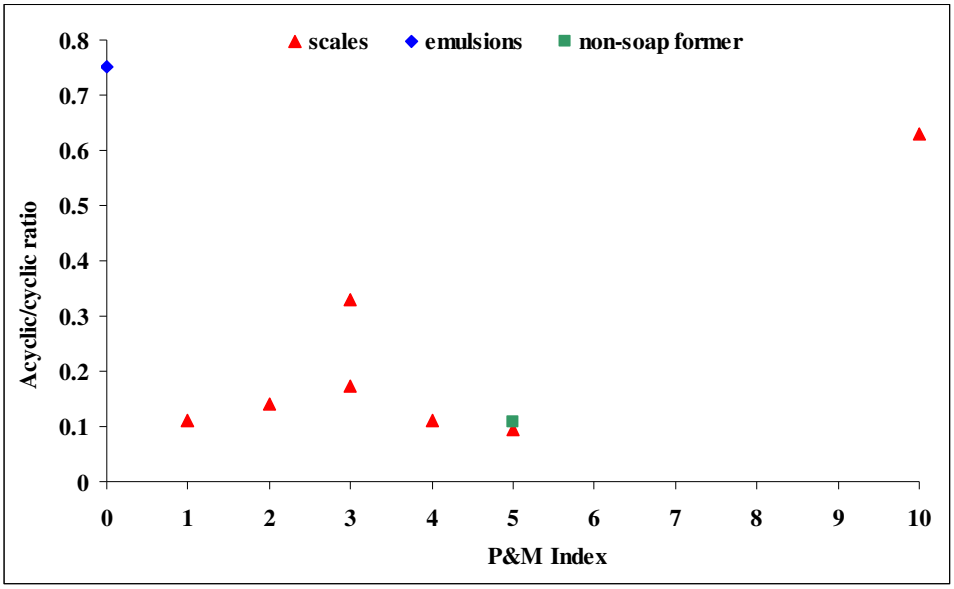

Figure 8.15. Acyclic/cyclic naphthenic acid ratio as a function of the Peters and Moldowan (P&M) index for selected crude oils. Scales refers to soap scale-forming crude oils, emulsions refers to soap emulsion-forming crude oils.

Many maturity parameters are also affected by biodegradation. Some correlations were attempted in this thesis with the relative concentration of C_{29} sterane ratios. The parameters which showed the best correlation are presented in Figure 8.16. There is a good correlation

between the sterane ratio and the TAN of the soap-forming crude oils. This is surprising, given that these crude oils are from different source rocks. It was however not possible to distinguish between soap emulsion-formers and soap scale-formers. This means that there is not much difference in crude oil maturity for the samples used in this thesis. However, data for non-soap-forming fields also falls in this region thus this type of parameter would need to be examined with additional non-soap-forming crude oil samples.

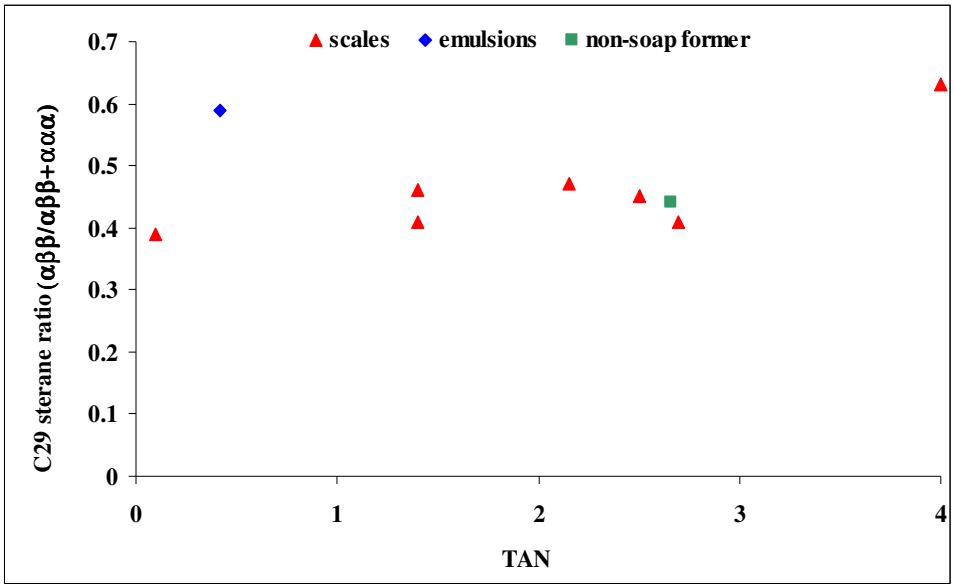

Figure 8.16. C_{29} stearane ratio (αββ/αββ+ααα) as a function of TAN for selected crude oils. Scales refers to soap scale-forming crude oils, emulsions refers to soap emulsion-forming crude oils.

SARA and wax.

Table 8.1 presents the SARA data obtained using the HPLC procedure described in Section 8.2.5. Soap scale-forming crude oils contained significantly more asphaltenes on average than the soap emulsion-forming crude oils. The relative asphaltene values range from 0.23 to 8.53 wt%. Yet the asphaltene/resin ratio showed some scatter in the data. Soap emulsion-forming samples showed mostly low asphaltene/resin ratio, but also higher saturate to aromatic ratios. Data from a non-soap-forming field is also presented and this also falls within the soap scale-forming data range. Despite some evident differences between the two major soap end-member cases, there are some major overlaps for the solubility fractions. Therefore, the use of this information for soap prediction purposed would not be recommended.

Sample	Saturates (wt%)	Aromatics (wt%)	Asphaltenes (wt%)	Resins (wt%)
Scale-former	27.7	53.7	3.8	14.7
Scale-former	42.8	51.0	0.7	5.5
Scale-former	67.3	30.9	0.5	1.2
Scale-former	37.5	56.1	0.4	6.1
Scale-former	44.7	45.3	2.0	8.0
Scale-former	41.2	54.2	0.7	3.9
Scale-former	69.2	29.7	0.2	0.9
Scale-former	43.1	43.4	0.7	13.1
Scale-former	30.1	53.0	8.5	8.4
Emulsion-former	55.9	32.8	0.0	11.4
Emulsion-former	56.5	33.9	0.3	9.3
Emulsion-former	74.2	18.2	0.4	7.2
Non-soap former	44.9	46.2	1.1	7.8

Table 8.1. SARA results.

Figure 8.17 presents the results of the acyclic and mono-cyclic content obtained by MS plotted as a function of the wax content of the crude oil samples used in this thesis. The data falls into two regions: soap emulsion-forming crude oils were observed to contain high amounts of wax and high amounts of acyclics plus mono-cyclic acids. A cut-off value observed for this group of crude oils was 50 % acyclic plus mono-cyclic acids. Soap-emulsion samples appear to have higher wax contents, but no clear cut off can be established for this variable. There was a large scatter in the data for soap scale-forming crude oils both in relation to wax content and acid content. The higher wax content reported for the soap emulsion-forming crude oil is in agreement with the work of Gallup *et al.* (2007). Thus this information could in principle be used to distinguish soap emulsion-forming crude oils from other systems. The non-soap-forming crude oil has the lowest wax content of the samples tested, but is close to those for scale-forming systems. More non-soap-forming samples would need to be tested or a detailed wax cut speciation performed to better delineate the flow assurance ranges.

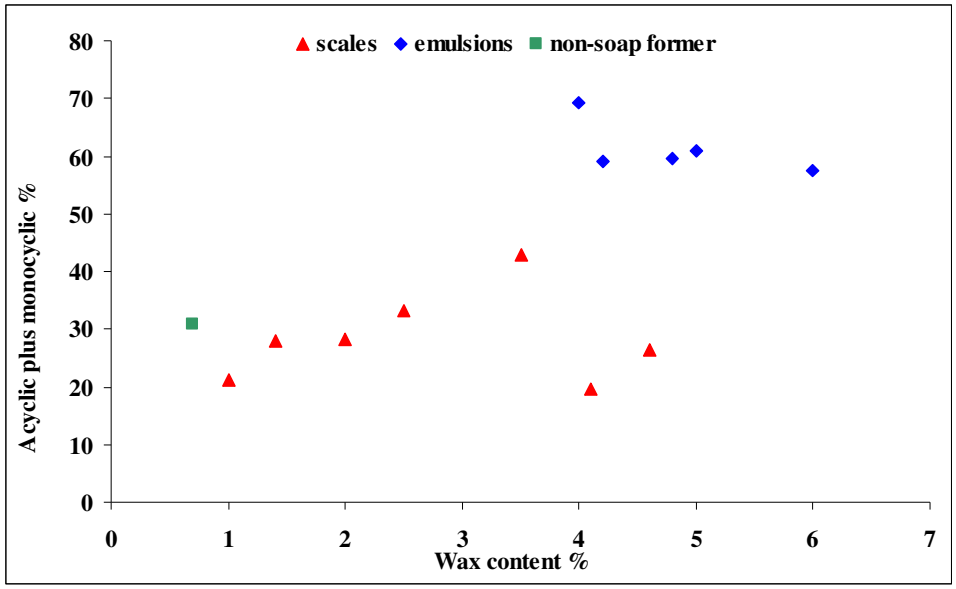

Figure 8.17. Acyclic plus mono-cyclic acid content as a function of wax content for selected crude oils. Scales refers to soap scale-forming crude oils, emulsions refers to soap emulsion-forming crude oils.

Sulphur, metal, chlorine and water content.

Figure 8.18 presents a plot of sulphur content as a function of TAN values for the oils analysed. There is no clear correlation between TAN and sulphur for the soap-forming samples. Yet a clear area exists which indicates an interesting fingerprint for the soap emulsion-forming samples. The results suggest that for low acidic crude oils, sulphur may be a major contributor to TAN, as opposed to high acidic crude oils (where the naphthenic acid content represents the main contribution). The results are in agreement with those of Meredith *et al.* (2000) and suggest that the variation in sulphur amounts is due to source effects and not TAN. Based on this information, the use of sulphur content for the prediction of soap problems in crude oils would be questionable. The results for a bound soap scale-forming sample are also presented in Figure 8.18, and this falls in an area of high TAN and lower sulphur values.

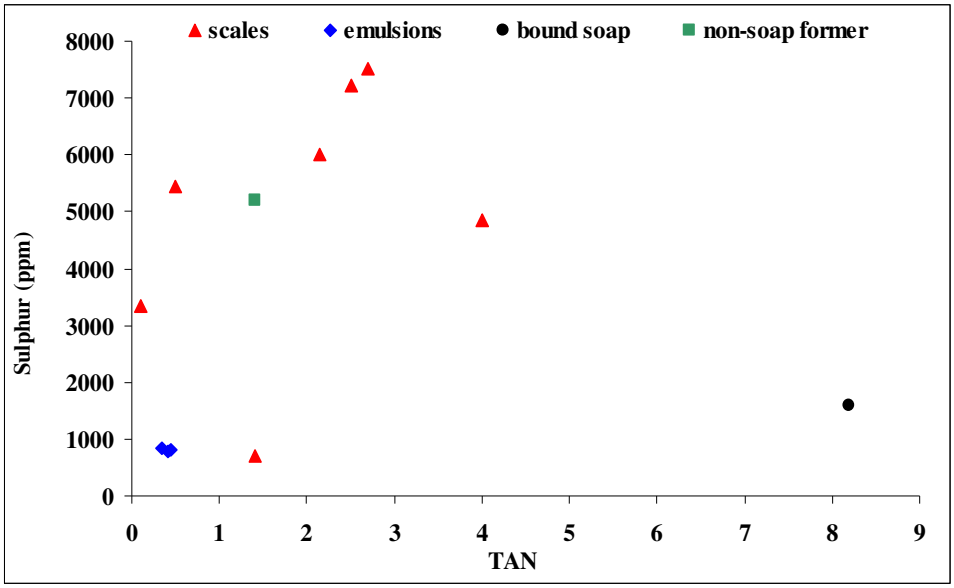

Figure 8.18. Sulphur content as a function of TAN of for selected crude oils. Scales refers to soap scale-forming crude oils, emulsions refers to soap emulsion-forming crude oils. Bound soap refers to bound soap scale-forming crude oils.

Figures 8.19 and 8.20 present attempts to correlate particular metal species in the soap-forming crude oils with soap-forming tendencies. Figure 8.19 shows the nickel content plotted as a function of vanadium content. It can be seen there is no clear correlation between these two metal species for the soap-forming crude oils. Thus it is not likely that these species could be used for soap prediction. This conclusion is not surprising given that the soap-forming crude oils used in this work were from different source rocks and have been exposed to different levels of biodegradation. Figure 8.20 presents the measured calcium concentration of the soap-forming crude oils plotted as a function of the total metal content. The calcium levels in these samples are low compared to the total metal content. Weers and Bieber (2005) presented data for high calcium-containing crude oils and suggested the high values were a result of the formation of salts in the crude oil. Calcium levels for a particular crude oil blend were reported to be between 250 and 435 ppm, which are more than two orders of magnitude larger than the values shown in Figure 8.20. In order to further establish the true origin of the calcium detected in the sample crude oils, total chlorine and water content of the crude oils were measured. If all the calcium detected in the crude oil is due to calcium chloride (dissolved in the dispersed water in the crude oil), then the relative molar ratio of chlorine/calcium in these samples would be 2. The measured chlorine/calcium ratio for these samples is plotted in Figure 8.21 and the majority of values are above 2. The results are probably an indication that most of the measured calcium is organic and results from naphthenic acid complexes. This suggests that the use of calcium

measurements in a crude oil could in principle be used for soap prediction in addition to the FTIR spectra proposed in Chapter 6, to accompany the soap formation reaction. Yet, for this to be carried out, different samples would need to be examined.

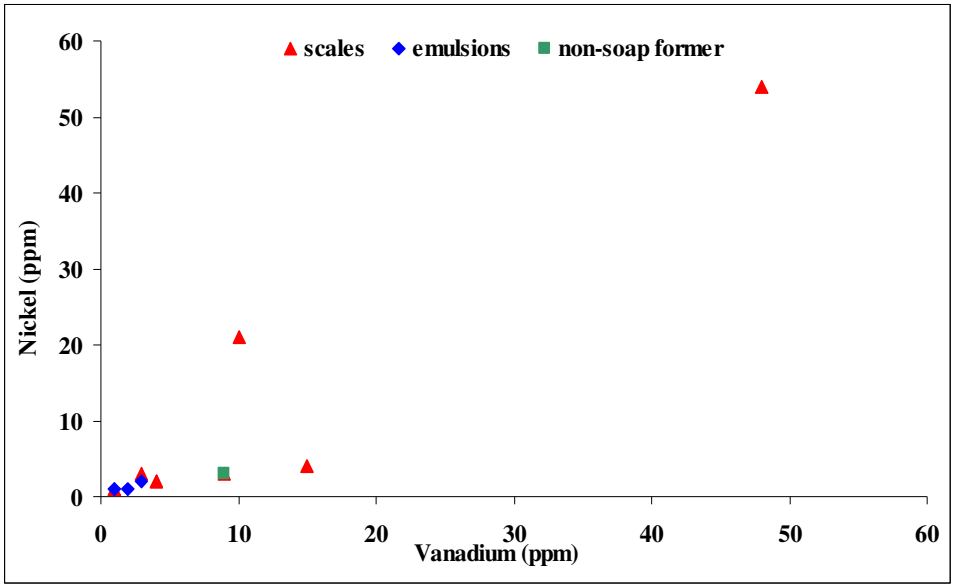

Figure 8.19. Nickel concentration as a function of vanadium concentration in selected crude oil samples. Scales refers to soap scale-forming crude oils, emulsions refers to soap emulsion-forming crude oils.

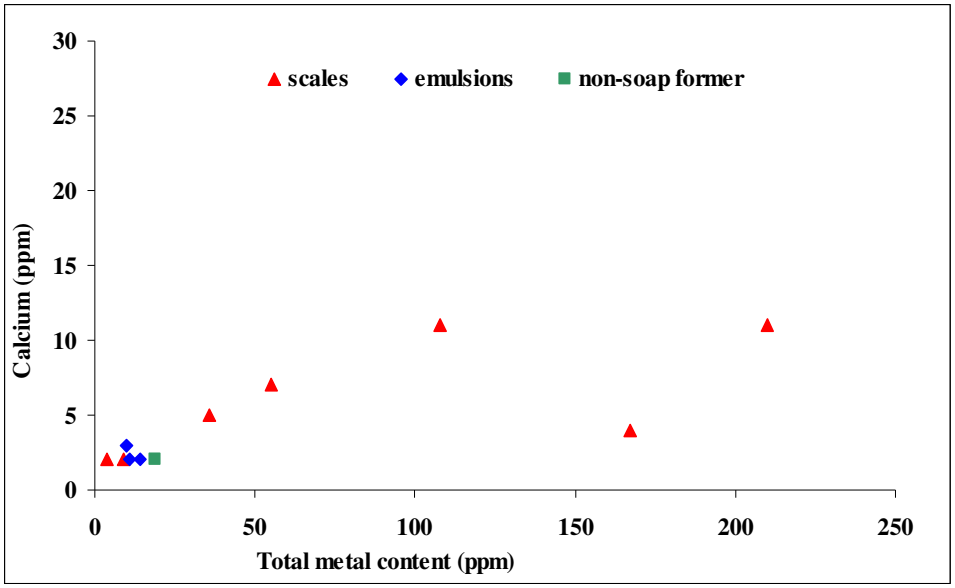

Figure 8.20. Calcium concentration as a function of total metal content in selected crude oil samples. Scales refers to soap scale-forming crude oils, emulsions refers to soap emulsion-forming crude oils.

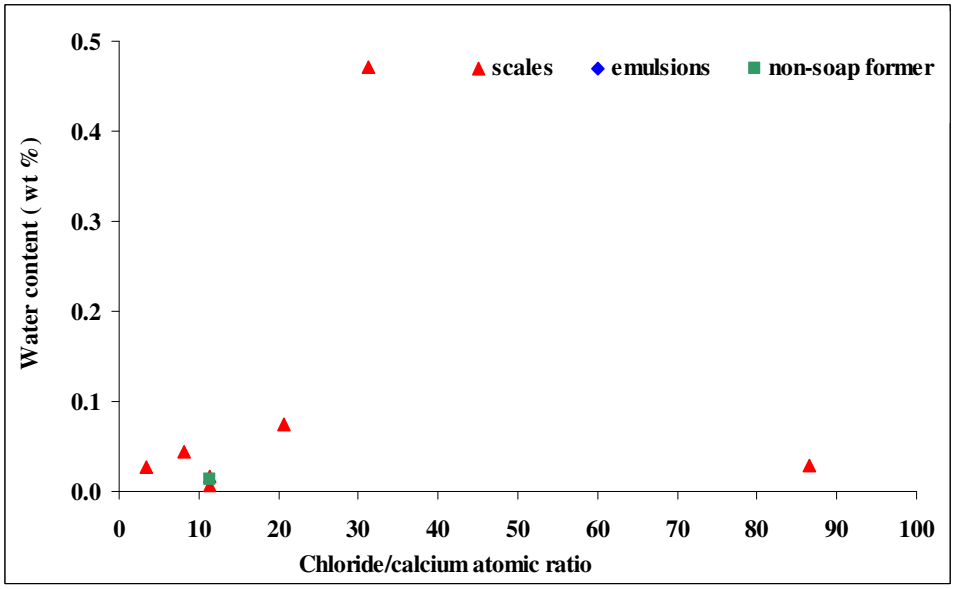

Figure 8.21. Water content as a function of chloride/calcium ratio in selected crude oil samples. Scales refers to soap scale-forming crude oils, emulsions refers to soap emulsion-forming crude oils. Note emulsions data falls outside of the chloride/calcium atomic ratio scale and hence is not shown.

Water properties.

The basic mechanism for soap deposition presented in Chapter 2 suggested that water data should be used in conjunction with the crude oil data for a more accurate soap prediction. The presence of naphthenic acid species alone is not sufficient for soap formation. Table 8.2 presents the surface pH values for a range of produced water samples.

pH	Sample	Bicarbonate (ppm)
8.5	Emulsion-former	2029
8.2	Emulsion-former	1900
8.0	Emulsion-former	1100
8.0	Bound soap scale-former	287
7.7	Emulsion-former	917
7.7	Emulsion-former	800
7.2	Non-former	440
7.1	Scale-former	714
7.0	Scale-former	900
6.8	Scale-former	1029
6.8	Scale-former	667
6.7	Scale-former	1418
6.5	Scale-former	600
6.4	Scale-former	700
6.3	Scale-former	530

Table 8.2. pH at surface and bicarbonate concentrations for produced water samples.

Surface pH can be seen to fall into two major groups, namely, high pH which represents all soap emulsion-forming produced waters, and lower pH which represents soap scale-forming produced waters. Based on this, the use of two critical pH values are suggested for prediction purposes. For soap scales, the value suggested is 6.2 (0.1 pH units below the lowest measured pH for these samples). For soap emulsions, the suggested value is 7.6 (0.1 pH units below the lowest measured pH for these samples). The value of 0.1 pH units is associated with the typical absolute error in pH meters. The produced water associated with the bound soap scale has high pH and falls within the soap emulsion-forming produced water range. Water from a non-soap-forming system has a pH value between those of the soap scale and soap emulsion systems. More information on these systems can be obtained by analysing the bicarbonate ion concentrations in Table 8.2. All soap emulsion-forming produced waters were observed to contain high bicarbonate concentrations. Thus, a critical value is suggested to be 800 ppm, below which a given system is unlikely to form a soap emulsion based on Table 8.2. Gallup *et al.* (2004) suggested that bicarbonate ions might be

an integral part of the soap emulsion structure. Data in Figure 6.30 also suggests this may be the case with the formation of laboratory soaps. There is a large scatter in the bicarbonate concentrations for soap scale-forming produced waters as shown in Table 8.2. Thus it is unlikely bicarbonate content could be used as a prediction variable. It is interesting to note that the lowest bicarbonate concentrations are for the produced water from the bound soap-scale and for the non-soap-forming produced water (Figure 8.22). Bicarbonate ions act as a buffer, so when naphthenic acids partition and dissociate from the oil phase to the water phase (which lowers the pH), bicarbonates help maintain high pH in the produced water (Rousseau *et al.,* 2001). When there are less bicarbonate ions in the produced waters, the soap-forming reaction might occur until there are no more buffer ions to keep the pH high, at which point the soap formation may cease. This would also be a function of the exact naphthenic species present in the crude oil. Rousseau *et al.* (2001) have shown that bicarbonate ions may control the amount of acids that can partition and dissociate into the water phase. This would also explain why bound soap scale does not drop out as solid under field conditions, despite a very high formation water pH. The bound soap scaling-crude oil contained the highest amount of naphthenic acids. Yet with the lowest bicarbonate concentrations in the produced waters (as shown in Figure 8.22), not enough naphthenic acids would be able to partition and dissociate at the oil-water interface.

Figure 8.23 presents the sodium ion concentration in the soap-forming waters as a function of calcium ion concentration. The data falls into two general categories: high sodium and low calcium concentrations (soap emulsion-forming produced waters), and high sodium and high calcium concentrations (soap scale-forming produced waters). Based on the data, characteristic values for soap emulsion systems are: less than 1000 ppm calcium and less than 10000 ppm sodium in the produced waters. The higher sodium to calcium requirements are in-line with the results shown for model naphthenic acid systems in Figures 6.24 and 6.25. It has been shown that acyclic fatty acids (such as those which are predominant in soap emulsion-forming systems), form stable soaps in the laboratory when in contact with brines having high sodium to calcium content (Figure 6.14). Calcium soaps may be formed from these fatty acids only when the calcium concentrations are higher. However, it was also shown that the average amounts of these calcium soaps are much less than the sodium soaps formed under the same conditions. The use of model solutions containing Arn naphthenic acids showed it was also possible to form sodium naphthenates with sodium-rich aqueous phases (Figure 6.64). However, the total amount of soap formed was much less than the calcium naphthenate laboratory deposits. This can be explained by the network effect caused by the interactions of (at least) two calcium ions, and one Arn

species. This requirement may therefore be used to explain the higher calcium concentrations found in soap scale-forming produced waters compared to the soap emulsion-forming waters. The formation of soap emulsions is therefore favoured by high sodium concentrations. Data from a non soap-forming system is also plotted in Figure 8.23 and falls in the soap scale region. Interestingly the bound soap-scaling crude oil data falls within the soap emulsion region. Thus if the crude oil properties are such that a precipitate is predicted to form, the observation of water properties would help to distinguish between soap scales and soap emulsions. It can be speculated that this water sample and the associated crude oil sample are co-mingled during production. Because of the high surface pH values, acids and calcium ions would become bound in the hydrocarbon phase, which would deplete the water of calcium ions.

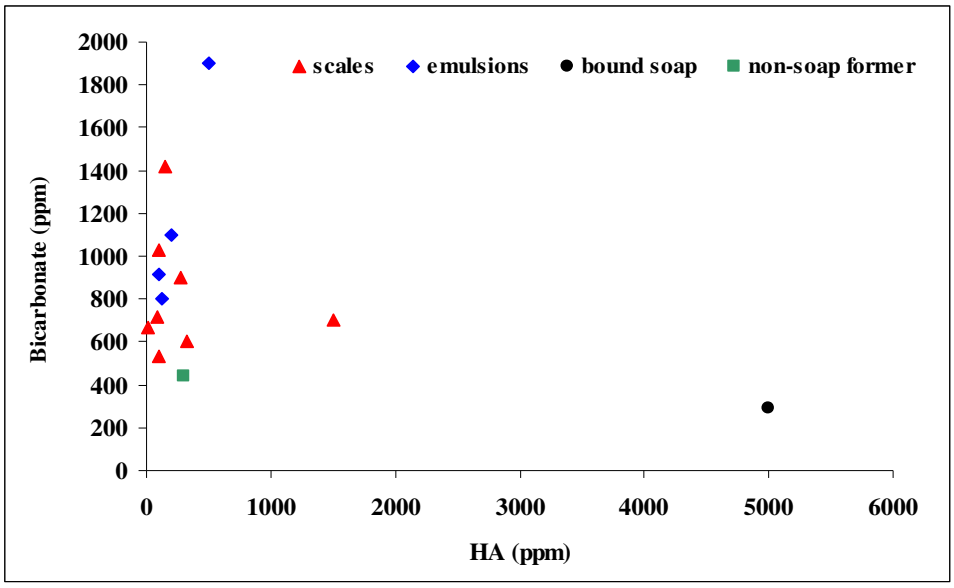

Figure 8.22. Bicarbonate concentration in produced waters as a function of naphthenic acid HA concentration (ppm) in the associated crude oils. Scales refers to soap scale-forming systems, emulsions refers to soap emulsion-forming systems, bound soap refers to bound soap scale-forming systems.

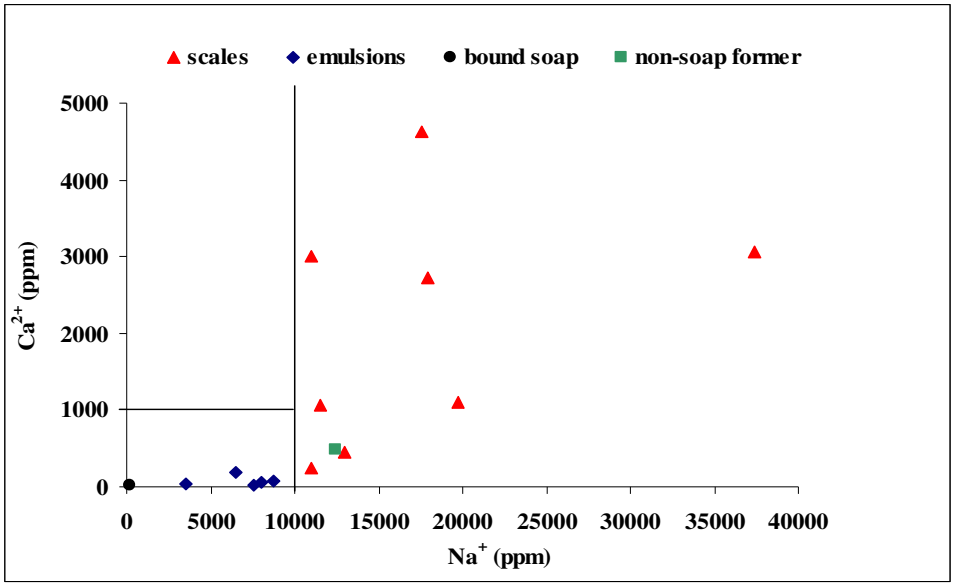

Figure 8.23. Calcium ion concentration as a function of sodium ion concentration for produced water samples from selected fields. Scales refers to soap scale-forming systems, emulsions refers to soap emulsion-forming systems, bound soap refers to bound soap scale-forming systems.

IFT trends.

Figure 8.24 presents the interfacial tension (IFT) data of the crude oils systems and synthetic brines, as a function of pH. A few interesting trends can be observed. The soap scale-forming crude oils show mostly bell-shaped IFT curves, with maximum values at pH close to 4. Certain crude oils also show a second maximum IFT at pH close to 8. These trends are a reflection of the various surface-active components (i.e. amines, phenols) as well as naphthenic acids which become charged as pH changes (Straasner, 1968; Acevedo *et al.,* 1992).

One particular soap scaling-system (Field Z) showed lower IFT trends than the other samples tested. However, the higher IFT at pH close to 4 can still be seen for this sample. The negative mode MS spectra for this sample were shown in Figures 8.6 and 8.7. This sample was the only soap-forming crude oil where the first ionisation of the Arn family was detected. Although the second ionisation of the Arn family was also observed in one additional crude sample, it can be speculated that the lower IFT values may be owing to the presence of this acid species. However in Figure 8.24, the IFT trends for indigenous acids are also presented (soap sample from Field Y). This soap sample was shown to contain up to 4 wt% Arn (Figure 6.38). It can be observed that the IFT values are much lower than the

soap scale-forming systems. Thus, the presence of Arn could be responsible for these trends.

The non-soap-forming crude oil IFT trend is also shown in Figure 8.24 and this sample presents a less defined IFT maximum. Thus, despite the fact that surface activity may be a consequence of Arn presence, it is unlikely that it could be used alone for soap prediction screening. The soap emulsion-forming crude oils present different IFT trends, where decreasing IFT values with increasing pH are observed. This can be interpreted by examining the IFT trends for fatty acid solutions presented in Figure 6.34. These acids also are the predominant species in the soap emulsion-forming crude oils. The sodium (predominant cation in the synthetic brine) and fatty acid pairs are believed to be packed at the oil water interface (Figure 6.13). When calcium naphthenate precipitates Arn acid is removed from the bulk of the crude oil to the oil water interface. This leads to low IFT values as shown in Figure 8.24. An attempt was made to correlate the maximum IFT at pH 4 with the soap formation tendency of the different crude oils. However, it was found that IFT ranged between 22 and 10 mN/m, and it was not possible to distinguish between the two main end-member soap varieties (soap scales and soap emulsions). It is thus suggested that the overall IFT trends be used as an additional qualitative guideline for the prediction of soaps from crude oil and water properties only.

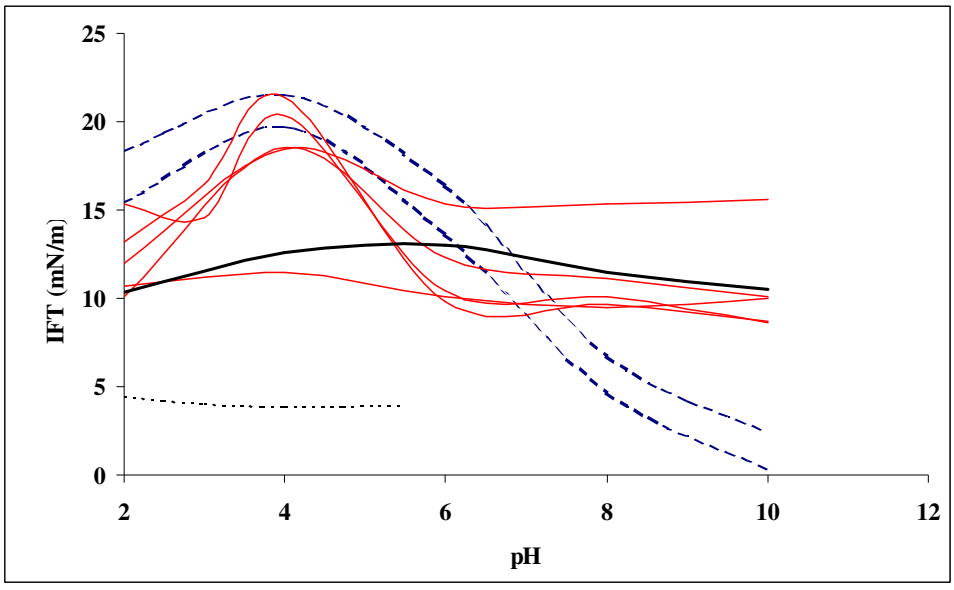

Figure 8.24. IFT values for selected crude oil and brine systems as a function of pH. The solid thin red lines refer to soap scale-forming systems, the dotted blue lines refer to soap emulsion-forming systems, the thick black like refers to a non-soap-forming system, the dotted thin black line refers to an indigenous acid system.

8.6. Conclusions.

The main contribution in this chapter is to the state-of-the-art of prediction of soaps from production fluids. Note that previous chapters presented analysis of soap deposits, where the concentration of naphthenic acids was relatively high. The challenge associated with identifying naphthenic acids in crude oils is low concentrations, particularly of species such as Arn.

A few guidelines were discussed in this chapter using naphthenic acid identification and other crude oil and water properties. Note however that due to the limited number (e.g. < 20) fluids used, data does not have true statistical significance.

It was difficult to fingerprint precisely soap scale-forming crude oils in regards to the crude oil and water properties. However, the fingerprinting of soap emulsion-forming crude oils was possible. Therefore two general end-member soap types can be distinguished. More data is required for a better understanding of the bound soap scale cases.

API gravity and TAN may be used as a preliminary indicator of soap formation tendency. Soap emulsions occur at high API, while soap scales occur at low API. Intermediate API values between 25 and 30 API must be used with caution.

Various different naphthenic acid families were observed in soap-forming crude oil samples. High-resolution mass spectrometry and ion-exchange separation of the naphthenic acids were unable to detect the Arn acid species in all but two soap scale-forming crude oil sample. It is concluded that this species was probably removed from the crude oil during deposition. Quantitative Arn identification would therefore be more suited on virgin, pristine crude oil samples which had not experienced precipitation.

The surprisingly low ion-exchange yields found in this thesis represent a major contribution in this chapter. Though the results do not discourage the total use of this method for further acid separation, results must be used with reservation for fingerprinting purposed. Further optimisation of the separation technique may lead to better performance and less biased effects as a function of naphthenic acid molecular weight.

In this chapter, a new naphthenic acid indicator was shown to distinguish between soap emulsion-forming crude oils and soap scale-forming crude oils: acyclic plus mono-cyclic acid percent plotted against the acyclic/cyclic naphthenic acid ratio. This also represents a major contribution of this chapter.

Whole oil GC and GCMS studies indicate soap emulsion-forming crude oils to be non-biodegraded samples having land plant organic matter as source material. Soap scale-forming crude oils have various degrees of biodegradation with predominantly siliciclastic source rock in normal marine environment. However, deltaic or land plant dominated

lacustrine facies source systems were also observed. C_{29} ratios also show potential for fingerprinting. Overall it would be of importance to distinguish parameters associated with both biodegradation and maturity.

Wax content as a function of acyclic acid plus mono-cyclic concentration (50 % threshold) can be used to distinguish soap emulsion-forming crude oils, as opposed to soap scale-forming crude oils.

The critical pH for soap emulsion systems was identified as 7.6. These systems were only seen to occur when bicarbonate concentrations in the water were above 800 ppm. Produced water critical calcium and sodium concentrations were found to be below 1000 and 10000 ppm, respectively. The critical pH for soap scale-forming systems was identified as 6.2. These were seen to occur with varying concentrations of bicarbonate ions. Calcium concentrations were found to be above 1000 ppm with higher calcium/sodium ratios for soap scales compared to soap emulsion-forming systems.

Analysis of metal content in the soap-forming crude oil suggested that most of the calcium ions dispersed in the samples were present in the form of complexed salts. The majority of the crude oils in this chapter have experienced some form of soap precipitation. The presence of complexed salts suggests that the mechanism of soap formation could be accompanied before the onset of precipitation. This supports the use of FTIR, as discussed in Chapter 6 for model systems.

Soap emulsion-forming crude oils show decreasing IFT values as a function of pH, and this is a direct function of the presence of acyclic acids and sodium ion pairing at the oil-water interface. Soap scale-forming crude oils present a bell-shaped IFT curve as a function of pH which is a reflection of the diversity of surface-active components present in the crude oil samples. The low IFT values as a function of pH in the soap-forming crude oil samples is very likely related to the presence of Arn.

The techniques used and presented in this chapter for soap analysis, were conducted and acquired from static measurements only on dead oil and water samples. Should data from a non-soap-forming field be available for comparison it would be advisable also to submit this crude oil (and associated produced water) to conditions which mimic field operations as closely as possible, e.g. shear, water cut, temperature, pressure. Thus, the use of deposition rigs similar to those reported by Rousseau *et al.,* 2001; Mediaas *et al.,* 2005; and Dyer *et al.,* 2006 would be suggested.

Table 8.3 presents a summary of the soap prediction information presented in this chapter.

Parameter	Soap Soap Scale	Type Soap Emulsion	Uncertainty
API *vs.* TAN	Low (< 25) and high (> 1)	High (> 30) and low (< 1)	25-30 API. TAN value < 0.5 also observed with soap scales
Naphthenic acid indicators			
Arn presence	A possible (but not necessary) indicator	Not associated	Low concentrations, contaminated samples
Acyclic/cyclic ratio *vs.* acyclic plus monocylic %	< 0.6 and < 50%	> 0.6 and > 50%	MS values given as % (assumed same ionization in ES run)
Geochemistry	Most are biodegraded with siliciclastic source rocks	Clear fingerprint of non-biodegraded deltaic or lacustrine with land plant matter	Deltaic and lacustrine also present in soap scales
Wax % *vs.* acyclic plus monocyclic %	> 4% and > 50%	< 4% and < 50%	MS values given as % (assumed same ionization in ES run). Assume pristine sample (no wax loss)
Water properties			
pH	> 6.3	> 7.6	Major uncertainty
Na^+ and Ca^{2+} (ppm)	> 10000 and > 1000	< 10000 and < 1000	
HCO_3^- (ppm)	n.a.	> 800	Effect of VFA's not computed

Table 8.3. Chapter guidelines for soap scale and soap emulsion fingerprinting. Note n.a. = not applicable.

CHAPTER 9 – CONCLUSIONS AND RECOMMENDATIONS FOR FUTURE WORK.

9.1. Conclusions.

The main objective of the work undertaken in this thesis was to study the formation of soap deposits through analysis of field samples, as well as mechanistic experiments with a variety of naphthenic acid systems under laboratory conditions.

Chapter 4 presented the results of a series of sensitivity tests carried out using deposit samples from a range of fields from Southeast Asia to West Africa. It was possible to distinguish clear characteristics that differentiate between calcium naphthenate soap scales and sodium carboxylate soap emulsions in field deposit samples. The analysis of naphthenic acid in the deposits using low-resolution mass spectrometry showed the presence of Arn species only in calcium naphthenate soap scales and not in sodium carboxylate soap emulsions. Acyclic species were detected in all field deposits, but were shown to be predominant in sodium carboxylate soap emulsion samples. It was also shown that detection of the naphthenic acid species, including Arn acids, was a function of the analysis method, which in this case involved the ionisation source, instrument settings and solvents employed in the mass spectrometry analysis. Overall detection was suggested to be a function of ionisation conditions, charge transfer, solvent polarity and viscosity (for non-derivatized naphthenic acids). Moreover, it was shown that clear differences exist between chemically treated deposits and deposits formed *in-situ* in the field without chemical treatment. It was concluded that chemically treated calcium naphthenate soap scale deposits contained less calcium ions in addition to less Arn species. There was evidence of relationships between the availability of naphthenic acids (given by use of production chemicals or solubility/thermodynamic effects of crude oil species) with the final composition found in the field deposit itself (*viz.* presence of Arn in non-calcium-containing deposits). For instance, when an inhibitor was used to prevent soap formation, the predominance of acyclic species as opposed to Arn in the deposits, suggested there was complexation with the former species present in the parent soap-forming crude oil. This resulted in a reduction of the Arn signal at m/z 1230, and an increase in low molecular weight naphthenic acid concentration in the field deposit. Overall the results in Chapter 4 present a novel combination of analytical techniques applicable to field deposits, which enable characterisation of both inorganic as well as organic portions.

The objective of the experiments described in Chapter 6 was to conduct a series of experiments using static bottle tests with model naphthenic acids, naphthenic acid extracts and crude oil samples. The formation of soaps in the laboratory was shown to be both a surface and a bulk phenomenon, which is a function of oil and water phase properties. It was shown that soaps may be formed using realistic aqueous phases and this is pH dependent; similar to that observed under field conditions. Acyclic species dissolved in toluene and sodium-rich aqueous phases were shown to lead to the formation of sodium carboxylate soap emulsions. Cyclic acids, on the other hand, were shown to react preferentially with calcium-rich aqueous phases. Cation effects were discussed in terms of hydration (given by the ionic radius) as well as the partitioning and dissociation of the naphthenic acids. Surface effects were also shown to be affected by combinations of these variables.

The role of Arn in soap deposition was also discussed in this thesis. These acids showed a high affinity towards calcium ions through the formation of a sticky network at the oil-water interface. This is probably owing to the four carboxylic groups identified in this thesis by MS/MS, which was first suggested by Baugh *et al.,* (2004). It was possible to form a calcium naphthenate soap scale in the laboratory which contained Arn, but only with calcium-rich and bicarbonate-containing aqueous phases. When sodium-rich or aqueous phases not containing bicarbonate were used, deposits were formed in the laboratory which did not contain Arn, but predominantly straight chain naphthenic acids. The role of bicarbonate ions in soap emulsion tests was suggested to be not only a buffer effect, but also an integral part of the naphthenic acid complex.

The formation of soaps from crude oils showed mixed results in this thesis. Although water-in-oil emulsions were seen to form from soap emulsion-forming crude oils, no soaps were obtained using soap scale-forming crude oils. It was suggested that this could be owing to insufficient pH variations during the static bottle test experiments and/or slow kinetics. Nevertheless, since Arn naphthenic acids were only identified in two of these crude oils, the influence of this species cannot be totally ruled out.

Static bottle tests described in Chapter 6 showed that, when mixed with other acids, Arn species are the predominant surface-active components within model systems. This conclusion was obtained using interfacial tension measurements, and aqueous phases containing pH and dissolved solids commonly found in produced waters. However the presence of different acids was shown to affect the final composition of the deposits formed as well as the amount of partitioning and dissociation. These tests were carried out with indigenous naphthenic acid species but evidence from a field deposition case was also

presented. The conclusions of these experiments point to a critical concentration of Arn acids for the formation of calcium naphthenate soap scale deposits.

Chapter 7 discussed in detail a series of prediction experiments and preliminary model for soap systems in the laboratory. At present, one of the biggest limitations is that the model is strictly dependent on one naphthenic acid in solution, not multi-component species. The challenge lies in obtaining parameters for multi-component systems, such as the dissociation constant (pK_a) or the solubility constant (K_{CaA2}) when more than one naphthenic acid is present in solution. Nevertheless, it was shown that the indigenous acids (including Arn) have two different pK_a values. Additional precipitation experiments are necessary to correlate the amount of soap formation encountered in field conditions. A further challenge lies in the quantification of soap emulsion quantities with model predictions, since these soaps do not form solids *per se*.

In Chapter 8 an attempt was made to correlate various crude oil and water parameters to the tendency for soap formation in a range of different soap-forming systems. A description of the limitations of one of the solid phase extraction techniques (QAE-sephadex) for the treatment of crude oil naphthenic acids was carried out (however no optimization of the method was attempted). The relationship of Arn presence in crude oil samples on resin selectivity was not addressed. It would be advisable to repeat tests with pristine soap-forming crude oil samples (possibly collected from downhole campaigns). Despite this, it was shown that Arn was only detected in two soap-forming samples. Nevertheless, using naphthenic acid speciation obtained from low-resolution instruments allowed for the differentiation of soap scale-forming and soap emulsion-forming crude oils. Particular geochemical aspects of soap-forming crude oils were identified, such as the link with biodegradation. The wax content of crude oils was also shown to correlate well with specific acyclic acid structures for the different soap-forming crude oils. Additional non-soap-forming samples are necessary to support the conclusions in this chapter.

9.2 Recommendations for future work.

Additional work on the naphthenic acids present in the field deposits could include developing new or improved methods for naphthenic acid characterisation, such as separation via more selective ion-exchange resins. This may benefit the detection of bad-actor acids such as Arn. Research in the literature has indicated that the detection of acids may be improved by the use of derivatization agents, such as BF_3/methanol. This agent has been employed extensively in the study of indigenous naphthenic acids from soap deposits (Lutnaes *et al.,* 2006), but the exact yields of derivatization as well as selectivity towards different naphthenic acids have not been discussed. It is suggested therefore, that a range of different derivatization agents be employed and their effect on the characterisation of acid, using different sources and solvents be carried out. Two-dimensional gas chromatography also has the potential to evaluate naphthenic acids from a molecular perspective. Only one reference exists in the literature that deals with this subject (Hao *et al.,* 2005). The technique does have limitations since acids with hydrogen deficiencies larger than 10 (five cyclic rings) cannot be analysed due to boiling points. The technique therefore would be more efficient if applied with a time-of-flight mass analyser (TOF), possibly with the use of derivatization agents, in GCMS. The analysis of Arn was briefly studied using LCMS in this thesis. Thus it would be advisable to repeat some of the above-mentioned experiments, with the LC fractions identified as being associated with the Arn acid. This would also help further characterisation studies such as 2D NMR which were not successful due to very complex spectra being produced, without the separation of the Arn from the other indigenous acid species.

It is also suggested that more tests be conducted using high-resolution mass spectrometry. This would be useful to distinguish carboxylic groups from other heteroatom-containing acidic species, currently not possible with the low-resolution instruments used in this thesis. The results presented in Chapter 6 with regards to bulk and surface property trends present good opportunities for molecular simulations. In particular, studies could be carried out to examine the behaviour of naphthenic acids at the oil-water interface as well as the simulation of chemical inhibitors. A more detailed analysis of the importance of liquid crystals (which were shown to be associated with the Arn acids under certain conditions in Chapter 6) is recommended. This could help provide further detail on stability mechanisms, by the mapping of the phase behaviour of the Arn acid in model systems. One of the issues involved in calcium naphthenate soap scale formation not addressed in this thesis is the

hardening of soap samples when exposed to air. It is not known if this is an oxidation or a curing process. Nevertheless, it would be an interesting aspect for future analysis. The benefit of such analysis would be to verify if the soap samples can be better treated or even flowed prior to handling (which may improve OPEX costs). Many viscosity measurements were carried out on chemically treated soaps, but these were not presented in this thesis. Values were high (of the order of 4500 cP). Viscosity values may also be used to follow inhibition reactions. Water contamination, as well as wax precipitation influence on these results cannot be ruled out. It is debatable if crude oil or interfacial viscosity analysis could be used to predict soap formation. In addition, if soap scales may be kept in sludge form when collected under field conditions, they may be easier to treat and transport on site, and this would bring economic benefits to field operations.

One of the areas for further work with soap-forming crude oils would be to examine more realistic pH adjusting systems. Both a tube blocking and a CO_2 rig were shown to lead to poor results, but better design of a deposition rig could be attempted, in particular, CO_2 mixing should be focused on. The open literature contains at least two references of naphthenate test rig designs that could be adapted for further work (Mediaas *et al.,* 2005; Dyer *et al.,* 2006). The use of live fluids would be a useful addition to these experiments since it would allow the examination of three phase (oil-gas-brine) systems at production conditions. Ultimately this would also enable the role of PVT properties on soap formation to be examined. During the experiments in this thesis, it was shown that FTIR has excellent potential as a prediction tool for the formation of soaps in the laboratory. It was suggested that depletion of naphthenic acids could be followed by FTIR measurements on oil phases. A natural progression of this work could be that the extension to crude oil systems to examine properties for indigenous acids and soap formation.

The action of dedicated chemical inhibitors on the formation of soaps was not investigated explicitly in this thesis, although the effects of chemical treatment on soap composition were shown in Chapter 4. Despite this, the development of the optimised static bottle tests has potential for the study of such production chemicals, and better insights into the deposition mechanism. Further work could focus on the testing of inhibitors using these procedures.

More experiments should be designed for the purpose of obtaining information associated with the naphthenate precipitation model discussed in Chapter 7. Further sensitivity modelling should be carried out to examine the effect of water-cut and different naphthenic acids on modelling results. In addition, the presence of bicarbonate buffers in solution was not considered in the modelling presented in Chapter 7. Ideally, the incorporation of a

deposition model in commercial software such as Multiscale or OLI would be of industrial interest. However, for this model to be validated, experiments would have to be conducted, preferably, with realistic feeds. The challenge here would be to match the PVT behaviour of reservoir fluids with soap deposition thermodynamics.

The correct speciation of n-paraffins present both in the soap-forming crude oils and particularly in soap emulsions, would be an interesting area to pursue in future work to build on the conclusions obtained in Chapter 8 (e.g. the influence on overall wax content on soap fingerprinting). For this purpose, high temperature gas chromatography (HTGC) would be most suitable. This would allow further verification of the particular effects of biodegradation of crude oils. It has been reported in the literature that fatty acids may be used as precursor for cyclic naphthenic acid structures and hydrocarbons (Philp, 1994). One possible biological route for the Arn acid from archaelbacteria has been already reported in the literature (Lutnaes *et al.,* 2006). No attempts have been carried out to support these claims using laboratory tests. The study of maturation/biodegradation or thermal effects on naphthenic acids would thus be a suitable route for studying the exact formation of high molecular weight Arn acids. Therefore the following could be addressed by this approach: the relationship between biodegradation and naphthenic acids and formation of naphthenic acids *in situ*. For this purpose, two non-biodegraded crude oils and one moderately biodegraded crude oil sample candidates could be examined. The crude oils could be treated under controlled laboratory conditions following the procedures described by Goodwin *et al.* (1981). In summary, these tests could be used to predict the formation of Arn acids in reservoir conditions and thus would serve as a valuable tool in new exploration and production projects.

REFERENCES.

Acevedo S., Mendez B., Rojas A., Layrisse I., Rivas H., *Asphaltenes and resins from the Orinoco Basin*, 1985, Fuel , 64, 1741-1747.

Acevedo S., Escobar G., Gutierrez L., Rivas H., *Isolation and characterization of natural surfactants from heavy crude oil, asphaltenes and maltenes. Interpretation of their interfacial tension-pH behaviour in terms of ion pair formation*, 1992, Fuel, 71, 619-623.

Acevedo S., Escobar G., Ranaudo M. A., Khazen J., Borges B., Pereira J. C., Mendez B., *Isolation and characterization of low and high molecular weight acidic compounds from Cerro Negro extra heavy crude oil. Role of these acids in the interfacial properties of the crude oil emulsions*, 1999, Energy and Fuels, 13, 333-335.

Acevedo S., Gutierrez X., Rivas H., *Bitumen-in-water emulsions stabilized with natural surfactants*, 2001, Journal of Colloid and Interface Science, 242, 230-238.

Acros, www.acros.com, this is a website of a manufacturer of commercial naphthenic acids, which contains physical and chemical information.

Adamson A. W., Gast A. P., *Physical chemistry of surfaces*, 1997, 6th edition, John Wiley and Sons.

Ali M. F., Alqam M. H., *The role of asphaltenes, resins and other solids in the stabilization of water in oil emulsions and its effects on oil production in Saudi oil fields*, 2000, Fuel, 79, 1309-1316.

American Petroleum Institute API., 2003, *Reclaimed substances – naphthenic acids report.*

Anchyeta J., Centeno G., Trijo F., Marroquin G., Garcia J. A., *Extraction and characterization of asphaltenes from different crude oils and solvents*, 2002, Energy and Fuels, 16, 1121-1127.

Arla D., Sinquin A., Palermo T., Hurtevent C., Gracida A., Dicharry C., *Influence of pH and water content on the type and stability of acidic crude oil emulsions*, 2007, Energy and Fuels, 21 (2), 1337-1342.

Aske N., Kallevik H., Sjoblom J., *Determination of saturate, aromatic, resin and asphaltenic (SARA) components in crude oils by means of infrared and near-infrared spectroscopy*, 2001, Energy and Fuels, 15, 1304-1312.

Babaian-Kibala E., *Phosphate ester inhibitors solve naphthenic acid corrosion problems*, 1994, Oil and Gas Journal, 92 (9), 31-35.

Barnard P. C., Bastow M. A., *Hydrocarbon generation, migration, alteration, entrapment and mixing in the Central and Northern North Sea*, 1991, Petroleum Migration, Geological Society, Special Publication, England W. A and Fleet A. J (editors), 167-190.

Barnes I., *Field measurement of alkalinity and pH*, 1964, U.S. Geological Survey Water-Supply Paper, 1535-H 7.

Barrow M. P., *Characterization of the naphthenic acid content in crude oil extracts using Fourier-Transform ion cyclotron resonance mass spectrometry*, 2003, internal presentation for Total at the Department of Chemistry, University of Warwick, UK.

Barth T., Bjorlikke K., *Organic acids from source rock maturation: generation potentials, transport mechanisms and relevance for mineral diagenesis*, 1993, Applied Geochemistry, 8, 325-337.

Barth T., Hoiland S., Fotland P., Askvik K. M., Pedersen B. S., Borgund A. E., *Acidic compounds in biodegraded petroleum*, 2004, Organic Geochemistry, 35, 1513-1525.

Baugh T. D., Wolf N. O., Mediaas H., Vindstad J. E., Grande K., *Characterization of a calcium naphthenate deposit – The Arn acid discovery*, 2004, American Chemical Society, Division of Petroleum Chemistry, 49 (3), 274-276.

Baugh T D., Grande K., Mediaas H., Vindstad J. E., Wolf N. O., *The discovery of high molecular weight naphthenic acids (Arn acid) responsible for calcium naphthenates deposits*, 2005, SPE 93011, presented at the 7th International Symposium on Oilfield Chemistry, Aberdeen, UK, May 11-12.

Baugh T., Grande K. V., Mediaas H., Vindstad J. E., Wolf N. O., The discovery of high molecular weight naphthenic acids (Arn acid) responsible for calcium naphthenate deposits", 2005, pproceedings of the Chemistry in the Oil Industry IX, RSC/EOSCA, Manchester, UK, October 31-November 2.

Becker J. R., *Crude oil waxes, emulsions and asphaltenes*, 1997, 1st edition, Pennwell Publishing Company.

Beneventi D., Carre B., Gandini A., *Precipitation and solubility of calcium soaps in basic aqueous media,* 2001, Journal of Colloid and Interface Science, 237, 142-144.

Beneventi D., Pugh R. J., Carre B., Gandini A., *Surface rheology and foaming properties of sodium oleate and C12(EO)6 aqueous solutions*, 2003, Journal of Colloid and Interface Science, 268, 221-229.

Berg J. M., Claesson P. M., *Forces between carboxylic acid layers in divalent salt solutions*, 1989, Thin Solid Films, 178, 261-270.

Bitsh-Larsen A., *Phase behaviour of naphthenic acid in mixture*, 2004, M.Sc thesis, Department of Chemical Engineering, Technical University of Denmark, Copenhagen, Denmark.

Bloch J. M., Yun W., *Condensation of monovalent and divalent metal ions on a Langmuir monolayer*, 1990, Physical Review A, 41 (2), 844-862.

Borgund, A. E., Erstad, K., Barth, T., *Fractionation of crude oil acids by HPLC and characterization of their properties and effects on gas hydrate surfaces*, 2007, Energy and Fuels, 21, 2816-2826.

Brandal O., Sjoblom J., Oye G., *Interfacial behavior of naphthenic acid and multivalent cations in systems with oil and water I. A pendant drop study of interactions between n-dodecyl benzoic acid and divalent cations*, 2004, Journal of Dispersion Science and Technology, 23 (3), 367-374.

Brandal O., *Interfacial (O/W) properties of naphthenic acids and metal naphthenates, naphthenic acid characterization and metal naphthenate inhibition*, 2005, PhD thesis, Department of Chemical Engineering, Norwegian University of Science and Technology, Trondheim, Norway.

Brient J. A., Wessner P. J., Doyle M. N., *Naphthenic acids*, 1995, in Encyclopedia of Chemical Technology Kirk-Othmer, 4th edition, volume 16, Kroschwitz J. I (editor), John Wiley and Sons, 1017-1029.

Brient J. A., *Commercial utility of naphthenic acids recovered from petroleum distillates*, 1998, presented before the Division of Petroleum Chemistry Inc. 215th National Meeting, American Chemical Society, Dallas, Texas, USA, March 29-April 3.

Brocart B., Hurtevent C., Volle J. L., *Analytical detection of Arn-type naphthenic acids in crudes*, 2005, presented at the 6th Petroleum Phase Behavior and Fouling Conference, Amsterdam, The Netherlands, June 25-29.

Campos M. C. V., Oliveira E. C., Filho P. J. S., C, Piatnicki C. M. S., Camarao E. B., *Analysis of tert-butyldimethylsilyl derivatives in heavy gas oil from Brazilian naphthenic acids by gas chromatography coupled to mass spectrometry with electron impact ionization*, 2006, Journal of Chromatography A, 1105 (1-2), 95-105.

Carroll J, J., Slupsky J. D., Mather A. E., *The solubility of carbon dioxide in water at low pressure*, 1991, Journal of Physical Chemistry Reference Data, 20, 1201-1209.

Cason J., Graham D. W., *Isolation of isoprenoid acids from a California petroleum*, 1965, Tetrahedron, 21, 471-483.

Castiglioni S., Bagnati R., Calamari D., Fanelli R., Zuccato E., *A multiresidue analytical method using solid-phase extraction and high-pressure liquid chromatography tandem mass spectrometry to measure pharmaceuticals of different therapeutic classes in urban wastewaters*, 2005, Journal of Chromatography A, 1092, 206-215.

Chan J., Forrest J. A., Torrie B. H., *Using a quartz crystal microbalance to probe formation of Xe hydrate in thin ice films*, 2004, Journal of Applied Physics, 96 (5), 2980-2984.

Clemente J. S., Prasad N. G. N., MacKinnon M. D., Fedorak P. M., *A statistical comparison of naphthenic acids characterized by gas chromatography-mass spectrometry*, 2003, Chemosphere, 50, 1265-1274.

Clemente J. S., Fedorak P. M., *Evaluation of tert-butyldimethylsilyl derivatives of naphthenic acids by gas chromatography-electron impact mass spectrometry*, 2004, Journal of Chromatography A, 1047, 117-128.

Collins R. N., *Separation of low-molecular mass organic-acid metal complexes by high-performance liquid chromatography*, 2004, Journal of Chromatography A, 1059, 1-12.

Cooper J. E., Bray E. E., *A postulated role of fatty acids in petroleum form*, 1963, Geochimica *et* Cosmochimica Acta, 27, 1113-1127.

Cotton F. A., Wilkinson G., *Advanced inorganic chemistry*, 1988, 5th edition, John Wiley and Sons.

Covey T. R., Lee E. D., Bruins A. P., Henion J. D., *Liquid chromatography mass spectrometry*, 1986, Analytical Chemistry, 58 (14), 1034-1045.

Cratin P. D., *Mathematical modeling of some pH-dependent surface and interfacial properties of stearic acid*, 1993, Journal of Dispersion Science and Technology, 14 (5), 559-602.

Cratin P. D., *Surface and interfacial dissociation constants: apparent vs. absolute,* 1994, Colloids and Surfaces A: Physicochemical and Engineering Aspects, 89, 103-108.

Crawford H. R., Neill G. H., Bucy B. J., Crawford P. B., *Carbon dioxide – a multipurpose additive for effective well stimulation*, 1963, Journal of Petroleum Technology, 15, 237-242.

Cressman P. R., Hurren M. L., Smith E. F., Holbrook D. L., *Caustic-free jet fuel Merox unit reduces waste disposal*, 1995, Oil and Gas Journal, 93 (12), 80-84.

Damas C., Vannier L., Naejus R., Couder R., *Influence of structural modifications near the polar head of sodium carboxylates on their aqueous solution behaviour*, 1999, Colloids and Surfaces A: Physicochemical and Engineering Aspects, 152, 183-187.

Dehkissia S., Larachi F., Rodrigue D., Chornet E., *Characterization of Doba-Chad heavy crude oil in relation with the feasibility of pipeline transportation*, 2004, Fuel, 83, 2157-2168.

Derungs W, A., *Naphthenic acid corrosion – an old enemy of the petroleum industry*, 1956, Corrosion, 12 (12), 617-622.

Dyer S, J., Graham G, M., Arnott C., *Naphthenate scale formation – examination of molecular controls in idealised systems*, 2003, SPE 80395, presented at the 5th International Symposium on Oilfield Scale, Aberdeen, UK, January 29-30.

Dyer S. J., Williams H. L., Graham G. M., Cummine C., Melvin, K B., Haider F., Gabb A. E., *Simulating calcium naphthenate formation and mitigation under laboratory conditions*, 2006, SPE 100632, presented at the 8th International Symposium on Oilfield Scale, Aberdeen, UK, May 31-June 1.

Dzidic I., Somerville A. C., Raia J. C., Hart H. V., *Determination of naphthenic acids in California crudes and refinery wastewaters by fluoride ion chemical ionization mass spectrometry*, 1988, Analytical Chemistry, 60, 1318-1323.

Earll M., *A guide to Log P and pKa measurements and their use*, 2006, http://www.raell.demon.co.uk/chem/logp/logppka.htm. This is an analytical chemistry website which gives in depth information on the measurement of dissociation constants and partition coefficients.

Ederth T., Claesson P. M., *Forces between carboxylic acid surfaces in divalent electrolyte solutions*, 2000, Journal of Colloid and Interface Science, 229, 123-128.

Ege S. N., *Organic chemistry – structure and reactivity*, 1994, 3rd edition, D. C and Heath Company.

Elvidge J. A., Sammes P. G., *A course in modern techniques of organic chemistry*, 1966, 2nd edition, Butterworths.

Enever R. P., Pilpel N., *Reaction between stearic acid and calcium ions at the air-water interface using surface viscometry*, 1967, Transactions of the Faraday Society, 63, 781-792.

Enever R. P., Pilpel N., *Reaction between stearic acid and calcium ions at the air-water interface using surface viscometry. Part 2-Mixed films of octadecanol and stearic acid*, 1967, Transactions of the Faraday Society, 63, 1559-1566.

Ekwall P., *Two types of micelle formation in organic solvents*, 1969, Journal of Colloid and Interface Science, 29 (1), 16-26.

Escobedo J., Mansoori G. A, *Heavy organic deposition and plugging of wells (analysis of Mexico's experience)*, 1992, SPE 23696, presented at the 2nd Latin American Petroleum Engineering Conference, Caracas, Venezuela, March 8-11.

Ese M. H., Kilpatrick P. K., *Stabilization of water-in-oil emulsion by naphthenic acids and their salts: model compounds, role of pH, and soap/acid ratio*, 2004, Journal of Dispersion Science and Technology, 25 (3), 253-261.

Fan T. P., *Characterisation of naphthenic acids in petroleum by Fast Atom Bombardment mass spectrometry*, 1991, Energy and Fuels, 5, 371-375.

Fitton J. G., Saunders A. D. Larsen L. M., Hardarson B. S., Norry M. J., *Volcanic rocks from the southeast Greenland margin at 63°N: composition, petrogenesis and mantle sources*, 1998, in proceedings of the Ocean Drilling Program Scientific Results, 152, 331–350.

Fitton J. G., X-*ray fluorescence spectrometry*, 2000, in Modern Analytical Geochemistry Longman Geochemistry, Gill R (editor), Chapter Six, Longman.

Fitton J. G., Godard M., *Origin and evolution of magmas on the Ontong Java Plateau*, 2004, Geological Society Special Publications, 229, 151-178.

Friberg S., Linden E. S., Saito, H., *Thin films from liquid crystals*, 1974, Nature, 251, 494-495.

Gaikar V. G., Maiti D., *Adsorptive recovery of naphthenic acids using ion-exchange resins*, 1996, Reactive and Functional Polymers, 31, 155-164.

Gallup D. G., Smith P. C., Chipponeri J., Abuyazid A., Mulyono D., *Formation and mitigation of metallic soap sludge, Attaka, Indonesia field*, 2002, SPE 73960, presented at the International Conference on Health Safety and Environment in Oil and Gas Exploration and Production, Kuala Lumpur, Malaysia, March 20-22.

Gallup D. G., Star J., *Soap sludges: aggravating factors and mitigation measures*, 2004, SPE 87471, presented at the 6th International Symposium on Oilfield Scale, Aberdeen, UK, May 26-27.

Gallup D. G., Smith P. C., Star J. F., Hamilton S. H., *West Seno deepwater development case history, production chemistry*, 2005, SPE 92969, presented at the International Symposium on Oilfield Chemistry, Houston, Texas, USA, February 2-4.

Gallup D. L., Curiale J. A., Smith P. C., *Characterization of sodium emulsion soaps formed from production fields of Kutei Basin, Indonesia*, 2007, Energy and Fuels, 21, 1741-1759.

Goldszal A., Hurtevent C., Rousseau G., *Scale and naphthenate inhibition in deep-offshore fields*, 2002, SPE 74661, presented at the 4th International Oilfield Scale Symposium, Aberdeen, UK, January 30-31.

Gomari, K. E. R., Hamouda, A.A., Effect of fatty acids, water composition and pH on the wettability alteration of calcite surface, 2006, Journal of Petroleum Science and Engineering, 50, 140-150.

Goodwin N. S., Park P. J. D., Rawlinson A. P., *Crude oil biodegradation under simulated and natural conditions*, 1981, Advances in Organic Geochemistry, proceedings of the 10th International Meeting on Organic Geochemistry, Bergen, Norway, 650-658.

Gorbaty M. L., Martella D. J. M, Sartori G., Savane D.W., Ballinger B. H., Blum S. C., Anderson M. P., Rammanarayanan T. A., *Process for neutralization of petroleum acids using overbased detergents*, 2000, US Patent 6054042.

Govindaraju K., *Compilation of working values and sample description for 383 geostandards*, 1994, Geostandards Newsletter, 18, 1–158.

Hao C., Headley J. H., Peru K. M., Frank R., Yang P., Solomon K. R., *Characterization and pattern recognition of oil-sand naphthenic acids using comprehensive two dimensional gas chromatography/time of flights mass spectrometry*, 2005, Journal of Chromatography A, 1067, 277-284.

Hajos P., Nagy L., *Retention behaviours and separation of carboxylic acids by ion-exchange chromatography*, 1998, Journal of Chromatography B, 717, 27-38.

Havre T, E., *Formation of calcium naphthenate in water/oil systems, naphthenic acid chemistry and emulsion stability*, 2002, PhD thesis, Department of Chemical Engineering, Norwegian University of Science and Technology, Trondheim, Norway.

Headley J. V., Peru K. M., MacMartin D. W., Winkler M., *Determination of dissolved naphthenic acids in natural water by using negative-ion electrospray mass spectrometry*, 2002, Journal of the AOAC International, 85 (1), 182-187.

Healey T. W., White L. R., *Ionizable surface group models of aqueous interfaces*, 1978, Advances in Colloid and Interface Science, 9, 303-345.

Heck A., *Introduction to Maple*, 2003, 3rd edition, Springer.

Hell C., Medinger E., *Uber das vorkommen und die zusammensetzung von sauren im rohpetroleum*, 1874, Berichte Der Deutschen Chemischen, Gesellschaft zu Berlin, Siebenter Jahrgang, 1957, Juli bis Dezember nachdruck, 1216-1223.

Hemmingsen P. V., Silset A., Hannisdal A., Sjoblom J., *Emulsions of heavy crude oils. I: influence of viscosity, temperature and dilution*, 2005, Journal of Dispersion Science and Technology, 26, 615-627.

Hoeiland S., Barth T., Blokhus A. M., Skauge A., *The effect of crude oil acid fractions on wettability as studies by interfacial tension and contact angles*, 2001, Journal of Petroleum Science and Engineering, 30, 91-103.

Holowenko F. M., MacKinnon M. D., Fedorak P. M., *Characterization of naphthenic acids in oil sands wastewaters by gas chromatography-mass spectroscopy*, 2002, Water Research, 36, 2843-2855.

Horvath-Szabo G., Czarnecki J., Masliyah J .H., *Phase behavior of sodium naphthenates, toluene and water*, 2001, Journal of Colloid and Interface Science, 242, 247-254.

Horvath-Szabo G., Czarnecki J., Masliyah J. H., *Liquid crystals in aqueous solutions of sodium naphthenates*, 2001, Journal of Colloid and Interface Science, 236, 233-241.

Horvath-Szabo G., Czarnecki J., Masliyah J. H., *Sandwich structures at oil-water interfaces under alkaline conditions*, 2002, Journal of Colloid and Interface Science, 253, 427-434.

Horvath-Szabo G., Czarnecki J., Masliyah J. H., *Emulsion stability based on phase behaviour in sodium naphthenates containing systems: Gels with a high organic solvent content*, 2003, Journal of Colloid and Interface Science, 257, 299-309.

Hsu C. S., Fukuda E., Roussis S. G., *Mass spectrometric characterization of acids in crude oils*, 1998, presented before the Division of Petroleum Chemistry Inc. 215th National Meeting, American Chemical Society, Dallas, Texas, USA, March 29-April 3.

Hsu C. S., Dechert G. J., Robbins W. K., Fukuda E. K., *Naphthenic acids in crude oils characterized by mass spectrometry*, 2000, Energy and Fuels, 14, 217-233.

Huang J., *Thermal degradation of asphaltene and infrared characterization of its degraded fractions*, 2006, Petroleum Science and Technology, 24 (9), 1089-1095.

Hughey C. A., Rodgers R. P., Marshall A. G., Qian K., Robbins W. K., Identification of acidic NSO compounds in crude oils of different geochemical origins by negative ion electrospray Fourier Transform ion cyclotron resonance mass spectrometry, 2002, Organic Geochemistry, 33, 743-759.

Hurtevent C., 2004, *personal communication.*

Hurtevent C., Ubbels S., *Preventing naphthenate stabilized emulsions and naphthenate deposits in fields producing acidic oils*, 2006, SPE 100430, presented at the 8th International Symposium on Oilfield Scale, Aberdeen, UK, May 31-June 01.

Idem R. O., Ibrahim H. H., *Kinetics of CO_2-induced asphaltene precipitation from various Saskatchewan crude oils during CO_2 miscible flooding*, 2002, Journal of Petroleum Science and Engineering, 35, 233-246.

Iupac, *Compendium of Chemical Terminology*, 1997, 2nd edition, www.iupac.org.

Jaffe R., Albrecht P., Oudin J. L., *Carboxylic acids as indicators of oil migration II. Case of Mahakam Delta, Indonesia*, 1988, Geochimica et Cosmochimica Acta, 52, 2599-2607.
Jaffe R., Gallardo M. T., *Application of carboxylic acid biomarkers as indicators of biodegradation and migration of crude oils from the Maracaibo Basin, Western Venezuela*, 1993, Organic Geochemistry, 20 (7), 973-984.

Jiang H., Jordan K. D., Taylor C. E., *Molecular dynamics simulations of methane hydrate using polarizable force fields*, 2007, Journal of Physical Chemistry B, 111 (23), 6486-6492.

Jochum K. P., Seufert H. M., Thirlwall M. F., *High-sensitivity Nb analysis by spark-source mass spectrometry (SSMS) and calibration of XRF Nb and Zr*, 1990, Chemical Geology, 81 (1-2), 1–16.

Johnson D., McAteer G., Zuk H., *Naphthenic acid corrosion field evaluation and mitigation studies*, 2002, presented at the European Refining Technical Conference, Paris, France, November 18-20.

Jones D. M., Watson J. S., Meredith W., Chen M., Bennett B., *Determination of naphthenic acids in crude oils using nonaqueous ion exchange solid phase extraction*, 2001, Analytical Chemistry, 73, 703-707.

Kanicky J. R., Lopez-Montilla J. C., Pandey S., Shah D. O., *Surface chemistry in the petroleum industry*, 2001, Handbook of Applied Surface and Colloid Chemistry, Chapter 11, Holmberg K (editor), John Wiley and Sons.

Kanicky J. R., Shah D. O., *Effect of degree, type, position of unsaturations on the pKa of long-chain fatty acids*, 2002, Journal of Colloid and Interface Science, 256, 201-207.

Kanicky J. R., Shah D.O., *Effect of premicellar aggregation on the pKa of fatty acid soap solutions*, 2003, Langmuir, 19, 2034-2038.

Kazanis J., *Isolation and structure determination of naphthenic acids*, 1971, PhD thesis, Department of Chemistry, University of Nebraska, Lincoln, Nebraska, USA.

Kim S., Stanford L., Rodgers R. P., Marshall A. G., Walters C. C., Qian K., Wenger L. M., Mankiewicz P., *Microbial alteration of the acidic and neutral polar NSO compounds revealed by Fourier transform ion cyclotron resonance mass spectrometry*, 2005, Organic Geochemistry, 36, 1117-1134.

Klein G, C., Rodgers R, P., Larter S. R., Bennett B., Marshall A. G., *A comprehensive comparison of the polar NSO compounds in a suite of biodegraded oils by ESI FTICR MS*, 2006, presented at the 17th International Mass Spectrometry Conference, Prague, Czech Republic, August 27- September 1.

Koike L., Reboucas L. M. C., Reis A. M, Marsaioli A. J., Richnow H. H., Michaelis W., *Naphthenic acids from crude oil of Campos Basin*, 1992, Organic Geochemistry, 18 (6), 851-860.

Kovalchuck V. I., Zholkovskiy E. K., Bondarenko N. P., Vollhardt D., *Dissociation of fatty acid and counterion binding at the Langmuir monolayer deposition: theoretical considerations*, 2001, Journal of Physical Chemistry B, 105, 9254-9265.

KSV, Sigma 70 surface tension/contact angle meter, 2004, http://www.ksvinc.com/sigma70.htm.

Kuzmanovic B., Kuipers N. J. M., De Haan A. B., Kwant G., *Reactive extraction of carboxylic acids from apolar hydrocarbons using aqueous sodium hydrogen carbonate with back-recovery using carbon dioxide under pressure*, 2005, Separation and Purification Technology, 47 (1-2), 58-72.

Lachance G. R., Claisse F., *Quantitative X-ray fluorescence analysis: theory and application*, 1995, John Wiley and Sons.

Lagendijk S., *Considerations for various methods for density and specific gravity,* 1998, *Report for the Institute for Interlaboratory Studies*, Dordrecht, the Netherlands.

Langmuir I., Schaefer V. J., *The effect of dissolved salts on insoluble monolayers*, 1937, Journal of the American Chemical Society, 59, 2400-2414.

Laredo G. C., Lopez C. R., Alvarez R. E., Cano J. L., *Naphthenic acids, total acid number and sulfur content profile characterization in Isthmus and Maya crude oils*, 2004, Fuel, 83 (11), 1689-1695.

Leenheer J. A., Rostad C. E., *Tannins and terpenoids as major precursors of Swanee River fulvic acid*, 2004, U.S. Geological Survey Scientific Investigations, Report 5276.

Li M., Lin M., Wu Z., Christy A. A., *The influence of NaOH on the stability of paraffinic crude oil emulsion*, 2004, Fuel, 84, 183-187.

Lutnaes B. J., Brandal O., Sjoblom J., Krane J., *Archaeal C80 isoprenoid tetracids responsible for naphthenate deposition in crude oil processing*, 2006, Organic and Biomolecular Chemistry, 4, 616-620.

Mackay E., Sorbie K. S., *Brine mixing in waterflooded reservoirs and the implications for scale prevention*, 2000, SPE 60193, presented at the 1st International Symposium on Oilfield Scale, Aberdeen, UK, January 26-27.

Mackay E. J., *The application of reservoir simulation calculations to oilfield scale management*, 2005, PhD thesis, Institute of Petroleum Engineering, Heriot Watt University, Edinburgh, UK.

Mcmullen N, D., *Flow assurance field solutions*, OTC 18381, 2006, presented at the Offshore Technology Conference, Houston, Texas, USA, May 1-4.

Malvern., *Basic principles of particle size analysis*, 2005, http://www.malvern.co.uk/LabEng/products/iwtn/particle_size.htm.

Masspec., *Introduction to mass spectrometry*, 2005, Scripps Centre for Mass Spectrometry, http://masspec.scripps.edu.

Marshall A. G., Hendrickson C. L., Jackson G. S., *Fourier transform ion cyclotron resonance mass spectrometry: a primer*, 1998, Mass Spectrometry Reviews, 17, 1-35.

McNaughton J. L., Mortimer C. T., *Differential Scanning Calorimetry*, 1975, IRS Physical Chemistry Series 2, volume 10, Butterworths.

Mediaas H., Grande K., Hustad B-M., Rasch A., Rueslatten H, G., Vindstad J. E., *The acid-ier method – a method for selective isolation of carboxylic acids from crude oils and other organic solvents*, 2003, SPE 80404, presented at the 5th International Symposium on Oilfield Scale, Aberdeen, UK, January 29-30.

Mediaas H., Grande K., Hustad B-M., Hovik K. R, Kummernes H., Nergard B., Vindstad J. E., *A unique laboratory test rig reduces the need for offshore tests to combat calcium naphthenate deposition in oilfield process equipment*, 2005, presented at Tekna Oilfield Chemistry Symposium, Geilo, Norway, March 13-16.

Mendez Z., Anton R. E., Salager J-L., *Surfactant oil water systems near the affinity inversion, Part XI, pH sensitive emulsions containing carboxylic acids*, 1999, Journal of Dispersion Science and Technology, 20 (3), 883-892.

Meredith W., Kelland S-J., Jones D. M., *Influence of biodegradation on crude oil acidity and carboxylic acid composition*, 2000, Organic Geochemistry, 31, 1059-1073.

Miller D. E., Holba A. G., Huges W. B., *Effects of biodegradation on crude oils, Exploration for Heavy Crude Oil and Natural Bitumen*, 1987, Studies in Geology #25: Tulsa, Oklahoma, AAPG, Meyer R. F (editor), 233-241.

Morrison R. T., Boyd R. N., *Organic Chemistry*, 1979, 3rd edition, Chapter 18 Carboxylic Acids, Allyn and Bacon Inc.

Mullins O. C., Sheu E. Y., Hammani A., Marshall A. G., *Asphaltenes, heavy oils, and petroleomics*, 2007, Springer.

Murkerjee P., *Dimerization of anions of long-chain fatty acids in aqueous solutions and the hydrophobic properties of the acids*, 1965, The Journal of Physical Chemistry, 69 (9), 2821-2827.

Nascimento L. R., Rebouças L. M. C., Koike L., Reis F, A. M., Soldan A. L., Cerqueira J. R., Marsaioli A. J., *Acidic biomarkers from Albacora oils, Campos basin, Brazil*, 1999, Organic Geochemistry, 30, 1175-1191.

Nikolov A. D., Wasan D. T., *Ordered micelle structuring in thin films formed from anionic surfactant solutions*, 1989, Journal of Colloid and Interface Science, 133 (1), 1-12.

New Objective., *What is electrospray?*, 2005, www.newobjective.com/electrospray. This is the website of on of the LCMS manufacturers which provides a wealth of information on instrument operation and calibration.

Norrish K., Hutton J. T., *An accurate X-ray spectrographic method for the analysis of a wide range of geological samples*, 1969, Geochimica et Cosmochimica. Acta, 33, 431-453.

Ogden P, H (editor), *Chemicals in the Oil Industry*, 1983, proceedings of a symposium organized by the North West Region of the Industrial Division of the Royal Society of Chemistry, Manchester, UK, March 22-23.

Ohlenbusch G., Zwiener C., Meckenstock R. U., Frimmel F. H., *Identification and quantification of polar naphthalene derivatives in contaminated groundwater of a former gas plant site by liquid chromatography-electrospray ionisation tandem mass spectrometry*, 2002, Journal of Chromatography A, 967, 201-207.

Oilplus., *Oilplus offers revolutionary oil screening technique for predicting calcium naphthenates*, 2006, Oilplus newsletter, June.

Patist A., Oh S. G., Leung R., Shah D. O., *Kinetic of micellization: its significance to technological processes*, 2001, Colloids and Surfaces A: Physicochemical an Engineering Aspects, 176, 3-16.

Pearson K, *Separator profiling: Kuito FPSO case study*, 2004, SPE 8847, presented at the 11th International Petroleum Exhibition and Conference, Abu Dhabi, UAE, October 10-13.

Peters K. E., Moldowan J. E., *The Biomarker Guide – Interpreting Molecular Fossils in Petroleum and Ancient Sediments*, 1993, Prentice Hall.

Petex, *Treating Oilfield Emulsions*, 1990, University of Texas at Austin, Petroleum Extension Service.

Philips, *Environmental scanning electron microscopy. An introduction to ESEM*, 1996, 2nd edition, Philips Electron Optics.

Philp R. P., *High temperature gas chromatography for the analysis of fossil fuels: a review*, 1994, Journal of High Resolution Chromatography, 17, 398-406.

Pickett J. M., Ellway K. A., *Gels in soap stabilized emulsions*, 1976, Journal of Pharmacy and Pharmaceuticals, 28, 625-628.

Piehl R. L., *Naphthenic acid corrosion in crude distillation units*, 1988, Materials Performance, 27 (1), 37-43.

Pope M. I., Judd M. D., *Differential Thermal Analysis*, 1980, Heyden & Son Ltd.

Qian K., Robbins W. K., Hughey C. A., Cooper H. J., Rodgers R. P., Marshall A. G., *Resolution and identification of elemental composition for more than 3000 crude acids in heavy petroleum by high-field Fourier-Transform ion cyclotron resonance mass spectrometry*, 2001, Energy and Fuels, 15, 1505-1511.

Ramstad K., *Grane field naphthenates*, 2001, presented at the Flow Assurance and Scale Team Steering Meeting, Institute of Petroleum Engineering, Heriot-Watt University, Edinburgh, UK, November 11-12.

Reinsel M. A., Borkowski J. J., Sears J, T., *Partition coefficients for acetic, propionic and butyric acids in crude oil/water system*, 1994, Journal of Chemical Engineering Data, 39, 513-516.

Riazi, M. R., *Chracterization and properties of petroleum fractions*, 2005, 1st edition, ASTM international.

Robbins W. K., *Challenges in the characterization of naphthenic acids in petroleum*, 1998, presented before the Division of Petroleum Chemistry Inc. 215th National Meeting, American Chemical Society, Dallas, Texas, USA, March 29-April 3.

Rodgers R. P., Rahimi O., Messer B., Phillips T., Marshall A. G., *Advanced evaluation of crude compositions for optimum corrosion resistance and processing capabilities*, 06582, 2006, presented at the 61st Annual Corrosion Nace Conference and Exposition, San Diego, California, USA, March 12-16.

Rogers V. V., Liber K., MacKinnon M. D., *Isolation and characterization of naphthenic acids from Athabasca oil sands tailings pond water*, 2002, Chemosphere, 48, 519-527.

Rousseau G., Zhou H., Hurtevent C., Calcium carbonate and naphthenate mixed scale in deep-offshore fields, 2001, SPE 68307, presented at the 3rd International Symposium on Oilfield Scale, Aberdeen, UK, January 30-31.

Roussis S. G., Lawlor L. J., *Direct determination of acid distributions in crude and crude fractions*, 2002, International Patent, WO 02/48698 A1.

Rudin J., Wasan D. T., *Mechanisms for lowering of interfacial tension in alkali/acidic oil systems 1. Experimental studies*, 1992, Colloids and Surfaces, 68, 67-79.

Rudzinski W. E., Oehlers L., Zhang Y., Najera B., *Tandem mass spectrometric characterization of commercial naphthenic acids and Maya crude oil*, 2002, Energy and Fuels, 16, 1178-1185.

Russell P. A., James R., *Determination of toxic elements in liquid hazardous waste using high-resolution energy dispersive X-ray fluorescence spectrometry*, 1997, Journal of Analytical Spectrometry, 12, 25-32.

Saab J., Mokbel A. C., Razzouk A. C., Ainous N., Zydowicz N., Jose J., *Quantitative extraction procedure of naphthenic acids contained in crude oils. Characterization with different spectroscopic methods*, 2005, Energy and Fuels, 19, 525-531.

Saunders J. K. M., Hunter B. K., *Modern NMR spectroscopy a guide for chemis*ts, 1993, 2nd edition, Oxford University Press.

Sartori G., Savage C. W., Ballinger B. H., Dalrymple D. C., *Process for extraction of naphthenic acids from crudes*, 2001, US Patent 6281328 B1.

Sato S., Takanohashi T., Tanaka R., *Molecular weight calibration of asphaltenes using gel permeation chromatography/mass spectrometry*, 2005, Energy Fuels, 19 (5), 1991-1994.

Schmitter J. M., Arpino P., Guiochon G., *Investigation of high-molecular weight carboxylic acids in petroleum by different combination of chromatography (gas and liquid) and mass spectrometry (electron impact and chemical ionization)*, 1978, Journal of Chromatography, 167, 149-158.

Schouten S., Wakeham S. G., Hopmans E. C., Damste J. S. S., *Biogeochemical evidence that thermophilic archaea mediate the anaerobic oxidation of methane*, 2003, Applied and Environmental Microbiology, 69, 1680-1686.

Seifert W. K., Howells W. G., *Interfacially active acids in a California crude oil. Isolation of carboxylic acids and phenols*, 1969, Analytical Chemistry, 41 (4), 554-562.

Seifert W. K., *Effect of phenols on the interfacial activity of crude oil (California). Carboxylic acids and the identification of carbazoles and indoles*, 1969, Analytical Chemistry, 41 (4), 562-568.

Seifert W., Gallegos E. J., Teeter, R., *Proof of structure of steroid carboxylic acids in a California petroleum by deuterium labelling, synthesis and mass spectrometry*, 1972, Journal of the American Chemical Society, 94, 5880-5887.

Silverstein R. M., Bassler G. C., Morrill T. C., *Spectrometric identification of organic compounds*, 1991, 5th edition, John Wiley and Sons.

Silverstein R. M., Webster F. X., Kiemle D. J., *Spectrometric identification of organic compounds*, 2005, 7th edition, John Wiley and Sons.

Sirius Analytical Instruments., *Applications and Theory Guide to pH-Metric pKa and logP determination,* 1993.

Sirius Analytical Instruments., STAN Sirius Technical Application notes, 1994, Volume 1.

Sjoblom J., Aske N., Auflem I, H., Brandal O., Havre T. E., Saether O., Westvik A., Johnsen E. E., Kallevik H., *Our current understanding of water-in-crude emulsions. Recent characterization techniques and high-pressure performance*, 2003, Advances in Colloid and Interface Science, 100, 399-473.

Skippins J., Johnson D., Davies R., *Corrosion-mitigation program*, 2000, Oil and Gas Journal, 98 (37), 64-68.

Smith B. E., Sutton P. A., Lewis A., Dunsmore B., Fowler G., Krane J., Lutnaes B. F., Brandal O., Sjöblom J., Rowland S. J., *Analysis of ARN naphthenic acids by high temperature gas chromatography and high performance liquid chromatography*, 2007, Journal of Separation Science, 30 (3), 375-380.

Smith E., Dent G., *Modern Raman Spectroscopy: A practical Approach*, 2005, Wiley.

Smith P. C., *Soap (naphthenates) scales management from deepwater flow assurance aspects to oil terminal sludge processing*, 2004, presented at IQPC Flow Assurance. A Holistic Approach Meeting, Kuala Lumpur, Malaysia, December 1-2.
Smith P. C., Turner M., 2004, *personal communication*.

Somasundaran P., Ananthapadmanabhan K. P., Ivanov I. B., *Dimerization of oleate in aqueous solutions*, 1984, Journal of Colloid and Interface Science, 99 (1), 128-135.

Sorbie, K., Mackay, E., Neville, A., Flow Assurance and Scale Team FAST 1. Progress Report, Presentations, Publicatios and Thesis, April 2001-March 2004, Heriot-Watt University, Edinburgh.

Speight J, G., *The chemistry and technology of petroleum*, 1991, 2nd edition, Marcel Dekker.

Speight J. G., *Petroleum asphaltenes part 1. Asphaltenes, resins and the structure of petroleum*, 2004, Oil and Gas Science and Technology – Rev IFP, 59 (5), 467-477.

Spildo K., Hoiland H., *Interfacial properties and partitioning of 4-heptylbenzoic acid between decane and water*, 1999, Journal of Colloid and Interface Science, 209, 99-108.

Standal S. H., Blokhus A. M., Haavik J., Skauge A., Barth T., *Partition coefficients and interfacial activity for polar components in oil/water model systems*, 1999, Journal of Colloid and Interface Science, 212, 33-41.

Stenius P., Zillacus C. H., *Association equilibria and micelle formation of fatty acid sodium salts. I. A survey of potentiometric measurements on salts with 2-6 carbon atoms at high ionic strength*, 1971, Acta Chimica Scandinavica, 25, 2232-2250.

Stenius P., *Association equilibria and micelle formation of fatty acid sodium salts. II. An investigation of straight-chain salts by vapour pressure osmometry*, 1973, Acta Chimica Scandinavica, 27, 3435-3451.

Stenius P., *Association equilibria and micelle formation of fatty acid sodium salts. III. The association of sodium butyrate at 40℃ in 3 M NaCl*, 1973, Acta Chimica Scandinavica, 27, 3452-3466.

Stenius P., *Association equilibria and micelle formation of fatty acid sodium salts. IV. A comparison between the association of sodium pentanoate, sodium 3-methylbutyrate and sodium trymethylacetate*, 1973, Acta Chimica Scandinavica, 27, 3897-3918.

Stenius, P., *Association equilibria and micelle formation of fatty acid sodium salts. V. Investigation of branched chain salts by vapour pressure osmometry*, 1978, Acta Chimica Scandinavica A, 32, 289-296.

St John W. P., Rughani J., Green S. A., McGinnis G. D., *Analysis and characterisation of naphthenic acids by gas chromatography-electron impact mass spectrometry of tert-butyldimethylsilyl derivatives*, 1998, Journal of Chromatography A, 807, 241-251.

Straasner J. E., *Effect of pH on interfacial films and stability of crude oil-water emulsion*, 1968, Journal of Petroleum Technology, 243, 303-312.

Tomczyk N. A., Winans R. E., Shinn J. H., Robinson R. C., *Results of treatment on acid content in a California heavy crude*, 1998, presented before the Division of Petroleum Chemistry Inc. 215th National Meeting, American Chemical Society, Dallas, Texas, USA, March 29-April 3.

Tomczyk N. A., Winans R. E., Shinn J. H., Robinson R. C., *On the nature and origin of acidic species in petroleum 1. Detailed acid type distribution in a California crude oil*, 2001, Energy and Fuels, 15, 1498-1504.

Trainer M., *The effects of particle shape on particle size resolution using angular scattering measurements*, 2001, presented at the 52nd Pittsburgh Conference, New Orleans, Louisiana, USA, March 4-9.

Trusovs S., *Method for preparation of metal organic acid chelates*, 2003, US Patent 6670494 B1.

Turnbull A., Slavcheva E, Shone B., *Factors controlling naphthenic acid corrosion*, 1998, Corrosion, 54 (11), 922-930.

Turner M., Smith C. P., *Controls on soap scale formation, including naphthenate soaps - drivers and mitigation*, 2005, SPE 94339, presented at the 7th International Symposium on Oilfield Scale, Aberdeen, UK, May 11-12.

Ubbels S. J., Turner M., *Diagnosing and preventing naphthenate stabilised emulsions and naphthenate deposits during crude oil processing,* 2005, presented at the 6th Petroleum Phase Behavior and Fouling Conference, Amsterdam, The Netherlands, June 25-29.

Ushikusa T., *Decomposition temperature of fatty acid metal salts used as the constituent molecules of molecular cognizance thin solid films*, 1990, Japanese Journal of Applied Physics, 29, 11, 2460-2464.

Verzaro F., Bourrel M., Garnier O., Zhou H. G., Argillier J. F., *Heavy acidic oil transportation by emulsion in water*, 2002, SPE 78959, presented at the International Thermal Operations and Heavy Oil Symposium and International Horizontal Well Technology Conference held in Calgary, Alberta, Canada, November 4-7.

Vindstad J. E., Bye A. S., Grande K. V., Hustad B. M., Hustvedt E., Nergard B., *Fighting naphthenate deposition at the Heidrun field*, 2003, SPE 80375, presented at the 5th International Symposium on Oilfield Scale, Aberdeen, UK, January 29-30.

Warren B. E., *X-ray diffraction*, 1969, 1st edition, General Publishing Company.

Water, Ionisation Sources, 2005, http://www.waters.com/watersdivision. This is a website of a manufacturer and supplier of LCMS equipment.

Weers J. J., Bieber S., *Calcium removal from high tan crudes*, 2005, Petroleum Technology Quarterly, 10 (4), 21-25.

Weiss H. H., Wilhelms A., Mills N., Scotchmer J., Hall P. B., Lind K., Brekket T., *NIGOGA – The Norwegian industry guide to organic geochemistry analysis*, 2000, published by the Norwegian Petroleum Directorate.

Williams B., *Refiners' future survival hinges on adapting to changing feedstocks, product species*, 2003, Oil and Gas Journal, 101 (31), 20-34.

Wolstenholme G. A., Schulman J. H., *Metal-monolayer interactions in aqueous systems. part I – the interaction of monolayers of long chain polar compounds with metal ions in the underlying solution*, 1950, Transactions of the Faraday Society, 46, 475-487.

Wolstenholme G. A., Schulman J. H., *Metal-monolayer interactions in aqueous systems. part III – steric effects with branched chain fatty acid monolayers*, 1951, Transactions of the Faraday Society, 47, 788-794.

Wong D. C., van Compernolle R., Nowlin J. G., O'Neal D. L., Johnson G. M., *Use of supercritical fluid extraction and fast ion bombardment mass spectrometry to identify toxic chemicals from a refinery effluent adsorbed onto granular activated carbons*, 1996, Chemosphere, 32, 1669-1679.

Yang X., Czarnecki J., *Tracing sodium naphthenate in asphaltenes precipitated from Athabasca bitumen*, 2005, Energy and Fuels, 19, 2455-2459.

Yazdanian M., Yu H., Zografi G., *Ionic interactions of fatty acid monolayers at the air/water interface*, 1990, Langmuir, 6, 1093-1098.

Ye X., *Gas oil desalting reduces chlorides in crude*, 2000, Oil and Gas Journal, 98 (42), 76-81.

Yen T. W., Marsh W. P., MacKinnon M. D., Fedorak P. M., *Measuring naphthenic acids concentrations in aqueous environmental samples by liquid chromatography*, 2004, Journal of Chromatography A, 1033, 83-90.

Yepez O., *Influence of different sulfur compounds on corrosion due to naphthenic acid*, 2005, Fuel, 84, 97-104.

Zhang Y., Shaw H., Farquhar R., Dawe R., *The kinetic of carbonate scaling – application for the prediction of downhole carbonate scaling*, 2001, Journal of Petroleum Science and Engineering, 29, 85-95.

Zyskowski, J., Kamdem, P. D., *Ultraviolet spectrophotometry and fourier transform infrared spectroscopy characterization of copper naphthenate*, 1999, Wood and Fiber Science, 31 (4), 441-446.